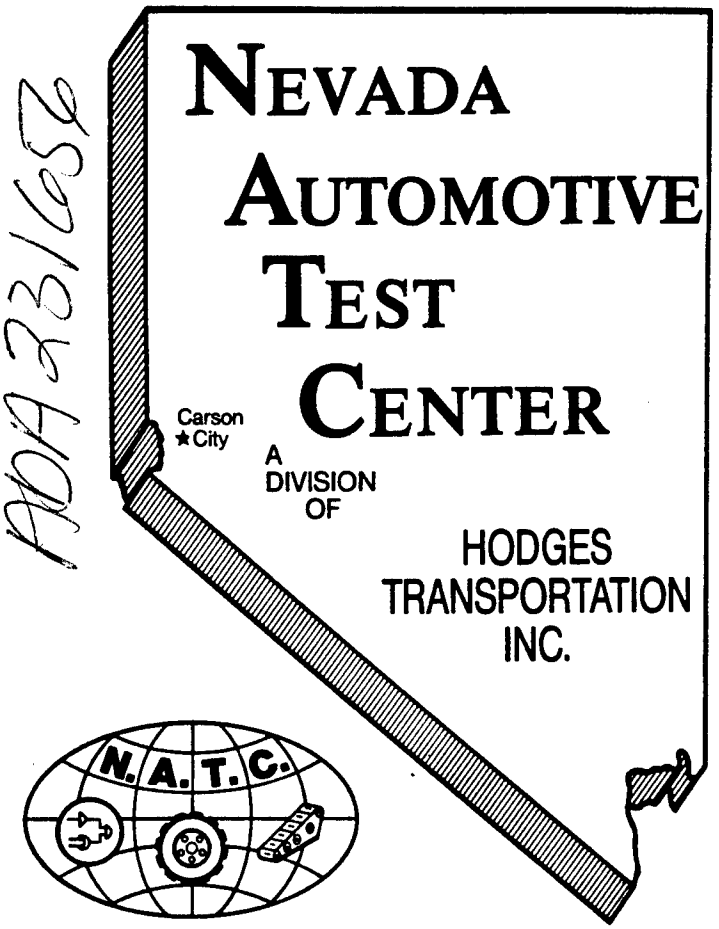

FINAL REPORT
FOR
U.S. ARMY TANK-AUTOMOTIVE COMMAND

TERRAIN SEVERITY DATA GENERATION AT YUMA PROVING GROUND

TACOM REPORT NO. 13491

AUTHORIZATION:
CONTRACT NO. DAAE07-89-C-R106

NATC PROJECT NO. 20-17-399

OCTOBER 1989 - NOVEMBER 1990

VOLUME I OF II

REPORT DOCUMENTATION PAGE	1. REPORT NO. 13491	2.	3. Recipient's Accession No.

4. Title and Subtitle	5. Report Date
TERRAIN SEVERITY DATA GENERATION AT YUMA PROVING GROUND	Approval Date: Nov 1990
	6.

7. Author(s)	8. Performing Organization Rept. No.
S. Colin Ashmore, Henry C. Hodges Jr., Matthew J. M. Prebeg	NATC 20-17-399

9. Performing Organization Name and Address	10. Project/Task/Work Unit No.
Nevada Automotive Test Center P.O. Box 234 Carson City, Nevada 89702 (702) 882-3261	11. Contract(C) or Grant(G) No. (C) DAAE07-89-C-R106 (G)

12. Sponsoring Organization Name and Address	13. Type of Report & Period Covered
U.S. Army Tank-Automotive Command AMSTA-QAT Warren, Michigan 48397-5000 Attn: Mr. Chester Kedzior (COTR)	Final - Volume I of II Oct 1989 - Nov 1990 14.

15. Supplementary Notes

This report consists of two volumes: Volume I contains the report narrative and supplementary charts; Volume II contains additional supplementary charts.

16. Abstract (Limit: 200 words)

This report details the results of a course profiling exercise conducted at the Yuma Proving Grounds (YPG) using the Nevada Automotive Test Center (NATC) Dynamic Force Measurement Vehicle (DFMV) methodology, the U.S. Army Waterways Experiment Station (WES) rod and level methodology and the Aberdeen Proving Ground (APG) inertial profilometer methodology. The rod and level methodology was used to establish the baseline for validation and comparison purposes. Eleven test courses were profiled at YPG. The test courses profiled included terrain representative of that used by the Army for ground-based vehicle durability testing. All data acquired was supplied to the U.S. Army Tank-Automotive Command (TACOM) for further analysis by their vehicle simulation department.

For each of the eleven courses, a left- and right-wheel path elevation versus distance profile, a left- and right-wheel path wave-number spectrum and coherence function plots were computed from the four wheels on the DFMV. This data was compared to equal data from the rod and level and the inertial profilometer.

Based upon the profiles and wave-number spectra computed using procedures in this report, techniques for measuring and monitoring road roughness characteristics are recommended. It is further recommended that a wave-number spectrum course roughness description replace the current RMS roughness index.

17. Document Analysis a. Descriptors

road roughness, test course roughness, terrain severity, road profile, profile measurement, wave-number spectra, spatial PSD, vehicle testing, vehicle simulation

b. Identifiers/Open-Ended Terms

Dynamic Force Measurement Vehicle, U.S. Army Waterways Experiment Station rod and level, Aberdeen Proving Ground inertial profilometer, Yuma Proving Ground RMS courses, Yuma Proving Ground Middle East Courses, Yuma Proving Ground Truck Hill courses

c. COSATI Field/Group

18. Availability Statement	19. Security Class (This Report)	21. No. of Pages
Unlimited	Unclassified	277
	20. Security Class (This Page)	22. Price
	None	

NOTICES

This report is not to be construed as an official Department of the Army position.

Mention of any trade names or manufacturers in this report shall not be construed as an official endorsement or approval of such products or companies by the U.S. Government.

Destroy this report when it is no longer needed. Do not return it to the originator.

TABLE OF CONTENTS

TABLE OF CONTENTS
(CONTINUED)

TABLE OF CONTENTS
(CONTINUED)

PAGE

LIST OF FIGURES

LIST OF FIGURES
(CONTINUED)

LIST OF FIGURES
(CONTINUED)

LIST OF TABLES

TERRAIN SEVERITY DATA GENERATION AT YUMA PROVING GROUND

1.0 SUMMARY

Two summaries are given, a nontechnical application summary and a project summary.

1.1 Nontechnical Application Summary of DFMV Profile Data

The data in this report details the results of a course profiling exercise conducted at the Yuma Proving Grounds (YPG) using the Nevada Automotive Test Center (NATC) Dynamic Force Measurement Vehicle (DFMV) methodology, the Waterways Experiment Station (WES) rod and level methodology and the Aberdeen Proving Ground (APG) inertial profilometer methodology. The objective of this nontechnical application summary is to explain in limited detail the concept of a wave-number spectrum and the application it has for measuring and monitoring roughness of the Army's durability test courses. However, it is more important to look beyond the details of the results and comparisons contained in this report and focus on the opportunities a terrain presentation of this format provides. Specifically, in addition to measuring and monitoring test course roughness, this methodology can be used for illustrating differences in test course roughness between different courses around the country, specifying mission profiles that can be utilized by both the design engineer and the procuring activity in vehicle buy specifications, accurately performing accelerated life cycle testing, conducting fatigue RAM analysis, providing terrain inputs for computer modeling, understanding terrain inputs to vehicle systems over a range of vehicle speeds and conducting vehicle comparisons. This summary expands on the potential use of wave-number spectra by the vehicle designer, developer, tester and end-user.

Wave-number spectra (spatial PSDs) are an efficient and very accurate technique for measuring and rapidly monitoring long sections of various terrain types, including paved road and off-road durability test courses. This technique is independent of the measurement methodology and can be applied to rod and level data, as well as more advanced systems such as the DFMV. Since the implementation of a wave-number spectrum format is recommended in this paper as a means of measuring and monitoring test course roughness, and since much of the historical literature reviewed contained erroneous analysis (e.g., aliasing problems at the shorter wavelengths and lack of proper detrending), great detail has been given to signal processing considerations and procedures. In addition to presenting the results of the DFMV methodology, it is hoped that this document can serve as a useful guideline for analyzing terrain roughness measurements.

Tremendous effort has been expended over the years addressing the issue of terrain inputs to ground vehicle systems. This document attempts to identify problem areas and provide recommendations for application of a validated measurement technique. For any user of terrain or roughness data, the method of analysis and basis for the results must be critically reviewed. For the Army, as a user of this type data, the signal-processing considerations addressed in this report have to be asked of every system and every spectrum produced by a profilometer system (including the rod and level). It is hoped that this document, through the presentation of valid engineering data, will assist in the development of a methodology that can be implemented into the procurement system, as well as to insure repeatable and representative vehicle durability test environments.

In 1979, U.S. Army Tank-Automotive Command (TACOM) requested that NATC utilize the DFMV methodology to measure and evaluate durability test courses at YPG, APG and NATC. Since that time, NATC has continued to upgrade its profiling methodology. NATC's current goal is integration of terrain roughness data into current vehicle dynamics modelling methodologies (Dynamic Analysis Design System, DADS). The data and analysis presented in this report represents the first step in a multi-task effort. For this program, NATC's DFMV was used to measure profiles of eleven courses located at YPG. The courses selected provided a range of roughness inputs, including standard WES RMS roughness courses and standard YPG vehicle durability courses. The intent of this phase was to provide a concurrent set of WES rod and level, APG inertial profilometer and NATC terrain severity data from which the individual methodologies could be assessed, with the WES data regarded as the reference.

To continuously measure the terrain, the DFMV is equipped with a vertical, longitudinal and lateral force transducer, a vertical accelerometer and a wheel speed sensor at each wheel end. The vertical elevation changes in the course are calculated at each wheel by determining what the course had to look like under the tire to cause the measured forces and accelerations at each wheel. From those measurements, the exact course can be calculated, in terms of elevation versus distance and a wave-number spectrum.

Consider a hypothetical road with only three wavelengths, as shown in the wave-number spectrum in Figure 1 (the dots in the dashed spectrum are the three wavelengths of interest). To visualize this road, first assume that the road is a continuous sine wave of 100-foot cycles. Overlaid on each 100-foot cycle are ten, 10-foot cycles. Also overlaid on each 100-foot cycle are 100, 1-foot cycles. The x-axis is cycle/foot. The inverse of cycle/foot is simply "foot" and represents the length of one cycle of a wave. Figure 1 shows three separate wavelengths, one 100-foot long, one 10-foot long and one 1-foot long. The amplitude of the 100-foot wave is much greater than the 1-foot wave and thus has a higher amplitude on the y-axis of the plot.

The cycle/foot presentation is called spatial frequency, a frequency dependent on distance rather than time. For example, a rod and level measurement of the road described above would show vertical elevation changes along the length of a course, sampled at discrete distance intervals. This data can be plotted as elevation (amplitude) versus distance. A wave-number spectrum plot of that same data would show normalized amplitude squared versus spatial frequency. The plot in Figure 1 is the result of measuring the hypothetical road with a rod and level or the DFMV, and presenting the data in a frequency-domain plot. A collection of many of these frequencies is called a wave-number spectrum (as shown in the dashed lines in Figure 1).

Since the world is much more random in nature than sinusoidal, it is important to know both the amplitude of the vertical disturbances, as well as their frequency. The single-number Root Mean Squared (RMS) value describes only the amplitude of the roughness of the road. The user knows nothing about how far apart the random vertical disturbances are or how their amplitudes vary over the range of frequencies present. A wave-number spectrum gives both amplitude and frequency and, therefore, gives a complete picture of the road. A wave-number spectrum represents the true input to a vehicle, whether wheeled or tracked.

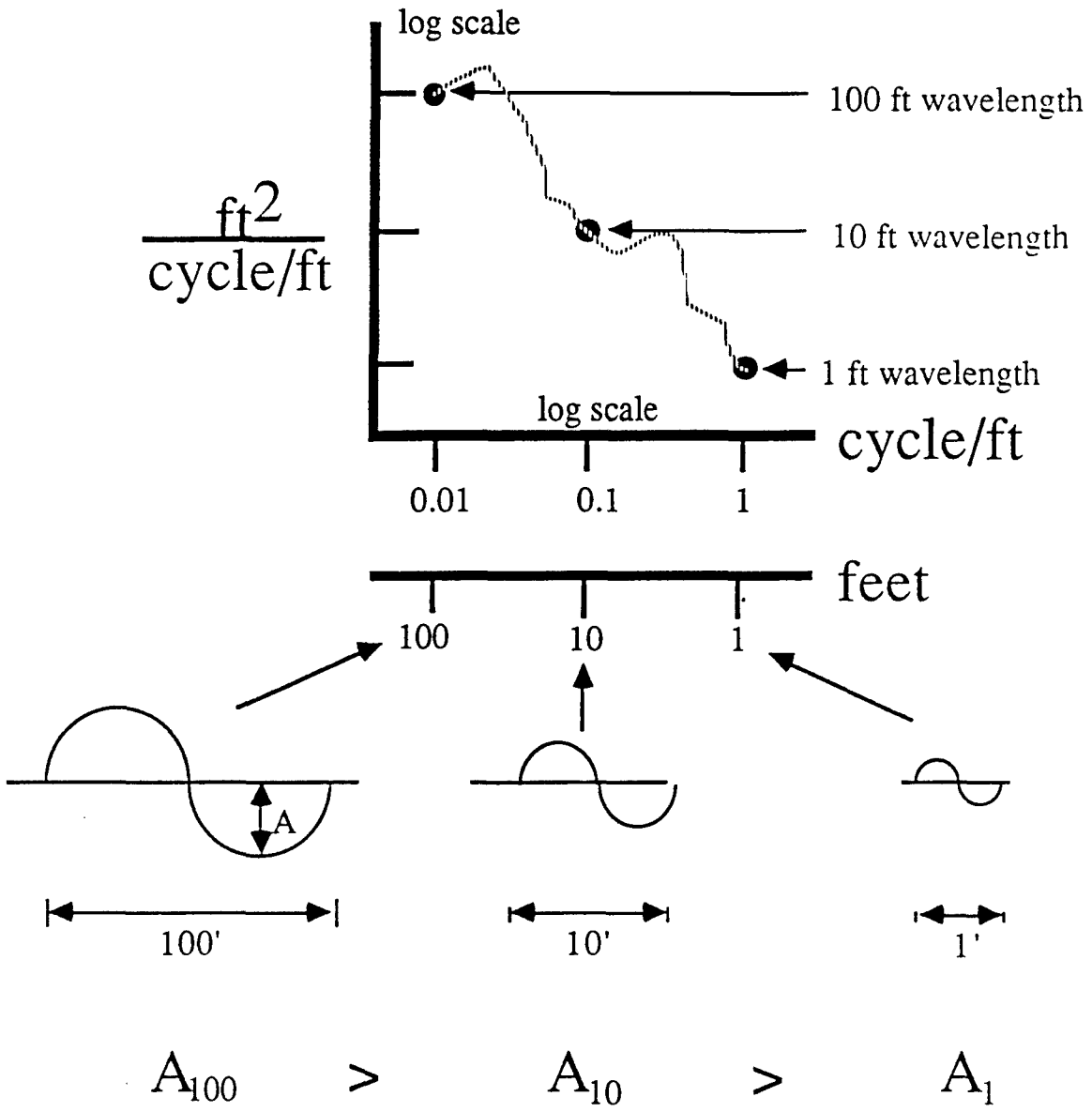

Figure 1. Wave-Number Spectrum Summary Plot

Vehicle traffic deteriorates a road over time, especially secondary and off-highway trails. On our public paved and well-maintained road networks, this deterioration happens very slowly and may be noticeable only after several years. In comparison, durability test courses used for wheeled- and tracked-vehicle evaluations can change much more rapidly, and depending on the weather and volume of traffic, can have significant changes daily. As the road changes, so does the input to the vehicle. The result of this change may tend to over-test or under-test the vehicle. In our example above, assume that heavy wheeled-vehicle traffic has little effect on the 100- and 10-foot waves, but does change the 1-foot waves. Whereas originally the 1-foot waves were at an amplitude unnoticed by the vehicle, the amplitudes of the 1-foot waves have increased by several factors due to washboarding and multiple 12-inch diameter potholes. As a result, the vertical disturbance input to the vehicle at 1 cycle/foot increases significantly and the test course roughness has a substantially different effect on the vehicle when compared to the start of the test when the course was much smoother. Assuming the test vehicle is traveling 15 MPH (22 ft/s), that would relate to a fundamental frequency input to the vehicle at 22 Hz, a potentially very damaging frequency for wheeled vehicle components. Although the vehicle may see a similar environment sometime over its life, the effect of the durability testing is ideally neither to over- or under-test the vehicle.

If the DFMV was employed to monitor the course, any changes in the course roughness would result in changes in amplitudes in the wave-number spectrum. Through established tolerances of each course, maintenance could be performed when the course was outside a baseline tolerance. In addition, a cross-country course at Aberdeen could be directly compared to one at Yuma, NATC or elsewhere. Equivalence techniques could be employed to compare a 20,000 mile durability test at APG to the YPG durability test environment. Accurate trade-offs in terms of equivalent miles could be made between the two proving grounds.

There is an important distinction between wavelengths that affect the powertrain of a vehicle versus those that affect the roughness input to the vehicle. For the High Mobility Multi-Purpose Wheeled Vehicle (HMMWV, the reference vehicle for this study), if differences exist in wavelengths greater than 100 feet, those differences can be addressed in terms of powertrain performance. These wavelengths add low-frequency inputs to a vehicle (and do not change significantly with heavy vehicle traffic), as shown in this example.

Example: The input of a 100-foot wave to a vehicle traveling 35 MPH (51 ft/sec) is 0.51 Hz.

100-foot wavelength = 0.01 cycle/foot

0.01 cycle/ft x 51 ft /sec = 0.51 cycle/sec (Hz)

It can be seen in this example that wavelengths less than 100 feet are the roughness seen by the vehicle; therefore, maintenance could be specified to keep a course within a tolerance or modifications could be specified for bringing the test courses to equal inputs between proving grounds. The vehicle and the speed of the vehicle over the durability course are the critical factors for selecting which wavelengths affect the drivetrain components and which affect fatigue damage.

In the past, representations of changes in test course roughness have been made by identifying the changes in vertical acceleration measured at the driver's location and at suspension components. This methodology addresses the changes in test course severity for that particular vehicle but does not address the effects of those changes on other vehicle systems. For example, accelerations measured at the wheel end of a HMMWV may indicate that there is no significant change to the test course. However , if the measurements were made on the Heavy Expanded Mobility Tactical Truck (HEMTT) or Heavy Equipment Transporter (HET) the results may be significantly different.

One of the common complaints of vehicle manufacturers is that it is impossible to know what the input to a vehicle in service will be. Typically a vehicle's RAM performance is judged in terms of failure rates at selected test and user evaluation sites. The environments at these sites may be very different. Obviously the conditions at YPG are different from those at APG, which are different from those at Fort Carson or Fort Lewis. These are different from the conditions found in potential system deployment areas worldwide. To accurately define the operational environment in engineering terms would insure that the Army gets a better product in a more timely and cost effective manner. For example, the mission profile of the HMMWV could be specified through an average wave-number spectrum for 30 percent primary, 30 percent secondary, and 40 percent cross-country (level and hilly) in as few as four curves (Figure 2). This information would represent all potential deployment areas and could be used in all phases of the vehicle development. In the early design phases, the vehicle developer could use wave-number spectra in computer model analysis to compare different suspension concepts and/or to verify the structural integrity of the modeled vehicle. In the shakedown phase, the developer could use the spectra to further tune suspension components or to accelerate durability testing, as described in the new Air Force MIL-STD-1784A. And finally, in the government testing phase, the government could adequately address whether the vehicle will meet its specified transport requirements. For the given mission profile of the vehicle, government testing could be scaled so that an exact number of "Belgian Block" miles are run to verify the structural integrity of the vehicle up to an expected life (in miles). This approach assumes that the spectrum of the "Belgian Block" course is known (and monitored if deformable) and that the material types on the vehicle are known. With those inputs and a few guidelines on how far to accelerate the test, the problem of accelerated life cycle testing is reduced to one equation. One of the recommendations of this program is that the procedures and guidelines for accelerated life cycle testing be developed based on the use of wave-number spectra to quantify the environment. As stated in the opening paragraph, wave-number spectra are an efficient and potentially very accurate measurement tool, however, they can lead to erroneous interpretation if guidelines are not strictly followed.

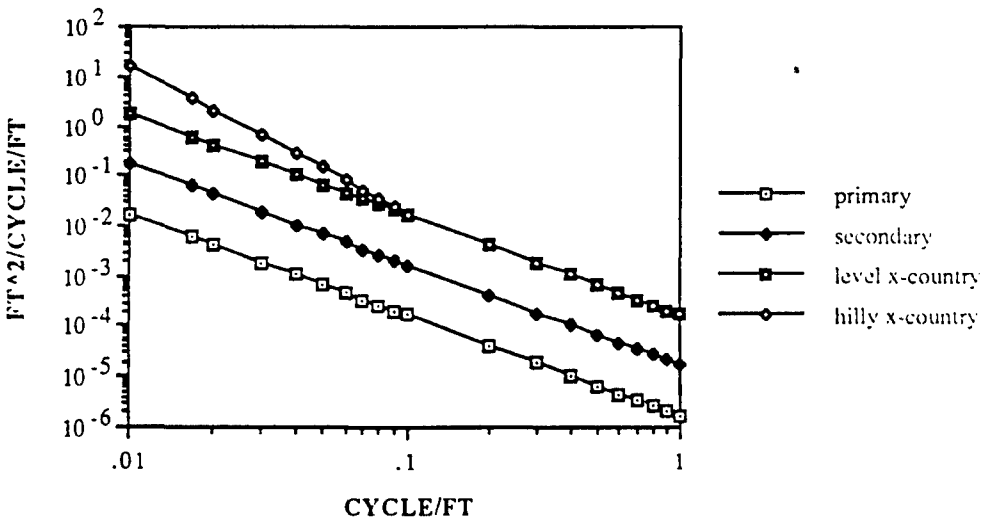

Figure 2. Hypothetical Mission Profile Environment of the HMMWV
Note: Wave-number magnitudes are not to scale

The DFMV is a unique tool for performing the wave-number concepts discussed above, as the results of this program show. Specifically, the summaries and conclusions of this program are:

1. The DFMV measurement methodology is vehicle independent, due to the location of the force transducers.

2. The DFMV measurement methodology is independent of speed, to the point the DFMV wheels do not leave the ground.

3. Because of the design characteristics, the DFMV is able to profile rough terrain at speeds appropriate for measuring and monitoring long sections of durability test courses. The DFMV is not limited by terrain severity or by sand and mud conditions.

4. Through the measurement at all four wheel ends, the DFMV has a built-in check for assessing the quality of the profile. A frequency-domain correlation, called a coherence function, should have a value near unity over the wave-number spectrum between the front and rear wheels on the same side of the DFMV (since they see the same road). Therefore, the sections of the wave-number spectrum where the coherence is poor indicates that the measurement may not be valid at those wave numbers.

5. In terms of the wave-number spectra for the courses profiled during this exercise, this quality check proved to be a valuable tool. Several of the courses profiled at YPG had a long grade with a relatively smooth surface (sections of the Truck Hill course). Once wavelengths longer than 100 foot were removed (by detrending operations), the overall roughness of the course was less than the measurement resolution of the rod and level or APG profilometer. For example, the vertical perturbations of the course roughness for the Truck Hill #2 course was less than ± 0.1 feet. At a 0.01 foot measurement resolution with the rod and level, the wave-number spectrum computation was dominated by noise in the rod and level measurement, and the course appeared to be much rougher than in actuality.

6. A wave-number spectrum is recommended as a replacement to the current RMS terrain descriptor because of the presentation of amplitude and frequency. It should be noted that for programs such as the NATO Reference Mobility Model (NRMM), the RMS of the course is easily calculated from the area under the wave-number spectrum curve.

7. The DFMV methodology accounts for terrain deformation (measures a loaded profile) and can be equipped with tires which are representative of the wheeled vehicle of interest, thus representing the true input to the vehicle. NATC has DFMV configurations that will profile with the PLS tires and measure the course input as seen by the PLS. For the profiling exercise at YPG, HMMWV tires were installed on the DFMV at the same wheel track and same deflection as a HMMWV. An instrumented M1025 HMMWV was run over the courses profiled at YPG and will serve as the final validation of each measurement methodology. NATC has developed methodologies for addressing the terrain effects on tracked vehicles as well. However, profiling deformable soils and providing inputs to tracked vehicles were not in the scope of this phase of the test.

8. The wave-number spectrum presentation of course data can replace the rod and level elevation versus distance inputs currently used in computer models of vehicles. In addition, there is extreme latitude as to the format of that input. For example, the inputs at the tire/ground interface could be elevation versus distance, elevation versus time, acceleration versus distance, acceleration versus time or a direct frequency-based model driver.

9. The DFMV methodology could be used to replace the tire in a computer model of a vehicle, thus saving many dollars of tire model development currently proposed by TACOM. NATC could provide the wave-number spectrum to describe the terrain. The tire could be described as a mathematical "black box", called a transfer function. The "black box" would contain all the transmissibility properties of the tire due to the interaction of load, inflation pressure, tread properties, temperature, radial or bias characteristics, hysteresis, etc. The DFMV is uniquely capable of developing this transfer function because of the position of the load cells in the measurements system. The development of a tire transfer function is a laboratory procedure independent of any road profiles. Once developed, the wave-number spectrum multiplied by the tire transfer function would give the vertical acceleration output at the vehicle spindle, as shown.

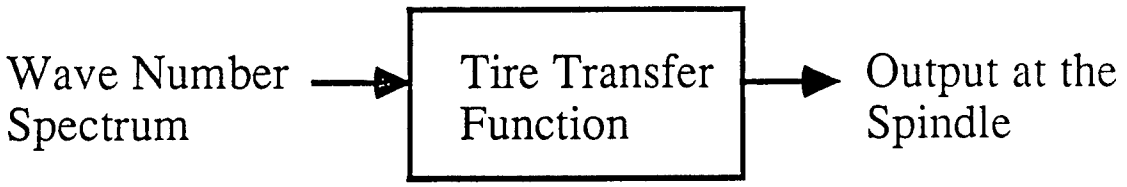

1.2 Project Summary

Eleven test courses were profiled at YPG using the NATC Dynamic Force Measurement Vehicle (DFMV). The same eleven test courses were profiled by WES, using the rod and level procedure to establish baseline profiles for validation purposes. An APG inertial profilometer was the third methodology in this evaluation. The test courses profiled included four WES RMS courses developed for the evaluation of the Hard Mobile Launcher, two Middle East courses typified by rocks and undulating terrain, four Truck Hill course sections selected from the YPG Rolling Hill Cross-Country course, and a washboarded section of road on old Hwy 95. For each of the 11 courses, a left- and right-wheel path elevation versus distance profile, a left- and right-wheel path wave-number spectrum and two coherence function plots were computed from the four wheels on the DFMV. The rod and level data, also measured for each wheel path, served as the validation of the DFMV and APG methodologies. NATC computed wave-number spectra and spatial coherence functions for all the rod and level profiles. Then profiles, wave-number spectra, and spatial coherences for all the test courses computed from the DFMV were compared to the equivalent results from the rod and level data (all wave-number spectrum data was put on the same scale for direct comparisons). DFMV runs at 2, 4, 6, 8, and 10 MPH showed that the wave-number spectra produced by the vehicle were independent of vehicle speed through the spatial presentation of the data.

The comparisons between the DFMV and the rod and level data are generally good, although some discrepancies do occur. The sources of the more significant discrepancies have been identified. These included accuracy limitations of the rod and level and known force variations in the DFMV tires. Based on theoretical expectations, coherence functions plots proved to be a valuable tool for determining the quality of a given profile. The results of this program indicate that no profile should be presented or used without the spatial coherence and coherence phase information between the left- and right-wheel tracks also given. Although not supplied by WES or APG, spatial coherence plots were generated by NATC for comparison and analytical purposes.

The results of this program suggest that the DFMV profiling procedure would be substantially improved by two simple modifications. The first modification, which is in process, is to drive the analog-to-digital converter (ADC) in the DFMV data acquisition system by the position indicator on the vehicle wheel, rather than a clock, so that the data are collected directly as a function of distance rather than time. This will reduce minor errors due to speed variations of the vehicle. The second modification is to replace the current piezoelectric accelerometer, used to establish an inertial reference for the vehicle axle position, with a higher quality, low noise level piezoresistive accelerometer. The low-frequency noise level of the current accelerometer is limiting the definition of accurate wave-number spectral values at the longer wavelengths when the vehicle speed is below 10 MPH, as was the case for the YPG tests.

The two correctable problems did not limit the usefulness of the YPG data. Driving the ADC with the optical encoders would be important to runway profiling where the exact location on the runway is very critical. Accurately measuring wavelengths greater than 100 foot would be important on less severe courses and roads where vehicle speeds might approach 55 MPH.

Excluding these two correctable problems, the DFMV measurement procedure and profiling algorithms produce excellent results compared to the rod and level. To produce rod and level data of comparable accuracy to the DFMV, the following rod measurements would be required:

1. 1,000 foot minimum course length (random error limitations)
2. 3-inch sample interval (required to quantify 1 ft cycles, the lowest wavelength of interest)
3. greater than 0.01 foot vertical rod resolution (due to signal-to-noise considerations of rod and level measurement on maintained unpaved roads, a resolution of 0.04 inches is recommended)
4. left- and right-wheel paths accurately aligned over length of course (required for coherence function analysis)

In a comparison of the single-number RMS value, the WES RMS calculations for the Truck Hill courses did not reflect the true roughness of the courses. The RMS value was severely biased by the grades in the courses, and thus indicated a roughness much greater than actually existed. The filter in the RMS program was unable to adequately detrend this data (remove the long wavelengths).

The DFMV terrain profiling methodology provides five major attributes that other terrain profiling devices do not possess; in summary, these are:

1. Although the DFMV has a suspension and sprung mass, the DFMV measurement procedure is not influenced by the vehicle dynamics, due to the placement of the load cells (as explained in Appendix J).

2. The DFMV measurement procedure allows the determination of terrain profiles at all four wheels. Through coherence function plots, the individual wheel measurements can be used to assess the quality of the profile over the entire wave-number range. Specifically, by computing the coherence function between the measured elevations at the front and rear wheels on each side of the vehicle, the actual signal-to-noise ratio and general accuracy for the elevation profile computations can be directly determined. A second-order estimate of the profile quality can be calculated through coherence plots between the left- and right-wheel path profiles. This second-order analysis would be used for verification of the rod and level measurements or any other technique which does not have two redundant measurement in each wheel path. This technique however, could not be used if severe phase changes in vertical elevation occurred between the left- and right-wheel paths (roll inputs).

3. The DFMV measurement procedure does not use a direct displacement measurement to determine the terrain profile. Whereas the majority of the profilometers use motion measurements to calculate the terrain, the DFMV uses force-motion measurements made at each wheel end to calculate the terrain.

4. The DFMV measurement procedure accounts for terrain deformability (e.g., the effects of sand and mud on test course roughness).

5. Accurate elevation profiles can be generated up to the maximum speed of the DFMV, restricted only by the requirement that the DFMV wheels do not leave the ground. This insures rapid test course measurement and analysis. For example, all of the standard truck and tank durability test courses at APG or YPG could be measured and compared to a reference requirement in a day.

Based upon the profiles and wave-number spectra computed using the DFMV procedure, possible techniques for specifying road roughness characteristics are recommended. The suggested roughness specification involves a two number index, which can be determined for any road, terrain, or test course, by a single pass of the road, terrain, or test course with the DFMV (or any other validated profiling device). Specific values of the two-number index for all eleven test courses are presented (Section 11.5). It is recommended that this course roughness description replace the current RMS roughness index.

1.3 Abbreviations and Definitions

APG - Aberdeen Proving Ground, U.S. Army Combat Systems Test Activity, Aberdeen, MD
DFMV - Dynamic Force Measurement Vehicle
NATC - Nevada Automotive Test Center, Carson City, NV
PSD -- Power Spectral Density. A spatial PSD is one dependent on distance rather than time. In this report, a wave-number spectrum and a spatial PSD are the same.
TACOM - U.S. Army Tank-Automotive Command
TACOM-RYA - Mail stop and in-house extension for TACOM's Vehicle Simulation Division
TACOM-QAT - Mail stop and in-house extension for TACOM's Product Assurance and Test Division
WES - U.S. Army Waterways Experiment Station Corps of Engineers, Vicksburg, MS
YPG - Yuma Proving Ground, Yuma, AZ

Aliasing - Aliasing is not normally of concern in the analysis of stationary signals, because signal processing analyzers generally have built-in low-pass filters that eliminate unwanted high-frequency signals before digitizing. Whereas the DFMV data was recorded analog and then filtered and digitized in post processing, the rod and level data was sampled digitally. In the case of the rod and level data, aliasing is an effect introduced by the discrete sampling of the elevation versus distance profile, whereby short wavelengths after sampling appear as longer wavelengths near the Nyquist or folding frequency. Aliasing constitutes a source of error in the rod and level data, because the amplitudes near the Nyquist frequency are higher due to the unwanted frequencies folding back into the spectrum. The aliasing effect is best described in Reference [4] as follows, "Those who have viewed a motion picture of the classic western vintage have undoubtedly observed the apparent reversal in the direction of rotation of the stage coach wheels as the stage coach slows down or speeds up. That observation is a simple illustration of an aliasing error caused by the analog-to-digital conversion operation performed by a motion picture camera". In that sense, the digital FFT algorithm can not distinguish between a wheel that rotates seven-eighths of a revolution between samples and one which rotates a negative one-eighths of a revolution between samples.

Detrend - Reference [4] and Section 9.6 contains discussions on trend removal. The reference to detrending or trend removal in this report applies to the removal of wavelengths that are longer than the course length. If the courses are further broken into smaller segments for ensemble averaging purposes (Section 9.4), then trend removal applies to wavelengths that are longer than the ensemble segment. For example, Truck Hill #2 had an approximate 10% grade that equated to a wavelength of several thousand feet if extended. The course length was 280 feet and two ensemble averages were used. That means that all wavelengths longer than 140 feet had to be removed from the blocks of data to avoid large distortions of the wave-number spectrum. The most common technique for trend removal is to fit a polynomial to the data using the least squares procedure.

Leakage - Leakage is a frequency-domain effect whereby the power in a single frequency component appears to leak into adjacent bands. Like aliasing, leakage it is a problem that applies primarily to data acquired digitally, like the rod and level. Leakage refers to two slightly different phenomena in this report. First, leakage occurs in the standard Army RMS program due to the roll-off characteristics of the moving exponential filter. Because the filter does not have an infinitely sharp cut off at 60', some of the power (amplitude) of the wavelengths shorter than 60' are attenuated, while components of the wavelengths longer than 60' are not completely removed by the analysis. When the single-number RMS value is calculated, the RMS value may be biased by this leakage. Ideally, the user could filter the data in the frequency domain by setting the frequency bins outside the integration limits to zero before an inverse FFT is performed to get back to the elevation versus distance profile. The second type of leakage used in this report refers to the use of different tapering or windowing processes during analysis and is discussed in Reference [4] and in Section 9.5.

Wave Number - Wave number is the reciprocal of wavelength and is a spatial equivalent of frequency. It has units of cycle/length. In this report, the units are cycle/foot.

Wavelength - The inverse of wave number. Represents the length of a wave in feet.

2.0 OBJECTIVE

This study was designed to show the application of NATC's Dynamic Force Measurement Vehicle for quantifying terrain severity. As such, the primary objective of this contract was to provide DFMV terrain profile data to TACOM for TACOM's use in computer modeling and analysis of the DFMV data. This report details the DFMV durability test course profile methodology and provides applications for monitoring test course severity and developing representative and validated inputs to vehicle computer models. Specifically, the individual contract tasks were as follows:

1. Perform DFMV characterization measurements for the purpose of computer model development.

2. Instrument the DFMV with 33 channels of sensor data. For the purposes of this study comparing only vertical roughness measurements, nine (9) channels were required. Twenty-three channels are required for complete terrain analysis. Ten additional channels were required for computer simulation comparisons of the DFMV operating over the YPG courses.

3. Perform positive bump computer simulation validation test runs with the DFMV.

4. Profile eleven test courses at YPG. For comparison between the methodologies and the profile data, WES (rod and level) and APG (inertial profilometer) profiled the same courses.

5. Analyze the data and supply both course profile and positive bump validation data to TACOM on magnetic media. In addition, hard copy and magnetic media (as applicable) profile data of the eleven courses was provided to TACOM by NATC, WES and APG as comparison data between the methodologies. The data was distributed by the COTR.

An instrumented M1025 configuration HMMWV, supplied by NATC, was operated over the same courses. In the evaluation of the three methodologies, the HMMWV will serve as the response vehicle. TACOM's vehicle simulation group (AMSTA-RYA) will show modeled versus actual test results for the HMMWV. The course inputs for the modeled HMMWV comparison will be the test courses as measured by NATC, APG and WES. The significance of the measurements as identified by the response of the HMMWV can be established.

3.0 BACKGROUND

In December 1989, NATC, WES and APG met at YPG to profile preselected test courses and to provide test data to TACOM's vehicle simulation group for evaluation of the three methodologies. An instrumented HMMWV vehicle was operated over the same test course and will serve as the response vehicle for the comparisons. The test courses were selected as representative of various types of macro and micro roughness. The courses were generally nondeformable, with the exception of short sections near the YPG Middle East test course area. NATC profiled the courses with the DFMV. APG profiled the courses with an inertial profilometer. WES profiled the courses with a rod and level. Details of the APG and WES systems can be found in the reports generated by those organizations.

The initial, unedited data produced by the DFMV profiling efforts at YPG were submitted by NATC in an interim draft report to TACOM (AMSTA-RYA and AMSTA-QAT), APG and WES and is contained in Volume II of this report. Upon receipt of these data by the COTR (Chester Kedzior), the data were exchanged so that the three profiling methodologies could be compared. The final data comparisons of the three methodologies, performed by NATC are presented in this report. Although submitted in the draft Characterization Measurements report, the final results of the DFMV characterization measurements will be submitted under a separate letter final report, as well as the DFMV and HMMWV model validation data and summary of the instrumentation installed on both.

4.0 INTRODUCTION

The following is excerpted from a typical current Army purchase description specifying terrain conditions:

Terrain Conditions

Primary Roads. Two or more lanes, all weather, maintained, hard surface (paved) roads with good driving visibility used for heavy and high density traffic. These roads have lanes with a minimum width of 108 inches (2.75 M), road crown to 20 degrees and the legal maximum GVW/GCW for the county and state is assured for all bridges. The roads have surfaces having Root Mean Square (RMS) value of 0.1 inches (2.54 mm).

Secondary Roads. Two lanes, all weather, occasionally maintained, hard or loose surface (e.g., large rock, paved, crushed rock, gravel) intended for medium-weight, low-density traffic. These roads have lanes with minimum width of 98.5 inches (2.5 M) and no guarantee that the legal maximum GVW/GCW for the county and state is assured for all bridges. These roads are surfaces having a RMS value varying between 0.3 inches (7.63mm) - 0.6 inches (15.24 mm).

Trails. One lane, dry weather, unimproved, seldom maintained loose surface roads, intended for low density traffic. Trails have a minimum width of 98.5 inches (2.5 M), no large obstacles (boulder, logs, stumps) and no bridging. These are surfaces having an RMS value varying between 0.5 inches (12.7mm) - 1.5 inches (38.1mm).

Rough Trails. Vehicle operations over terrain not subject to repeated traffic in addition, no roads, routes, well-worn trails or man-made improvements exist (This definition does not apply to vehicle test courses which are made to simulate cross-country terrain). These are surfaces having an RMS value varying between 1.5 inches (38.1mm) - 2.0 inches (50.8mm).

The Root Mean Squared (RMS) value is an established methodology for identifying road roughness; however, the RMS description describes a road as a wave (of unknown length) with an RMS amplitude. In reality, a road or terrain is a random environment with multitudes of different frequencies, often with amplitude varying per frequency. Therefore, a terrain or road should be described in terms of both the amplitude and frequency of the vertical disturbances, and in a format useful to designers, testers, and users. A wave-number spectrum is such a descriptor; it offers a complete representation of terrain roughness as it affects vehicle systems, and can be used as a direct comparison of terrains. Given that, an average wave-number spectrum could be given for each of the terrain conditions above, replacing the underlined sections of the paragraphs. Simplified further, the four terrain conditions could be given as an average of many spectra, ideally described as a linear relation on a log-log wave-number spectrum plot. The underlined sections in the above paragraphs could be replaced, as follows. The numerical example for primary roads was calculated from data in Reference 3 and match previously used Air Force data.

Primary Roads.

$$G_{XX}(\text{wave number}) \sim \text{roughness coefficient } (\text{wave number})^{-\text{slope}}$$

For example: $G_{XX}(n) = 1.66e^{-6}\ (n)^{-2.0}$

where:

$G_{XX}(n)$ = wave-number spectrum of the road elevation in ft^2/cycle/ft

n = wave number in cycle/ft

$1.66e^{-6}$ = roughness coefficient (amplitude of spectrum at 1 cycle/foot)

-2.0 = slope of the wave-number spectrum

Secondary Roads.

$$G_{XX}(\text{wave number}) \sim \text{roughness coefficient } (\text{wave number})^{-\text{slope}}$$

With the following note: "Washboarded secondary roads can often have a peak amplitude of 0.1 ft^2/cycle/ft at 0.5 cycle/ft."

Trails and Rough Trails

$$G_{XX}(\text{wave number}) \sim \text{roughness coefficient } (\text{wave number})^{-\text{slope}}$$

With the following note: "The trails and rough trails can often have a peak amplitude of 5 ft^2/cycle/ft at 0.03 cycle/ft."

The RMS roughness (in inches of displacement) is calculated from a set of vertical height versus distance measurements (the rougher the course, the higher the RMS number). These vertical displacements are typically measured with a surveyor's rod and level. In order to develop a representative single value from the rod and level readings (the "RMS" of the course), the low-frequency (long wavelength) components are filtered out, since they add large values to the RMS magnitude at frequencies which are assumed to be too low to produce a significant vehicle response. The WES digital filtering techniques (moving exponential filter) typically filter out frequencies greater than 60 feet, for vehicle lengths that are 20 to 30 feet. However, the filter does not have a sharp cut-off. Depending on the quality of the analysis, the filtering process may remove shorter wavelength components due to filter leakage and the resulting RMS number (the standard deviation after filtering) may not reflect the true severity of the terrain. Also, as a single number, there is no indication as to the frequency at which the disturbance inputs occurred, other than the fact that the longer wavelengths have been removed.

A frequency-domain presentation of the data allows for efficient filtering, where the filter is unity in the pass-band and zero in the stop-band. This will eliminate leakage of the longer wavelengths and establish defined integration limits to the RMS value. It is proposed that integration limits between 100' and 1' be used for a vehicle similar to the HMMWV.

At the U.S. Army proving grounds and at other proving grounds used for government and commercial testing, there are miles of paved, secondary and unimproved roads, as well as specialized test courses. Typically, due to vehicle traffic (wheeled or tracked) and weather variations, these test courses require maintenance. However, there is currently no established vehicle independent procedure for monitoring the courses to ensure that the test vehicle is not being either over- or under-tested [Reference 1, 2]. Often, course titles like "Tank Course," "Perryman III," "Middle East Desert" and "Truck Hill - Level" are generic descriptors of courses that have no quantitative basis as to their roughness, much less the tolerance of that roughness over a given year or test. Due to the length of the test courses and the frequency of the measurements required to monitor them, the rod and level has not been a feasible tool for test course monitoring. For rough durability test courses, the rod and level can serve as a validation tool for profilometer systems, as it has for the tests reported herein. It is evident from the course types at the different proving grounds that the ability to measure washboard and severe roughness is a prerequisite of a profilometer system.

Although limited, most of the literature reviewed presented terrain profile data as plots of elevation versus distance, or as spatial power spectral density (PSD) function plots (called a wave-number spectrum in this report). A wave-number spectrum is nothing more than a frequency-domain representation of an elevation versus distance profile typically generated with a rod and level. The y-axis represents displacement spectral density normalized to vehicle velocity, while the x-axis represents frequency similarly normalized. As the WES profile data proposed, road roughness data can be presented as plots of elevation versus distance with the RMS, cone index, and moisture content values to describe the course roughness (Appendix A, p. 98). Wave-number spectra offer a more complete picture of the course roughness and allow for monitoring of that roughness. Specifically, wave-number spectra provide information as to the magnitude and frequency of vertical disturbances, and can be used as a direct comparison of test course roughness. In contrast to a single-number analysis, wave-number spectra allow additional information describing the interaction between the vehicle and the terrain, and thus have many applications beyond a course roughness measurement. Several possible approaches to data analysis utilizing wave-number spectra include course replication, terrain input to computer models, equivalence studies, accelerated life cycle testing, instrumented vehicle evaluations, etc. Additional discussions on the approach utilized by NATC are presented in Sections 11.5 and 12.

A second objective of this overall TACOM study is to provide a more efficient terrain descriptor for TACOM's vehicle simulation group (TACOM-RYA). The individual data points from the rod and level elevation profile can be used as displacement inputs to a model of a vehicle. Usually, these data are input via an extensive table of vertical displacements for each incremental distance of travel. The table is unique to the specific course profiled and is not necessarily correlatable to other courses containing similar displacement input spectra. From the standpoint of test course severity, the individual rod and level data points must be translated into a more succinct analysis due to the volume of information. Further, the rod and level data points cannot provide any indication as to the deformable nature of the terrain. Finally, due to the lack of repetitive rod and level measurements (primarily due to cost), the modeler has to assume that the course does not vary with time.

Reference 3 provides a discussion on time-domain, frequency-domain and steady-state simulation analysis requiring inputs in the form of one or more spatial functions. When considering multi-wheeled vehicles following the same wheel track (such as a motorcycle), a single wave-number spectrum is sufficient for describing the road input, because the different wheels are just time delayed inputs (if the course is nondeformable). When considering a three-dimensional model, the spatial coherence and phase relationships between the left- and right-wheel path inputs are needed at the wheel track of the vehicle being modeled. The DFMV can supply three-dimensional inputs to a vehicle dynamics model, as can the rod and level and APG inertial profilometer. However, the DFMV is better equipped to ensuring that the measurements are made in parallel paths with a separation equal to the track width of the response vehicle. The same wheel tracks ensure that the correct spatial coherence between the DFMV and the HMMWV is measured (roll and longitudinal twist inputs). It is important that the coherence between measured and modeled profiles be the same for input into a three-dimensional model.

5.0 LITERATURE REVIEW

The following literature review is limited and does not represent a complete coverage of all the road profiling literature. For example, a complete review of highway profilometers and the use of highway roughness indices was excluded from this discussion. To better understand the discussions on wave-number spectra and profiling methodologies, References 3, 4, 5 and 6 are necessary documents. References 3 and 6 expand on the use of wave-number spectra as a road profiling tool and discuss highway profiling methodologies used throughout the world. References 4 and 5 discuss random data and the use of frequency-domain routines to present that data. It should be noted that the use of wave-number spectra for road roughness quantification is well documented in previously published papers [1, 2, 3, 6, 7, 8, and 9]. In addition, NATC has used and assisted the Air Force in developing design documents with wave-number spectra specified for road transport analysis. The data envelopes typically produce two distinct curves, one for primary roads and one for secondary roads.

There are a number of different road roughness measurement systems in use worldwide. These systems can be classified into two groups: (1) systems that measure the profile directly, such as the surface dynamics profilometer (DFMV, APG profilometer or one of the highway profilometer systems) or the rod and level method, and (2) systems which measure vehicle cumulative response to road roughness, such as the Mays meter or the Bureau of Public Roads (BPR) Roughometer [3, p. 55]. As shown, the DFMV fits into the first category; however, it is unique to that category. Whereas the majority of the profilometers use pure motion measurements to calculate the terrain (based on a design from General Motors), the DFMV uses force-motion measurements made at each wheel end to calculate the terrain roughness.

References 3 and 6 compare 13 different highway profile systems in use throughout the world and discuss their performance limits. Most of the systems were limited at low-wave numbers. All the spatial PSD (wave-number spectra) comparisons in Reference 3 use slope (velocity) data computed from the difference of adjacent elevation values divided by the sample interval [3, pp. 105-107]. This is a differential procedure that suppresses trends in the data due to grades and tends to make the wave-number spectrum for the road profile cover a smaller dynamic range. The reduced dynamic range does suppress the "leakage" problem in the spectral analysis of the data, but "leakage," as well as trends, can be adequately suppressed in the spectral analysis of elevation data by appropriate tapering and detrending procedures prior to the spectral computations [4, pp. 362-365, 393-398]. The slope (velocity) wave-number spectra in [3, 6] are readily converted to elevation wave-number spectra through a division by $(2\pi n)^2$, where n is wave number.

Gillespie [8] thoroughly discusses the ride dynamics of large trucks and discusses inputs due to road roughness. The wave-number spectrum is developed as an excitation input for evaluating the ride of a vehicle. In general, a slope of n^{-2}, where n is wave number, appears to fit most road surfaces, with the spectral values increasing as the roughness of the road increases. Gillespie [8] discusses three major types of tire/wheel assembly nonuniformities, namely (1) dimensional variations, (2) mass imbalance, and (3) stiffness variations. "These nonuniformities all combine in a tire/wheel assembly, causing it to experience variations in the forces and moments at the ground" [8, p. 8]. Because these imbalances occur, it is important that they are understood and minimized if the intent of the profiling is to calculate the actual elevation versus distance profile. When the DFMV is used for profiling, force variations can appear as peaks in the wave-number spectra at the circumference of the tire and all multiples thereof.

Bekker [7] has a thorough discussion on wave-number spectra as a ground roughness descriptor, and references most all the past work in this area up to 1969. Bekker's review proposes that a ground profile can be approximated by an exponential equation, which gives a linear fit on a log-log wave-number spectrum (i.e., an equation of the form $G_{XX}(n) \sim A\, n^{-w}$, as described in Section 4.0).

A 1963 TACOM Land Locomotion Laboratory report concluded that the principal problems of characterizing ground roughness by spatial PSD (wave-number spectrum) methods had been solved and the efforts must be focused on the more difficult task of relating the measurements to the suspension system design [16, p. 9]. A 1966 TACOM Land Locomotion Laboratory report provided an atlas of off-road ground roughness PSD's [17]. Given the improved accuracy of PSD computation and digital computers, a current atlas of course roughness could be developed for durability test courses at APG, YPG and other test sites.

Dodds and Robson [9] discuss spatial coherence, and further the development of a linear fit (using two lines) of the wave-number spectrum on a log-log plot. Coherence functions between left- and right-wheel tracks are used to test the hypothesis of isotropy (similar roughness characteristics in orthoganal directions). For the roads investigated by Dodds and Robson, isotropy was confirmed, but this property should not be anticipated on the RMS test courses used in this study. The RMS courses are designed to have only two dimensional (nonisotropic) roughness . The Middle East #1 course used in this study, however, is a good example of isotropic roughness.

6.0 DYNAMIC FORCE MEASUREMENT VEHICLE (DFMV) DESCRIPTION

The DFMV is an instrumented four-wheel-drive chassis with several modifications made by NATC, as follows (see photographs in Appendix I):

1. Profiling instrumentation including a triaxial force transducer, a vertical accelerometer and an optical speed encoder at each wheel end.

2. Front steerable axle with 0° camber and 0° caster. The rear-drive axle has the same camber and caster.

3. Air-assisted shock absorbers for adjustment of the spring rate between the sprung and unsprung mass for better ride control.

4. Adapters for different tire sizes and track widths.

The DFMV measures and records the dynamic vertical, longitudinal and side forces at the tire/ground interface. Wheel velocity and wheel vertical acceleration are also measured for terrain elevation profiles. Finally, front-wheel steering angle (course curvature) and sprung-mass inclination angle (to define long wavelengths) are also measured. The force measurements are accomplished through nonrotating triaxial load cells located at each wheel end of the vehicle. Each triaxial load cell has 28 strain gauges mounted on a proving ring that is calibrated for forces up to 6,000 pounds, and is moment-compensated for different size tires. Optical encoders (300 counts/revolution) are used for the wheel velocity (wheel end) measurements. Given a HMMWV tire circumference of 9.4 foot, 300 counts/revolution represents a distance measurement every 0.38 inches. The motion response of the tire system is measured with a vertical accelerometer mounted at each wheel end. To record the outputs from the various sensors, a 14-channel TEAC XR-5000 tape recorder with three PCM cards (35 channels total data acquisition capability) was installed in the vehicle.

For this study, the DFMV was used for measuring terrain elevation profiles, however, the DFMV is used for numerous additional studies. Some of these include:

1. Dynamic tire response and mobility measurements

2. Quantification of drivetrain performance and integration of tire and suspension dynamics for optimum performance

3. Accelerated treadwear measurements

4. Catastrophic tire failure force measurements

5. Separation of bound and unbound tire-slip energy.

The DFMV can also be used as a dynamometer for tire/surface friction measurements. In some highway or runway profiling applications, the texture of the surface is a required measurement. For example, μ-measurement devices quantify the surface friction properties of a road through the use of a standard reference tire. If that standard reference tire were mounted on the DFMV, these surface friction measurements could be made. To further describing the terrain and the performance of the response HMMWV on a given terrain, the μ-slip (longitudinal traction) and μ-alpha (cornering traction) relationships are important. The DFMV quantifies these relationships and establishes the shear characteristics at the tire/surface interface. The DFMV has locking hubs on the front and rear axles so that the wheels can be driven in front- or rear-wheel drive, or both. For the μ-slip measurements required on the test surface, the vehicle acts as its own dynamometer. The front tires are braked while the rear tires spin-up through the range of slip. For the μ-alpha measurements, the front axle is varied through different angles of toe-in and toe-out while driven on the test surface.

When the DFMV is used for measuring terrain elevation profiles at higher speeds (i.e., highway profiling), several speeds can be used to define wave numbers from 0.005 to 1.0 ft^{-1} (1 to 200 ft), each speed defining a different range of the spectra. The resulting wave-number spectra, combined with the μ-slip properties of the course to define surface texture, give a complete description of the parameters affecting terrain/vehicle interaction. In addition, key parameters needed for modeling the terrain features are also given.

There is an important distinction between wavelengths that effect vehicle fatigue versus those that effect vehicle powertrain performance. If differences exist in wavelengths greater than 100 feet, those differences can be addressed in terms of powertrain performance. The 100-foot cut-off is in reference to the HMMWV, were vehicle speeds are generally below 35 MPH. Wavelengths greater than 100 foot do not contribute to the fatigue cycling because they represent a low-frequency input to the HMMWV. For example, a 100-foot wave will input a 0.51 Hz input into a HMMWV traveling at 35 MPH (0.01 cycle/ft x 51 ft/sec = 0.51 cycle/sec). Hence, vehicle performance must be evaluated as a function of both roughness and grade to determine the overall capability of the vehicle. The drivetrain load resulting from the grade can be introduced as a function of vehicle motion resistance. Motion resistance is a function of the interaction of the vehicle and the terrain. For this study, the effects of motion resistance due to soil, soil sinkage, and grades were not addressed. The DFMV has the capability to quantify these conditions through the longitudinal and lateral force measurements made with the DFMV during profiling and through the inclinometer located at the cg of the DFMV.

7.0 TERRAIN ELEVATION MEASUREMENT METHODOLOGY

The DFMV has been used for numerous studies; however, one of the functions of the DFMV is to measure terrain elevation profiles. The basic principle behind the DFMV terrain elevation measurement procedure is uniquely different from all other known terrain profiling procedures in that it uses force-motion measurements, rather than motion measurements alone, to define the terrain elevation. This principle is schematically modelled in Figure 3. Note that the model requires certain parameters of the tire, namely, stiffness under load (k), damping (c), and effective mass (m outside the load cell). However, as will be demonstrated later in Section 10.3, the actual road elevation computation is insensitive to these parameters, so relatively large errors in the definition of the tire have very little influence on the final results. NATC has special fixtures for measuring the spring and damping rates of tires, so these parameters can be easily and accurately measured.

The DFMV methodology is actually quite simple. Specifically, assume each wheel of the vehicle, as modelled in Figure 3, is moving across a rough terrain at constant speed. The differential equation of motion for the tire/wheel/hub assembly mass can be written as follows:

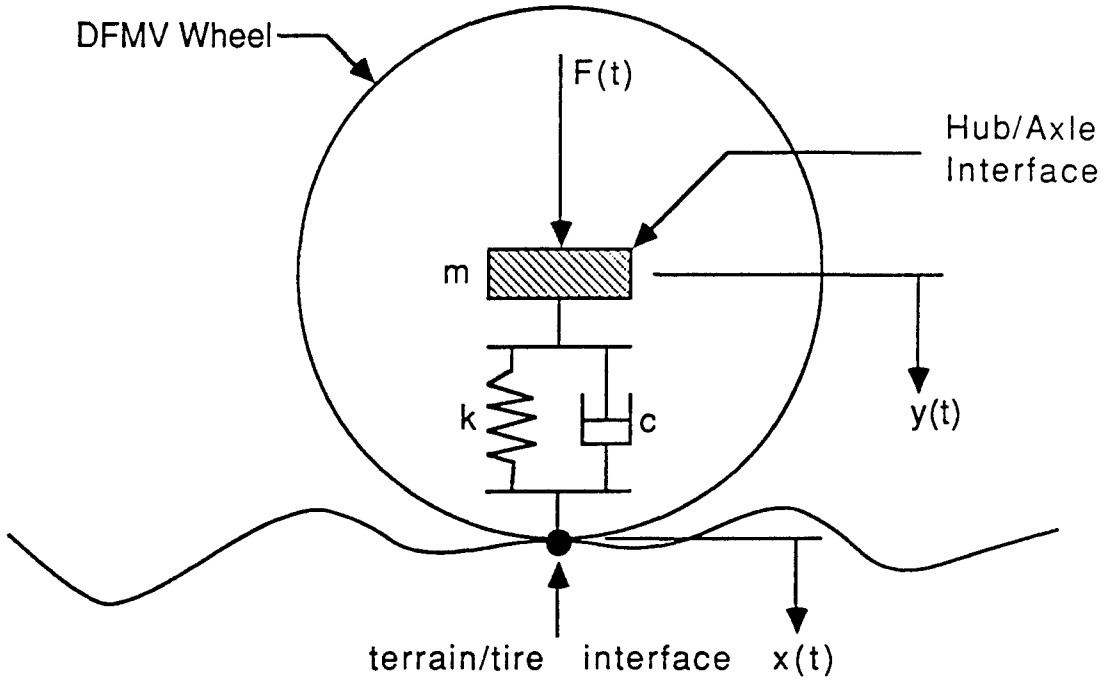

Figure 3. Physical Model for DFMV Wheel Hub/Axle Interface

$$c\frac{dx(t)}{dt} + k\,x(t) = m\frac{d^2y(t)}{dt^2} + c\frac{dy(t)}{dt} + k\,y(t) - F(t) \qquad (1)$$

where

x(t) = displacement at tire/ground interface
y(t) = displacement at wheel hub/axle interface
F(t) = force at wheel hub/axle interface
m = mass of tire/wheel/hub assembly
k = stiffness of loaded tire
c = damping coefficient of tire (computed with m)

Equation (1) can be solved directly for the displacement, x(t), at the tire/ground interface to yield the terrain elevation as seen by the vehicle tire as a function of time, t (the actual algorithms for solving Equation (1) are detailed in the next section). If it is assumed that the vehicle moves at a constant speed, V, then time can be replaced as the independent variable in Equation (1) by distance, d = tV, to obtain the terrain elevation as a function of distance. Note that Equation (1) can be solved independently for the elevation profile at each of the four wheels. Further note Equation (1) is valid independent of the dynamics (both rigid body and elastic) of the vehicle above the measurement location for f(t) and y(t); the vehicle response is fully defined in the force and motion measurements at the wheel-vehicle interface. Over the years, NATC has had to explain in great detail why the measurement methodology is independent of the chassis above the load cells. A further explanation of Equation (1) is given in Appendix J of this report. It should be noted that Equation 1 can be solved as a function of either time or distance.

7.1 Unique Features and Attributes of The DFMV Methodology

The DFMV terrain profiling methodology provides four major attributes over other terrain profiling procedures known to be in current use, as follows:

1. The DFMV measurement procedure is not influenced by the vehicle dynamics; i,e., the suspension system response, the normal modes of vibration of the vehicle and/or its cargo, and on-board vehicle excitations, have no influence on the resulting terrain elevation profile measurements. Also, the terrain elevation at each wheel is measured accurately, independent of the terrain inputs at the other wheels and the vehicle pitching and rolling they might produce. This important result occurs because the force and acceleration measurements at each wheel end provide a measure of the interface impedance between the wheel assembly and the remainder of the vehicle above the force and acceleration measurement location. All dynamic activity of the vehicle above this location is accounted for in the force and acceleration measurements, and hence, is accounted for in the tire/ground input displacement computation.

   The load cell at each wheel end measuring the interface impedance is the same principle that is widely used to measure the normal modes of structures, where the shaker used to apply the excitation may be heavy relative to the structure and significantly load it. As long as a force measurement is made at the shaker-structure interface, the normal modes of the unloaded structure can be accurately determined, even through the observed vibration characteristics of the structure might be significantly influenced by the shaker weight [15, pp. 23-33].

   If the interface impedance example or modal analysis example given above are not familiar to the reader, a detailed description of why the DFMV is vehicle independent is given in Appendix J. It is important to the discussions of this report that the reader understand that the four wheel-end measurements are independent of each other and of the chassis. For courses that do not deform with each wheel pass, as was the case for the YPG courses, the front-to-rear measurements are redundant and have no other use than the front-to-rear coherence function measurements (discussed later in Section 11.3).

   It should also be mentioned that, because the load cells at each wheel-end measure the wheel-vehicle interface impedance, the DFMV can be used for vehicle dynamics studies. For example, the frequency response functions between the wheel attachment and any location on the vehicle structure can be easily and accurately computed using the wheel-axle interface force measurements as the input. It follows that the complete normal mode characteristics of the vehicle structure can be determined, without interference from the tire dynamics, using the input force and response acceleration data obtained by driving the vehicle over any rough road. This same approach could be used to develop a transfer function between the ground and the wheel end to describe the tire, thus eliminating the need to have a tire in a wheeled-vehicle simulation model. This would be a laboratory procedure independent of any road profiles. The advantage to this procedure is that the transmissibility characteristics of a tire are included in the transfer function, as well as tire inflation pressure, tire temperature, etc. A complex model to describe a tire and all its variations is eliminated. A series of transfer functions could be developed for a vehicle system with a Central Tire Inflation (CTI) system to easily model the effects of CTI on axle or sprung-mass acceleration. The natural filtering (with increased footprint length), increased bridging of the macro and micro deviations in the road and changes in spring and damping rates could easily be quantified.

2. The DFMV measurement procedure allows the determination of terrain profiles at all four wheels; i.e., terrain profiles are independently determined at the front and rear wheels on both sides of the vehicle. Assuming the vehicle is traversing a straight path, and the rear wheels do not cause significant soil deformation over that caused by the front wheels, then the measured terrain profiles for the front and rear wheels on either side of the vehicle should be identical, except for a displacement in distance corresponding to the wheel base of the vehicle. Hence, the measurements at the front and rear wheels can be used to assess the quality of the resulting elevation data. Specifically, by computing the coherence function (to be defined later in Section 10.4) between the measured elevations at the front and rear wheels on each side of the vehicle, the actual signal-to-noise ratio and general accuracy for the elevation profile computations can be directly determined. Through coherence function plots, NATC can accurately determine the quality of the road profile over its entire wave-number range.

3. The DFMV uses a combination of force and acceleration measurements to calculate the terrain. In comparison, other surface dynamic profilometers use direct displacement measurement to determine the terrain profile, including the rod and level and APG inertial profilometer procedures. The spectra for terrain elevation profiles tend to fall monotonically with increasing wave number, meaning the magnitude of the terrain variations at large wave numbers (short wavelengths) becomes very small, causing poor signal-to-noise ratios in direct displacement measurements (as can be seen in the data from the rod and level and APG profilometer). Since the DFMV procedure uses both acceleration and force measurements, the signal-to-noise problem at the high wave numbers are greatly reduced. On the other hand, the DFMV procedure does have a potential signal-to-noise problem at the low wave numbers, which is discussed in the next section. However, this signal-to-noise problem at the low end can be eliminated through the use of a higher-quality accelerometer.

4. The DFMV measurement procedure accounts for terrain deformability; i.e., the profile measured is the actual terrain elevation seen by the vehicle tire as it loads the terrain. Different size tires can be mounted on the DFMV. If tires of the same size and contact patch area (equal deflection) are used on the DFMV and test vehicle of interest, then they will potentially deform the soil equally. The resulting terrain profile measured by the DFMV is then the true profile seen by the test vehicle. This means the elevation, as seen by the vehicle, can be described without any knowledge or understanding of the terrain deformation/load characteristics within a comparable ground speed range.

At YPG, the same size tire as that used on the HMMWV was installed on the DFMV. With 37X12.50R16.5LT radial-ply tires on the DFMV at the same deflection and spaced at the same wheel track as the HMMWV, the resulting terrain elevation measurements provide the true input for the HMMWV. This advantage is particularly important to addressing the issue of tire filtering and the roughness of terrain that deforms under vehicle load. It should be noted that the 37X12.50R16.5LT radial-ply tires were installed on the DFMV and set at the same deflection and wheel track as the HMMWV in order to best approximate the true input to the HMMWV. If NATC's desired profiling effort was to provide the best possible match to the rod and level data, a smaller tire with a shorter footprint would have been used. This would yield better agreement at higher wave numbers to the rod and level data. As the photographs and video show, the HMMWV tires on the DFMV are extremely oversized. The standard profiling tire for the DFMV is a specially designed P235/75R15 4-ply radial tire with extremely low force variations. In order to prove the accuracy of the DFMV system in analyzing the interaction between the HMMWV and the ground, the tires used on the DFMV and HMMWV were nonproduction tires with known high force variations (dimensional variations, mass imbalance and stiffness variations were know to be largely present). The DFMV data can identify the effect of these force variations, and the data is presented in a manner which allows either inclusion of the force variation in the analysis or exclusion of this information. (It should be noted that if the standard DFMV profile tire is used on a nondeformable terrain, the same profile would be calculated; however, the tire filtering and force variation effects shown in Figure 5 would be different).

A fifth advantage of the DFMV methodology, which is not unique but nevertheless important, is the speed with which road profiling can be accomplished. Specifically, accurate elevation profiles can be generated up to the maximum speed of the DFMV, restricted only by the requirement that the DFMV wheels do not leave the ground. As previously identified, all of the YPG or APG durability test courses could be profiled in one day.

7.2 DFMV Spectra Versus Rod Spectra, Comparative Differences

Although the DFMV terrain profiling methodology offers the important attributes outlined in Section 7.1, it also has three important distinctions that make the DFMV spectra differ from rod spectra. Two of these are unique to the DFMV procedure, and a third common to all procedures that use accelerometers to measure motion. These differences may vary in importance depending on the end use of the wave-number spectra, and in some cases, may be advantages. Items 1 and 2 are DFMV advantages, given that the HMMWV is the response vehicle for this study. The differences between the DFMV and rod must be understood to utilize the resulting wave-number spectra. The differences are as follows:

1. Since the tire/ground interface motion into the vehicle is used as the measure of terrain elevation, the measurement procedure is limited at the high wave numbers (short wavelengths) by the length of the tire footprint in contact with the terrain. Specifically, variations in the terrain elevation with a wavelength equal to or less than the length of the tire footprint clearly cannot be measured, since the elevation seen by the tire at that wavelength is at maximum attenuation. Hence, the tire acts as a low-pass filter of the terrain elevation data, with a full cut-off wave number of $n_c = 1/W$, where W is the length of the tire footprint. For the tires used on the DFMV for the YPG tests (see Section 7.1, Item 4), the footprint was $W \approx 0.8$ ft, meaning $n_c \approx 1.2$ ft^{-1}.

Reference 3 and 13 reports the use of a moving average to approximate the low-pass filtering effects of a tire. When a moving average is translated into the wave-number spectrum domain (fourier transform), the low-pass filter can be approximated by $[\sin(\pi n/n_c)/(\pi n/n_c)]^2$, as plotted in Figure 4. Note in Figure 4 that the theoretical reduction in the computed elevation values starts well before the full cut-off wave number. Specifically, the elevation value is attenuated by about 50% at $n \approx 0.42\ n_c \approx 0.5\ ft^{-1}$.

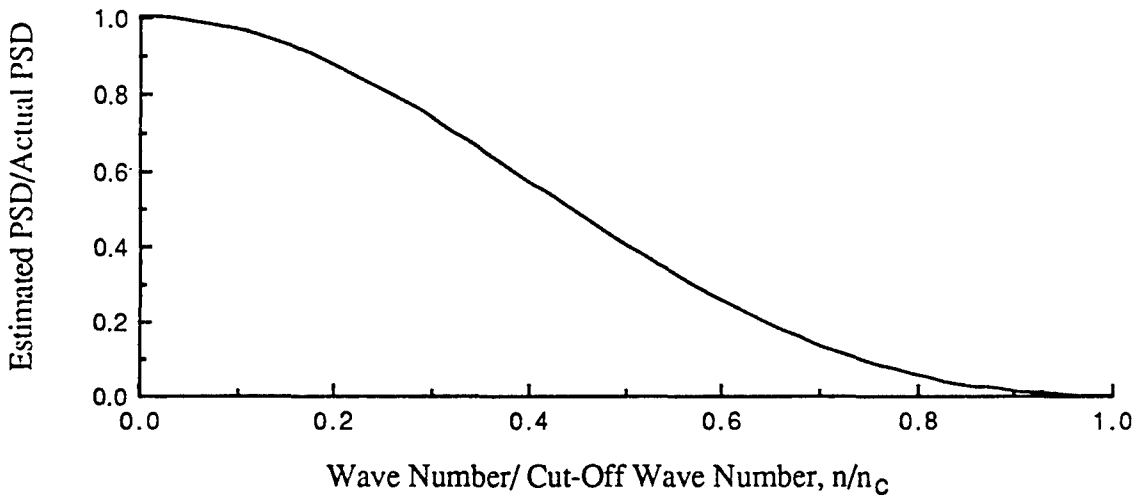

Figure 4. Theoretical Low-Pass Filter of Wave-Number Spectrum Due to Tire Footprint

Figure 5 shows the actual filtering effects of the HMMWV tire (the amplitude reduction is at wave numbers between 0.22 and 1 ft^{-1}) for RMS #5 course. Note that the filtering effect of the HMMWV tire starts well before the theoretical $[\sin(\pi n/n_c)/(\pi n/n_c)]^2$ relation.

Figures 4 and 5 are ratios (H_{xy}) between the wave-number spectrum generated for the DFMV and the rod and level. Since the y-axis on the spectra are squared values, the square root of the ratio was taken. Therefore, the tire filter relation would work similar to a transfer function, namely:

$$G_{xx(rod)} \times \left|H_{xy}^2\right| = G_{yy(DFMV)}$$

From Figures 4 and 5, the DFMV procedure in the YPG test configuration is not capable of providing accurate elevation profile data at wave numbers above about 0.22 ft^{-1} (at wavelengths less than about 4.5 feet) for direct comparisons to rod and level data. Of course, the actual excitations to the vehicle are attenuated at these wave numbers as well, so this filtering effect is not really an error in terms of the vehicle loads seen by the HMMWV model, which has the same tires. However, it will cause the DFMV generated wave-number spectra to be lower near the cut-off wave number than the spectra produced by other profile measuring procedures. In comparison, the tire footprint on the Aberdeen profilometer was approximately one-inch long, so the data has effectively no filtering. This is a moot point, however, due to the fact that the Aberdeen profilometer data was adversely affected by system noise at wave numbers of 0.4 cycles/foot (2.5 feet) or less.

One of the specific goals of this study was to show the applicability of the terrain profiling methodology to specific vehicles. If the HEMTT had been chosen as the reference vehicle, then the DFMV would have been equipped with tires which represented the HEMTT. The results of the profile would have changed at the higher wave numbers, due to the relationship shown in Figures 4 and 5. While this is not important to terrain profiling and test course monitoring per se, it is very important to an accurate computer model of the subject vehicle's interaction with the terrain.

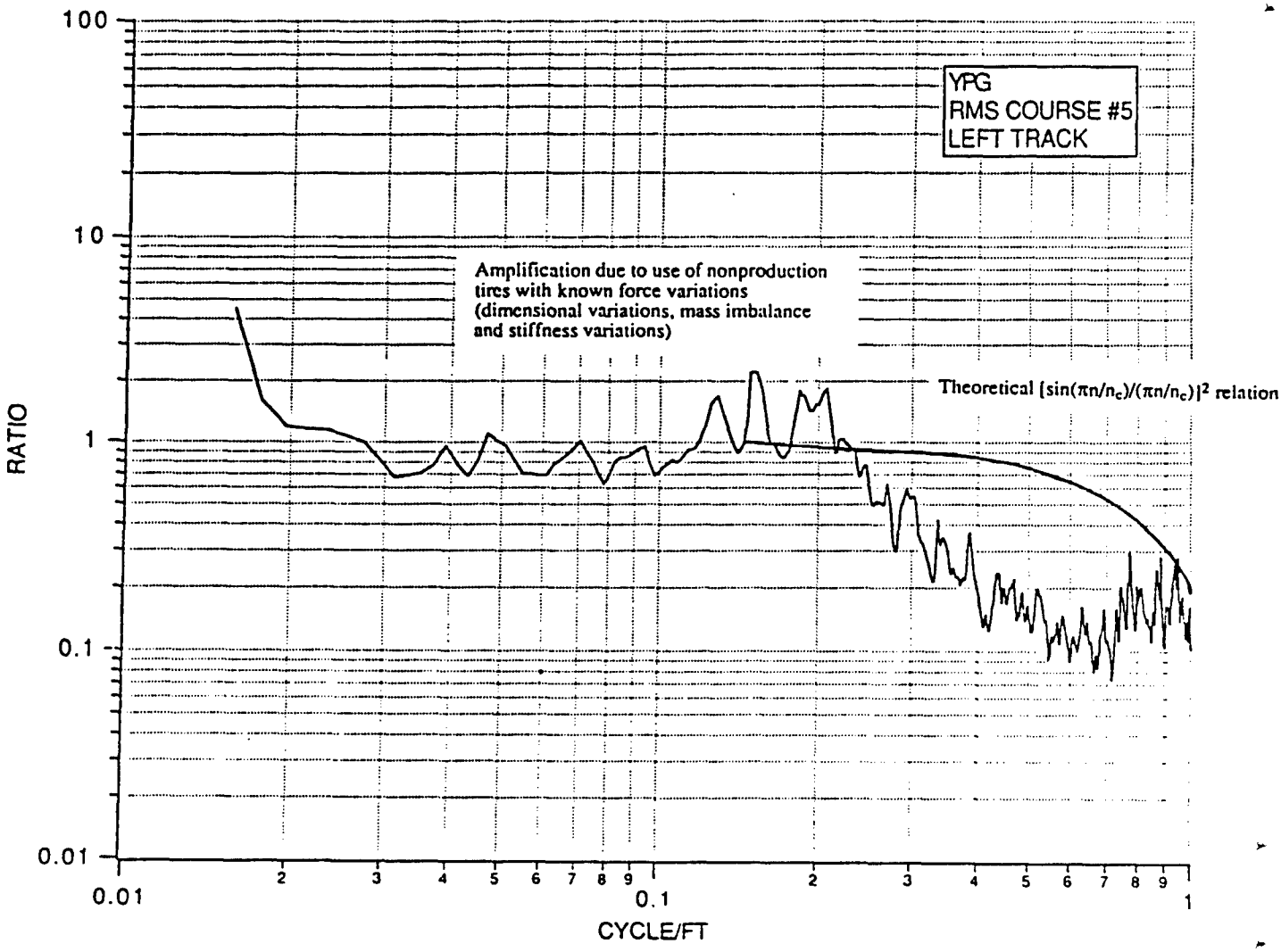

Figure 5. Actual Low-Pass Filter of Wave-Number Spectrum Due to Tire Footprint, RMS #5, DFMV Speed = 6 MPH, Left Front Tire

2. Referring to Figure 3, Equation (1) and Section 7.1, Item 4, since the wheel and tire are below the force and acceleration measurement location, their properties appear in the governing differential equation for the profiling technique. As will be shown in Section 10, substantial errors in the wheel/tire parameters (k and c measurements) produce a negligible error in the resulting profile computation, which is an attribute of the DFMV methodology given the standard DFMV profile tires. However, any forces produced in the wheel/tire assembly due to imbalance and force variations within the tire will cause an apparent increase in amplitude at wave numbers equal to the tire's circumference and first harmonics (as shown in Figure 5). Hence, for pure test-course profiling efforts, it is desirable that the wheels of the DFMV be carefully balanced and that tires with low-force variations be used, particularly when profiling is done at high speeds (e.g., use of the standard DFMV profile tire). On the other hand, when analyzing the dynamic interaction between the vehicle and the terrain, the influence of wheel imbalance (dimensional variations, mass imbalance and stiffness variations) can be detected as peaks in the wave-number Fourier transforms computed from the resulting profiles. These peaks can best be detected when profiling primary roads at high speeds (i.e., an interstate highway at 55 MPH, as shown in Figure 6). The defined peaks are not evident in the wave-number spectra data in this report for two reasons, (1) the speeds were below 10 MPH and (2) the amplitude of the course roughness is greater than the amplitude of the imbalance.

   For this study, NATC wanted to emphasize the effects (if any) of tire filtering and tire imbalance on a tire model, therefore, HMMWV tires were used on the DFMV. The DFMV and HMMWV tires were installed, with bead retainers, according to procedure; however, they were not balanced.

3. As is true of all terrain profiling procedures that use an accelerometer to measure a motion parameter required in the elevation calculation, the accuracy of the DFMV procedure is limited at the low frequencies (corresponding to low wave numbers or long wavelengths) by the noise floor of the accelerometer; i.e., at very low frequencies, even large variations in terrain elevation translate into a small acceleration level. This is normally not a problem for the DFMV because it is ideally used at higher speeds where the lowest wave number of common interest (usually $n = 0.01$ ft^{-1}) corresponds to a frequency where significant accelerations occur; e.g., at 55 MPH (81 ft/sec), $n = 0.01$ ft^{-1} corresponds to a frequency of $f \approx 0.8$ Hz, where the acceleration induced by even small variations in elevation is well above the accelerometer noise floor. However, for the YPG tests, the vehicle velocities were between 2 and 10 MPH. Assuming a profile measurement at 6 MPH (8.8 ft/sec), $n = 0.01$ ft^{-1} corresponds to a frequency of only $f = 0.088$ Hz. The cut-off of the piezoelectric accelerometer used for this study was 0.2 Hz, although advertised to 0.05 Hz. Hence, in the YPG tests, the lower wave-number limit for accurate elevation data was often limited by the accelerometer noise floor to wave number greater than $n = 0.01$ ft^{-1}, as will be noted in the spectral results for the measurements (Table 1). For speeds less than 10 MPH, a piezoresistive or a force-balance accelerometer would provide an accurate measure at the low end of the wave-number spectrum. This change has been implemented and the data sheets on the accelerometer used (PCB 348M30) and the replacement accelerometer (Endevco 7290-10) are shown in Appendix L.

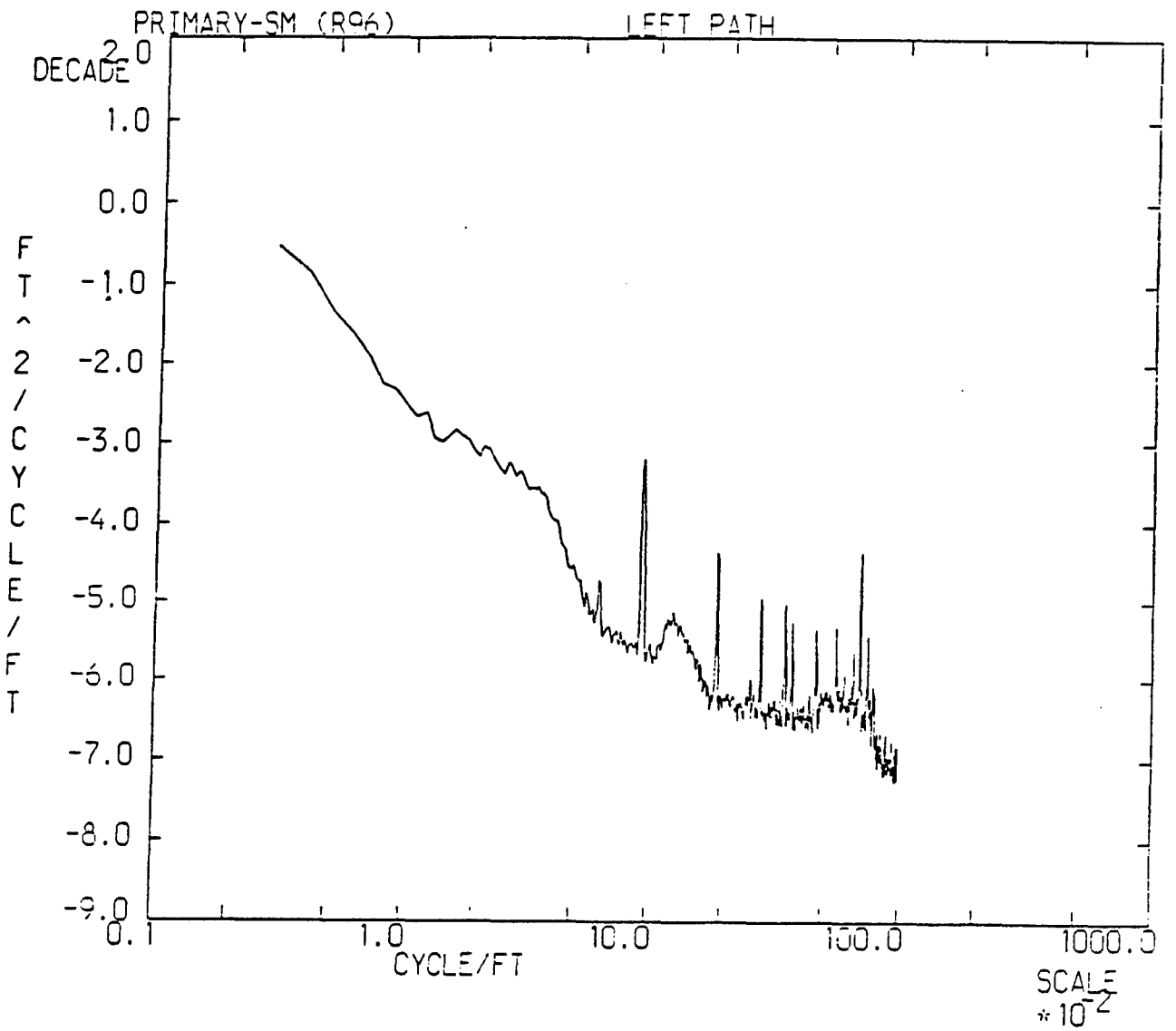

Figure 6. Wave-Number Spectrum of an Interstate Highway at 55 MPH Showing Tire Imbalances

Table 1. DFMV Actual Versus Predicted Wavelength Limits

DFMV Speed MPH	Expected Wavelength Resolution*	Actual Wavelength Resolution**
2	60	15
4	120	30
6	180	45
8	240	60
10	300	75

* Based on the advertised low-end frequency range for the accelerometer used
** Based on actual low-end frequency range for the accelerometer used

There is a fourth difference on the accuracy of the DFMV measurements for the YPG tests that will not apply in the near future. Specifically, although the DFMV data include optical encoder signals that define the spatial position of the vehicle at any time, the analysis software used at the time of the YPG data reduction was unable to use the encoder signals to drive the analog-to-digital converter (ADC). Hence, the ADC was driven by a clock, meaning the conversion from time to distance is vulnerable to errors due to DFMV speed variations during the tests. However, as will be seen later in the data evaluations, these errors are minor.

8.0 DATA ANALYSIS ALGORITHMS

A MASSCOMP 5550 computer with the Cranfield Data Systems (CDS) software (now a Scientific Atlanta Spectral Dynamics package) was used for the data analysis. The MASSCOMP is a 32-channel system with a high-speed A/D front end and programmable elliptical filters. Using FORTRAN and the CDS software, code was written around the data analysis procedure detailed in this section. Using the MASSCOMP, the force, acceleration and speed analog signals reproduced from the TEAC XR-5000 tape recorder were digitized and stored as a function of time, t (i.e., time histories). The overall data analysis system is schematically illustrated in Figure 7.

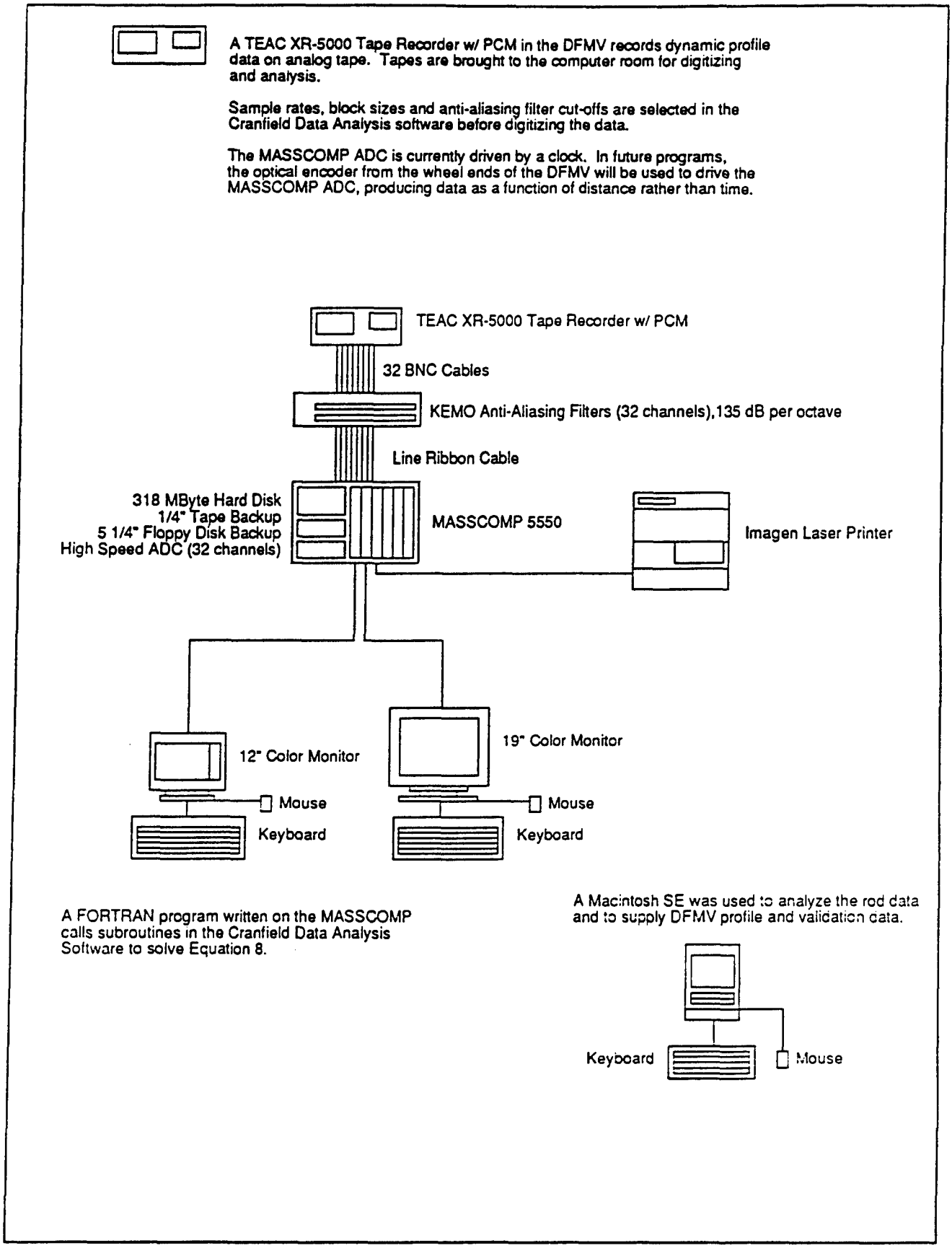

Figure 7. Schematic Diagram of DFMV Data Acquisition and Analysis System

The force and acceleration signals used to compute terrain profiles were acquired as records of terrain elevation as a function of time, t in seconds (time histories), which produce spectral values as a function of frequency, f in cycles per second (Hz). The final presentation of all data, however, is desired in terms of terrain elevation as a function of distance, d in feet, producing spectral values as a function of wave number, n in cycles per foot (ft^{-1}). For convenience, all data analysis algorithms are presented in terms of operations on time histories. The resulting time and frequency functions are readily converted to functions of distance and wave number through the following relationships:

$$d = tV \; ; \; n = \frac{f}{V} \tag{2}$$

where V is the DFMV velocity in ft/sec. Of course, these straightforward conversions from the time (frequency) domain to the distance (wave number) domain assume the speed of the vehicle is constant. As noted in Section 7.2, every effort was made to keep the vehicle speed constant over the length of each run. However, some speed variations did occur, especially on the RMS courses.

8.1 Computation of Elevation Profiles

Referring back to Section 7 and Figure 3, for each of the four wheels on the DFMV, the formula relating the vertical displacement at the tire/ground interface (the elevation), denoted by x(t), and the vertical force and displacement on the axle, denoted by f(t) and y(t), respectively, can be written as the following differential equation:

$$c\frac{dx(t)}{dt} + k\,x(t) = m\frac{d^2y(t)}{dt^2} + c\frac{dy(t)}{dt} + k\,y(t) - F(t) \tag{3}$$

Note the sign conventions of Figure 3 apply; it is important that the forces and accelerations be analyzed with that sign convention. In addition, the resulting course profile will have the same convention.

Taking the Fourier transform of Equation (3) over a long but finite time duration, T, yields

$$j2\pi fc\,X(f,T) + k\,X(f,T) = -(2\pi f)^2 m\,Y(f,T) + j2\pi fc\,Y(f,T) + k\,Y(f,T) - F(f,T) \tag{4a}$$

or

$$[k + j2\pi fc]\,X(f,T) = [k - (2\pi f)^2 m + j2\pi fc]\,Y(f,T) - F(f,T) \tag{4b}$$

where

$$X(f,T) = \int_0^T x(t)e^{-j2\pi ft}dt \; ; \; Y(f,T) = \int_0^T y(t)e^{-j2\pi ft}dt \; ; \; F(f,T) = \int_0^T F(t)e^{-j2\pi ft}dt$$

To simplify the notation, let the following frequency response functions be defined:

$$H_1(f) = \frac{1}{[k - (2\pi f)^2 m + j2\pi fc]} \; ; \; H_2(f) = \frac{[k + j2\pi fc]}{[k - (2\pi f)^2 m + j2\pi fc]} \tag{5}$$

From [4, p. 41], $H_1(f)$ is the frequency response function of the tire system (modelled by a single degree-of-freedom system) with a force excitation, and $H_2(f)$ is the frequency response function of the tire system with a displacement excitation. Using the definitions in Equation (5), Equation (4) may now be written as

$$X(f,T) = \frac{1}{H_2(f)} [Y(f,T) - H_1(f)\, F(f,T)] \tag{6}$$

On the DFMV, the motion response of the tire system was measured with an accelerometer. Noting that the Fourier transform of acceleration, A(f), is given by

$$A(f,T) = - (2\pi f)^2\, Y(f,T) \tag{7}$$

It follows that

$$X(f,T) = \frac{- 1}{H_2(f)} \left[\frac{A(f,T)}{(2\pi f)^2} + H_1(f)\, F(f,T) \right] \tag{8}$$

Using a FORTRAN program and the Cranfield Data Systems (CDS) software on a MASSCOMP computer (Figure 7), the Fourier transforms, A(f,T) and F(f,T), were computed from the simultaneously measured axle acceleration, a(t), and tire system force, f(t), on each of the four wheels. The two frequency response functions, $H_1(f)$ and $H_2(f)$, could be determined experimentally with an air-bearing plate and a shaker. However, for the purposes of this report, the individual tire parameters were calculated using NATC's fixture for determining spring and damping rates. NATC has specialized fixtures for measuring the spring and damping characteristics of tires. From those measurements, the following parameters were calculated as inputs to Equation (5).

m = mass of tire/wheel/hub assembly = 5.1 slugs (lb-s^2/ft)

Assuming 17.5% deflection (See Appendix O),
k = spring rate of tire = 8,470 lb/ft
c = damping rate of tire = 19.75 lb-s/ft

As will be demonstrated in Section 10, the Fourier transform computed in Equation (8) is relatively insensitive to these analysis model parameters, which is a major virtue of the DFMV terrain profiling system. Note that these tire parameters are not the same as those in the Interim Data Summary, due to a error in calculating c, the tire damping (see characterization report and Volume II).

After solving Equation (8) with the appropriate tire parameters, the vertical displacement (elevation) time history of the course is obtained by computing the inverse Fourier transform of Equation (8), given by

$$x(t) = \int_0^{f_c} X(f,T)e^{j2\pi ft}df \tag{9}$$

where f_c is the upper cut-off frequency of the computation (the Nyquist frequency). This upper cut-off frequency, f_c, is established by the sampling rate used to convert the analog signals to a digital format, as detailed later in Section 10. The elevation versus time history yielded by Equation (9) is readily converted to an elevation versus distance history (terrain profile) using the relationships in Equation (2).

The duration, T in seconds, of the Fourier transform computations in Equation (7.3) is fixed by the length, L in feet, of the test course. Specifically,

$$T = \frac{L}{V} \tag{10}$$

where V is the DFMV velocity in ft/sec. Because the duration of the Fourier transform is finite (L is finite), the equality in Equation (8) is only approximate. For this approximation to be acceptable, the duration, T, must be long compared to the memory scale, τ_1, of the $H_1(f)$ system defined in terms of its unit impulse response function, given by [5]

$$h_1(\tau) = \int_0^{\infty} H_1(f)e^{j2\pi f\tau}df = C\, e^{-2\pi f_n\zeta\tau}\sin(2\pi f_d\tau) \tag{11}$$

where

$$C = \frac{2\pi f_n}{k\sqrt{1-\zeta^2}} \;;\; f_d = f_n\sqrt{1-\zeta^2} \;;\; f_n = \frac{1}{2\pi}\sqrt{\frac{k}{m}}$$

m = mass of tire/wheel/hub assembly = 5.1 slugs (lb-s^2/ft)

k = spring rate of tire = 8,470 lb/ft

$\zeta = \frac{c}{2\sqrt{km}}$ = damping ratio = 0.047

$f_n = \frac{1}{2\pi}\sqrt{\frac{k}{m}}$ = 6.5 Hz

It should be emphasized that the undamped natural frequency of f_n = 6.5 Hz in Equation (11) is physically fictitious; i.e., it is simply a parameter of the mathematical model in Figure 3, and will not appear as a natural frequency in the actual vehicle dynamics.

Equation (11) was solved for the integration time of all Fourier transform computations (τ = T), and was found to be negligible, meaning the approximation provided by Equation (8) is excellent.

8.2 Computation of Elevation Power Spectra

It is a common practice to describe the spectral characteristics of terrain and road roughness data in terms of the power (auto) spectral density function (PSD), which is a function first developed by statistical communication engineers to describe the spectral content of random processes [4]. To apply this function to road roughness data, it is assumed that each test course represents a single sample of a collection of test courses of the same design that might be constructed, meaning that the elevation data for each test course can be viewed as a single physical realization of a random process. It is further assumed that each test course, excluding its mean elevation, is homogeneous (stationary in space) [4, p. 109] so that the ergodic theorem can be invoked [4, p. 144] to allow the spatial PSD of the terrain profile over a single test course to be interpreted as an estimate of the average terrain spatial PSD for all test courses of the same design. The homogeneity assumption is justified even for the test courses with systematic bumps (the RMS Test Courses), if it is assumed the distance between the start of the test course and the first bump for all possible test courses of the same design is a uniformly distributed random variable [4, p. 147]. These philosophical considerations, although rarely stated, are the theoretical justification for using wave-number spectra (spatial PSD) to describe road and terrain roughness data.

With the above assumptions in mind, the PSD of the terrain elevation versus time, x(t), for each test course was computed based upon the definition of the power (auto) spectral density function given by [4]

$$G_{xx}(f) = \lim_{T \to \infty} \frac{2}{T} E[X^*(f,T)X(f,T)] \tag{12}$$

where E[ ] denoted the expected value of [ ], and the asterisk (*) denotes complex conjugate. Substituting from Equation (8),

$$X^*(f,T)X(f,T) = \left\{ \frac{1}{H_2^*(f)} [Y^*(f,T) - H_1^*(f)\, F^*(f,T)] \right\} \left\{ \frac{1}{H_2(f)} [Y(f,T) - H_1(f)\, F(f,T)] \right\}$$

$$= \frac{1}{|H_2(f)|^2} [|Y(f,T)|^2 + |H_1(f)|^2 |F(f,T)|^2 - H_1(f)\, Y^*(f,T)\, F(f,T) - H_1^*(f)\, Y(f,T)\, F^*(f,T)] \tag{13}$$

The cross-spectral density function between the response displacement, y(t), and the force, f(t), is given by

$$G_{yf}(f) = \lim_{T\to\infty} \frac{2}{T} E[Y^*(f,T)F(f,T)] \tag{14}$$

Furthermore,

$$G_{fy}(f) = G_{yf}^*(f) \text{ and } G_{yf}(f) + G_{yf}^*(f) = 2 \text{ Re } [G_{yf}(f)] \tag{15}$$

where Re [ ] is the real part of the complex quantity, $G_{yf}(f)$. Then, taking the expected value of Equation (13) with the limits defined in Equations (12) and (14) yields

$$G_{xx}(f) = \frac{1}{|H_2(f)|^2} \{G_{yy}(f) + |H_1(f)|^2 G_{ff}(f) - 2 \text{ Re } [H_1(f) G_{yf}(f)]\} \tag{16}$$

In terms of the acceleration response of the axle, a(t), the PSD of the tire/ground interface vertical displacement is given using Equation (7) by

$$G_{xx}(f) = \frac{1}{|H_2(f)|^2} \{[G_{aa}(f)/(2\pi f)^4] + |H_1(f)|^2 G_{ff}(f) + 2 \text{ Re } [H_1(f) G_{af}(f)/(2\pi f)^2]\} \tag{17}$$

Of course, the spectral terms in Equations (16) and (17), as defined in Equations (12) and (14), cannot be computed precisely, because it is not possible to fully execute the expected value and limiting operations in Equations (12) and (14). However, these quantities can be estimated to any desired level of precision by subdividing the available data record into n_d contiguous segments, each of duration (length) T, and computing

$$G_{xx}(f) = \frac{2}{T} \sum_{i=0}^{n_d} X_i^*(f,T) X_i(f,T) \tag{18}$$

The CDS software and most commercial signal processing programs execute these procedures. The values of n_d and T for the PSD computations on the data analyzed in this report are detailed in Sections 9 and 10.

The description of the terrain elevation in terms of a PSD, as opposed to the simple Fourier spectrum of Equation (8), offers the following advantages:

1. The PSD is consistent with the usual descriptions of terrain roughness; e.g., [4].

2. The cross-spectrum portion of the computation in Equation (16) or (17) provides the best linear approximation, in the least squares sense, for nonlinear properties in the tire response [4, pp. 181-185].

3. The cross-spectrum portion of the computation in Equation (16) or (17) suppresses the extraneous measurement noise in the instrumentation. However, extraneous noise will sum into the power spectra terms, so good signal-to-noise ratios in the measurements are important.

The only major disadvantage of the PSD analysis procedure is that it eliminates the ability to reconstruct the time histories represented by the PSDs. However, for applications as a roughness index, this is not important. The response of vehicle structures to terrain roughness induced dynamic loads is highly dependent on frequency. Hence, the primary information of interest to assess the damage potential of a terrain is PSD of the motion that the terrain roughness will input at the vehicle wheels, which is given by the wave-number spectrum, $G_{xx}(n)$, where $n = f/V$. It follows that the PSD provides a meaningful measure of terrain roughness, from a vehicle damage potential viewpoint.

8.3 Computation of Coherence Functions

A full description of the terrain roughness requires not only the spectrum of the terrain elevation at each of the individual wheels of the test vehicle, but also a measure of the relationships among the terrain elevations at all four wheels. This spatial relationship can be described by the coherence function between the terrain elevations measured at the various wheels. The coherence function (in frequency domain terms) is defined by

$$\gamma_{ij}^2(f) = \frac{|G_{ij}(f)|^2}{G_{ii}(f)\, G_{jj}(f)} \tag{19}$$

where

$G_{ij}(f)$ = cross-spectrum between the terrain elevations at the ith and jth wheels

$G_{ii}(f)$ = PSD of the terrain elevation at the ith wheel

$G_{jj}(f)$ = PSD of the terrain elevation at the jth wheel

The coherence function is a frequency (wave number) dependent real number bounded by zero and one, where $\gamma_{ij}^2(f) = 0$ indicates there is no linear relationship between the two measurements, and $\gamma_{ij}^2(f) = 1$ means there is a perfect linear relationship between the two measurements. For the front and rear wheels on either side of the vehicle, the coherence must be close to one at all frequencies, since the rear wheel traverses the exact path of the front wheel (assuming no turns) and, hence, sees the same elevation profile with only a translation in time (distance). On the other hand, for the left and right wheels on either the front or rear of the vehicle, the coherence at all frequencies (wave numbers) can vary from $\gamma_{ij}^2(f) = 0$, as might occur on "Belgian Block", to $\gamma_{ij}^2(f) = 1$, as would occur on a road with one-dimensional roughness. See [4, pp. 172-176] for details. As discussed in Section 10.4, for the wave-number spectrum range in interest, coherence values greater than 0.7 are assumed good, while values less than 0.4 are assumed poor.

Using the Fourier spectra of the terrain elevations at the tire/ground interface for the four wheels, as computed in Equation (19), the coherence function between the left and right wheel was computed with the CDS software using Equations (14) and (16) with the appropriate Fourier spectra. A complete description of the spatial characteristics of the terrain roughness is thus provided from the DFMV measurements.

9.0 ROD AND LEVEL VALIDATION DATA ANALYSIS

The rod and level validation data, hereafter referred to simply as the "rod data," constitute the base line against which the DFMV elevation data are to be compared in terms of both elevation versus distance (course profiles) and wave-number spectra (spatial PSDs). Hence, it is

9.0 ROD AND LEVEL VALIDATION DATA ANALYSIS

The rod and level validation data, hereafter referred to simply as the "rod data," constitute the base line against which the DFMV elevation data are to be compared in terms of both elevation versus distance (course profiles) and wave-number spectra (spatial PSDs). Hence, it is important that the wave-number spectra of the rod data be computed in a meaningful and well-defined manner. It is also important that all plots from the three methodologies be on the exact same scales for exact comparisons between the systems. NATC has performed this exercise for the wave-number spectra and the data are contained in the Appendices of this report (Appendix C, D, and E). A spectrum from the rod and level can be overlaid on a spectrum of the DFMV for direct comparison.

Following from the discussions in Section 8.2, the wave-number spectrum computed for a single test course of finite length should be interpreted as an estimate of the average wave-number spectrum for all courses of that design. With this in mind, there are six basic considerations in the computation of statistically reliable wave-number spectra, as follows:

1. Lowest wave number at which spectral values can be determined in the computations.

2. Highest wave number at which spectral values can be determined in the computations.

3. Wave-number resolution, which determines the spectral bias error in the computations.

4. Number of averages, which determines the random error in the computations.

5. Tapering operations, which determine the spectral "leakage" in the computations.

6. Detrending operations, which suppress trend induced errors in the computations.

Each of these matters are now discussed, followed by a summary of the data analysis parameters and the analyzed wave-number spectra for the rod data.

9.1 Lowest Wave-Number

The lowest possible wave number, n_{lp}, for which an elevation spectral density value can be computed from a test course (excluding n = 0) is

$$n_{lp} = \frac{1}{L} \tag{20}$$

where L is the total length of the test course. For the test courses in this study, L = 280 to 1000 ft, meaning n_{lp} = 0.0036 to 0.001 ft^{-1}. However, to enhance the statistical stability of wave-number spectra estimates, it is desirable to perform averaging over independent blocks of data, as indicated in Equation (14). Hence, much shorter block lengths are desirable for computational purposes. Also, the RMS test courses in this study have systematic bumps that are spaced approximately 30 ft apart, meaning a block length of 100 ft, which will cover about three systematic bumps, should be adequate to describe the principle spectral features of the elevation data of concern. Based upon these considerations, the lower wave-number limit for the spectra analyses of the rod data was selected to be n_l = 0.01 ft^{-1}, corresponding to a maximum wavelength of λ_h = 100 ft. It should be noted that the longer the course, the better the estimate at the lower wave numbers. In future studies, it is recommended that the length of the profile segment be at least 10 times greater than the longest wavelength of interest (e.g., 1,000 feet for a 100 foot wavelength in the spectrum). A course length of 1,028 feet is normally the standard WES test course length, however, course lengths of 280 feet were allowed on the Truck Hill course.

9.2 Highest Wave-Number (Aliasing and Noise)

The highest possible wave number, n_h, for which an elevation spectral value can be computed from the rod data is fixed by the distance, Δd in feet, between the sample values describing the elevation profile (or the sampling rate, $1/\Delta d$ in samples/ft); specifically,

$$n_h = \frac{1}{2\Delta d} \tag{21}$$

where n_h is called the Nyquist wave number (frequency), or the folding wave number (frequency) [4, p. 337]. Beyond defining the highest wave number at which a spectral component can be defined in digital elevation data, all spectral values in the actual elevation versus distance function for the test course above the Nyquist wave number, n_h, are folded down and appear at a wave number below n_h due to an effect called "aliasing" [4, p. 337]. The result can be a severe distortion of the wave-number spectral values computed below the Nyquist wave number.

For those cases where elevation data are collected in the form of a continuous analog signal (as is true for the DFMV data), the aliasing problem is easily avoided by eliminating all analog signal values above the Nyquist wave number, using a low-pass analog filter (called the "anti-aliasing filter") prior to digitizing the elevation data for analysis. For the rod data, however, the original data acquisition was made directly in digital form. In most cases where data are collected directly in digital form, the sampling rate is selected to be much higher than the highest frequency of interest, so that digital filters can be used for anti-aliasing purposes. Noting that the maximum sampling rate for the rod data was only 2 samples/ft ($\Delta d = 0.5$ ft), corresponding to an upper wave-number limit of only $n_h = 1$ ft^{-1}, it follows that digital anti-aliasing filters cannot be used to suppress aliasing in the rod data without losing much of the wave-number spectral information of interest. On the other hand, there is a major factor that naturally suppresses aliasing in digitized terrain elevation data, namely, the wave-number spectra for terrain elevation data tend to decrease monotonically in value with increasing wave number (examples to the contrary seen in most all published spectra for road and terrain elevation data commonly reflect aliasing errors or background instrument noise). Hence, aliasing errors in terrain elevation data, even when they have not been low-pass filtered, are usually not very severe below about 50% of the Nyquist wave number.

On the other hand, the fact that the wave-number spectra for terrain decrease rapidly with increasing wave number introduces a signal-to-noise ratio problem at the higher wave numbers, which also may limit the highest wave number for accurate data. For the rod and level procedure, the elevation values are rounded off to 0.01 ft. Even excluding the other errors associated with the rod and level profiling procedure (such as rod tilt errors [11], which were observed), this round off error will translate into background measurement noise at the higher wave numbers.

For relatively smooth terrain (like the Truck Hill courses), this noise could come in at wave numbers well below the Nyquist wave number, n_h.

In summary, the plots of wave-number spectra for the rod data to follow will show spectral values out to the Nyquist wave number of $n_h = 1/(2\Delta d)$ ft^{-1}. However, it should be understood that the spectral values from the rod data at wave numbers below n_h may be erroneously high due to aliasing and/or measurement noise. In future studies, it is recommended that a minimum sample interval of 6 inches be used, giving a high end wave-number cut-off of 1 ft^{-1} (as was done for all the courses except the Truck Hill courses). If funds and time allow, a sample interval of 3 inches should be used for comparisons to other profilometer systems and for accurately estimating wave-number spectra. A 3-inch interval would minimize aliasing and measurement noise at the high end wave-number cut-off of 1 ft^{-1}.

9.3 Wave-Number Resolution (Bias Errors)

The narrowest possible resolution, D, with which an elevation wave-number spectrum can be computed from a test course is D = 1/L, where L is the length of the test course, although a more logical minimum resolution would be $D = n_1$, where n_1 is the lowest wave number for the analysis determined in Section 9.1. However, two other factors influence the selection of the wave-number spectral analysis resolution, as follows:

1. The resolution needed to suppress resolution bias errors in the resulting wave-number spectrum; i.e., the ability to correctly define peaks and valleys in the wave-number spectrum [4, p. 280]. An example would be a severely washboarded road, which will produce a well-defined peak in the wave-number spectrum.

2. The resolution needed to allow a sufficient number of averages to obtain the needed statistical reliability in the resulting wave-number spectrum; i.e., a narrower resolution must be traded off against a reduced number of averages, as discussed in Section 9.4.

Although both of the above-noted considerations are important, the first is the dominant factor in the selection of a resolution. The usual rule for an adequate spectral resolution, from the viewpoint of resolution bias errors, is that there be at least four spectral estimates between the half-power points of each peak or value in the wave-number spectrum [4, p. 282]. The only test courses that will predictably produce a peak in the wave-number spectrum are those with the systematic bumps (the RMS courses and the Washboard course). A preliminary evaluation of the wave-number spectra for the rod data from the various test courses indicates RMS No. 5 produces the best defined spectral peak at $n \approx 0.033$ ft^{-1}, corresponding to a bump separation distance of about $\lambda \approx 30$ ft. Wave-number spectra for these data were computed with two different resolution bandwidths; (a) D = 0.0078 ft^{-1} and (b) D = 0.0039 ft^{-1}. The results are shown in Figure 8. Note that the spectrum with a resolution of D = 0.0078 ft^{-1} does not comply with the criterion of at least four spectral values between the half-power points of the spectral peak at $n \approx 0.033$ ft^{-1}. On the other hand, there is no significant difference in the peak spectral values computed with the two resolutions, and the spectrum with the resolution of D = 0.0078 ft^{-1} is much smoother due to the higher number of averages (8 versus 4) allowed in the computations, which reduces the random error, discussed in Section 9.4 (a half power point area under the curve calculation would reveal that the two curves in Figure 8 are the same). Nevertheless, to assure a negligible resolution bias error, the resolution of D = 0.0039 ft^{-1} was selected for the wave-number spectral computations of the rod data from those test courses with systematic bumps. However, for the other test courses where a strong peak in the wave-number spectra is not anticipated (Middle East and Truck Hill courses), the spectral computations were performed using the wider resolution of 0.0078 ft^{-1}.

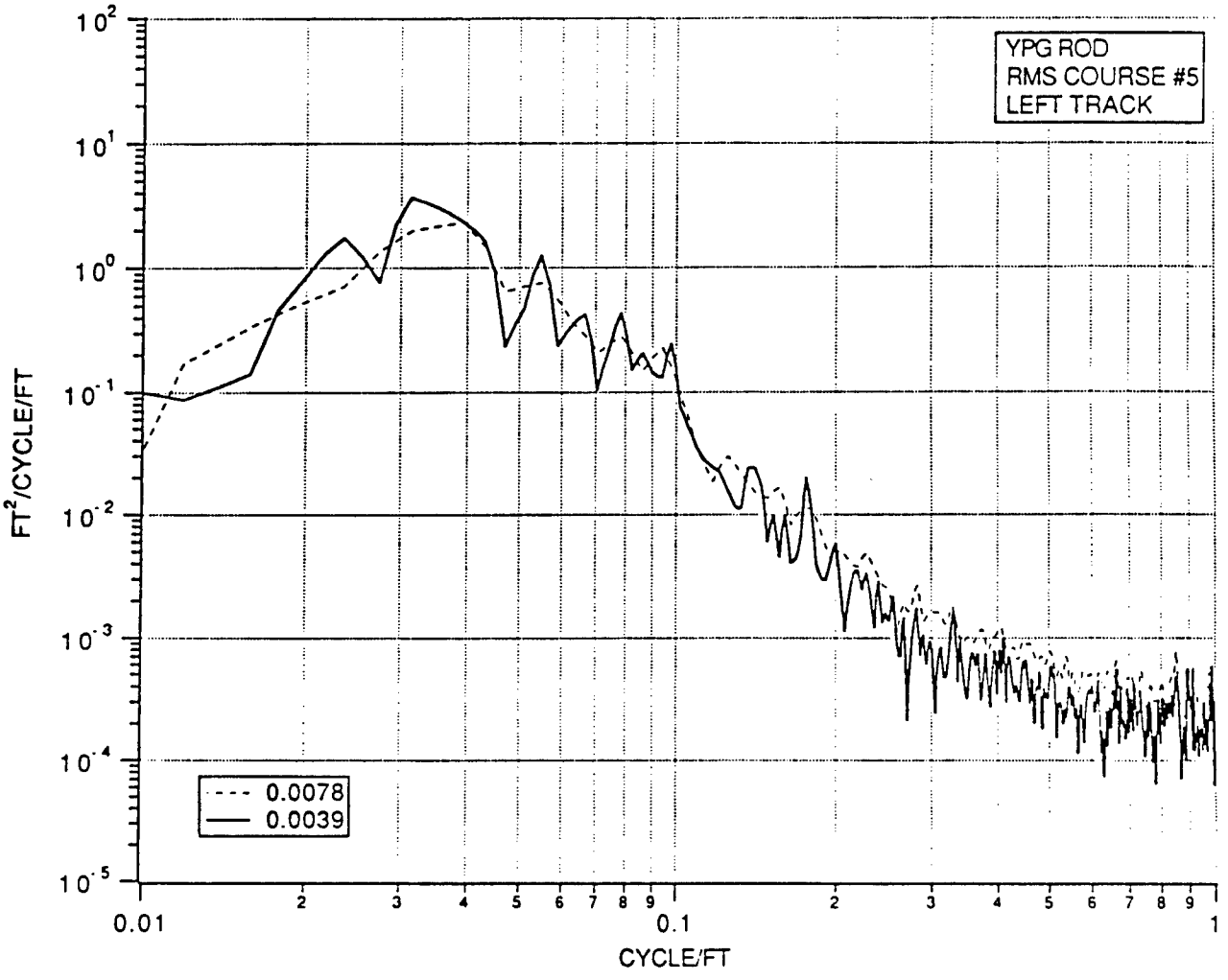

Figure 8. Wave-Number Spectrum for RMS Test Course No. 5 Computed With Resolutions of D = 0.0039 ft^{-1} and D = 0.0078 ft^{-1}, Rod and Level Data.

9.4 Number of Averages (Random Errors)

Viewing the elevation data for each test course as a single physical realization of a homogeneous random process (see Section 8.2), the normalized random error (coefficient of variation) in the resulting wave-number spectral computations is approximated by [4, p. 283]

$$\varepsilon \approx \frac{1}{\sqrt{n_d}} = \frac{1}{\sqrt{DL}} \tag{22}$$

where n_d is the number of disjoint data segments (called data "blocks") used for the wave-number spectral density computations, as detailed in Equation (18). Assuming contiguous data blocks, it is clear that $n_d \leq DL$, where D is the resolution bandwidth of the analysis, and L is the length of the test course. For the resolution of $D = 0.0039$ ft^{-1} determined in Section 9.3, which applies to test courses where L = 900 or 1000 ft (extended to 1024 ft by adding zeros for Fourier transform purposes and adding the appropriate correction factor), it follows that $n_d = 4$, corresponding to a normalized random error of $\varepsilon = 0.50$. From [4, p. 255], the interpretation of this random error is as follows: as a first order of approximation, about two-thirds of the spectral values at the different wave numbers will be within 50% of the average spectral value for all courses of the same design. For the analysis of the data from the shorter test courses with the wider resolution of $D = 0.0078$ ft^{-1}, different numbers of averages are used, as summarized in Table 2, but always $n_d \leq 6$. Random error limitations is another reason that it is recommended that the length of the profile segment be at least 10 times greater than the longest wavelength of interest (i.e., 1,000 feet for a 0.01 ft^{-1} wave-number cut-off).

Table 2. Computation Parameters for Wave-Number Spectra of Rod and Level Data

Course	Length* (L, ft)	Spacing (Δd, ft)	Highest Wave Number† (n_h, ft^{-1})	Lowest Wave Number, (n_l, ft^{-1})	Resolution Wave Number (D, ft^{-1})	Number of Averages‡ (n_d)
RMS #2	1000	0.5	1.0	.01	0.0039	4
RMS #3	1000	0.5	1.0	.01	0.0039	4
RMS #4	1000	0.5	1.0	.01	0.0039	4
RMS #5	1000	0.5	1.0	.01	0.0039	4
Washboard	900	0.5	1.0	.01	0.0039	4
Muggins Mesa 45° to wash (Middle East #2)	591	0.5	1.0	.01	0.0078	5
Muggins Mesa 90° to wash (Middle East #1)	591	0.5	1.0	.01	0.0078	5
Truck Hill #1	740	1	0.5	.01	0.0078	6
Truck Hill #2	280	1	0.5	.01	0.0078**	2
Truck Hill #3	400 (L) 410 (R)	1	0.5	.01	0.0078	3
Truck Hill #4	490 (L) 480 (R)	1	0.5	.01	0.0078**	4

† Wave-number limit based on Nyquist frequency, some aliasing and noise errors present. Divide this column by two for wave-number limit with negligible errors.

‡ Zeros are added to the data sequence where required (factor applied to wave-number spectra to correct for additional zeros)
An n_d of 4 equals a random error of 0.50 without overlap processing, 0.38 with overlap processing (Also see Appendix M)

* Based on data supplied by WES rod and level survey

** Does not apply to Figures 10 and 11; resolution presented in these Figures (D=0.0039 ft^{-1}) will not change detrending results

9.5 Tapering Operations (Leakage Errors)

Side-lobe leakage errors are an inherent problem in the computation of spectra for any random data sequence of finite duration in time, or finite length in space; they are analogous to the truncation errors that occur when a Fourier transform is computed for a periodic function of period, P, over a finite length, L, where $L \neq nP$; $n = 1, 2, 3, \ldots$ Leakage errors are most severe at the smaller spectral values in data that have strong spectral peaks and valleys. The leakage problem can be suppressed by a tapering operation on the data to modify the spectral window associated with the analysis (the most common tapering operation is the "cosine-squared" window, often called the "Hanning" window). However, tapering operations introduce problems, including the following (see [4, pp. 393-400] for details and illustrations):

1. They make the effective resolution of the analysis wider (by about 50% for Hanning).

2. They increase the random error in the resulting spectral estimates (by about 40% for Hanning).

3. They can lead to erroneous high or low values at all wave numbers if the data are not truly homogeneous within each data block.

Referring to Item 1 and the discussions in Section 9.3, the 50% increase in the effective resolution of the analysis is considered acceptable. Referring to Item 2 and the discussions in Section 9.4, the 40% increase in the random error of the analysis is not considered acceptable, but this increased error can be nearly eliminated by overlapped processing [4, p. 398]. Referring to Item 3, although the test courses are not truly homogeneous, a visual inspection of the detrended rod elevation data indicates the homogeneity assumption is acceptable.

To check on the extent of the leakage errors that might occur without tapering, the wave-number spectrum for RMS Course No. 5, which has the strongest spectral peak of any of the rod elevation data, was analyzed with and without a Hanning window, with the results shown in Figure 9. Note that the Hanning window has very little impact on the spectral values at the lowest and highest wave numbers, indicating that the leakage errors without tapering (with a rectangular window) would be relatively small. Nevertheless, to guarantee against possible leakage problems, all the rod elevation data blocks were tapered with a cosine-squared (Hanning) window for the wave-number spectral computations, and a 50% overlap of the data blocks was employed to suppress the increase in the random error due to the tapering.

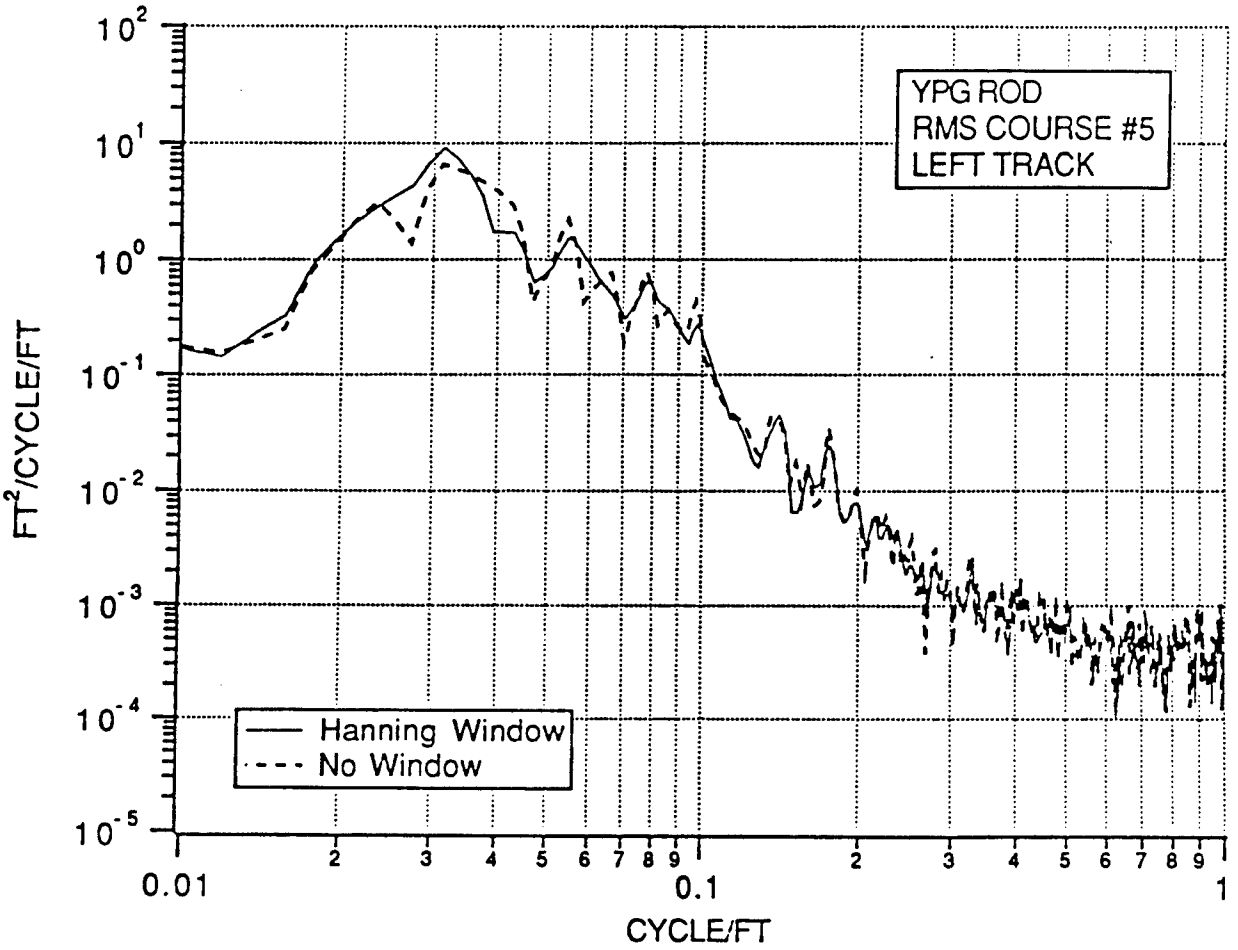

Note: The ft^2/cycle/ft amplitude in this figure is not the same as Figure 8. This is because the software used to compute the wave-number spectra did not automatically apply the Hanning window correction factor. This figure has the correction factor applied, Figure 8 does not.

Figure 9. Wave-Number Spectrum for RMS Test Course No. 5 Computed With and Without Tapering (Hanning Window) - Resolution D = 0.0039 ft^{-1}, Rod and Level Data.

9.6 Detrending Operations (Trend Errors)

The rod data were measured over some courses with substantial, monotonic changes in the elevation (grades), which appear in the elevation versus distance data as mean value trends (see Appendix A). These trends might be viewed as a very long wavelength component in the data, but because their wavelength is longer than the entire data sequence (the length of the test course), they cannot be properly defined by a finite Fourier transform of the data values over the test course needed to compute a wave-number spectrum. In fact, these trends become a major error term in the finite Fourier transform [5], which contaminates the spectral values at the lower wave numbers, due to effects essentially equivalent to the leakage problem discussed in Section 9.5. Hence, the trends in the rod elevation data must be removed prior to performing the finite Fourier transform operations needed to compute wave-number spectra.

For the data from all test courses excluding the Truck Hill test courses, trend removal was accomplished on each block of the rod elevation data by fitting a third-order polynomial to the data values by least squares procedures, and subtracting the trend from the data values (see [4, p. 362-365] for the details of polynomial trend removal and the applicable algorithms). A third-order polynomial will fit a trend of up to one cycle over the data block, which for most of the data corresponds to a wave number of $n = 0.0039$ ft^{-1} (a wavelength of $\lambda = 256$ ft). Hence, the actual elevation variations that are removed by the detrending operation are well below $n_1 = 0.01$ ft^{-1}, the lower wave-number limit for the analysis.

For the Truck Hill data, the trends were too extreme to be effectively removed by a third-order polynomial. Hence, higher-order polynomials (up to 14th order) were used, which removed the actual wave-number spectral values in the data below $n = 0.02$ ft^{-1}. The analysis of the Truck Hill data was also accomplished using the slope-domain procedure in [3, pp. 105-107] with third-order polynomial detrending. The slope procedure alone strongly suppresses, at least, linear trends.

The importance of trend removal is clearly illustrated in Figure 10 and 11, which shows the wave-number spectra computed for Truck Hill Test Course No. 2 and 4, with and without detrending of the data. There is a three order of magnitude difference between the data with and without the trend. In Figure 10 (Truck Hill #4), note the dramatic errors caused by the trend in the wave-number range below $n = 0.02$ ft^{-1}. Again, these represent waves removed by the higher-order polynomial detrending. Figure 11 shows the difference between four levels of detrending for Truck Hill #2. Figure 11 shows the wave-number spectrum computed using the slope procedure suggested in [3], after correcting the spectrum to elevation units (integral of slope PSD). Note that the results for the detrended elevation data and the slope data corrected back to elevation units are similar at wave numbers above $n = 0.04$ ft^{-1}. Below this wave number, the spectrum for the detrended elevation data shows much lower values due to the removal of actual spectral components by the high order polynomial fit (3rd order only). This indicates the importance of selecting the appropriate order polynomial in detrending operations.

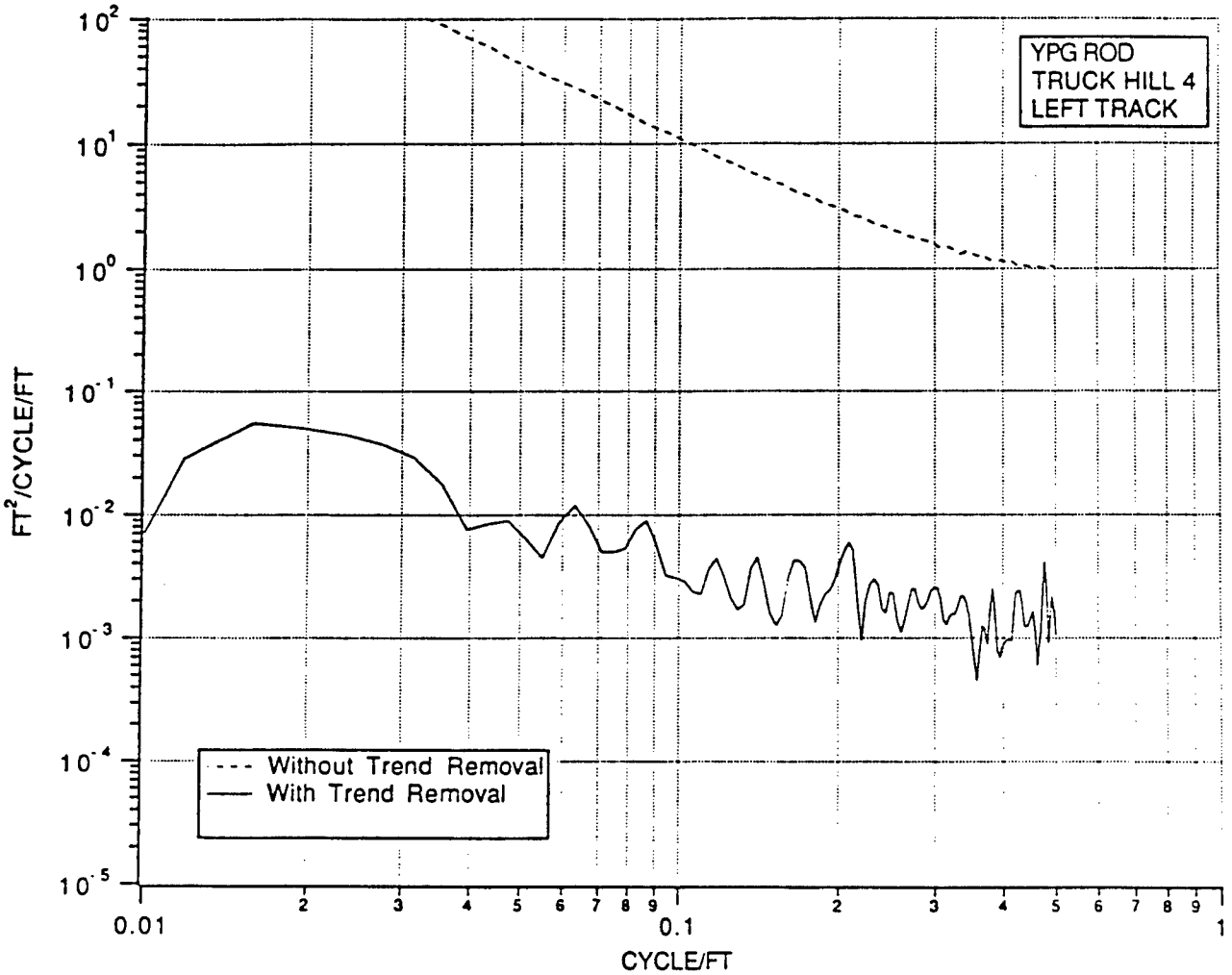

Figure 10. Wave-Number Spectrum for Truck Hill No. 4 Computed With and Without Detrending - Resolution D = 0.0039 ft^{-1}, Rod and Level Data.

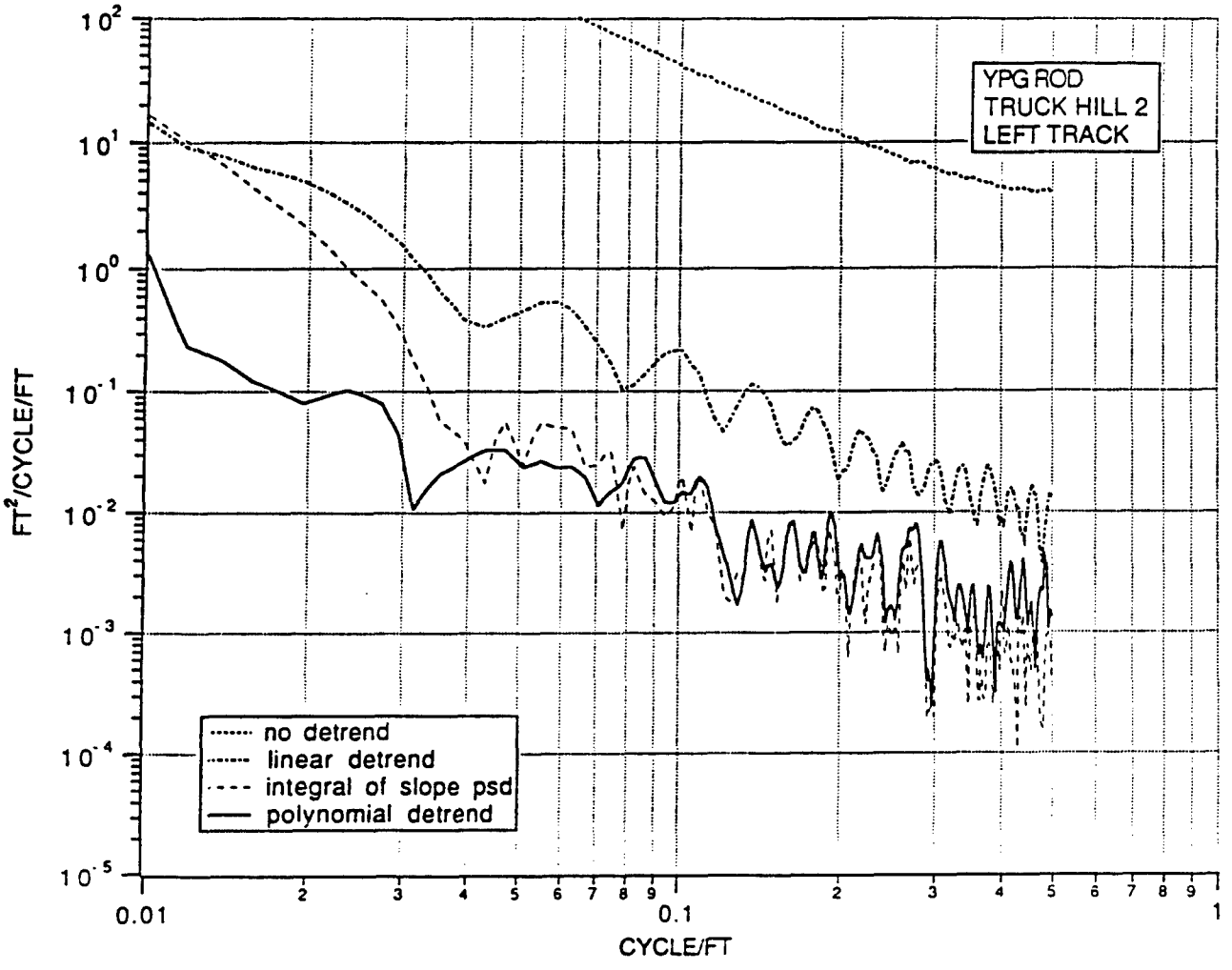

Figure 11. Wave-Number Spectrum for Truck Hill No. 2 Computed With and Without Detrending of Various Types - Resolution D = 0.0039 ft^{-1}, Rod and Level Data.

9.7 Summary of Wave-Number Spectrum Data

Based upon the considerations discussed in Sections 9.1 through 9.6, the wave-number spectral density functions for the rod data were computed using an FFT algorithm, as modified by the tapering and detrending operations summarized in Sections 9.5 and 9.6, using the analysis parameters summarized in Table 2. The coherence functions between the left- and right-wheel paths were also computed using Equation (19). The resulting wave-number spectra and coherence functions for the rod data are detailed in Appendices C and F, respectively.

10.0 DFMV DATA ANALYSIS

The DFMV data were analyzed to yield elevation versus distance profiles, wave-number spectrum, and coherence functions for each of the test courses. Coherence function plots were calculated for the front-to-rear and left-to-right wheels. To accomplish this, nine channels of data from the DFMV instrumentation were used, as follows:

1. Left-front-vertical force
2. Right-front-vertical force
3. Left-rear-vertical force
4. Right-rear-vertical force
5. Left-front-wheel speed (nondriven wheel)
6. Left-front-vertical acceleration
7. Right-front-vertical acceleration
8. Left-rear-vertical acceleration
9. Right-rear-vertical acceleration

As noted in Section 2.0, 33 channels of sensor data were recorded for each course. For example, DFMV steering angle was recorded to permit the curvature of the courses to be defined, if desired. All courses except Truck Hill #3 and #4 were straight, so an analysis of course curvature was not conducted. Also, sprung-mass inclination angle was recorded to permit the analysis of the wavelengths greater than 100 feet, if desired. Wavelengths greater than 100 feet contribute to drivetrain durability and are beyond the scope of this study. Appendix L discusses the instrumentation installed on the DFMV for TACOM's use in computer modeling and analysis of the DFMV data. Appendix L also discusses the instrumentation installed on the M1025 HMMWV, the reference vehicle for this study. Finally, Appendix L discusses the signal-to-noise and recording sensitivities for the instrumentation on the DFMV and HMMWV.

10.1 Summary of Tests

Eleven courses were profiled at YPG. The vehicle speeds used for the profiling are summarized in Table 3. Per the contract, courses were covered at various speeds ranging from 2 MPH to 10 MPH.

Table 3. Summary of DFMV Tests at the Yuma Proving Grounds

COURSE	SPEED	COMMENTS AND LOCATIONS
RMS #3	2, 4, 6, 8	Tire/ground contact lost at speeds above 6 MPH. Date: 5 Dec 1989
RMS #4	2, 4, 6, 8	Tire/ground contact lost at speeds above 6 MPH. Date: 5 Dec 1989
RMS #5	2, 4, 5, 6, 8	Tire/ground contact lost at speeds above 6 MPH. Date: 5 Dec 1989
RMS #2	2, 4, 6, 8, 10	Negative bump RMS course (discrete event). Date: 5 Dec 1989
Washboard	2, 4, 6, 8, 10	Slight washboard, loose gravel on top. Date: 7 Dec 1989
Middle East #1	2, 4, 6, 8, 10	Course parallel to mountain. Date: 7 Dec 1989.
Middle East #2	2, 4, 6, 8, 10	Course diagonal to mountain. Date: 7 Dec 1989
Truck Hill #1	2, 4, 6, 8, 10	0.0 to 0.1 mile marker, clockwise. Date: 8 Dec 1989
Truck Hill #2	2, 4, 6, 8, 10	0.35 to 0.4 mile marker, clockwise. Date: 8 Dec 1989
Truck Hill #3	2, 4, 6, 8, 10	0.5 mile marker, clockwise. Date: 8 Dec 1989
Truck Hill #4	2, 4, 6, 8, 10	1.65 to 1.75 mile marker, clockwise. Date: 8 Dec 1989

The elevation versus distance profile and the wave-number spectrum for each test course were computed by separate operations, to optimize the results for each function (i.e., one block of data is optimal for the elevation versus distance analysis, whereas the average of many blocks is optimal for the wave-number spectrum analysis, as discussed in Sections 10.2 and 10.3). Due to the severity of the RMS courses, 6 MPH was the limiting profile speed. On all other courses, the highest speed run under this contract was used (i.e., 10 MPH). The wave-number spectra for all speeds over all courses are shown in Volume II, and are available upon request. For this report, all elevation versus distance plots were processed at 6 MPH because this was the best speed on the RMS courses and consistence was desired for Table 4 and Appendix B. The wave-number spectra were processed at 6 MPH on the RMS test courses and 10 MPH on all other test courses. From the discussions in Section 7.2, Item 3, the higher speeds provide the best spectral data at the lower wave numbers. Other than better definition of the lower wave numbers with increasing DFMV speed, a wave-number spectrum and DFMV measurement methodology is independent of vehicle speed, as shown in Figure 12. Statistically, the 2, 4, 6, and 8 MPH curves in Figure 12 are the same, however, a full discussion of Figure 12 and the associated random error is given in Appendix M.

Table 4. Summary of Analysis Parameters for Elevation Profile Computations

Course	Length, L* ft	DFMV Speed MPH (ft/sec)	Sampling Rate samples/sec (samples/ft)	Block Size, N
RMS #2	1000	6.9 (10.0)	20 (2.0)	2048
RMS #3	1000	5.8 (8.5)	17 (2.0)	2048
RMS #4	1000	6.0 (8.8)	18 (2.0)	2048
RMS #5	1000	6.5 (9.5)	19 (2.0)	2048
Washboard	900	6.5 (9.5)	20 (2.1)	2048
Middle East #1	591	6.4 (9.4)	32 (3.4)	2048
Middle East #2	591	6.1 (8.9)	28 (3.1)	2048
Truck Hill #1	740	6.3 (9.2)	24 (2.6)	2048
Truck Hill #2	280	5.5 (8.1)	55 (6.8)	2048
Truck Hill #3	400 (L) 410 (R)	5.9 (8.6)	39 (4.5)	2048
Truck Hill #4	490 (L) 480 (R)	6.1 (8.9)	34 (3.8)	2048

* Actual length as surveyed by WES. The DFMV measurement may be shorter or longer, as calculated from columns 3 through 5.

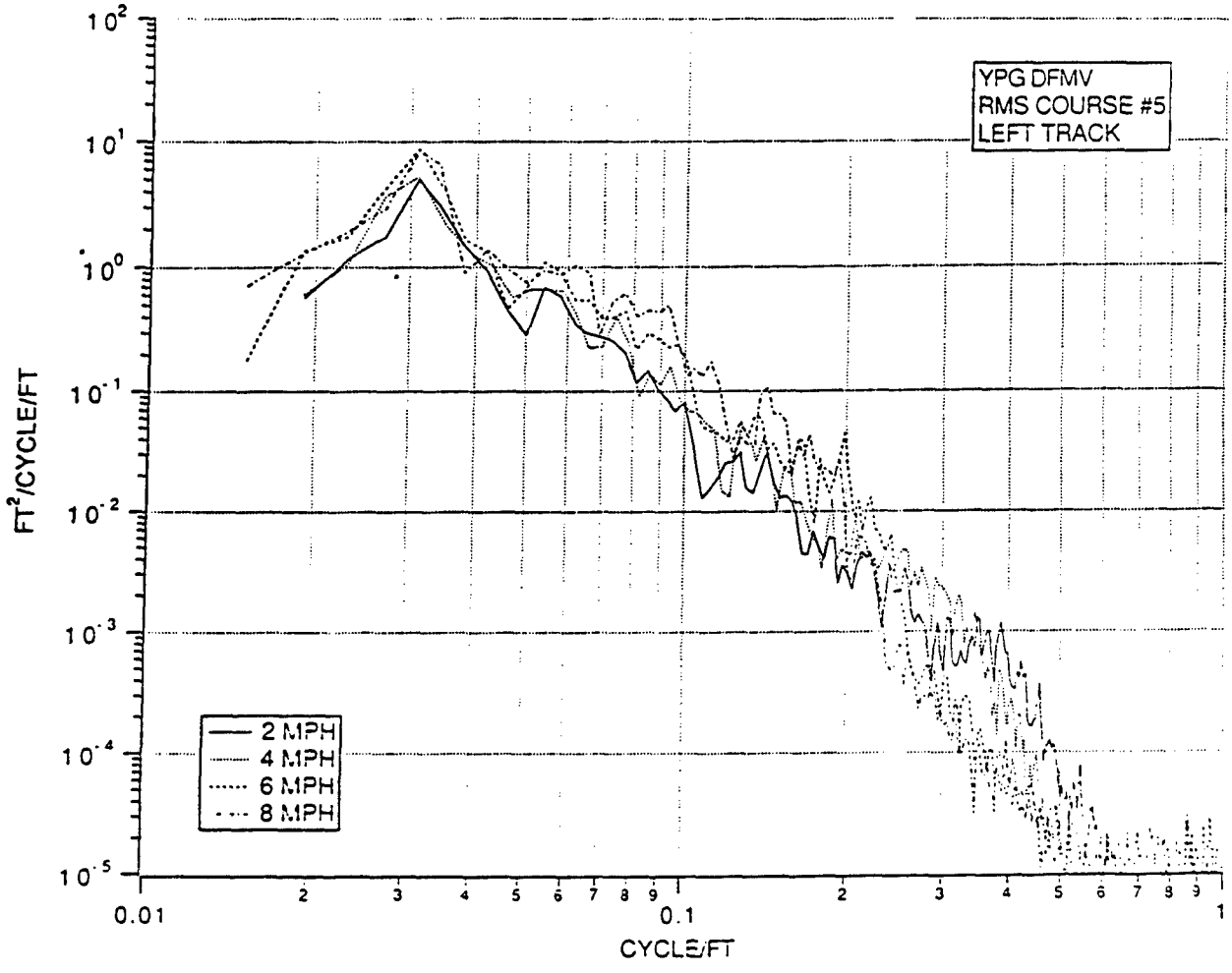

Figure 12. Wave-Number Spectrum for RMS Test Course No. 5 Computed For DFMV Speeds of 2, 4, 6 and 8 MPH.

10.2 Computation of Elevation Profiles

The elevation profiles of the test courses were computed at each wheel of the DFMV using Equations (8) and (9). All profiles were computed using a single block of data for the Fourier transform computations. The sampling rate was always set to provide exactly 2048 points over the time duration required to cover the test course, which resulted in at least two samples/ft for each test course. The cut-off frequency of the anti-aliasing low-pass filters was always set to correspond (as closely as permitted by the available filter selections) to $n = 1.0$ ft^{-1}. Many of the data sequences were also highpass filtered prior to computing the inverse Fourier transform in Equation (18) to eliminate spurious low frequency trends caused by accelerometer noise, as is discussed later. No tapering operations are used for the profile elevation computations. (This procedure is different than that used on the elevation versus distance plots presented in the Interim Data Report submitted 16 January 1990. For that data, multiple blocks were used and mean differences between blocks may have appeared as discrete elevation jumps in the elevation plots.)

Preliminary elevation profiles were computed at different speeds on the test courses. However, no major differences were found in the results obtained at different speeds, so the final profiles were computed only for a nominal speed of 6 MPH. The actual speeds (averaged over the test course) and other analysis parameters used to compute the final elevation profiles are also shown in Table 4. In all cases, the anti-aliasing filter was set to the closest frequency corresponding to a wave number of 1 ft^{-1}, as allowed by the available low-pass filter selections. For the RMS test courses, this resulted in the anti-aliasing filter cut-off being near or at the Nyquist wave number. Since the anti-aliasing filter does not have an infinitely sharp cut-off, a small amount of aliasing might be present at wave numbers above 0.5 ft^{-1} (Note: This cut-off limit was only true for the runs digitized to get the elevation versus distance plots) The computed profiles are presented in Appendix B.

10.3 Computation of Wave-Number Spectra

The wave-number spectra of the test courses were computed at each wheel of the DFMV using Equation (17), as approximated by Equation (18). The spectra for the DFMV data and for that of the rod and level data were computed using the same analysis parameters.

1. Lowest Wave Number - The spectra were computed to a lower wave-number limit of $n_l = 0.01$ ft^{-1} or the lower wave-number limit for valid data, whichever was lower. The lower wave-number limit for valid data was determined by inspection of the coherence functions between the front and rear wheels, as described in Section 10.4.

2. Highest Wave Number - The spectra were computed to an upper wave-number limit of $n_h = 1.0$ ft^{-1}. This was done by fixing the sampling rate of the analog-to-digital converter at the closest available rate for each vehicle speed that would yield 4 samples/ft (a Nyquist wave number of 2.0 ft^{-1}). The signals were low-pass filtered prior to digitizing (for anti-aliasing purposes) with a cut-off frequency selected to correspond to a wave number of $n_h = 1.0$ ft^{-1}.

   Although the cut-off frequency for the DFMV spectral analysis was set at $n_h = 1.0$ ft^{-1}, it is understood from Figure 4 and 5 that the spectral values above $n = 0.5$ ft^{-1} under-estimate the correct spectral value by more than 50%. Remembering from Section 9.2 that the spectra for the rod data probably over estimated above $n = 0.5$ ft^{-1} in some cases, and $n = 0.25$ ft^{-1} in other cases, due to aliasing and possible measurement noise, substantial discrepancies between the DFMV and rod data above the upper wave-number limits in Table 2 should be expected.

3. Wave Number Resolution - The resolution, D, for the spectral computations was selected to be exactly the same as used for the rod data in Table 2; i.e., either $D = 0.0039\ ft^{-1}$, or $D = 0.0078\ ft^{-1}$.

4. Number of Averages - The number of averages, n_d, for the spectral computations was selected to be exactly the same as used for the rod data in Table 2; i.e., from $n_d = 2$ to $n_d = 6$.

5. Tapering Operations - All data blocks were tapered by a Hanning window prior to the Fourier transform computations to suppress side-lobe leakage errors, same as for the rod data (see Section 9.5).

6. Detrending Operations - No detrending operations were required for the DFMV data due to the data acquisition and processing technique (as discussed in Section 9.6, the rod and level data was detrended before processing). The DFMV data is automatically detrended in the data processing due to block length considerations, as discussed in Section 9.1. For example, RMS #5 was 1,000 feet long, however, 4 blocks of data was used to improve the random error of the wave-number spectrum estimate. Therefore, wavelengths greater than 250 feet are removed from the analysis. In addition, a piezoelectric accelerometer was used to measure the motion response of the axle and a piezoelectric accelerometer does not measure inclination angle (zero frequencies). If a profile of the long wavelengths is required, a piezoresistive accelerometer or an inclinometer is used. For this study, an inclinometer was used to measure grade effects. This data is shown in Appendix N. The measured roughness could be added to the grade measurement to provide trends to the DFMV data. However, recall that wavelengths greater than approximately 250 feet represent a low frequency input to a vehicle and effect powertrain performance rather than fatigue performance.

Wave-number spectra for each test course were computed for the various DFMV speeds and were found to be essentially identical except at the lower wave numbers, where the higher vehicle speeds provided the best results, as anticipated (see Section 7.2, Item 3). Hence, for this report, the final spectra were computed for the highest vehicle speed producing valid data, as follows:

1. For the RMS Test Courses - nominally 6 MPH.
2. For all other test courses - nominally 10 MPH.

The computed spectra are presented in Appendix D.

During the processing of the wave-number spectral computations, a sensitivity study was performed to determine how much the spectra are influenced by possible errors in the tire/hub/wheel parameters used in the analytical model, which is the basis for the terrain profile computations by the DFMV procedure. Specifically, stiffness (k), and damping (c), were changed by ± 50% from the nominal values detailed in Section 8.1. As seen in Equation 6, varying k and c together by either ±50% is worst case. This was confirmed graphically for RMS #5, but not plotted for this report. The results for RMS Course No. 5 are shown in Figure 13. Note that the variations in the parameter values for the analytical model produce negligible errors, except at wave numbers above about 0.5 ft-1, which is beyond the range of accurate measurements due to the filtering caused by the footprint of the tire (see Section 7.2, Item 1).

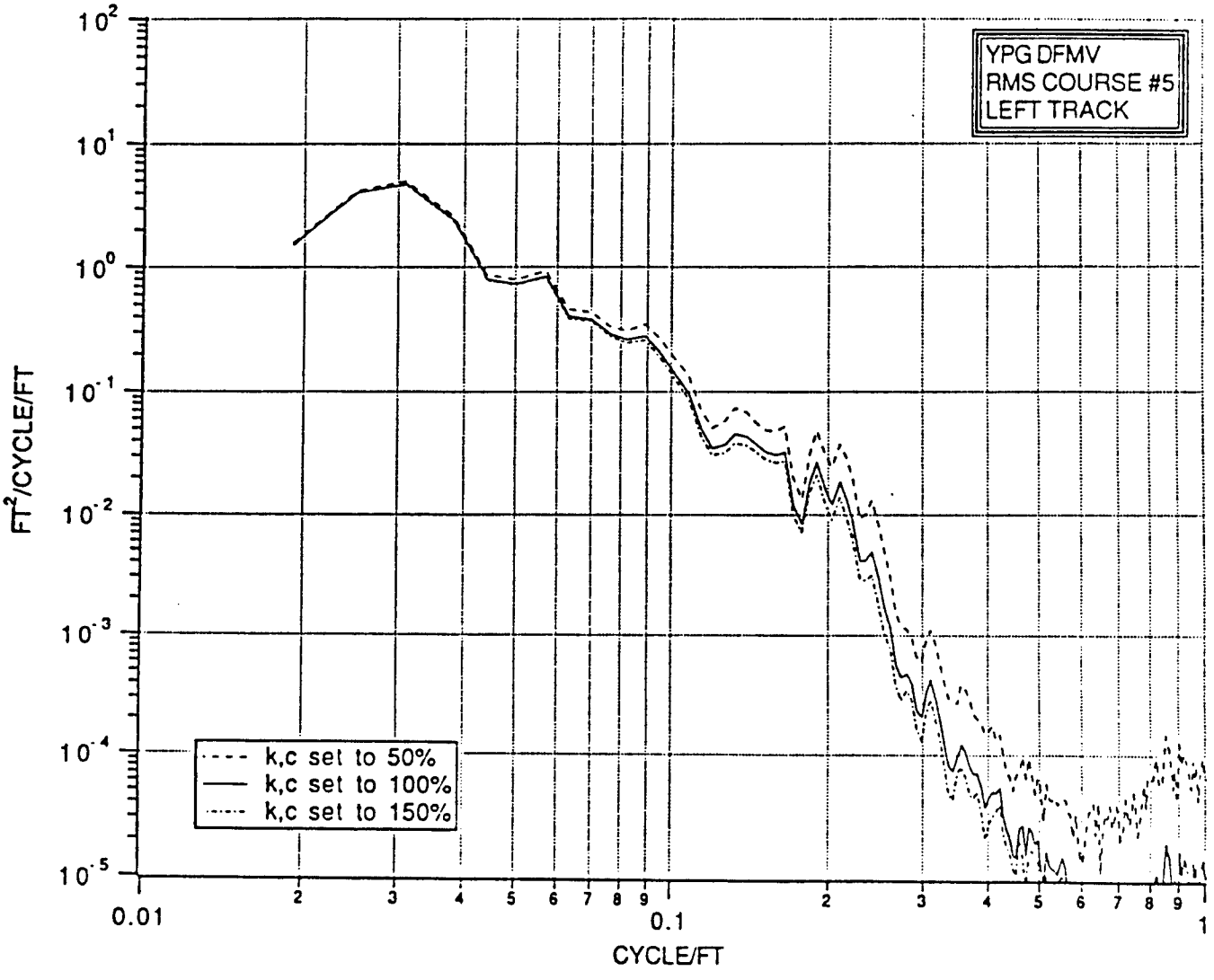

Figure 13. Wave-Number Spectrum for RMS Test Course No. 5 Computed With Variations of Tire Parameter Values in Analytical Model, DFMV Speed = 6 MPH, Left Front Tire

10.4 Computation of Coherence Functions

Spatial coherence functions and their associated phase angles were computed using Equation (19) between two pairs of wheels on the DFMV, as follows:

1. Left-front wheel to left-rear wheel (labeled "LF TO LR")
2. Left-front wheel to right-front wheel (labeled "LF TO RF")

The computed coherence and phase functions are presented in Appendix G.

As discussed earlier in Section 7.1, Item 2, the coherence function between the front and rear wheel on the same side of the vehicle should ideally be unity, assuming the vehicle moves in a straight line, and the front wheel does not cause significant soil deformation. This makes the front-to-rear wheel coherence function computed during each test a powerful measure of the signal-to-noise ratio and general accuracy of the measured terrain profile. Coherence plots between the front-to-rear wheels on the same side of the DFMV and left-to-right across an axle always vary with wave number, with the value of perfect unity applying to very low wave numbers (profiles show high correlation when considering long wavelengths such as large hills, where wave numbers are less than 0.01 ft^{-1}). It is also expected that the coherence at very high wave numbers is zero, due to the short wavelengths being uncorrelated and the tire filtering properties of the DFMV. Over the range of wave numbers to which a vehicle responds, the coherence lies between these two values [3, p. 22]. When comparing wave numbers between 0.01 and 0.1 ft^{-1}, a coherence value of 0.7 or better is good and below 0.4 indicates measurement limitations (as a general rule). Between 0.1 and 1 ft^{-1}, the coherence is expected to fall, with increasing scatter shown in the plots. Again this is due to the properties of the short wavelengths in the road and the fact that the spectral density of terrain elevation tends to fall rapidly with increasing wave number (potentially approaching the noise level of the measurement system). Therefore, between 0.1 and 1 ft^{-1}, the user has to know the characteristics of their system (e.g., background instrumentation noise) and have a feel for expected roll-off and scatter in the plots.

Additional tire/ground interactions that cause the coherence to drop between 0.1 and 1 ft^{-1} are (1) tire filtering, (2) powered rear wheel versus an unpowered front wheel (potential differences in wheel slip), and (3) slight steering inputs even though the vehicle is traveling straight. If a wheel leaves the ground during profiling, this will also be identified through poor coherence.

As shown in Appendix G, the DFMV front-to-rear coherence diminishes at the lower wave numbers, and generally drops below 0.7. This is due to the accelerometer noise that becomes dominant in the wave-number spectra computed from data signals measured at the relatively low speeds used for the YPG tests. Again, the measurement at low wave numbers will not be a problem with the future use of a piezoresistive accelerometer. For the purposes of this report, the low wave number where the drop-off in coherence occurs can be directly interpreted as the lower limit for valid spectral data. This was the basis for establishing the lower wave-number limit for the spectra presented in Appendix D.

There are additional locations in the coherence plots where the coherence value is expected to fall. For example, if the profile tire is out of balance or has high force variations, the coherence will be zero at a wave number equal to the circumference of the tire and all harmonics of that wave number. This is because at higher speeds (speeds greater than that used at YPG), tire force variations appear as sharp spikes in the wave-number spectrum. Another example is a terrain with roll inputs. The left-to-right coherence will go to zero when roll is present between the left- and right-wheelpaths.

11.0 EVALUATION OF RESULTS AND DISCUSSION

Four matters are of interest in the evaluation of the DFMV data, as follows:

1. Validation of the DFMV measurement procedure by direct comparisons of the DFMV generated elevation profiles with those measured by the rod and level procedure.

2. Validation of the DFMV measurement procedure by direct comparisons of the DFMV generated elevation wave-number spectra with those computed from the profiles measured by the rod and level procedure.

3. Comparisons of the spatial coherence functions between left and right wheels measured by the DFMV with those determined from the rod and level procedure and the interpretation of these coherence functions.

4. Interpretation of the DFMV data from the viewpoint of defining a measure of "roughness" for the test courses and general terrain.

11.1 Evaluation Of Profile Results

The elevation profiles computed by the DFMV in Appendix B include no grade information and, hence, must be compared to the rod and level elevation profiles in Appendix A, in terms of their dynamic components only. To facilitate a direct comparison, the rod and level profile for RMS Course No. 5 was detrended and replotted with the grade removed. A direct comparison of these results with the elevation profile computed from the DFMV data is shown in Figure 14. Note that the agreement between the rod and level and the DFMV results is good. In particular the indicated elevation of the humps are similar. The slight discrepancies in the location of some humps can be attributed to speed variations of the DFMV over the test course, or to position variations in the rod measurements (as discussed in Section 11.2, rod measurements were erroneously displaced as much as 12 feet between the left- and right-wheel paths on RMS #5 on the data initially submitted by WES. Corrected data was supplied and is replotted in Appendix K). Referring to Section 7.2, DFMV speed errors of this type can be eliminated when the appropriate software is implemented to drive the DFMV data acquisition analog-to-digital converter with the optical encoder signal from the vehicle wheel, rather than a clock.

Recall that wavelengths less than three feet will be underestimated in the elevation versus distance plots unless the wave-number spectra are corrected by the tire filtering relation shown in Figure 5. This will apply to the analysis of all courses except the RMS courses (where the longer wavelengths were the primary input). For the objectives of this study, the question has to be asked, "What is the true elevation versus distance profile to input into the M1025 HMMWV model?" Does the DADS tire model account for footprint filtering and, and if so, is the $[\sin(\pi n/n_c)/(\pi n/n_c)]^2$ function used? Does the DADS model account for force variations in the tire? Again, this supports the use of a tire transfer function as the required input to the M1025 HMMWV model to account for the true high-frequency road inputs.

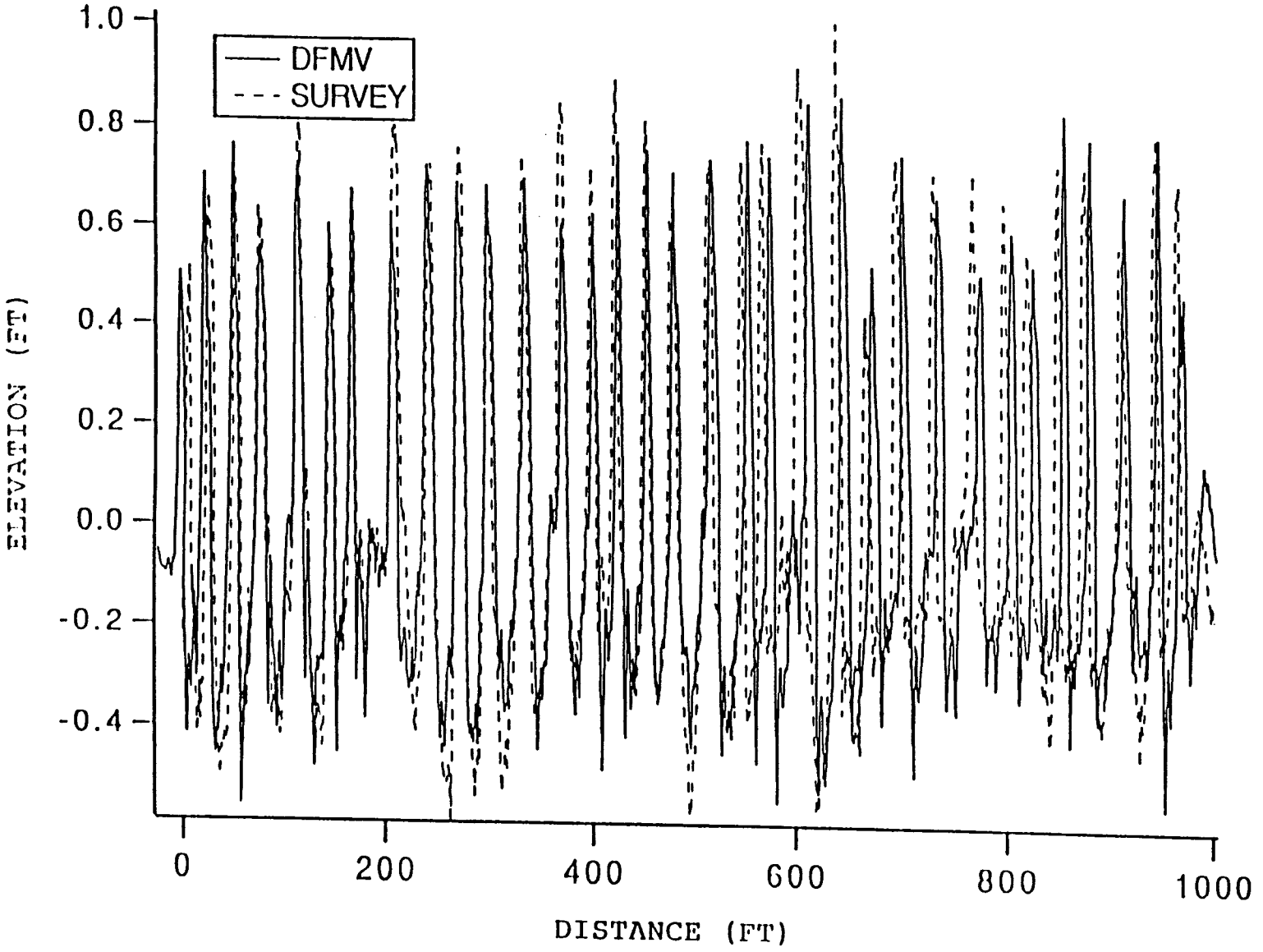

Figure 14. Profile Elevation for RMS Test Course No. 5 Computed from DFMV and Rod Data, DFMV Speed=6 MPH, Left Front Tire

Appendix A, p. 98 shows the data for the WES test course analysis. The data for the Truck Hill courses shows that the grades in the profiles severely biased the WES RMS calculations and indicated a roughness much greater than actually existed. This is confirmed by the Truck Hill #1 course value versus those for the other three Truck Hill courses. Specifically, Truck Hill #1 had an average RMS value of 0.2 inches and was relatively flat. Truck Hill courses #2, #3 and #4 had large grade changes over the length of the course (approximately 10 percent) and had average RMS values of 0.8, 1.5 and 1.0 inches, respectively. Once detrended, the overall roughness of these three Truck Hill courses was closer to that of Truck Hill #1 (or approximately 0.3 - 0.6 inches RMS).

It should be noted that for programs such as the NATO Reference Mobility Model (NRMM), the RMS of the course is easily calculated from the area under the wave-number spectrum curve. Integrating the wave-number spectrum over the frequency range (the area under the curve between set integration limits) yields ft^2. Taking the square root and converting to inches yields "inches RMS," theoretically the same value calculated via the traditional WES RMS program. However, as discussed in Section 4.0, the WES RMS filter does not have a sharp cut-off and filter leakage may remove shorter wavelength components. In addition, the WES RMS filter has detrending limitations, due to the way it attenuates longer wavelengths. A wave-number spectrum presentation of the data allows for efficient filtering, where the filter is unity in the pass-band and zero in the stop-band; however, the user has to define the integration limits. For example, if the user applies a 60-foot cut-off to the spectrum, 60-foot wavelengths are included, but 61-foot wavelengths are not. Defined integration limits without leakage will eliminate the discrepancy in the RMS calculation for the Truck Hill courses. In addition, it is proposed that integration limits between 0.01 and 1 ft^{-1} (100' and 1' wavelengths) be used for a vehicle similar to the HMMWV.

11.2 Evaluation of Spectral Results

The wave-number spectra for the RMS test courses generally provide the best agreement between the DFMV data and the rod data, undoubtedly because they have the most severe roughness characteristics producing the best signal-to-noise ratio in the DFMV and rod measurements. A direct comparison of the results for RMS Test Course No. 5 are shown in Figure 15. A half power point area under the curve calculation would reveal that the two curves in Figure 15 are the same.

Referring to Figure 15, it is seen that there is good agreement between the spectra produced by the DFMV and the rod data, except above a wave number of about $n = 0.3$ ft^{-1}, where the spectral values for the DFMV data fall rapidly relative to the rod data. This difference at the higher wave numbers is anticipated for all the spectral comparisons between the DFMV and rod data because the spectral values are lower for the DFMV data, and too high for the rod data, for the following reasons:

1. The spectral values for the DFMV data are reduced at the higher wave numbers due to the low-pass filtering effect of the tire footprint (see Section 7.2 and Figure 5).

2. The spectral values for the rod data are increased at the higher wave numbers due to the aliasing of power about the Nyquist wave number of $n_h = 1.0$ ft^{-1}, and possible measurement noise (see Section 9.2).

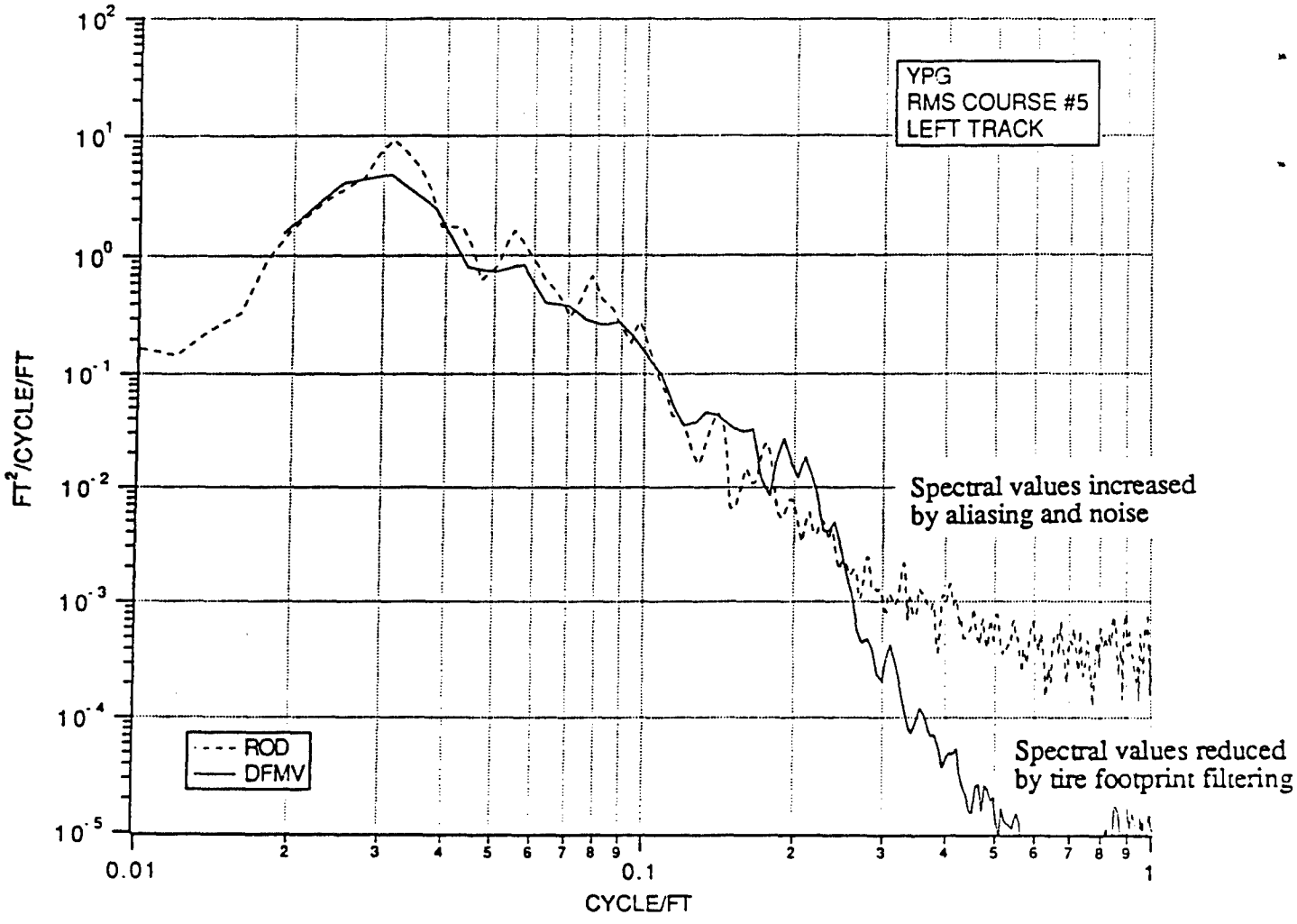

Figure 15. Wave-Number Spectrum for RMS Test Course No. 5 Computed from DFMV and Rod Data - Resolution D = 0.0039 ft^{-1}, DFMV Speed=6 MPH, Left Front Tire

The DFMV methodology strives to measure the terrain accurately and provide data that best meets the analysis requirements of the profiling effort. The tire filter relation shown in Figure 5 is always a direct discrepancy to rod and level data. Since the HMMWV was used as the reference vehicle for this study, the tire size chosen for the profile efforts was that of the HMMWV. Therefore, the DFMV profile is precise for the HMMWV vehicle. From the viewpoint of the influence of the terrain roughness on the vehicle dynamics, the DFMV wave-number spectra are more meaningful than the rod and level data, because of the tire filtering relation (see Section 7.2, Item 1). Note: if the user had a tire model that accurately accounted for tire filtering, the DFMV spectrum would be corrected through the filter relation given in Figure 5.

There is another significant difference between the wave-number spectra computed from the DFMV and the rod data for RMS Test Course No. 2 which was typified by negative bumps put into the course with a grader blade. Specifically, the DFMV spectra reveal higher values than the rod data spectra at $n = 0.22$ ft^{-1}, as illustrated in Figure 16. From Table 4, the vehicle speed for this test averaged V = 6.9 MPH (10 ft/sec). Dividing $n = 0.22$ ft^{-1} by V = 10 ft/sec gives a frequency of 2.2 Hz, which corresponds to the natural frequency of the HMMWV tire. As detailed in Section 7, the accuracy of the DFMV profiling procedure is dependent on a rather simple linear model for the tire dynamics. It is hypothesized that the model (see Figure 3) fails to account for the probable nonlinear response characteristics of the tire to the severe impact of the negative bumps on RMS Test Course No. 2 at that speed. This is supported by the observation that the higher values at $n = 0.22$ ft^{-1} are not present at the 2 MPH run. If discrete obstacles are to be profiled by the DFMV, it is recommended that the lowest speed possible be used. A further improvement to profiling courses with multiple discrete obstacles that potentially excite the resonance of the tire would be to develop a true tire-to-axle transfer function, replacing the linear values for k, the spring rate and c, the damping rate. This would eliminate some of the differences identified as tire nonlinearities. A true tire-to-axle transfer function would replace the two frequency response functions given in Equation 5 and enhance the signal processing of the DFMV data. This transfer function would be unique to the profile tire and several curves could be generated to account for different tire deflections. The development of this transfer function is a laboratory procedure involving a shaker at the axle and the air bearing plate used to calibrate the DFMV.

It should be noted that RMS Course #2 is not a "true" RMS test course but is rather a series of discrete events. This is confirmed by the wave-number spectra in Figure 16 and Appendix C, p. 129 and 130. Note that the spectra are flat between 0.0167 and 0.125 ft^{-1}, meaning that all the bumps between 8 feet and 60 feet apart have the same amplitude (either height or depth). In accordance with what NATC perceives a "true" RMS course to be, the spectrum should have a slope of approximately n^{-2} to n^{-3} between wave numbers of 0.0167 and 1 ft^{-1} (60- to 1-foot wavelengths) for a short wheel-based vehicle (i.e., WES would use a 60' RMS filter in the analysis of the HMMWV) [14]. In ride analysis work, pioneered by WES, discrete obstacles are handled in a different manner than are random terrain or sinusoidal events (RMS courses), therefore, RMS course #2 should be analyzed as a discrete event course.

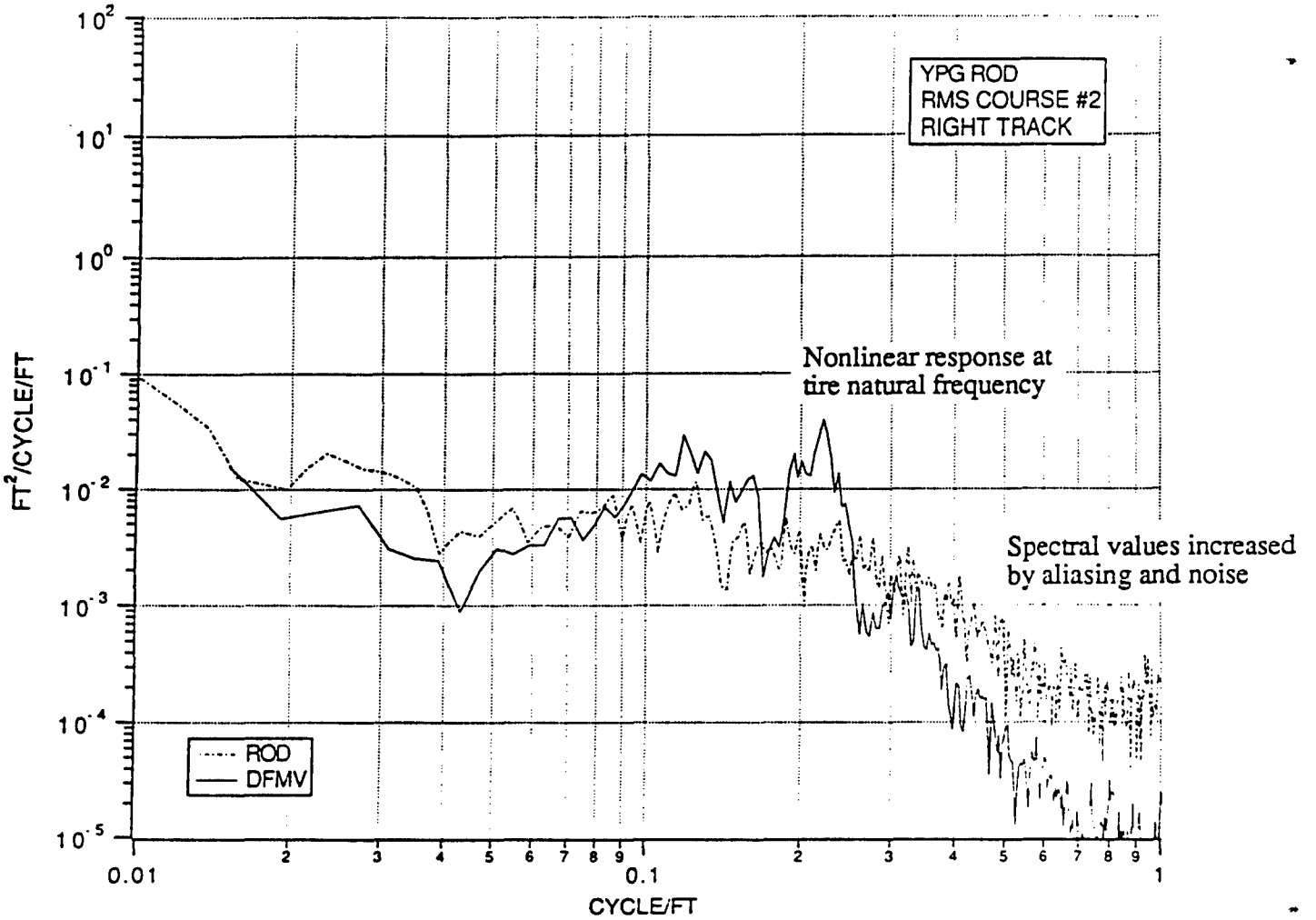

Figure 16. Wave-Number Spectrum for RMS Test Course No. 2 Computed from DFMV and Rod Data - Resolution D = 0.0039 ft^{-1}, DFMV Speed=6 MPH, Right Front Tire

The comparisons of the wave-number spectra computed from the DFMV and rod data for the other test courses are mixed, with the agreement varying from good (below n = 0.3 ft^{-1}) for Middle East Test Course No. 1, to poor for Truck Hill Test Course No. 2. A comparison of the spectra from the DFMV versus the rod data for Truck Hill Course No. 2 is shown in Figure 17. Note that the spectra computed from the DFMV data are about a half-decade lower than the values computed from the rod data. From the DFMV data, the RMS value of the elevation variations about the grade on Truck Hill Course No. 2 are less than 0.01 ft, which is the resolution of the rod and level procedure. Referring back to Section 9.2, it is believed likely that the dynamic portion of the rod data is dominated by round-off errors, causing the spectral values to be too high. This supposition is supported by the coherence measurement between the two tracks for the rod data in Appendix F. Specifically, coherence functions for turbulence phenomena, such as terrain roughness, should approach unity as the wave number approaches zero (as the wavelength approaches infinity). This anticipated result is observed in coherence functions computed from the rod data for most of the more severe test courses (RMS Course No. 5 is an unexpected exception to be discussed shortly). For Truck Hill Course No. 2, however, the coherence values in Appendix F are small even at the lowest wave number of n = 0.01 ft^{-1} (Figure 19). Hence, it is believed that the discrepancies between the wave-number spectra for the DFMV and rod data measured on the Truck Hill Course No. 2 is due to an inadequate signal-to-noise in the rod data. This indicates that the rod and level is not adequate for wave-number spectra calculations where a smooth surface overlays a grade of approximately 5 to 10 percent with the resolution used in this study (0.01 feet). Table 5 was excerpted from a draft ASTM standard for measuring road roughness by the rod and level method and references [3, 8, 11]. The proposed standard also suggests using a bubble level to keep rod perpendicular to ground. Rod tilt errors can be a source of error in the rod and level measurement procedure [11], and significant rod tilt was observed at YPG.

Table 5. Rod and Level Required Precision

General Roughness Category	Rod and Level Required Precision (Inches)	
	Class 1*	Class 2**
Airport runways	0.005	0.01
New pavements	0.01	0.02
Older pavements	0.02	0.04
Maintained unpaved roads†	0.04	0.08
Damaged pavements	0.06	0.12
Rough unpaved roads‡	0.08	0.16
Used for measurements at YPG	0.12	

† Representative of the Truck Hill courses
‡ Representative of the RMS and Middle East courses
* Class 1 - reduces the measurement to less than 2%
** Class 2 - reduces the measurement to less than 5%

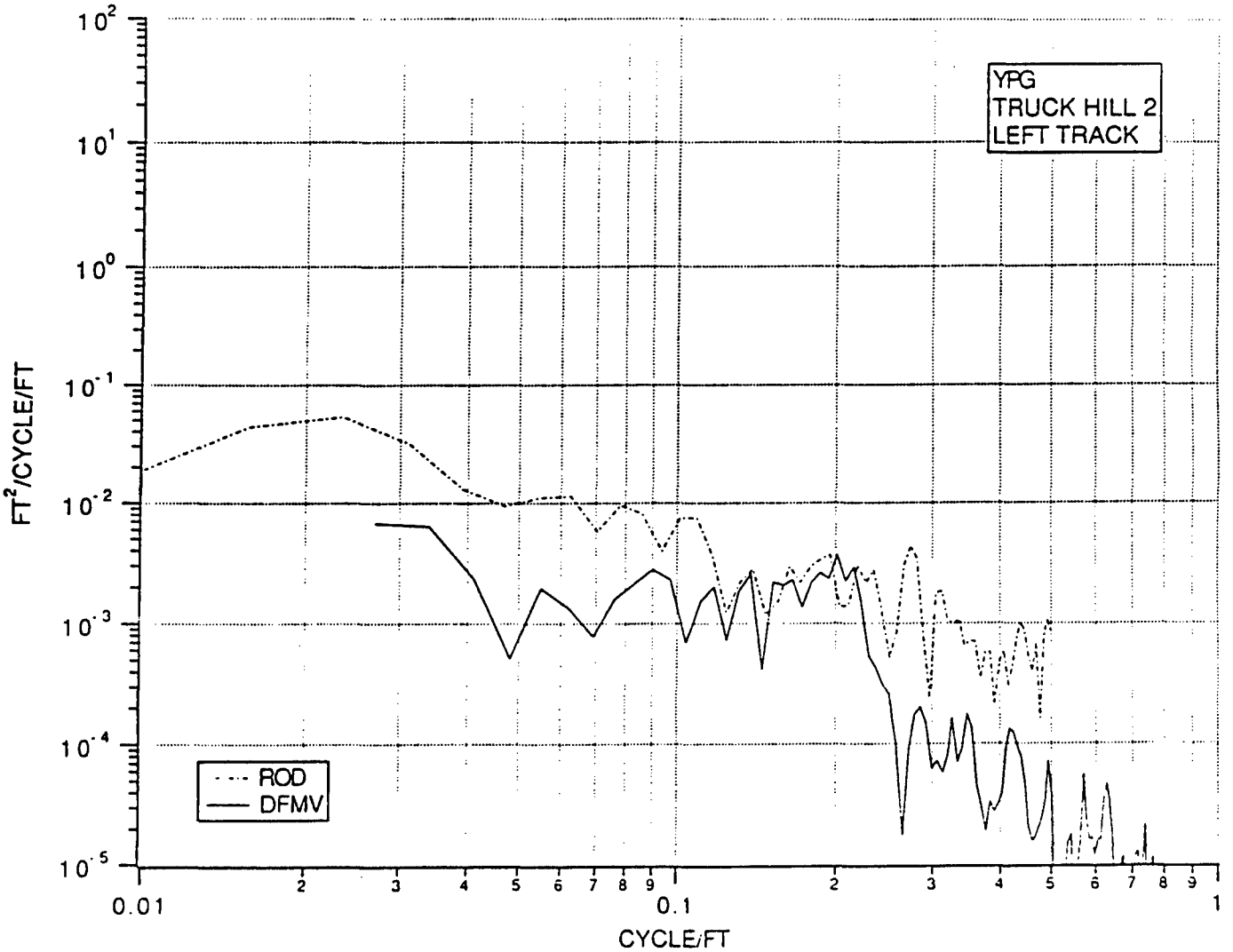

Figure 17. Wave-Number Spectrum for Truck Hill Course No. 2 Computed from DFMV and Rod Data - Resolution D = 0.0039 ft^{-1}, DFMV Speed=10 MPH, Left Front Tire

As a final point of discrepancy, RMS Test Course No. 5 for the original rod data reveals a poor coherence at the lower wave numbers, even though it is one of the more severe test courses with systematic bumps that should produce a very strong coherence at the lower wave numbers (Appendix F). To evaluate this result (because it was not present on the other RMS courses), the two initially supplied profiles for RMS Test Course No. 5 produced by the two tracks of rod data were overlaid and found to have major discrepancies (up to 12.5 ft) in the location of the bumps in the middle third of the test course. Since the two rod profiling tracks are only 6.25 ft apart on the RMS test courses, and since the bumps are nominally perpendicular to the profiling path, it appears a distance measurement error was made in the profiling of this course. It is critical to the modeling analysis that the left- and right-wheel paths stay aligned over the length of the course. (Note: After NATC identified this discrepancy, WES supplied corrected data. The corrected elevation versus distance and coherence plots are shown in Appendix K.)

11.3 Evaluation of Coherence Results

Coherence (normalized cross-spectral density) functions were computed from the DFMV data between the front and rear wheels to identify the signal-to-noise ratio and general accuracy of the DFMV measurements (see Section 10.4), but otherwise these front-to-rear coherence values are of no interest. On the other hand, the coherence functions between the left and right wheels are of interest, since they identify the spatial correlation of the input loads to the vehicle from the left and right wheels. This information is needed to define the total response of the vehicle, including the response to torsional loads. As discussed in Section 10.4, all spatial coherence functions must approach unity as the wave number approaches zero; i.e., the left-to-right spatial coherence for any separation distance must be unity for an infinite wavelength. Similarly, the spatial coherence at any wave number must approach unity as the wheel (track) separation distance approaches zero. The wave number where the coherence falls off in value for any given track separation distance essentially defines a "scale" for the terrain roughness; the wave number where torsional loads to the vehicle become relevant. For terrain that has isotropic roughness characteristics (a similar spatial coherence functions in all directions), the coherence function between the left and right wheels can be computed from a single elevation profile measurement at one wheel [9]. Many of the YPG test courses, however, are clearly nonisotropic; e.g., the Middle East #2 course. Hence, the spatial coherence between the left-to-right wheels must be measured using data from the two wheels.

From the rod data, which represent a track separation distance of 6.3 ft, RMS Test Course No. 2 yielded coherence values near unity to the highest wave number, namely, about 0.1 ft^{-1}. The coherence data for RMS Test Course No. 2 produced by the rod data are compared directly to the DFMV data in Figure 18. Since the track separation distances for the DFMV and rod data are similar (6 ft versus 6.3 ft), these results are directly comparable. From Figure 18, it is seen that the coherence values for the DFMV data drop at the lower wave numbers due to the accelerometer noise problem detailed in Section 7.2, Item 3, and again drop around the wave number of $n \approx 0.5$ ft-1 due to the footprint filtering detailed in Section 7.2, Item 1. The rod and level coherence starts to drop at the higher wave numbers due to the vertical measurement resolution. Given these known reasons for loss of coherence, the trend of the coherence results for RMS Course #2 are similar (recall from Section 10.4 that a coherence of 0.7 is acceptable). The coherence functions for the Middle East and Truck Hill test course drop off at smaller wave numbers in a manner similar to that measured in [Reference 9]. In some cases (e.g., Truck Hill Course No. 2), the coherence values computed from the rod data are low at all wave numbers due to resolution errors in the rod measurements (see Section 11.2 and Figure 19).

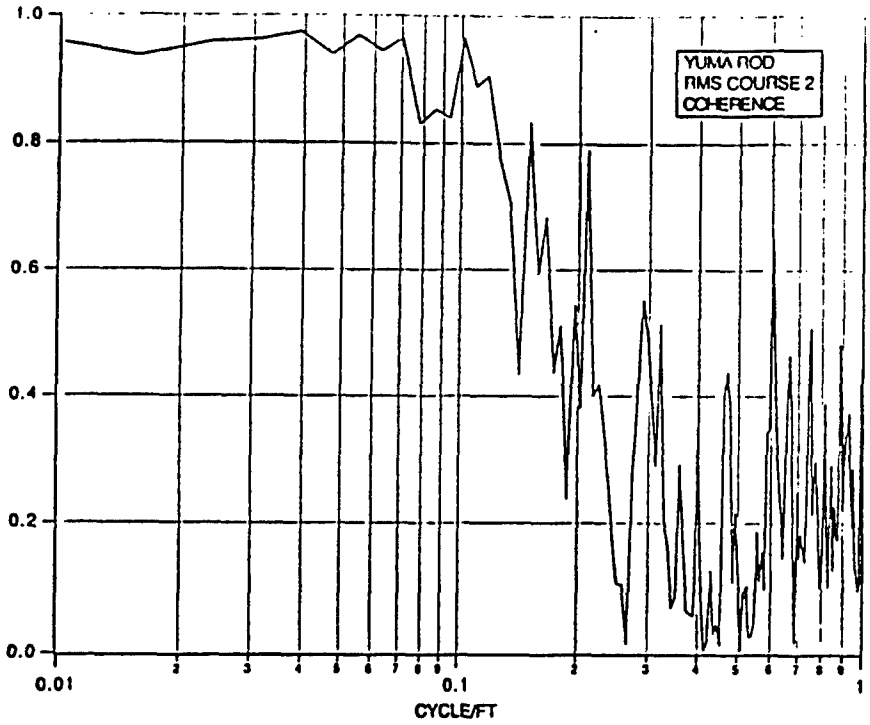

Rod and Level

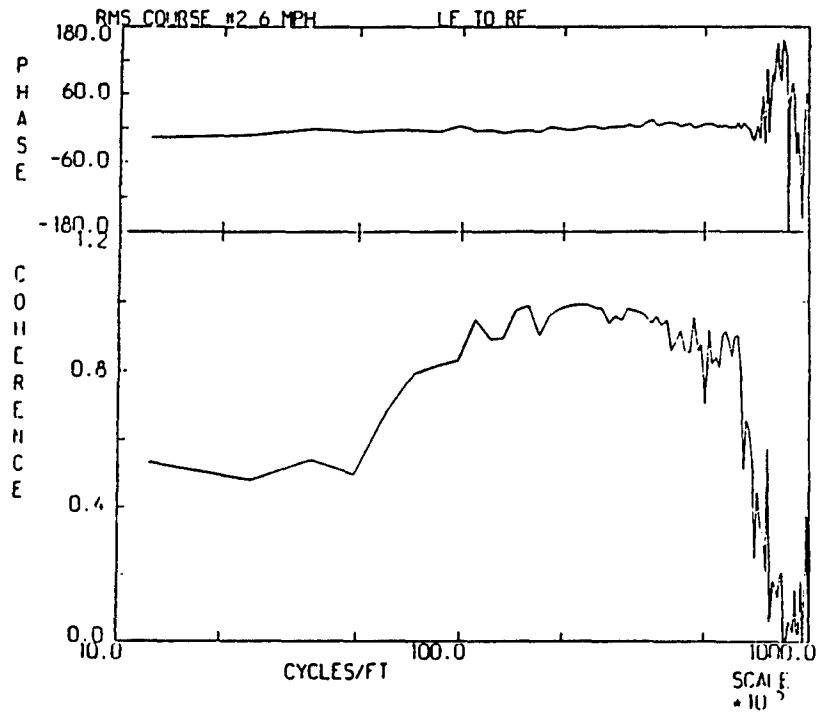

DFMV

Figure 18. Coherence Functions for RMS Course No. 2 Computed from DFMV and Rod Data, DFMV Speed= 6 MPH, Left-Front to Right-Front Coherence

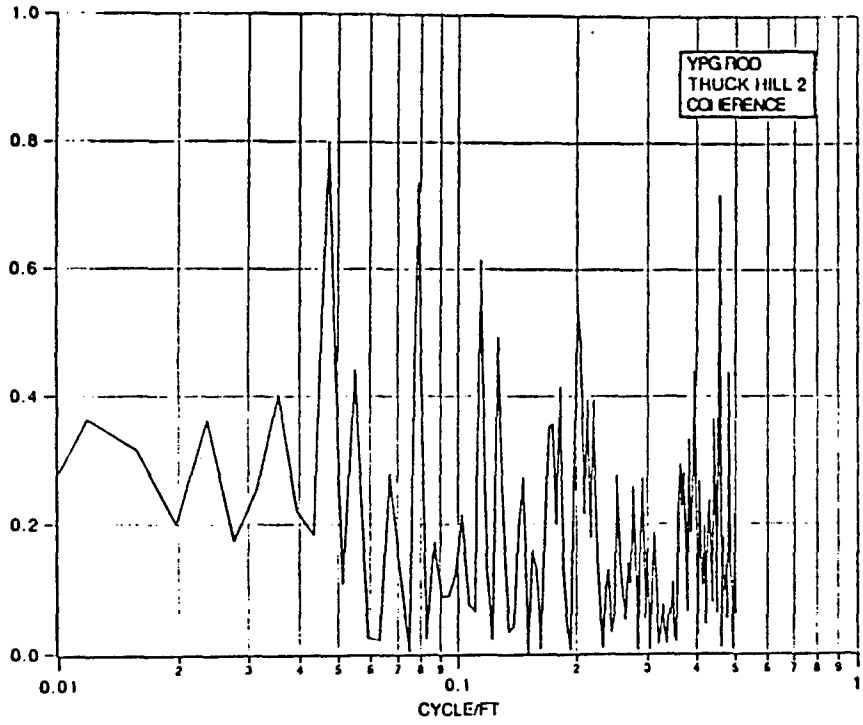

Rod and Level

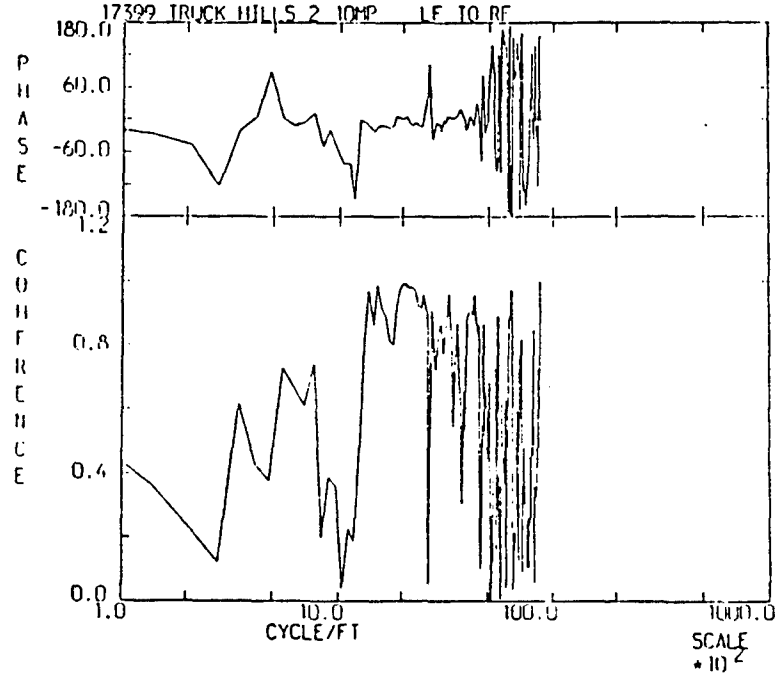

DFMV

Figure 19. Coherence Functions for Truck Hill No. 2 Computed from DFMV and Rod Data, DFMV Speed= 10 MPH, Left-Front to Right-Front Coherence

In three-dimensional model development, the coherence phase information is invaluable. For example, the M1025 HMMWV model with the left and right inputs from the original rod data for RMS #5 will show the HMMWV going over 1 foot high bumps aligned at various angles (0 to 63°) to the direction of travel. In actuality, the bumps on RMS #5 were always perpendicular to vehicle traffic and little roll input was present (as shown in the phase plot in Appendix G, p. 208). As discussed in Section 11.2, even slight alignment errors of this type in the rod data will produce significant response differences in the model of the M1025 HMMWV. With the DFMV, this alignment problem could never occur. If such differences exist, it indicates vehicle roll, which can be easily detected and modeled through the coherence phase plot. The coherence phase plot for RMS #5 shows that both wheel tracks are in-phase over the entire spectrum range (Appendix G, p. 208). (Note: After NATC identified the alignment discrepancy on RMS #5, WES supplied corrected data. The corrected elevation versus distance and coherence plots are shown in Appendix K. Its reference was left in the report to stress the importance of coherence and phase plots accompanying a profile.)

A specific example of roll input to the M1025 HMMWV model is the Middle East #2 course, where the washes were at a diagonal to the direction of vehicle traffic. The coherence phase data shows that the left-to-right wheel paths were 90° out of phase for wavelengths of approximately 10 foot (this could be calculated to a distance through the wheel-track spacing on the DFMV). This indicates that the phase information between the left- and right-wheel paths is required to predict roll inputs into a vehicle (a three-dimensional vehicle model) and that without this phase information, the modeler knows nothing about the correlation between the left- and right-wheel paths (Appendix G, p. 216).

In summary, the coherence plots are often the last information plotted. However, these are a useful tool for assessing the quality of a given profile, whether with the DFMV, an inertial profilometer or the rod and level. In future programs, it is recommended that coherence and coherence phase plots accompany all WES and APG profiles. Their interpretation is valuable to understanding wave number representations of test course and road roughness from any profilometer system.

11.4 Scaling of Coherence Function

The track widths between the APG profilometer, the WES rod and level, and the NATC DFMV were different, as shown in Table 6. (Since the HMMWV was the reference vehicle, the DFMV was configured to provide a similar track width to the HMMWV.) As a result, the left-to-right coherence functions between the three systems are not directly comparable in their current presentation. In addition, if the DFMV was used to profile a torsional-type course for a model of a vehicle with a wider wheel track, the left-to-right coherence functions would have to be adjusted to account for the differences in track separation distances. This is also very applicable to a track vehicle, which would have a different track width than the DFMV. An investigation of this matter suggests that the Strouhal number, which is widely used to scale turbulence phenomena of various types [12] should be applicable to this problem as well, assuming that there are no ruts in the road or test-course surface.

Table 6. Summary of Track Widths Between the Three Systems

Course	WES Rod and Level ft	DFMV ft	HMMWV ft	APG profilometer ft
RMS (2-5)	6.3	6	6	4
Washboard	5	6	6	4
Middle East #1&2	5	6	6	4
Truck Hills (1-4)	5	6	6	4

For cross-correlation and cross-spectra functions, including coherence functions, the Strouhal number is defined for wave numbers as:

$$S=nL \tag{23}$$

where, n=wave number in cycles/foot and L=separation distance in feet. The Strouhal number is technically dimensionless, although it can be interpreted as having the units of cycles. In regards to the coherence functions between tracks of terrain roughness, a scaling on Strouhal number means the coherence between the two tracks is really a function of the number of cycles between the two tracks. Hence, it is recommended that coherence data in the future be presented as a function of Strouhal number (the product of wave number and track separation distance).

11.5 Interpretations for Roughness Index

For the RMS test courses and the Washboard course, which have systematic bumps that cause a peak in the wave-number spectrum, the current U.S. Army procedure of defining roughness in terms of an RMS value is reasonable (as long as the distance between the bumps is also stated), since the test courses are all similar except for the height or depth of the bumps and their spacing. However, a better procedure might be to specify roughness in terms of a maximum spectral density value at the wave number corresponding to the average separation distance between the bumps on the wave-number spectrum. From the DFMV and rod data, these values at the time of the measurements are as shown in Table 7.

Table 7. Proposed Test Course Severity Index for Courses with Systematic Bumps

Course	Average Spectral Value, ft^2/cycle/ft	Wave Number, cycle/ft (ft^{-1})
Washboard	5×10^{-3} †	0.33
RMS #2	5×10^{-3}	0.0167 - 0.125‡
RMS #3	2×10^{-1}	0.01 - 0.085‡
RMS #4	1.2	0.027
RMS #5	6	0.033

† Taken from rod and level data because the DFMV tire filter attenuated the amplitude
‡ A range is given because the spectra indicated that all the bumps were the same height

However, as noted in this report, this methodology cannot be used consistently on the standard durability courses due to the randomness of the input and the fact that the roughness of the courses is not uniform across a lateral profile. For the other test courses profiled in this exercise (and all courses random in nature), an assessment of roughness in terms of RMS values is not meaningful. Here, it is believed the procedure recommended by Dodds and Robson [9] for assessing road roughness might be more effective. Assume the wave-number spectrum for the test course can be approximated by a straight line on a log-log plot (Dodds and Robson use two lines, but that is not considered warranted here), such that

$$G_{XX}(n) \sim G_{XX}(n_o) \left(\frac{n}{n_o}\right)^{-w} \tag{24}$$

where

$G_{XX}(n)$ = wave number PSD of the road elevation in ft^2/cycle/ft
n = wave number in ft^{-1}
$G_{XX}(n_o)$ = wave number PSD of road at wave number $n_o = \frac{1}{2\pi}$ cycles/m ≈ 0.05 ft^{-1}
w = constant

The reason for normalizing the equation to 0.05 ft^{-1} (20 foot wavelength) is because rod and level data is typically aliased at 1 ft^{-1} (1 foot wavelength) and the DFMV data is at a maximum attenuation due to tire filtering at 1 ft^{-1}.

The wave-number spectra computed from the DFMV data for the Middle East and the Truck Hill test courses were interpreted in this fashion to obtain the results shown in Table 8.

Table 8. Proposed Test Course Severity Index for Test Courses Without Systematic Bumps

Course	$G_{XX}(n_o)^{\dagger}$, ft^2/cycle/ft	w
Middle East #1 and 2	5×10^{-5}	3.4
Truck Hill #1	1×10^{-4}	1.0
Truck Hill #2, 3, and 4	1×10^{-4}	2.0

† $n_o = 0.05$ ft^{-1}

12.0 CONCLUSIONS

The DFMV was used to develop wave-number spectra of the courses used in this evaluation. A wave-number spectra is nothing more than a frequency-domain representation of an elevation versus distance profile typically generated with a rod and level, however, wave-number spectra offer a complete picture of the course roughness. If the test vehicle tires are used on the DFMV, the wave-number spectra measurement is the true input to the test vehicle.

The primary concern with using wave-number spectra descriptions, of course, is ensuring that the course measurement is not a function of the vehicle response or otherwise affected by the vehicle doing the measuring. This report expands on the use of the DFMV as a profilometer, the advantages it has over profile devices, and explains why the profile measurement is independent of the vehicle dynamics. In addition, this report expands on signal processing considerations and limitations associated with the calculation of wave-number spectra from the DFMV and rod and level data.

For the Army's use in specifying and monitoring road roughness, wave-number spectra offer the following advantages:

1. **Direct measurement of the course that contains both amplitude and frequency data.**

   Mission profiles of vehicles can be easily specified in government contract specifications. For example, an average spectra for 30 percent highway, 30 percent secondary, and 40 percent cross-country (level and hilly) could be specified in as few as 4 curves. This would eliminate the use of generic test course titles or RMS values to describe the course roughness. Because the operating environment is known, the vehicle manufacturer could design the vehicle to a warranty specified by the Army.

2. **Once understood, wave-number spectra are easily used for monitoring test-course roughness.**

   Wave-number spectra are less confusing than other presentations found in the literature, especially wave-number spectra in the slope domain [3]. Wave-number spectra can easily be used for monitoring test course severity. Based on a course tolerance for wheeled- or tracked-vehicle traffic, course maintenance can be performed to bring the course back to a base line.

3. **Wave-number spectra have a historical precedence.**

Published literature in 1962 used wave-number spectra to analyze the ride dynamics of vehicles traveling over a road with a known profile.

4. **Easier to use in dynamic modeling.**

The profile data can be used as wave-number spectra (frequency-domain input) or converted to elevation versus distance plots, elevation versus time plots, acceleration PSD plots, acceleration versus distance plots or acceleration versus time plots. Through a tire transfer function, the wave-number spectra could be converted to acceleration versus time inputs at the spindle or hub.

5. **Directly useable in current accelerated life scaling.**

Data presented in a wave-number spectrum format allows equivalence studies between different test environments. Equivalence techniques could be employed to compare a 20,000 mile durability test to the YPG durability test environment. The next step is to apply scaling techniques to the accelerated life cycle requirements of the new MIL-STD-1784(A). A complex service environment (Figure 2) at different speeds can be collapsed to one spectrum at one speed. That spectrum can be scaled to a test course spectrum at a given speed to determine the number of miles required to input the same energy. Given the sinusoidal S/N curves for the different material types on the vehicle, a complex service environment can be accurately accelerated.

6. **Represent the input to the tire in vehicle evaluations.**

Because the wave-number spectra can be easily converted to an acceleration PSDs at the tire/ground interface, it can be used as an input to vehicle evaluations and then compared to different acceleration PSD outputs on the vehicle. Response ratios between the input and output can be calculated.

7. **Easily identifies washboard-type phenomenons.**

Wave-number spectra are able to identify and measure such terrain properties as washboard and highway corrugations. These are very destructive inputs to the vehicle and accurate measurement is critical to representative vehicle durability testing.

8. **Presentation of road roughness is independent of profile speed.**

9. **DFMV is a robust measurement technique.**

It is shown that the DFMV methodology used to calculate wave-number spectra offers a robust measurement technique. The resulting profile is driven by the force and acceleration inputs from the road surface. A sensitivity study on the three tire inputs (k, c and m) showed little change in the spectra with changes of k, c and m of up to 50 percent. Although NATC has accurate measurements of k, c and m, it is reassuring that missing their values does not significantly effect the road spectra.

Another robust feature of this methodology is that the effects of the signal-to-noise ratio of the recording system are understood and can be quantified in the analysis. In all profiles measured, the DFMV signal to noise was better than the rod and level and APG inertial profilometer. This is because the sensitivity of the instrumentation can be set to measure inputs with very low forces and accelerations. In addition, any tire harmonics can be quantified and removed from the wave-number analysis through interpolation. For the profiling at YPG, speeds were below 10 MPH, so the removal of tire harmonics was not required. However, their removal would be required for highway profiling at a speed of 55 MPH .

13.0 RECOMMENDATIONS

Based on the results of this study, the DFMV methodology is an accurate and established profile technique which can be used to measure and monitor test course severity. Further, the terrain data generated can be input into dynamic vehicle computer models, either in a time- or frequency-domain format. Finally, the methodology presented in this report can be utilized in vehicle evaluations to establish pass-fail criteria for U.S. Army acquisitions. It is recommended that steps be taken to integrate this methodology into the durability test standards and into system acquisition requirements.

Recommendations 1 and 4 are immediate applications for wave-number spectrum of road surfaces beyond the course monitoring and model input objectives of this study.

1. One of the advantages of the DFMV methodology over the other methodologies explored is the fact that the technique accounts for terrain deformability. None of the courses profiled at YPG adequately addressed deformable soils, by test design (all courses profiled at YPG were purposely chosen because of their nondeformability). It is recommended that the impedance of the course surface be investigated through an additional study. This is particularly important in the evaluation of the APG test courses which experience greater seasonal changes due to moisture than do the courses at YPG.

2. Beyond using the DFMV as a course measurement and monitoring tool, and as a measurement device for generating road inputs to computer models of vehicles, NATC sees the DFMV having immediate application to accelerated life testing for the Army's current vehicle buys. Through wave-number spectra defining the operating environment and S-N curves (material fatigue curves) defining the vehicle structural components, fatigue life predictions can be generated with greater confidence and accelerated durability input levels can be calculated with greater accuracy for accelerated endurance testing. NATC is currently using this procedure for accelerated life testing for the USAF. It is recommended that guidelines be developed for using road spectra data for accelerated life testing.

3. Wave-number spectra and motion-resistance data can be provided directly to the manufacturers as design guidelines. Further, this information can adequately define the test environments at the various proving grounds and user test sites. These sites can be evaluated against mission profiles and against an established standard to determine the effect of changing test conditions on test results. It is recommended that a program be initiated to address these issues.

4. Tolerances on a baseline spectra could be specified through the use of Equation 23. For example, the government could specify that a vehicle successfully negotiate 1,000 miles of the Truck Hill course. The description of the Truck Hill course could be either the wave-number spectra with ± tolerance given or

$$G_{xx}(n) \sim 1 \times 10^{-4} \left(\frac{n}{0.52}\right)^{-2} \qquad (25)$$

with tolerances on the constants in the equation, w and $G_{xx}(n_o)$. A developmental program is needed to determine acceptable tolerances for test courses based on specifying a baseline and then determining the profile changes of the course after the course has changed the dynamics into the vehicle.

Recommendations 5 and 6 are made to reduce processing time and cost and to increase the accuracy at the low wave numbers in future studies. After preparation, NATC estimates approximately 30 minutes to profile a mile of test course, process the data and compare the course data to a base line. This estimate is based on the Truck Hill type course profiled at 10 MPH. If paved or smooth gravel surfaces were required, the time per mile would decrease. For severe courses requiring slower speeds, more time would be required. In general, all the durability test courses at APG or YPG could be profiled and processed within a day.

5. The use of digital pulses from the optical encoders on the DFMV (wheel-speed measurement) to externally drive the A/D converter on the MASSCOMP computer would further enhance the data. This would eliminate small speed variation averaging from the wave-number spectra plots and give exact measurement of distance in plots of elevation versus distance. Version 9.0 of the Cranfield Data Software will support a digital input to drive the A/D on the MASSCOMP computer, and this version is to be made available to NATC for evaluation by the end of February 1990. In addition, 300 pulse per revolution wheel encoders were used for the data presented in this report. For future studies, it is recommended that a higher-count optical encoder be investigated.

6. A piezoelectric accelerometer with a low-frequency cutoff of 0.05 Hz on the wheel end of the DFMV limits the high wavelength measurement. A DC coupled strain gage or force-balance accelerometer with a very low noise level would provide spatial PSDs to much lower wave numbers than the current system.

14.0 REFERENCES

1. Final Report on Special Study of Technique and Study of Automotive Test Course Index, Phase III, TECOM Project No. 9-CO-081-000-007, Feb. 1972 through March 1974, USAAPG, APG, MD 21005.

2. Profiling the Yuma Proving Ground Mid-East Desert Analog Test Course, TECOM Project No. 7-CO-RD3-AP1-012, Report No. APG-MT-5882, September 1983, USAAPG, APG, MD 21005.

3. Sayers, M.W., Dynamic Terrain Inputs to Predict Structural Integrity of Ground Vehicles, University of Michigan Transportation Research Institute Report No. UMTRI-88-16, April 1988.

4. Bendat, J. S., and Piersol, A. G., RANDOM DATA: Analysis and Measurement Procedures, 2nd edition, Wiley, New York, 1986.

5. Bendat, J. S., and Piersol, A. G., Engineering Applications of Correlation and Spectral Analysis, Wiley, New York, 1980.

6. Sayers, M.W. and T.D. Gillespie, The Ann Arbor Road Profilometer Meeting, FHWA Report FHWA/RD-86/100, April 1986.

7. Bekker, M.G., Introduction to Terrain Vehicle Systems, The University of Michigan Press, 1969

8. Gillespie, T.D., Heavy Truck Ride, SAE SP-607.

9. Dodds, C. J., and Robson, J. D., The Description of Road Surface Roughness, Journal of Sound and Vibration, Vol. 31, No. 2, pp. 175-183, 1973.

10. Sayers, M.W., T.D. Gillespie, and W.D.O. Paterson, Guidelines for Conducting and Calibrating Roughness Measurements, World Bank Technical Paper Number 46, 1986.

11. Srinarawat, M., A Method to Calibrate and Correlate Road Roughness Devices using Road Profiles, dissertation, University of Texas, Austin, TX 1982

12. Dyer, I., Estimation of Sound Induced Missile Vibrations, Ch. 9, pp. 9-11, Random Vibration (ed: S.H. Crandall), MIT Press, Cambridge, MA, 1958.

13. Gillespie, T.D., M.W. Sayers, and L. Segal, Calibration of Response-Type Road Roughness Measuring Systems, National Cooperative Highway Research program Report No. 228, December 1980, 88 pp.

14. Murphy, N.R. Jr, A Method For Determining Terrain Surface Roughness, U.S. Army Engineer Waterways Experiment Station, Geotechnical Laboratory Report, September 1984.

15. Ewins, D.J., Measurement and Applications of Mechanical Impedance Data - 2. Measurement Techniques, Journal of the Soci[illegible]f Environmental Engineers, Vol. 15, No. 1, pp. 23-33, March 1976.

16. Kozin F., L.J. Cote and J.L. Bogdanoff, Statistical Studies of Stable Ground Roughness, U.S. Army Tank-Automotive Center, Land Locomotion Laboratory, Warren, MI, Report No. 8391, November 1963, 149 pp.

17. Bogdanoff, J.L., F. Kozin, and L.J. Cote, Atlas of Off-Road Ground Roughness PSD's and Report on Data Acquisition Technique, U.S. Army Tank-Automotive Center, Land Locomotion Laboratory, Warren, MI, Technical Report No. AD802503, 1966.

APPENDIX A

ROD AND LEVEL ELEVATION VERSUS DISTANCE PLOTS

PAGE 98 WES TEST COURSE DATA (SUMMARY LISTING)

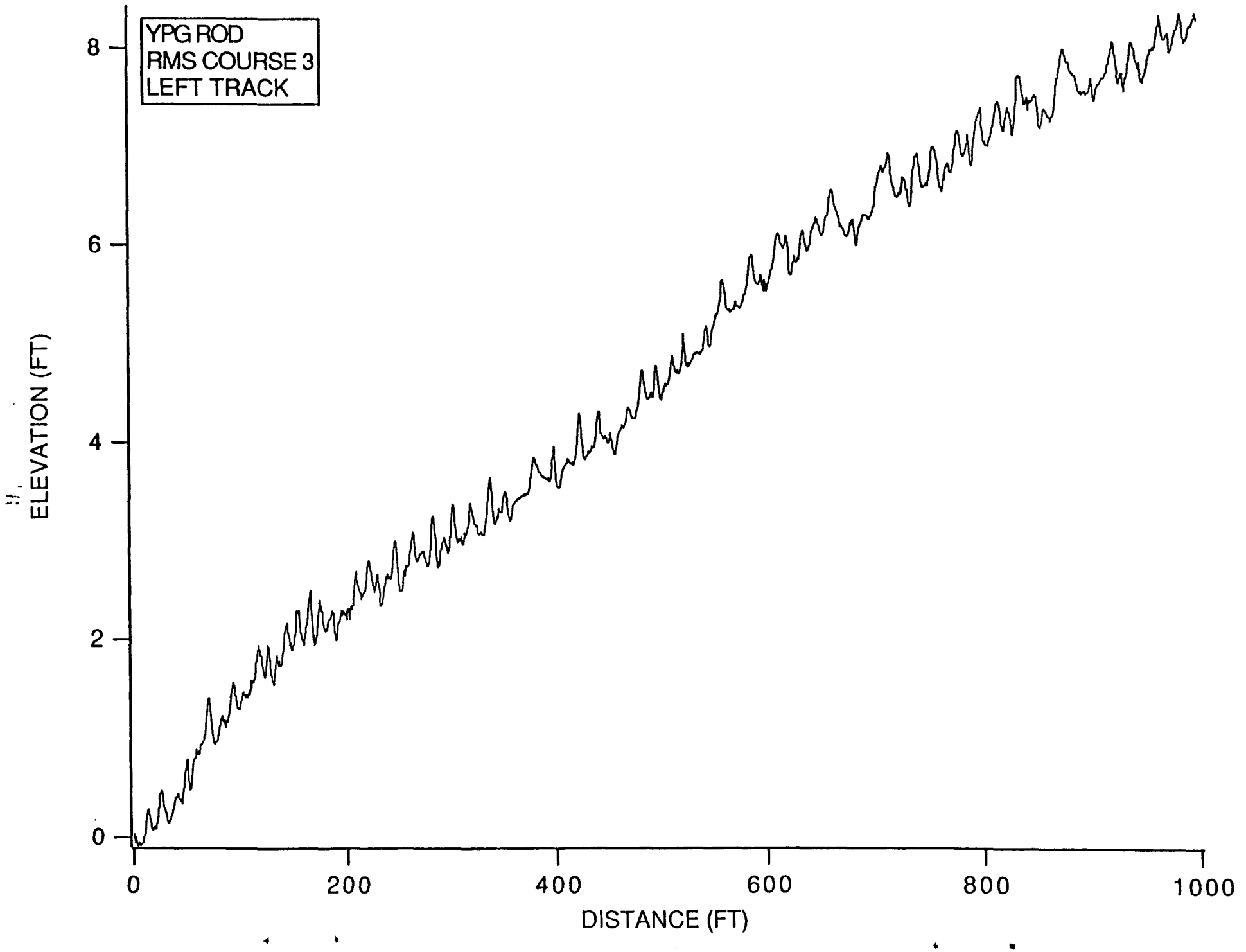
YPG ROD
RMS COURSE 3
LEFT TRACK
ELEVATION (FT)
8
6
4
2
0
0
200
400
600
800
1000
DISTANCE (FT)

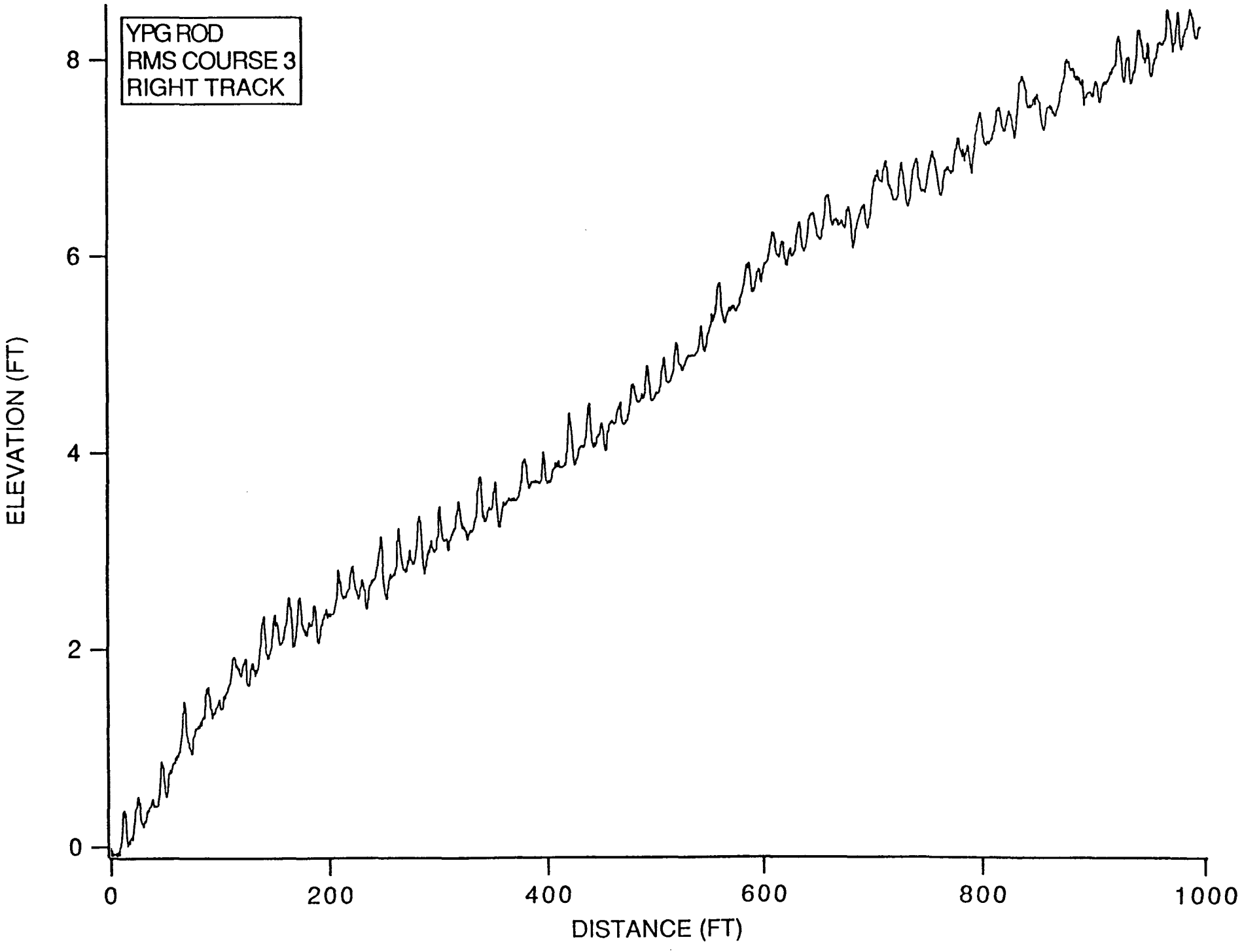
YPG ROD
RMS COURSE 3
RIGHT TRACK
8
6
4
2
0
ELEVATION (FT)
0
200
400
600
800
1000
DISTANCE (FT)

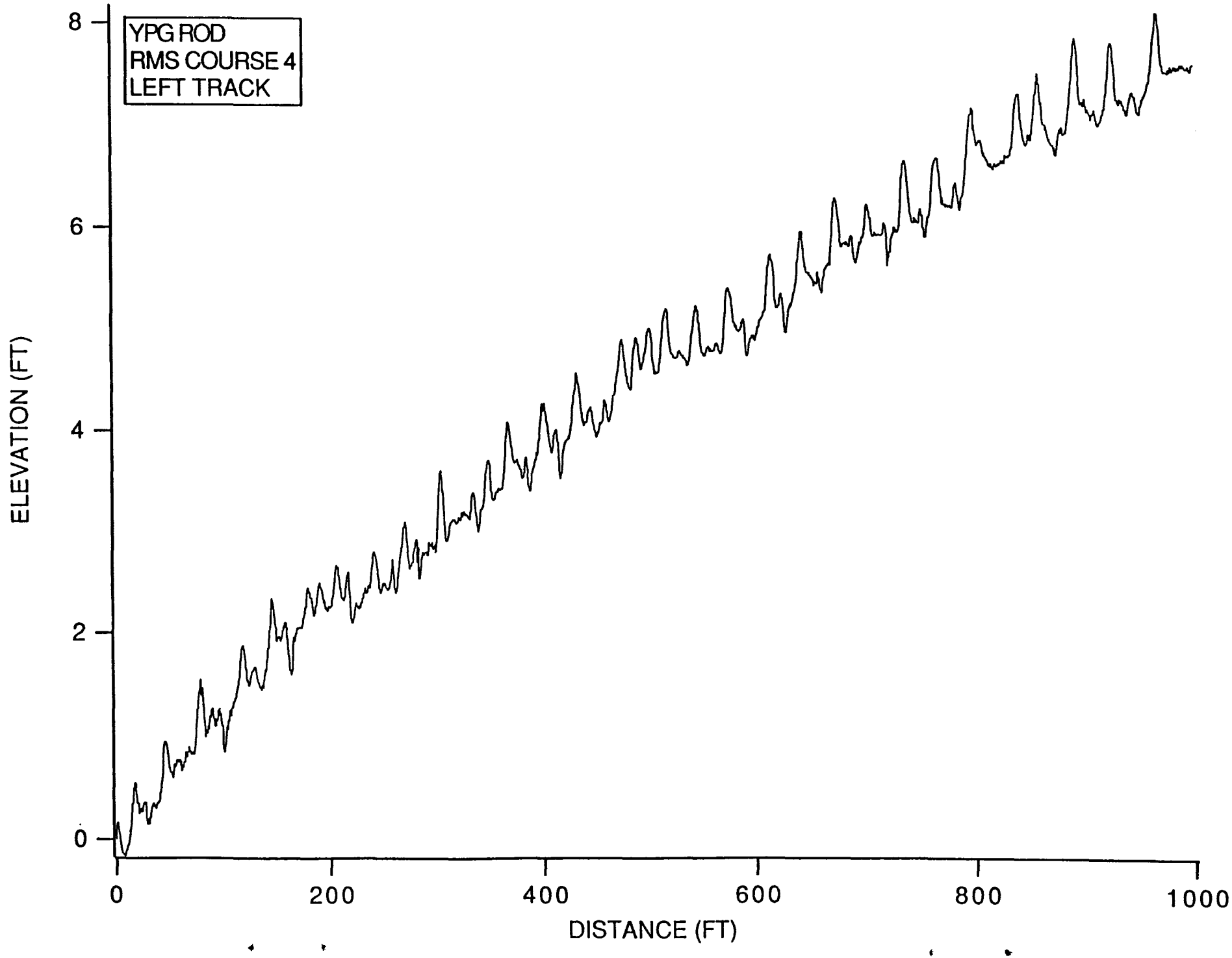
YPG ROD
RMS COURSE 4
LEFT TRACK
8
6
4
2
0
ELEVATION (FT)
0
200
400
600
800
1000
DISTANCE (FT)

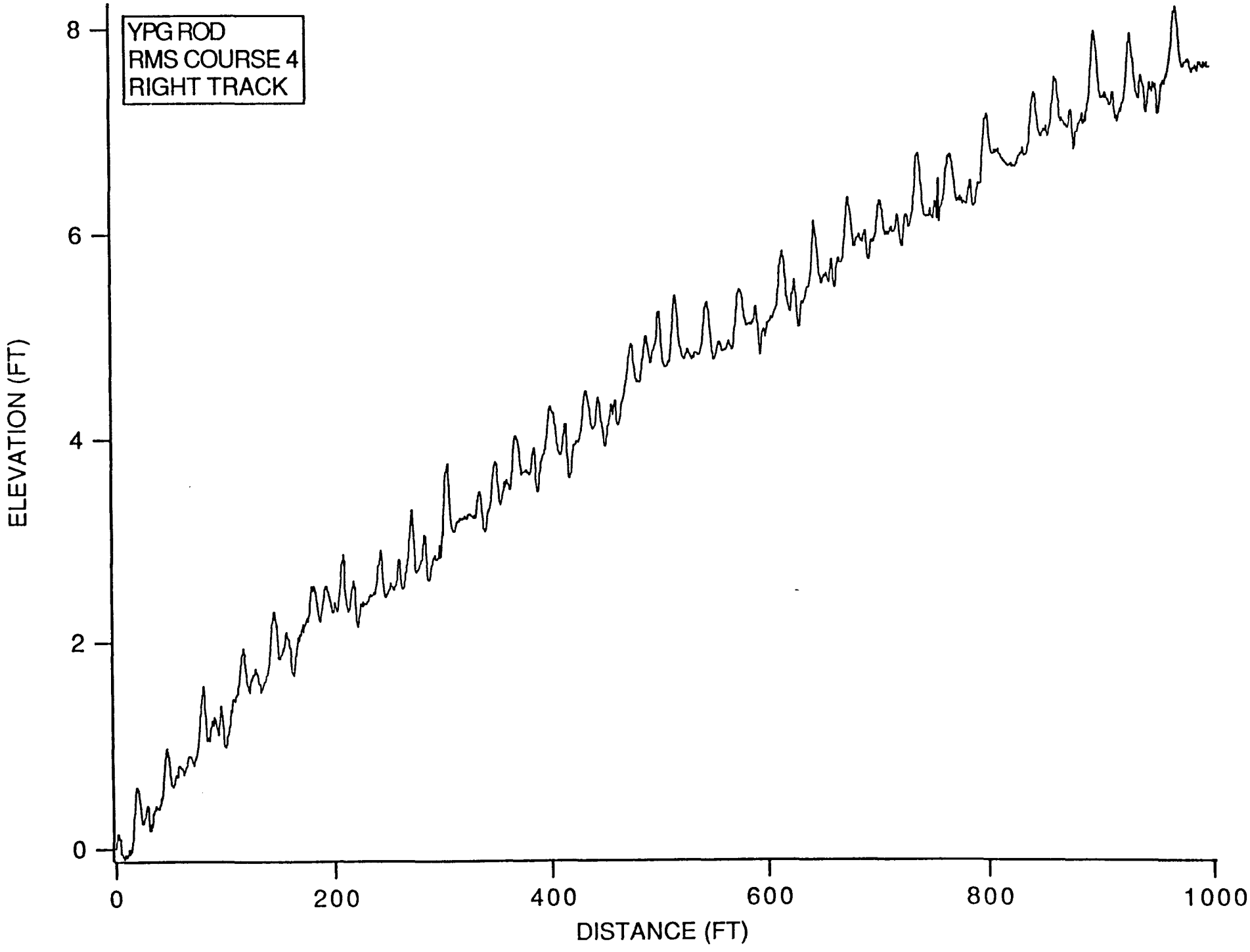
YPG ROD
RMS COURSE 4
RIGHT TRACK
8
6
4
2
0
ELEVATION (FT)
0
200
400
600
800
1000
DISTANCE (FT)

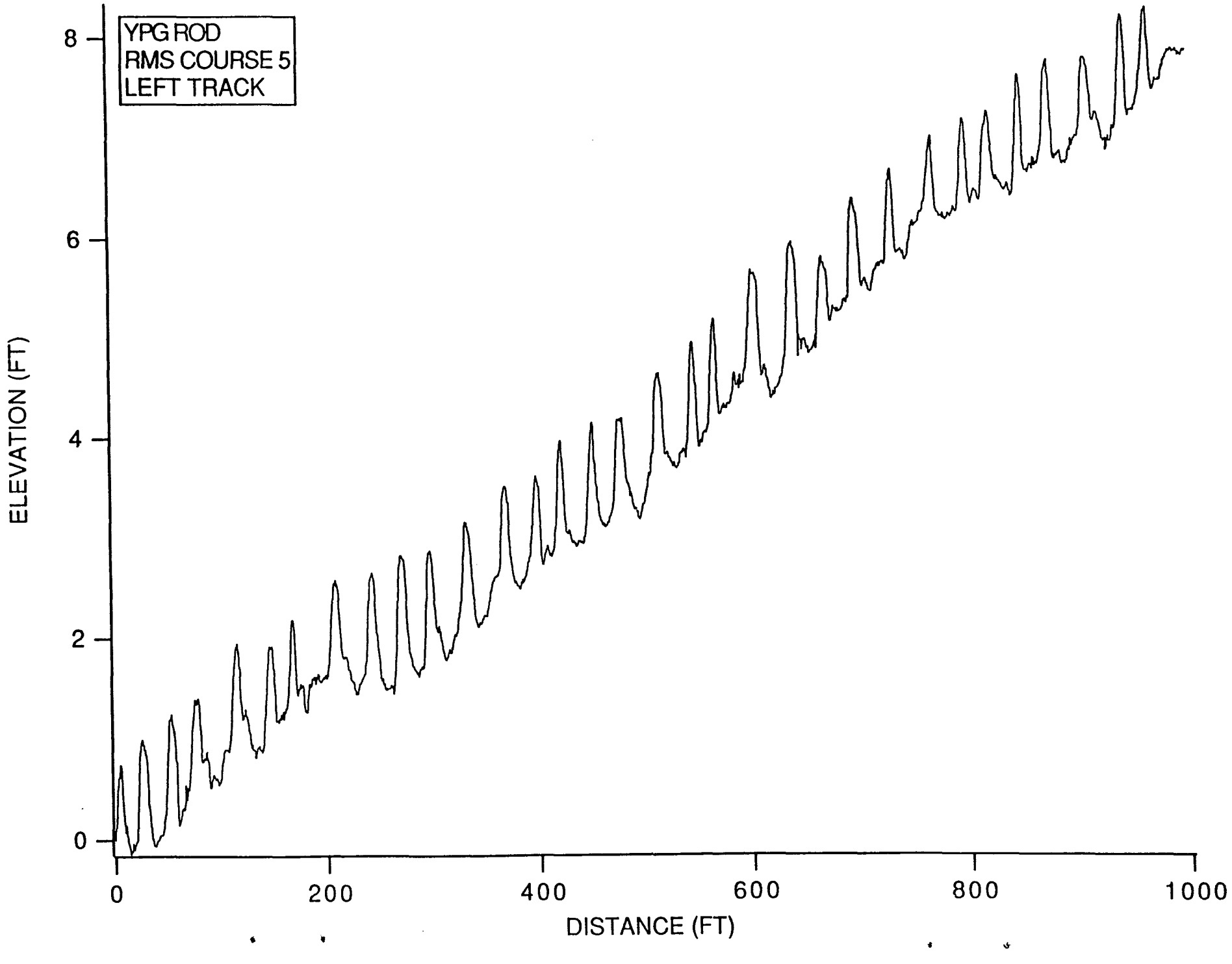
YPG ROD
RMS COURSE 5
LEFT TRACK
8
6
4
2
0
ELEVATION (FT)
0
200
400
600
800
1000
DISTANCE (FT)

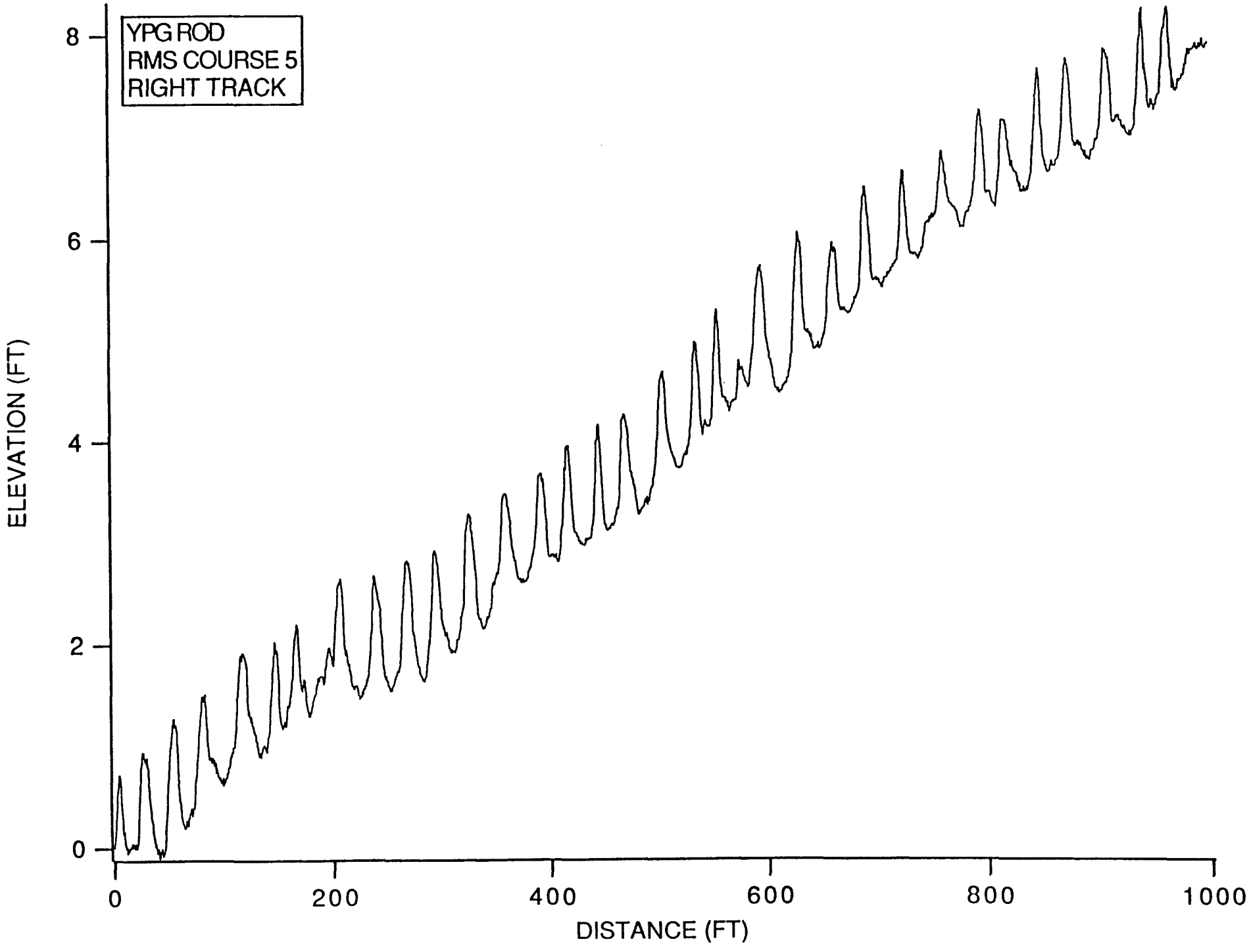
YPG ROD
RMS COURSE 5
RIGHT TRACK
8
6
4
2
0
ELEVATION (FT)
0
200
400
600
800
1000
DISTANCE (FT)

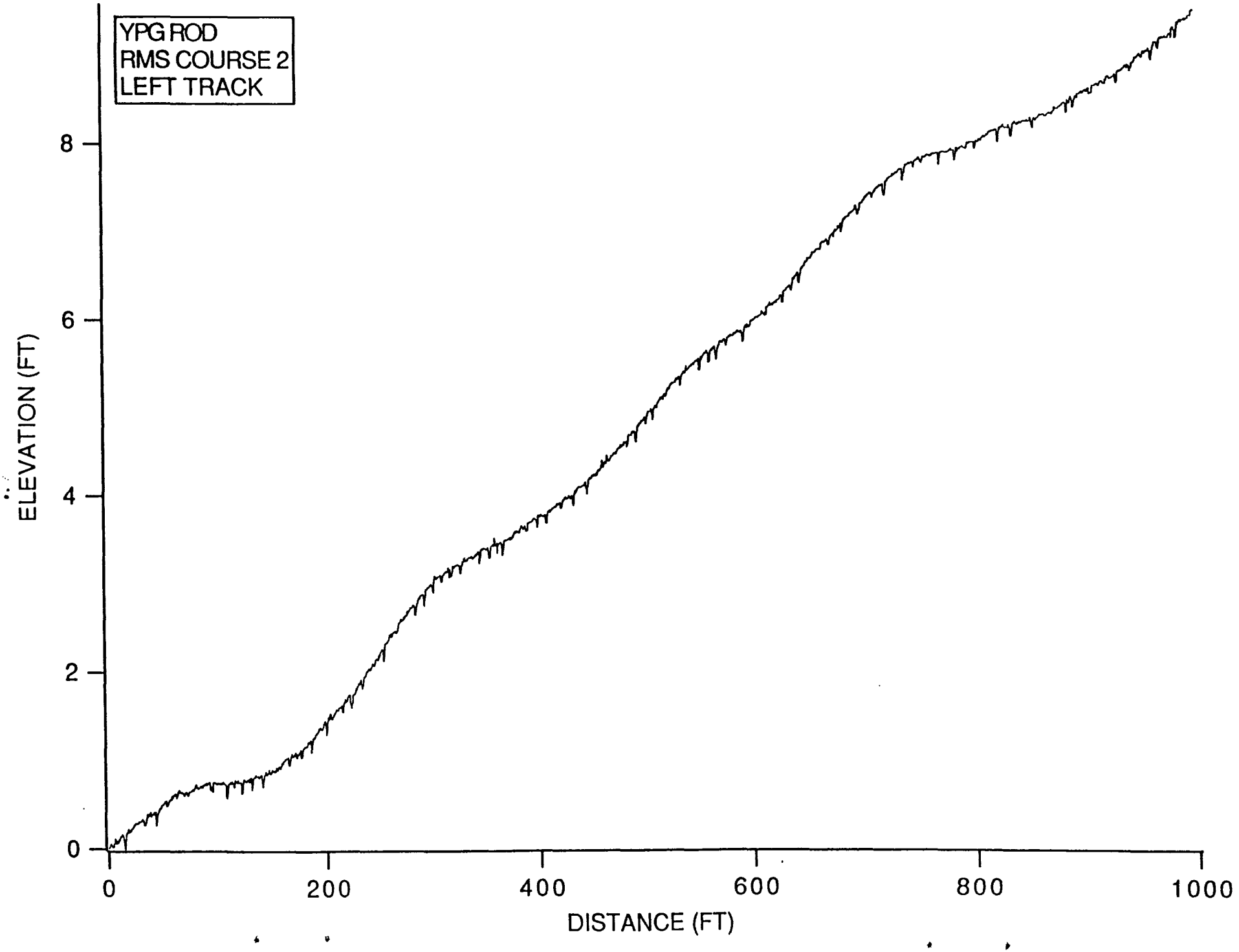
YPG ROD
RMS COURSE 2
LEFT TRACK
ELEVATION (FT)
0
2
4
6
8
0
200
400
600
800
1000
DISTANCE (FT)

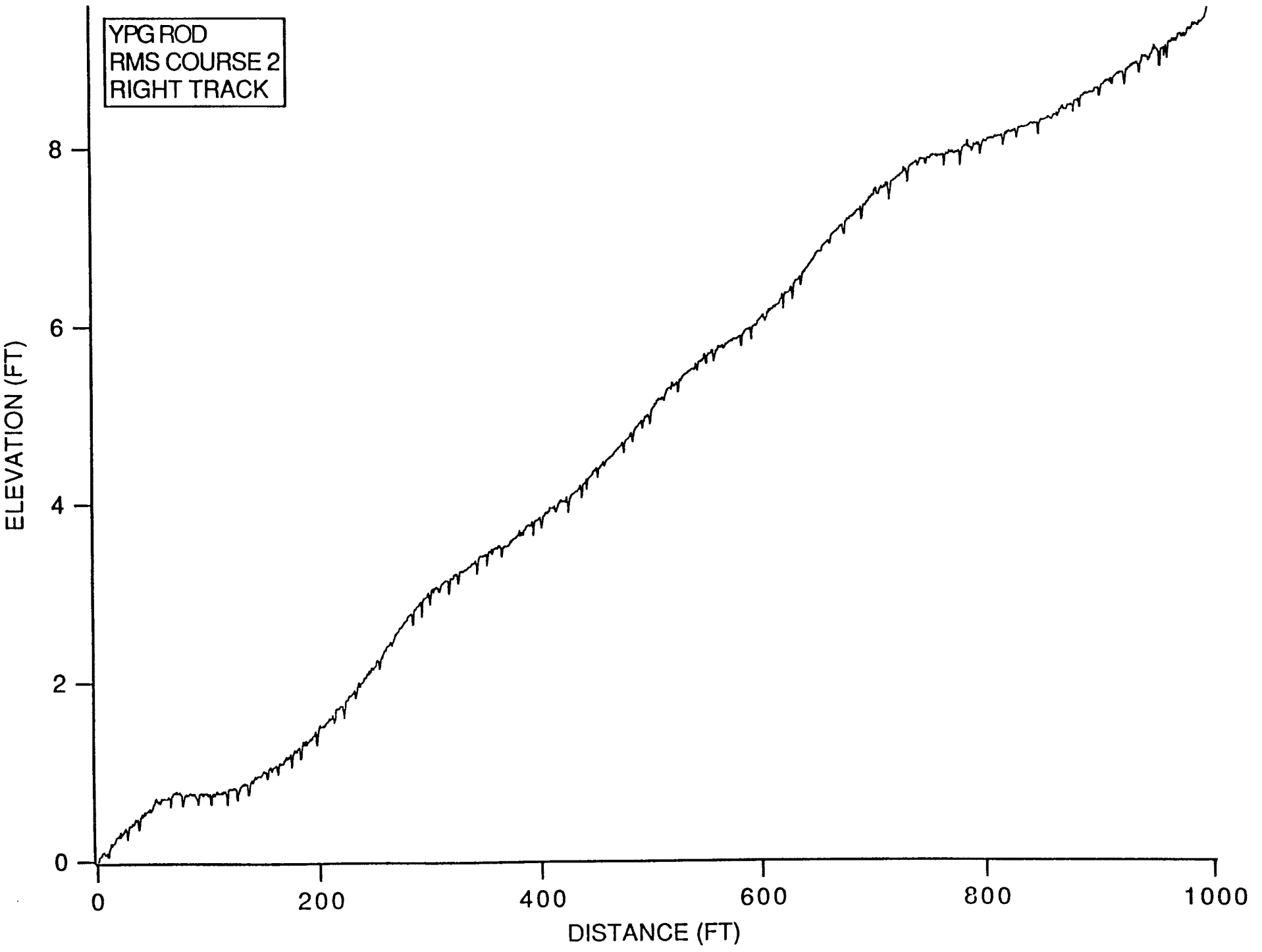
YPG ROD
RMS COURSE 2
RIGHT TRACK
ELEVATION (FT)
0
2
4
6
8
0
200
400
600
800
1000
DISTANCE (FT)

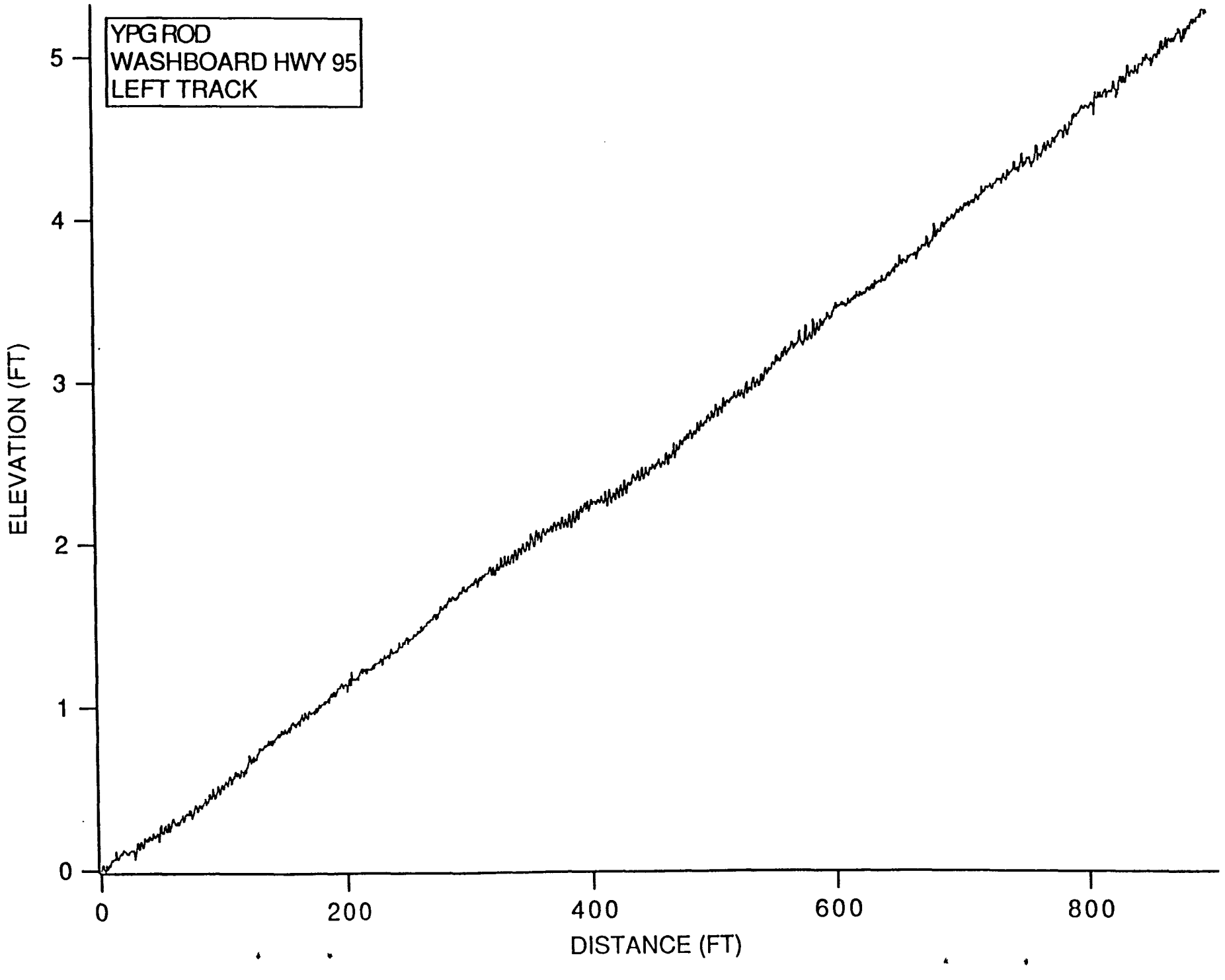
YPG ROD
WASHBOARD HWY 95
LEFT TRACK
ELEVATION (FT)
0
1
2
3
4
5
0
200
400
600
800
DISTANCE (FT)

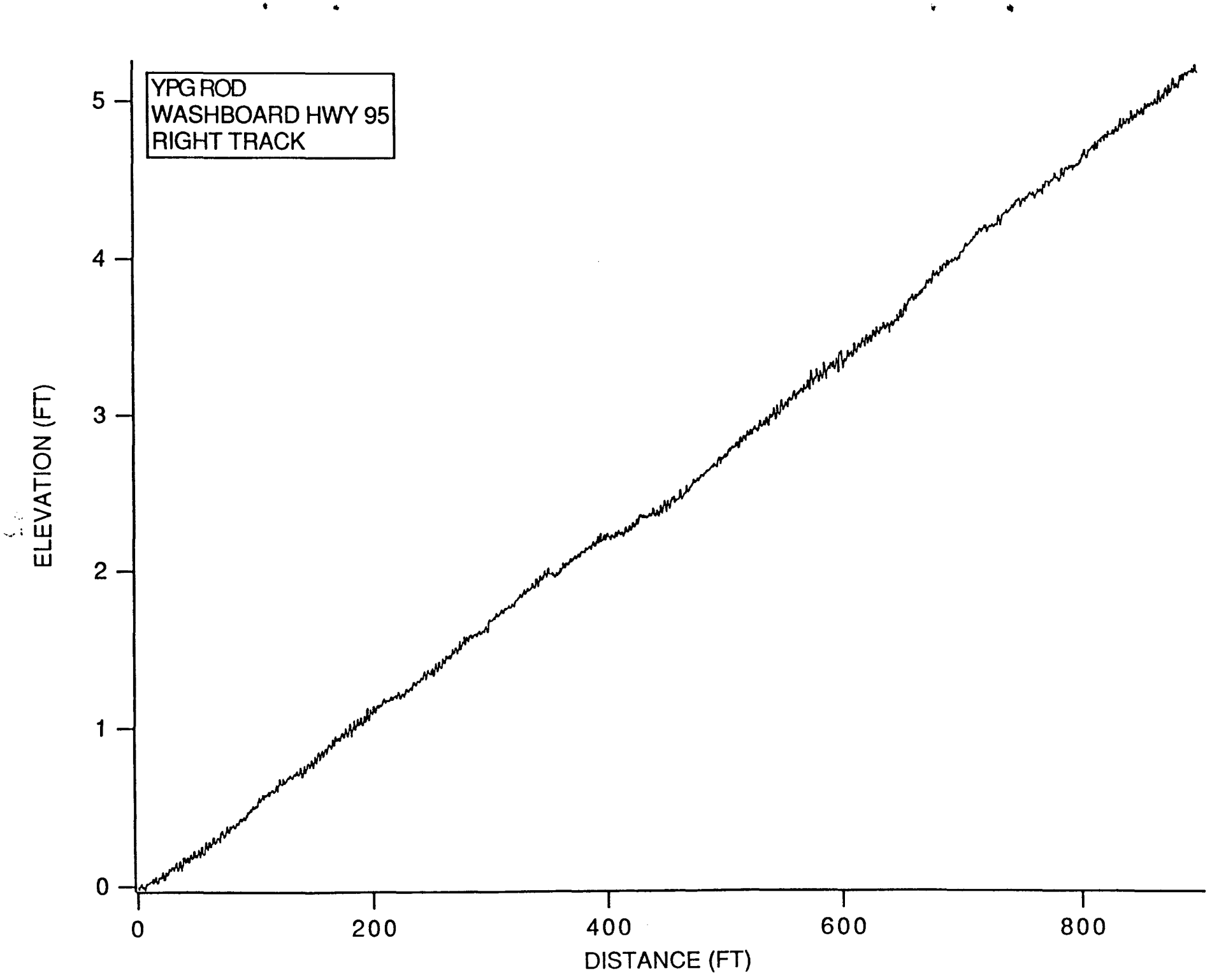
YPG ROD
WASHBOARD HWY 95
RIGHT TRACK
ELEVATION (FT)
0
1
2
3
4
5
0
200
400
600
800
DISTANCE (FT)

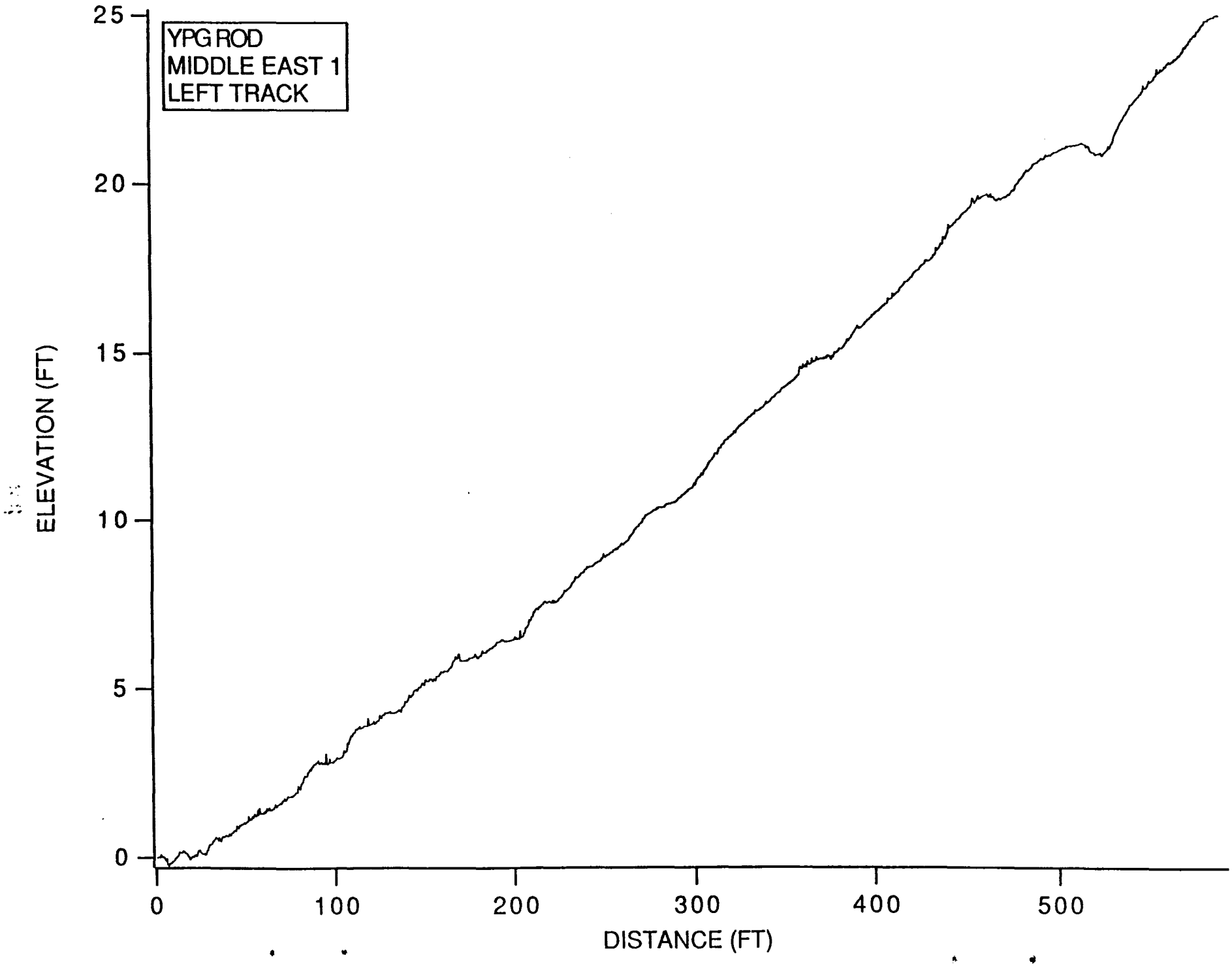
YPG ROD
MIDDLE EAST 1
LEFT TRACK
ELEVATION (FT)
25
20
15
10
5
0
0
100
200
300
400
500
DISTANCE (FT)

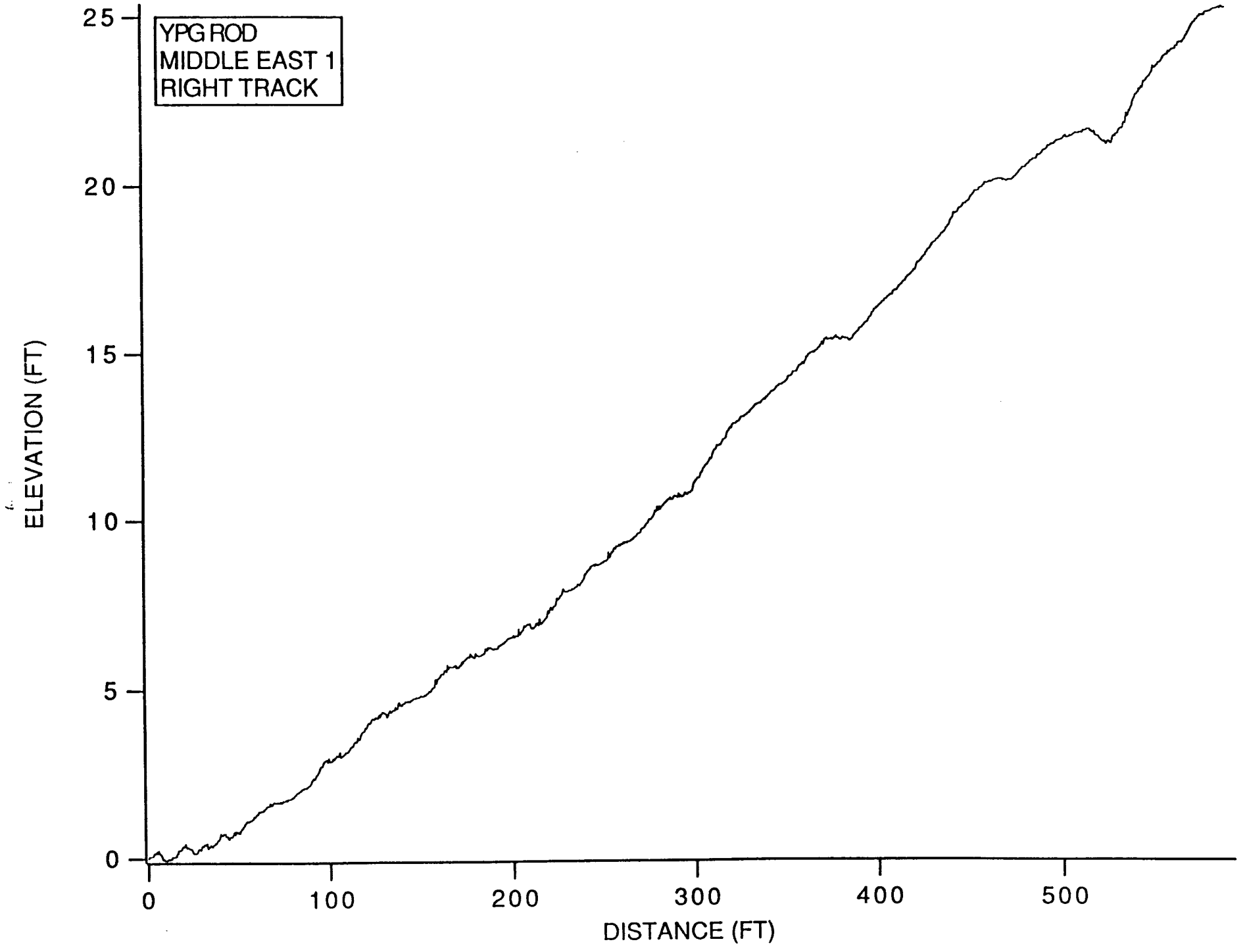
YPG ROD
MIDDLE EAST 1
RIGHT TRACK
ELEVATION (FT)
25
20
15
10
5
0
0
100
200
300
400
500
DISTANCE (FT)

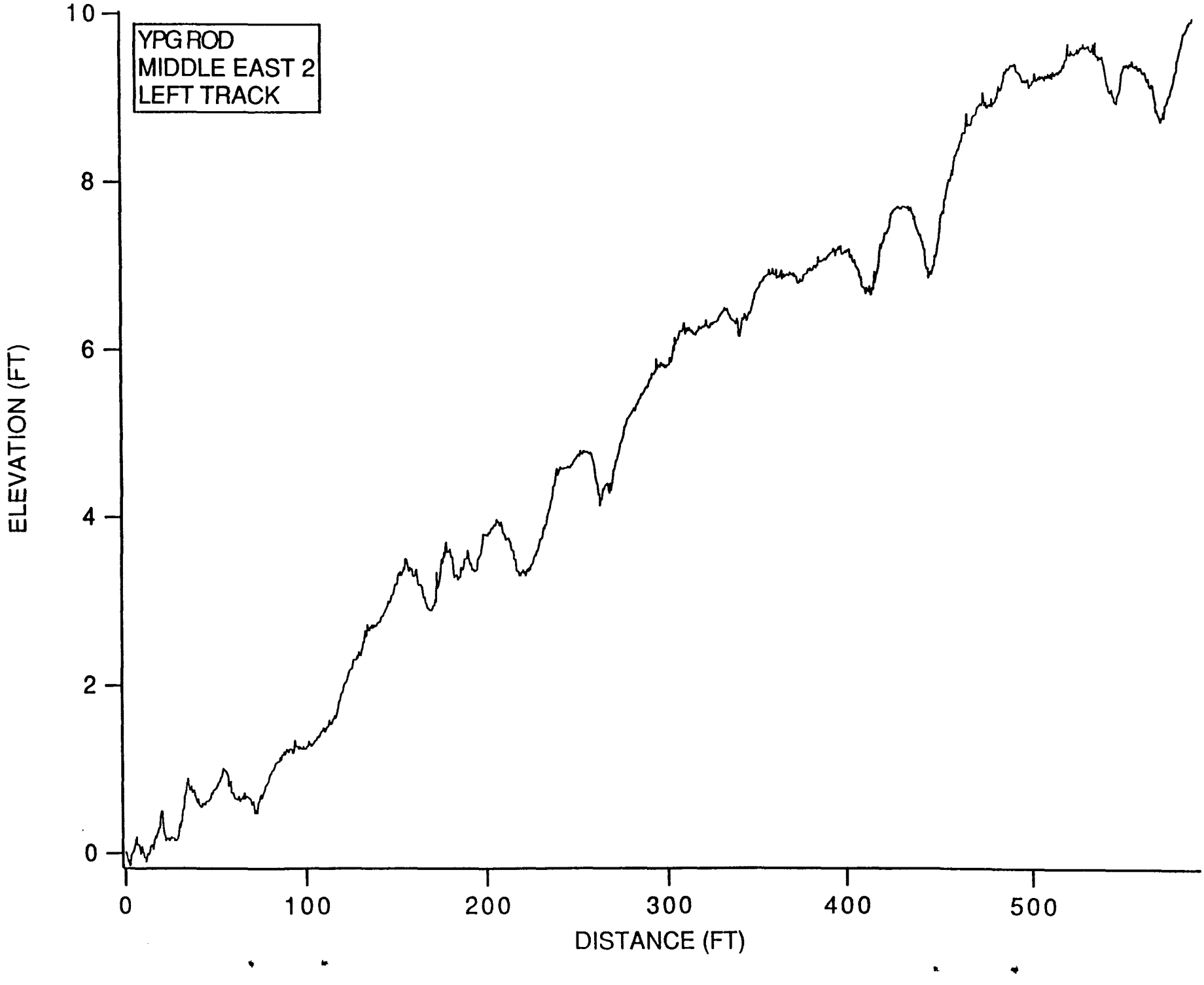
YPG ROD
MIDDLE EAST 2
LEFT TRACK
ELEVATION (FT)
10
8
6
4
2
0
0
100
200
300
400
500
DISTANCE (FT)

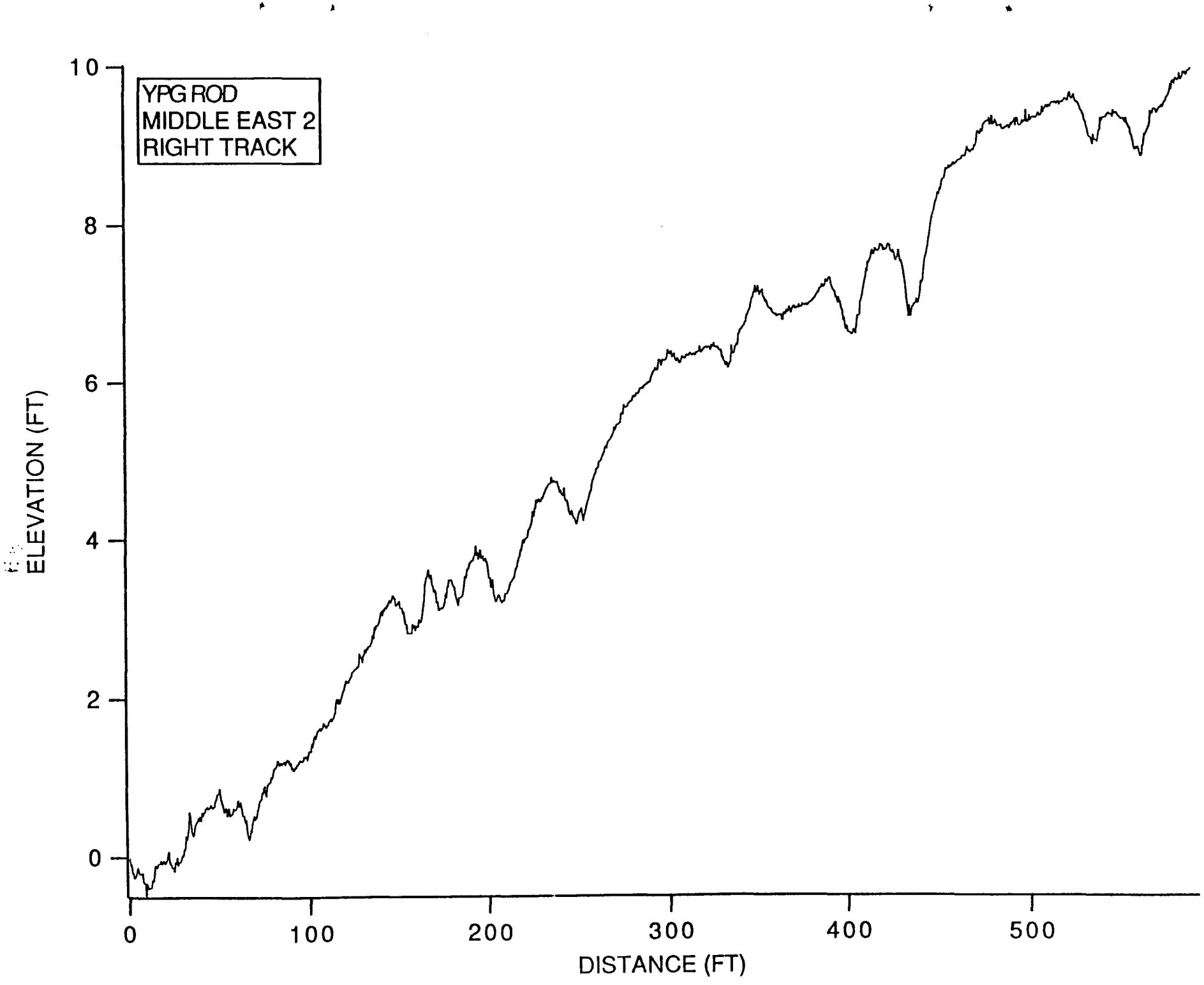
YPG ROD
MIDDLE EAST 2
RIGHT TRACK
ELEVATION (FT)
10
8
6
4
2
0
0
100
200
300
400
500
DISTANCE (FT)

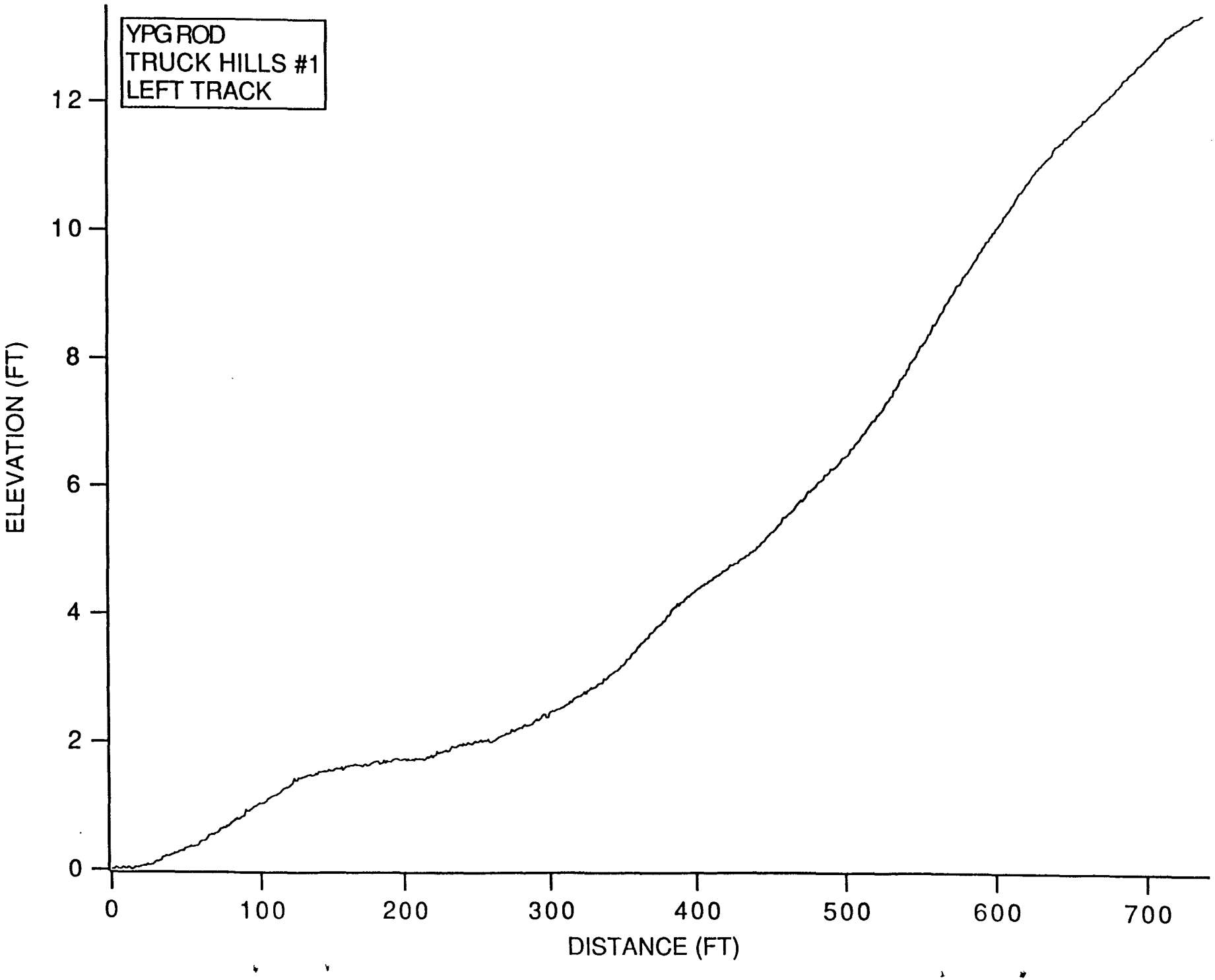
YPG ROD
TRUCK HILLS #1
LEFT TRACK
ELEVATION (FT)
0
2
4
6
8
10
12
0
100
200
300
400
500
600
700
DISTANCE (FT)

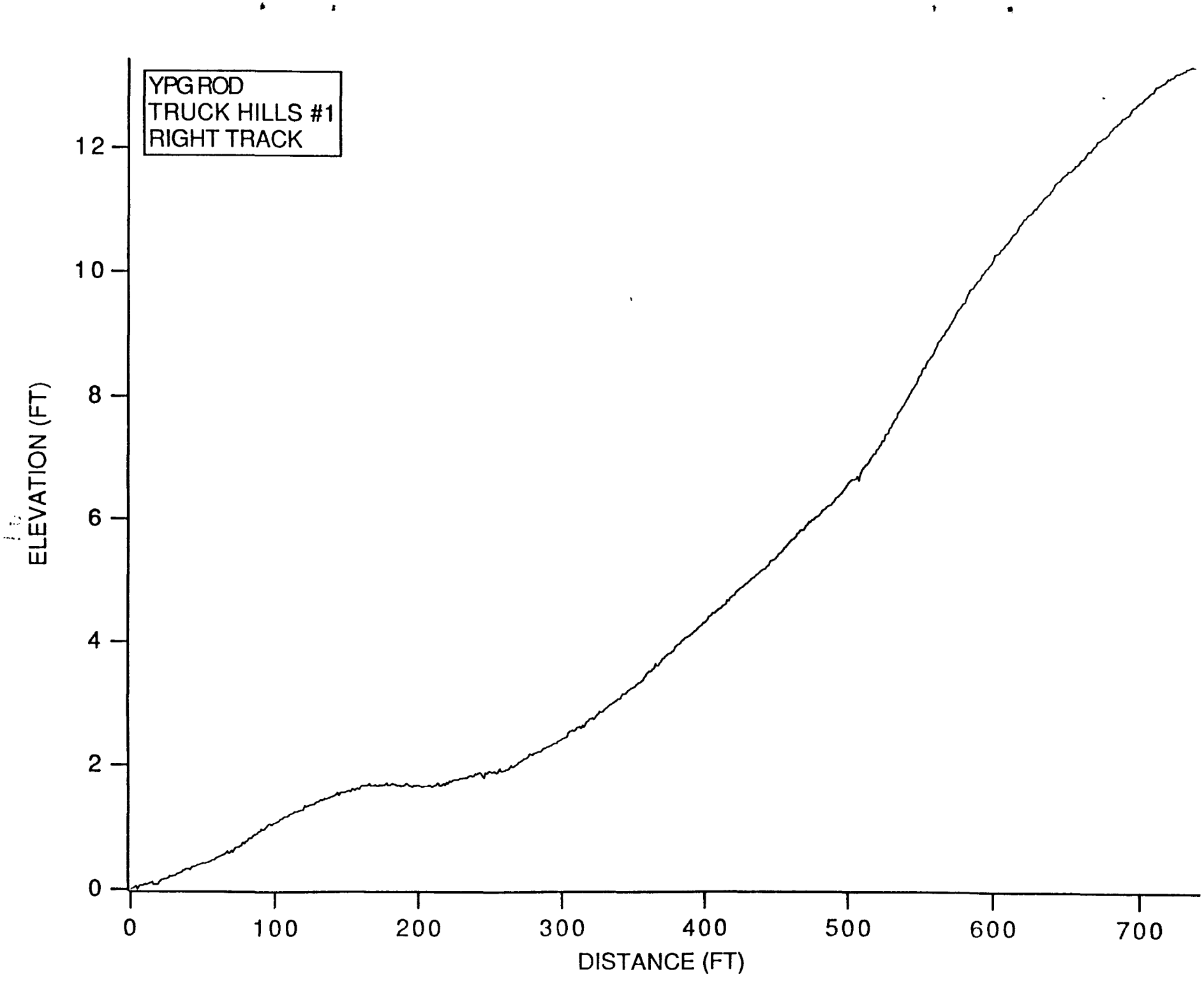
YPG ROD
TRUCK HILLS #1
RIGHT TRACK
ELEVATION (FT)
0
2
4
6
8
10
12
0
100
200
300
400
500
600
700
DISTANCE (FT)

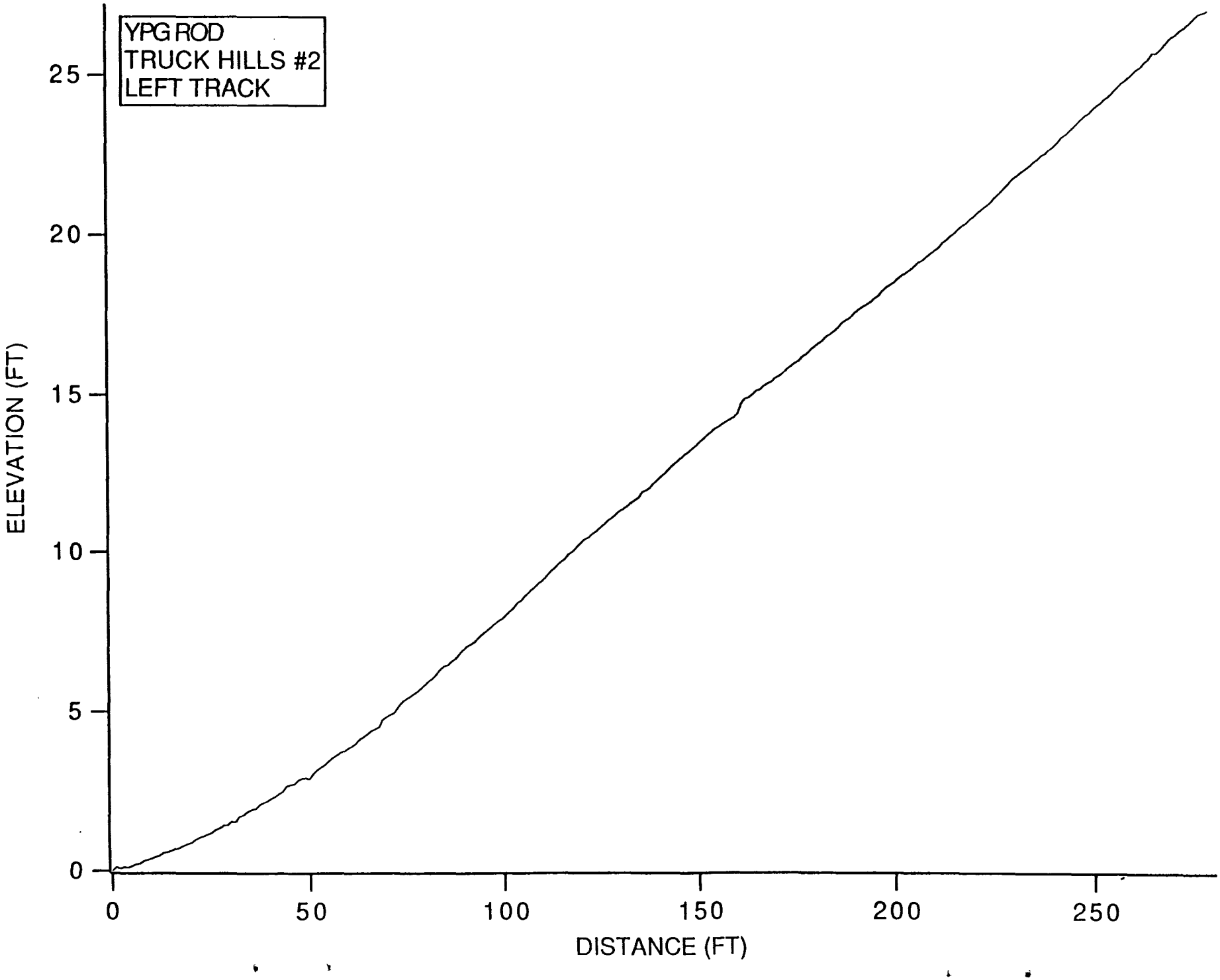
YPG ROD
TRUCK HILLS #2
LEFT TRACK
25
20
15
10
5
0
ELEVATION (FT)
0
50
100
150
200
250
DISTANCE (FT)

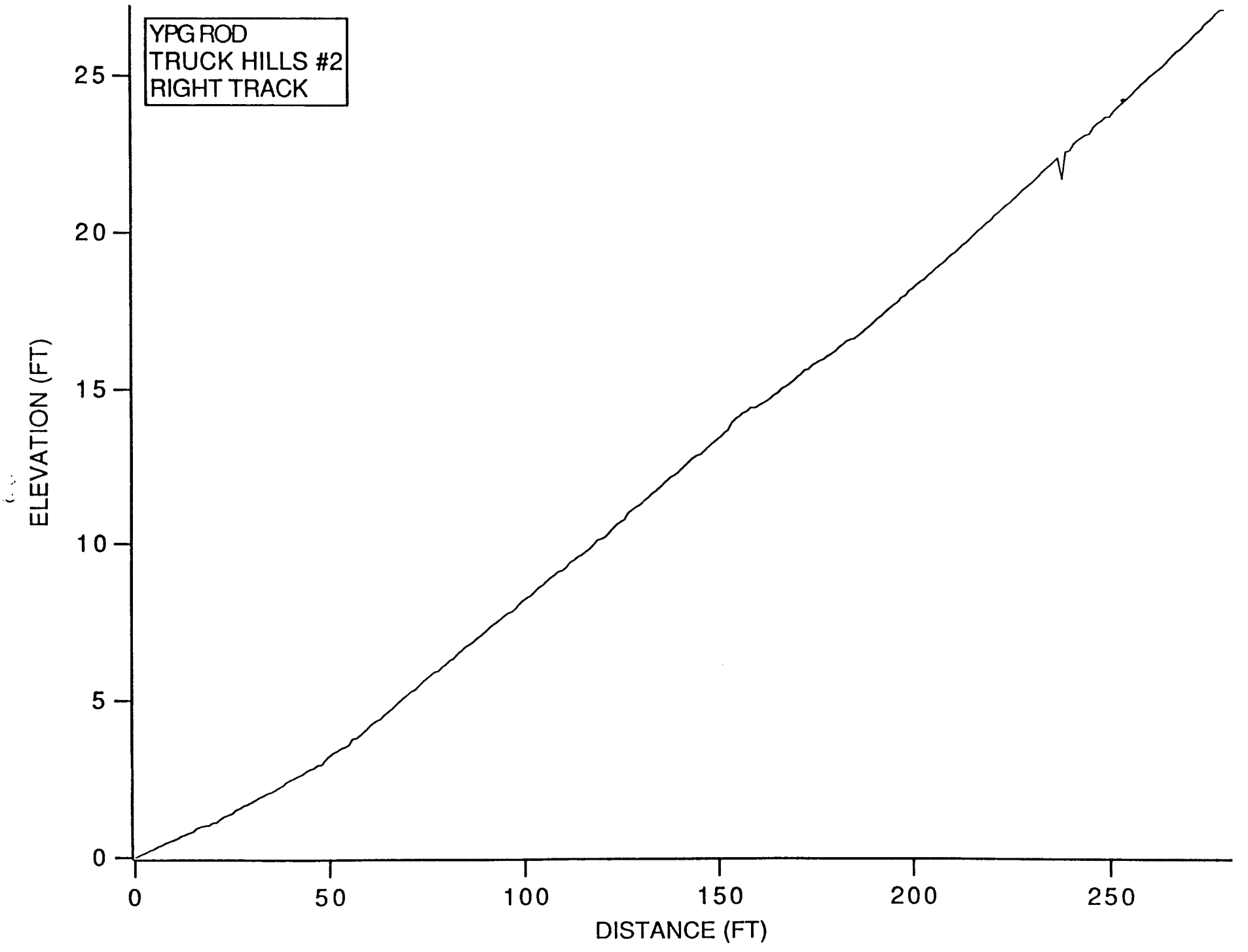
YPG ROD
TRUCK HILLS #2
RIGHT TRACK
25
20
15
10
5
0
ELEVATION (FT)
0
50
100
150
200
250
DISTANCE (FT)

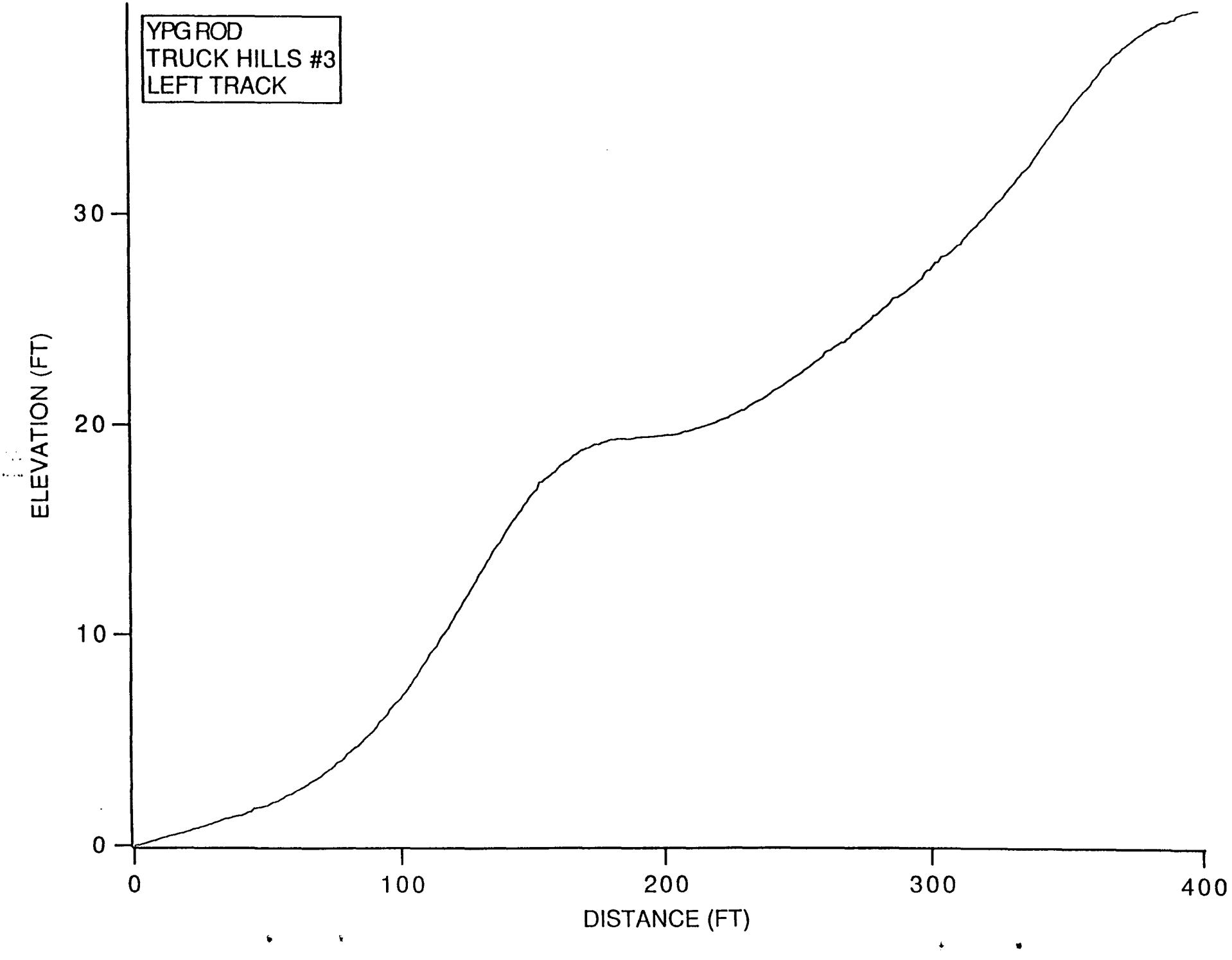
YPG ROD
TRUCK HILLS #3
LEFT TRACK
ELEVATION (FT)
30
20
10
0
0
100
200
300
400
DISTANCE (FT)

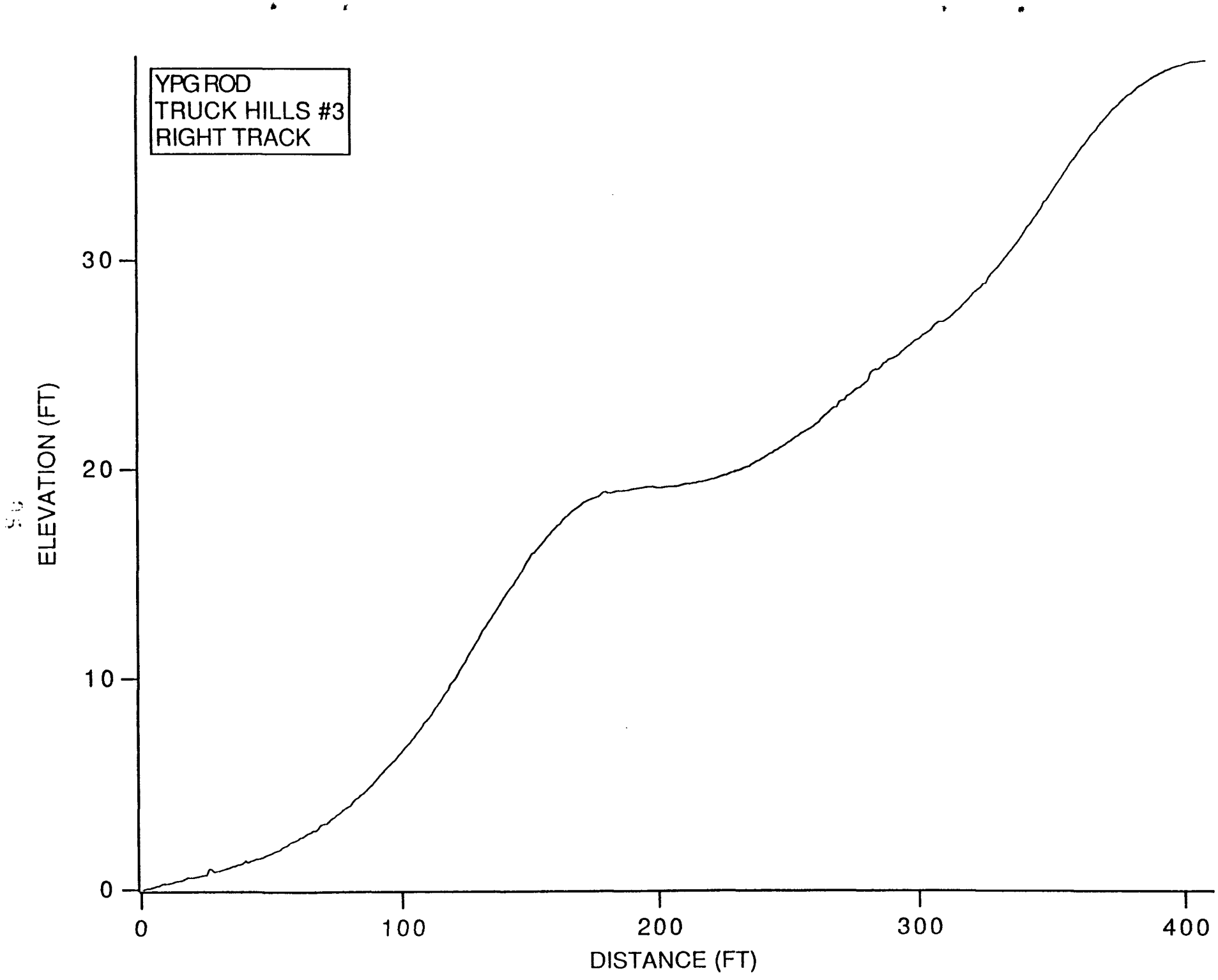
YPG ROD
TRUCK HILLS #3
RIGHT TRACK
ELEVATION (FT)
30
20
10
0
0
100
200
300
400
DISTANCE (FT)

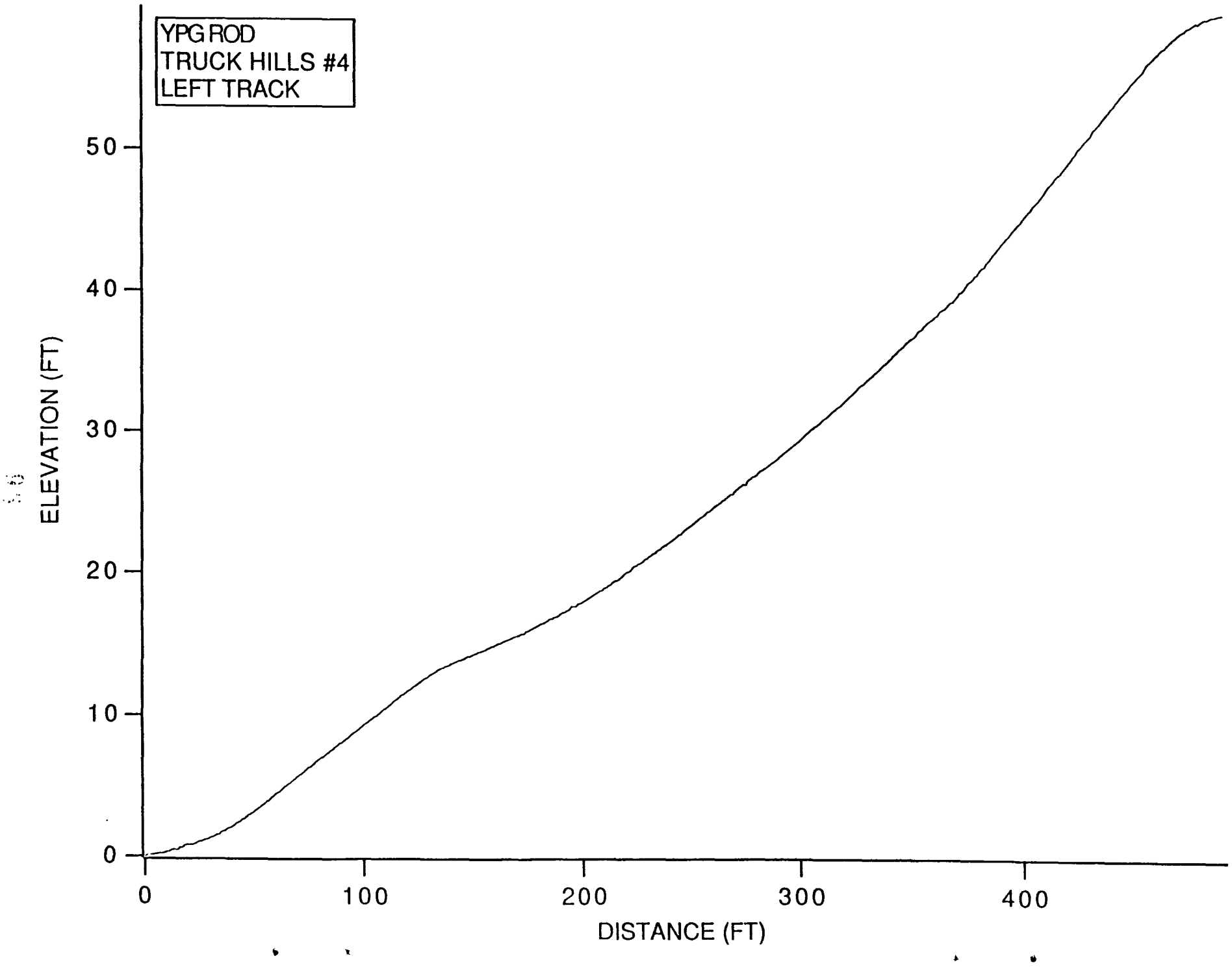
YPG ROD
TRUCK HILLS #4
LEFT TRACK
ELEVATION (FT)
50
40
30
20
10
0
0
100
200
300
400
DISTANCE (FT)

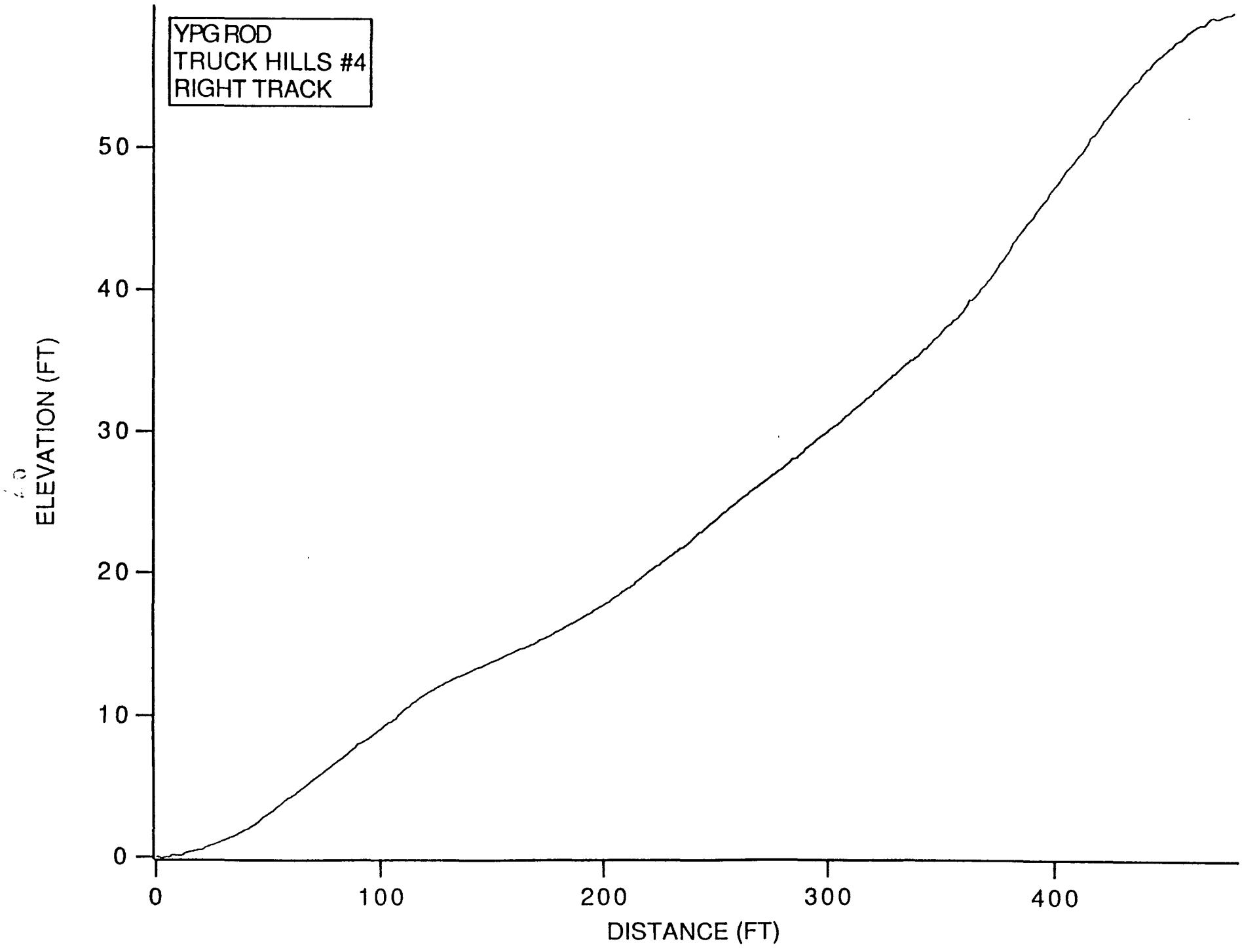
YPG ROD
TRUCK HILLS #4
RIGHT TRACK
ELEVATION (FT)
50
40
30
20
10
0
0
100
200
300
400
DISTANCE (FT)

Test Course Data

Course	Length ft.	Track	RMS in.	Spacing in.	Surface Moisture percent	Cone Index sfc	Cone Index 0-6 in.
RMS #2	1000	L	0.4	6	0.6	750+	750+
		R	0.4		0.7	750+	750+
RMS #3	1000	L	1.4	6	0.6	750+	750+
		R	1.4		0.5	750+	750+
RMS #4	1000	L	2.0	6	0.5	750+	750+
		R	1.9		0.4	750+	750+
RMS #5	1000	L	3.6	6	0.5	750+	750+
		R	3.5		0.5	750+	750+
WASHBOARD on old Hwy 95	900	L	0.2	6	0.2	750+	750+
		R	0.3		0.2	750+	750+
MUGGINS MESA 45 Deg. to Wash	591	L	1.3	6	0.6	83	610
		R	1.2		0.3	83	610
MUGGINS MESA 90 Deg. to Wash	591	L	1.9	6	0.4	90	700
		R	1.9		0.5	90	700
TRUCK HILLS #1	740	L	0.2	12	0.2	750+	750+
		R	0.2		0.5	750+	750+
TRUCK HILLS #2	280	L	0.7	12	0.1	750+	750+
		R	0.9		0.1	750+	750+
TRUCK HILLS #3	400	L	1.5	12	0.1	750+	750+
	410	R	1.5		0.2	750+	750+
TRUCK HILLS #4	490	L	0.9	12	0.2	750+	750+
	480	R	1.1		0.1	750+	750+

APPENDIX B

DFMV DETRENDED ELEVATION VERSUS DISTANCE PLOTS (ROUGHNESS)

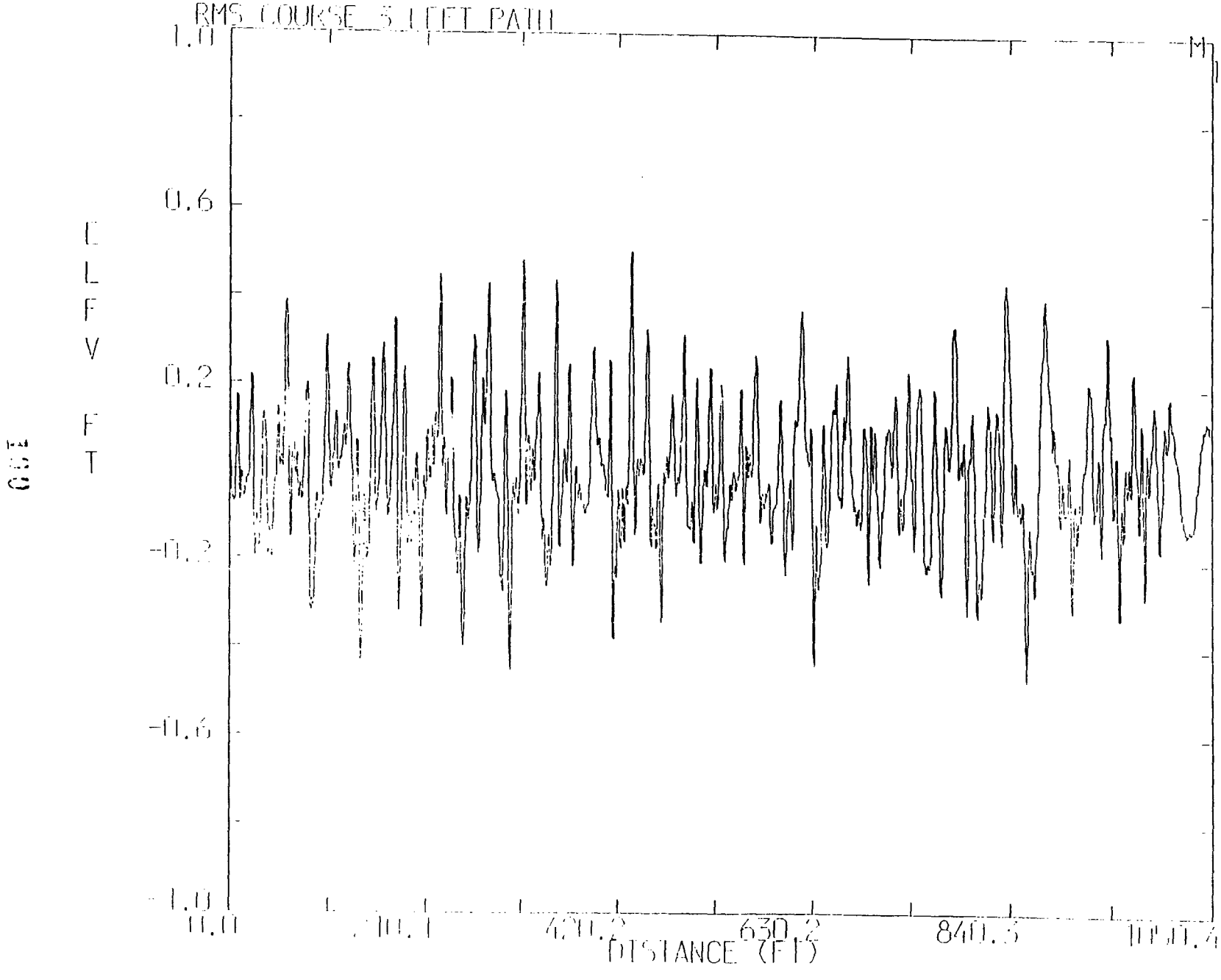
RMS COURSE 5 FEET PATH
1.0
0.6
0.2
-0.2
-0.6
-1.0
ELEVATION FT
0.0
210.1
420.2
630.2
840.3
1050.4
DISTANCE (FT)

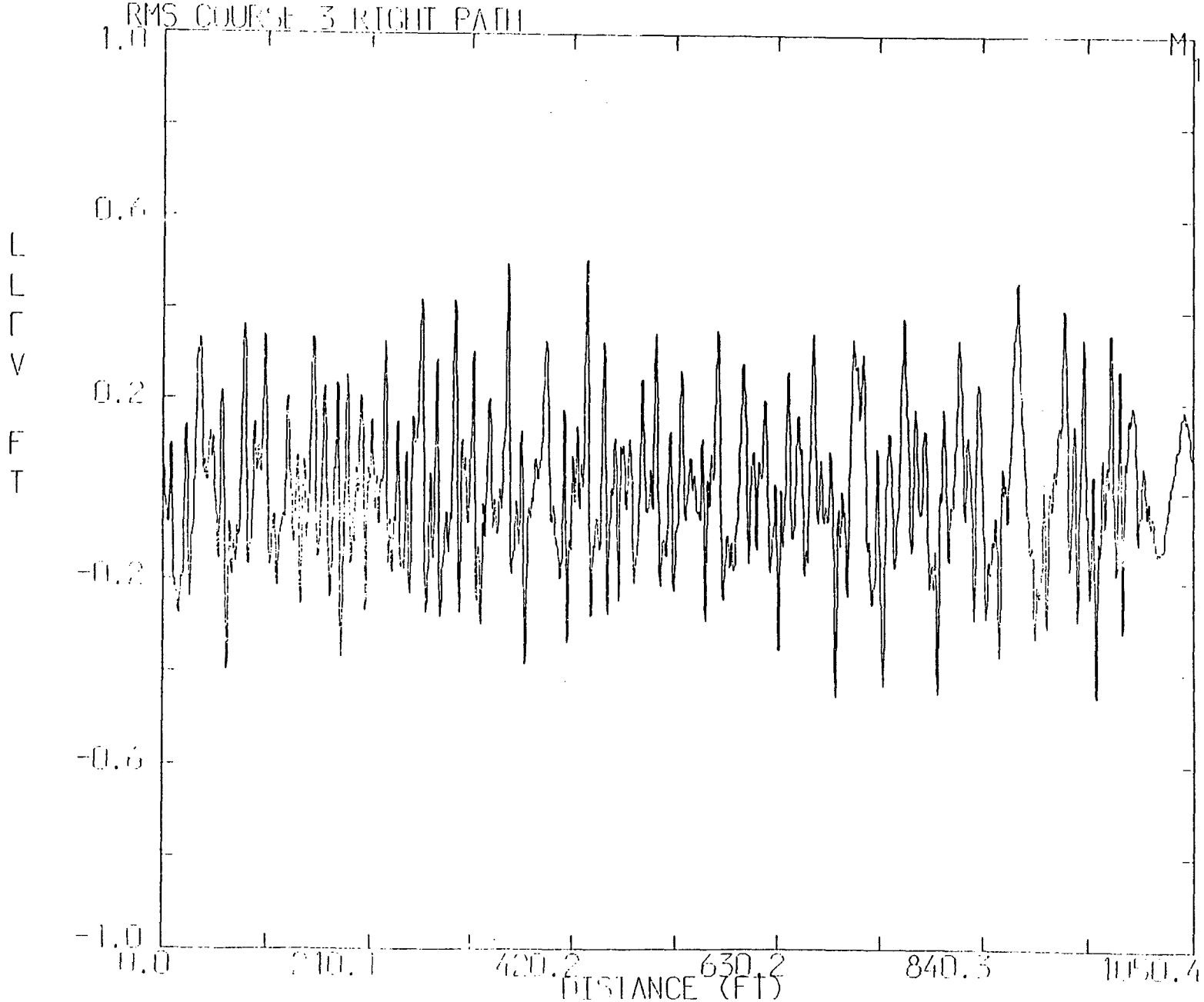
RMS COURSE 3 RIGHT PATH
1.0
0.6
0.2
-0.2
-0.6
-1.0
LEVEL FT
0.0
210.1
420.2
630.2
840.3
1050.4
DISTANCE (FT)

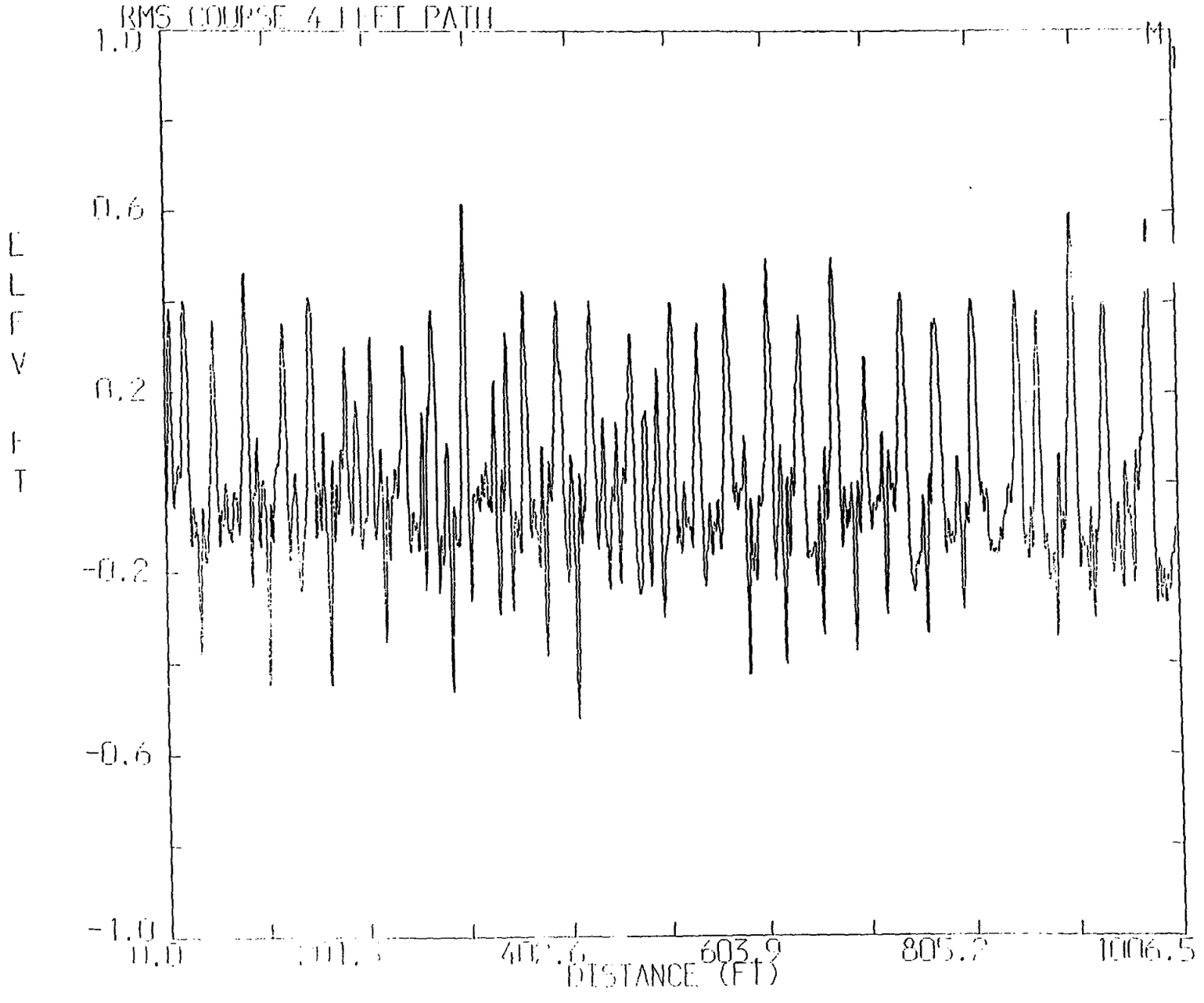
RMS COURSE 4 FEET PATH
1.0
0.6
0.2
-0.2
-0.6
-1.0
ELEV FT
0.0
201.3
402.6
603.9
805.2
1006.5
DISTANCE (FT)

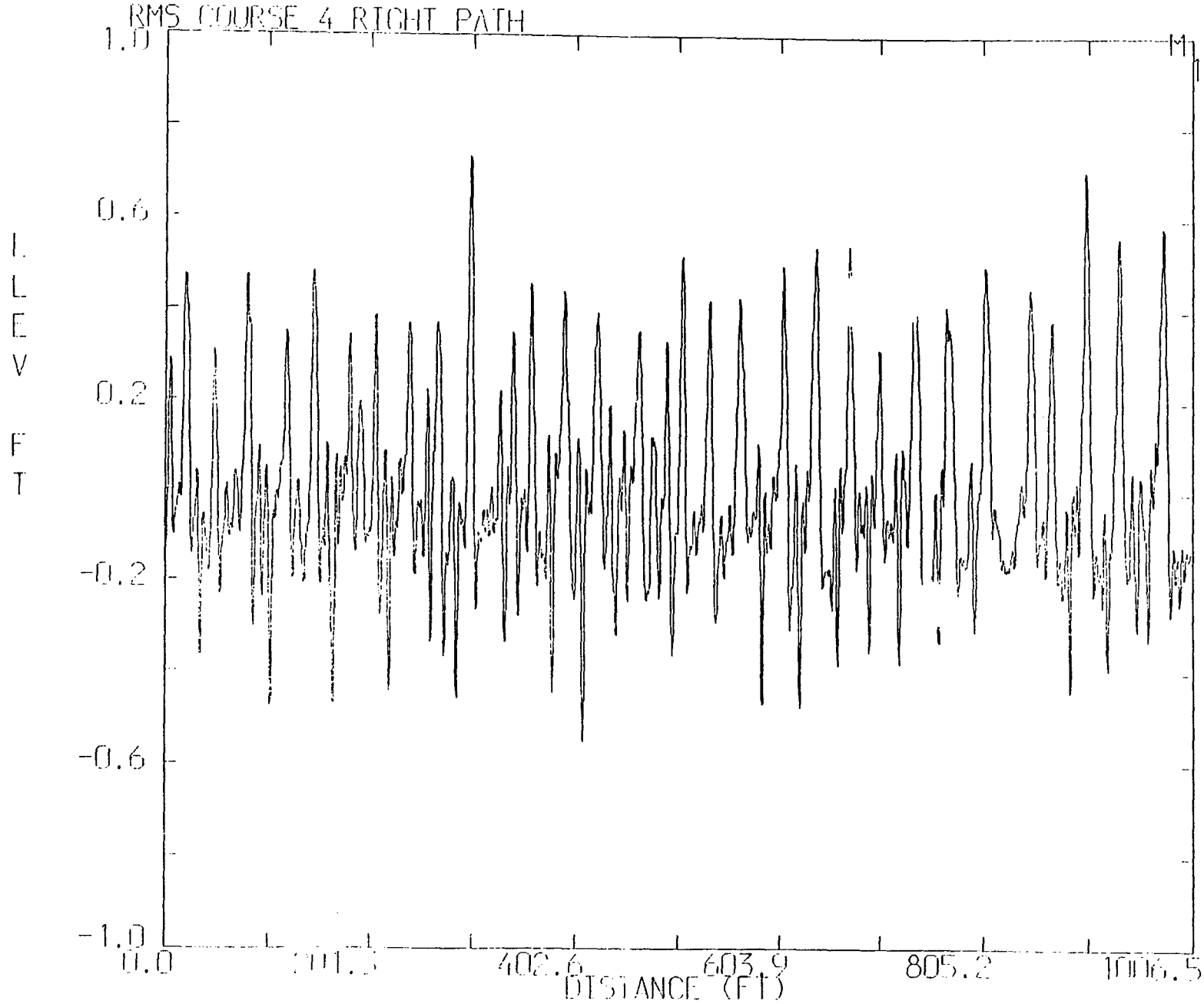
RMS COURSE 4 RIGHT PATH
1.0
0.6
0.2
-0.2
-0.6
-1.0
LEVEL FT
0.0
201.3
402.6
603.9
805.2
1006.5
DISTANCE (FT)

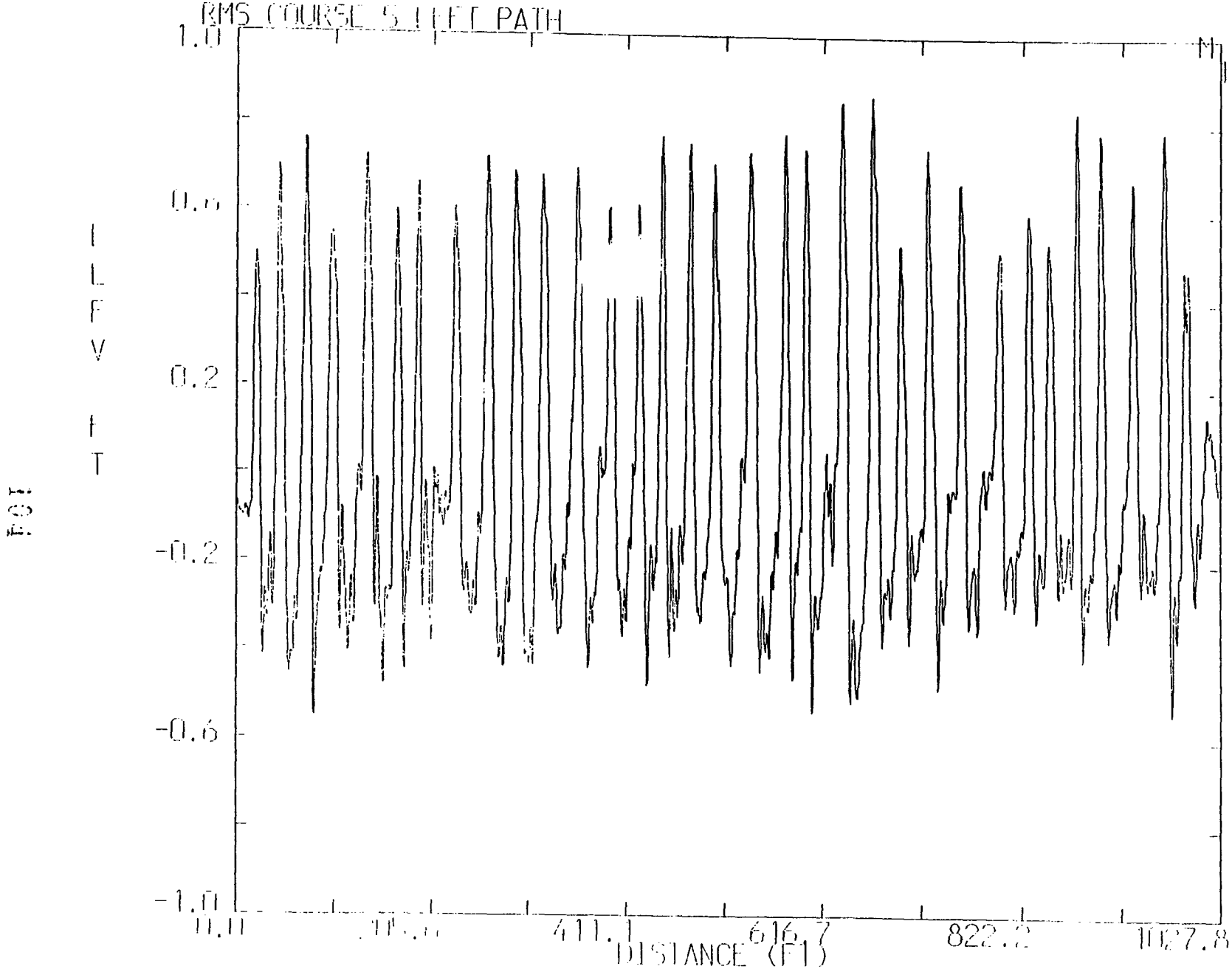
RMS COURSE SHEET PATH
1.0
0.6
0.2
-0.2
-0.6
-1.0
411.1
616.7
822.2
DISTANCE (FT)

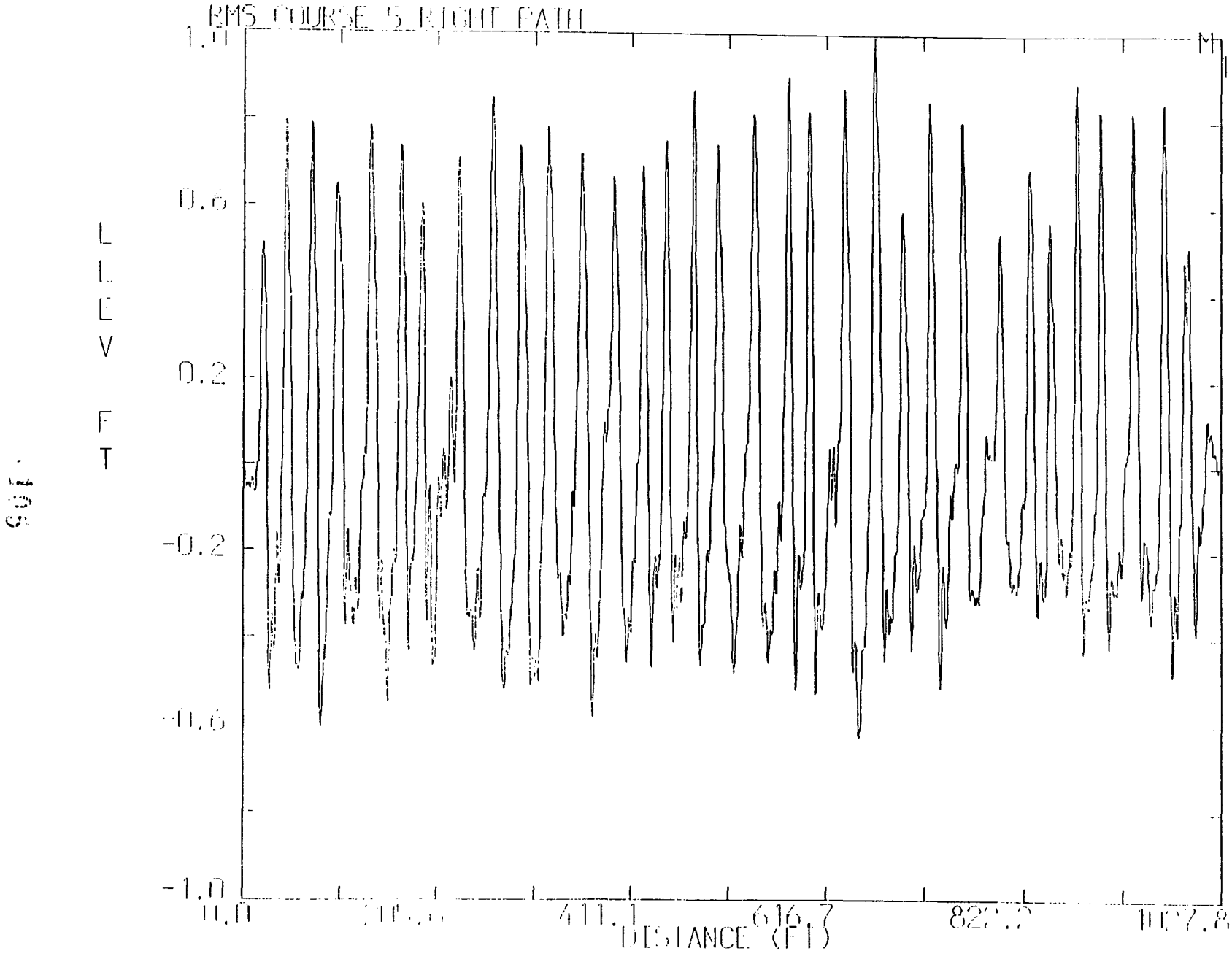
RMS COURSE 5 RIGHT PATH
1.0
0.6
0.2
-0.2
-0.6
-1.0
LEVEL FT
411.1
616.7
DISTANCE (FT)

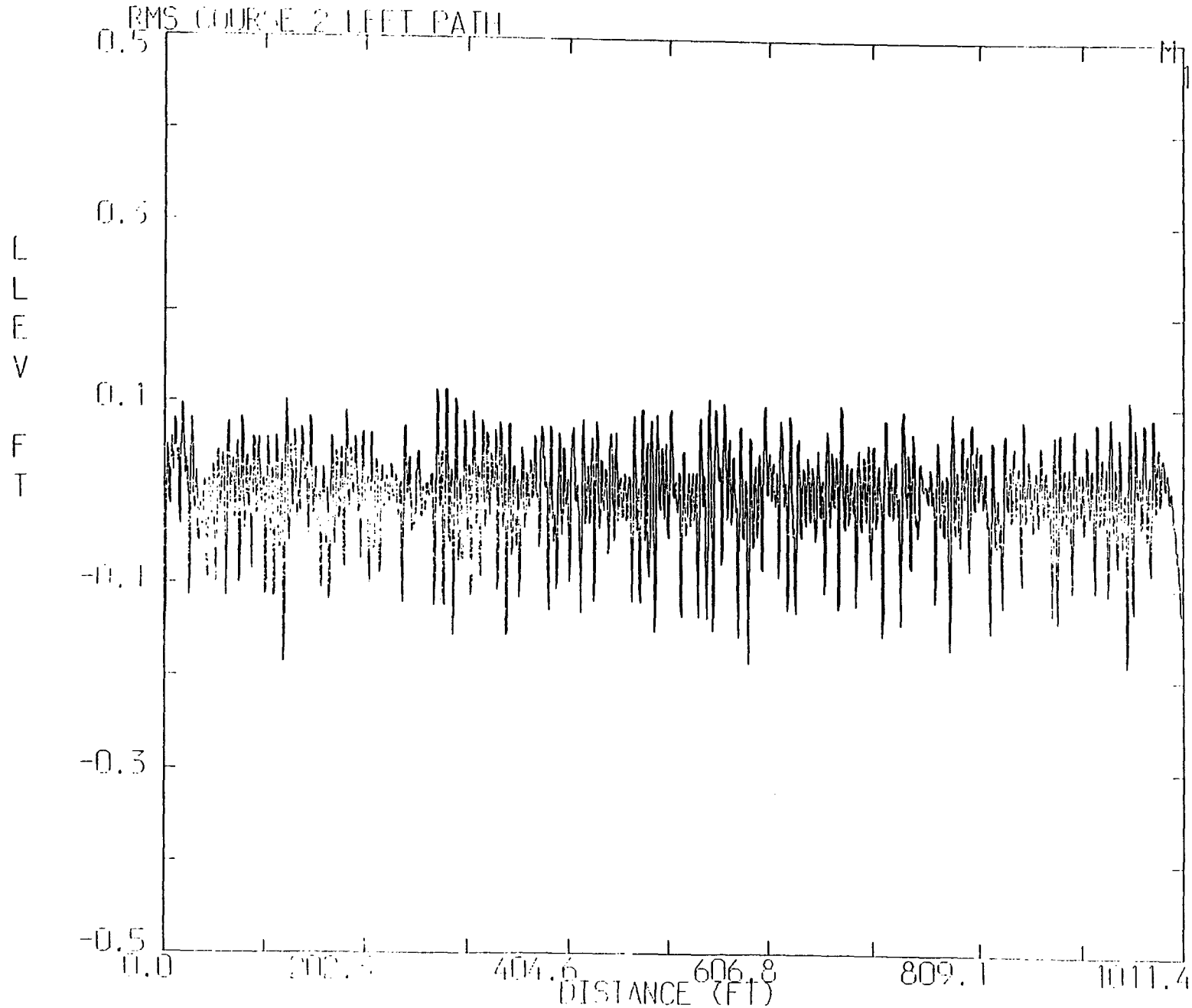
RMS COURSE 2 LEFT PATH
0.5
0.3
0.1
-0.1
-0.3
-0.5
LEVEL FT
0.0
202.3
404.6
606.8
809.1
1011.4
DISTANCE (FT)

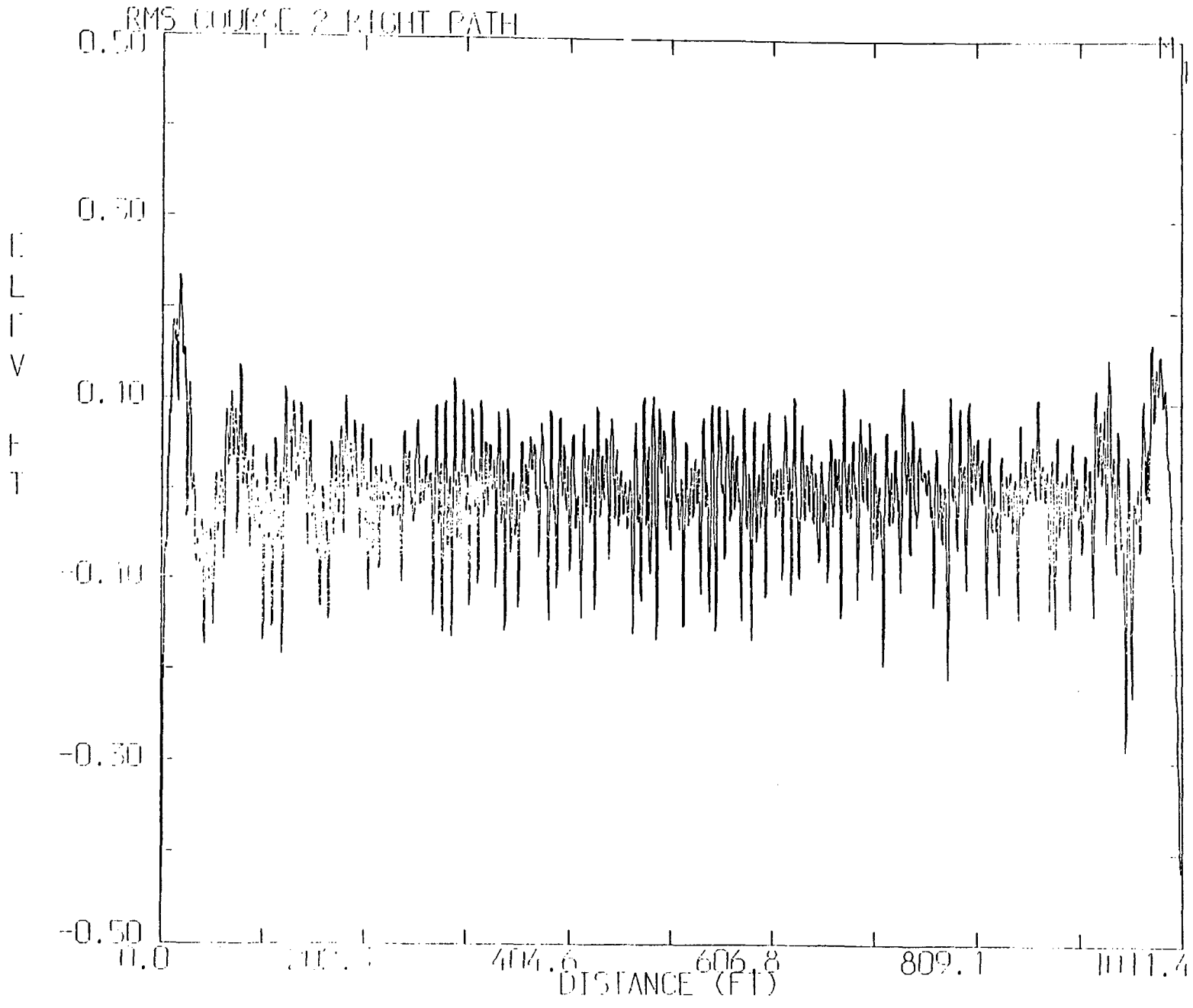
RMS COURSE 2 RIGHT PATH
0.50
0.30
0.10
-0.10
-0.30
-0.50
ELEV FT
0.0
404.6
606.8
809.1
1011.4
DISTANCE (FT)

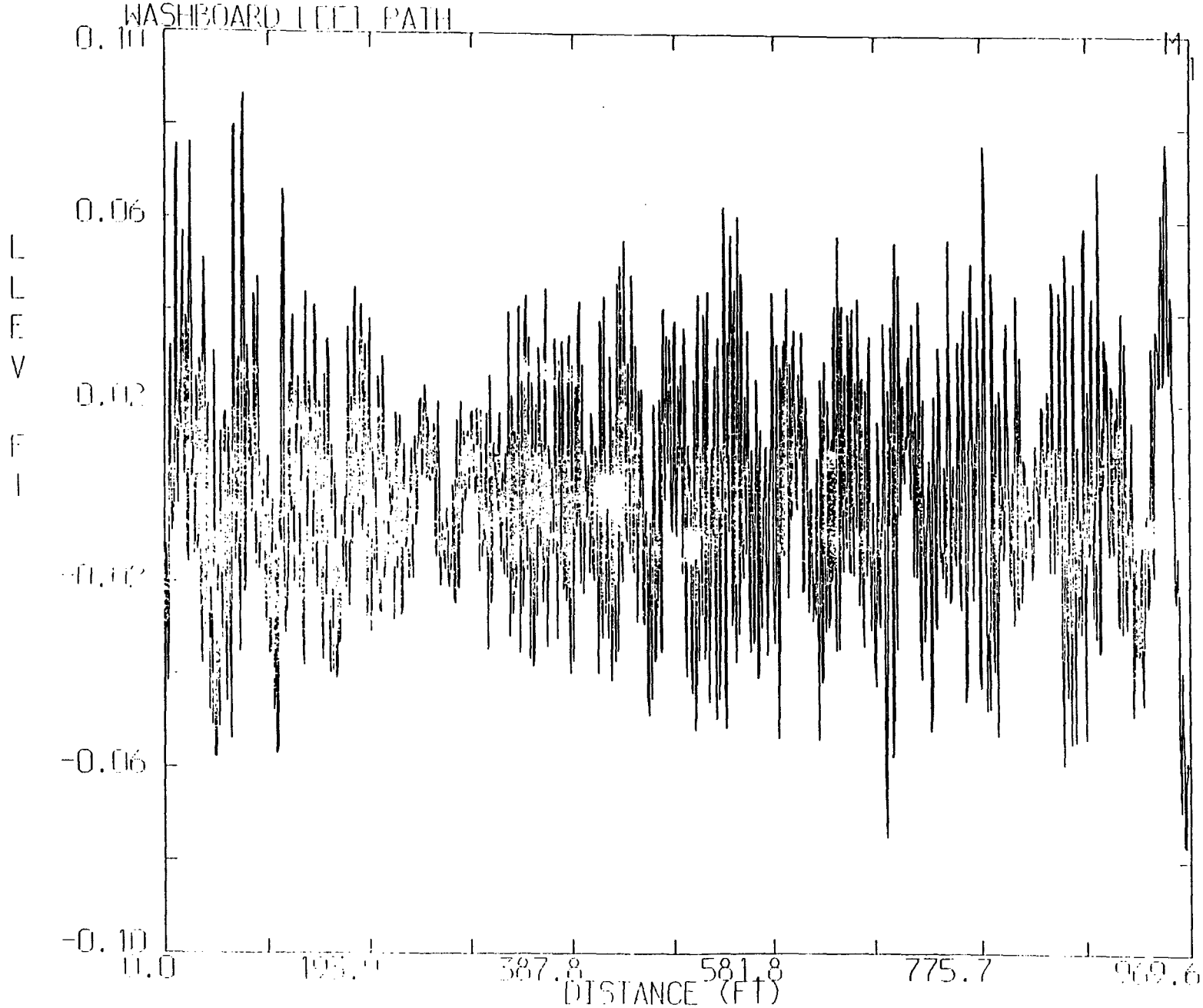
WASHBOARD TEST PATH
0.10
0.06
0.02
-0.06
-0.10
ELEV FT
0.0
193.9
387.8
581.8
775.7
969.6
DISTANCE (FT)

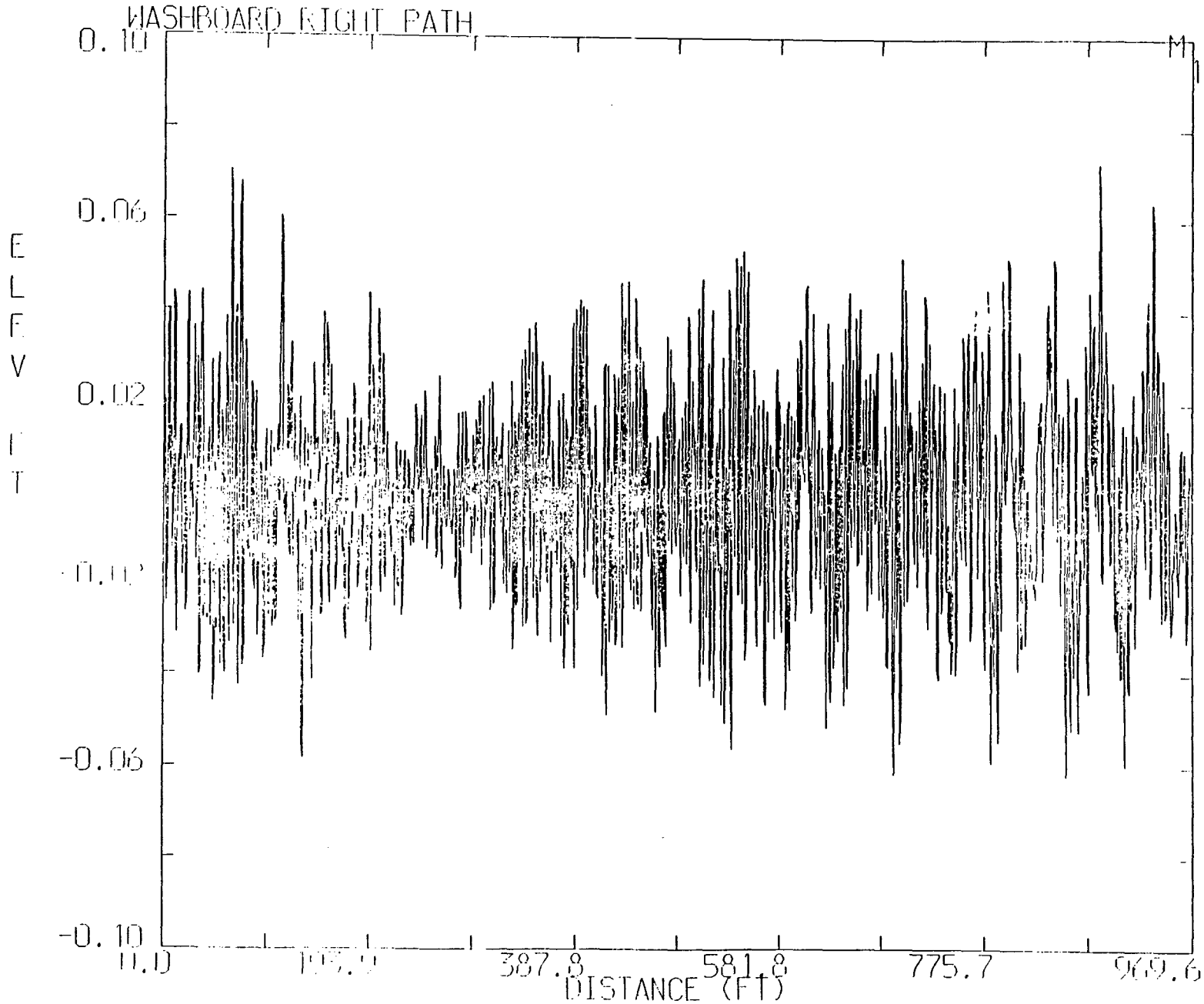
WASHBOARD RIGHT PATH
0.10
0.06
0.02
-0.06
-0.10
ELEVATION
0.0
387.8
581.8
775.7
969.6
DISTANCE (Ft)

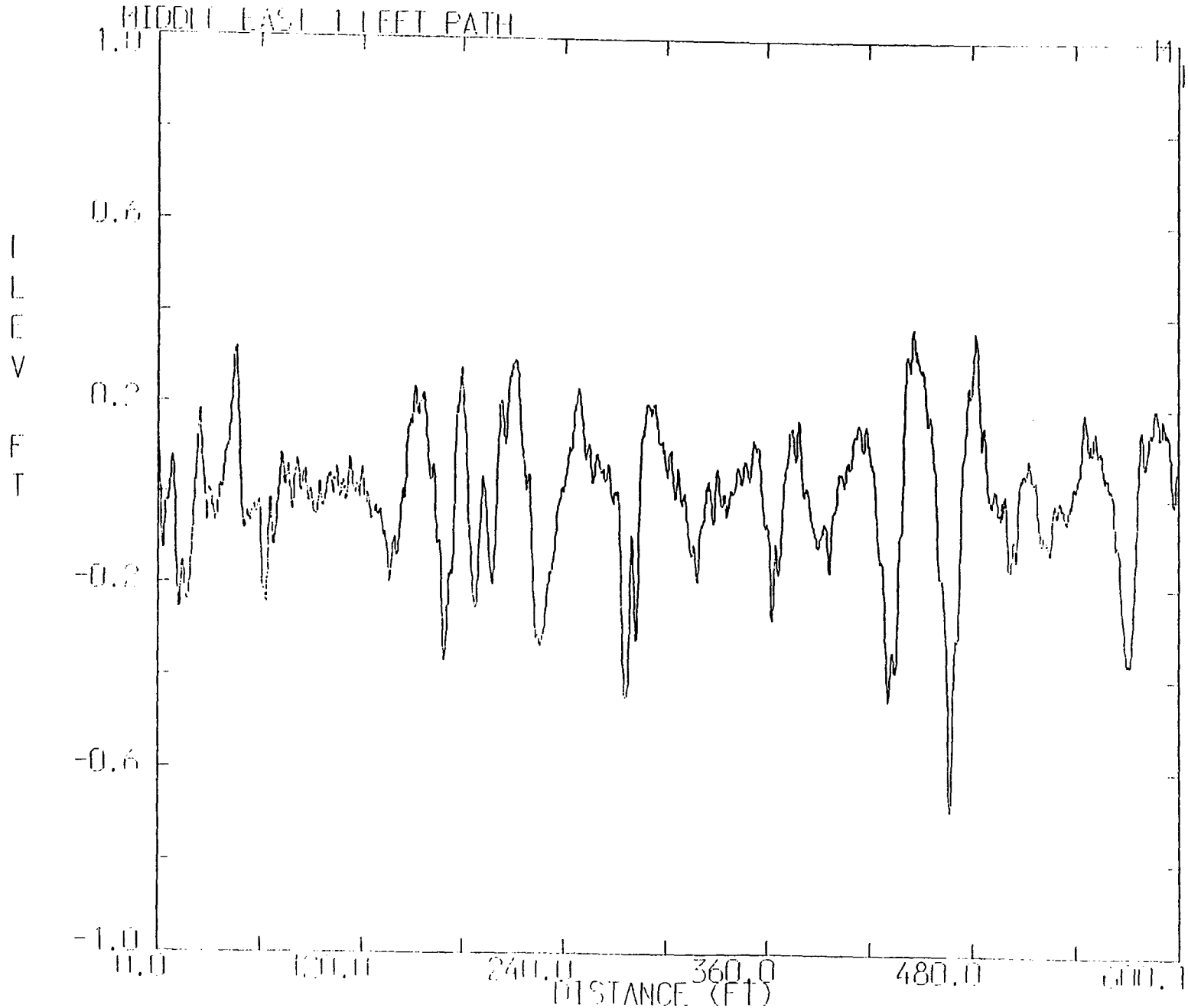
MIDDLE EAST LEFT PATH
1.0
0.6
0.2
-0.2
-0.6
-1.0
ELEV FT
0.0
120.0
240.0
360.0
480.0
600.0
DISTANCE (FT)

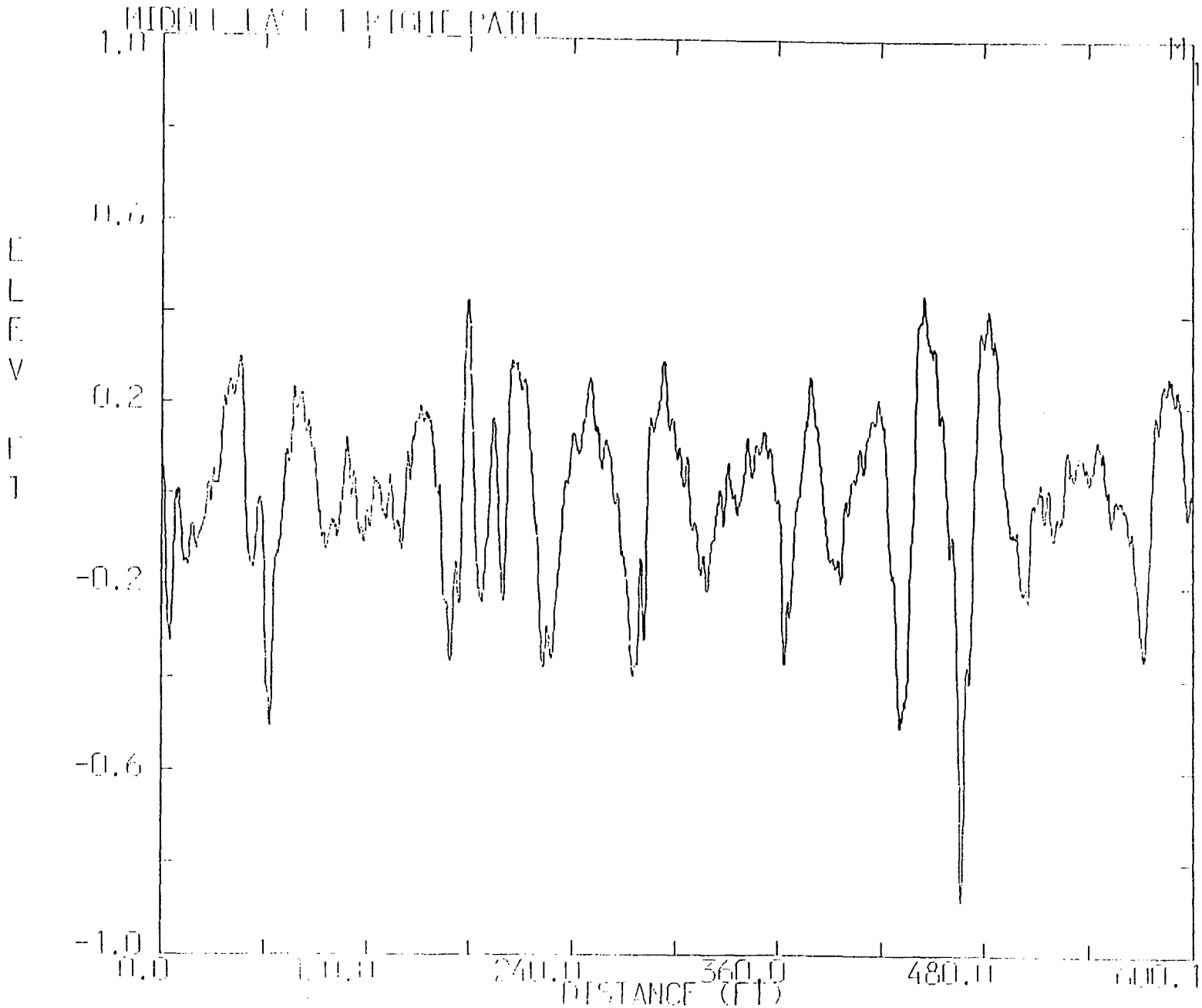
MIDDLE_LANE_FLIGHT_PATH
1.0
0.6
0.2
-0.2
-0.6
-1.0
ELEV FT
0.0
240.0
360.0
480.0
DISTANCE (FT)

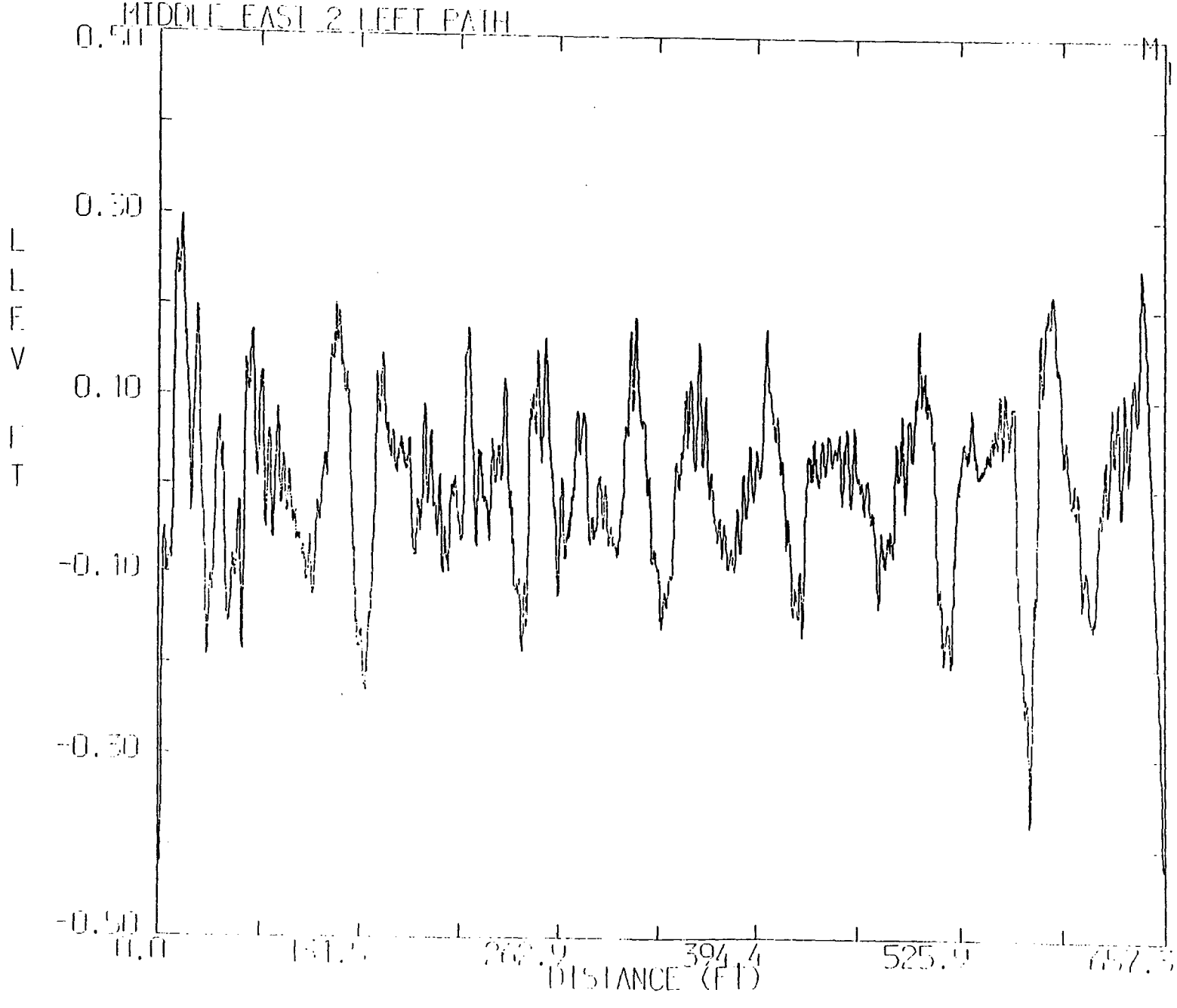
MIDDLE EAST 2 FEET PATH
0.50
0.30
0.10
-0.10
-0.30
-0.50
LEVEL FT
0.0
131.2
262.5
394.4
525.9
657.5
DISTANCE (FT)

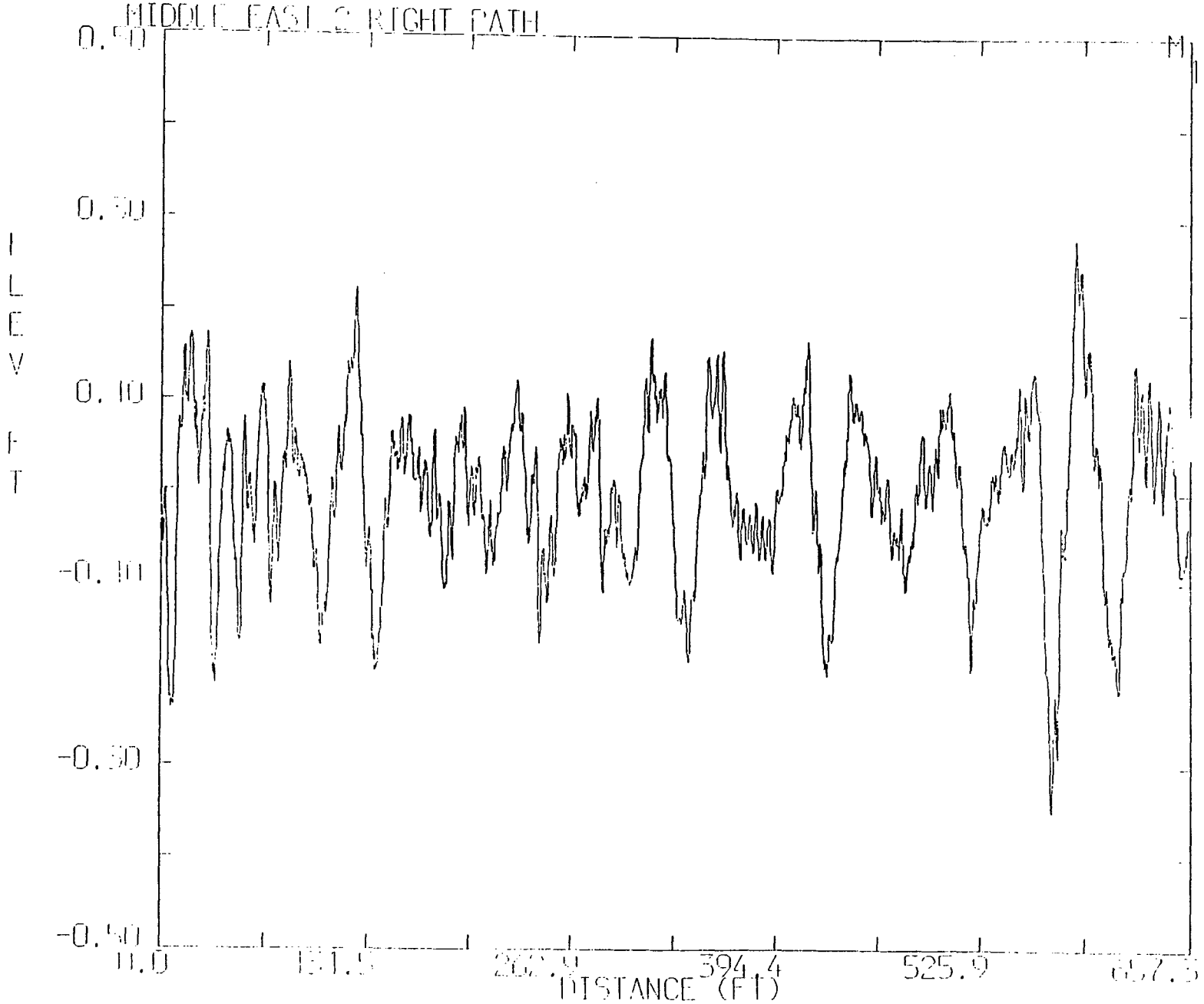
MIDDLE EAST RIGHT PATH
0.50
0.30
0.10
-0.10
-0.30
-0.50
ELEV FT
11.0
131.5
263.9
394.4
525.9
657.3
DISTANCE (FT)

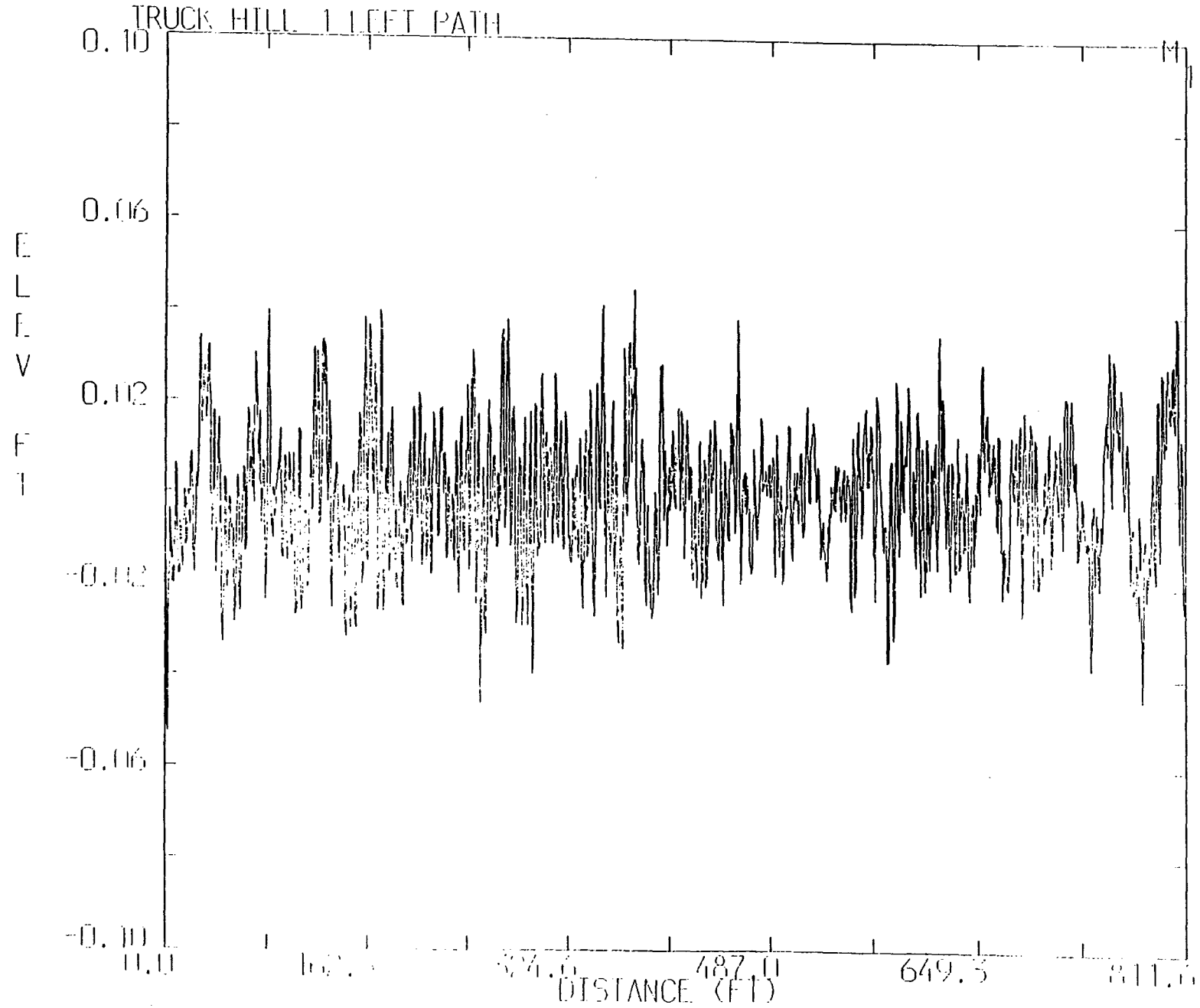
TRUCK HILL 1 LEFT PATH
0.10
0.06
0.02
-0.02
-0.06
-0.10
ELEV FT
0.0
324.0
487.0
649.5
811.0
DISTANCE (FT)

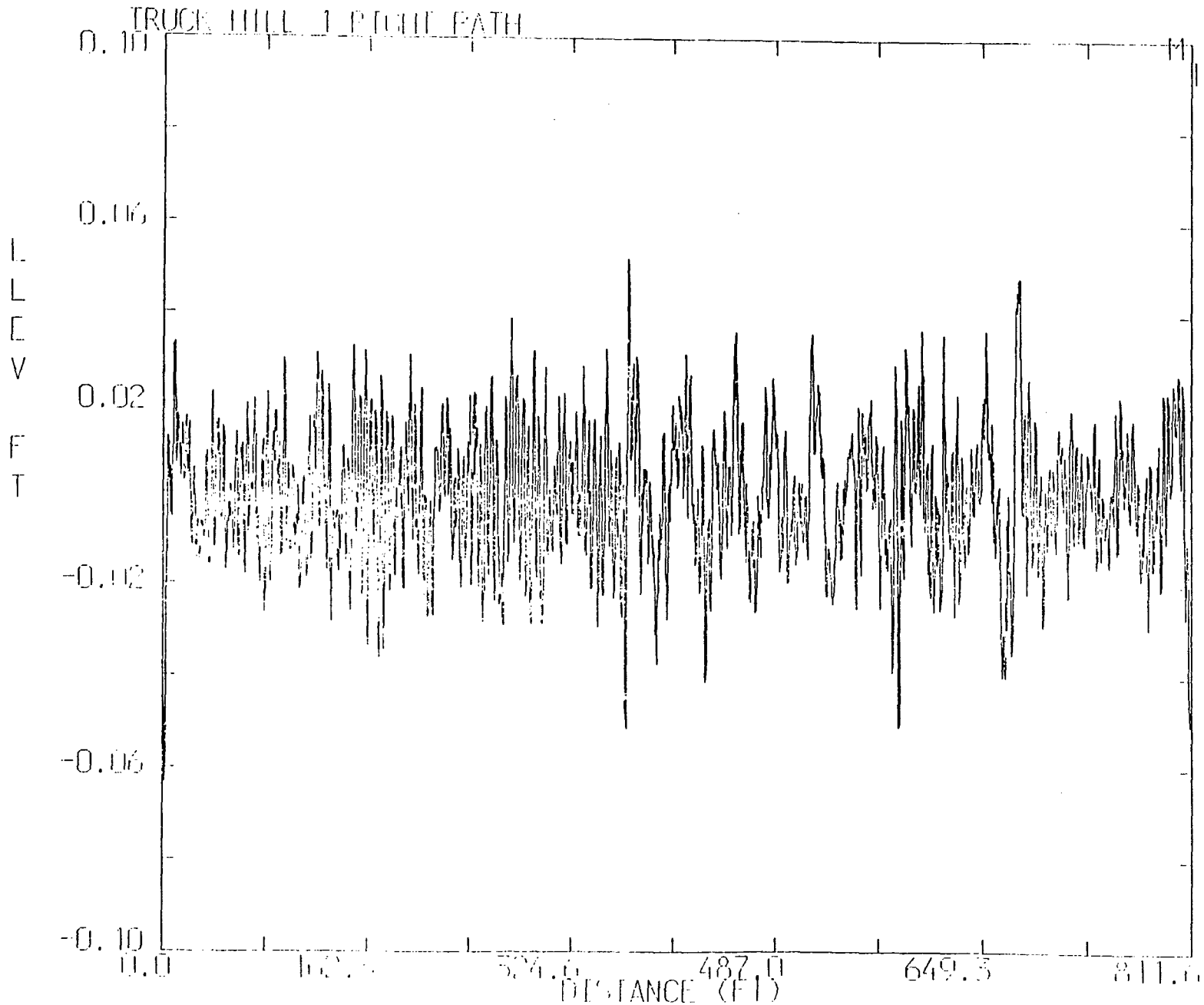
TRUCK HILL 1 PROFILE PATH
0.10
0.06
0.02
-0.02
-0.06
-0.10
LEVEL FT
0.0
324.6
487.0
649.3
811.6
DISTANCE (FT)

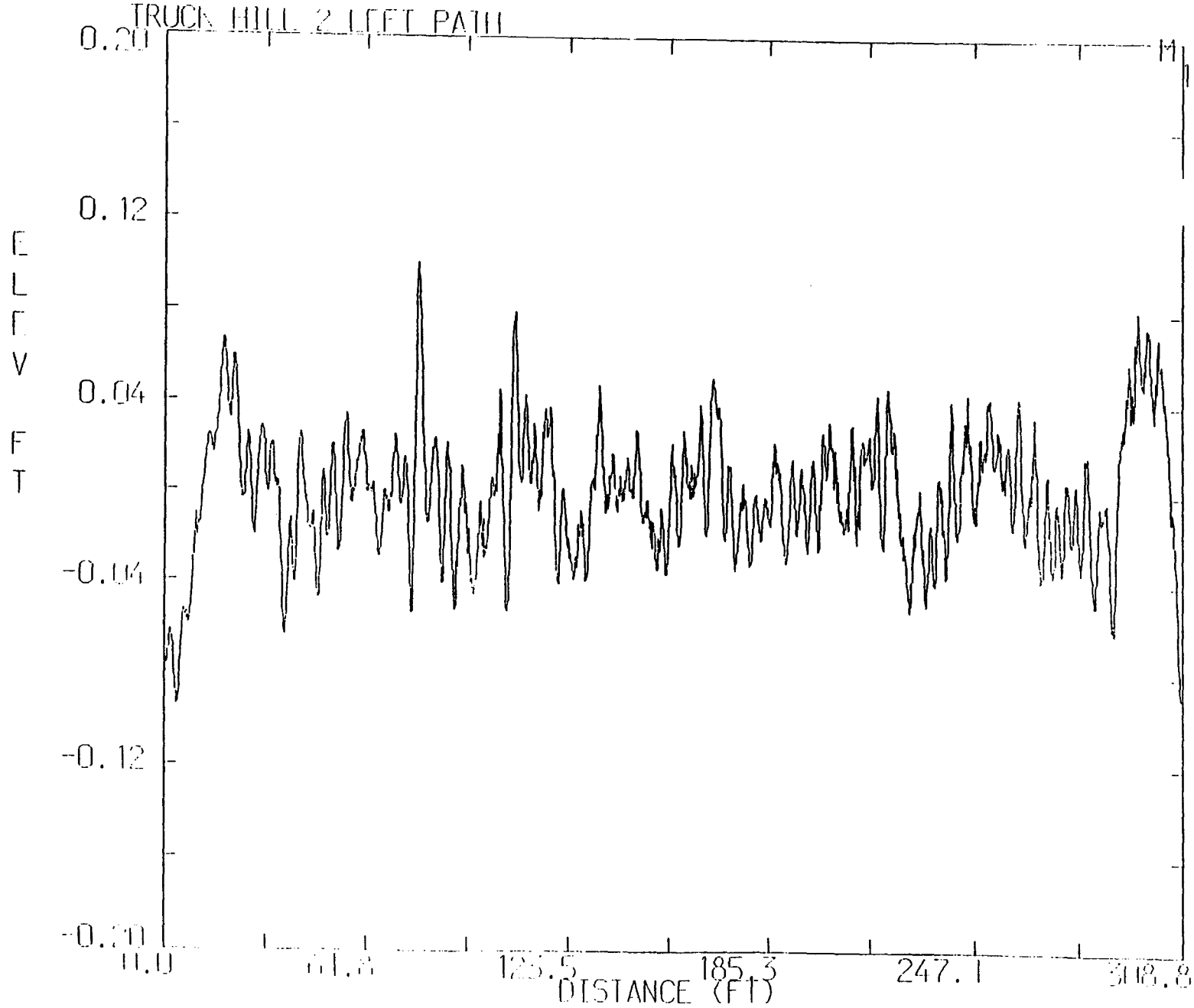
TRUCK HILL 2 LEFT PATH
0.20
0.12
0.04
-0.04
-0.12
-0.20
ELEV FT
0.0
61.8
123.5
185.3
247.1
308.8
DISTANCE (FT)

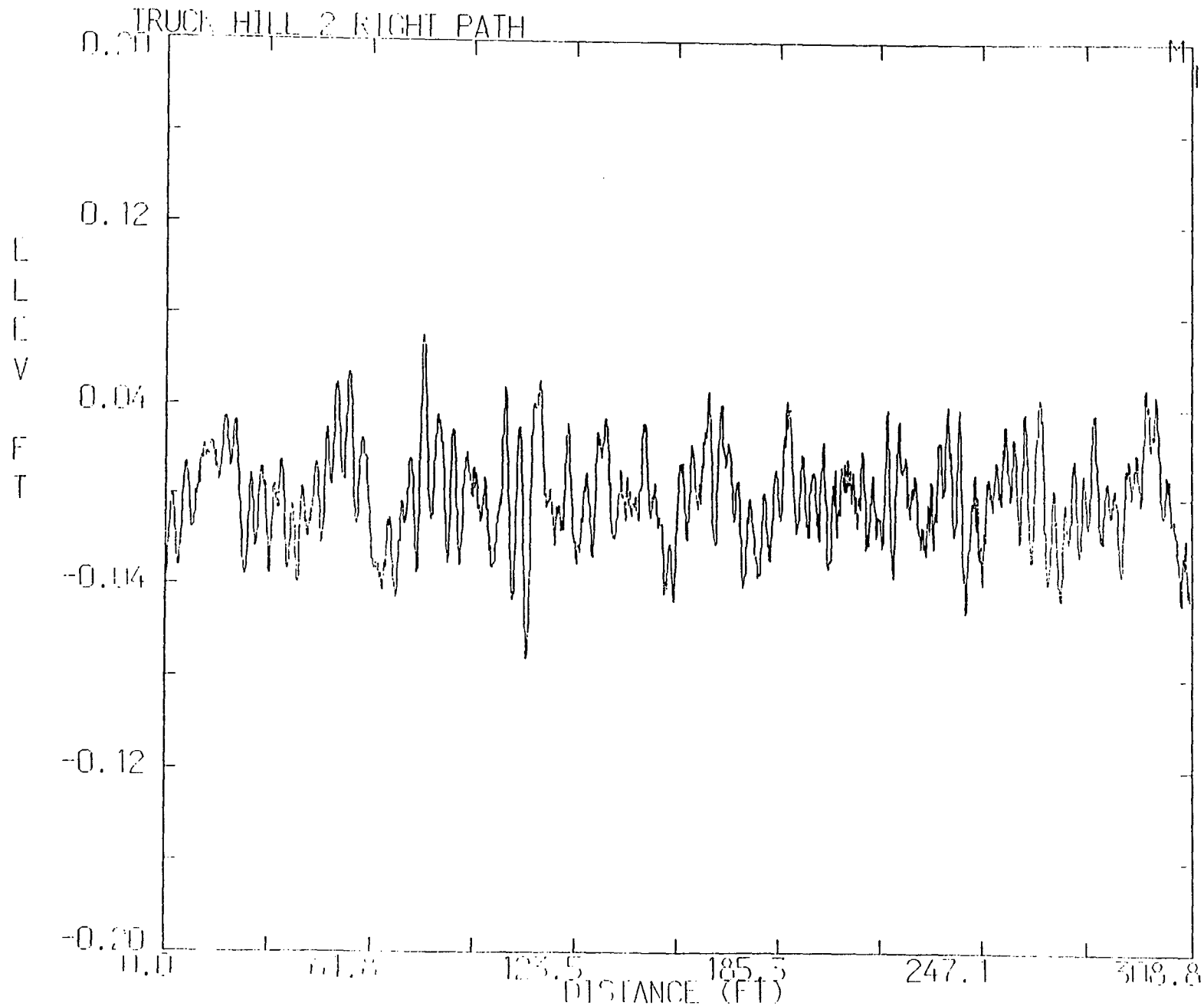
TRUCK HILL 2 RIGHT PATH
0.20
0.12
0.04
-0.04
-0.12
-0.20
ELEV FT
0.0
61.8
123.5
185.3
247.1
308.8
DISTANCE (FT)

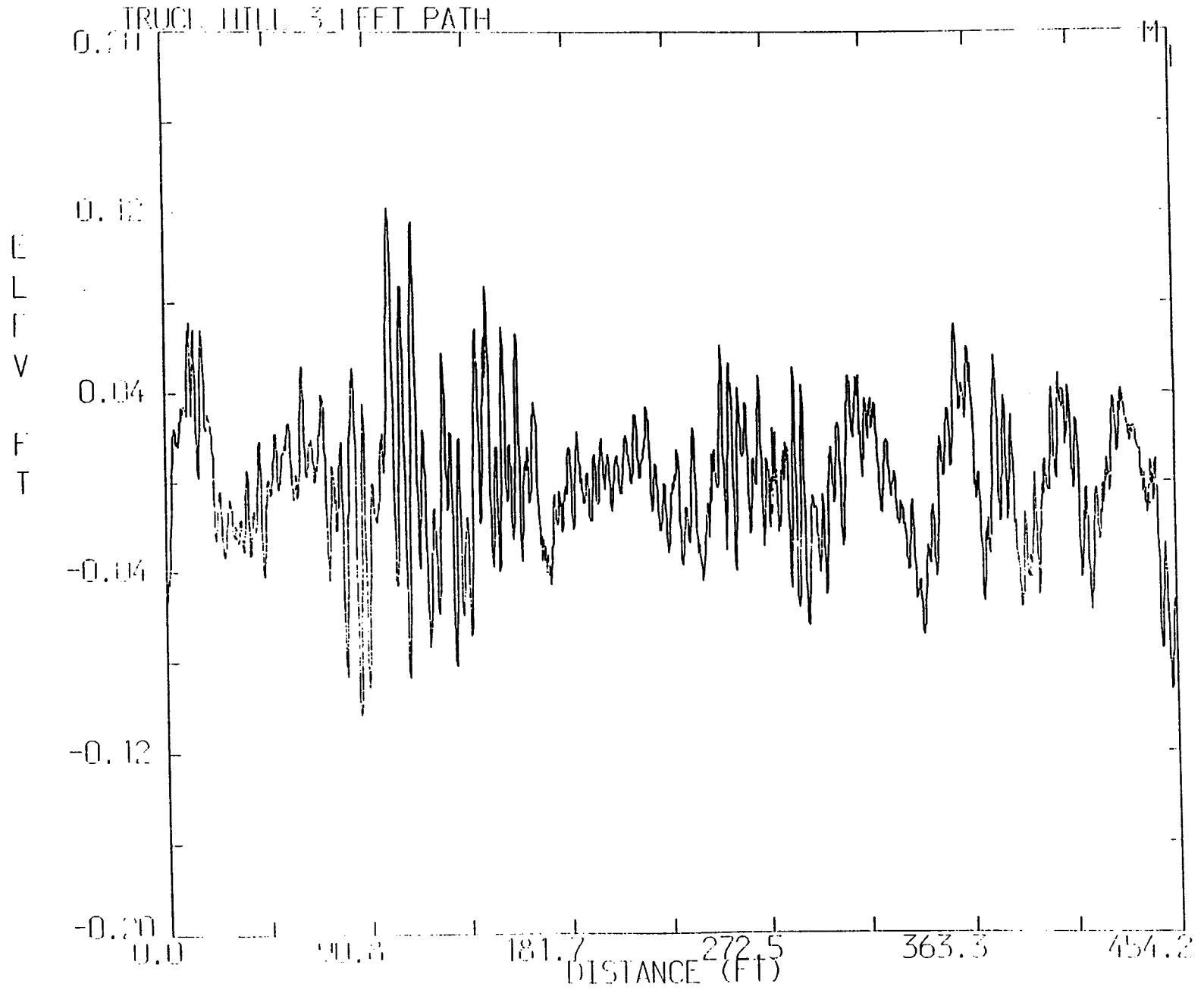
TRUCK HILL 3 LEFT PATH
0.20
0.12
0.04
-0.04
-0.12
-0.20
ELEVATION FT
0.0
90.8
181.7
272.5
363.3
454.2
DISTANCE (FT)

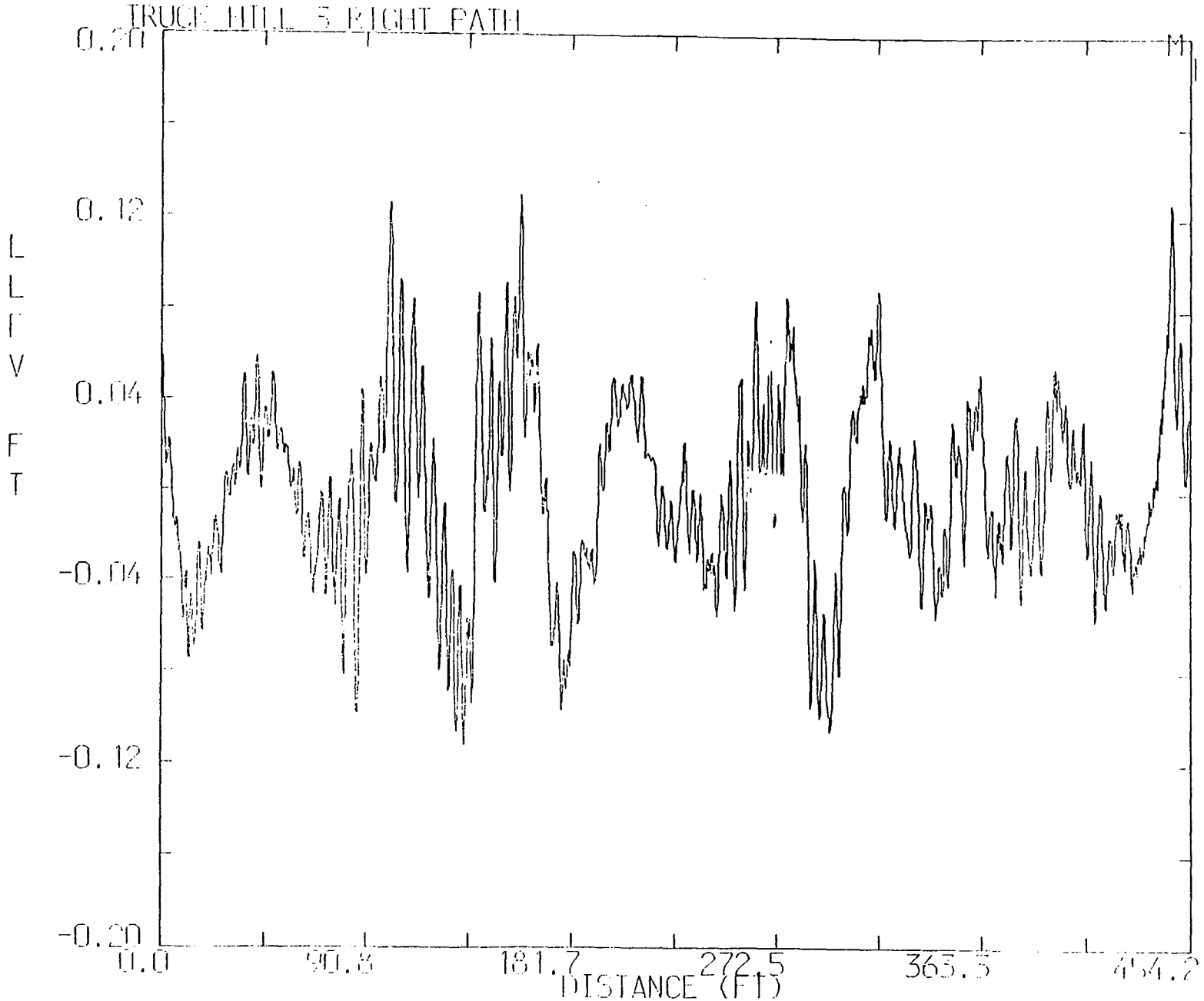
TRUCK HILL 5 RIGHT PATH
0.20
0.12
0.04
-0.04
-0.12
-0.20
LEVEL FT
0.0
90.8
181.7
272.5
363.3
454.2
DISTANCE (FT)

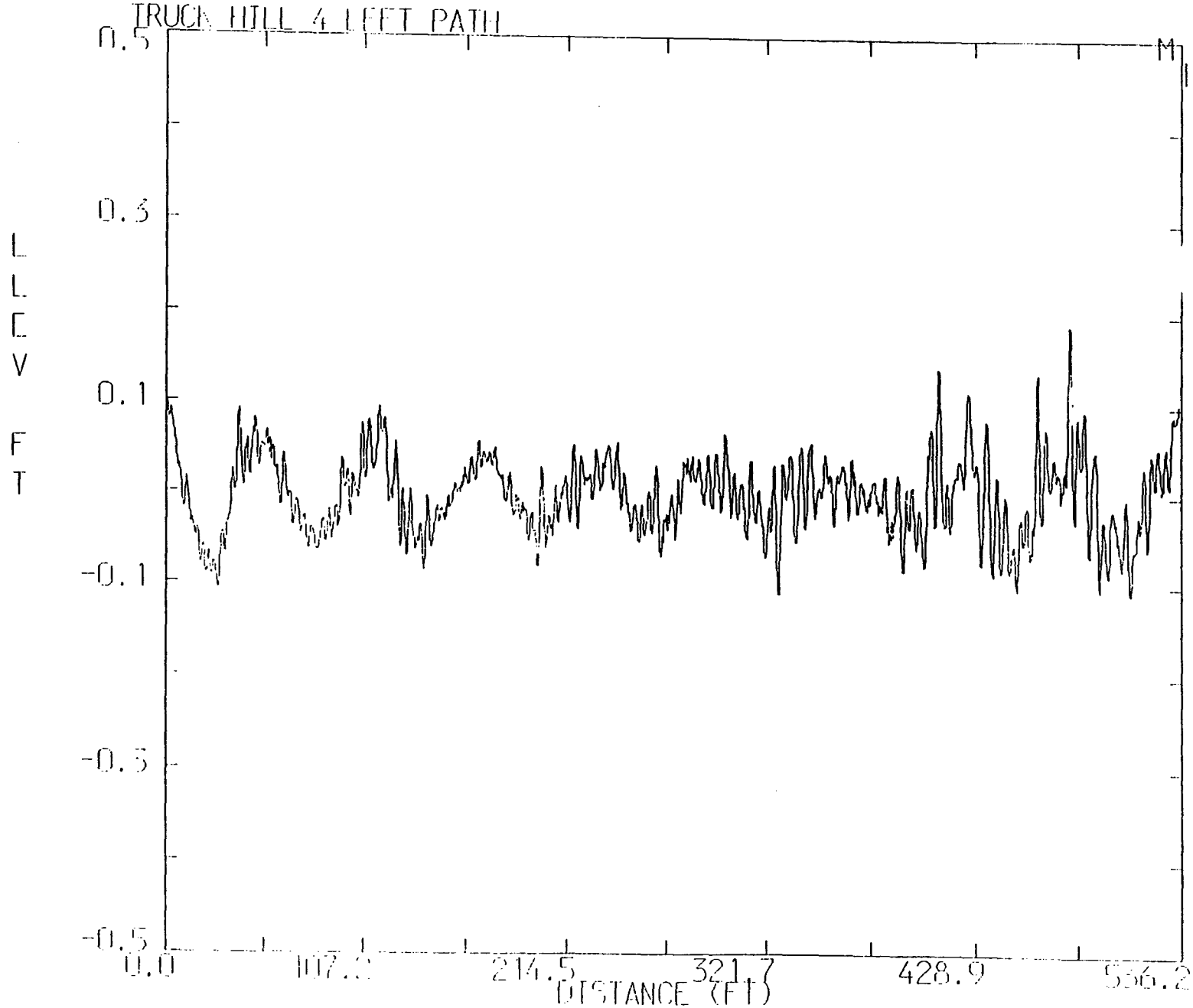
TRUCK HILL 4 LEFT PATH
0.5
0.3
0.1
-0.1
-0.3
-0.5
LEVEL FT
0.0
107.2
214.5
321.7
428.9
536.2
DISTANCE (FT)

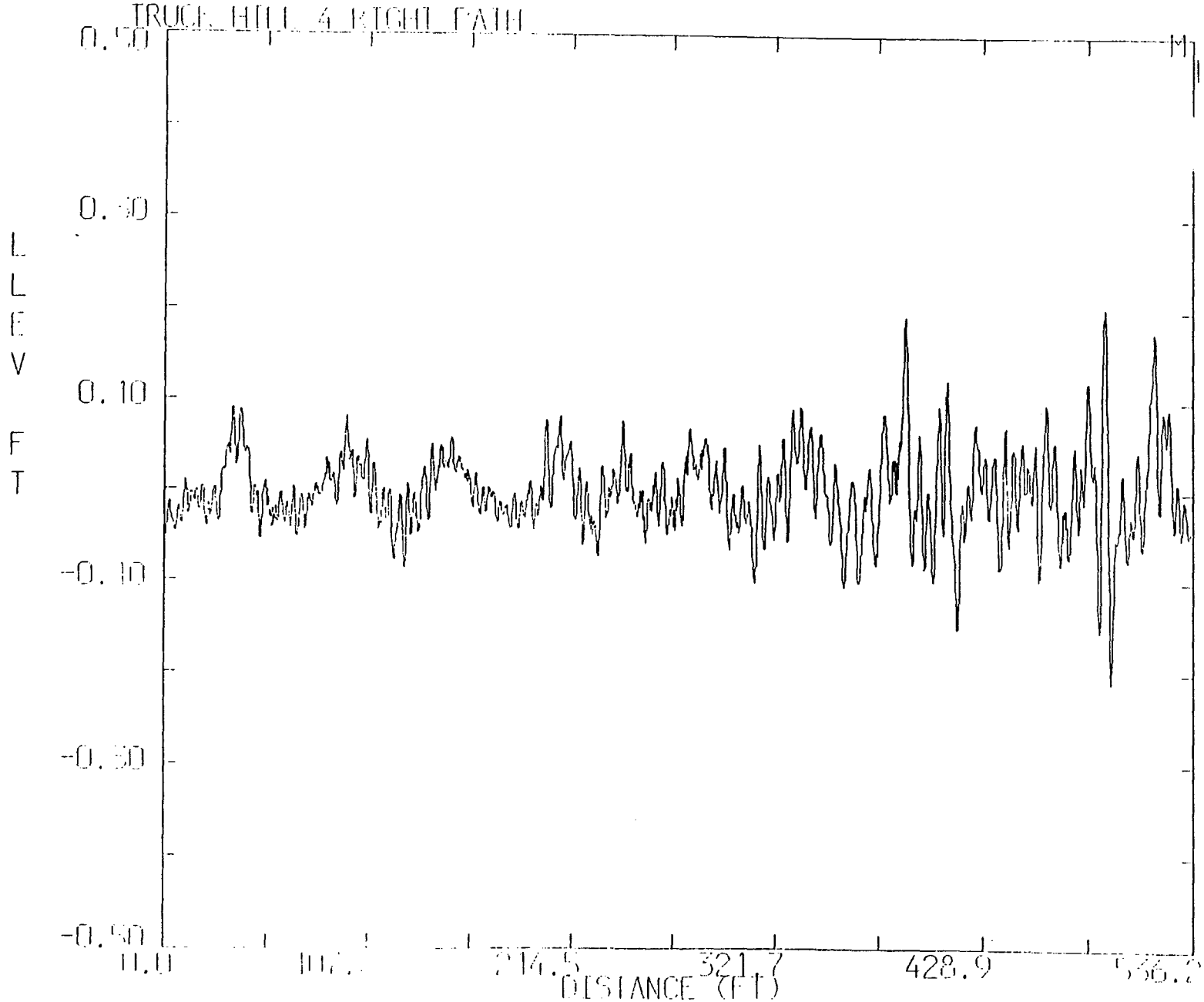
TRUCK HILL 4 RIGHT PATH
0.50
0.30
0.10
-0.10
-0.30
-0.50
LEVEL FT
214.5
321.7
428.9
DISTANCE (FT)

APPENDIX C

WAVE-NUMBER SPECTRA - ROD AND LEVEL

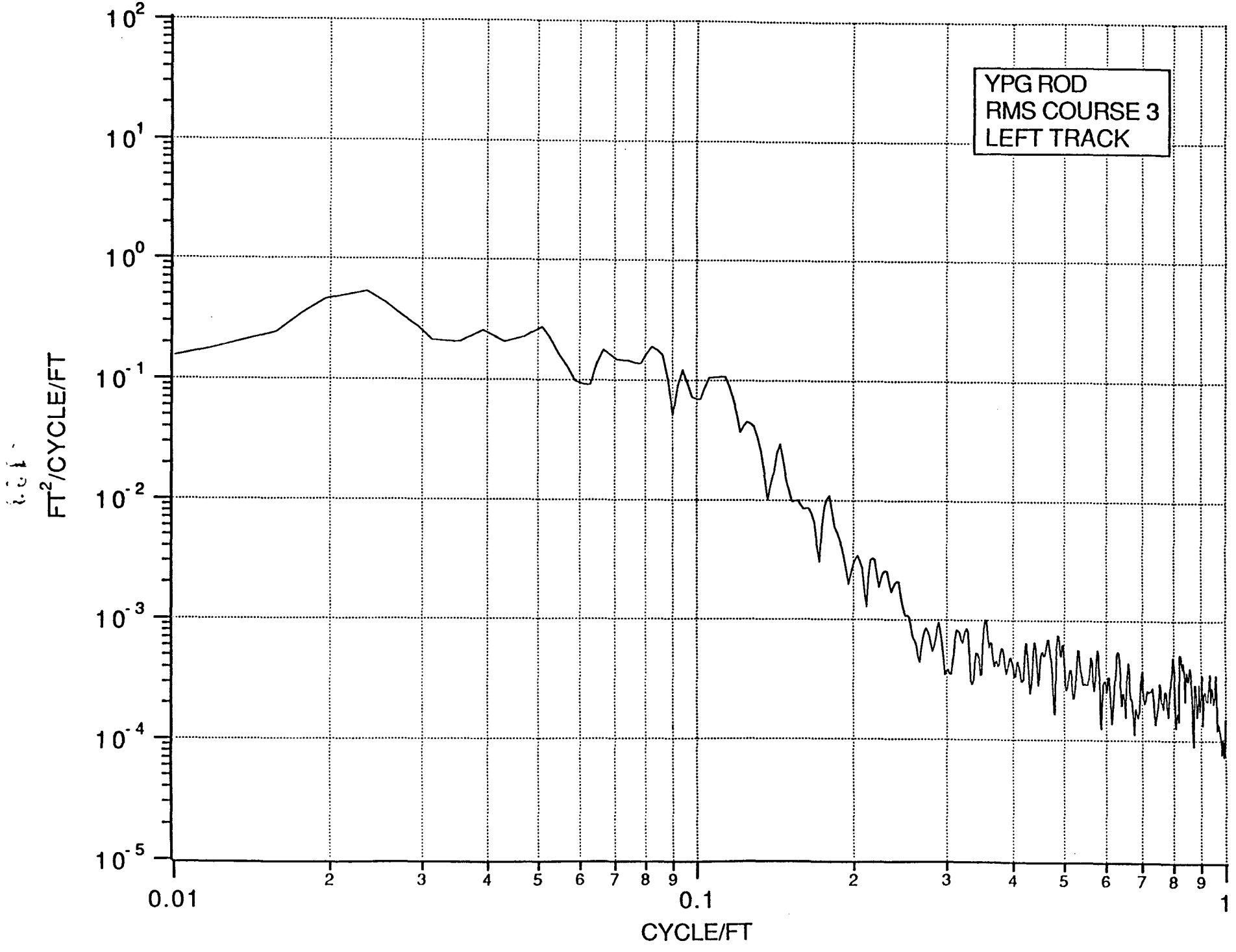
YPG ROD
RMS COURSE 3
LEFT TRACK
10^2
10^1
10^0
10^{-1}
10^{-2}
10^{-3}
10^{-4}
10^{-5}
FT^2/CYCLE/FT
0.01
0.1
1
2 3 4 5 6 7 8 9
2 3 4 5 6 7 8 9
CYCLE/FT

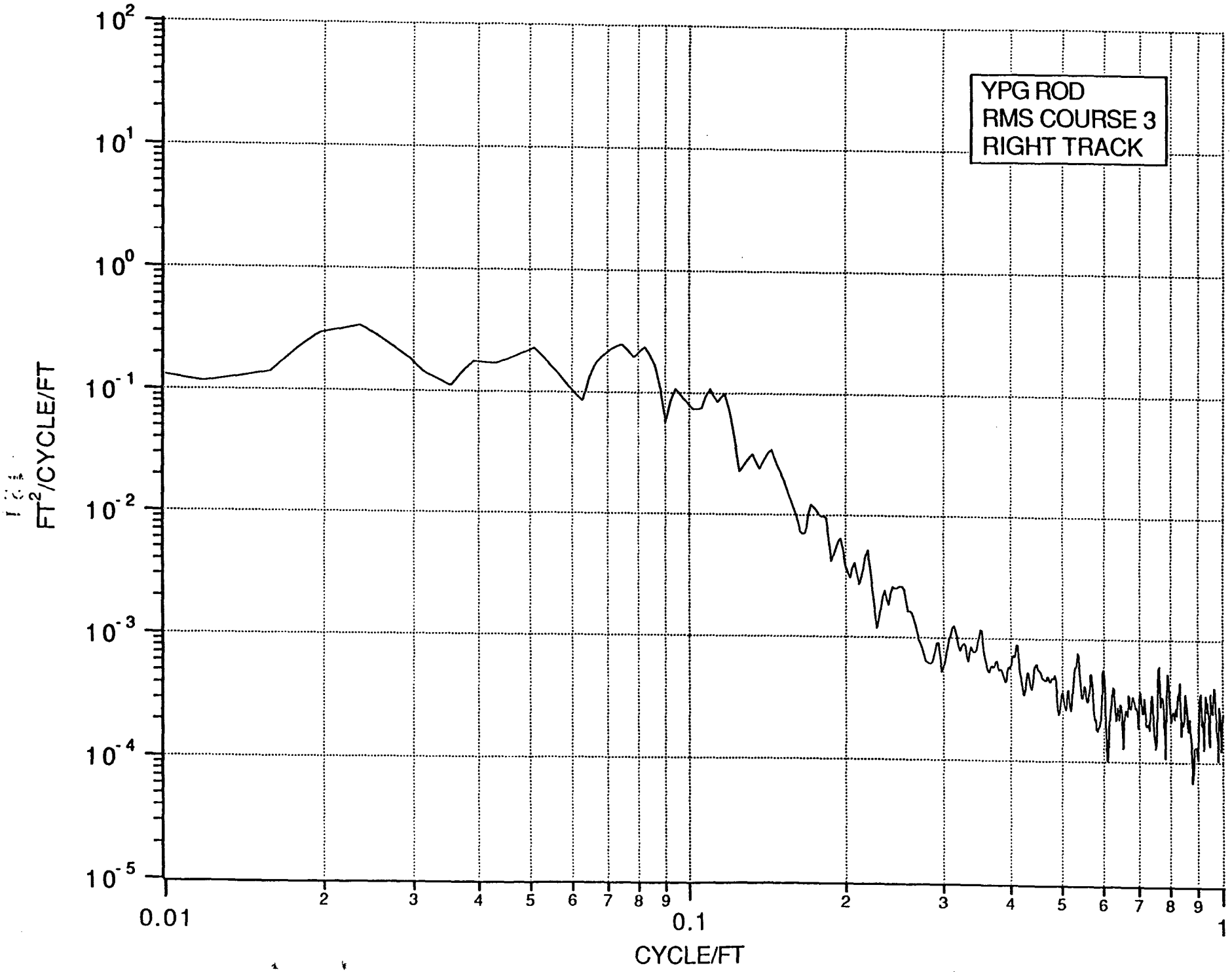
YPG ROD
RMS COURSE 3
RIGHT TRACK
10^2
10^1
10^0
10^{-1}
10^{-2}
10^{-3}
10^{-4}
10^{-5}
FT^2/CYCLE/FT
0.01
0.1
1
2
3
4
5
6
7
8
9
CYCLE/FT

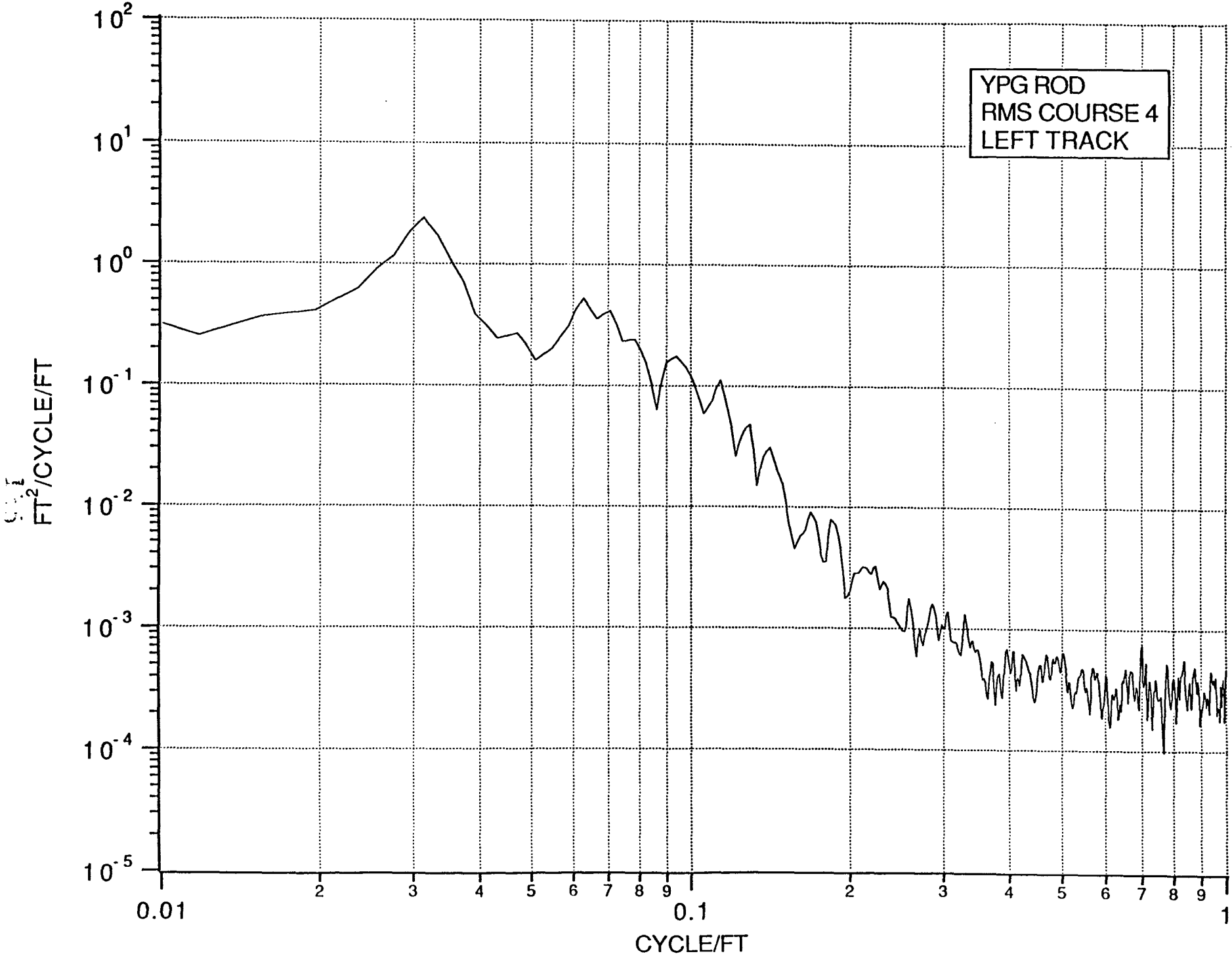
YPG ROD
RMS COURSE 4
LEFT TRACK
10^2
10^1
10^0
10^{-1}
10^{-2}
10^{-3}
10^{-4}
10^{-5}
FT²/CYCLE/FT
0.01
0.1
1
2 3 4 5 6 7 8 9
2 3 4 5 6 7 8 9
CYCLE/FT

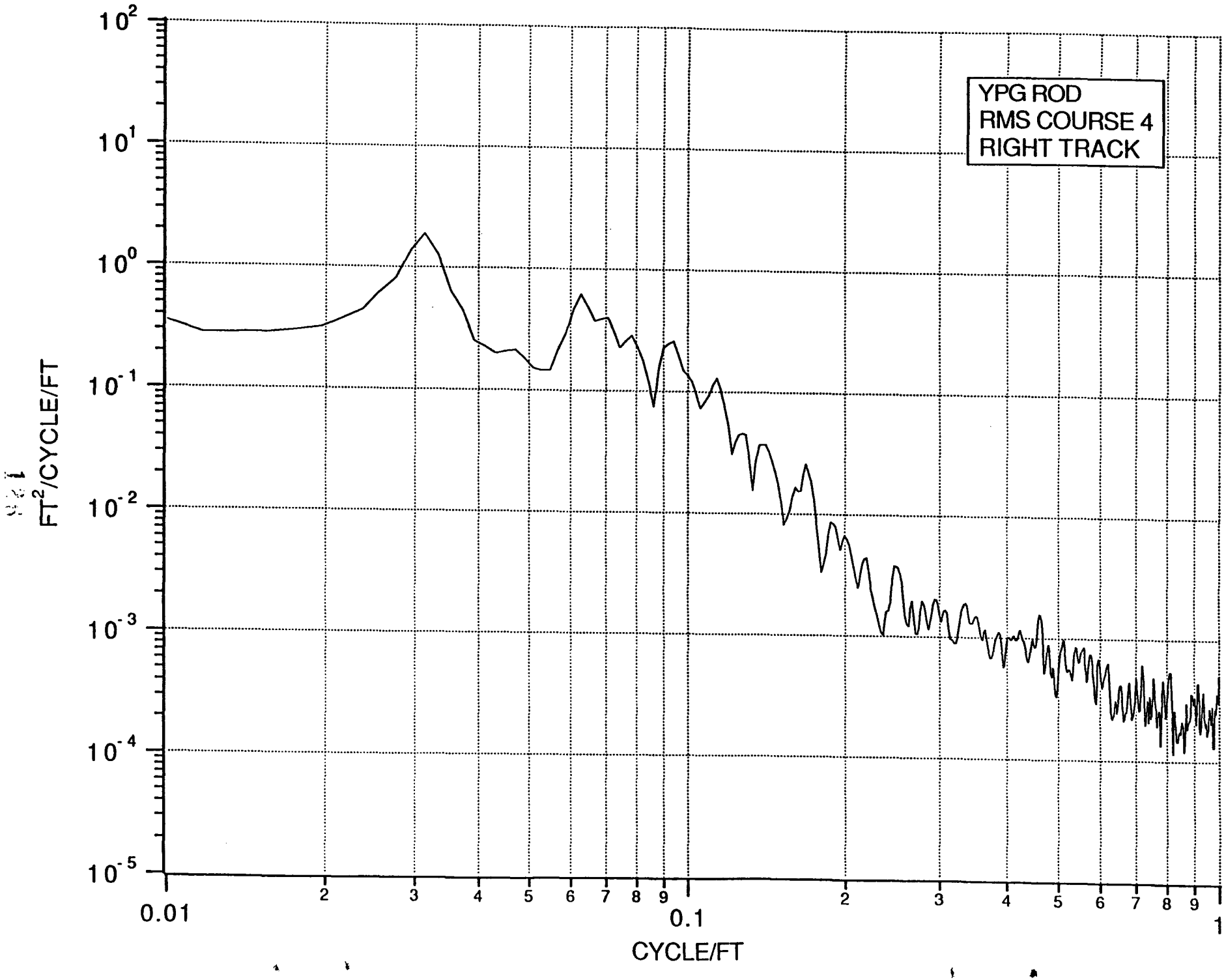
YPG ROD
RMS COURSE 4
RIGHT TRACK
10^2
10^1
10^0
10^{-1}
10^{-2}
10^{-3}
10^{-4}
10^{-5}
FT^2/CYCLE/FT
0.01
0.1
1
2 3 4 5 6 7 8 9
2 3 4 5 6 7 8 9
CYCLE/FT

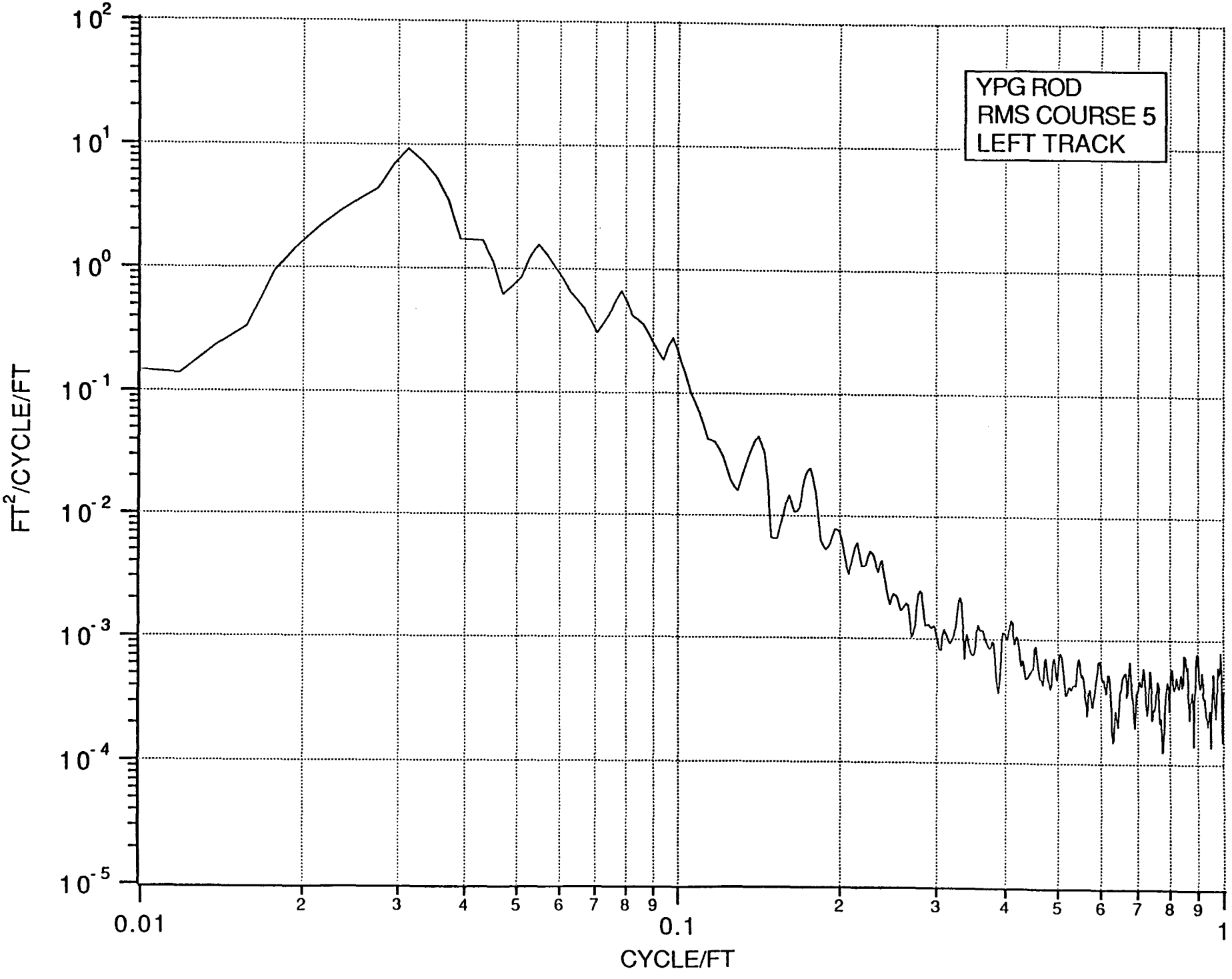
YPG ROD
RMS COURSE 5
LEFT TRACK
FT²/CYCLE/FT
CYCLE/FT
10²
10¹
10⁰
10⁻¹
10⁻²
10⁻³
10⁻⁴
10⁻⁵
0.01
0.1
1
2 3 4 5 6 7 8 9
2 3 4 5 6 7 8 9

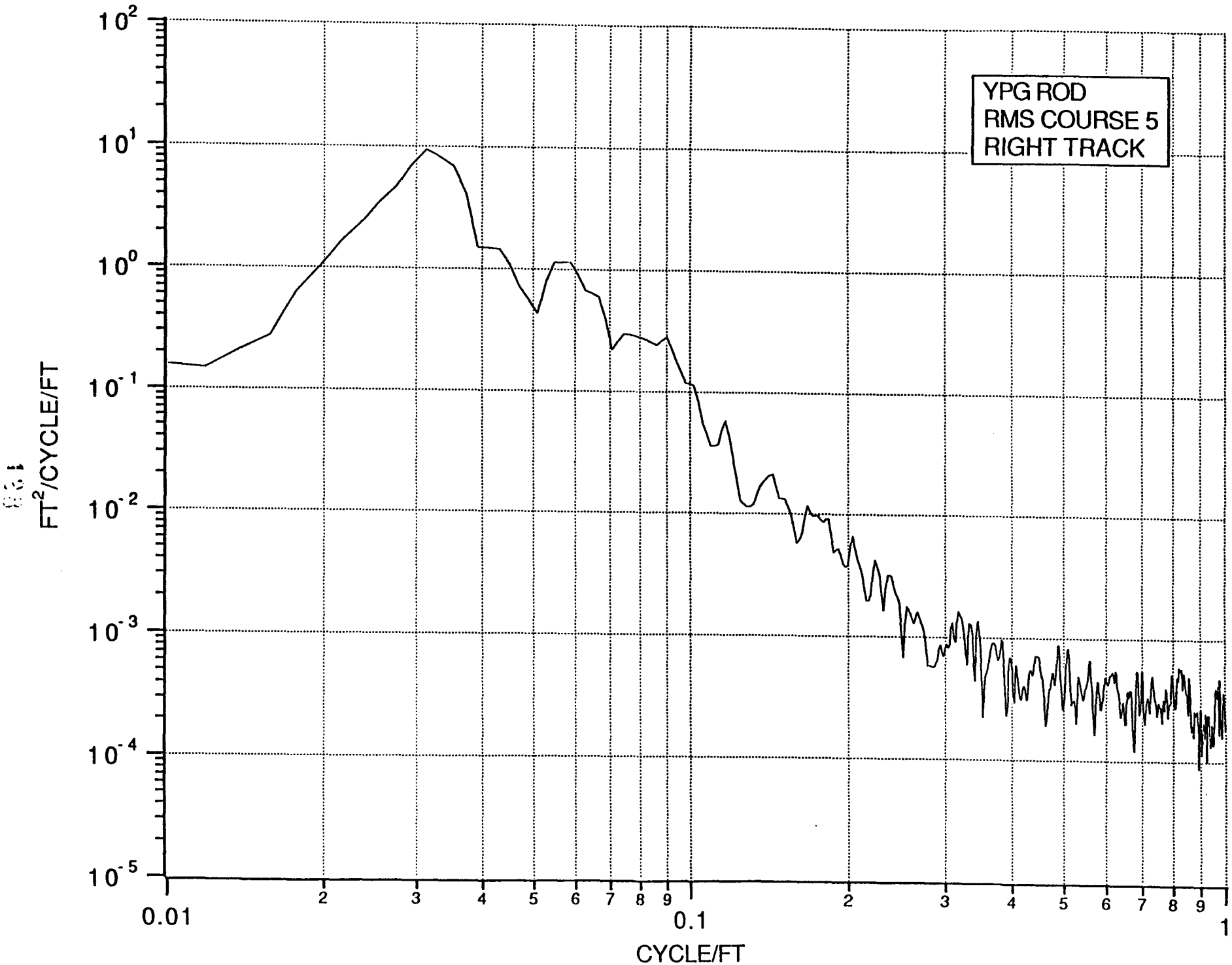
YPG ROD
RMS COURSE 5
RIGHT TRACK
10^2
10^1
10^0
10^{-1}
10^{-2}
10^{-3}
10^{-4}
10^{-5}
FT²/CYCLE/FT
0.01
2 3 4 5 6 7 8 9
0.1
2 3 4 5 6 7 8 9
1
CYCLE/FT

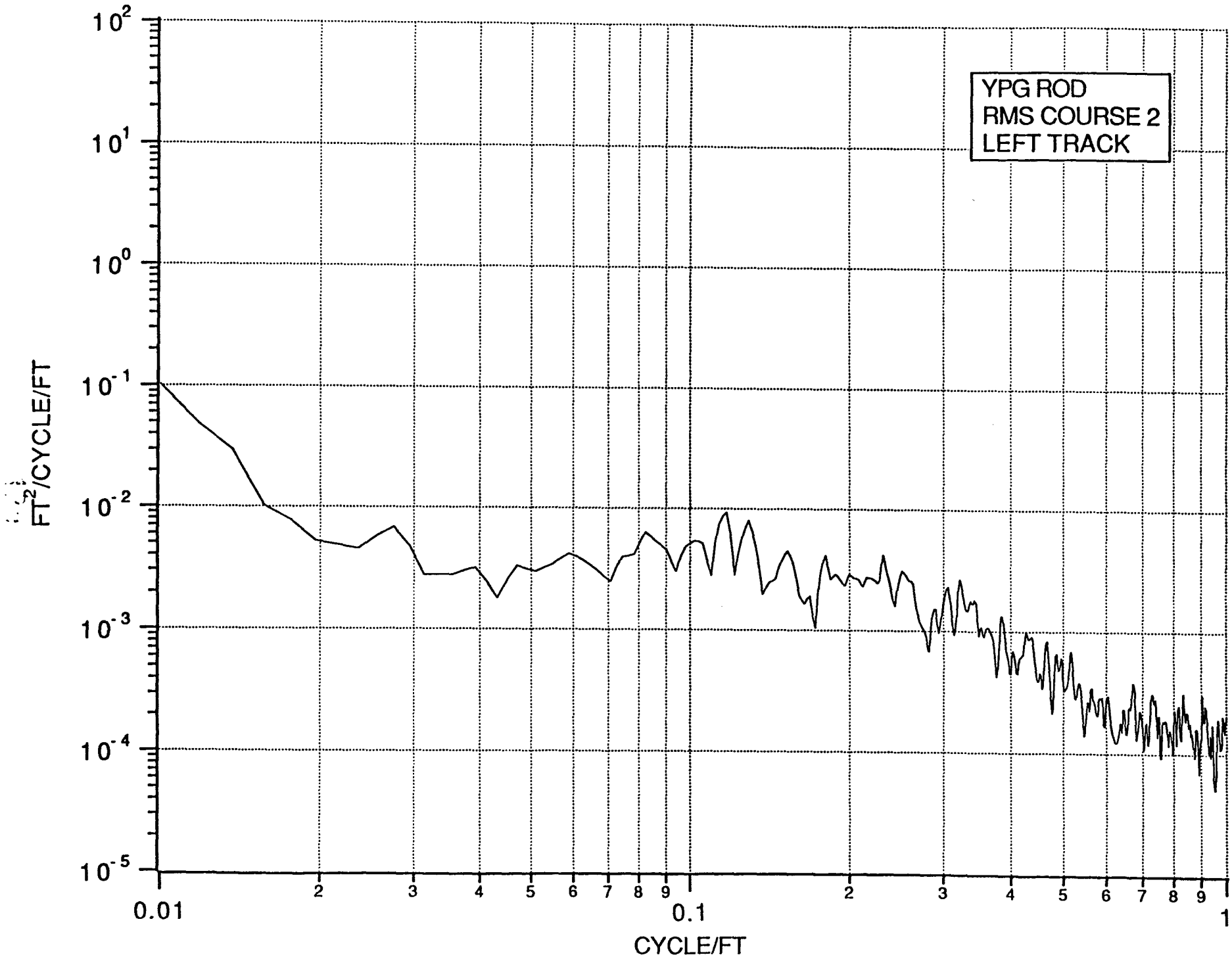
YPG ROD
RMS COURSE 2
LEFT TRACK
10^2
10^1
10^0
10^{-1}
10^{-2}
10^{-3}
10^{-4}
10^{-5}
FT^2/CYCLE/FT
0.01
2 3 4 5 6 7 8 9
0.1
2 3 4 5 6 7 8 9
1
CYCLE/FT

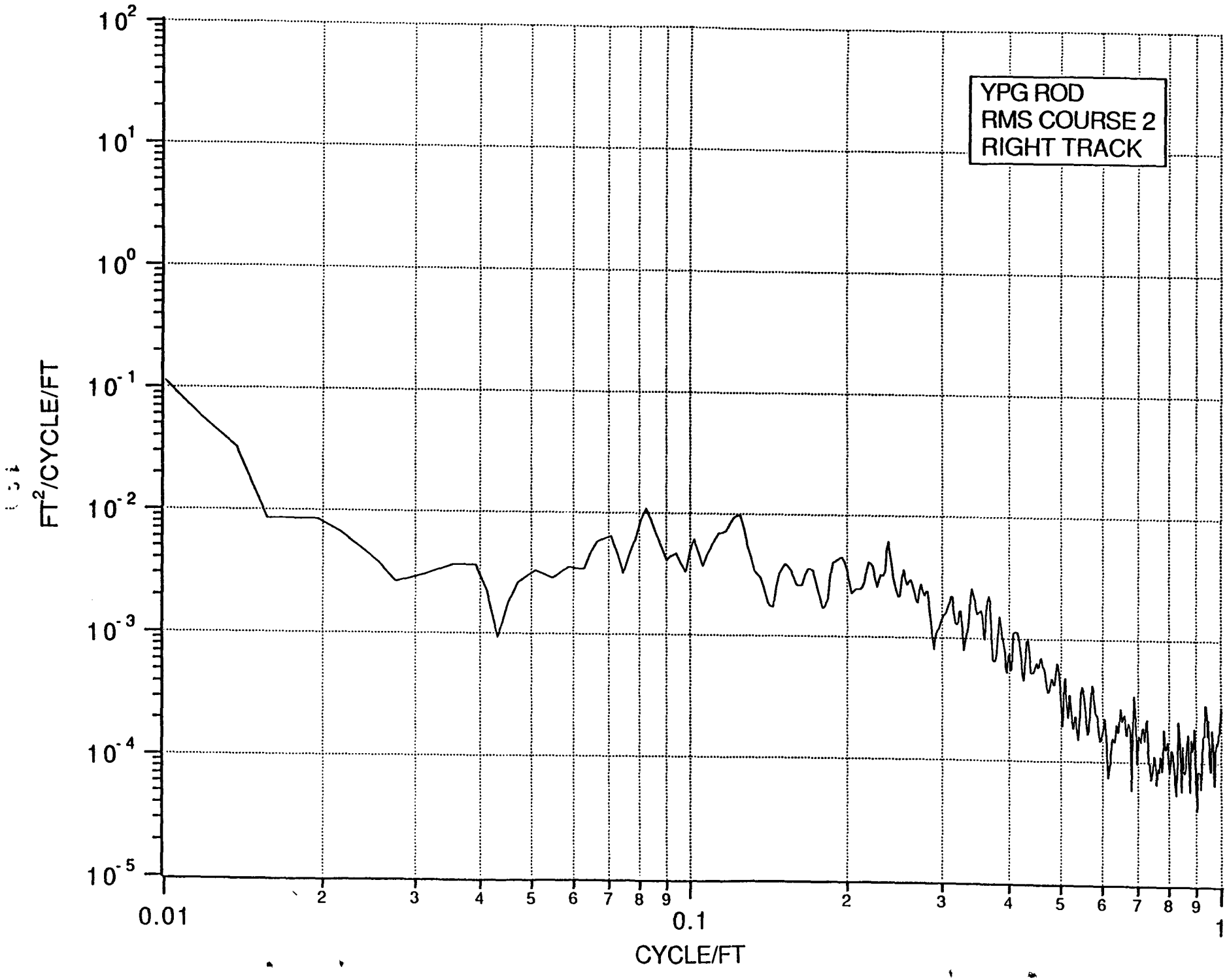
YPG ROD
RMS COURSE 2
RIGHT TRACK
FT²/CYCLE/FT
CYCLE/FT
10²
10¹
10⁰
10⁻¹
10⁻²
10⁻³
10⁻⁴
10⁻⁵
0.01
0.1
1
2
3
4
5
6
7
8
9

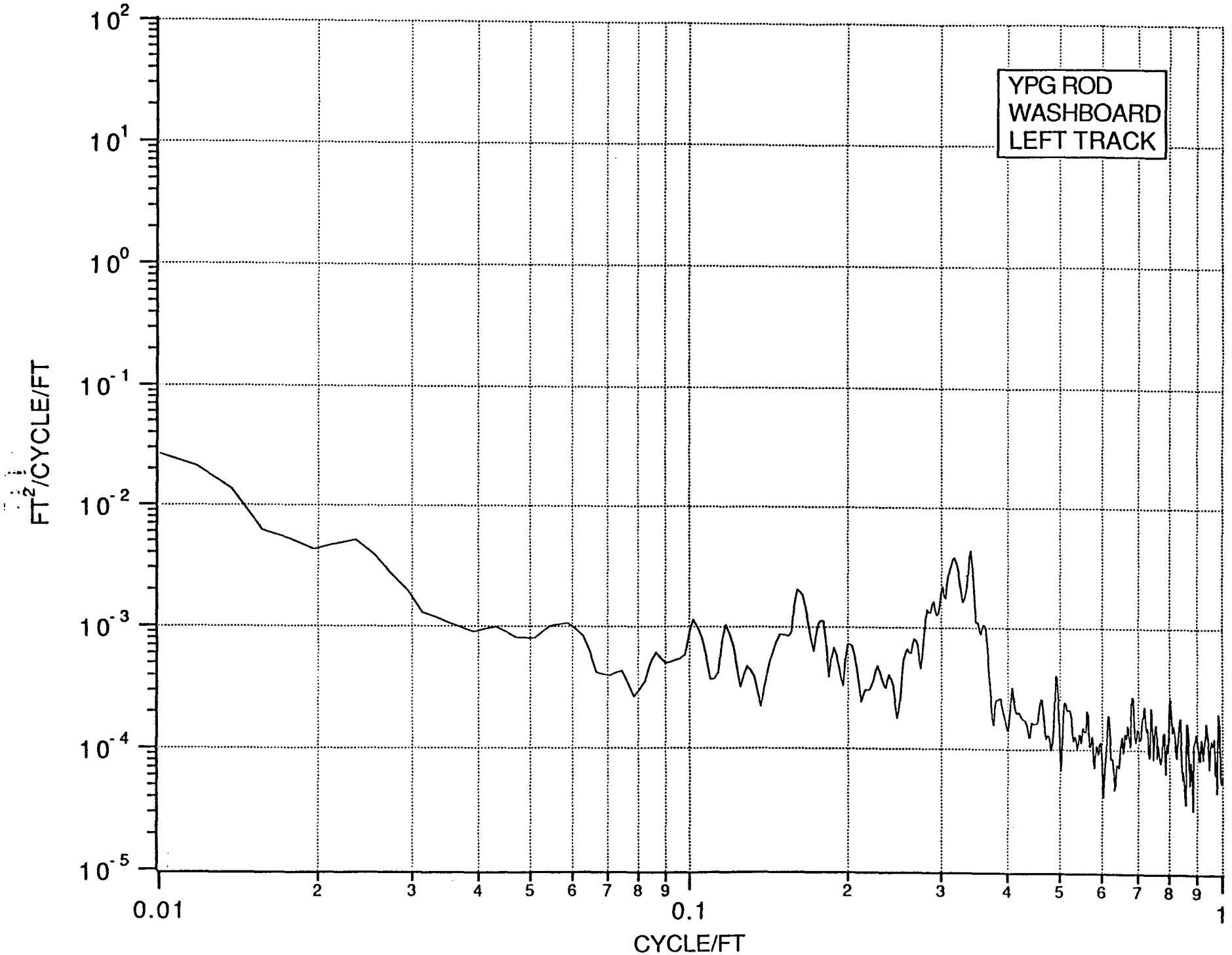
YPG ROD
WASHBOARD
LEFT TRACK
FT²/CYCLE/FT
CYCLE/FT
10²
10¹
10⁰
10⁻¹
10⁻²
10⁻³
10⁻⁴
10⁻⁵
0.01
0.1
1
2
3
4
5
6
7
8
9

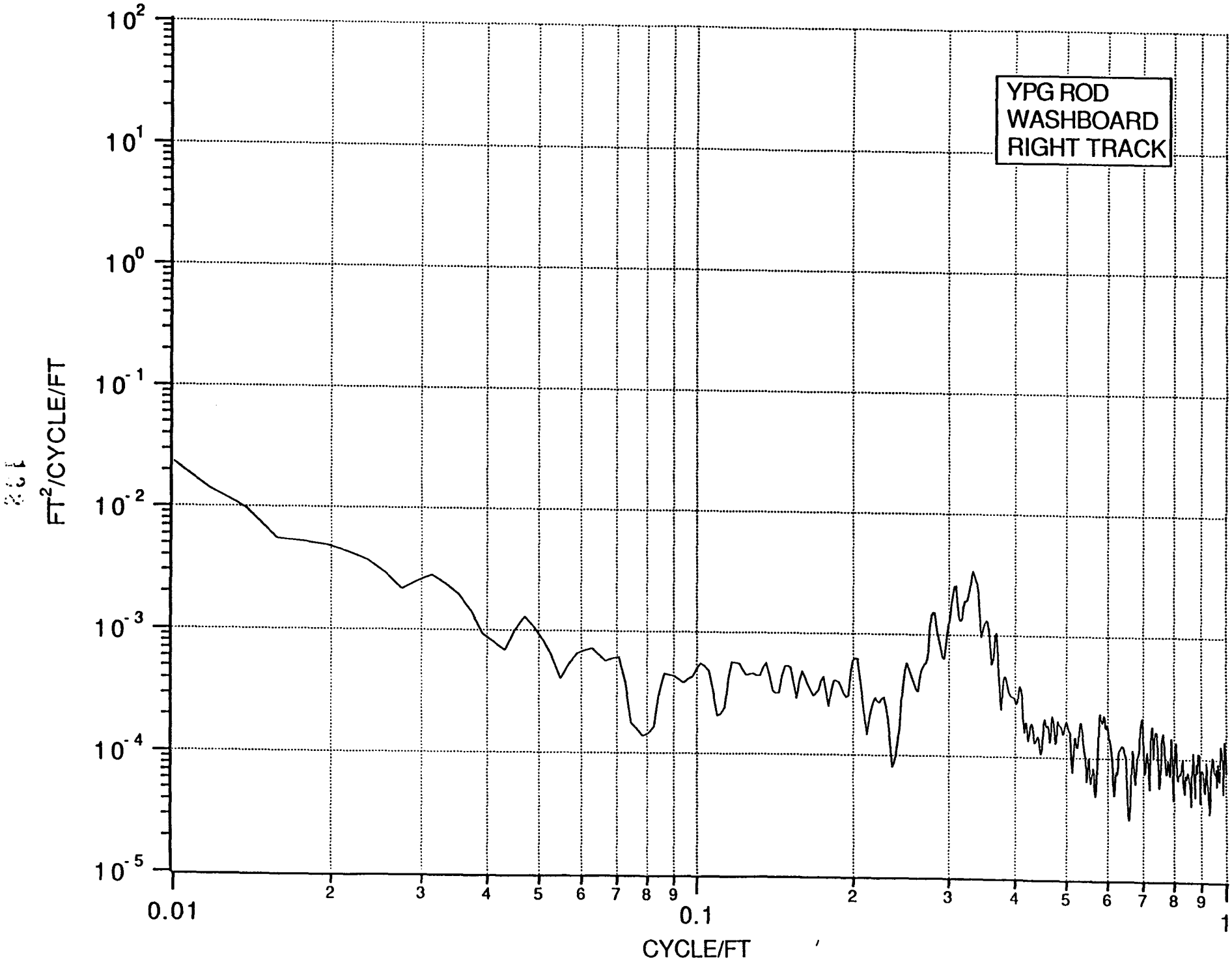
YPG ROD
WASHBOARD
RIGHT TRACK
10^2
10^1
10^0
10^{-1}
10^{-2}
10^{-3}
10^{-4}
10^{-5}
FT^2/CYCLE/FT
0.01
0.1
1
2 3 4 5 6 7 8 9
2 3 4 5 6 7 8 9
CYCLE/FT

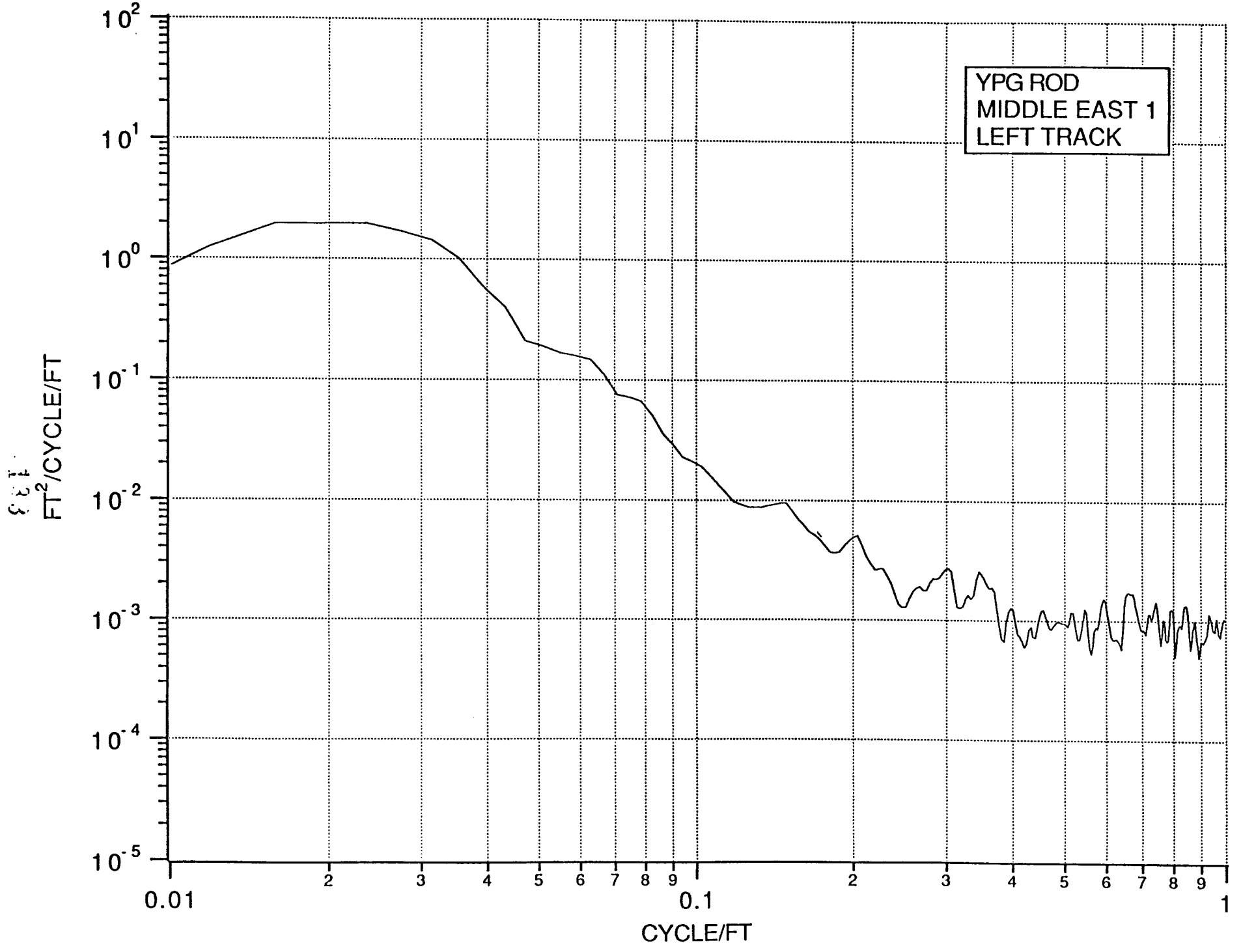
YPG ROD
MIDDLE EAST 1
LEFT TRACK
10^2
10^1
10^0
10^{-1}
10^{-2}
10^{-3}
10^{-4}
10^{-5}
FT²/CYCLE/FT
0.01
0.1
1
2 3 4 5 6 7 8 9
2 3 4 5 6 7 8 9
CYCLE/FT

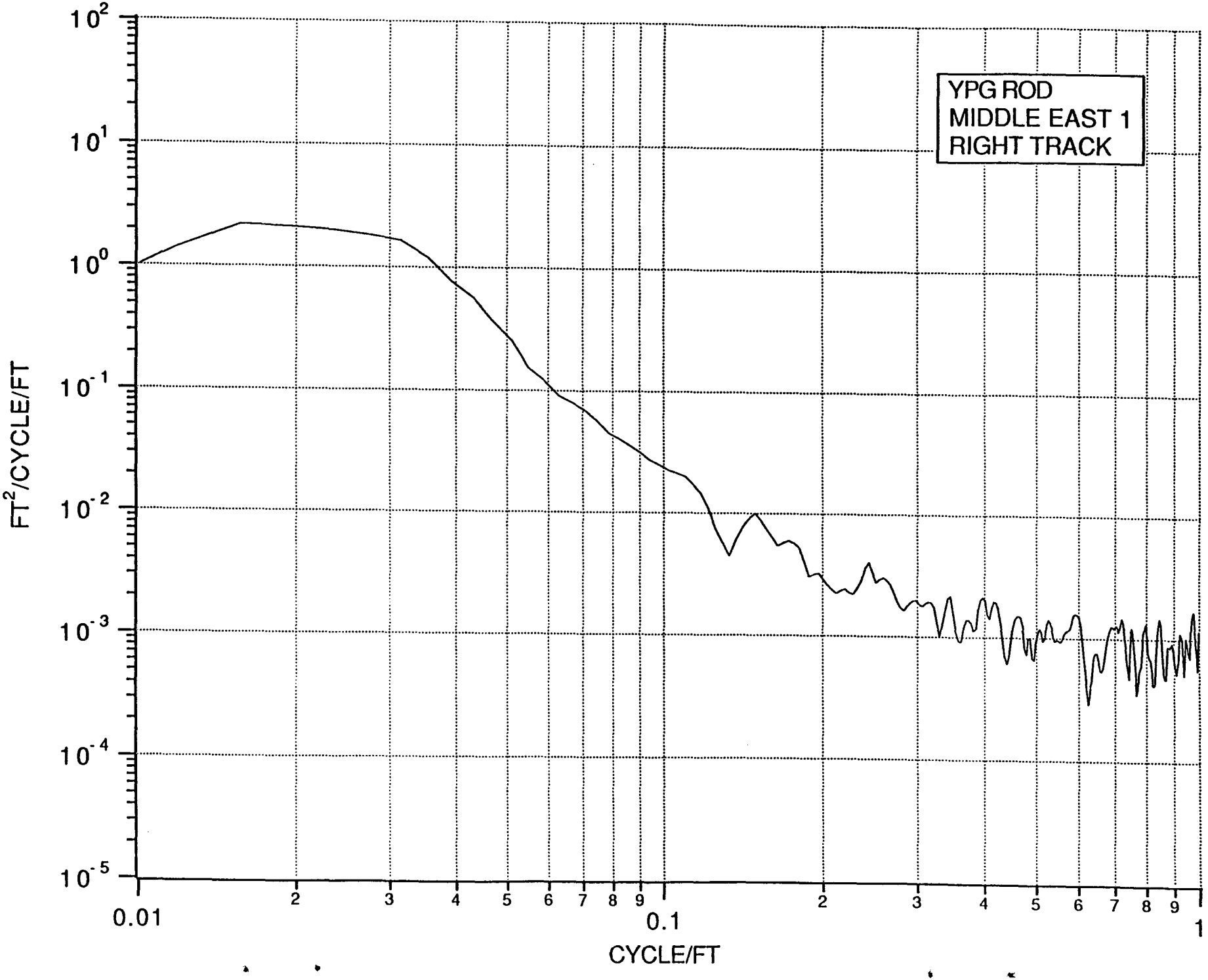
YPG ROD
MIDDLE EAST 1
RIGHT TRACK
10^2
10^1
10^0
10^{-1}
10^{-2}
10^{-3}
10^{-4}
10^{-5}
FT^2/CYCLE/FT
0.01
2 3 4 5 6 7 8 9
0.1
2 3 4 5 6 7 8 9
1
CYCLE/FT

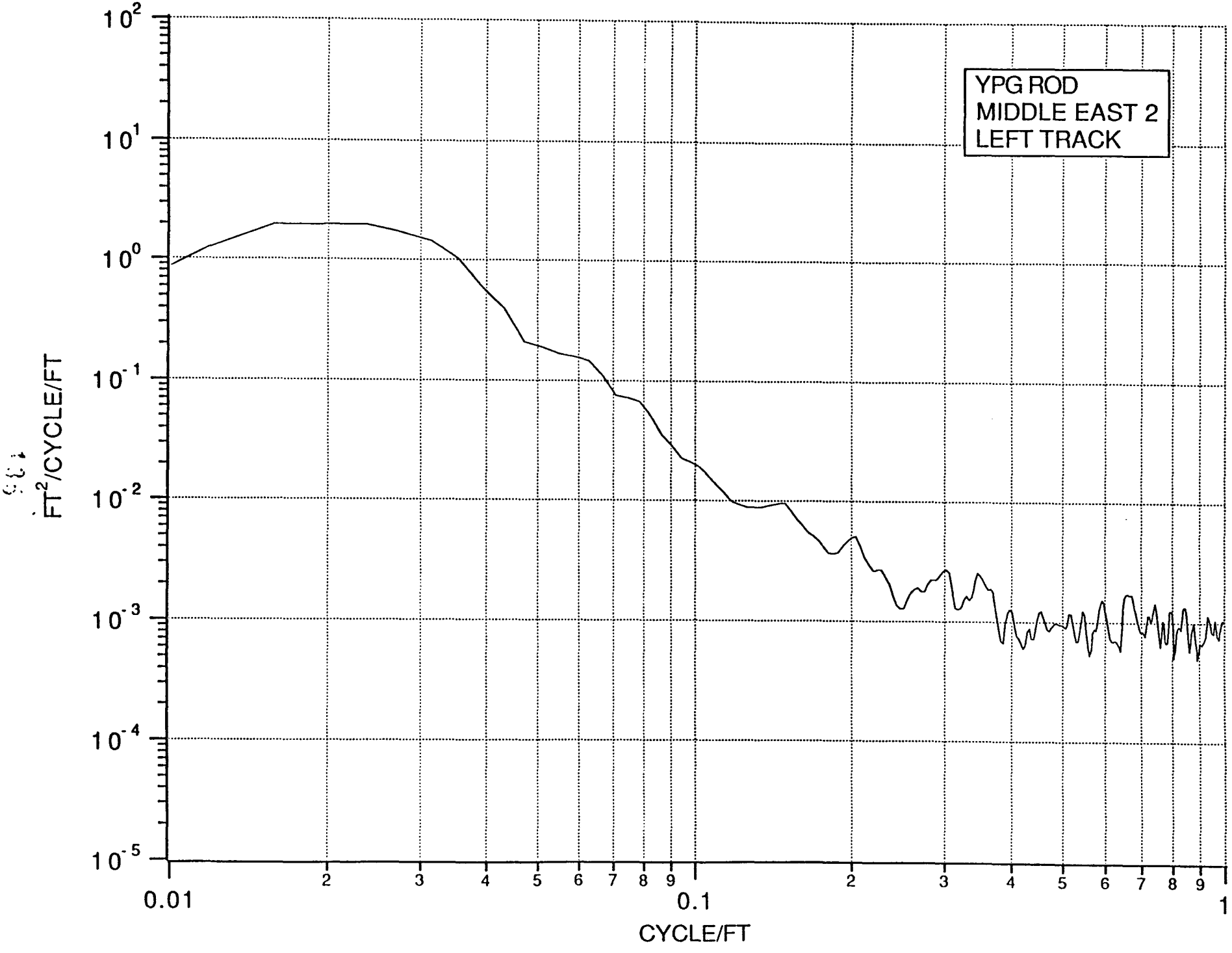
YPG ROD
MIDDLE EAST 2
LEFT TRACK
10^2
10^1
10^0
10^{-1}
10^{-2}
10^{-3}
10^{-4}
10^{-5}
FT^2/CYCLE/FT
0.01
2 3 4 5 6 7 8 9
0.1
2 3 4 5 6 7 8 9
1
CYCLE/FT

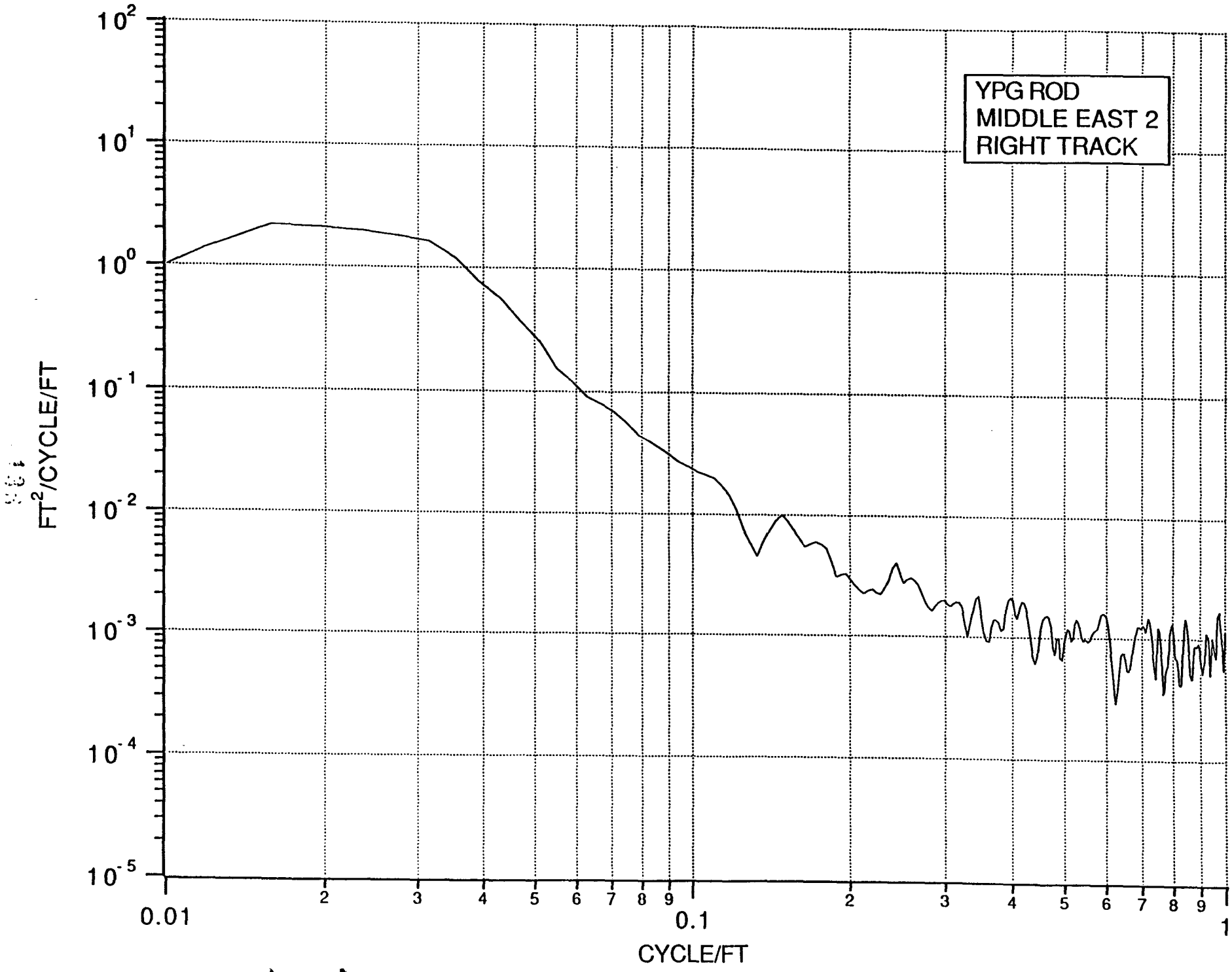
YPG ROD
MIDDLE EAST 2
RIGHT TRACK
10^2
10^1
10^0
10^{-1}
10^{-2}
10^{-3}
10^{-4}
10^{-5}
FT^2/CYCLE/FT
0.01
2 3 4 5 6 7 8 9
0.1
2 3 4 5 6 7 8 9
1
CYCLE/FT

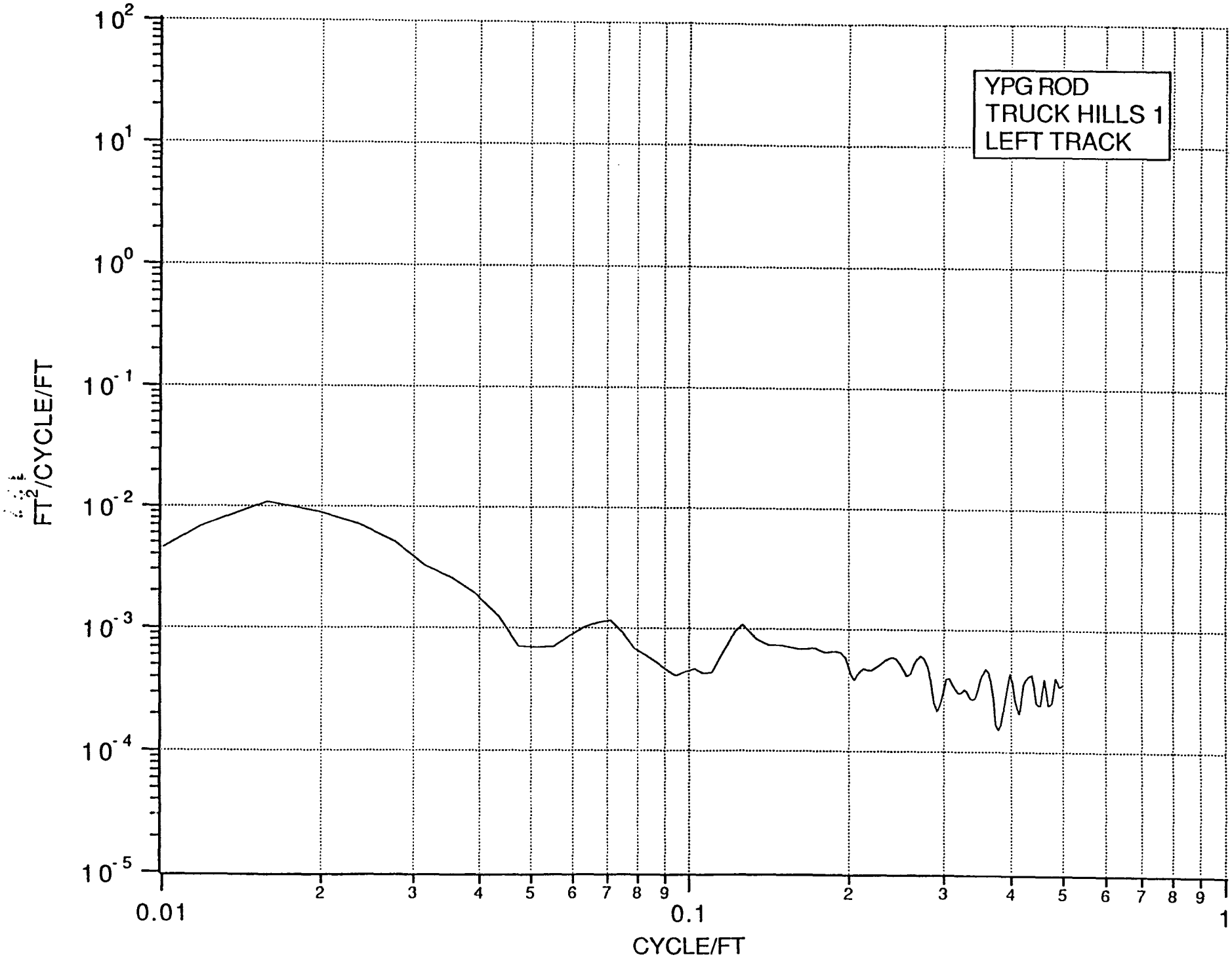
YPG ROD
TRUCK HILLS 1
LEFT TRACK
10^2
10^1
10^0
10^{-1}
10^{-2}
10^{-3}
10^{-4}
10^{-5}
FT²/CYCLE/FT
0.01
2 3 4 5 6 7 8 9
0.1
2 3 4 5 6 7 8 9
1
CYCLE/FT

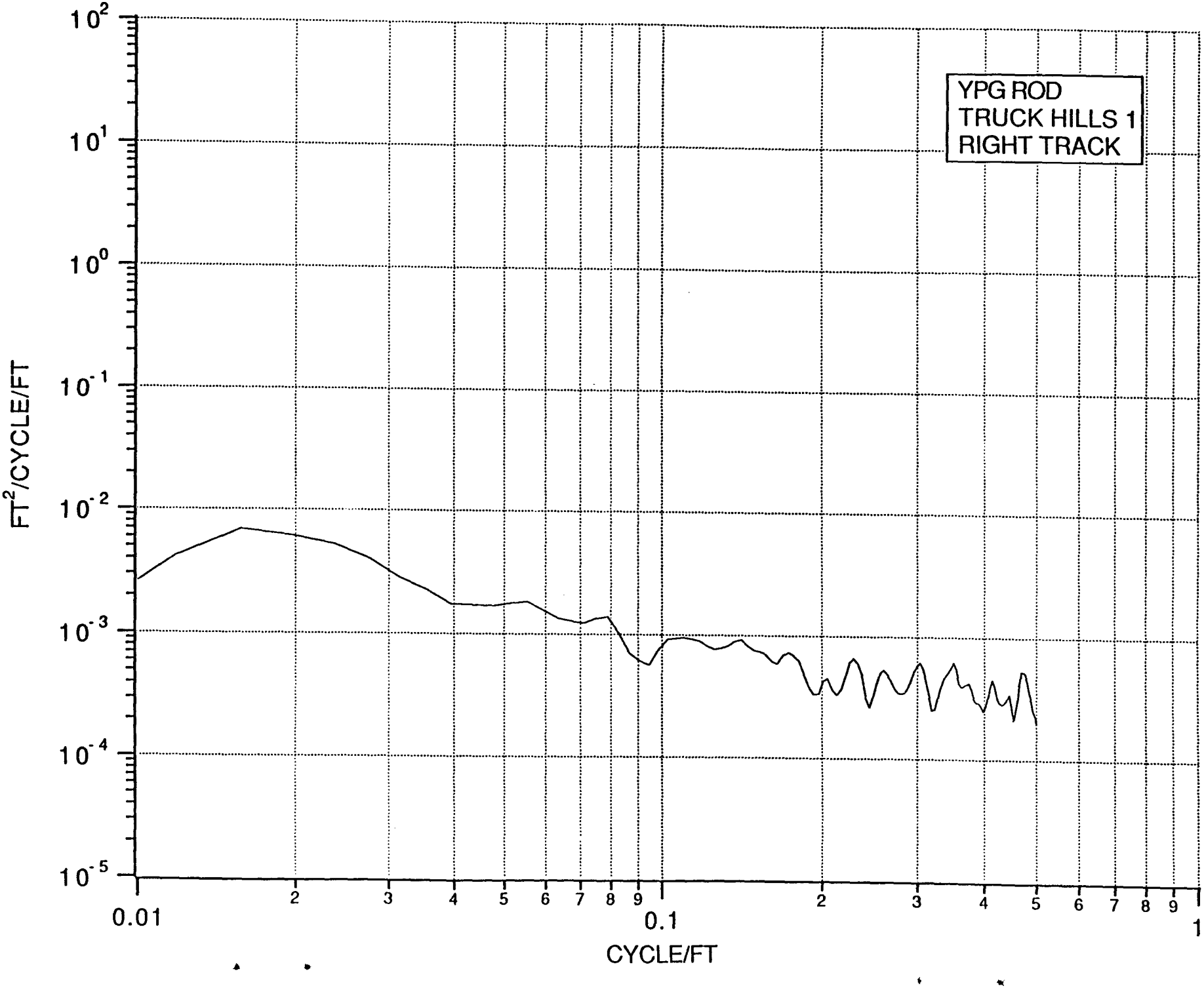
YPG ROD
TRUCK HILLS 1
RIGHT TRACK
10^2
10^1
10^0
10^{-1}
10^{-2}
10^{-3}
10^{-4}
10^{-5}
FT^2/CYCLE/FT
0.01
2 3 4 5 6 7 8 9
0.1
2 3 4 5 6 7 8 9
1
CYCLE/FT

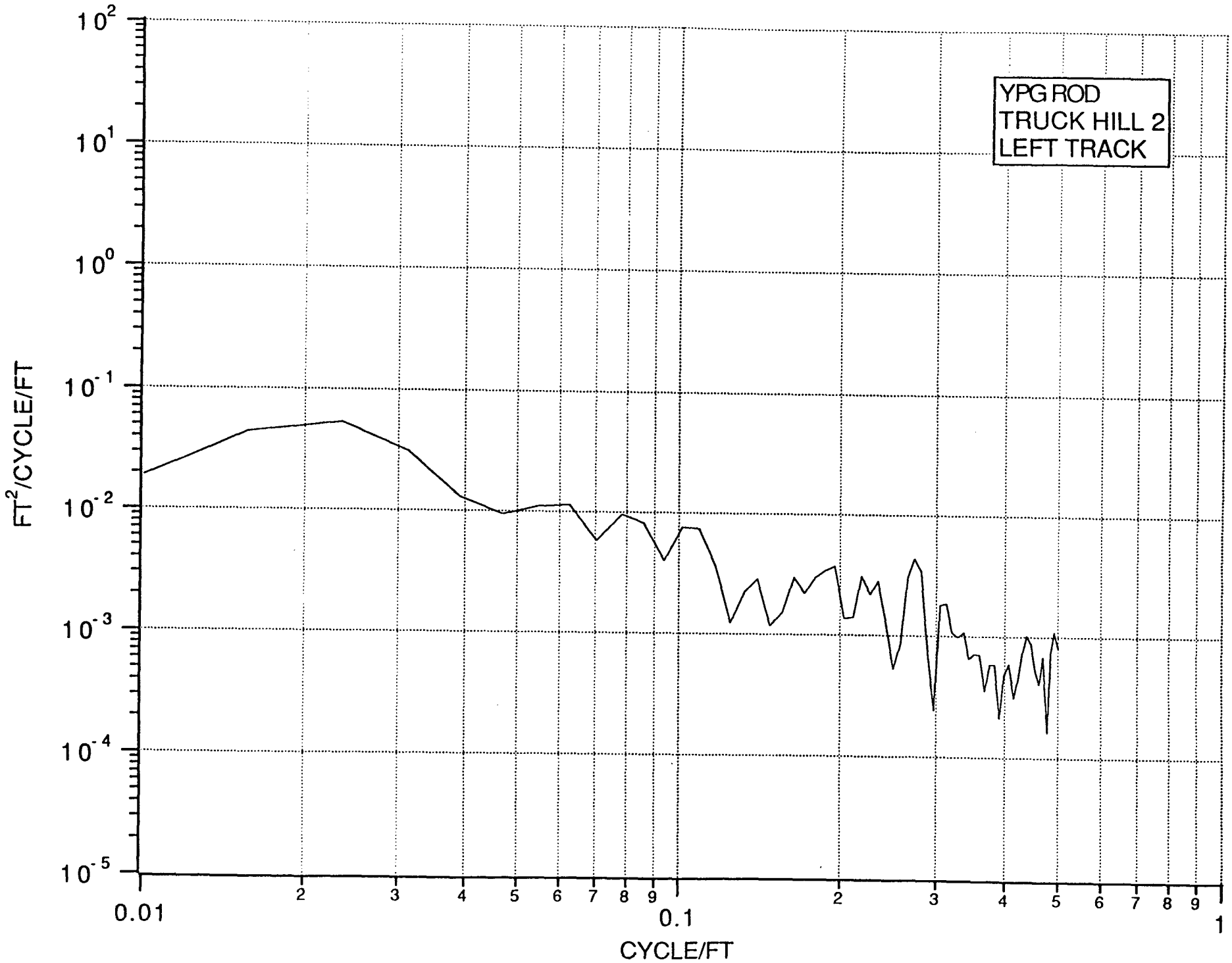
YPG ROD
TRUCK HILL 2
LEFT TRACK
10^2
10^1
10^0
10^{-1}
10^{-2}
10^{-3}
10^{-4}
10^{-5}
FT^2/CYCLE/FT
0.01
2 3 4 5 6 7 8 9
0.1
2 3 4 5 6 7 8 9
1
CYCLE/FT

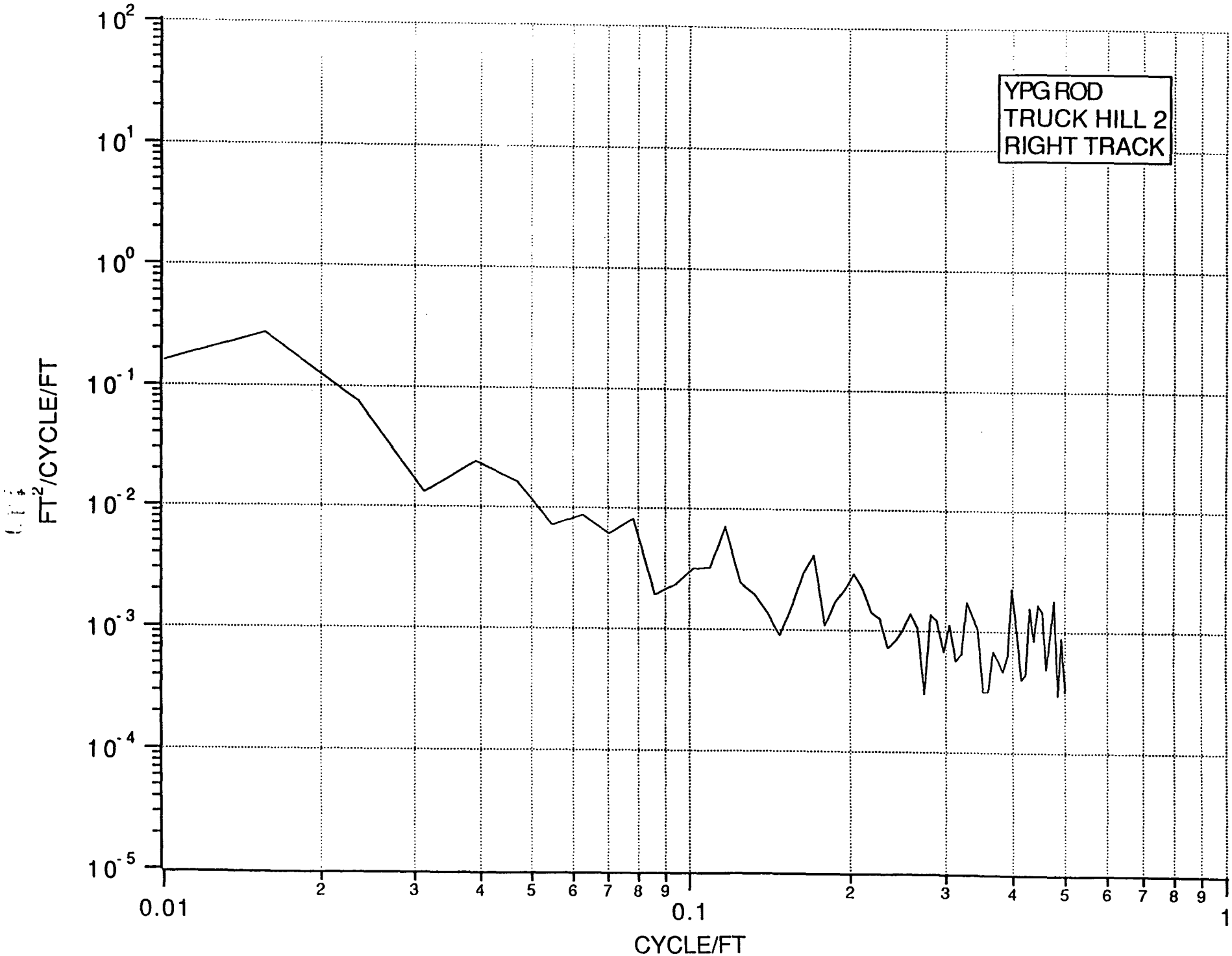
YPG ROD
TRUCK HILL 2
RIGHT TRACK
10^2
10^1
10^0
10^{-1}
10^{-2}
10^{-3}
10^{-4}
10^{-5}
FT^2/CYCLE/FT
0.01
2 3 4 5 6 7 8 9
0.1
2 3 4 5 6 7 8 9
1
CYCLE/FT

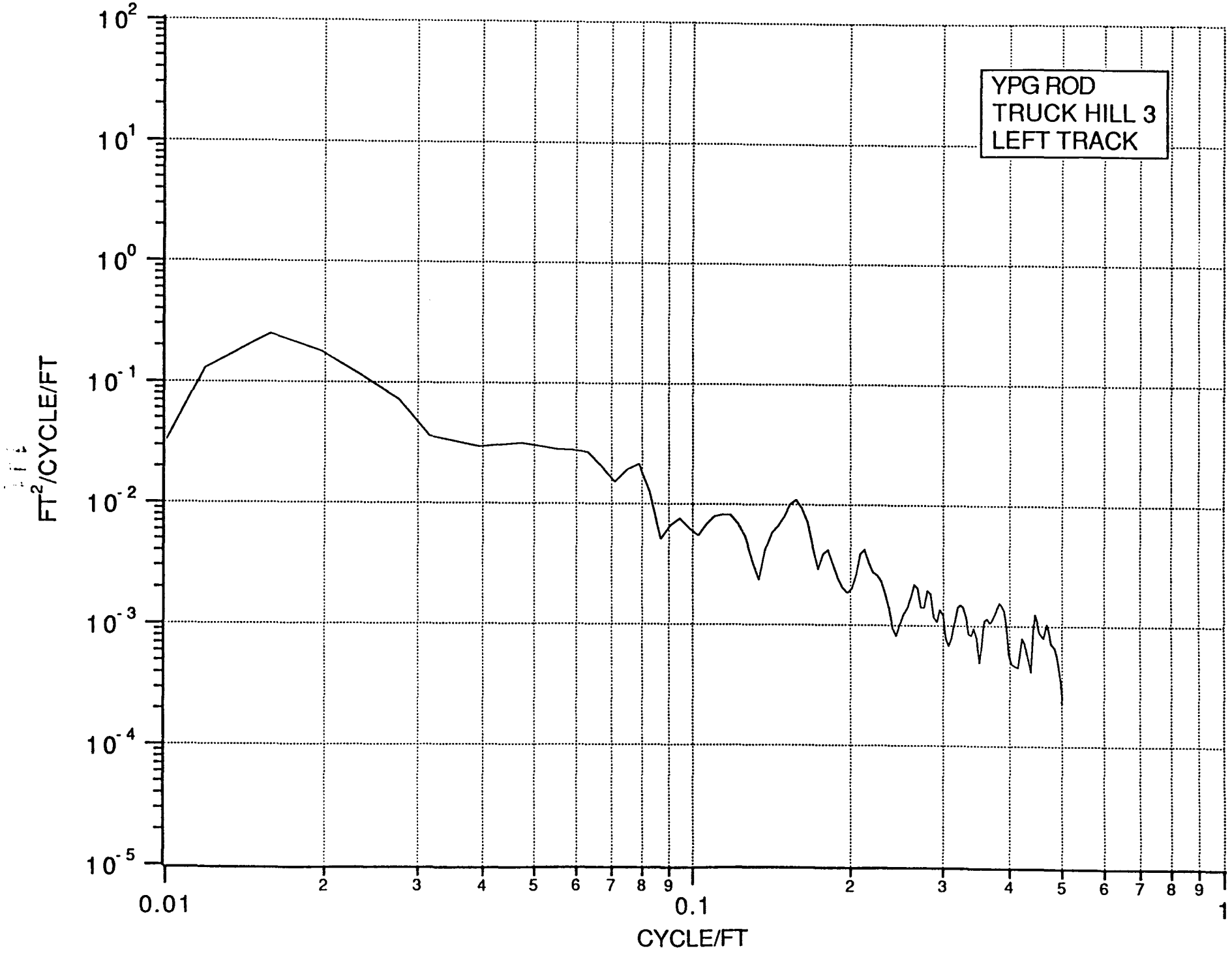
YPG ROD
TRUCK HILL 3
LEFT TRACK
10^2
10^1
10^0
10^{-1}
10^{-2}
10^{-3}
10^{-4}
10^{-5}
FT^2/CYCLE/FT
0.01
2
3
4
5
6
7
8
9
0.1
2
3
4
5
6
7
8
9
1
CYCLE/FT

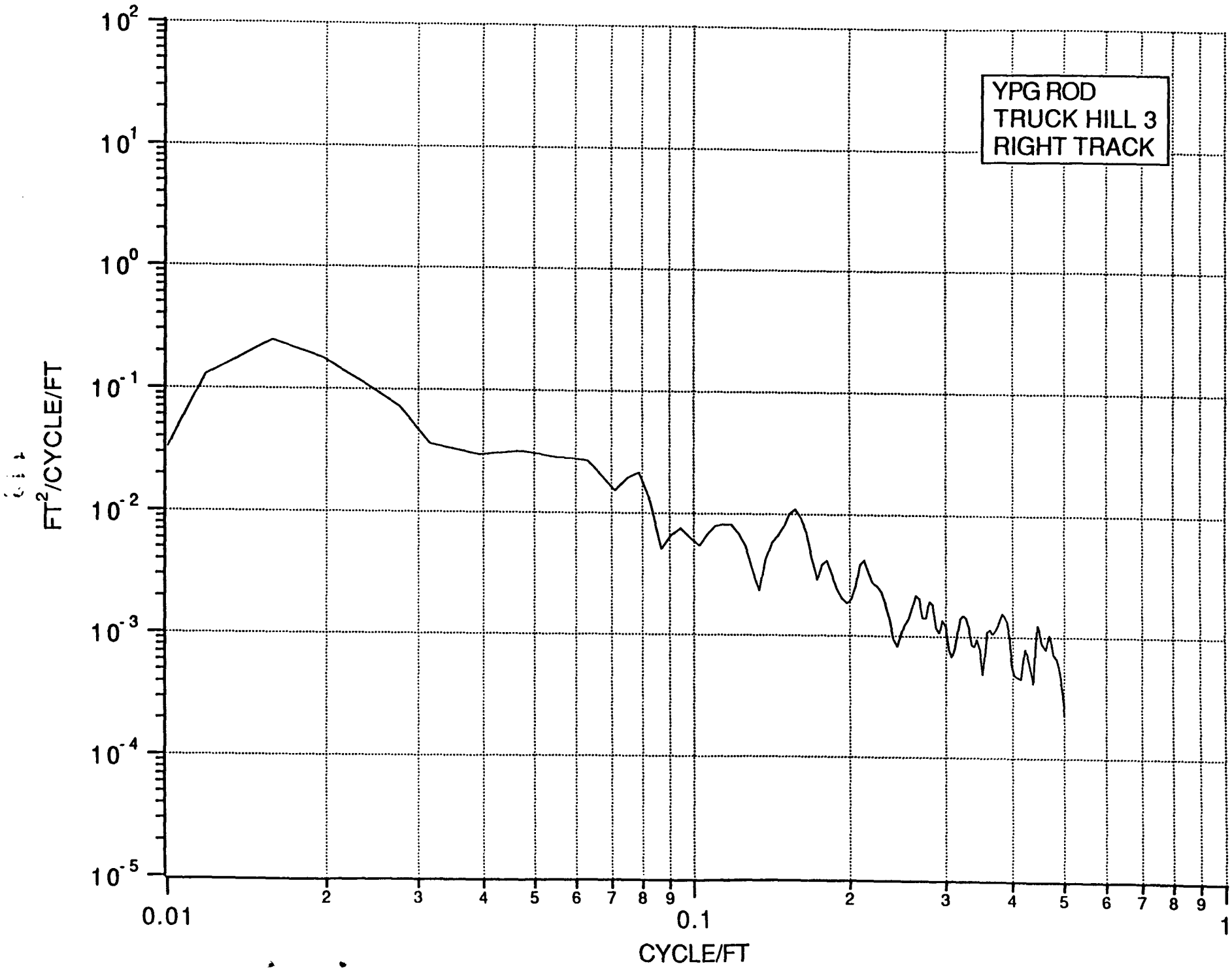
YPG ROD
TRUCK HILL 3
RIGHT TRACK
10^2
10^1
10^0
10^{-1}
10^{-2}
10^{-3}
10^{-4}
10^{-5}
FT^2/CYCLE/FT
0.01
2 3 4 5 6 7 8 9
0.1
2 3 4 5 6 7 8 9
1
CYCLE/FT

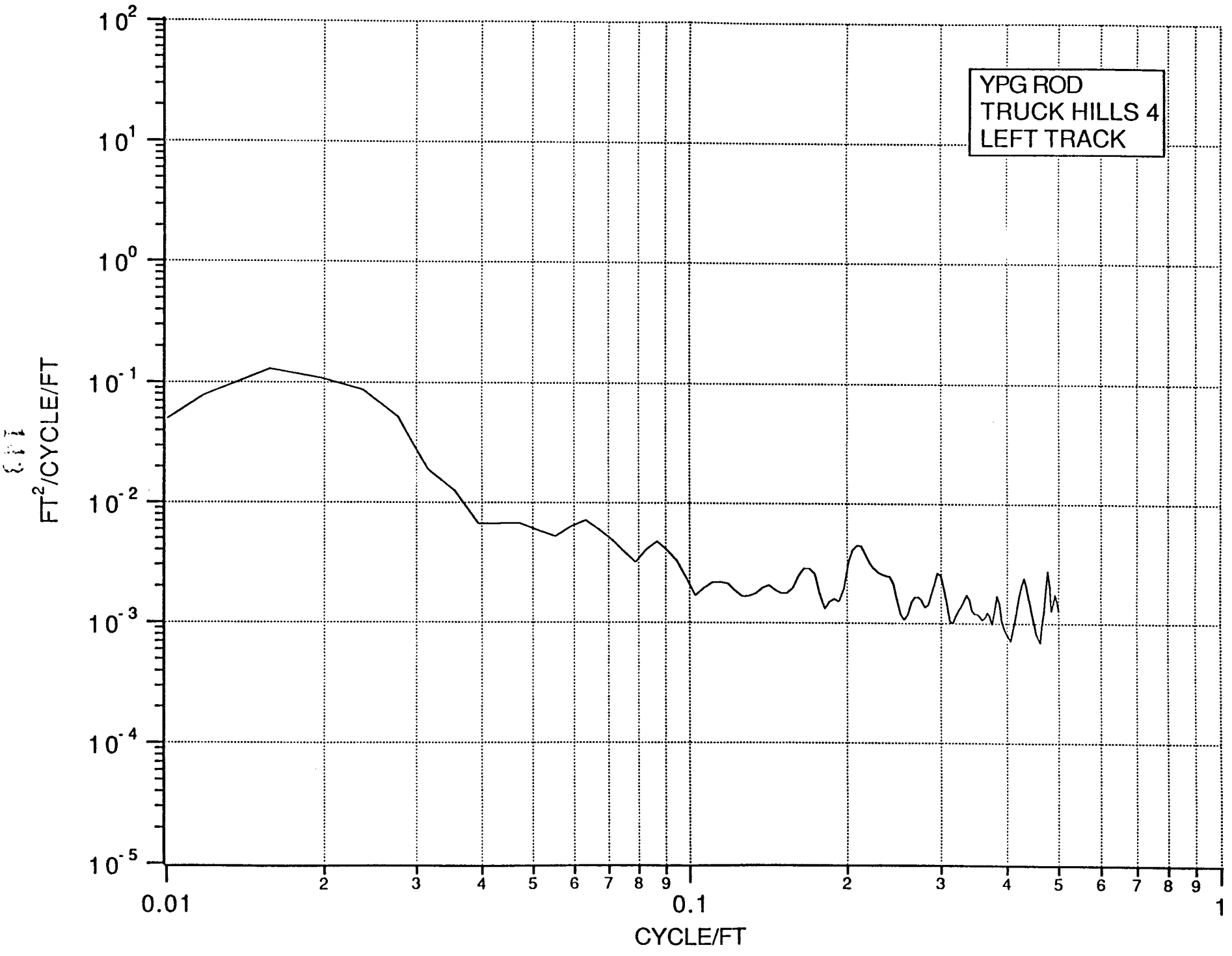
YPG ROD
TRUCK HILLS 4
LEFT TRACK
FT²/CYCLE/FT
CYCLE/FT
10²
10¹
10⁰
10⁻¹
10⁻²
10⁻³
10⁻⁴
10⁻⁵
0.01
0.1
1
2
3
4
5
6
7
8
9

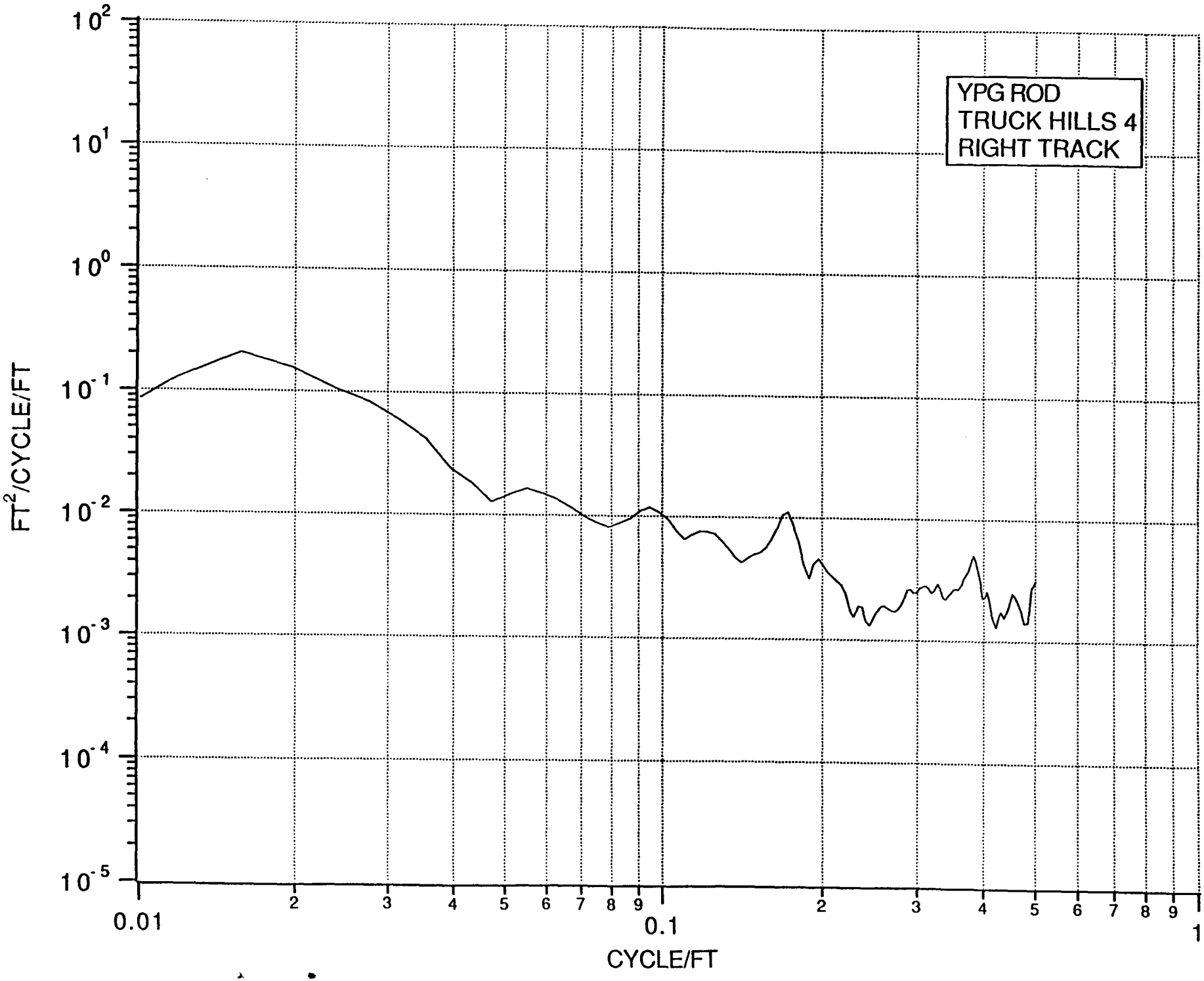
YPG ROD
TRUCK HILLS 4
RIGHT TRACK
10^2
10^1
10^0
10^{-1}
10^{-2}
10^{-3}
10^{-4}
10^{-5}
FT^2/CYCLE/FT
0.01
0.1
1
CYCLE/FT

APPENDIX D

WAVE-NUMBER SPECTRA - DFMV

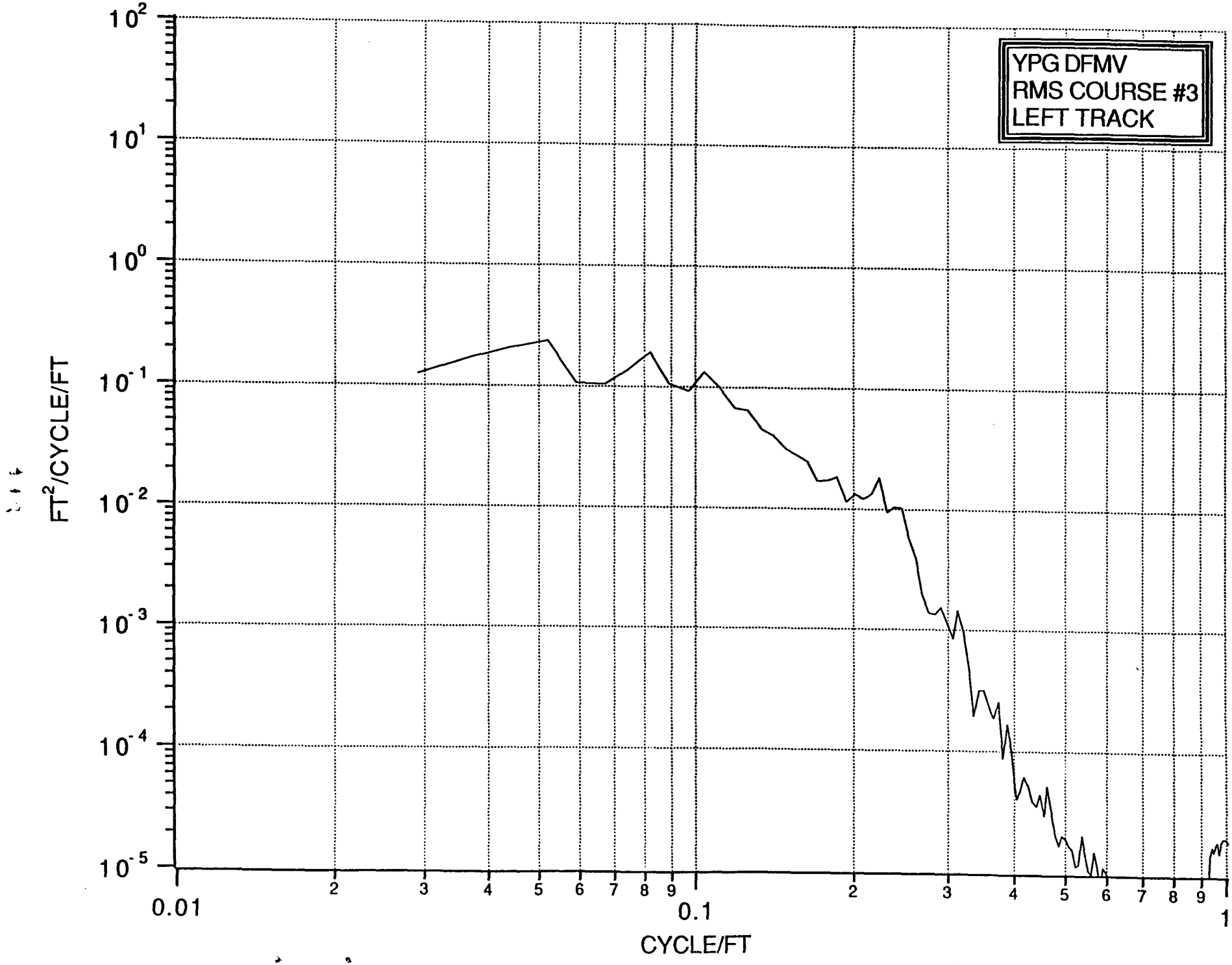
YPG DFMV
RMS COURSE #3
LEFT TRACK
10^2
10^1
10^0
10^{-1}
10^{-2}
10^{-3}
10^{-4}
10^{-5}
FT^2/CYCLE/FT
0.01
2 3 4 5 6 7 8 9
0.1
2 3 4 5 6 7 8 9
1
CYCLE/FT

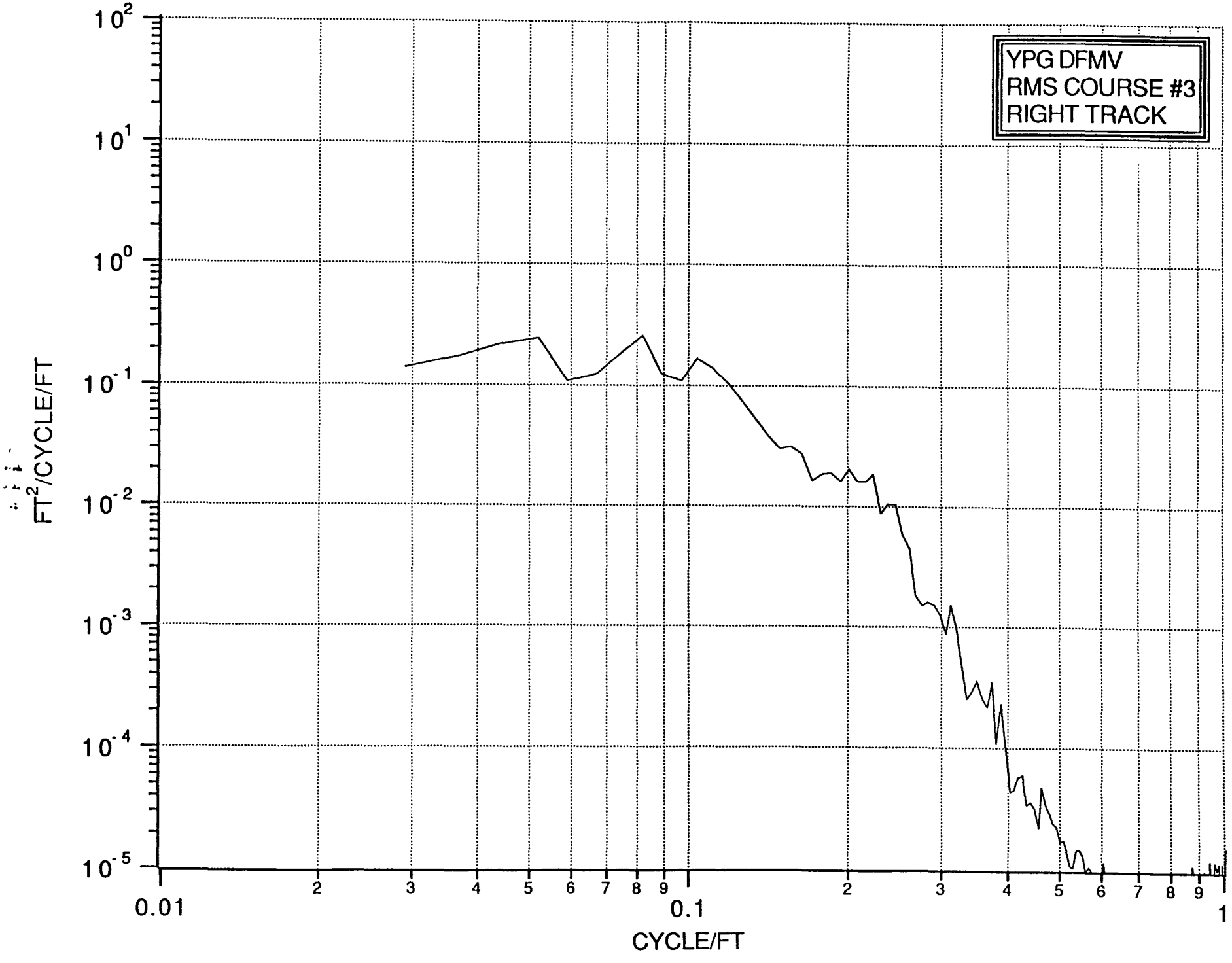
YPG DFMV
RMS COURSE #3
RIGHT TRACK
10^2
10^1
10^0
10^{-1}
10^{-2}
10^{-3}
10^{-4}
10^{-5}
FT^2/CYCLE/FT
0.01
2 3 4 5 6 7 8 9
0.1
2 3 4 5 6 7 8 9
1
CYCLE/FT

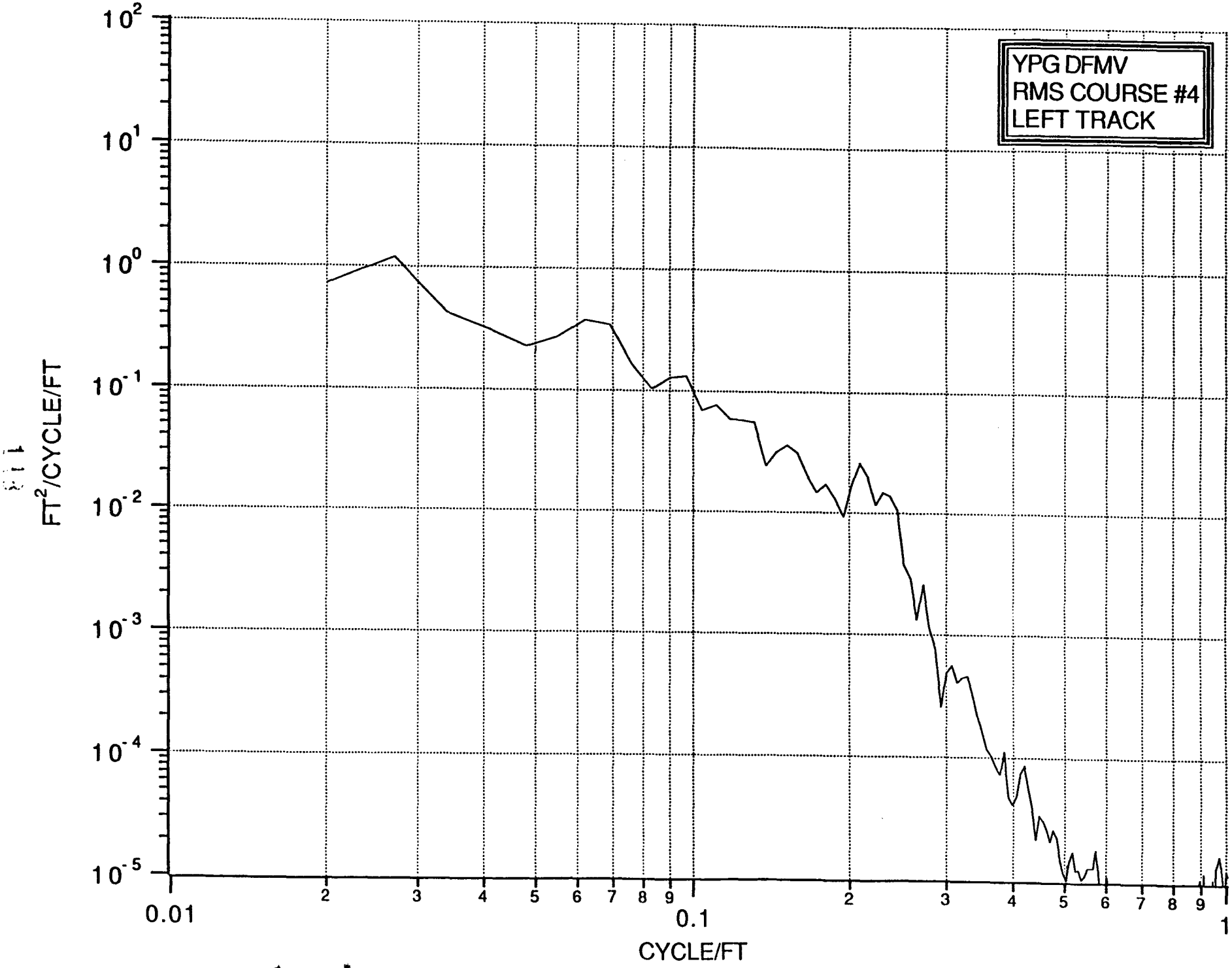
YPG DFMV
RMS COURSE #4
LEFT TRACK
10^2
10^1
10^0
10^{-1}
10^{-2}
10^{-3}
10^{-4}
10^{-5}
FT^2/CYCLE/FT
0.01
0.1
1
2 3 4 5 6 7 8 9
2 3 4 5 6 7 8 9
CYCLE/FT

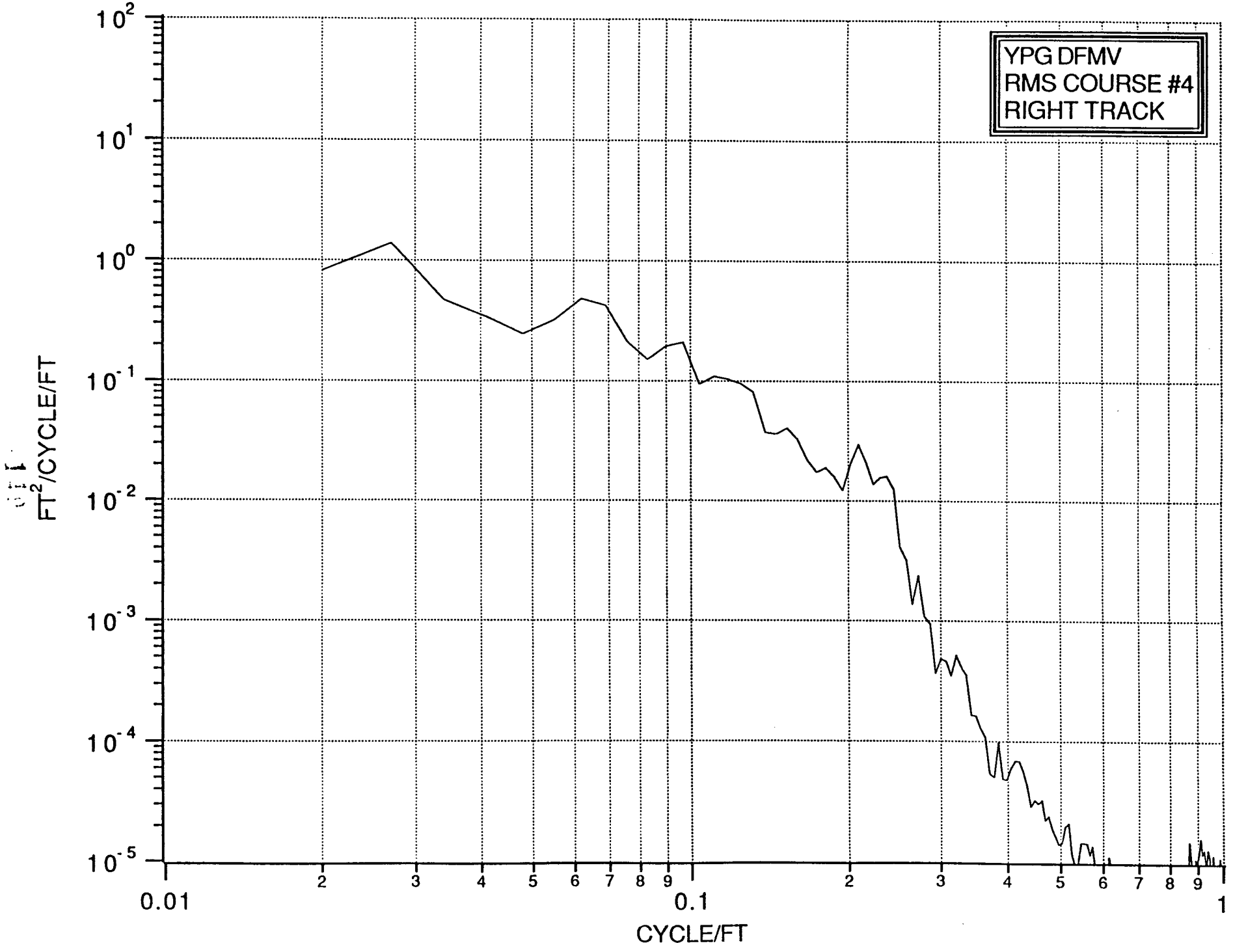
YPG DFMV
RMS COURSE #4
RIGHT TRACK
10^2
10^1
10^0
10^{-1}
10^{-2}
10^{-3}
10^{-4}
10^{-5}
FT^2/CYCLE/FT
0.01
0.1
1
2 3 4 5 6 7 8 9
2 3 4 5 6 7 8 9
CYCLE/FT

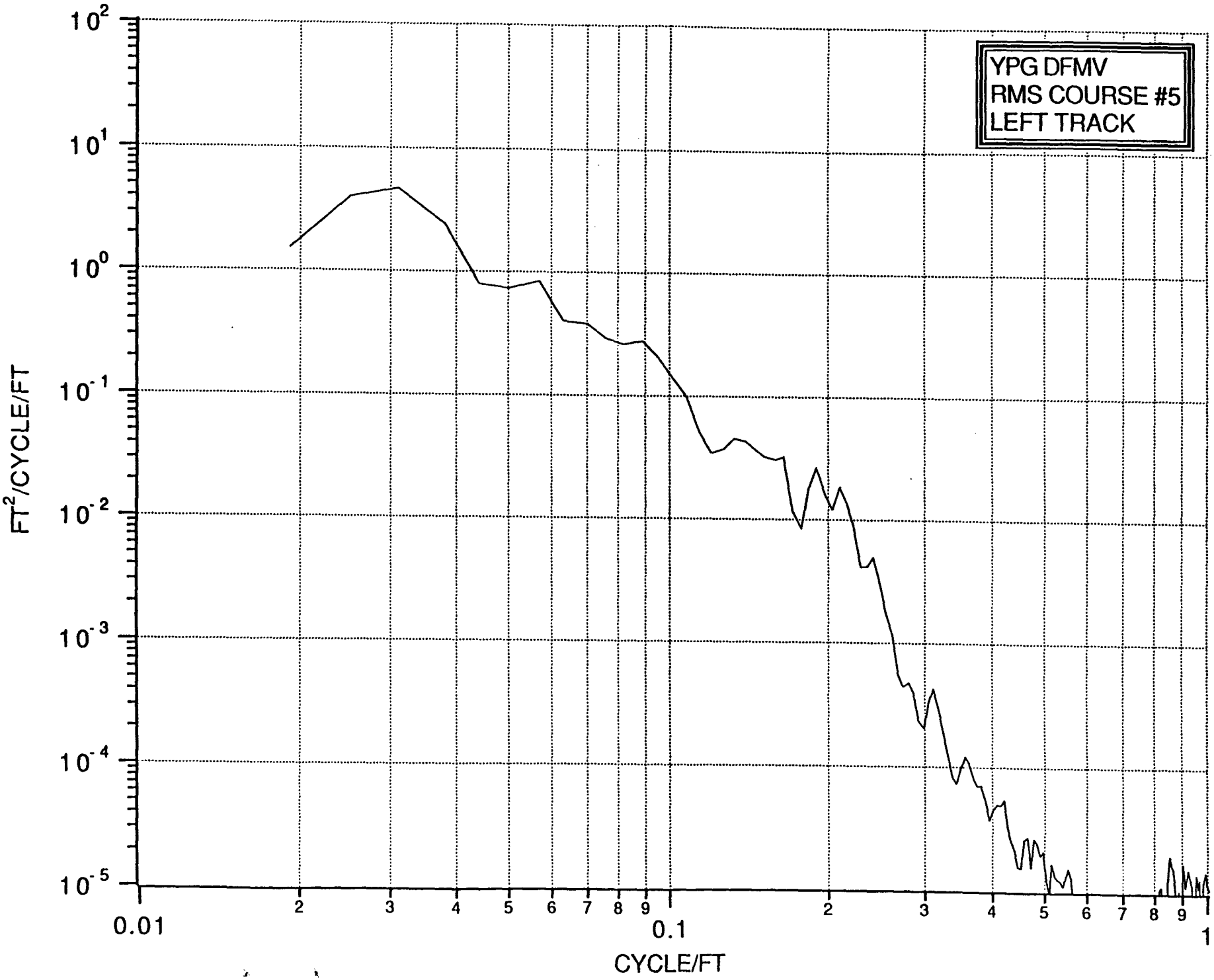
YPG DFMV
RMS COURSE #5
LEFT TRACK
10^2
10^1
10^0
10^{-1}
10^{-2}
10^{-3}
10^{-4}
10^{-5}
FT^2/CYCLE/FT
0.01
2 3 4 5 6 7 8 9
0.1
2 3 4 5 6 7 8 9
1
CYCLE/FT

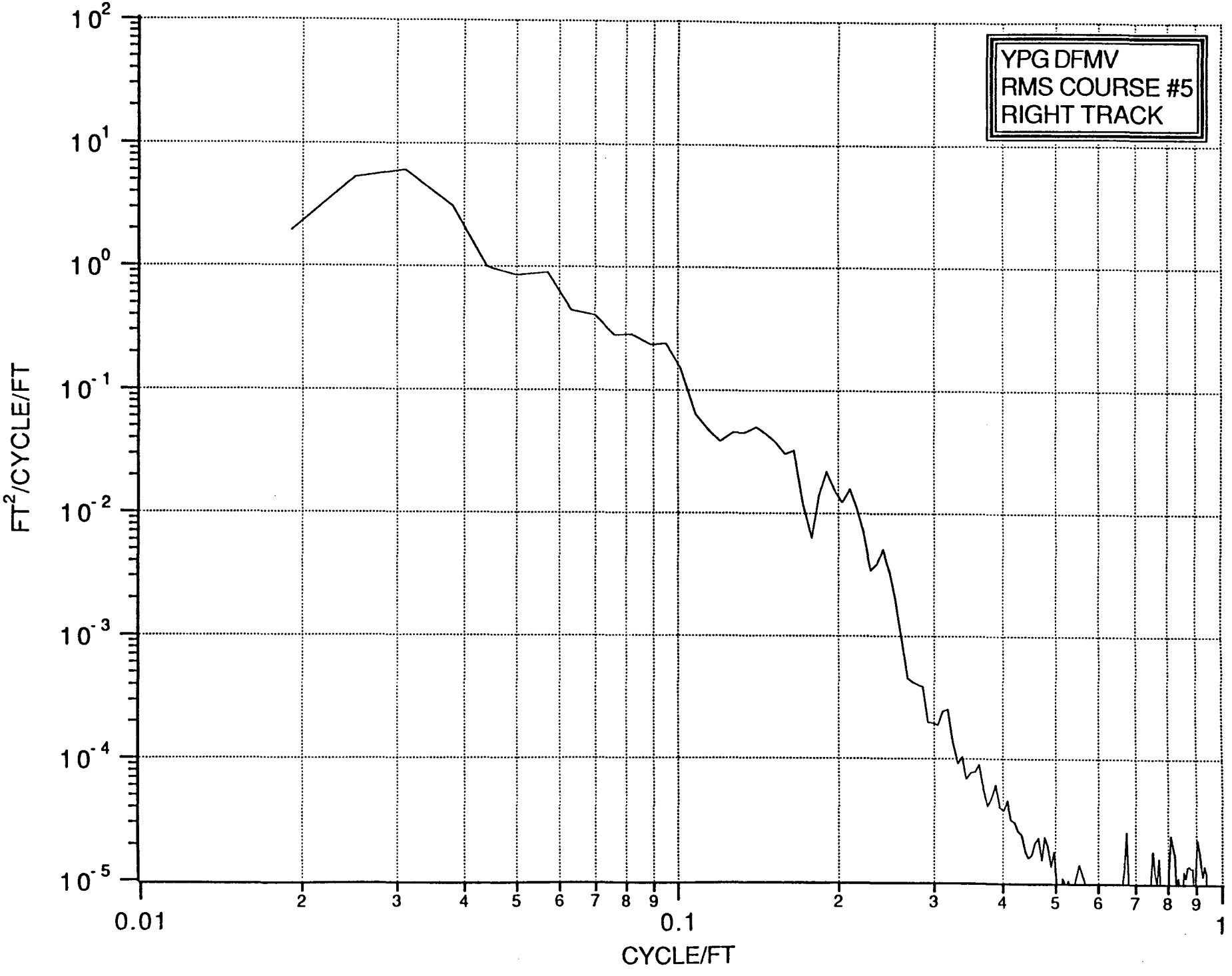
YPG DFMV
RMS COURSE #5
RIGHT TRACK
10^2
10^1
10^0
10^{-1}
10^{-2}
10^{-3}
10^{-4}
10^{-5}
FT^2/CYCLE/FT
0.01
0.1
1
2 3 4 5 6 7 8 9
2 3 4 5 6 7 8 9
CYCLE/FT

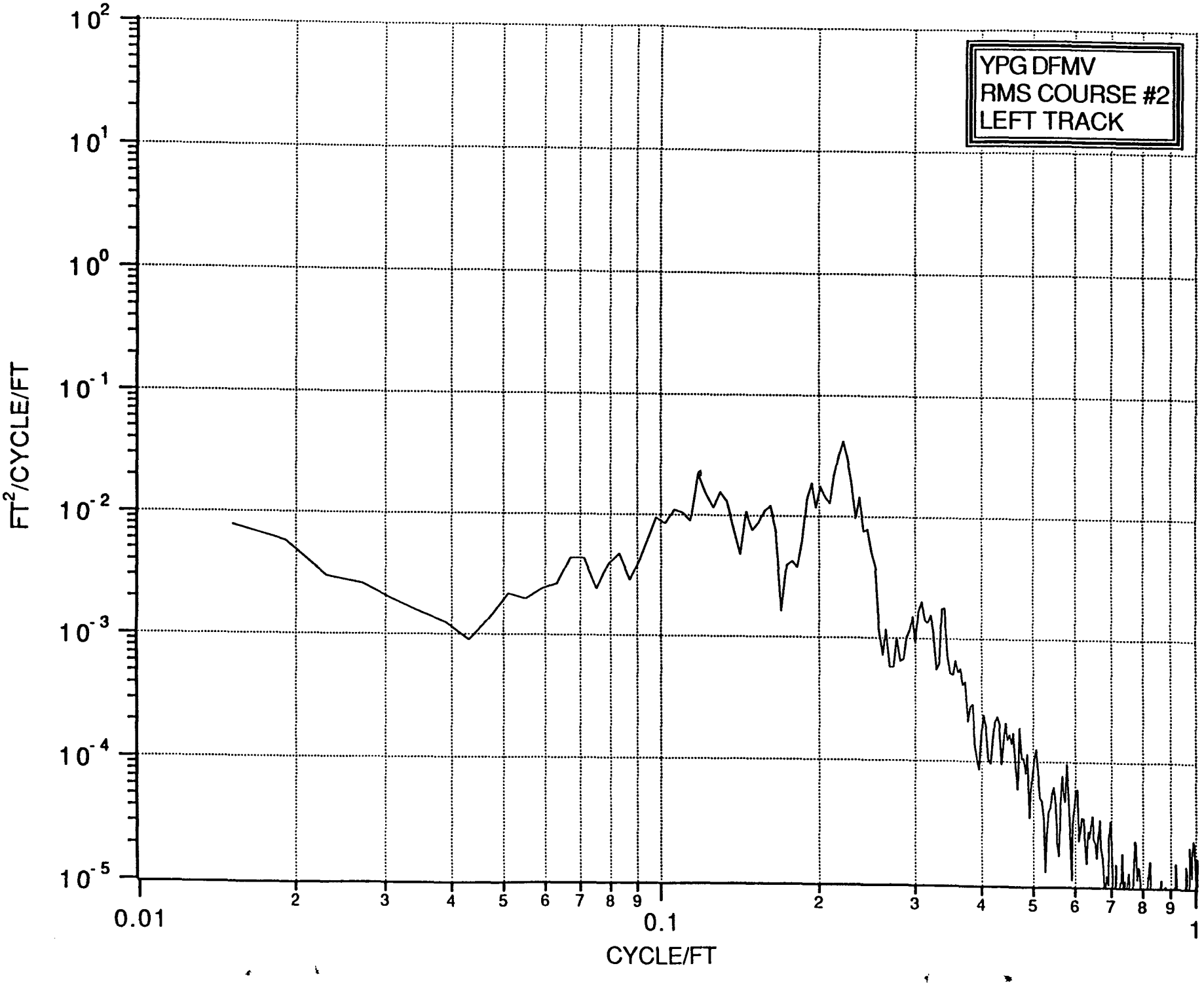
YPG DFMV
RMS COURSE #2
LEFT TRACK
10^2
10^1
10^0
10^{-1}
10^{-2}
10^{-3}
10^{-4}
10^{-5}
FT^2/CYCLE/FT
0.01
0.1
1
CYCLE/FT

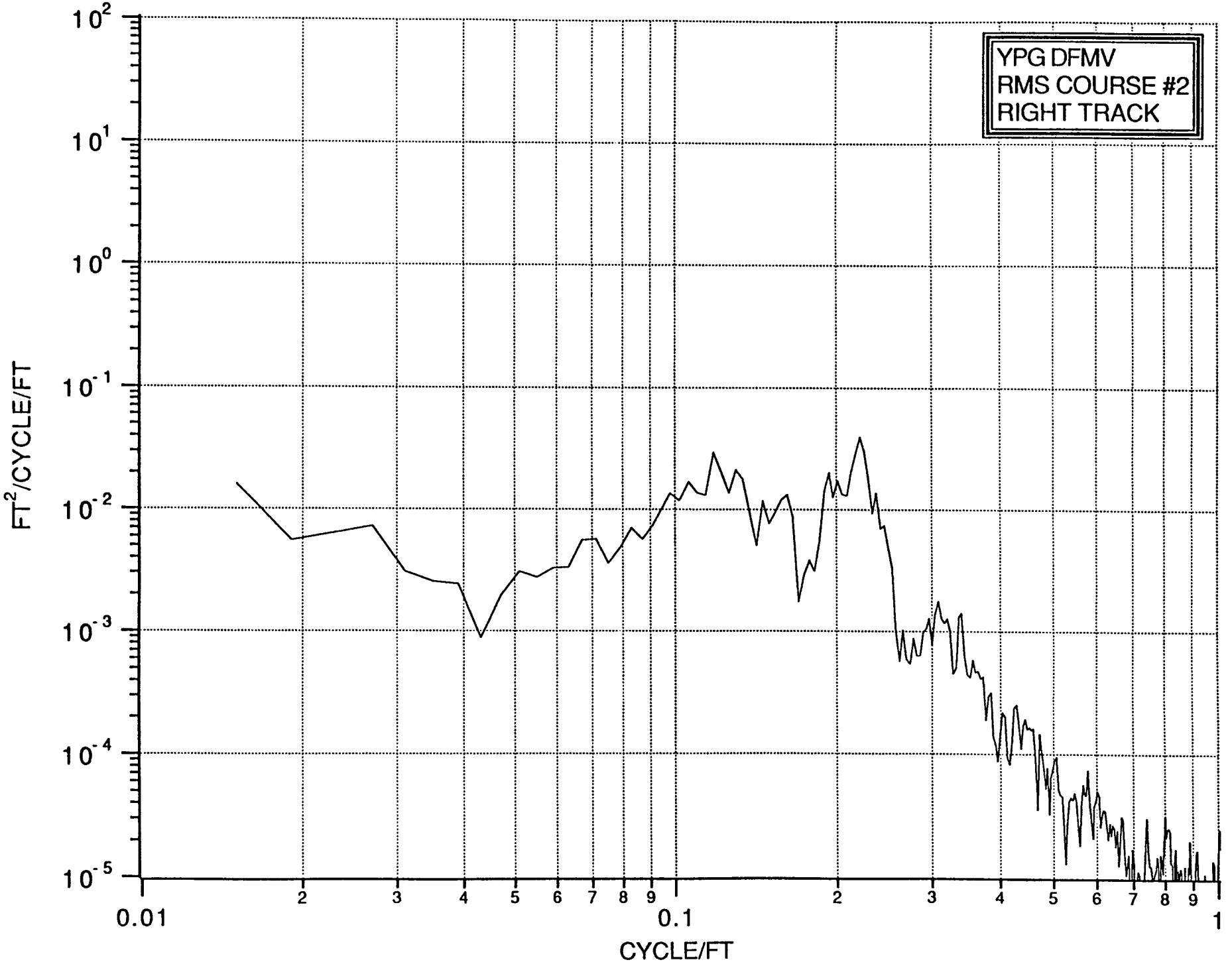
YPG DFMV
RMS COURSE #2
RIGHT TRACK
10^2
10^1
10^0
10^{-1}
10^{-2}
10^{-3}
10^{-4}
10^{-5}
FT^2/CYCLE/FT
0.01
0.1
1
CYCLE/FT

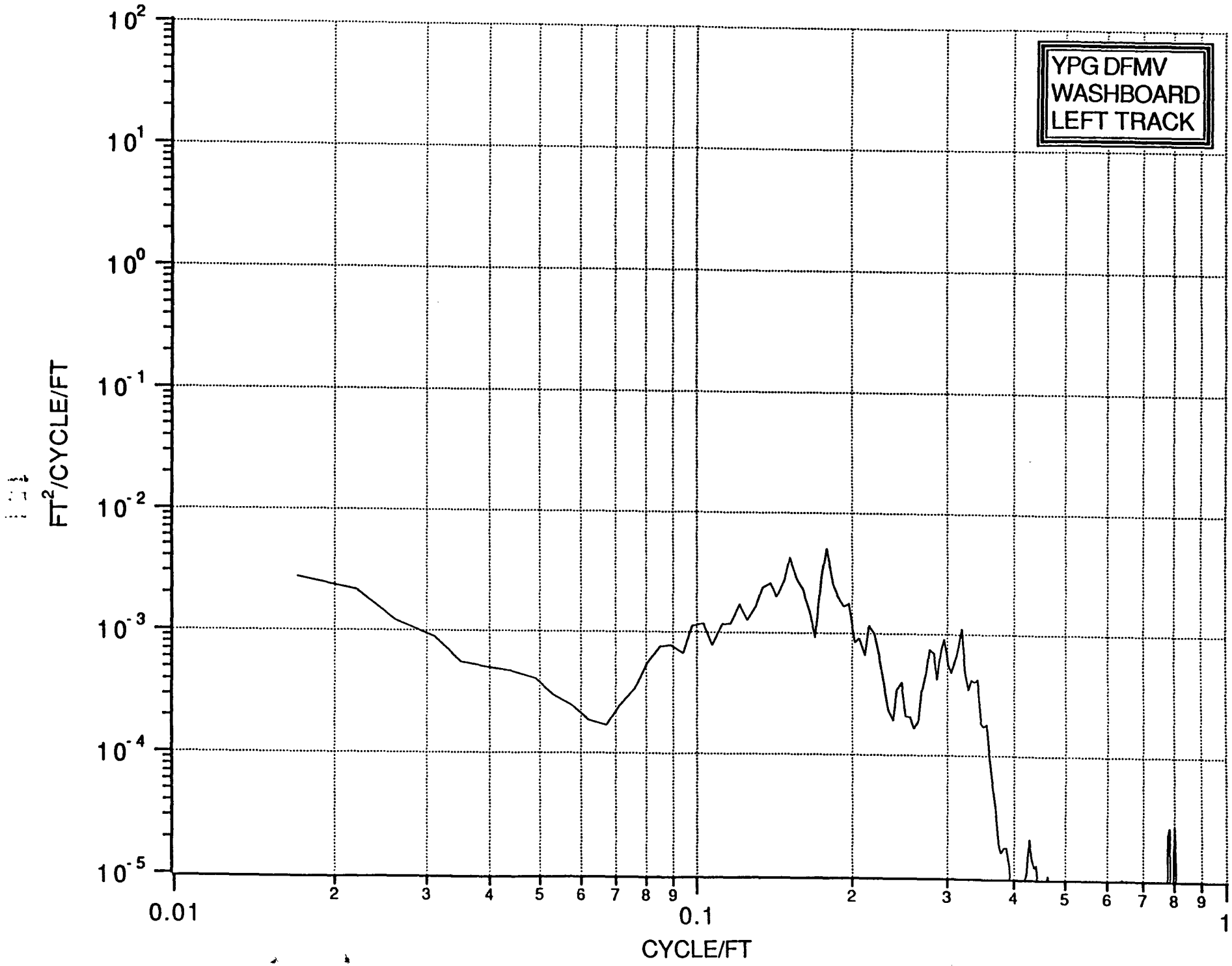
YPG DFMV
WASHBOARD
LEFT TRACK
FT²/CYCLE/FT
10²
10¹
10⁰
10⁻¹
10⁻²
10⁻³
10⁻⁴
10⁻⁵
0.01
0.1
1
2 3 4 5 6 7 8 9
2 3 4 5 6 7 8 9
CYCLE/FT

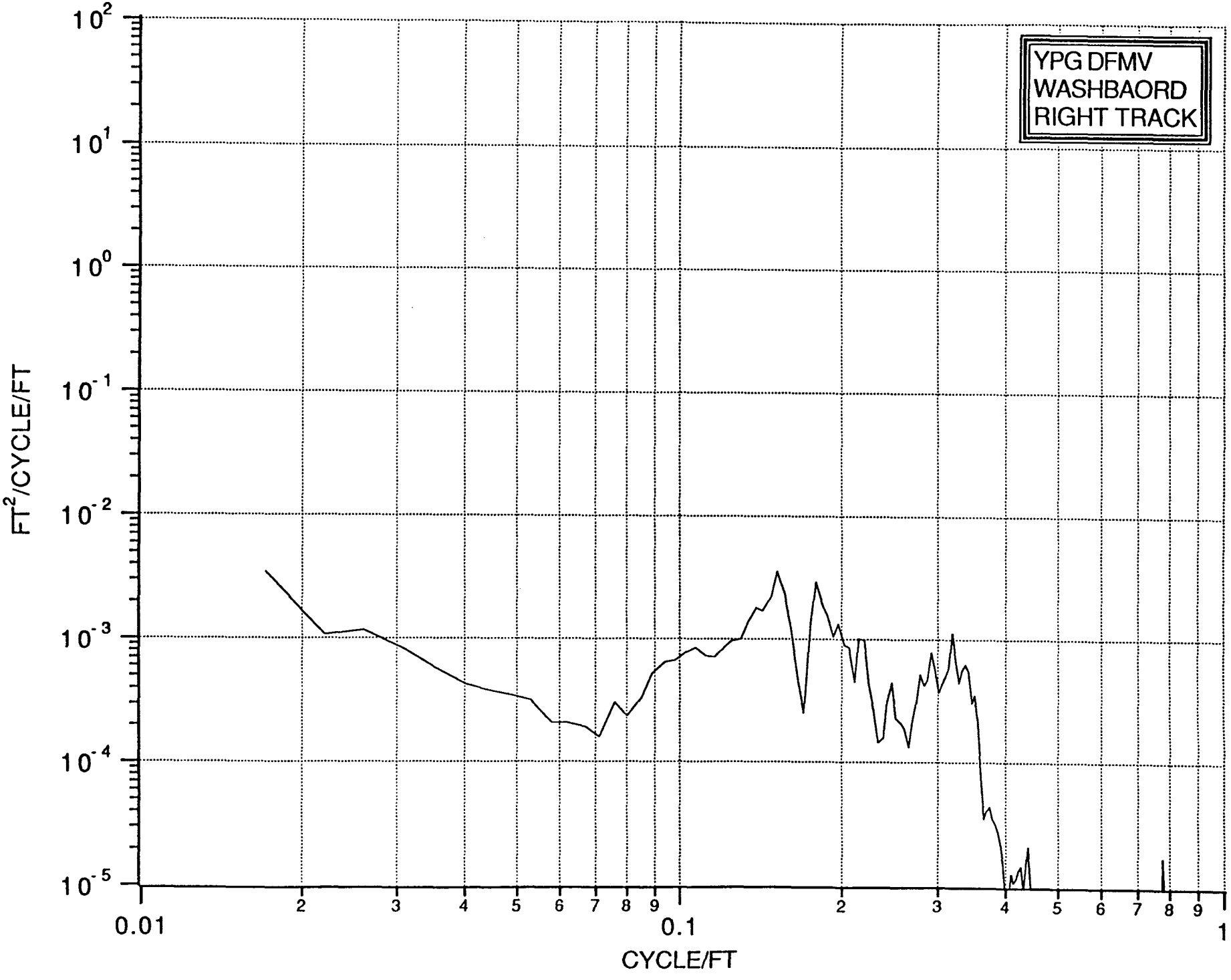
YPG DFMV
WASHBAORD
RIGHT TRACK
10^2
10^1
10^0
10^{-1}
10^{-2}
10^{-3}
10^{-4}
10^{-5}
FT^2/CYCLE/FT
0.01
0.1
1
2 3 4 5 6 7 8 9
2 3 4 5 6 7 8 9
CYCLE/FT

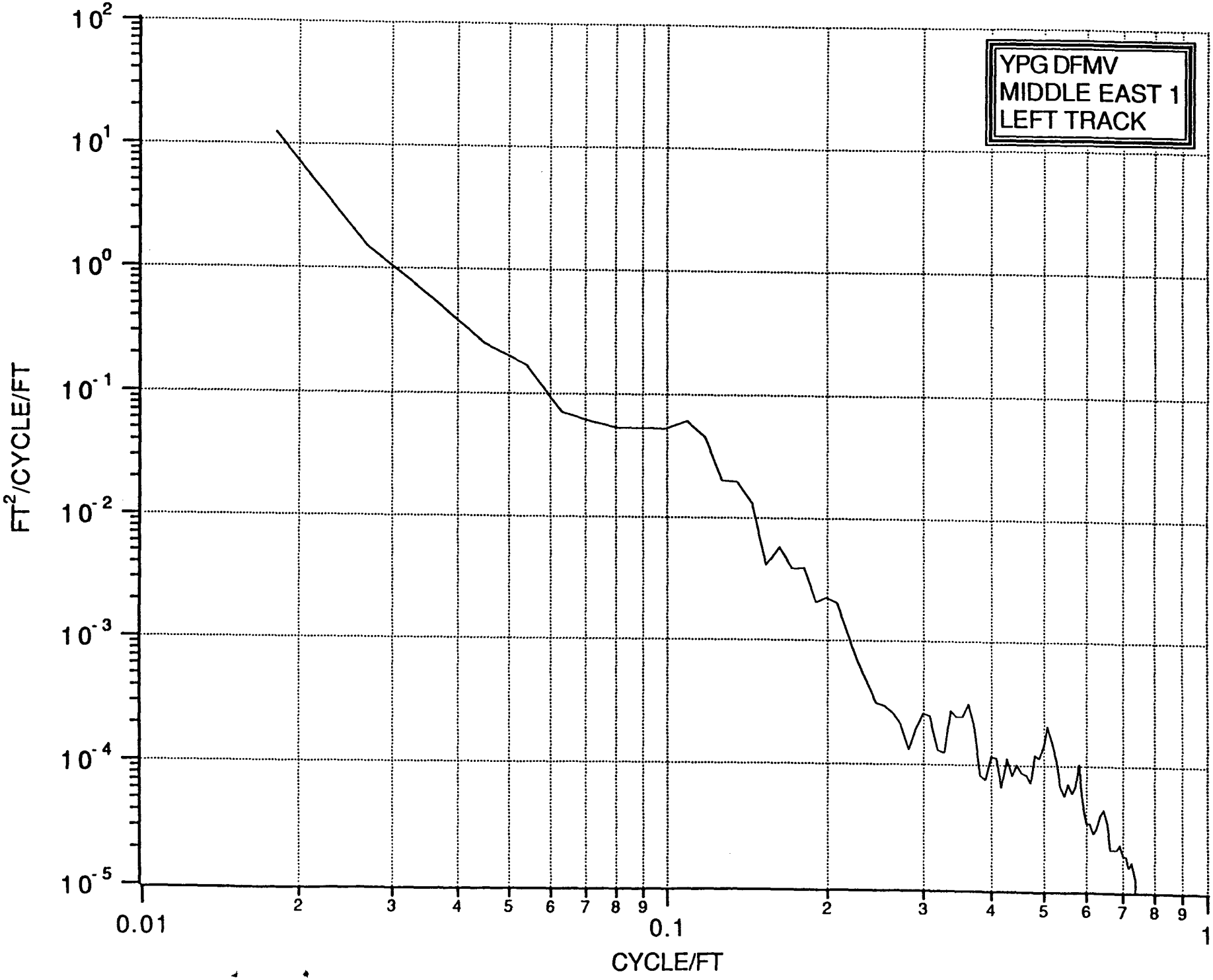
YPG DFMV
MIDDLE EAST 1
LEFT TRACK
FT²/CYCLE/FT
CYCLE/FT
10²
10¹
10⁰
10⁻¹
10⁻²
10⁻³
10⁻⁴
10⁻⁵
0.01
0.1
1
2 3 4 5 6 7 8 9
2 3 4 5 6 7 8 9

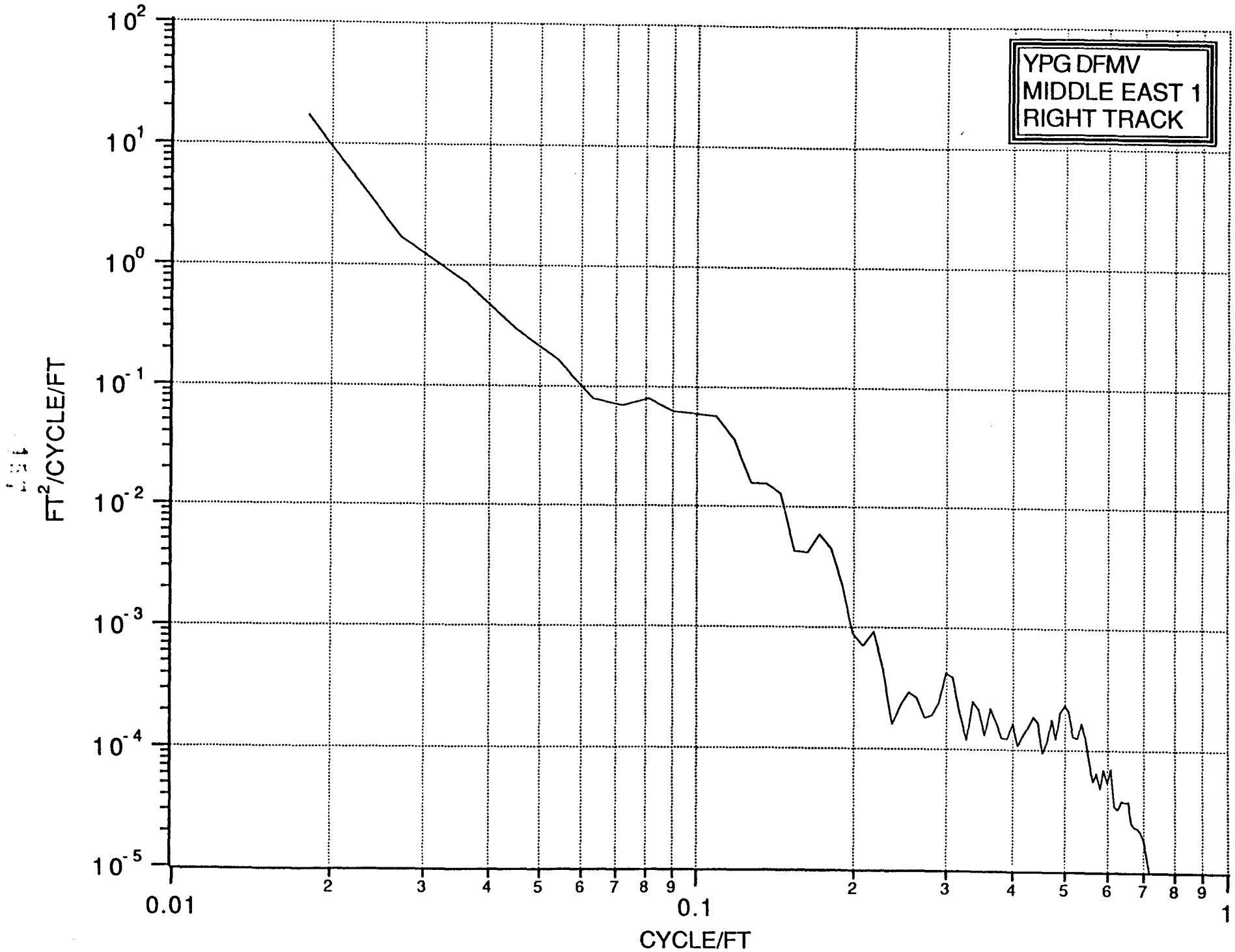
YPG DFMV
MIDDLE EAST 1
RIGHT TRACK
10^2
10^1
10^0
10^{-1}
10^{-2}
10^{-3}
10^{-4}
10^{-5}
FT^2/CYCLE/FT
0.01
2 3 4 5 6 7 8 9
0.1
2 3 4 5 6 7 8 9
1
CYCLE/FT

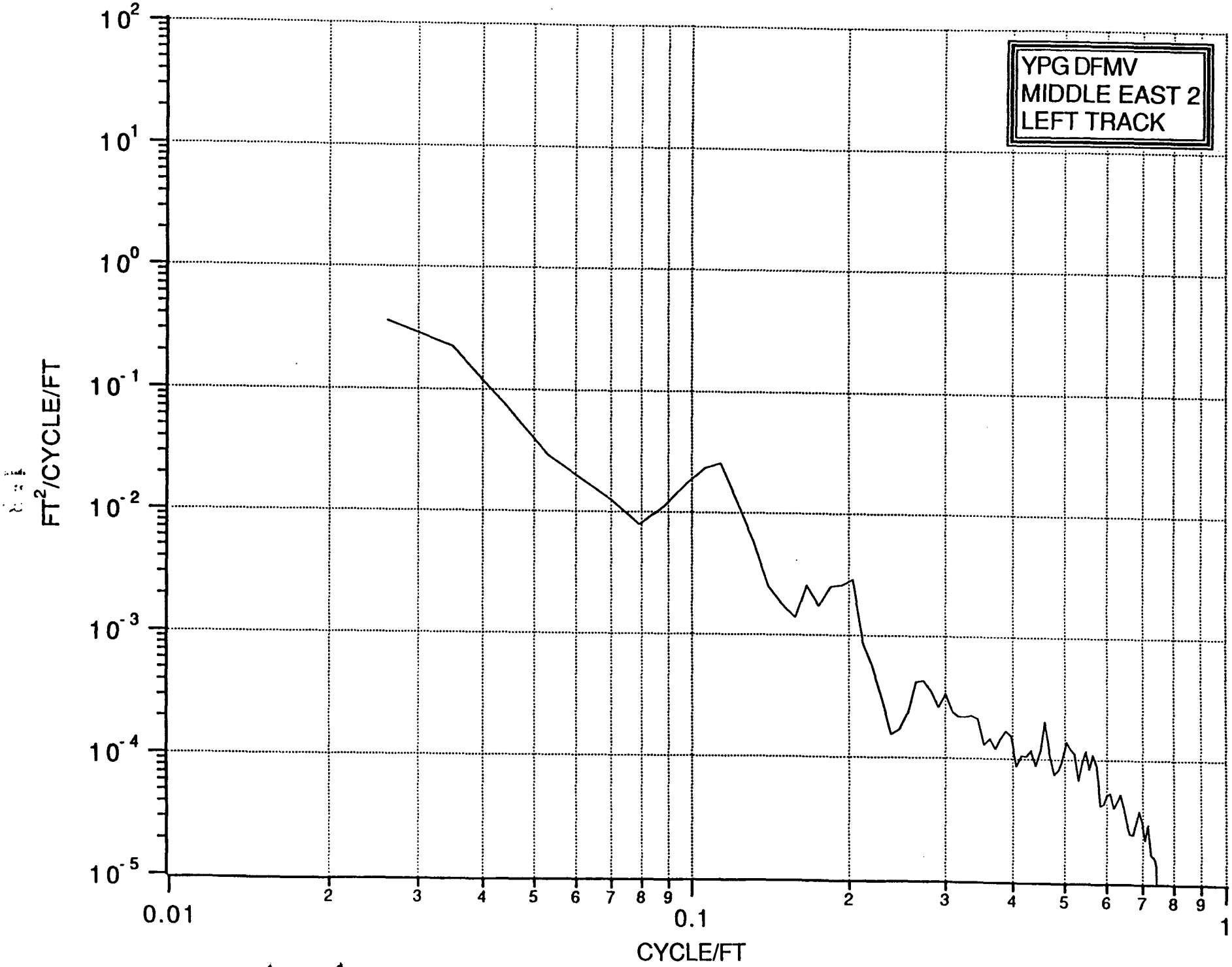
YPG DFMV
MIDDLE EAST 2
LEFT TRACK
10^2
10^1
10^0
10^{-1}
10^{-2}
10^{-3}
10^{-4}
10^{-5}
FT^2/CYCLE/FT
0.01
0.1
1
2 3 4 5 6 7 8 9
2 3 4 5 6 7 8 9
CYCLE/FT

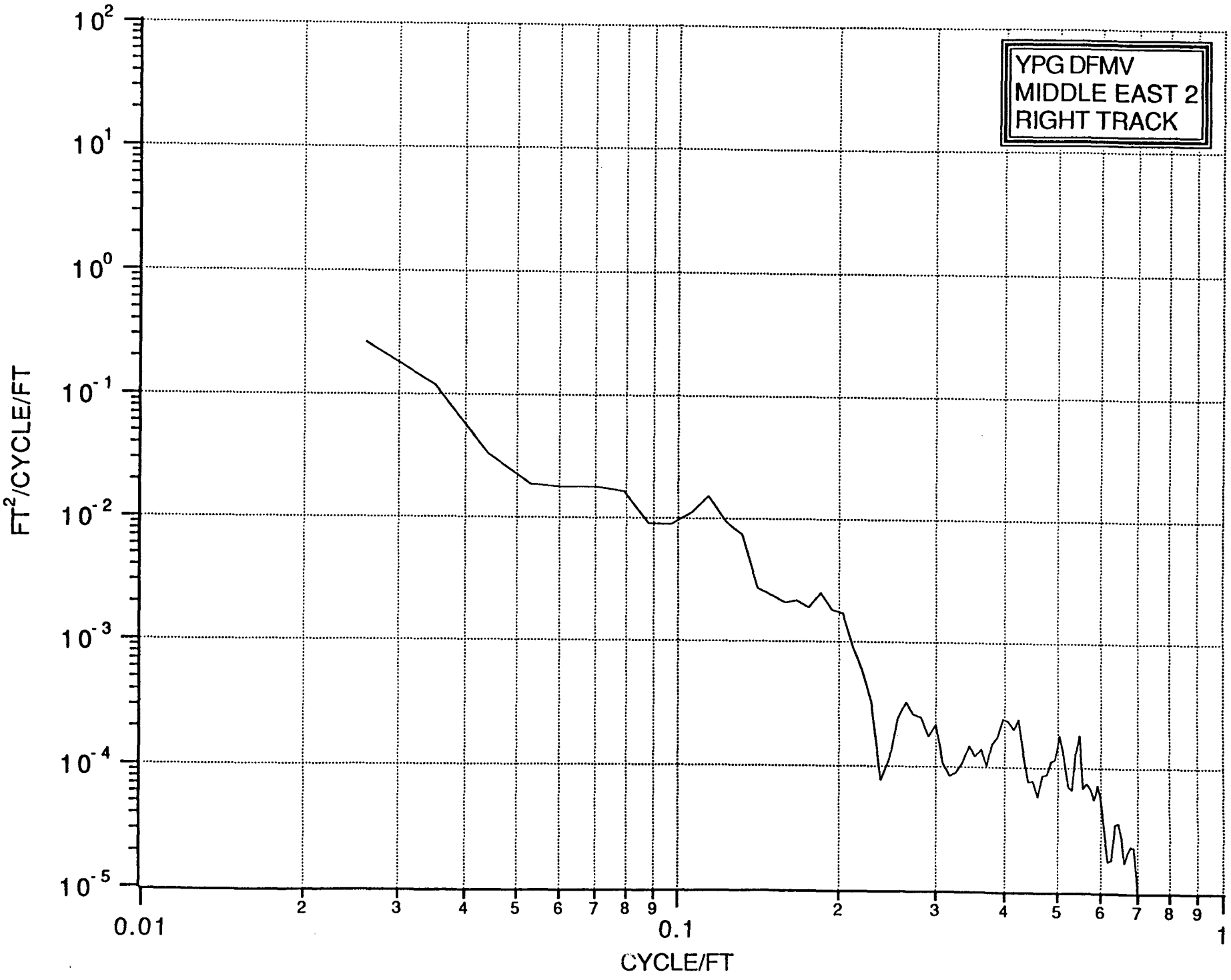
YPG DFMV
MIDDLE EAST 2
RIGHT TRACK
10^2
10^1
10^0
10^{-1}
10^{-2}
10^{-3}
10^{-4}
10^{-5}
FT^2/CYCLE/FT
0.01
2 3 4 5 6 7 8 9
0.1
2 3 4 5 6 7 8 9
1
CYCLE/FT

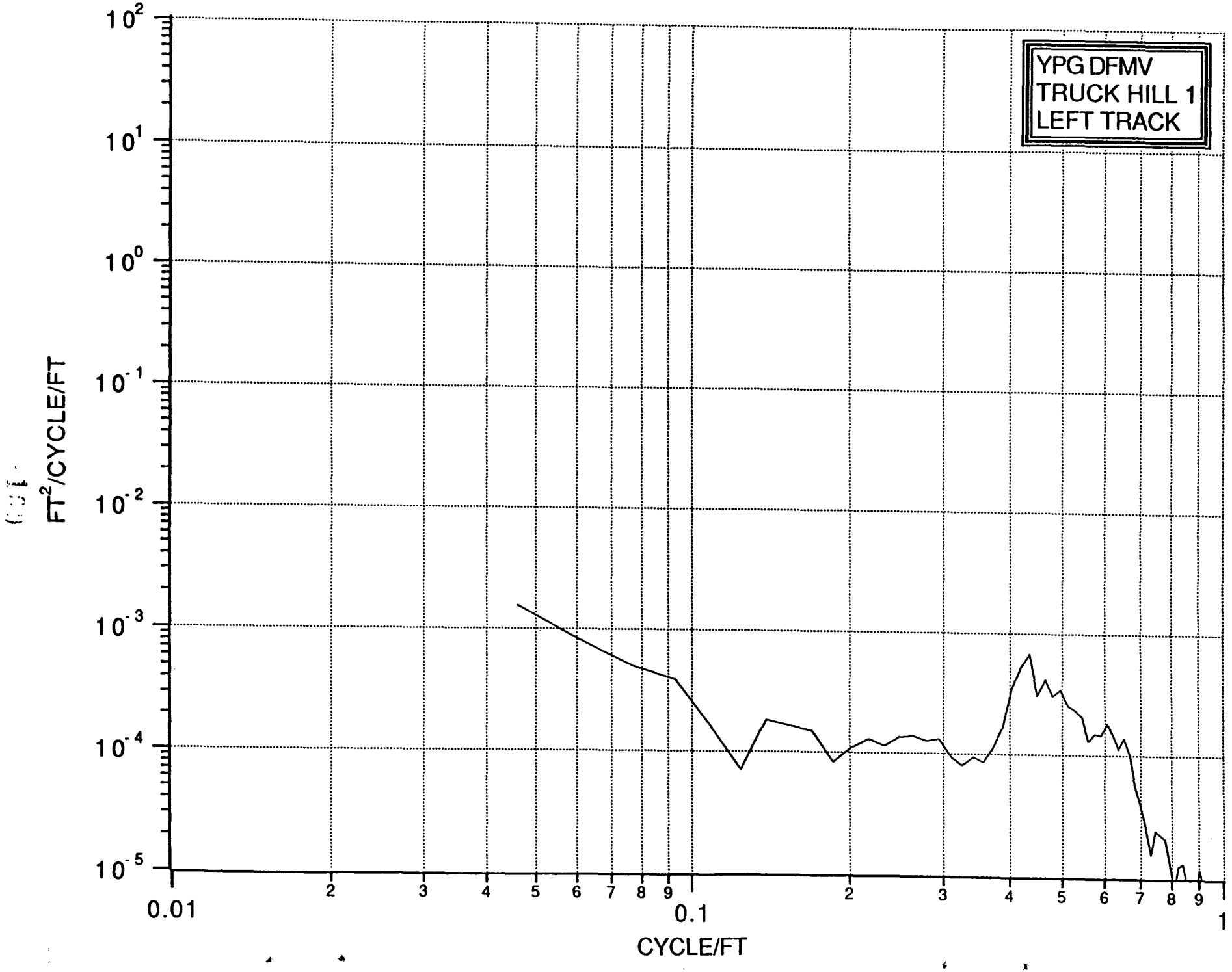
YPG DFMV
TRUCK HILL 1
LEFT TRACK
FT²/CYCLE/FT
CYCLE/FT
10²
10¹
10⁰
10⁻¹
10⁻²
10⁻³
10⁻⁴
10⁻⁵
0.01
0.1
1
2
3
4
5
6
7
8
9

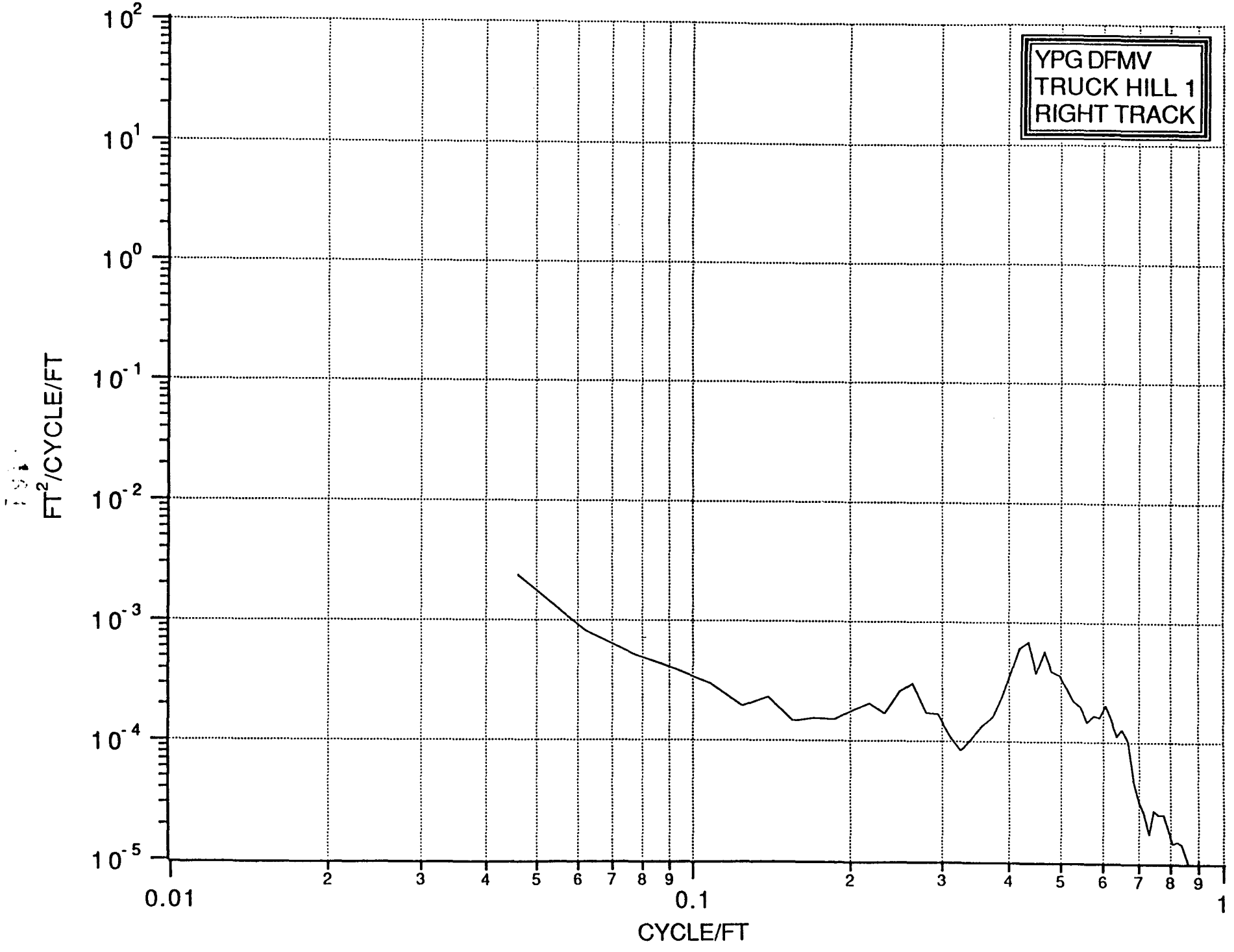
YPG DFMV
TRUCK HILL 1
RIGHT TRACK
10^2
10^1
10^0
10^{-1}
10^{-2}
10^{-3}
10^{-4}
10^{-5}
FT^2/CYCLE/FT
0.01
2 3 4 5 6 7 8 9
0.1
2 3 4 5 6 7 8 9
1
CYCLE/FT

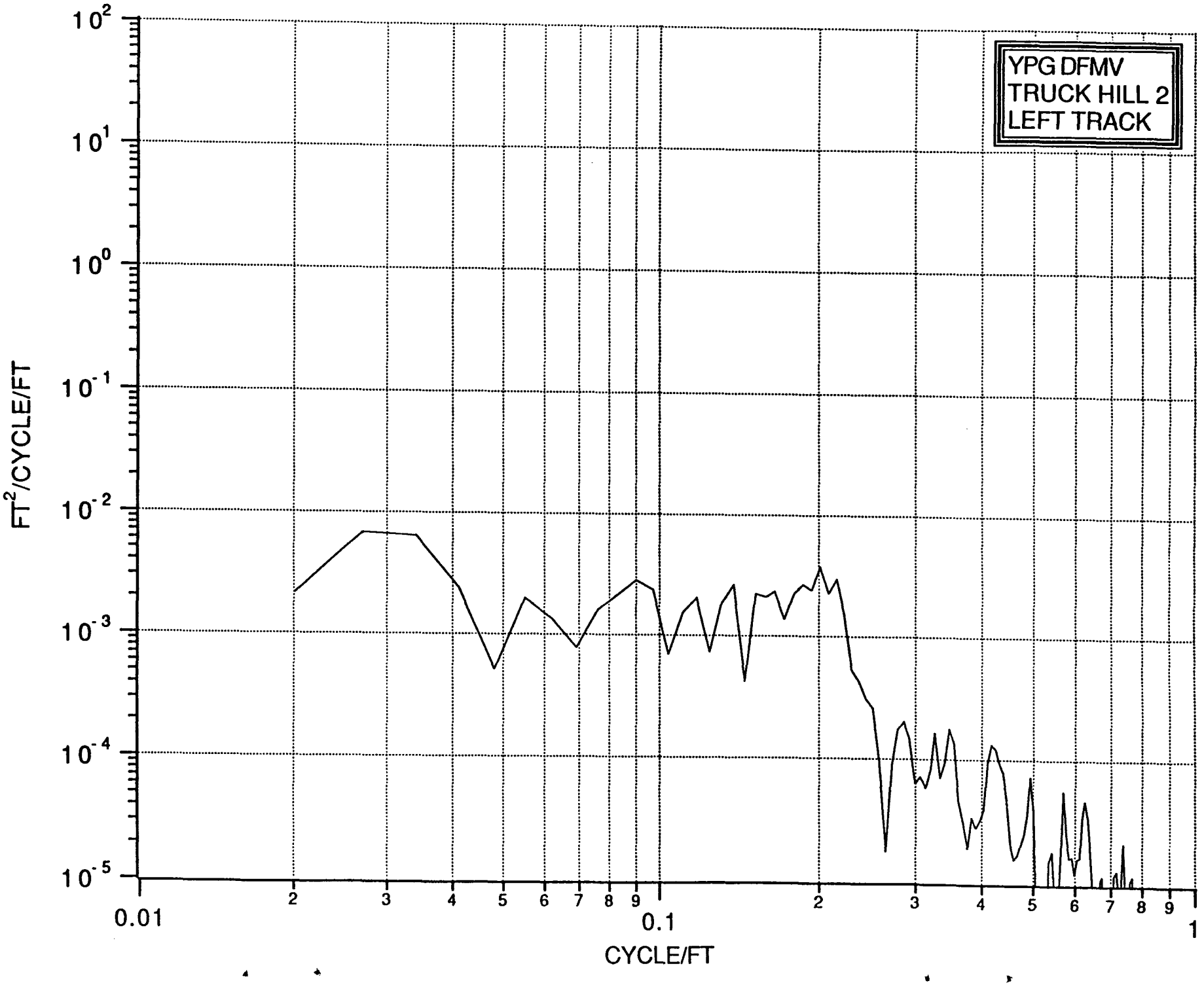
YPG DFMV
TRUCK HILL 2
LEFT TRACK
10^2
10^1
10^0
10^{-1}
10^{-2}
10^{-3}
10^{-4}
10^{-5}
FT^2/CYCLE/FT
0.01
0.1
1
2 3 4 5 6 7 8 9
2 3 4 5 6 7 8 9
CYCLE/FT

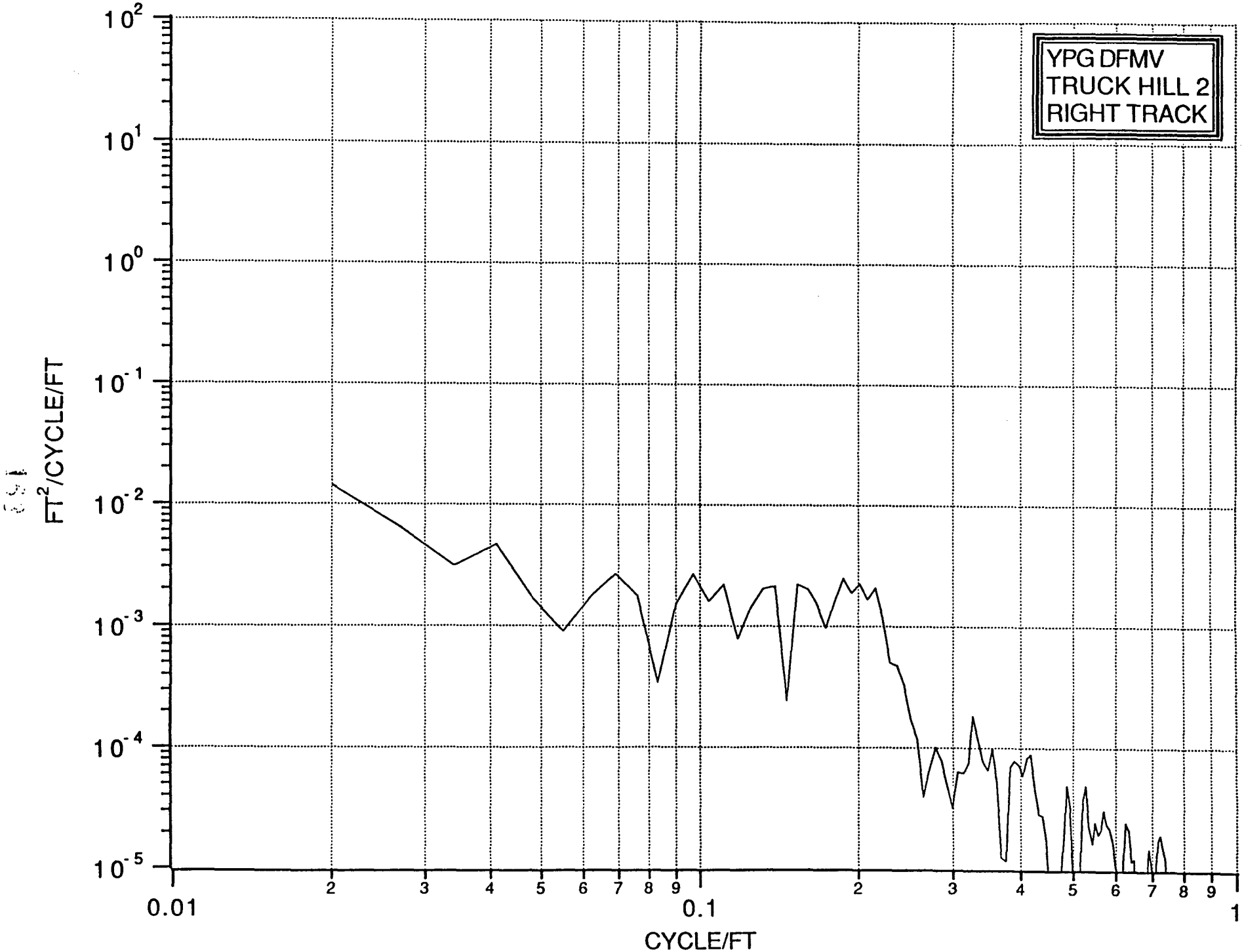
YPG DFMV
TRUCK HILL 2
RIGHT TRACK
10^2
10^1
10^0
10^{-1}
10^{-2}
10^{-3}
10^{-4}
10^{-5}
FT^2/CYCLE/FT
0.01
0.1
1
2 3 4 5 6 7 8 9
2 3 4 5 6 7 8 9
CYCLE/FT

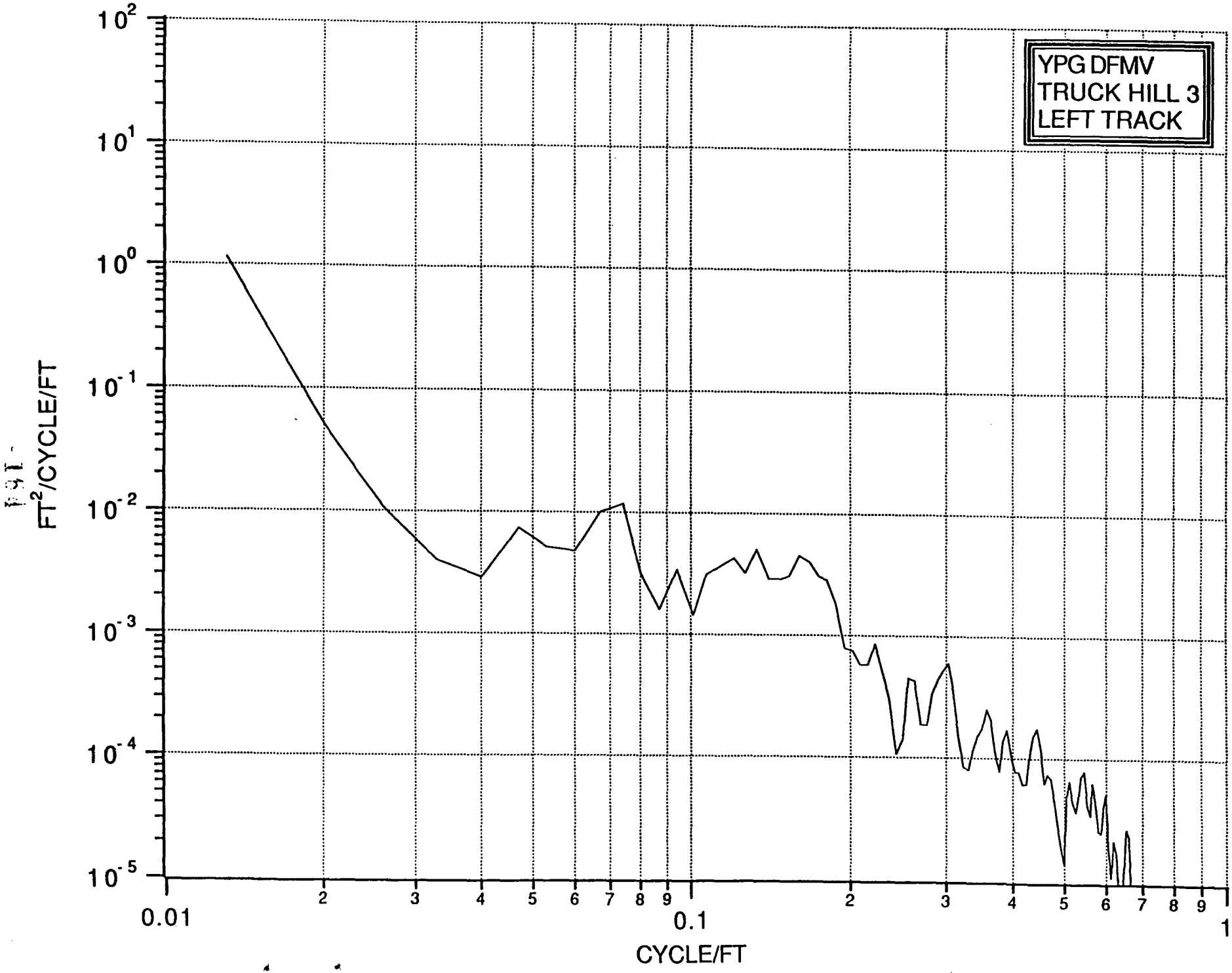
YPG DFMV
TRUCK HILL 3
LEFT TRACK
FT²/CYCLE/FT
CYCLE/FT
10²
10¹
10⁰
10⁻¹
10⁻²
10⁻³
10⁻⁴
10⁻⁵
0.01
0.1
1
2 3 4 5 6 7 8 9
2 3 4 5 6 7 8 9

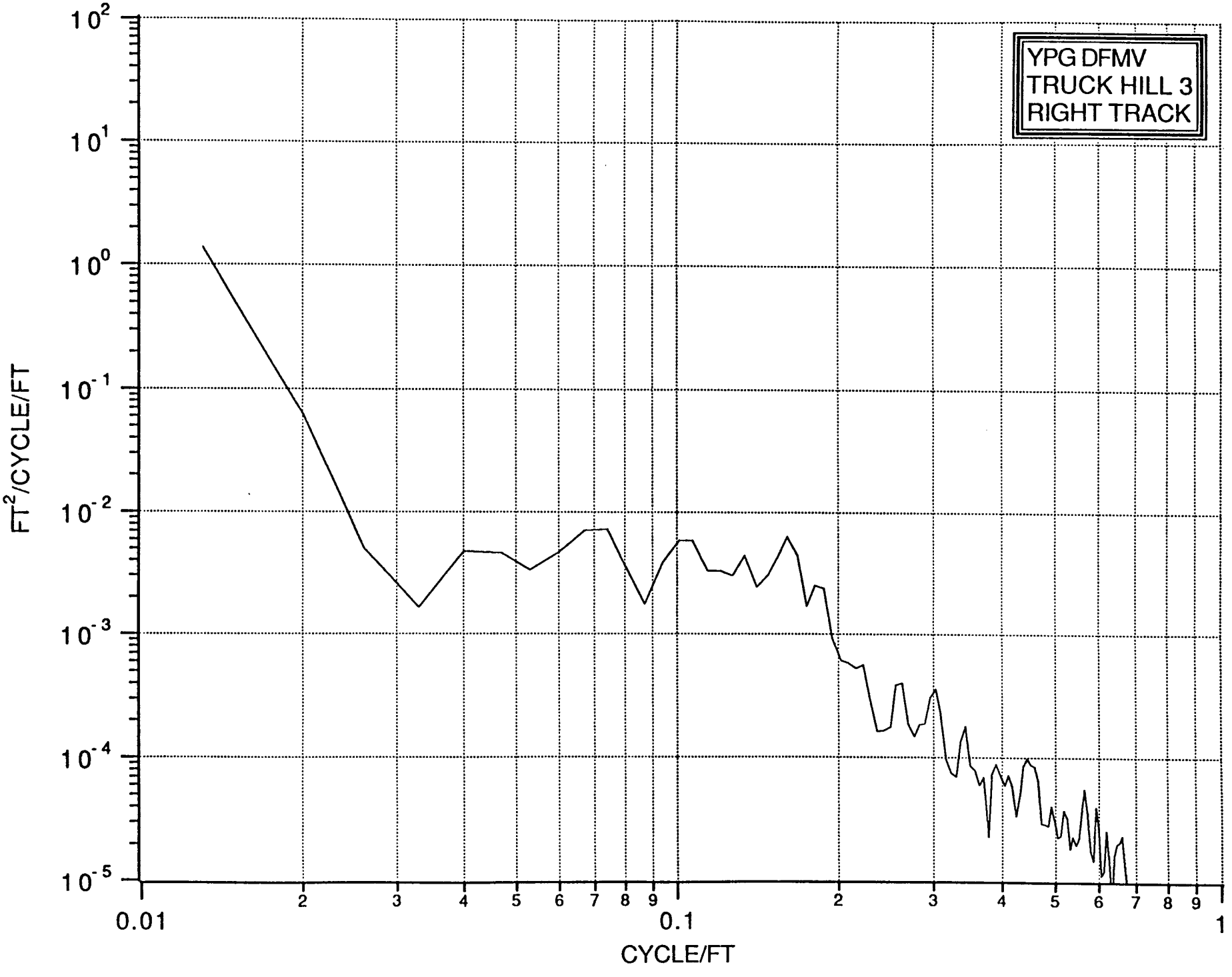
YPG DFMV
TRUCK HILL 3
RIGHT TRACK
10^2
10^1
10^0
10^{-1}
10^{-2}
10^{-3}
10^{-4}
10^{-5}
FT^2/CYCLE/FT
0.01
2
3
4
5
6
7
8
9
0.1
2
3
4
5
6
7
8
9
1
CYCLE/FT

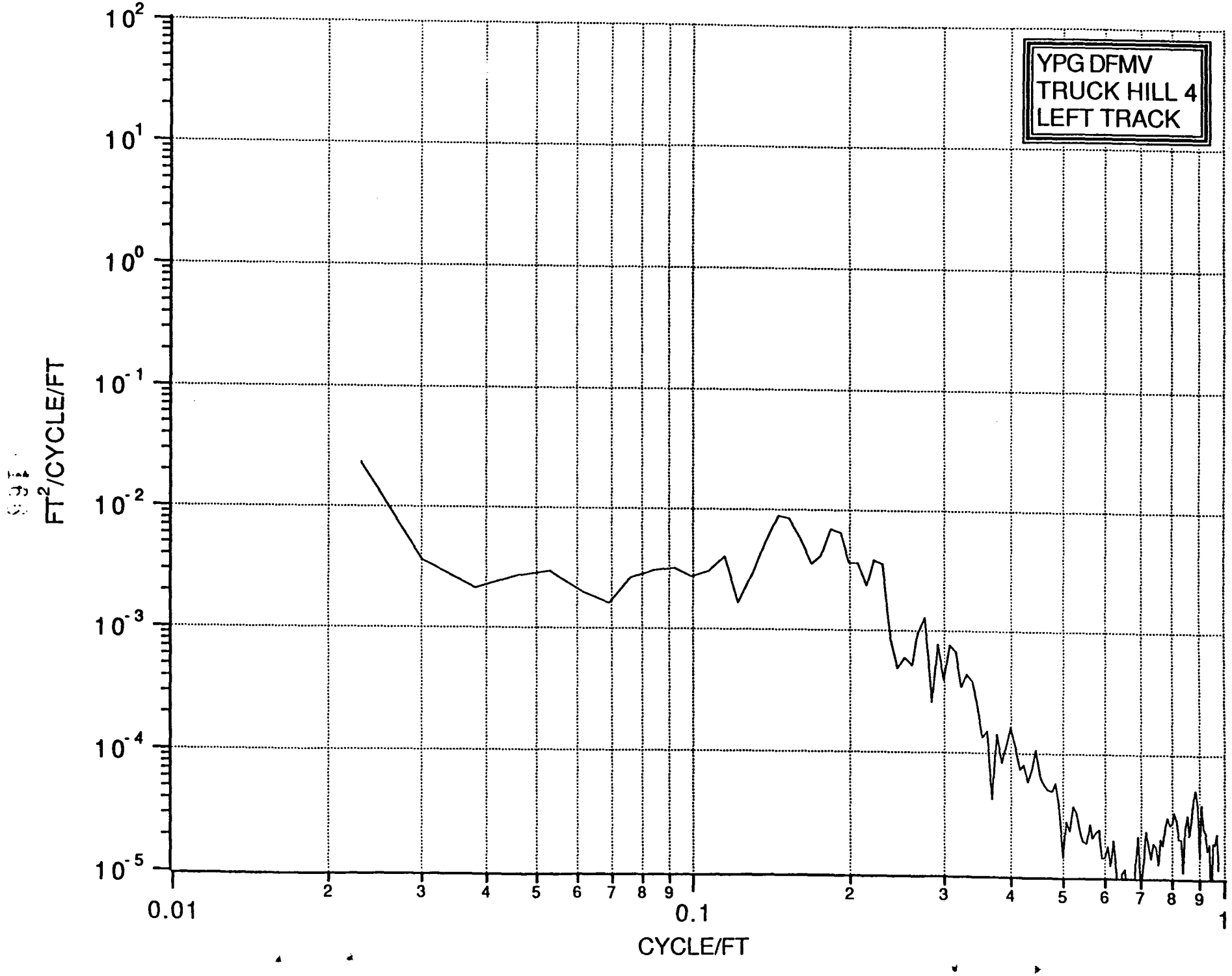
YPG DFMV
TRUCK HILL 4
LEFT TRACK
10^2
10^1
10^0
10^{-1}
10^{-2}
10^{-3}
10^{-4}
10^{-5}
FT^2/CYCLE/FT
0.01
2 3 4 5 6 7 8 9
0.1
2 3 4 5 6 7 8 9
1
CYCLE/FT

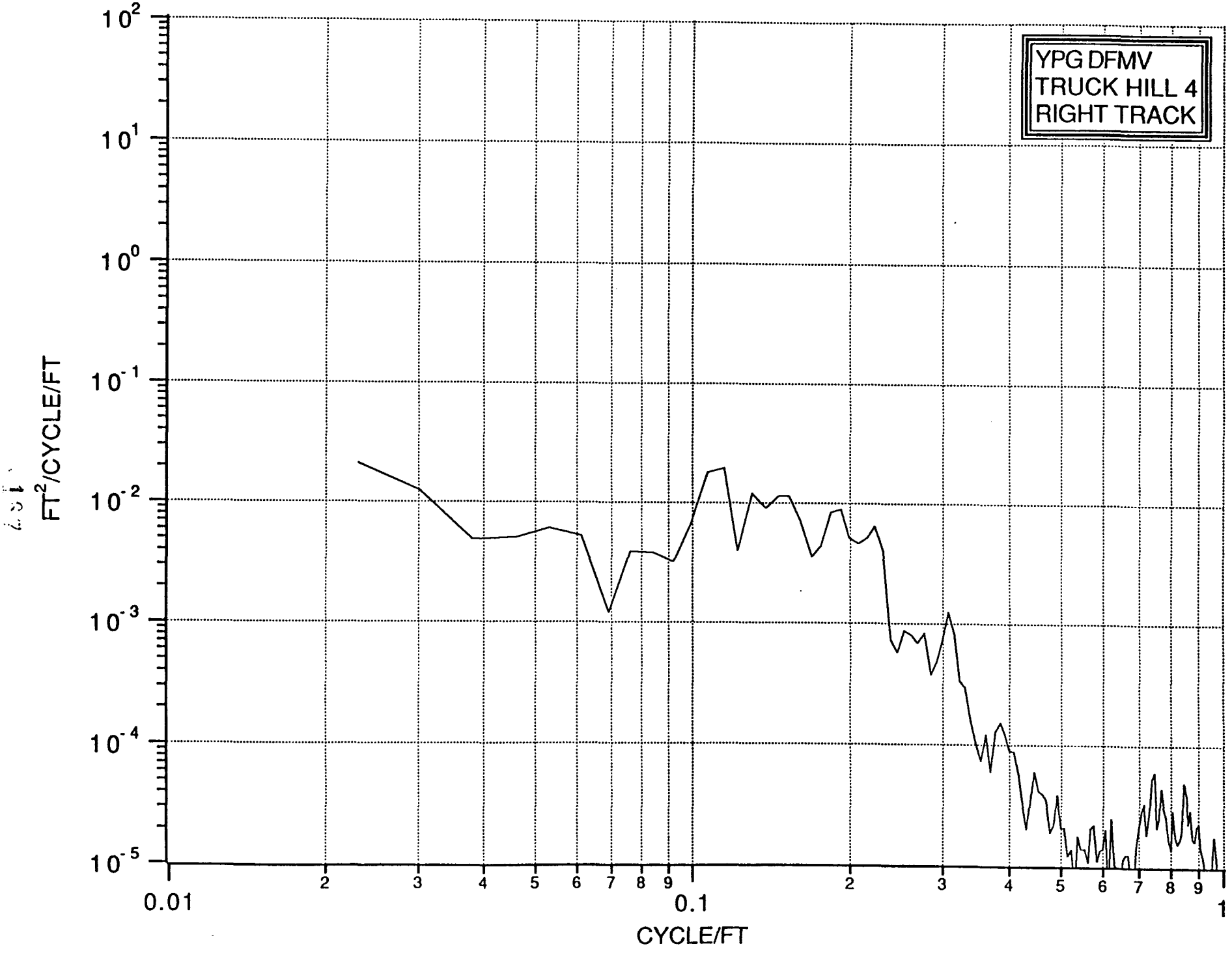
YPG DFMV
TRUCK HILL 4
RIGHT TRACK
10^2
10^1
10^0
10^{-1}
10^{-2}
10^{-3}
10^{-4}
10^{-5}
FT^2/CYCLE/FT
0.01
0.1
1
2 3 4 5 6 7 8 9
2 3 4 5 6 7 8 9
CYCLE/FT

APPENDIX E

WAVE-NUMBER SPECTRA - APG PROFILOMETER

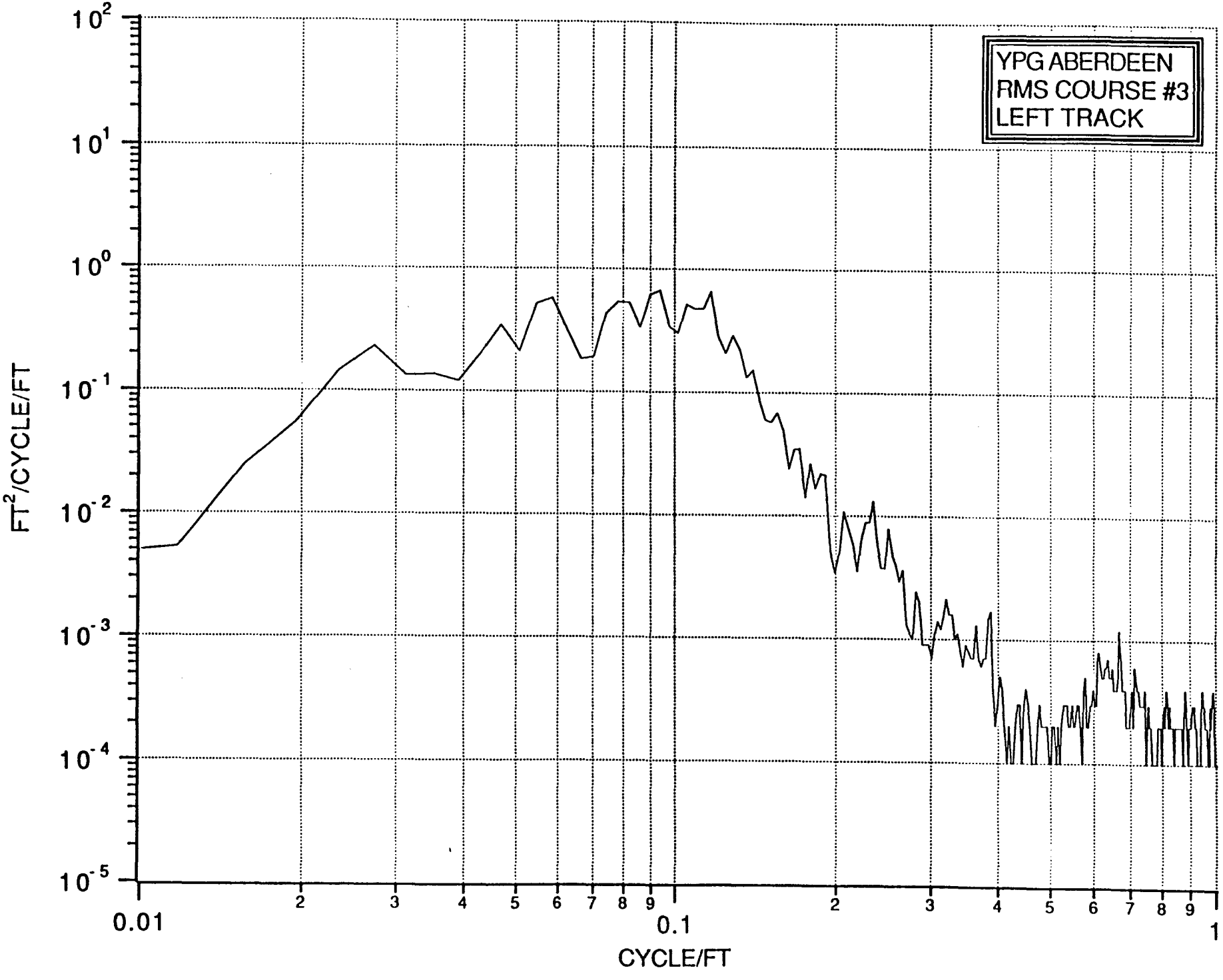
YPG ABERDEEN
RMS COURSE #3
LEFT TRACK
10^2
10^1
10^0
10^{-1}
10^{-2}
10^{-3}
10^{-4}
10^{-5}
FT^2/CYCLE/FT
0.01
2
3
4
5
6
7
8
9
0.1
2
3
4
5
6
7
8
9
1
CYCLE/FT

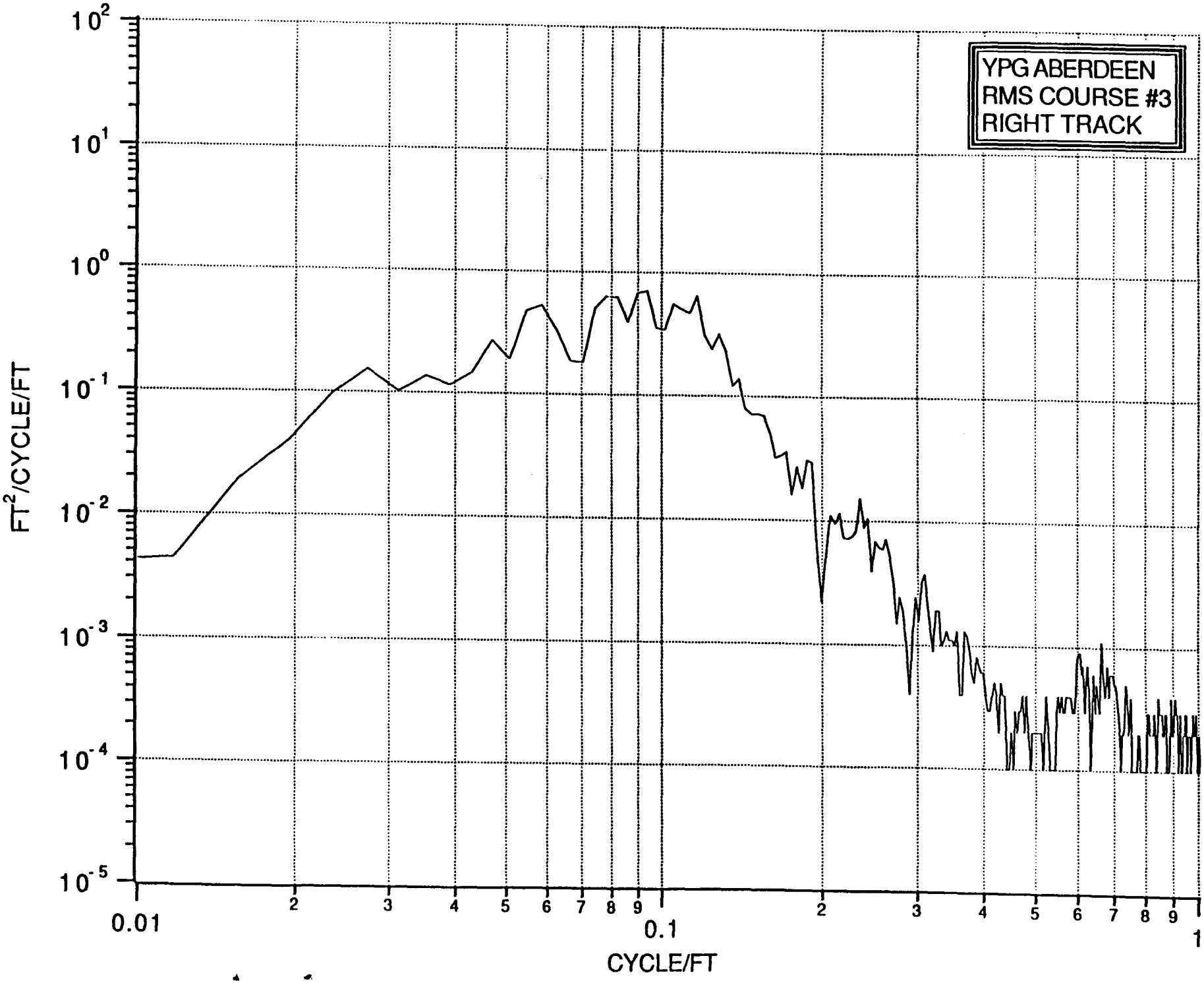
YPG ABERDEEN
RMS COURSE #3
RIGHT TRACK
10^2
10^1
10^0
10^{-1}
10^{-2}
10^{-3}
10^{-4}
10^{-5}
FT^2/CYCLE/FT
0.01
2 3 4 5 6 7 8 9
0.1
2 3 4 5 6 7 8 9
1
CYCLE/FT

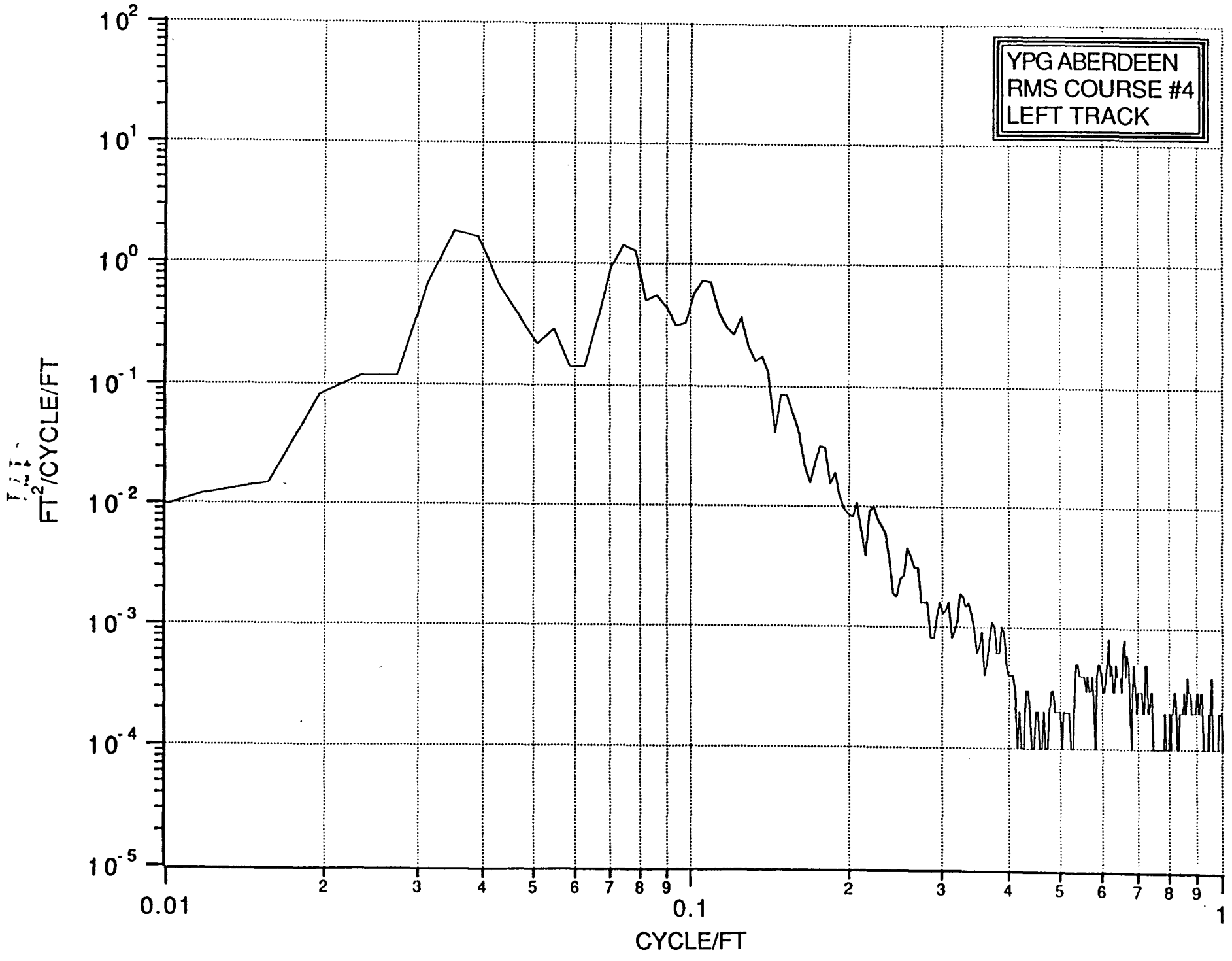
YPG ABERDEEN
RMS COURSE #4
LEFT TRACK
10^2
10^1
10^0
10^{-1}
10^{-2}
10^{-3}
10^{-4}
10^{-5}
FT²/CYCLE/FT
0.01
2 3 4 5 6 7 8 9
0.1
2 3 4 5 6 7 8 9
1
CYCLE/FT

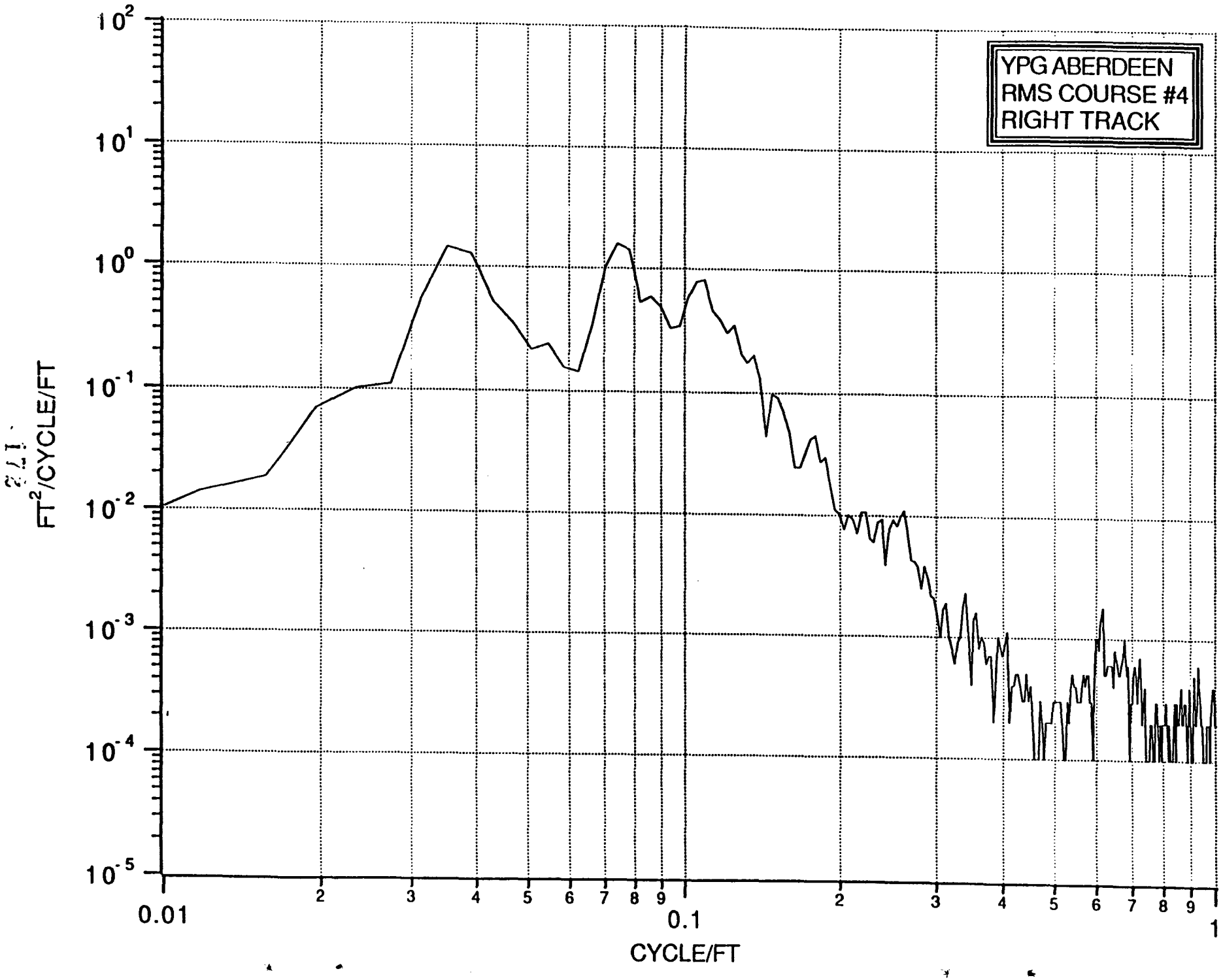
YPG ABERDEEN
RMS COURSE #4
RIGHT TRACK
10^2
10^1
10^0
10^{-1}
10^{-2}
10^{-3}
10^{-4}
10^{-5}
FT^2/CYCLE/FT
0.01
0.1
1
2 3 4 5 6 7 8 9
2 3 4 5 6 7 8 9
CYCLE/FT

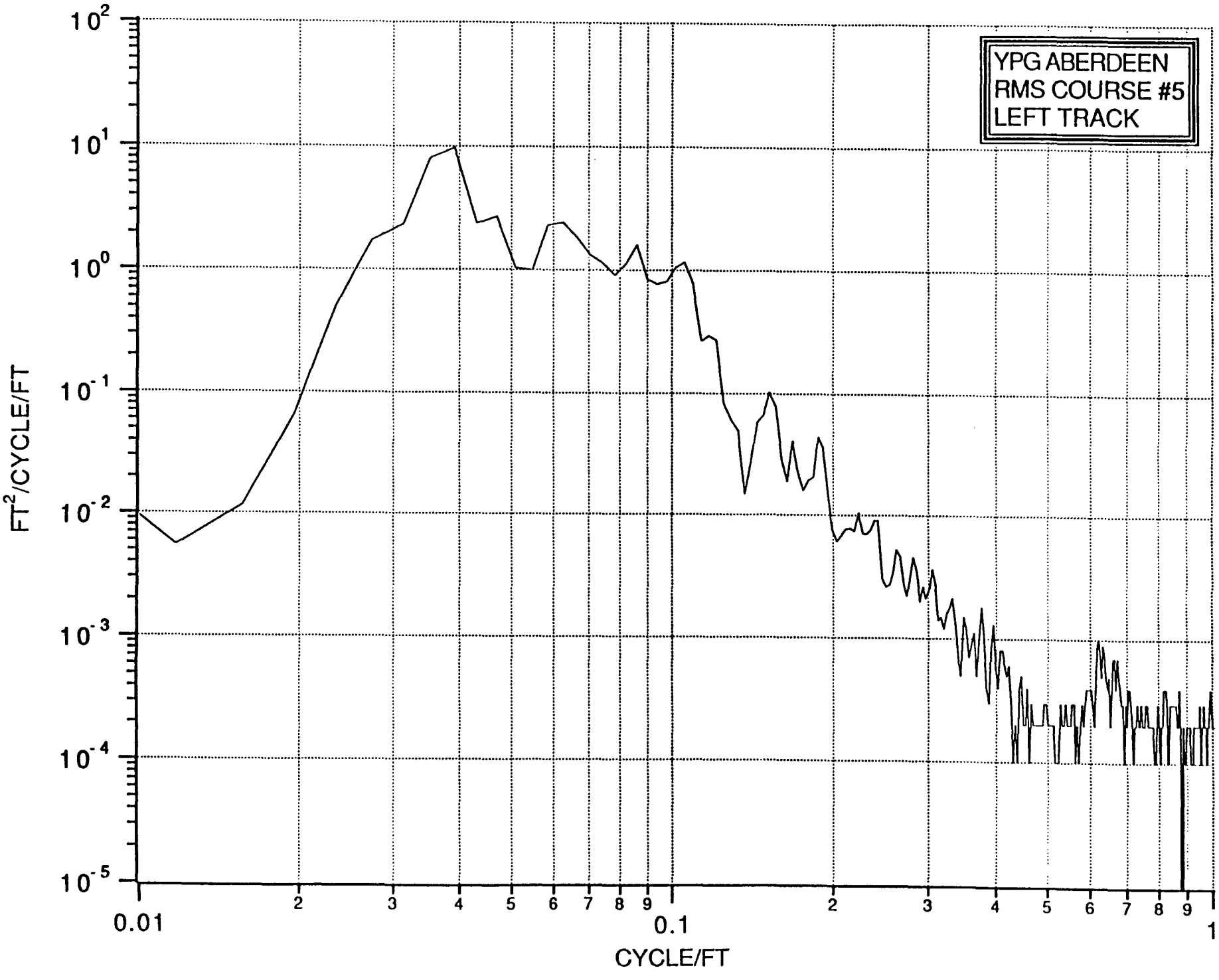
YPG ABERDEEN
RMS COURSE #5
LEFT TRACK
10^2
10^1
10^0
10^{-1}
10^{-2}
10^{-3}
10^{-4}
10^{-5}
FT^2/CYCLE/FT
0.01
2 3 4 5 6 7 8 9
0.1
2 3 4 5 6 7 8 9
1
CYCLE/FT

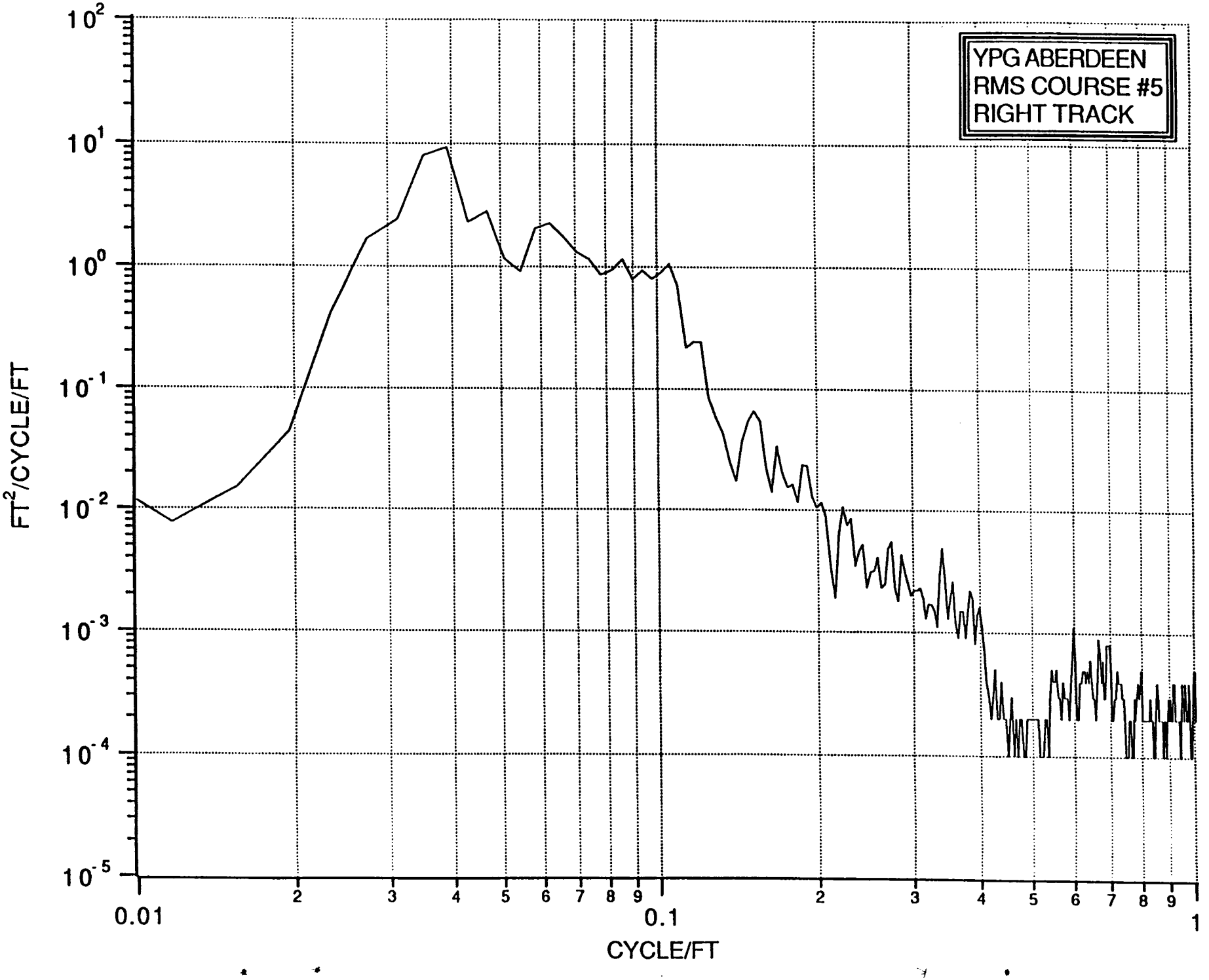
YPG ABERDEEN
RMS COURSE #5
RIGHT TRACK
10^2
10^1
10^0
10^{-1}
10^{-2}
10^{-3}
10^{-4}
10^{-5}
FT^2/CYCLE/FT
0.01
0.1
1
2 3 4 5 6 7 8 9
2 3 4 5 6 7 8 9
CYCLE/FT

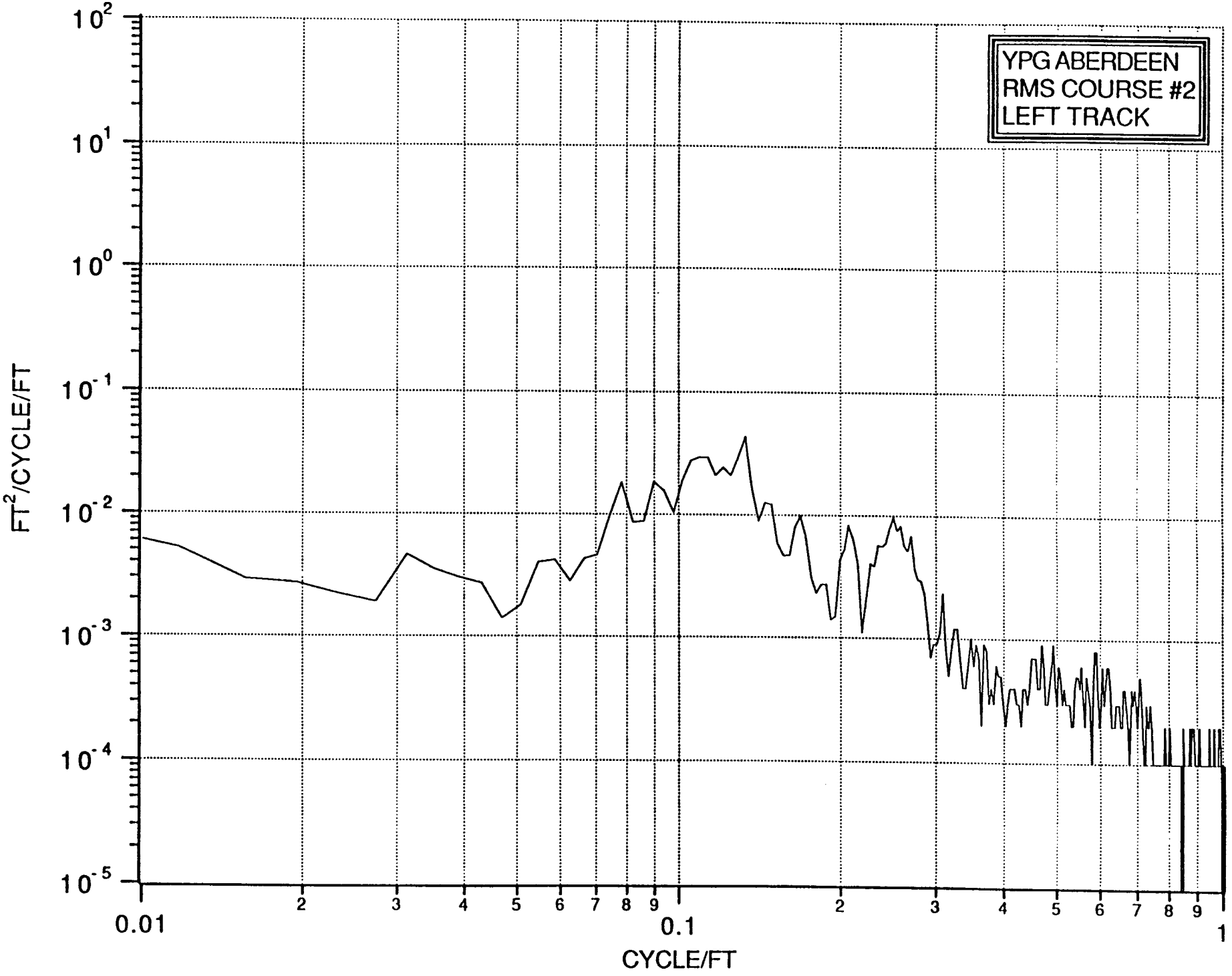
YPG ABERDEEN
RMS COURSE #2
LEFT TRACK
10^2
10^1
10^0
10^{-1}
10^{-2}
10^{-3}
10^{-4}
10^{-5}
FT^2/CYCLE/FT
0.01
2 3 4 5 6 7 8 9
0.1
2 3 4 5 6 7 8 9
1
CYCLE/FT

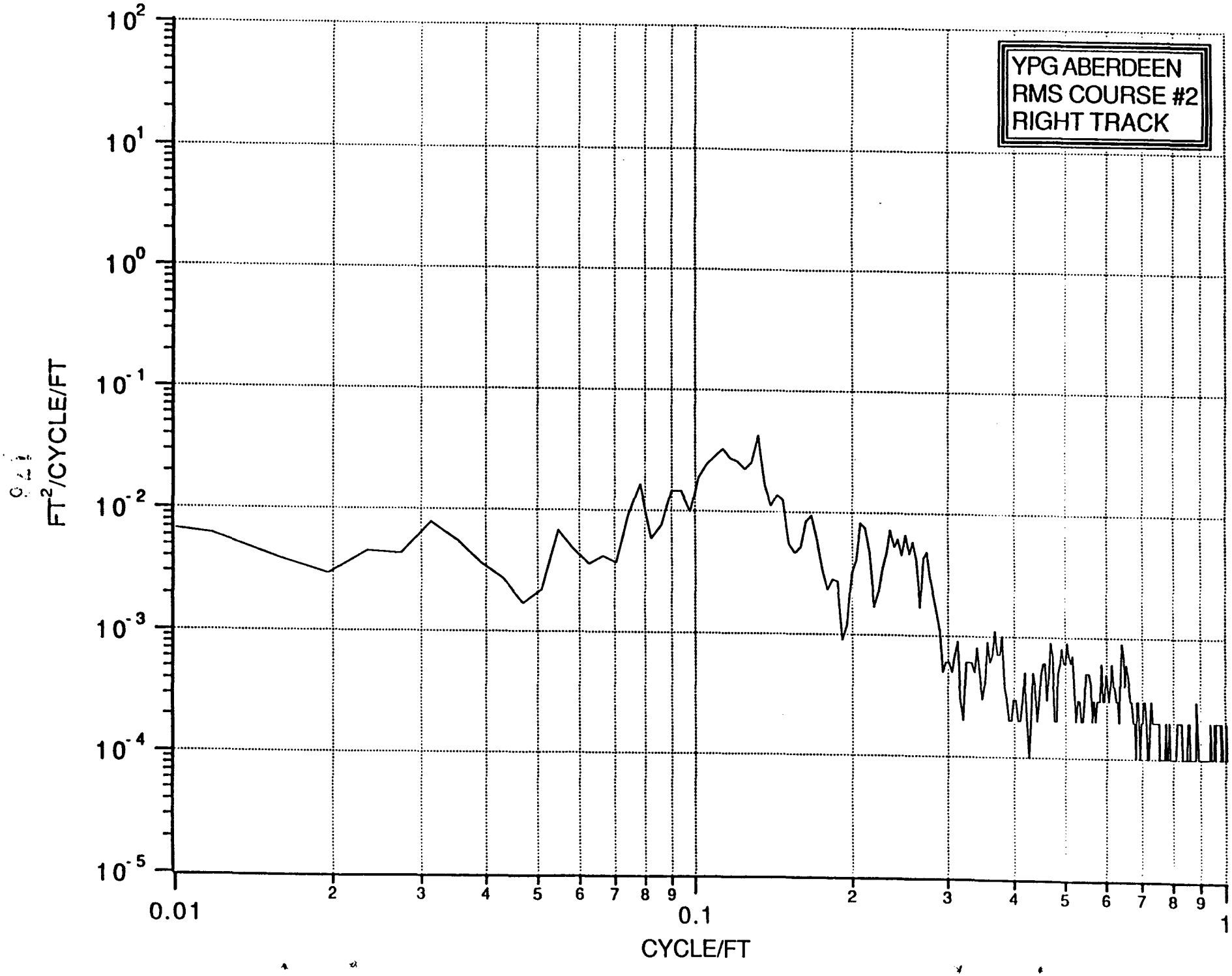
YPG ABERDEEN
RMS COURSE #2
RIGHT TRACK
10^2
10^1
10^0
10^{-1}
10^{-2}
10^{-3}
10^{-4}
10^{-5}
FT^2/CYCLE/FT
0.01
2 3 4 5 6 7 8 9
0.1
2 3 4 5 6 7 8 9
1
CYCLE/FT

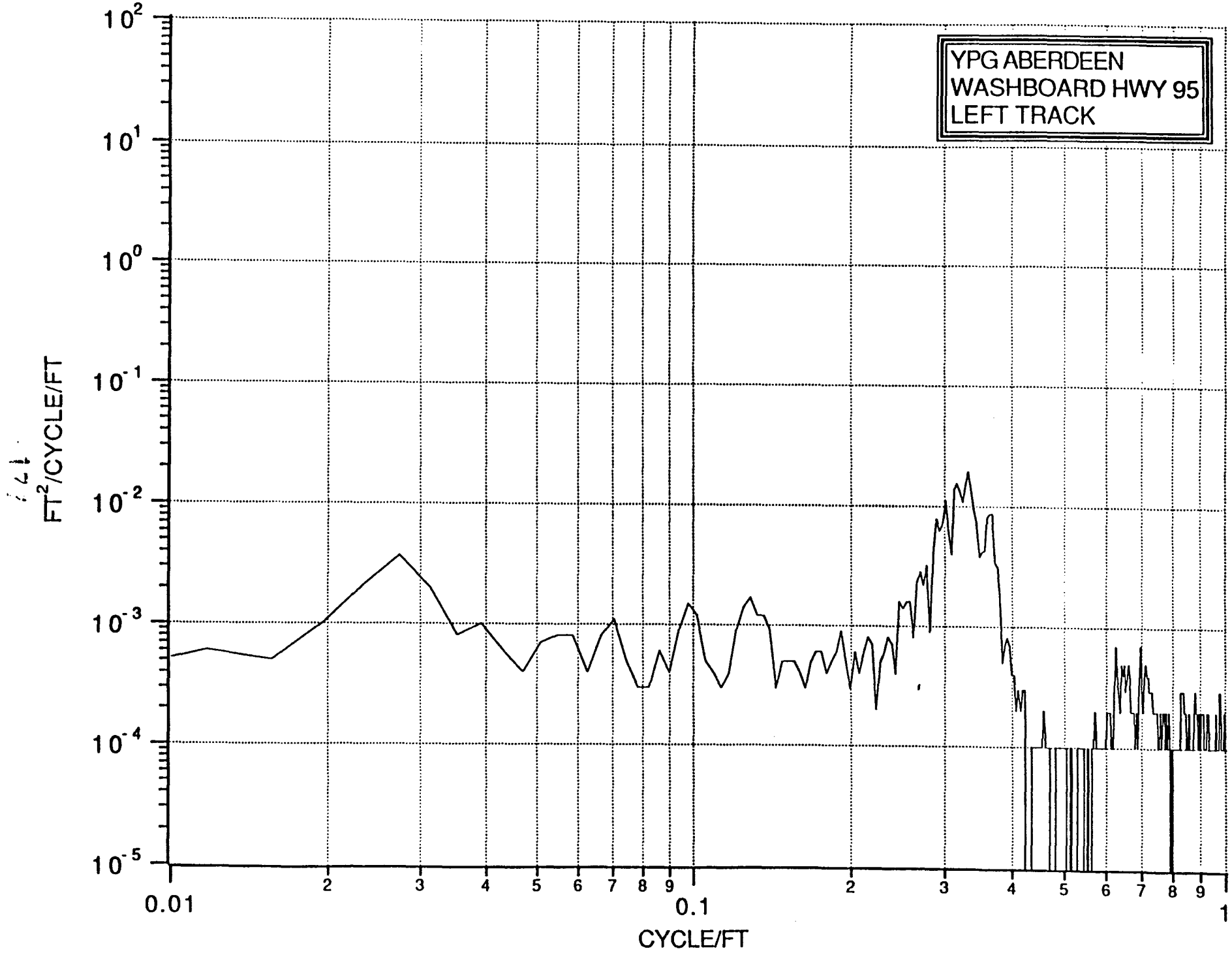
YPG ABERDEEN
WASHBOARD HWY 95
LEFT TRACK
10^2
10^1
10^0
10^{-1}
10^{-2}
10^{-3}
10^{-4}
10^{-5}
FT^2/CYCLE/FT
0.01
2 3 4 5 6 7 8 9
0.1
2 3 4 5 6 7 8 9
1
CYCLE/FT

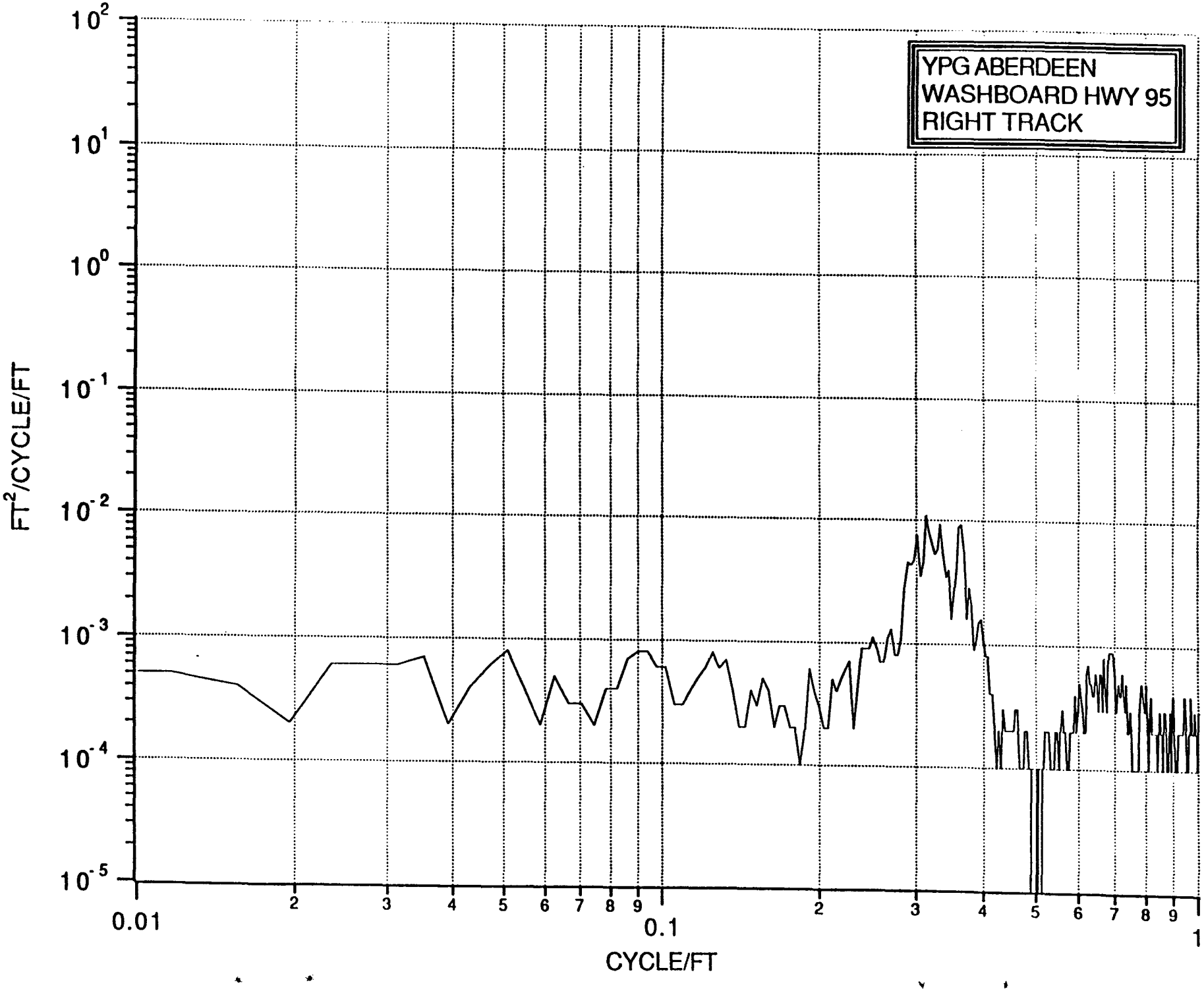
YPG ABERDEEN
WASHBOARD HWY 95
RIGHT TRACK
10^2
10^1
10^0
10^{-1}
10^{-2}
10^{-3}
10^{-4}
10^{-5}
FT^2/CYCLE/FT
0.01
2 3 4 5 6 7 8 9
0.1
2 3 4 5 6 7 8 9
1
CYCLE/FT

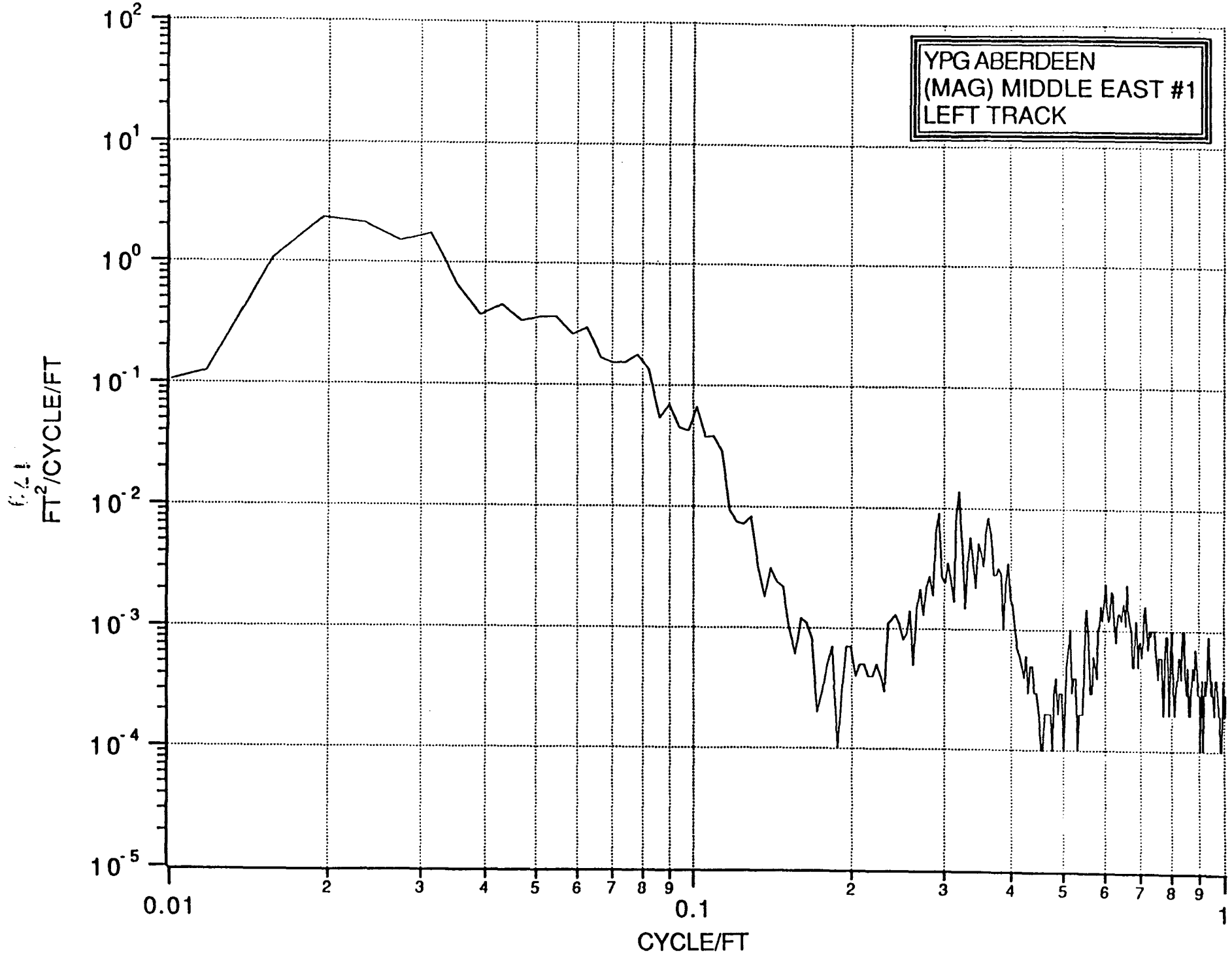
YPG ABERDEEN
(MAG) MIDDLE EAST #1
LEFT TRACK
10^2
10^1
10^0
10^{-1}
10^{-2}
10^{-3}
10^{-4}
10^{-5}
FT²/CYCLE/FT
0.01
2 3 4 5 6 7 8 9
0.1
2 3 4 5 6 7 8 9
1
CYCLE/FT

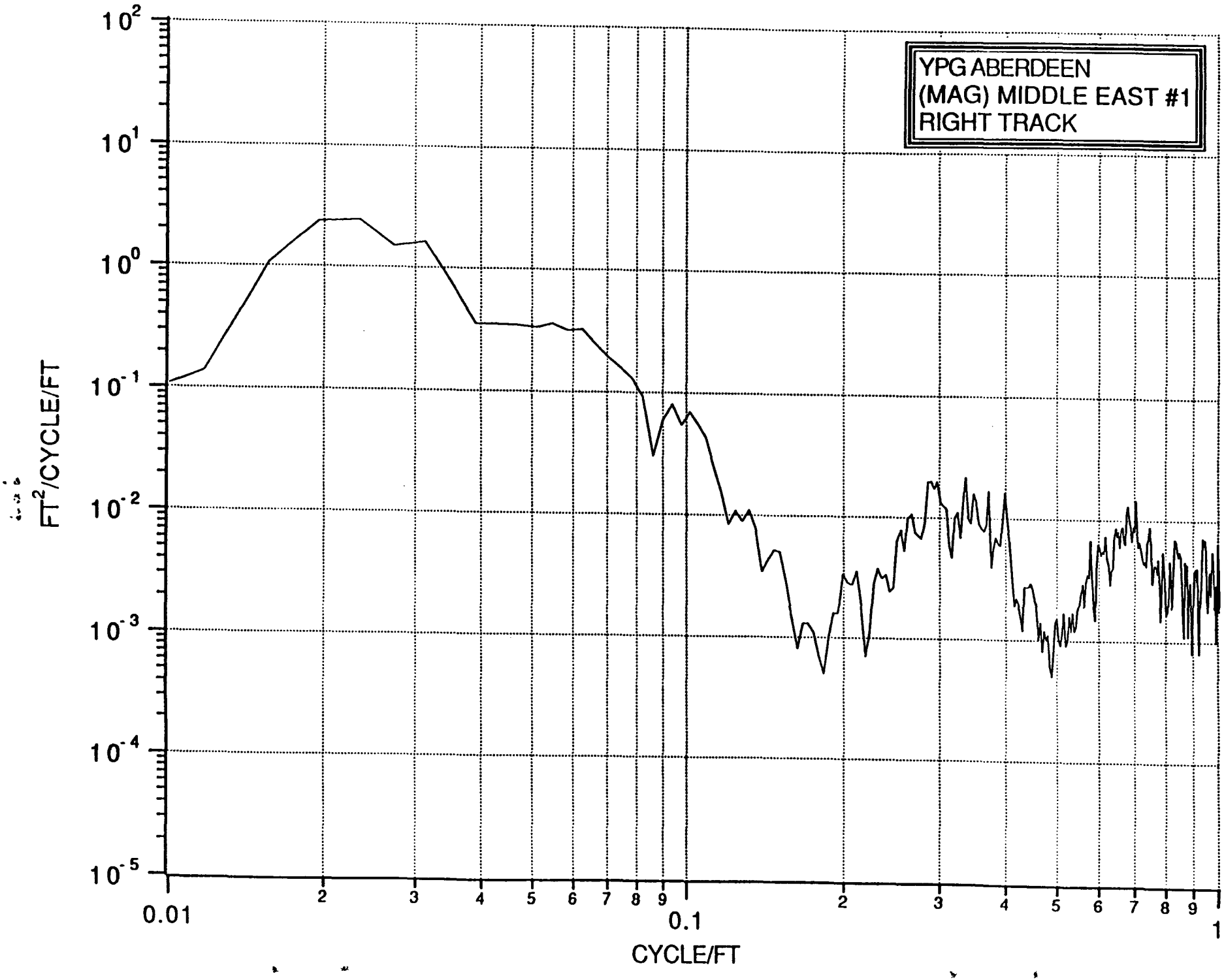
YPG ABERDEEN
(MAG) MIDDLE EAST #1
RIGHT TRACK
FT²/CYCLE/FT
10²
10¹
10⁰
10⁻¹
10⁻²
10⁻³
10⁻⁴
10⁻⁵
0.01
0.1
1
2 3 4 5 6 7 8 9
CYCLE/FT

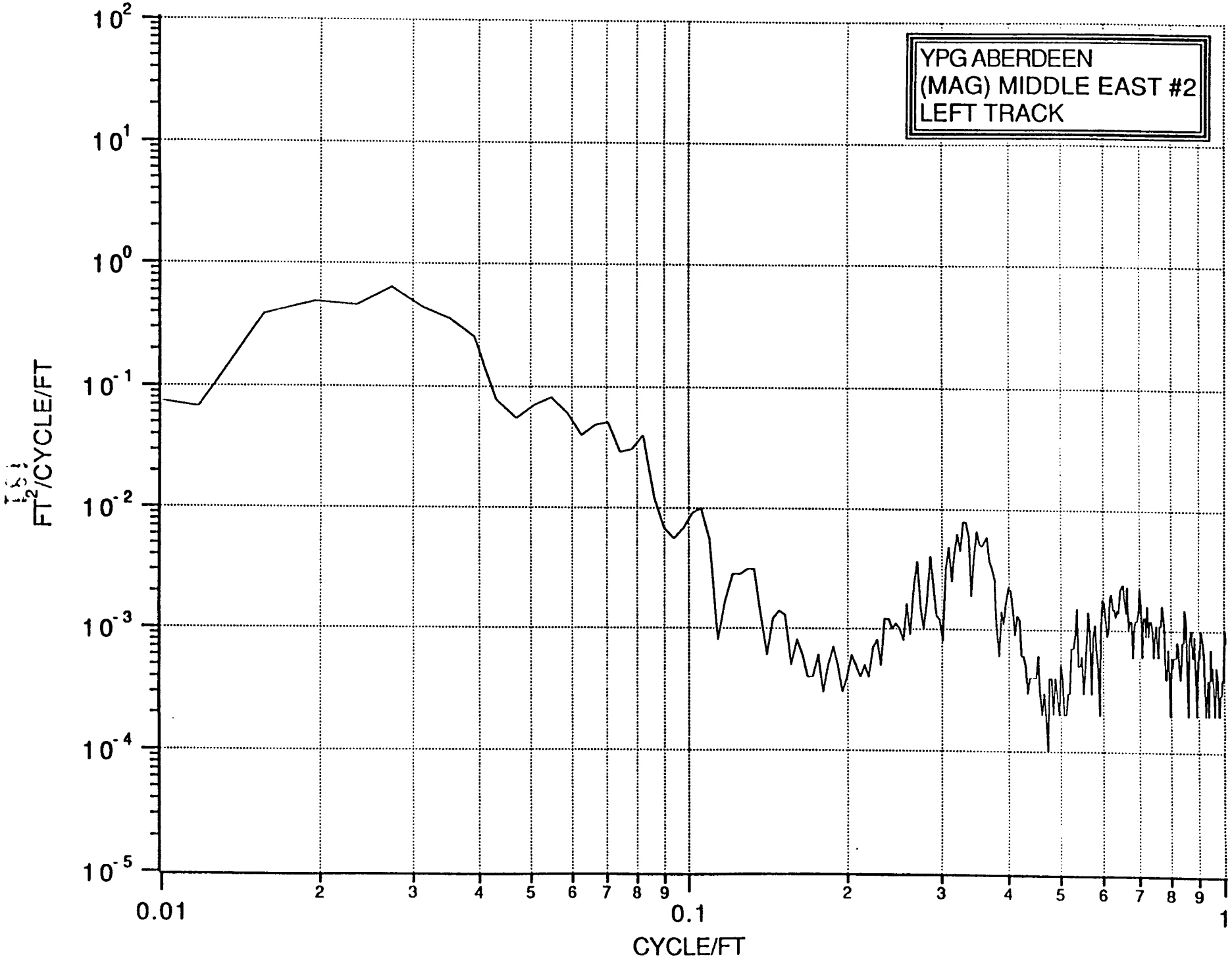
YPG ABERDEEN
(MAG) MIDDLE EAST #2
LEFT TRACK
FT²/CYCLE/FT
CYCLE/FT
10²
10¹
10⁰
10⁻¹
10⁻²
10⁻³
10⁻⁴
10⁻⁵
0.01
0.1
1
2
3
4
5
6
7
8
9

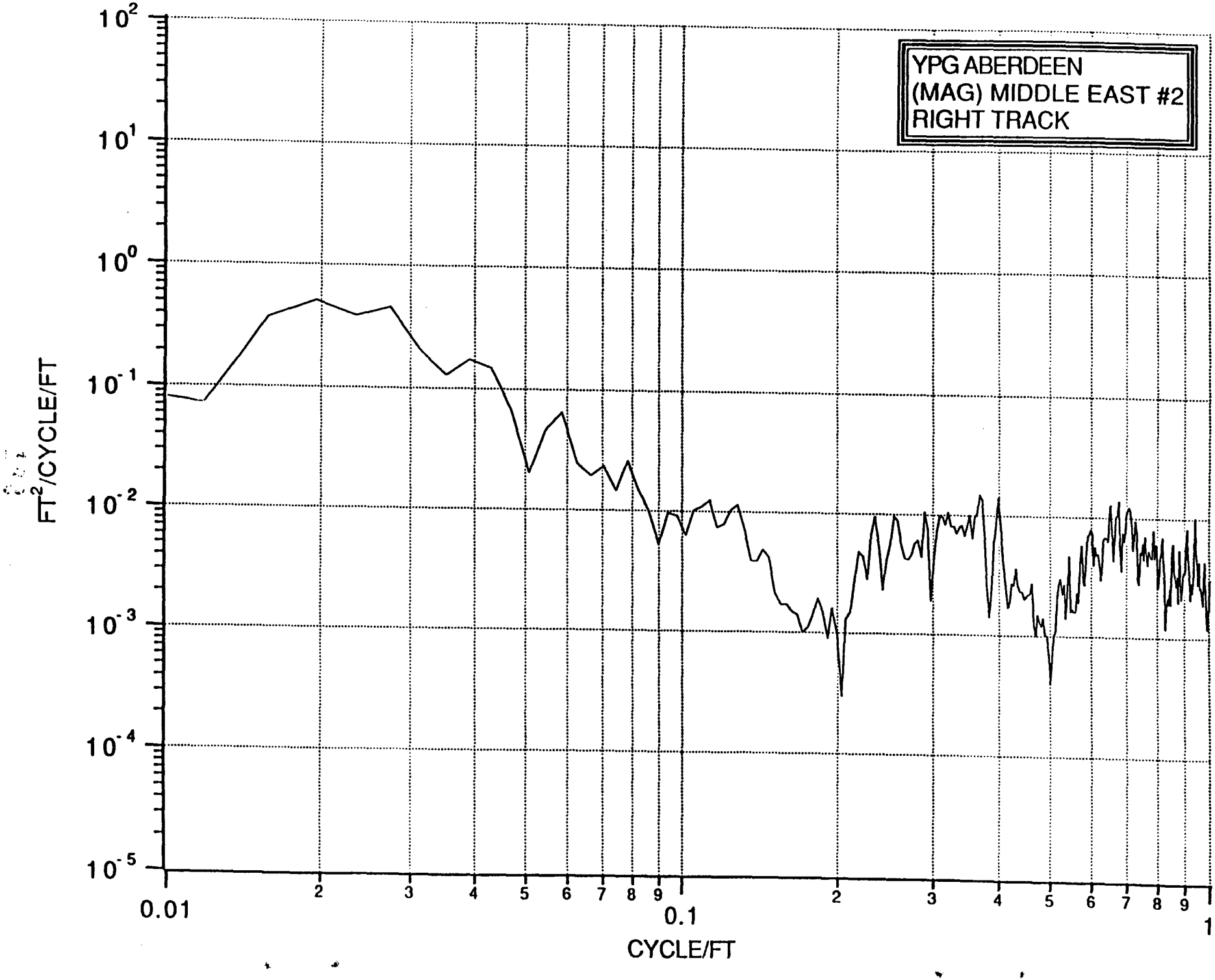
YPG ABERDEEN
(MAG) MIDDLE EAST #2
RIGHT TRACK
10^2
10^1
10^0
10^{-1}
10^{-2}
10^{-3}
10^{-4}
10^{-5}
FT^2/CYCLE/FT
0.01
2 3 4 5 6 7 8 9
0.1
2 3 4 5 6 7 8 9
1
CYCLE/FT

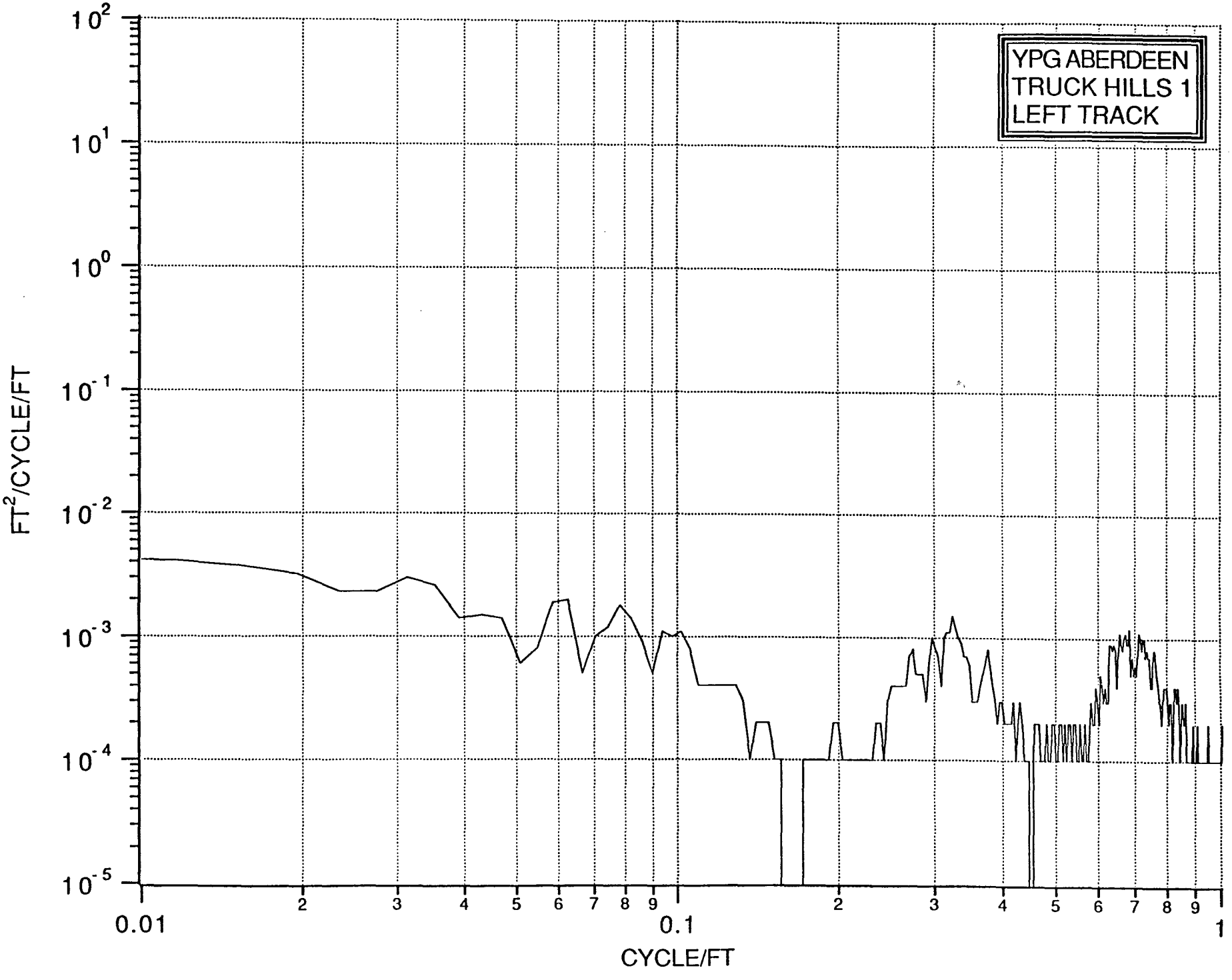
YPG ABERDEEN
TRUCK HILLS 1
LEFT TRACK
10^2
10^1
10^0
10^{-1}
10^{-2}
10^{-3}
10^{-4}
10^{-5}
FT^2/CYCLE/FT
0.01
2 3 4 5 6 7 8 9
0.1
2 3 4 5 6 7 8 9
1
CYCLE/FT

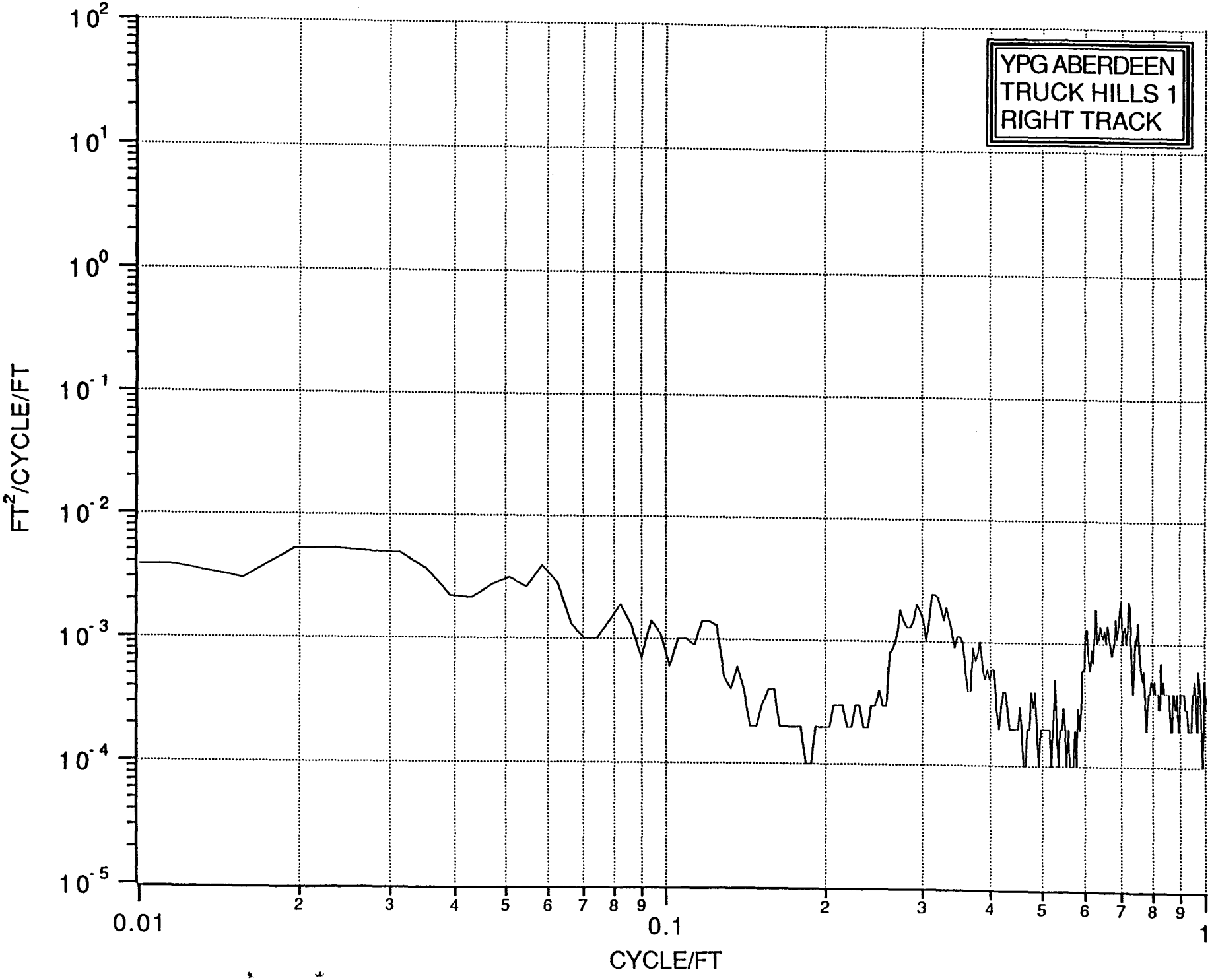
YPG ABERDEEN
TRUCK HILLS 1
RIGHT TRACK
10^2
10^1
10^0
10^{-1}
10^{-2}
10^{-3}
10^{-4}
10^{-5}
$FT^2/CYCLE/FT$
0.01
2 3 4 5 6 7 8 9
0.1
2 3 4 5 6 7 8 9
1
CYCLE/FT

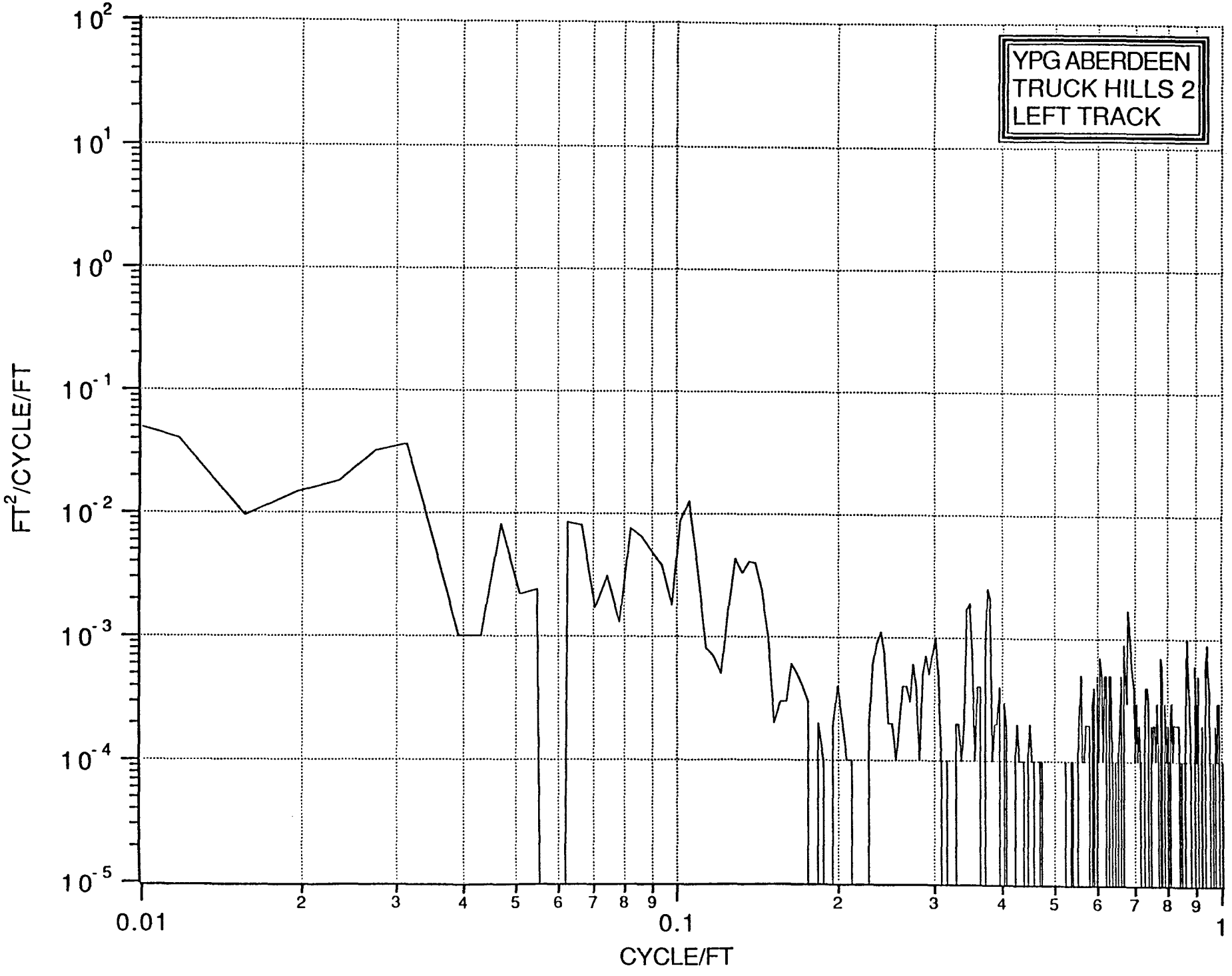
YPG ABERDEEN
TRUCK HILLS 2
LEFT TRACK
10^2
10^1
10^0
10^{-1}
10^{-2}
10^{-3}
10^{-4}
10^{-5}
FT^2/CYCLE/FT
0.01
2 3 4 5 6 7 8 9
0.1
2 3 4 5 6 7 8 9
1
CYCLE/FT

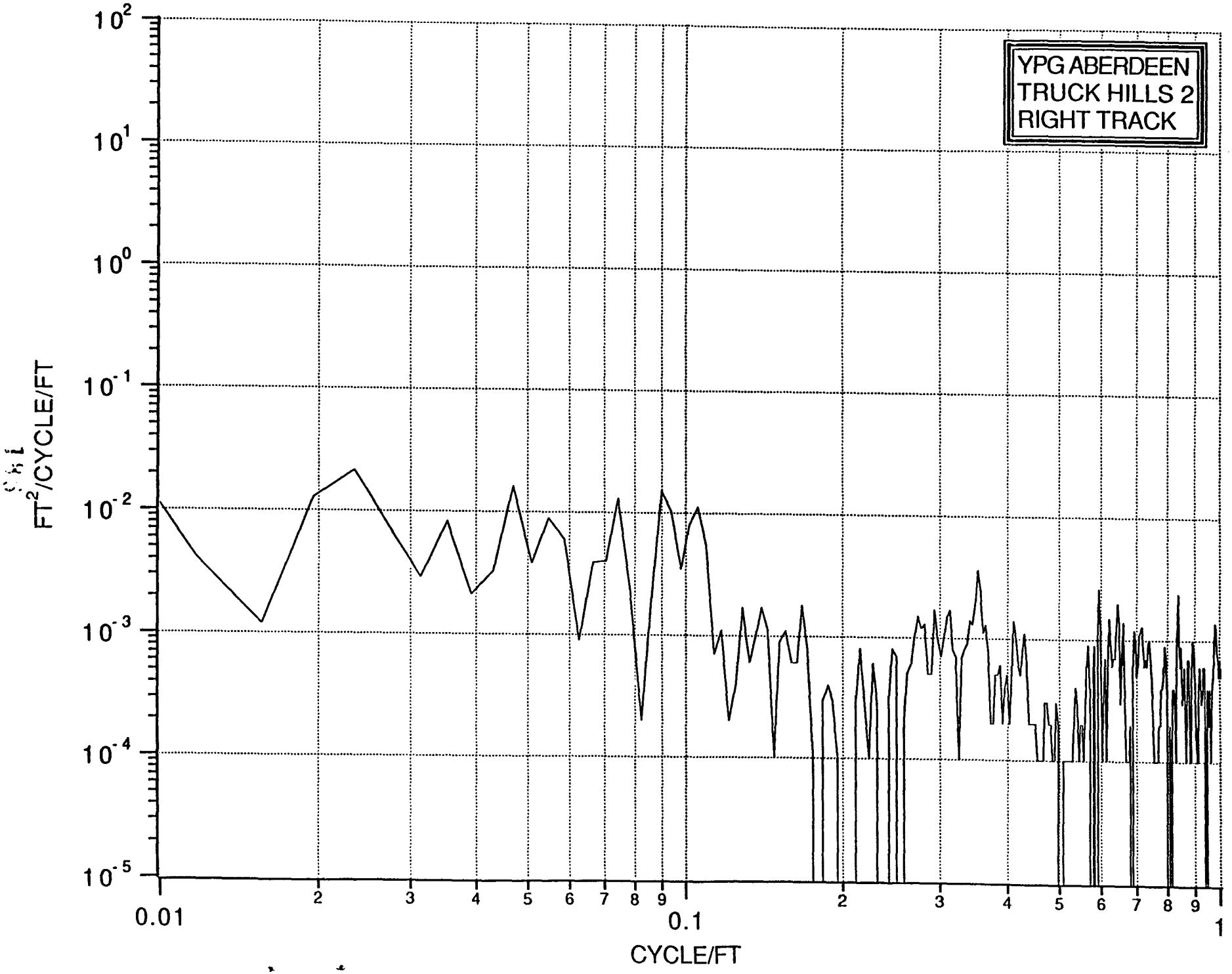
YPG ABERDEEN
TRUCK HILLS 2
RIGHT TRACK
10^2
10^1
10^0
10^{-1}
10^{-2}
10^{-3}
10^{-4}
10^{-5}
FT^2/CYCLE/FT
0.01
0.1
1
2 3 4 5 6 7 8 9
2 3 4 5 6 7 8 9
CYCLE/FT

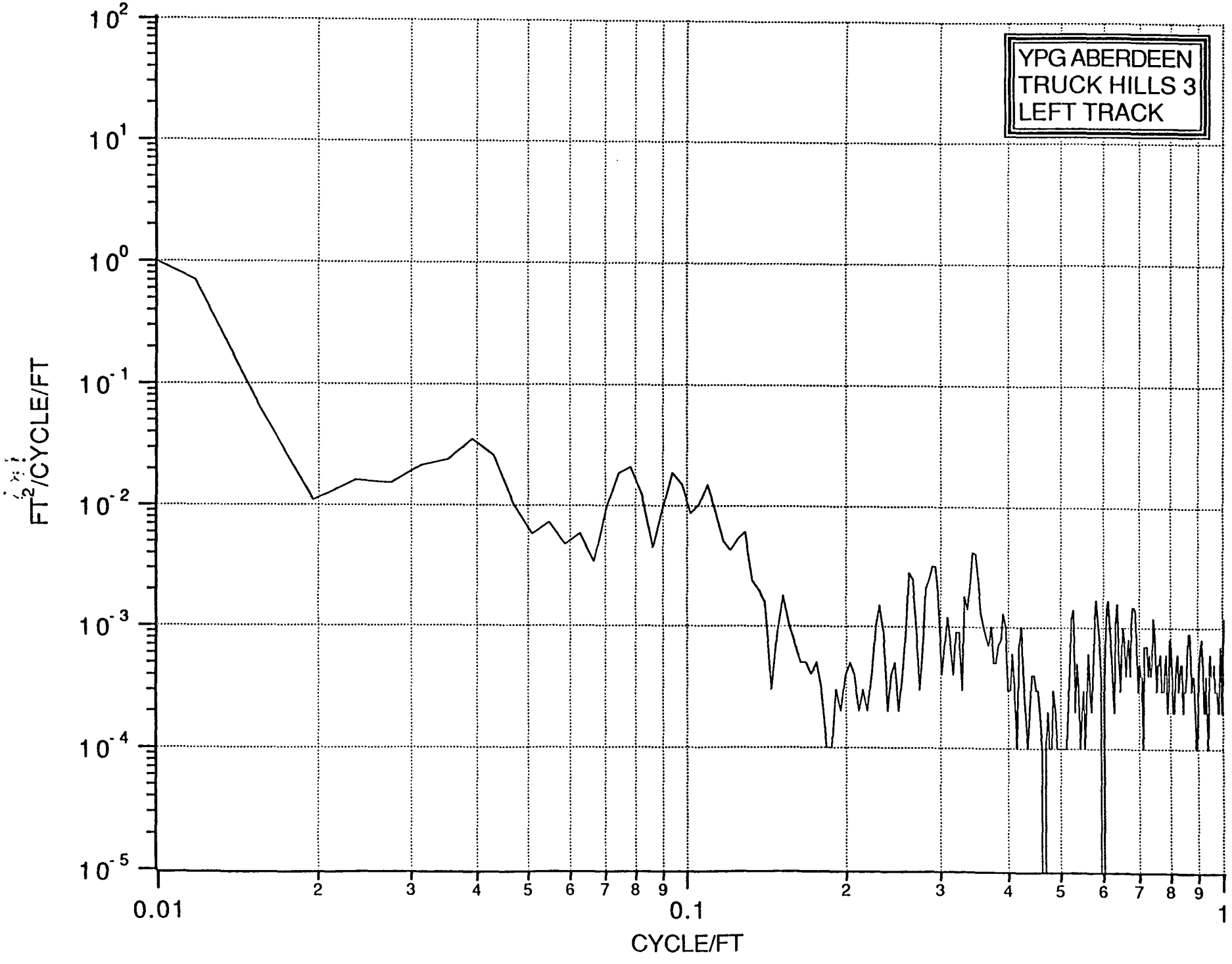
YPG ABERDEEN
TRUCK HILLS 3
LEFT TRACK
10^2
10^1
10^0
10^{-1}
10^{-2}
10^{-3}
10^{-4}
10^{-5}
FT²/CYCLE/FT
0.01
2 3 4 5 6 7 8 9
0.1
2 3 4 5 6 7 8 9
1
CYCLE/FT

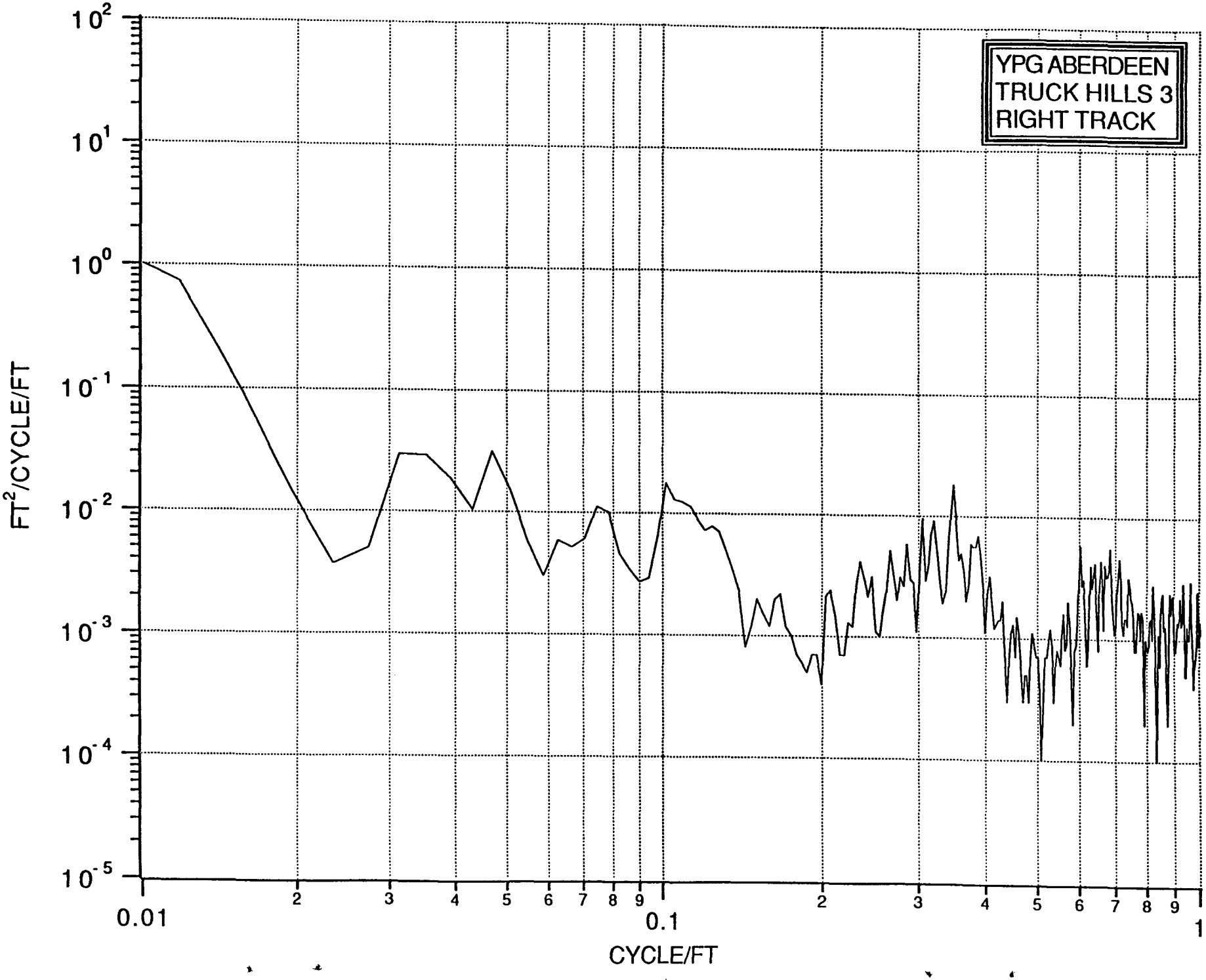
YPG ABERDEEN
TRUCK HILLS 3
RIGHT TRACK
10^2
10^1
10^0
10^{-1}
10^{-2}
10^{-3}
10^{-4}
10^{-5}
FT^2/CYCLE/FT
0.01
0.1
1
2 3 4 5 6 7 8 9
2 3 4 5 6 7 8 9
CYCLE/FT

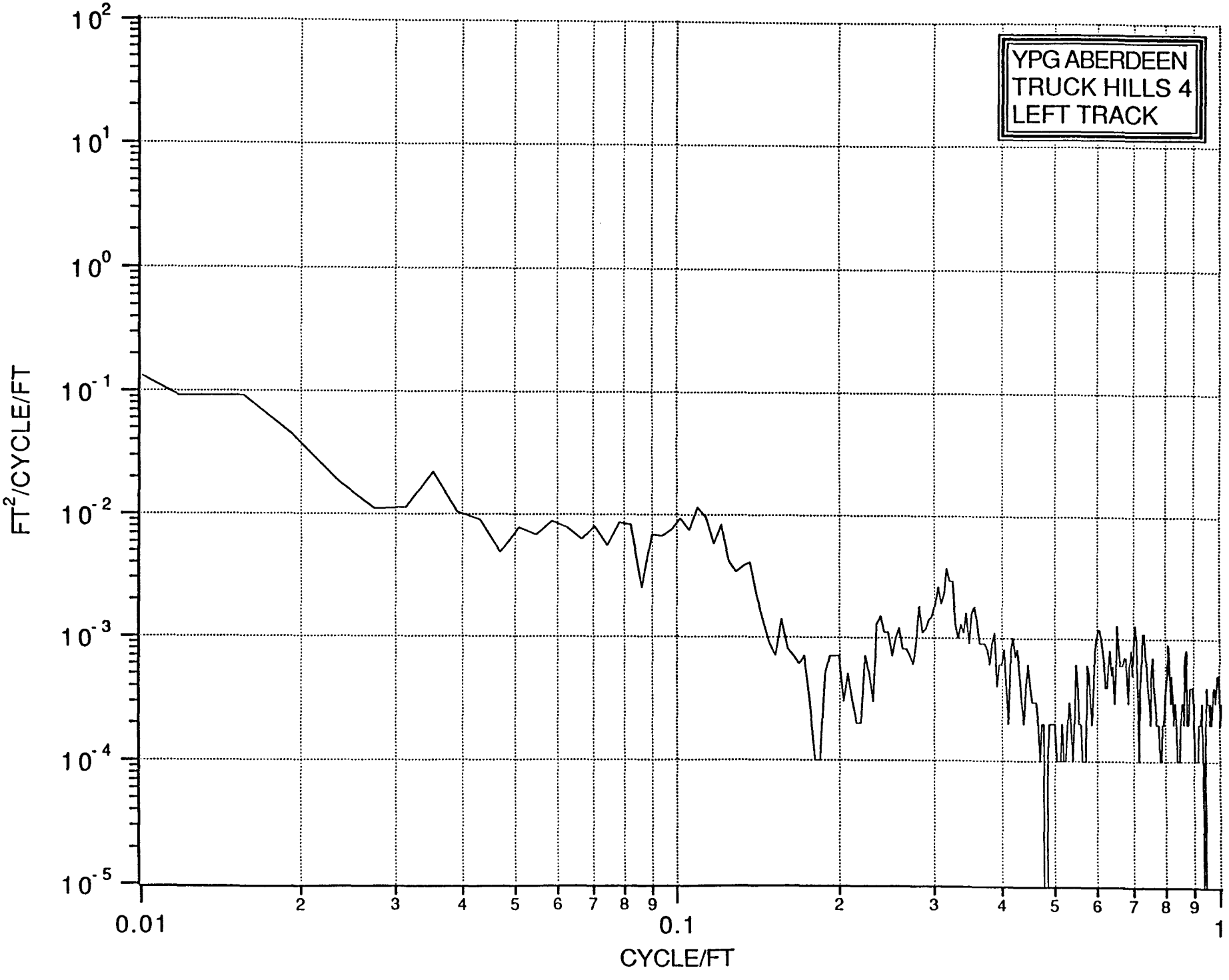
YPG ABERDEEN
TRUCK HILLS 4
LEFT TRACK
10^2
10^1
10^0
10^{-1}
10^{-2}
10^{-3}
10^{-4}
10^{-5}
FT^2/CYCLE/FT
0.01
2 3 4 5 6 7 8 9
0.1
2 3 4 5 6 7 8 9
1
CYCLE/FT

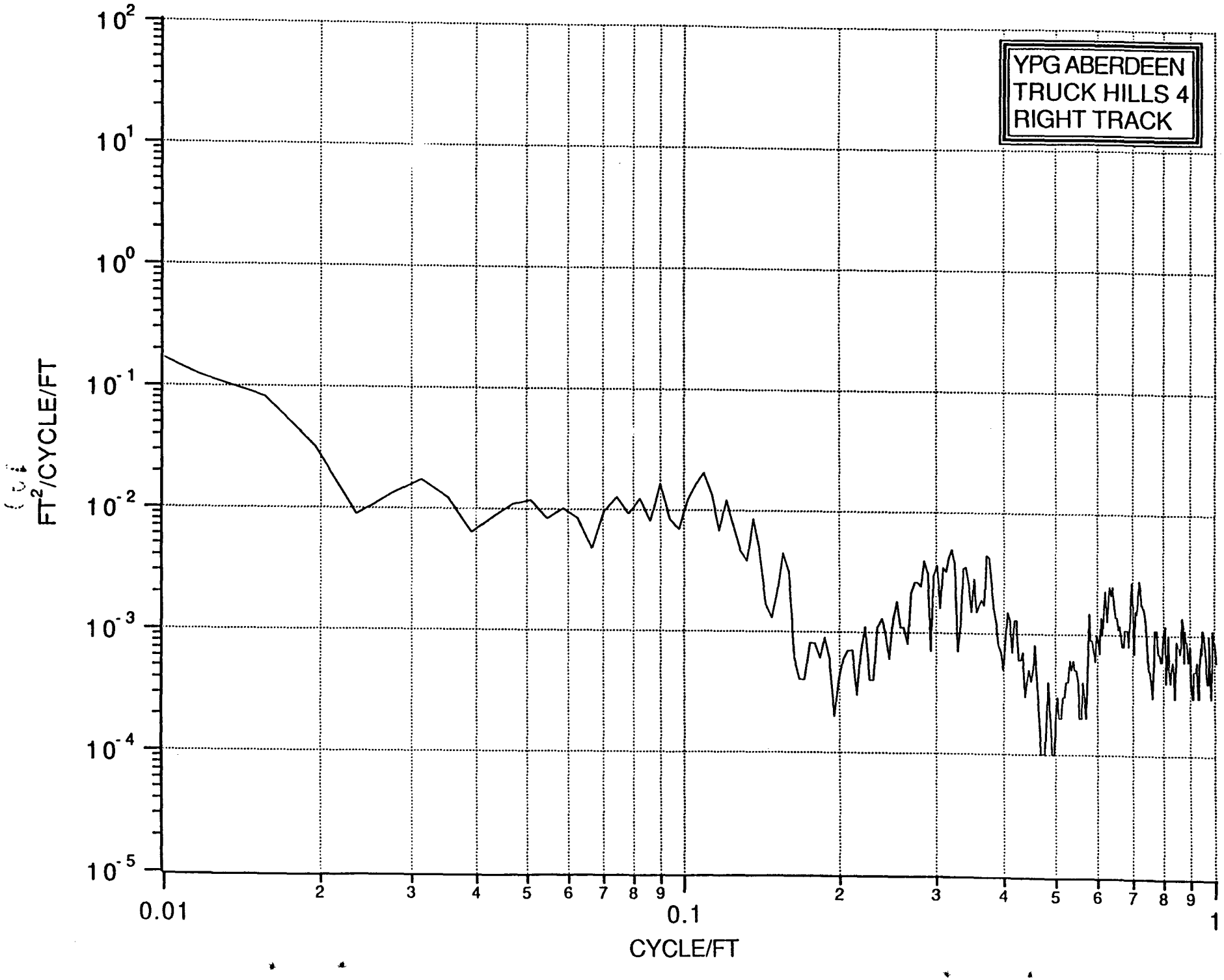
YPG ABERDEEN
TRUCK HILLS 4
RIGHT TRACK
10^2
10^1
10^0
10^{-1}
10^{-2}
10^{-3}
10^{-4}
10^{-5}
FT²/CYCLE/FT
0.01
2 3 4 5 6 7 8 9
0.1
2 3 4 5 6 7 8 9
1
CYCLE/FT

APPENDIX F

COHERENCE FUNCTION PLOTS - ROD AND LEVEL

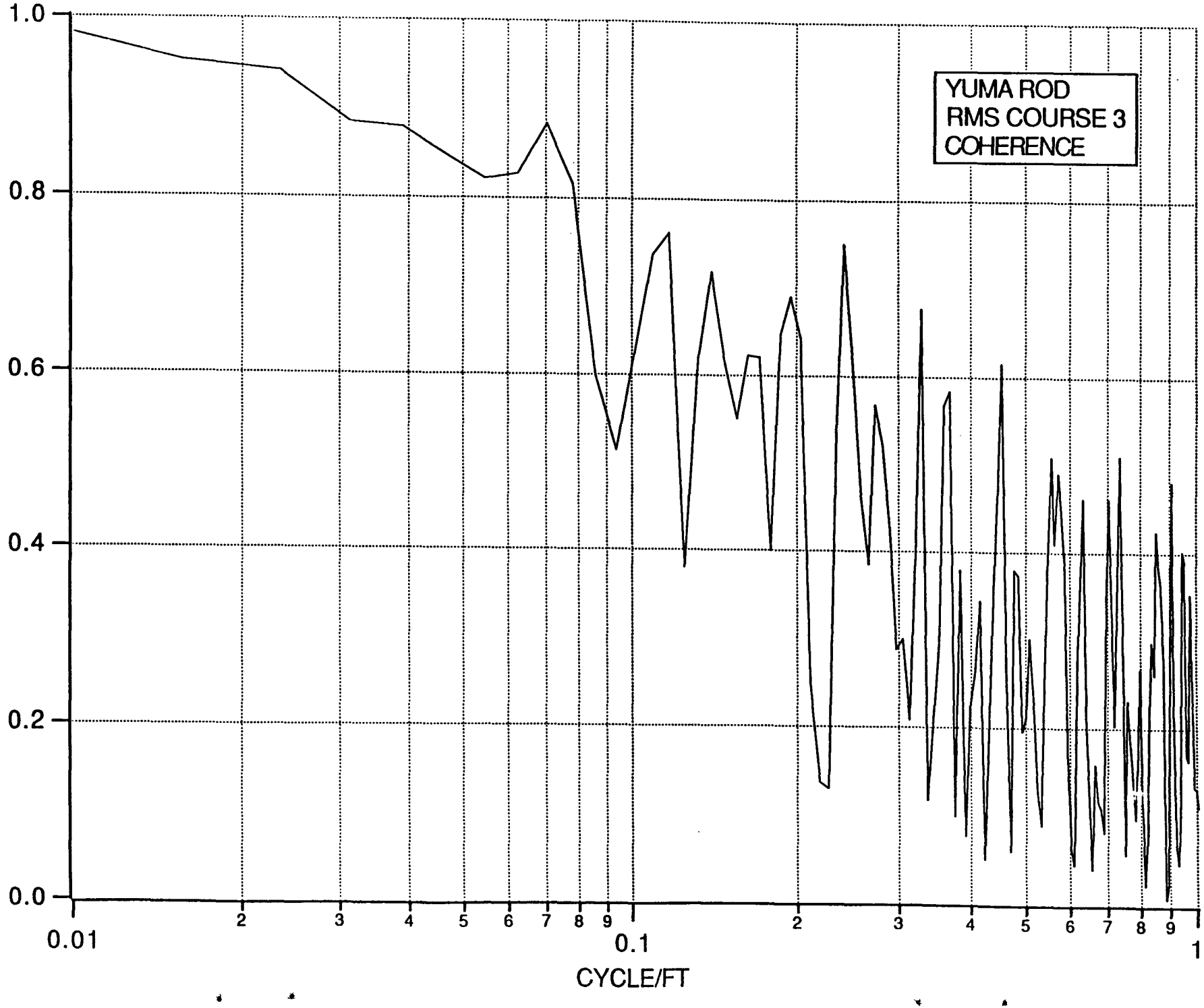
YUMA ROD
RMS COURSE 3
COHERENCE
1.0
0.8
0.6
0.4
0.2
0.0
0.01
2
3
4
5
6
7
8
9
0.1
2
3
4
5
6
7
8
9
1
CYCLE/FT

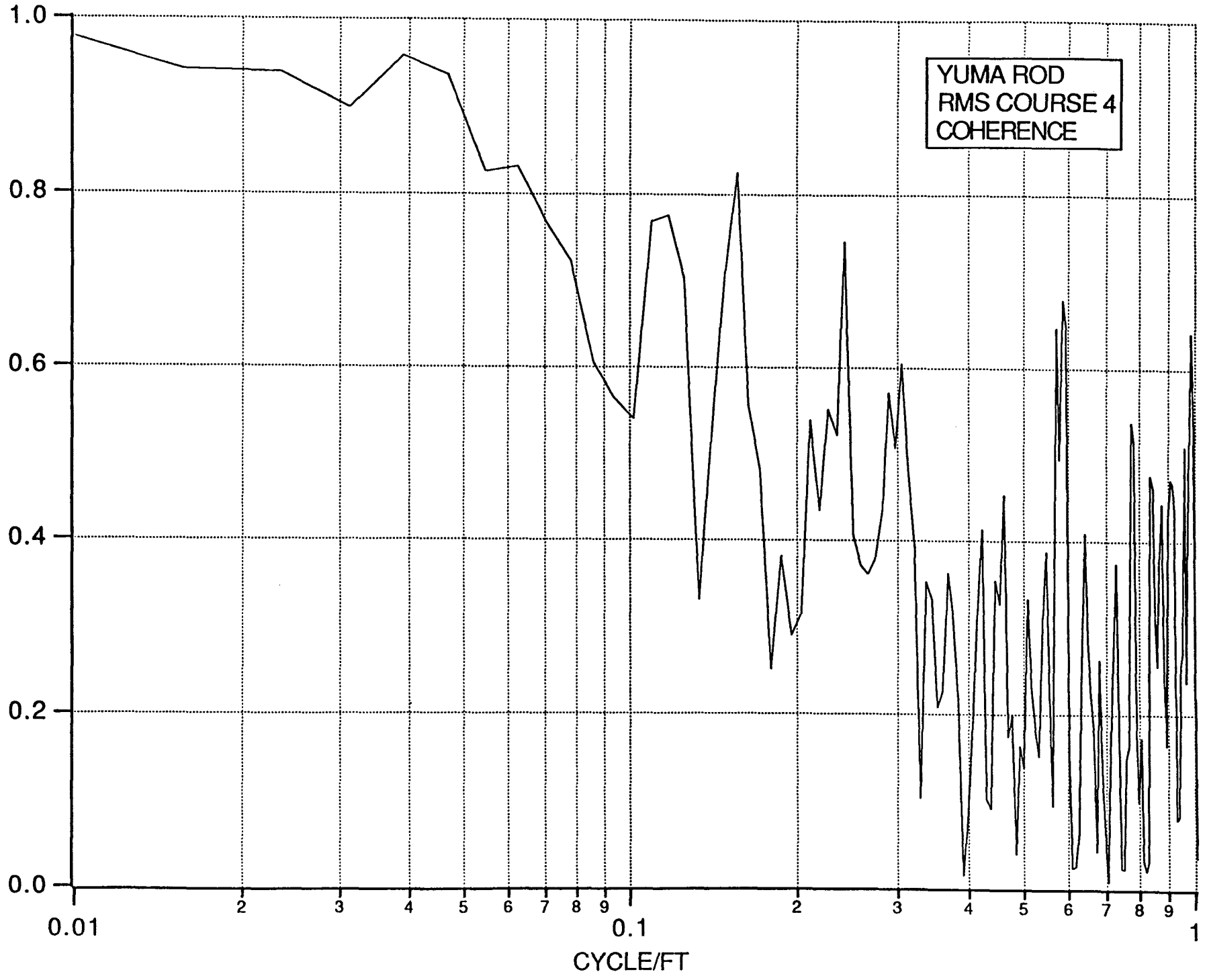
YUMA ROD
RMS COURSE 4
COHERENCE
1.0
0.8
0.6
0.4
0.2
0.0
0.01
2
3
4
5
6
7
8
9
0.1
2
3
4
5
6
7
8
9
1
CYCLE/FT

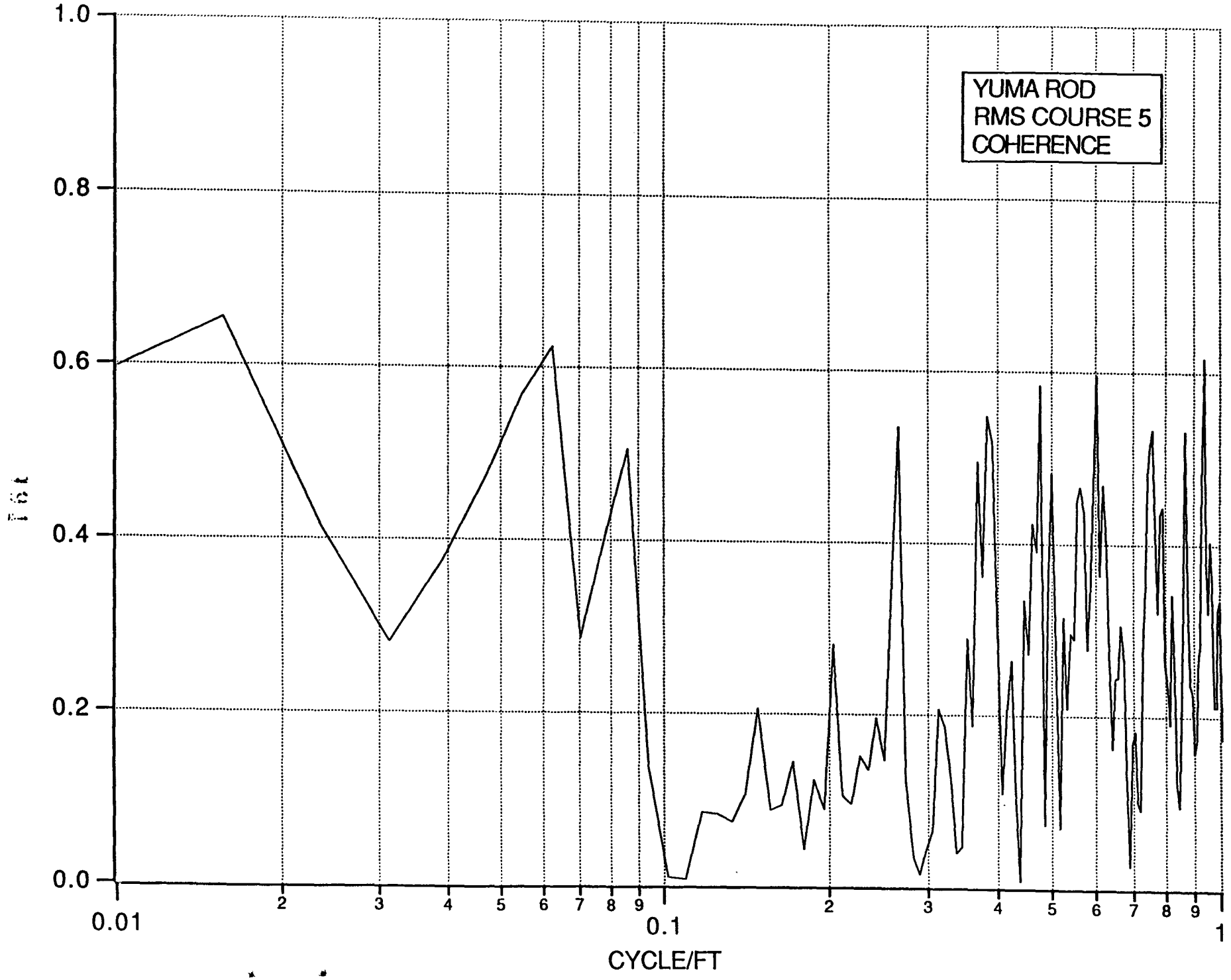
YUMA ROD
RMS COURSE 5
COHERENCE
1.0
0.8
0.6
0.4
0.2
0.0
Feet
0.01
2
3
4
5
6
7
8
9
0.1
2
3
4
5
6
7
8
9
1
CYCLE/FT

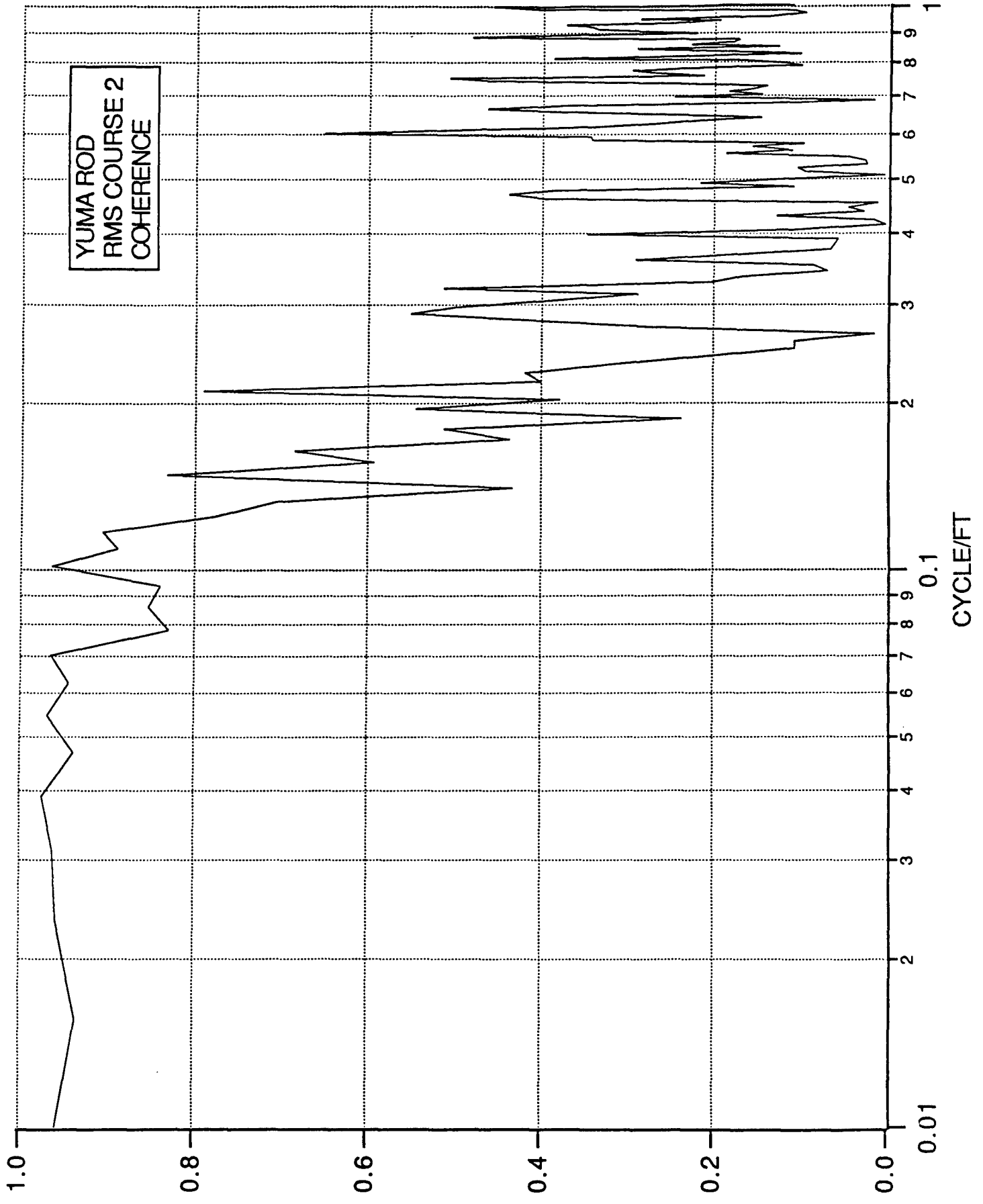
YUMA ROD
RMS COURSE 2
COHERENCE
1.0
0.8
0.6
0.4
0.2
0.0
0.01
0.1
1
2
3
4
5
6
7
8
9
CYCLE/FT

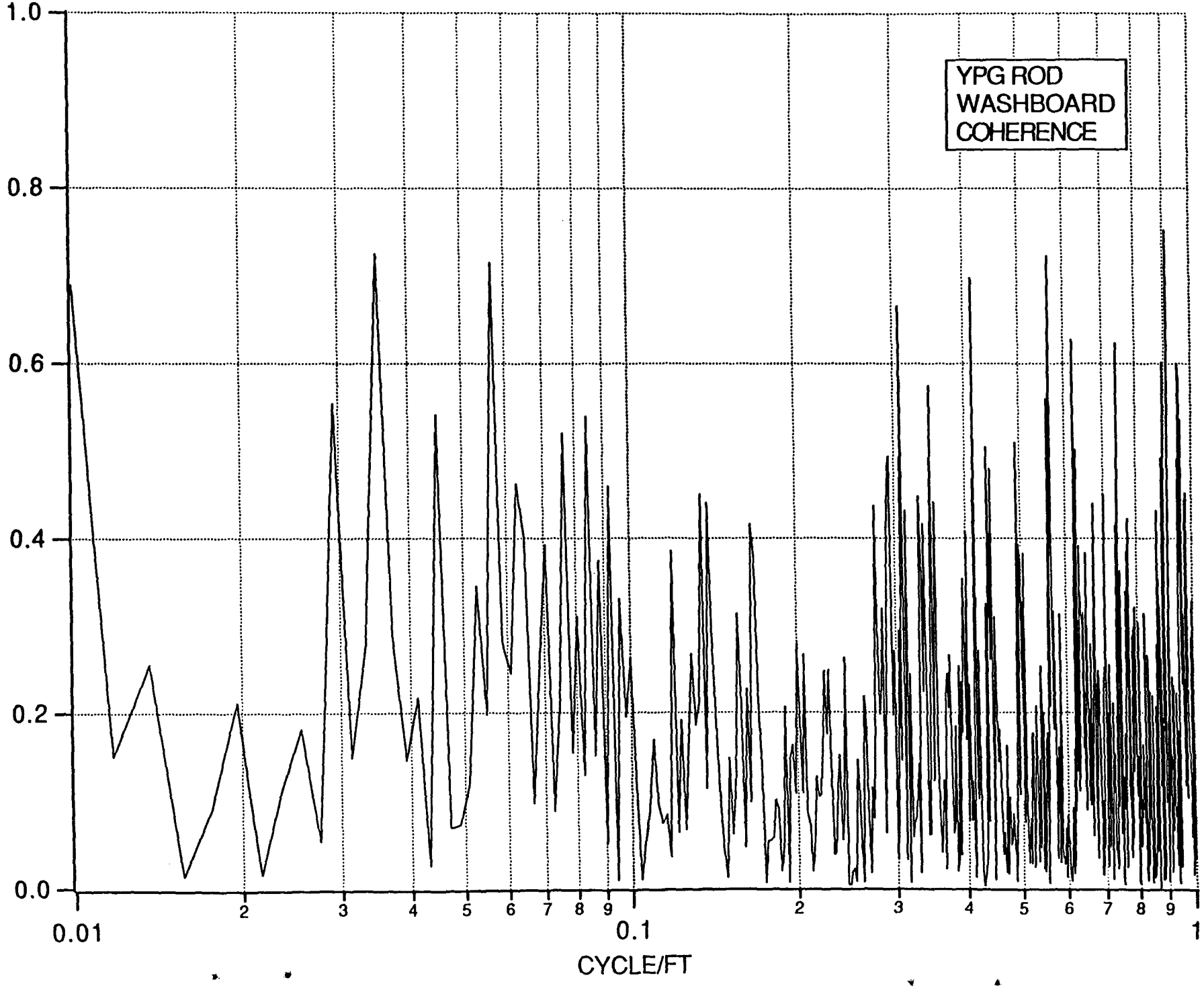
YPG ROD
WASHBOARD
COHERENCE
1.0
0.8
0.6
0.4
0.2
0.0
0.01
2
3
4
5
6
7
8
9
0.1
2
3
4
5
6
7
8
9
1
CYCLE/FT

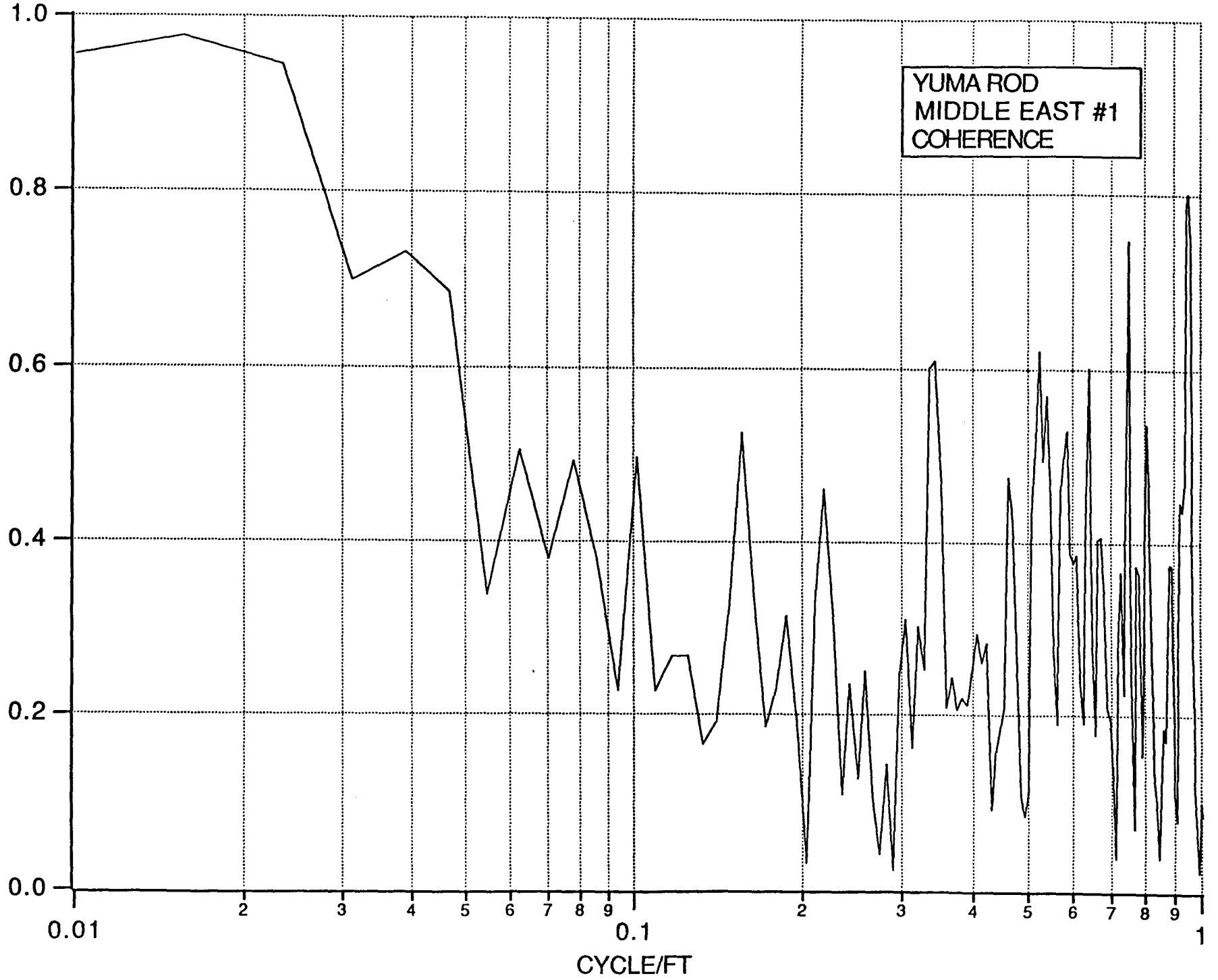
YUMA ROD
MIDDLE EAST #1
COHERENCE
1.0
0.8
0.6
0.4
0.2
0.0
0.01
2
3
4
5
6
7
8
9
0.1
2
3
4
5
6
7
8
9
1
CYCLE/FT

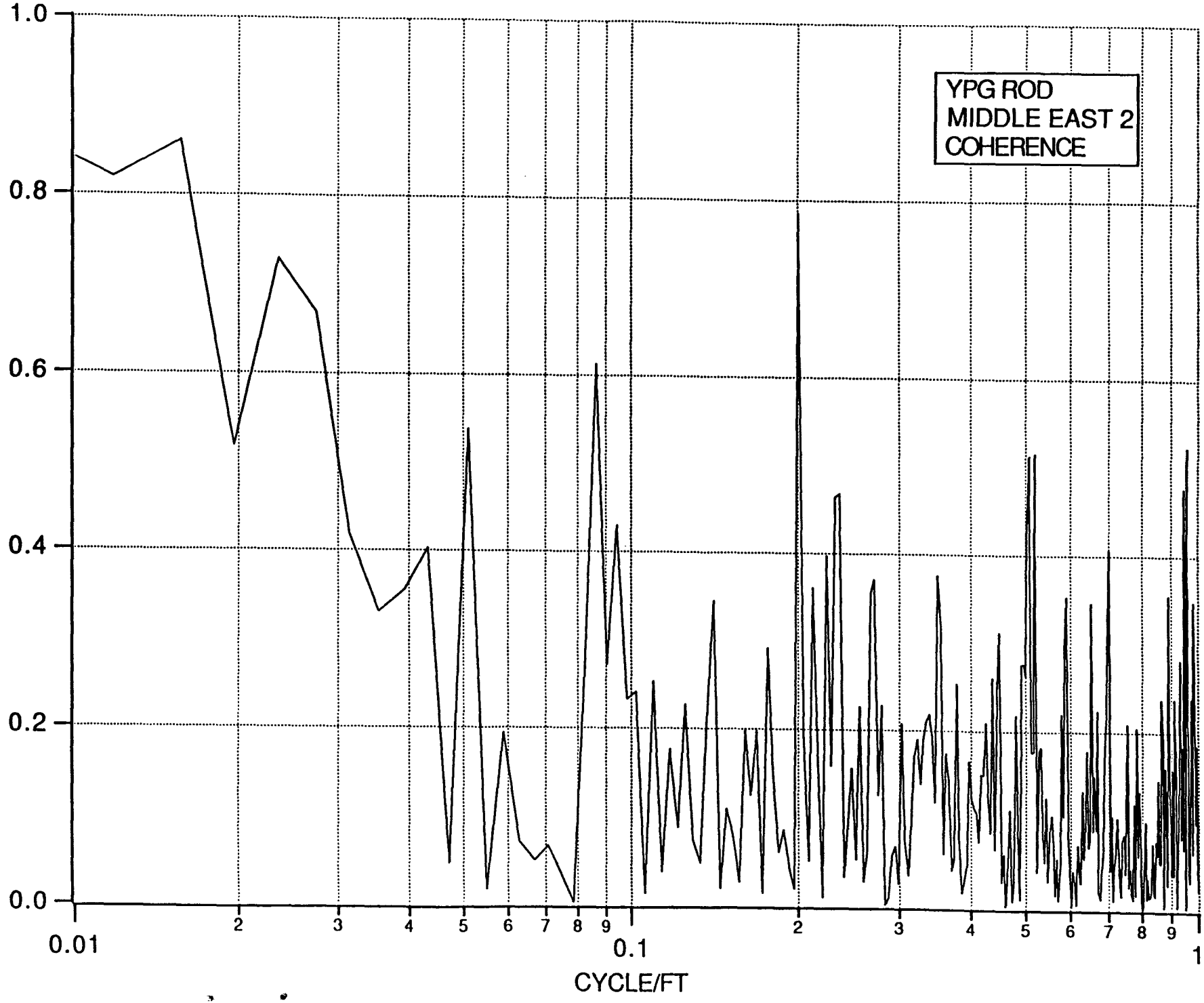
YPG ROD
MIDDLE EAST 2
COHERENCE
1.0
0.8
0.6
0.4
0.2
0.0
0.01
0.1
1
2
3
4
5
6
7
8
9
CYCLE/FT

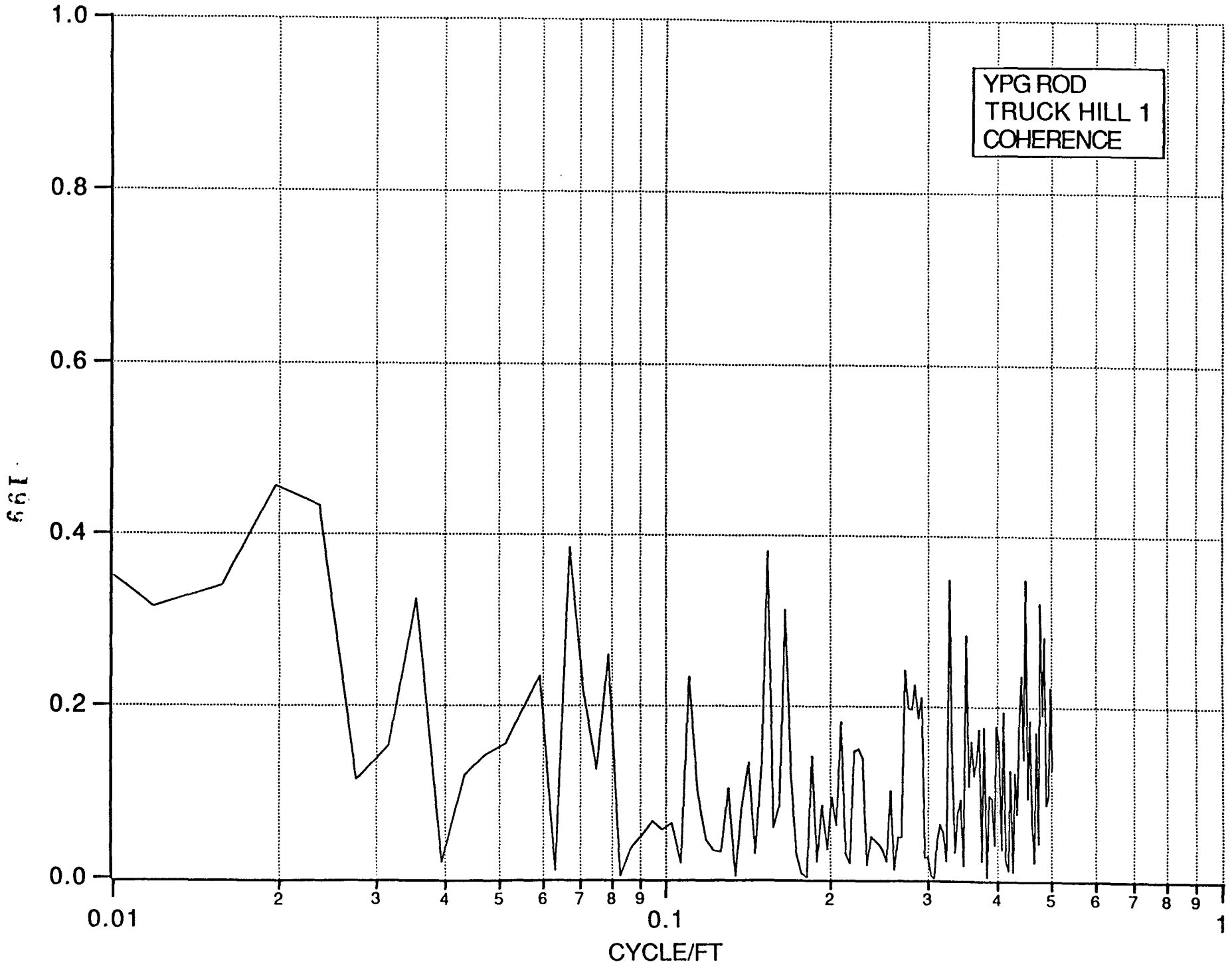
YPG ROD
TRUCK HILL 1
COHERENCE
1.0
0.8
0.6
0.4
0.2
0.0
0.01
0.1
1
CYCLE/FT

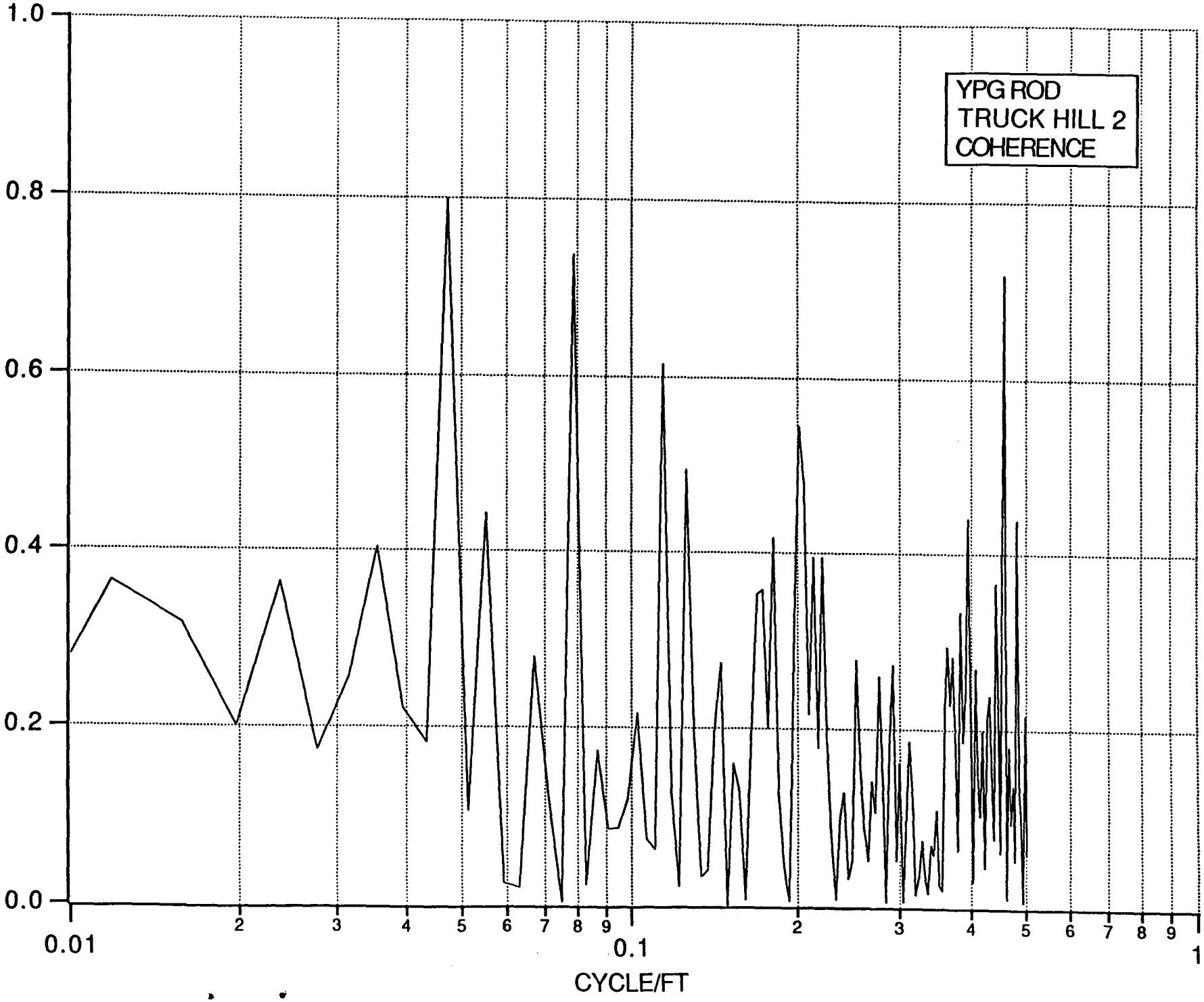
YPG ROD
TRUCK HILL 2
COHERENCE
1.0
0.8
0.6
0.4
0.2
0.0
0.01
2
3
4
5
6
7
8
9
0.1
2
3
4
5
6
7
8
9
1
CYCLE/FT

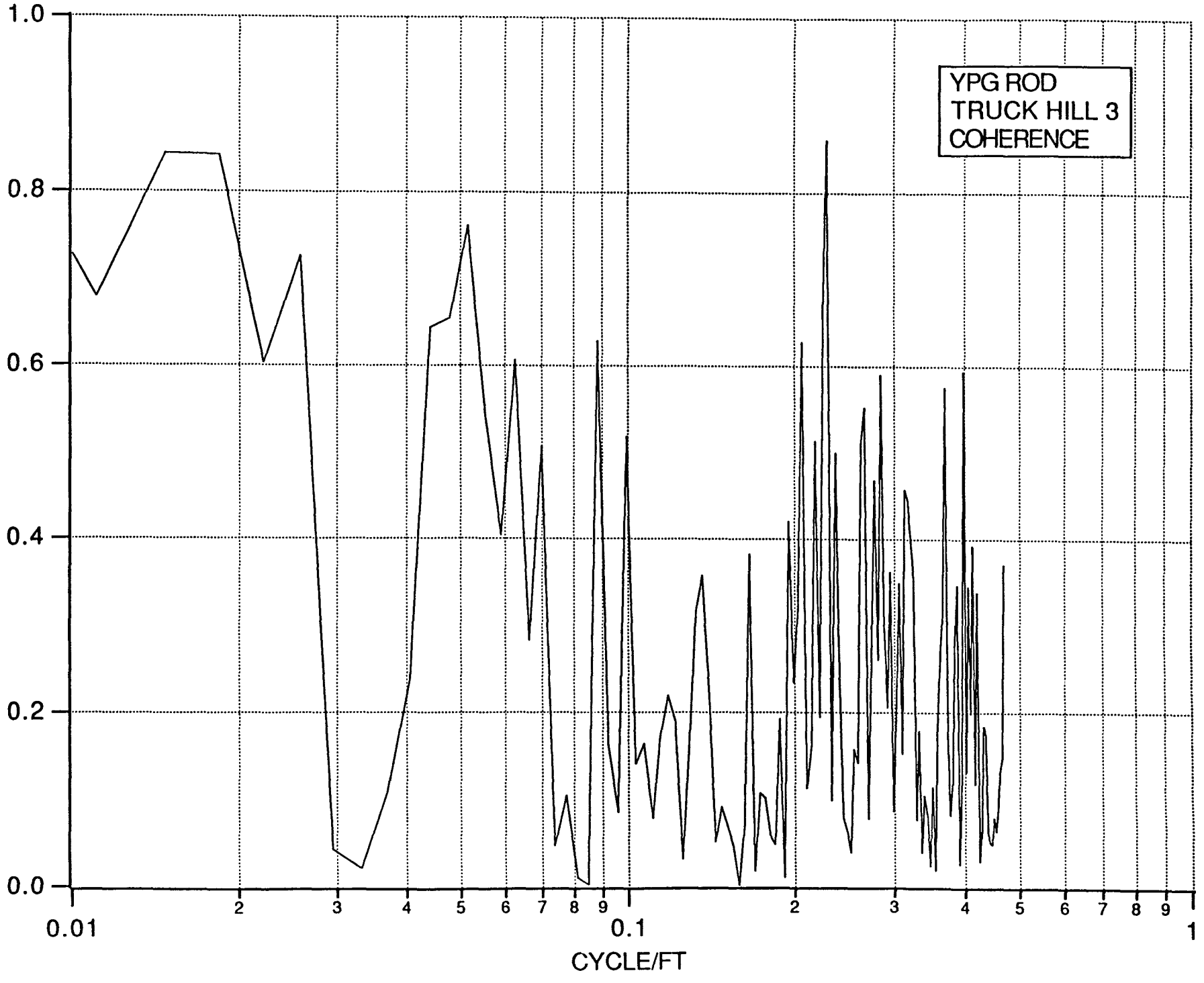
YPG ROD
TRUCK HILL 3
COHERENCE
1.0
0.8
0.6
0.4
0.2
0.0
0.01
0.1
1
2
3
4
5
6
7
8
9
CYCLE/FT

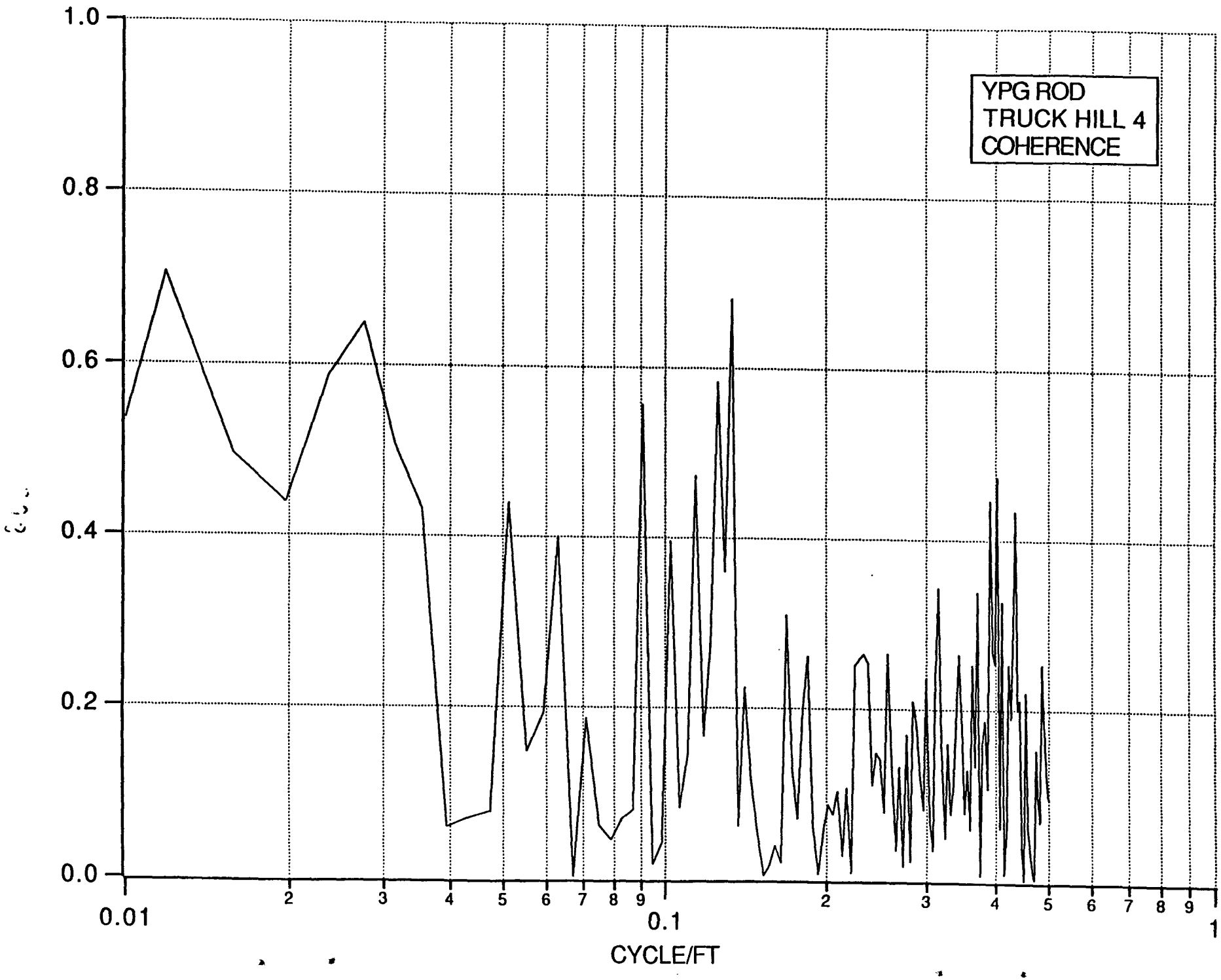
YPG ROD
TRUCK HILL 4
COHERENCE
1.0
0.8
0.6
0.4
0.2
0.0
0.01
0.1
1
2
3
4
5
6
7
8
9
CYCLE/FT

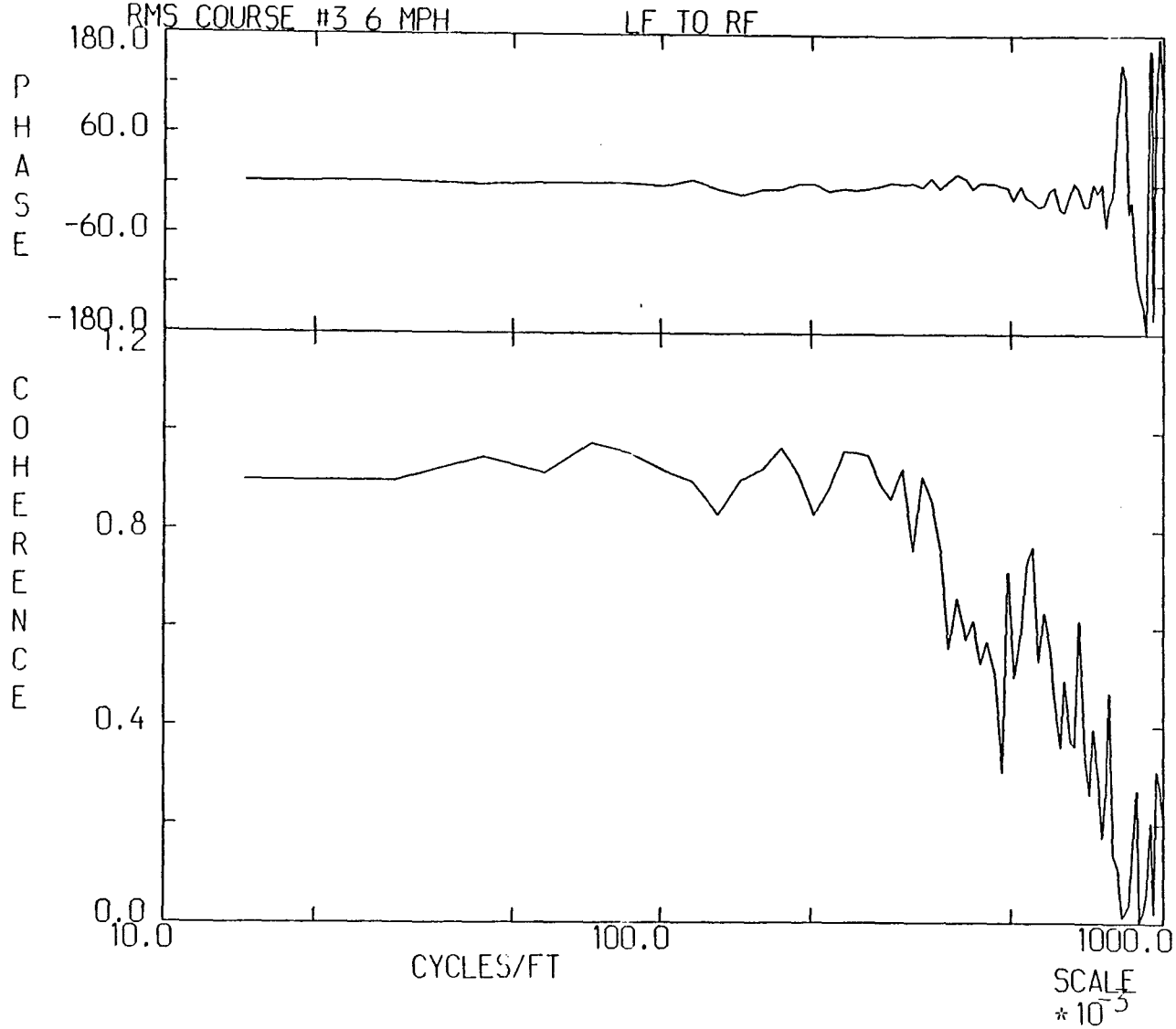
RMS COURSE #3 6 MPH
LF TO RF
PHASE
180.0
60.0
-60.0
-180.0
COHERENCE
1.2
0.8
0.4
0.0
10.0
100.0
1000.0
CYCLES/FT
SCALE
* 10^-3

APPENDIX G

COHERENCE FUNCTION PLOTS - DFMV

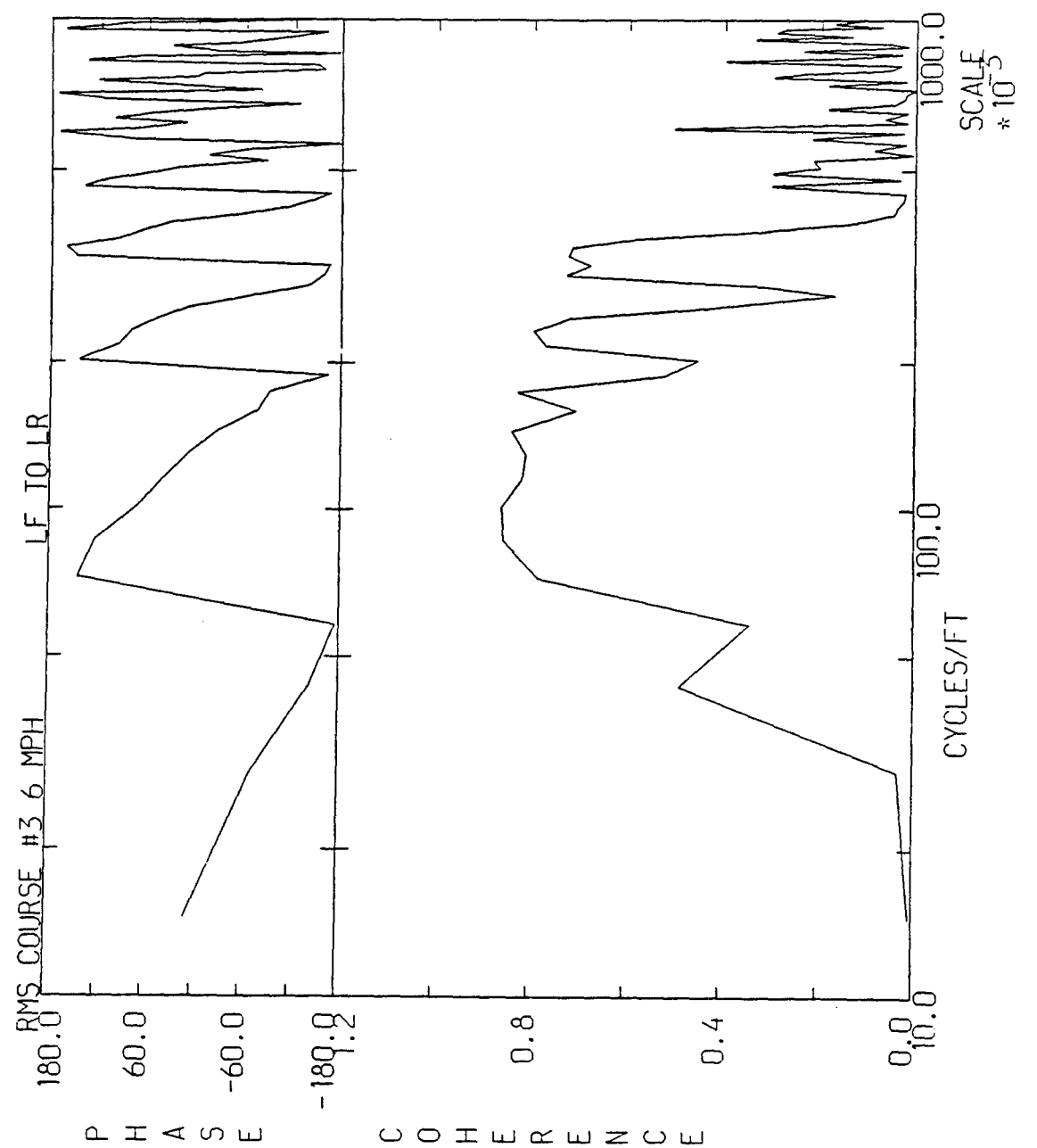
RMS COURSE #3 6 MPH
LF TO LR
180.0
60.0
-60.0
-180.0
PHASE
1.2
0.8
0.4
0.0
COHERENCE
10.0
100.0
1000.0
CYCLES/FT
SCALE
*10^-5

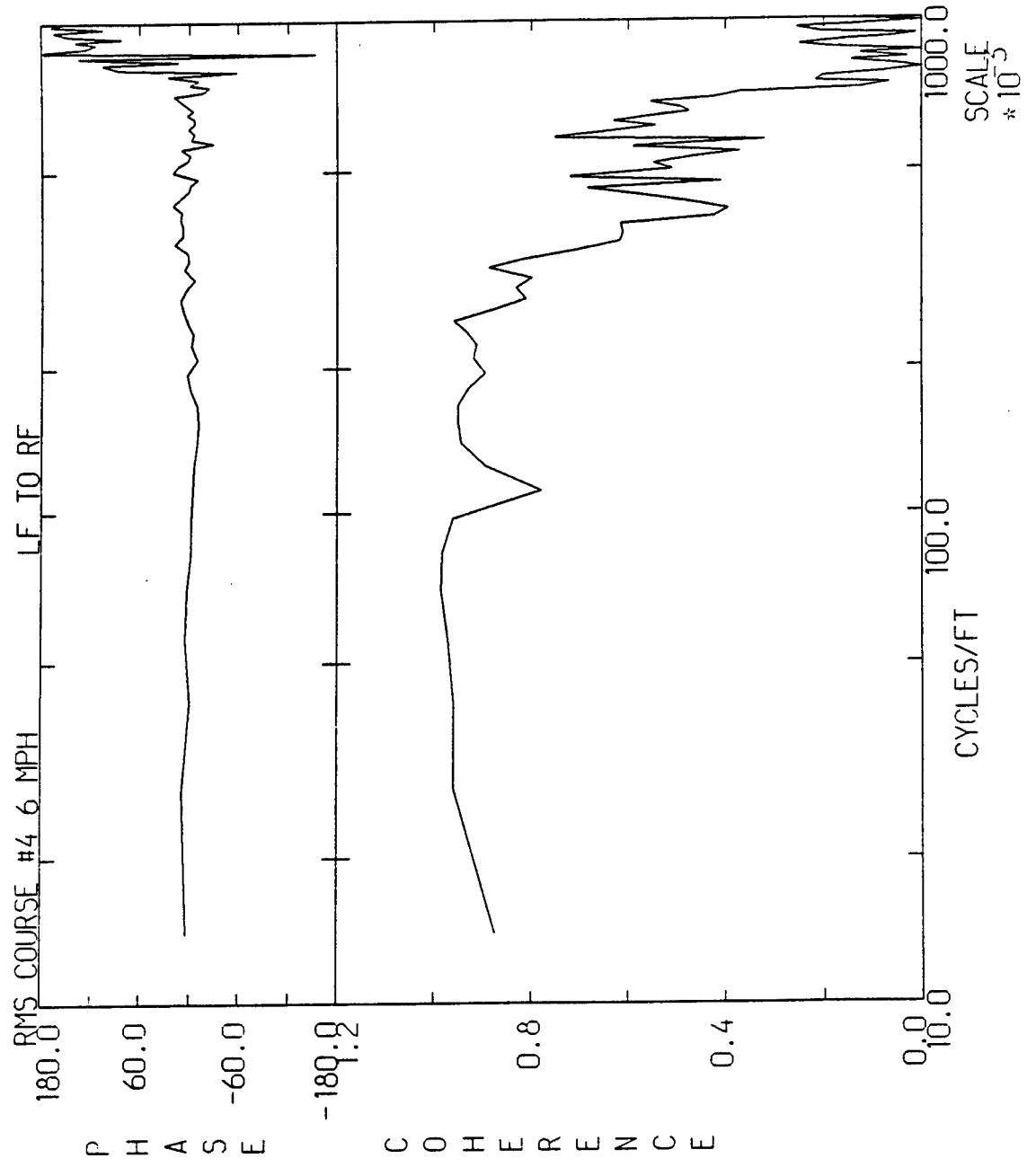
RMS COURSE #4 6 MPH
LF TO RF
180.0
60.0
-60.0
-180.0
PHASE
1.2
0.8
0.4
0.0
COHERENCE
10.0
100.0
1000.0
CYCLES/FT
SCALE
*10^-5

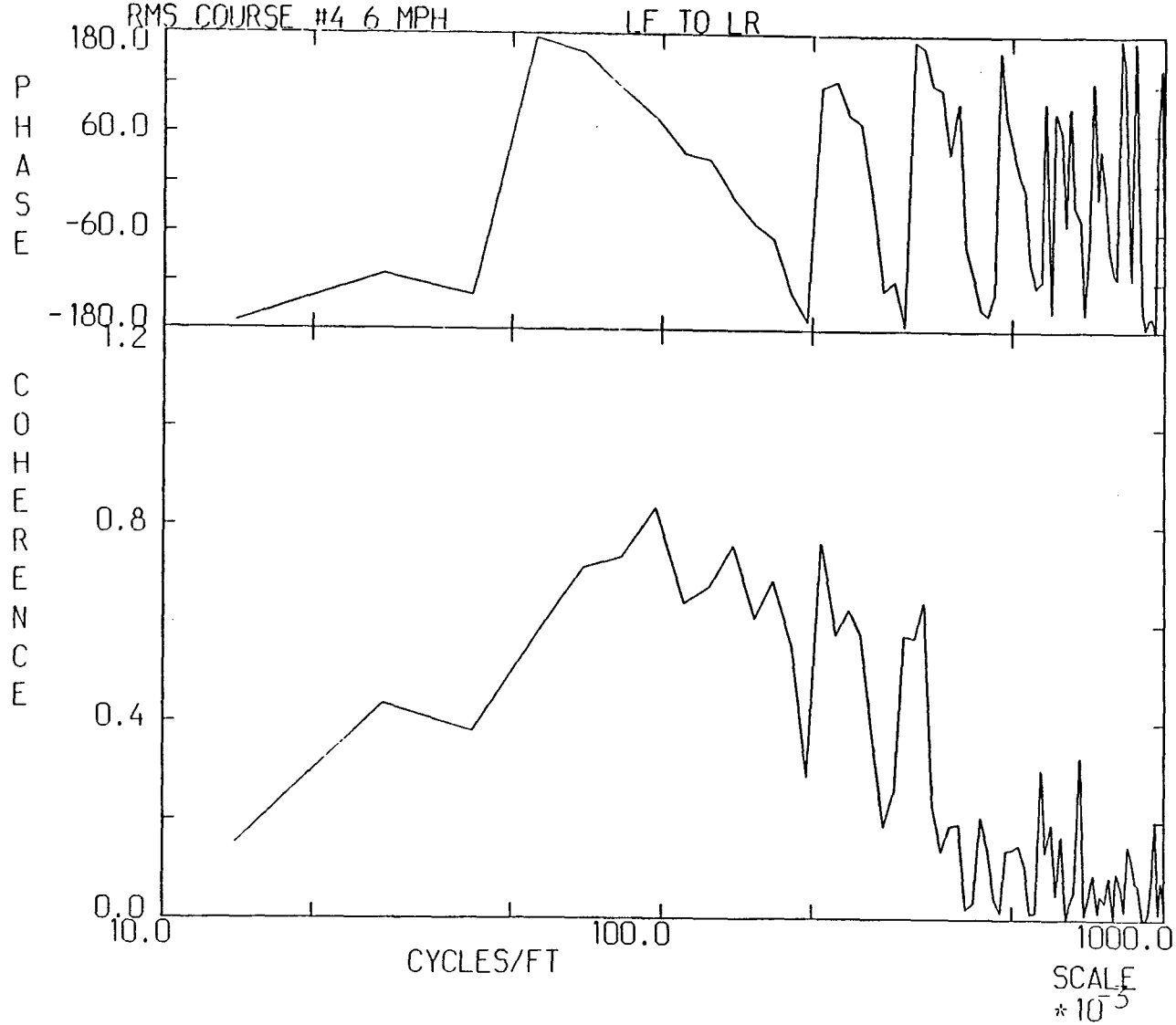
RMS COURSE #4 6 MPH
LF TO LR
180.0
60.0
-60.0
-180.0
PHASE
1.2
0.8
0.4
0.0
COHERENCE
10.0
100.0
1000.0
CYCLES/FT
SCALE
*10⁻⁵

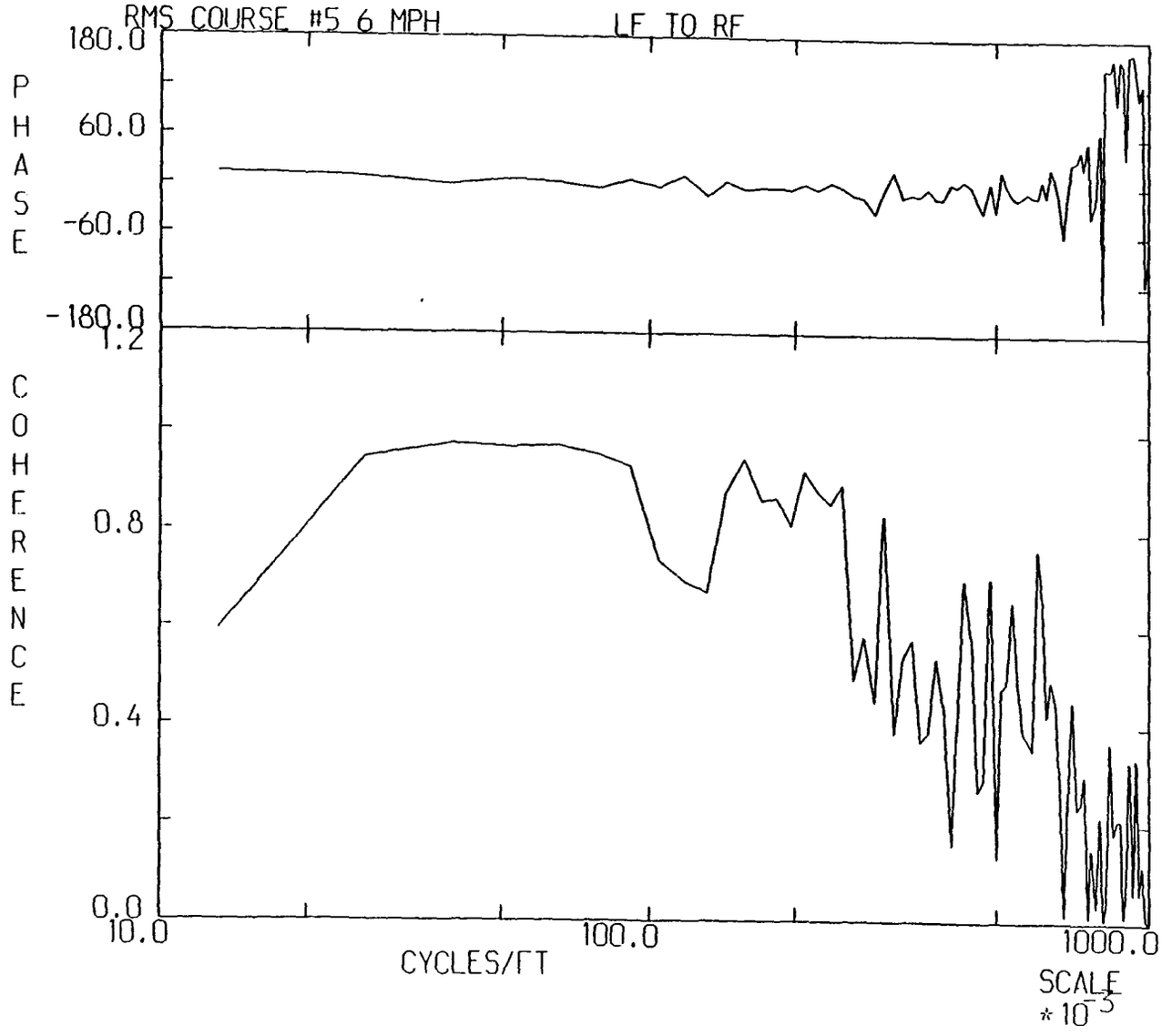
RMS COURSE #5 6 MPH
LF TO RF
180.0
60.0
-60.0
-180.0
PHASE
1.2
0.8
0.4
0.0
COHERENCE
10.0
100.0
1000.0
CYCLES/FT
SCALE
*10⁻³

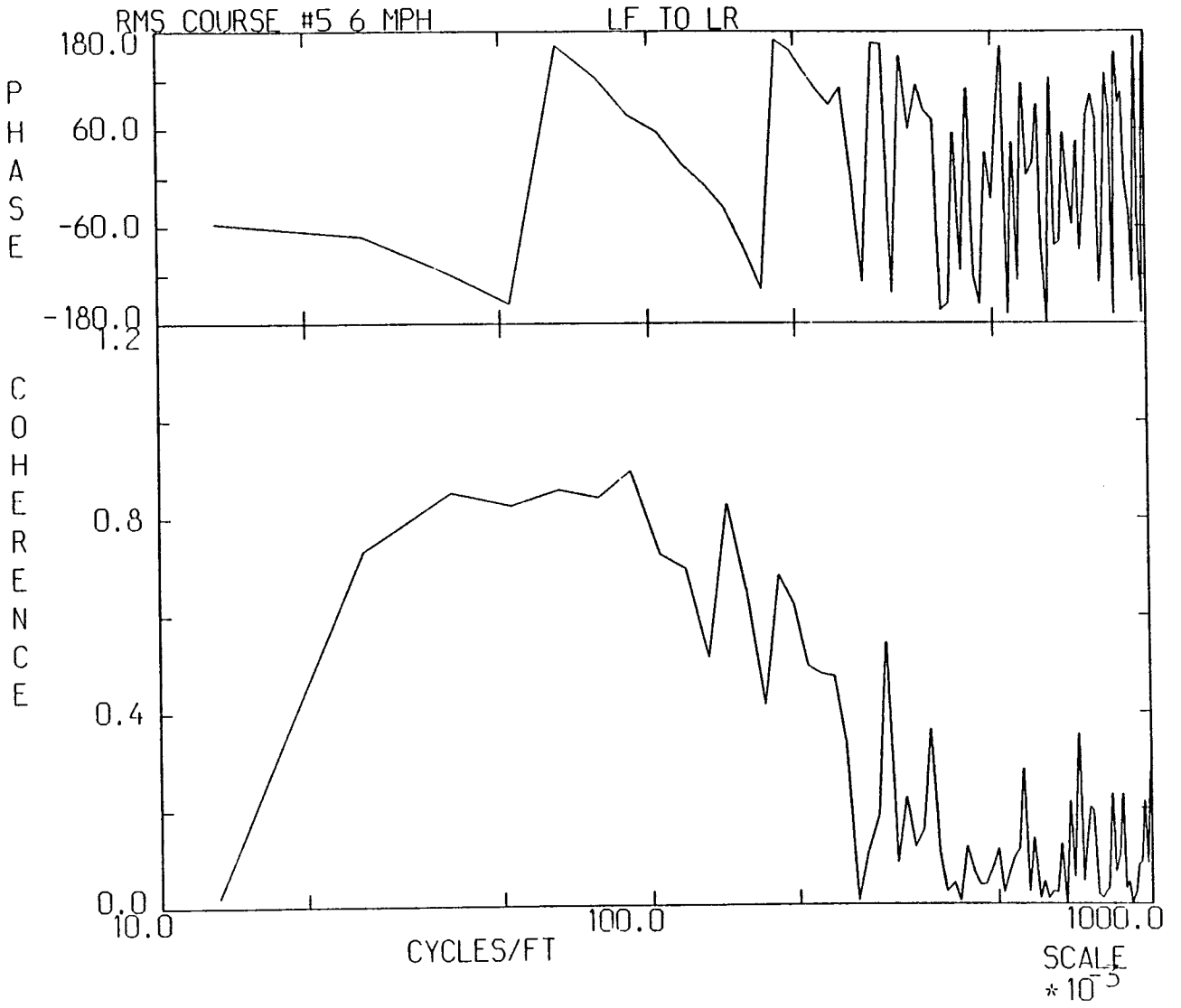
RMS COURSE #5 6 MPH
LF TO LR
PHASE
180.0
60.0
-60.0
-180.0
COHERENCE
1.2
0.8
0.4
0.0
10.0
100.0
1000.0
CYCLES/FT
SCALE
*10^-5

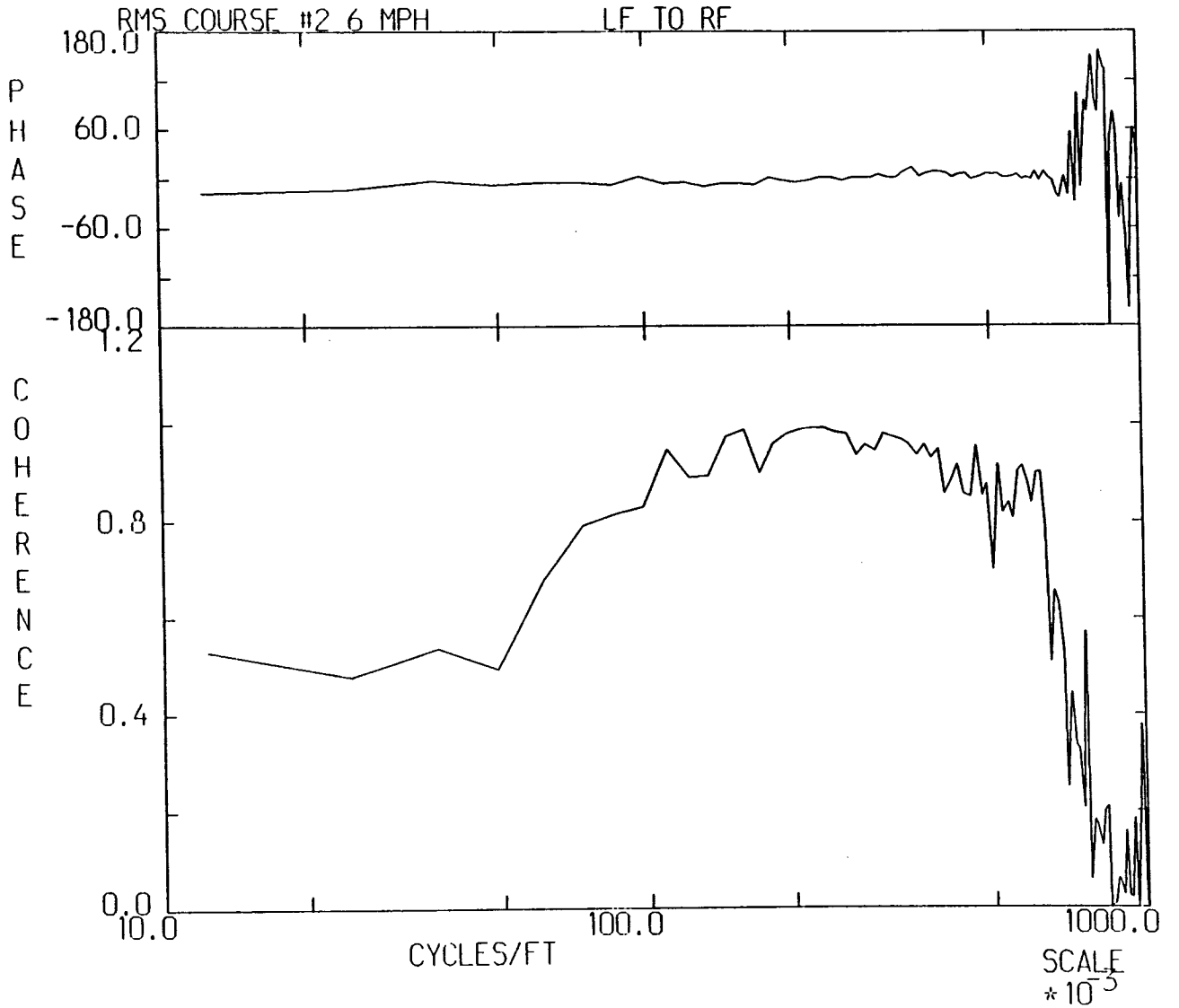
RMS COURSE #2 6 MPH
LF TO RF
180.0
60.0
-60.0
-180.0
PHASE
1.2
0.8
0.4
0.0
COHERENCE
10.0
100.0
1000.0
CYCLES/FT
SCALE
*10^-5

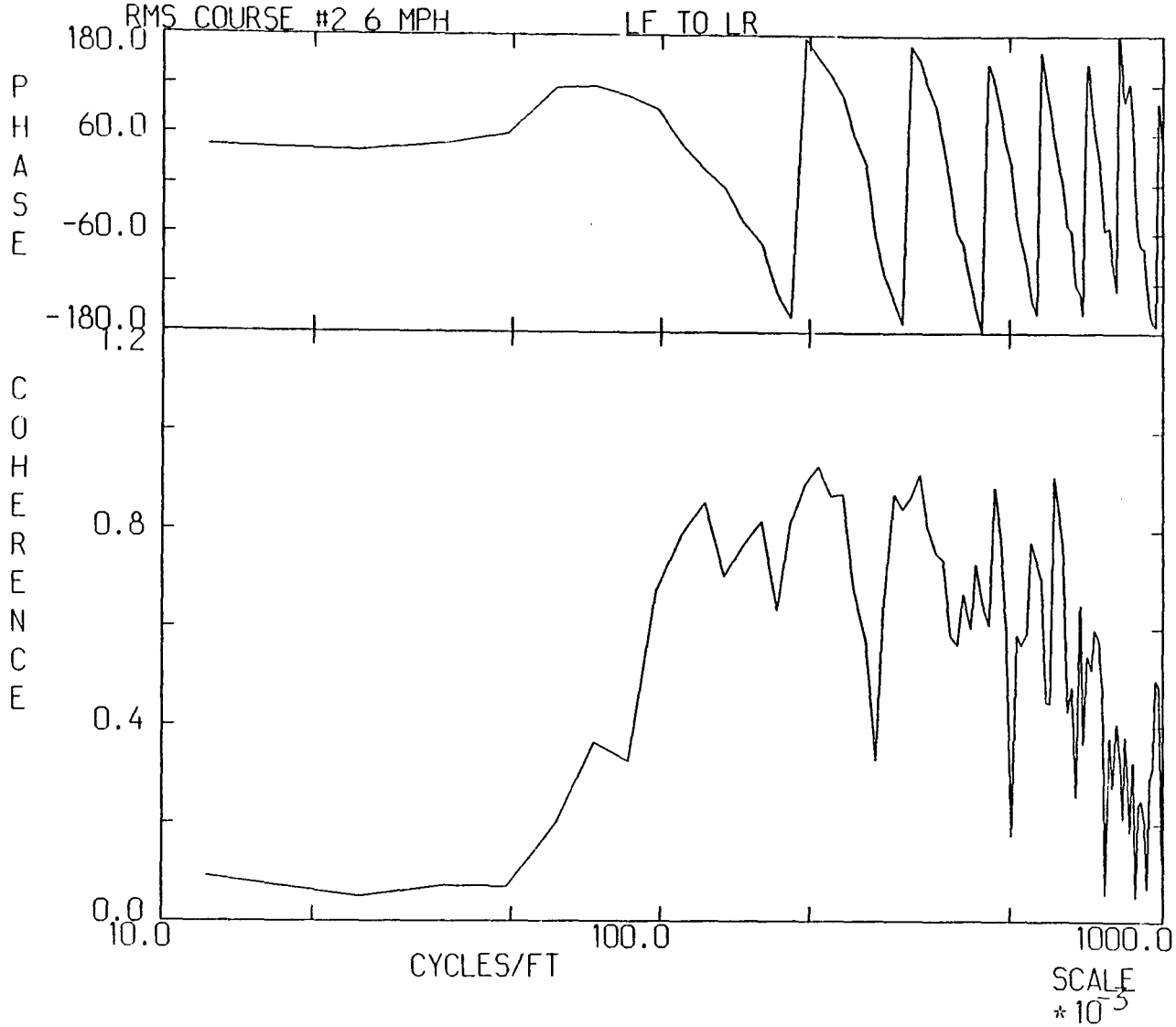
RMS COURSE #2 6 MPH
LF TO LR
PHASE
180.0
60.0
-60.0
-180.0
COHERENCE
1.2
0.8
0.4
0.0
10.0
100.0
1000.0
CYCLES/FT
SCALE
* 10^-3

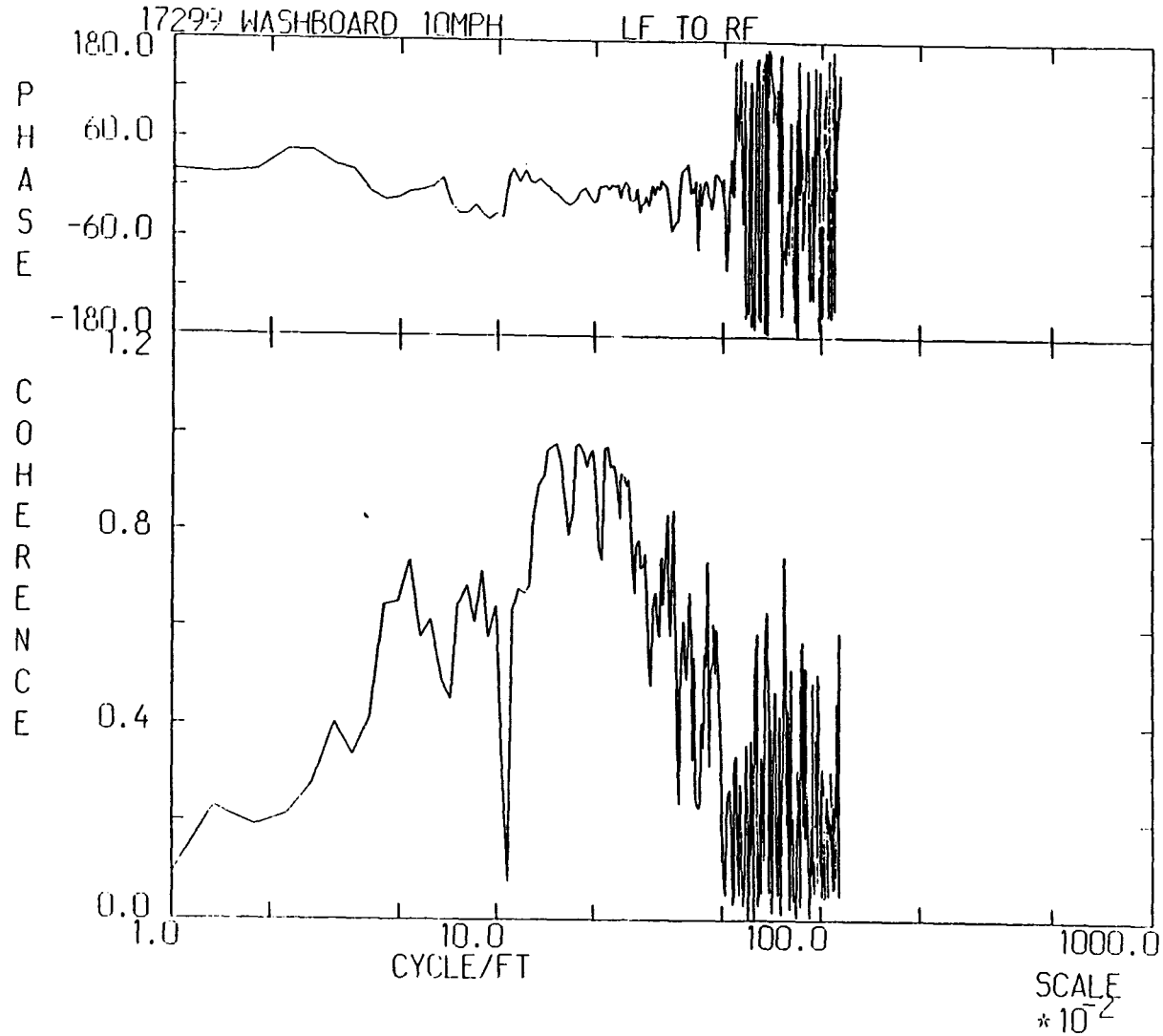
17299 WASHBOARD 10MPH
LF TO RF
PHASE
180.0
60.0
-60.0
-180.0
COHERENCE
1.2
0.8
0.4
0.0
1.0
10.0
100.0
1000.0
CYCLE/FT
SCALE
*10^-2

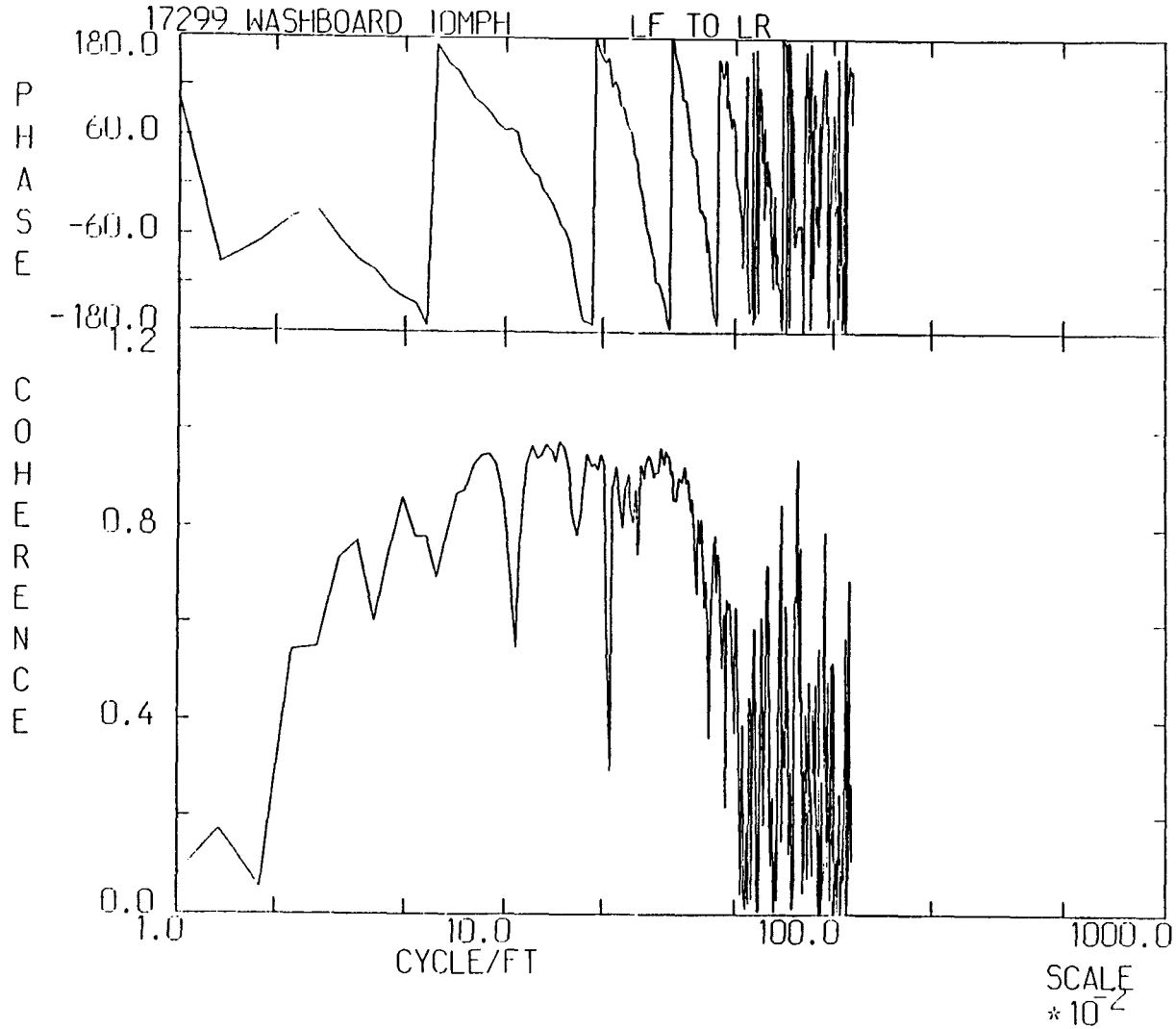
17299 WASHBOARD 10MPH
LF TO LR
180.0
60.0
-60.0
-180.0
PHASE
1.2
COHERENCE
0.8
0.4
0.0
1.0
10.0
100.0
1000.0
CYCLE/FT
SCALE
*10⁻²

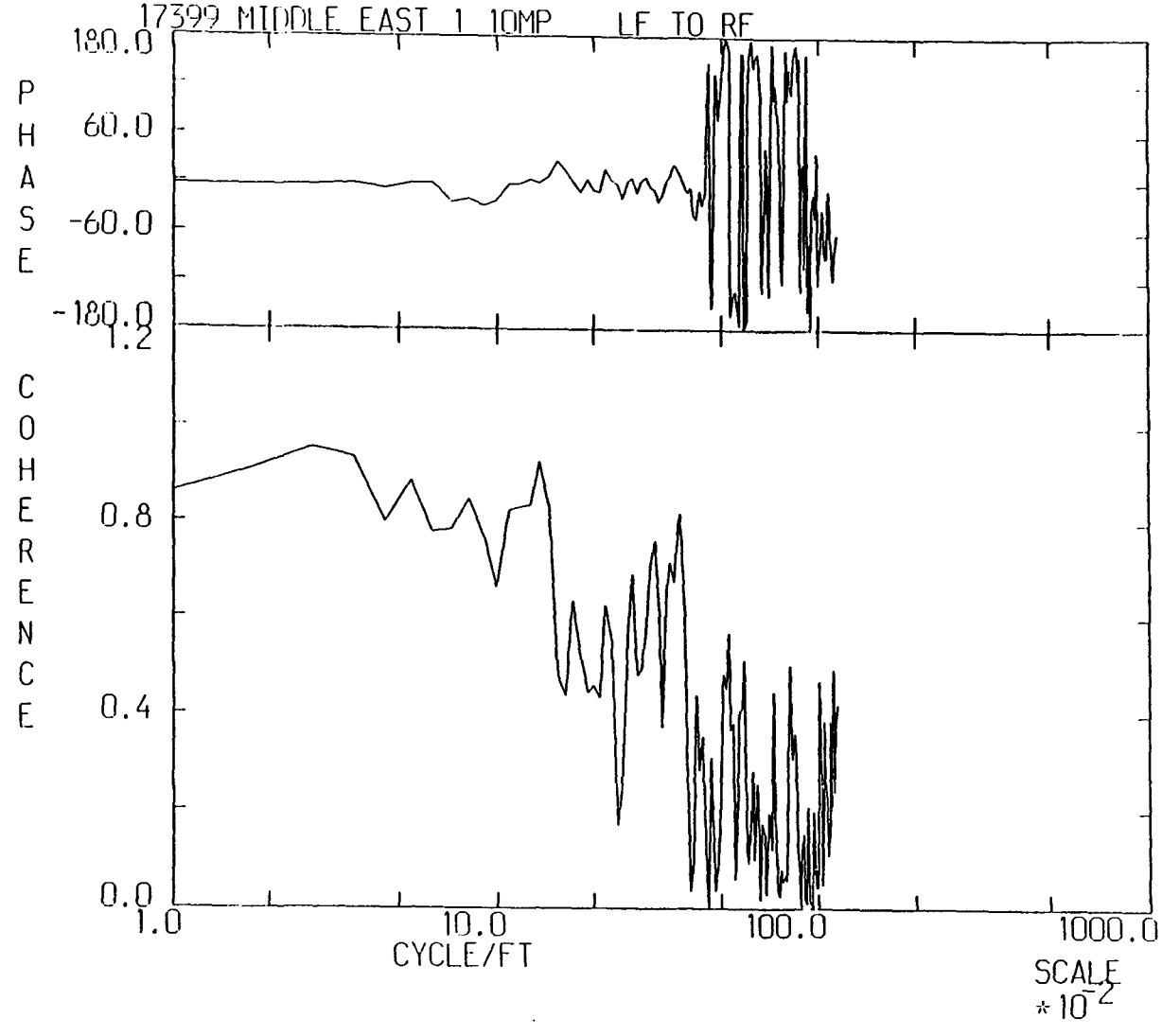
17399 MIDDLE EAST 1 10MP LF TO RF
180.0
60.0
-60.0
-180.0
PHASE
1.2
0.8
0.4
0.0
COHERENCE
1.0
10.0
100.0
1000.0
CYCLE/FT
SCALE
*10-2

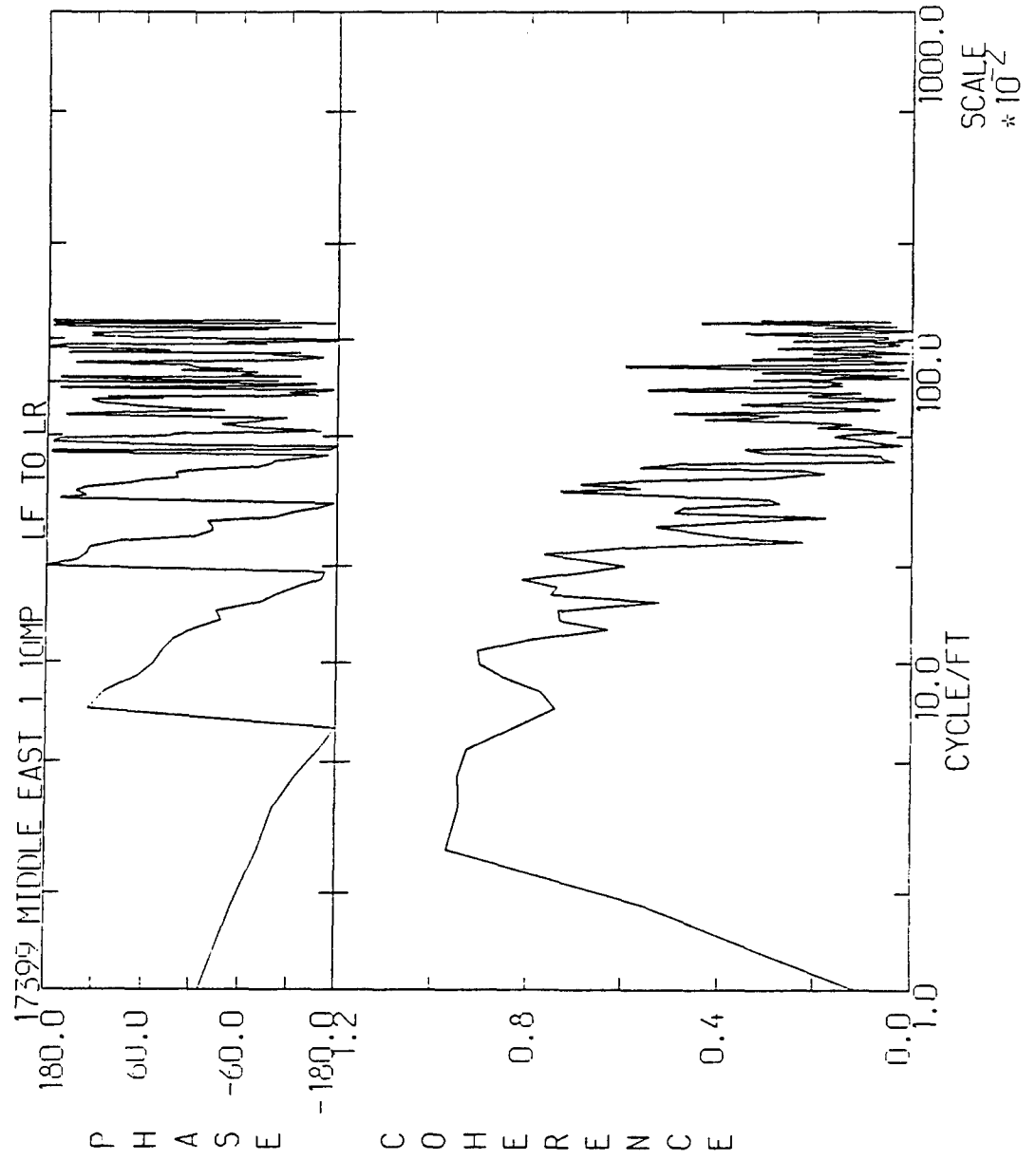
17399 MIDDLE EAST 1 10MP LF TO LR
180.0
60.0
-60.0
-180.0
PHASE
1.2
0.8
0.4
0.0
COHERENCE
1.0
10.0
100.0
1000.0
CYCLE/FT
SCALE
*10^-2

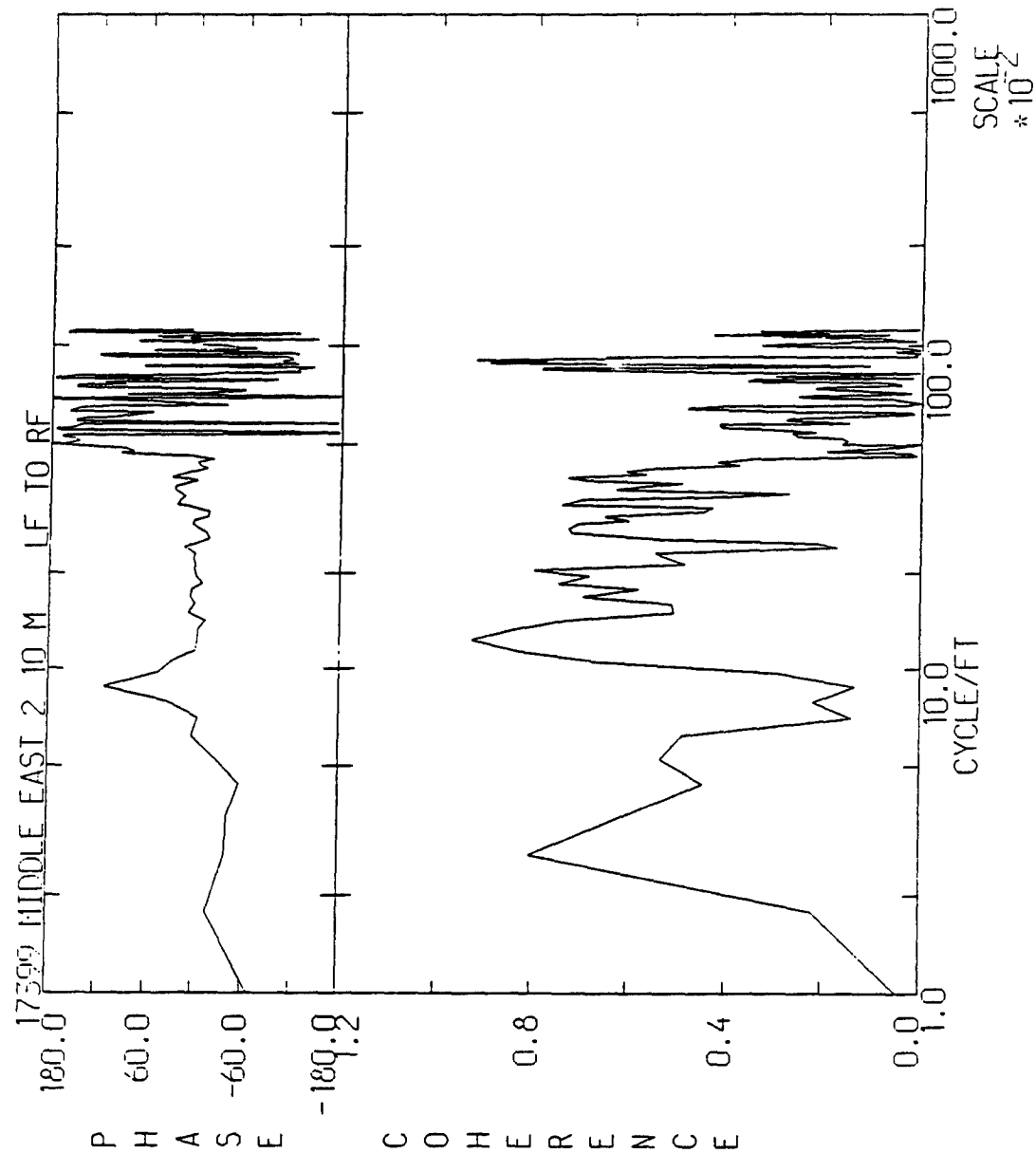
17399 MIDDLE EAST 2 10 M LF TO RF
180.0
60.0
-60.0
-180.0
PHASE
1.2
0.8
0.4
0.0
COHERENCE
1.0
10.0
100.0
1000.0
CYCLE/FT
SCALE
*10^-2

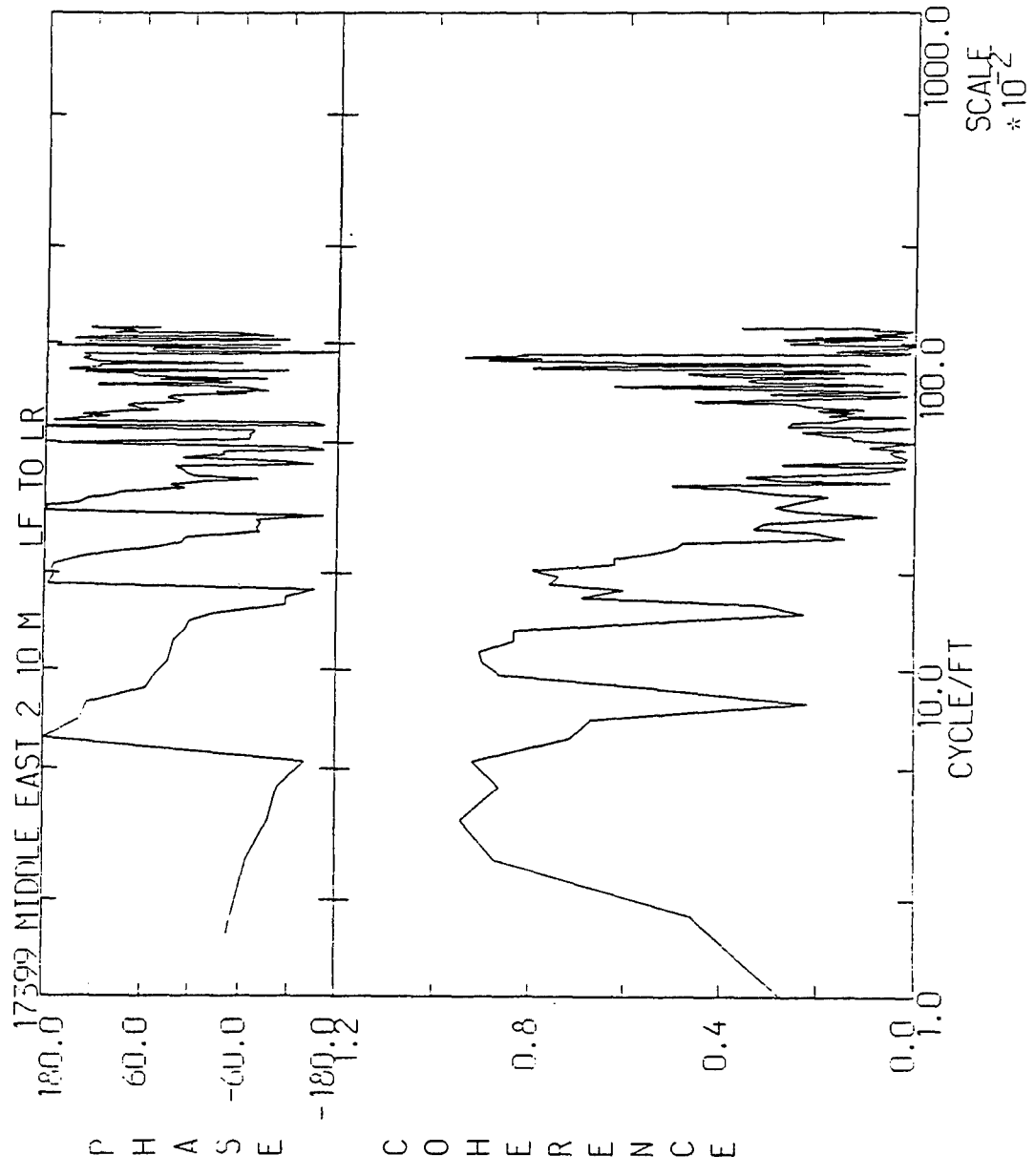
17599 MIDDLE EAST 2 10 M LF TO LR
180.0
60.0
-60.0
-180.0
PHASE
1.2
0.8
0.4
0.0
COHERENCE
1.0
10.0
100.0
1000.0
CYCLE/FT
SCALE
*10^-2

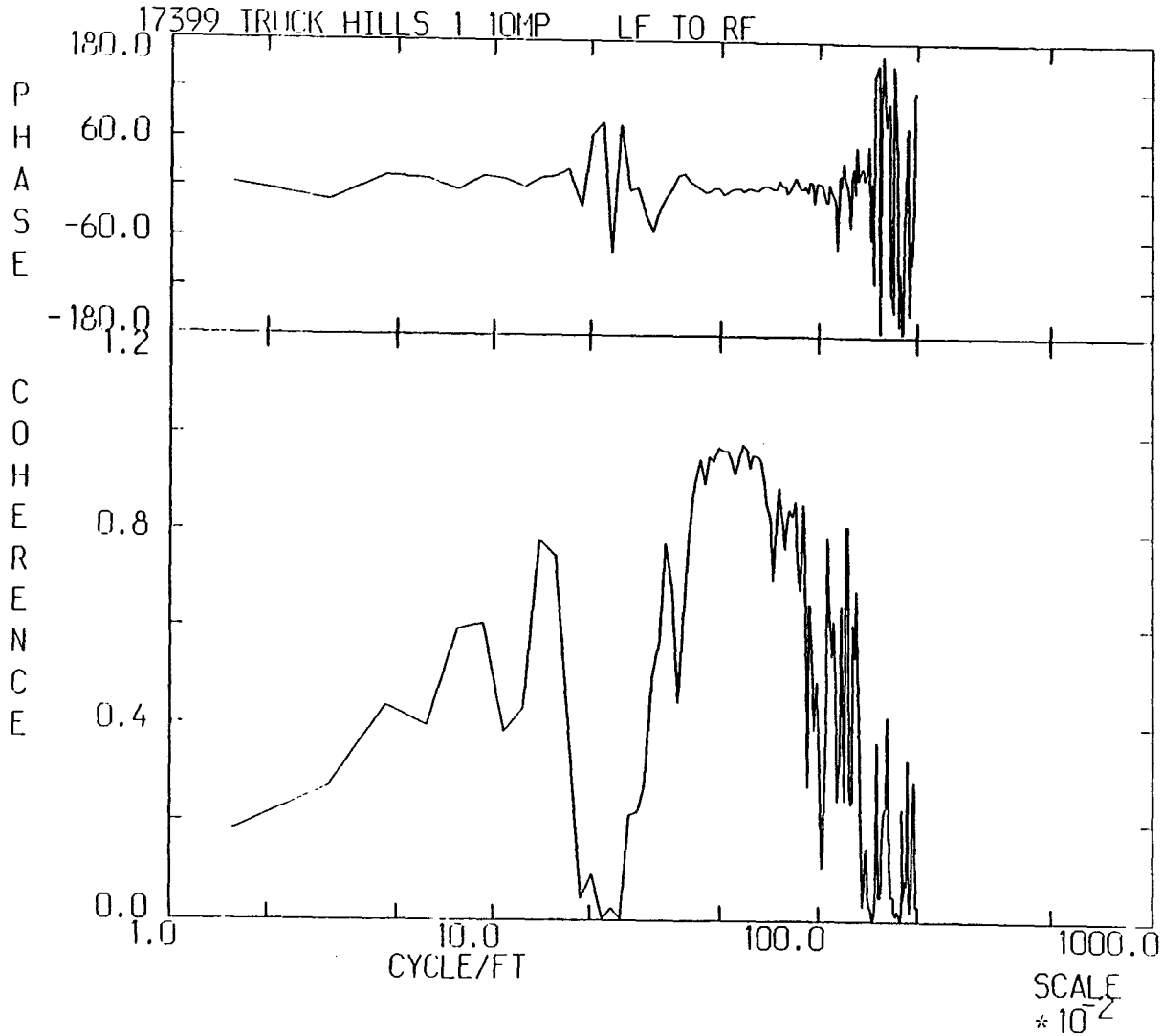
17399 TRUCK HILLS 1 10MP LF TO RF
PHASE
180.0
60.0
-60.0
-180.0
COHERENCE
1.2
0.8
0.4
0.0
1.0
10.0
100.0
1000.0
CYCLE/FT
SCALE
*10-2

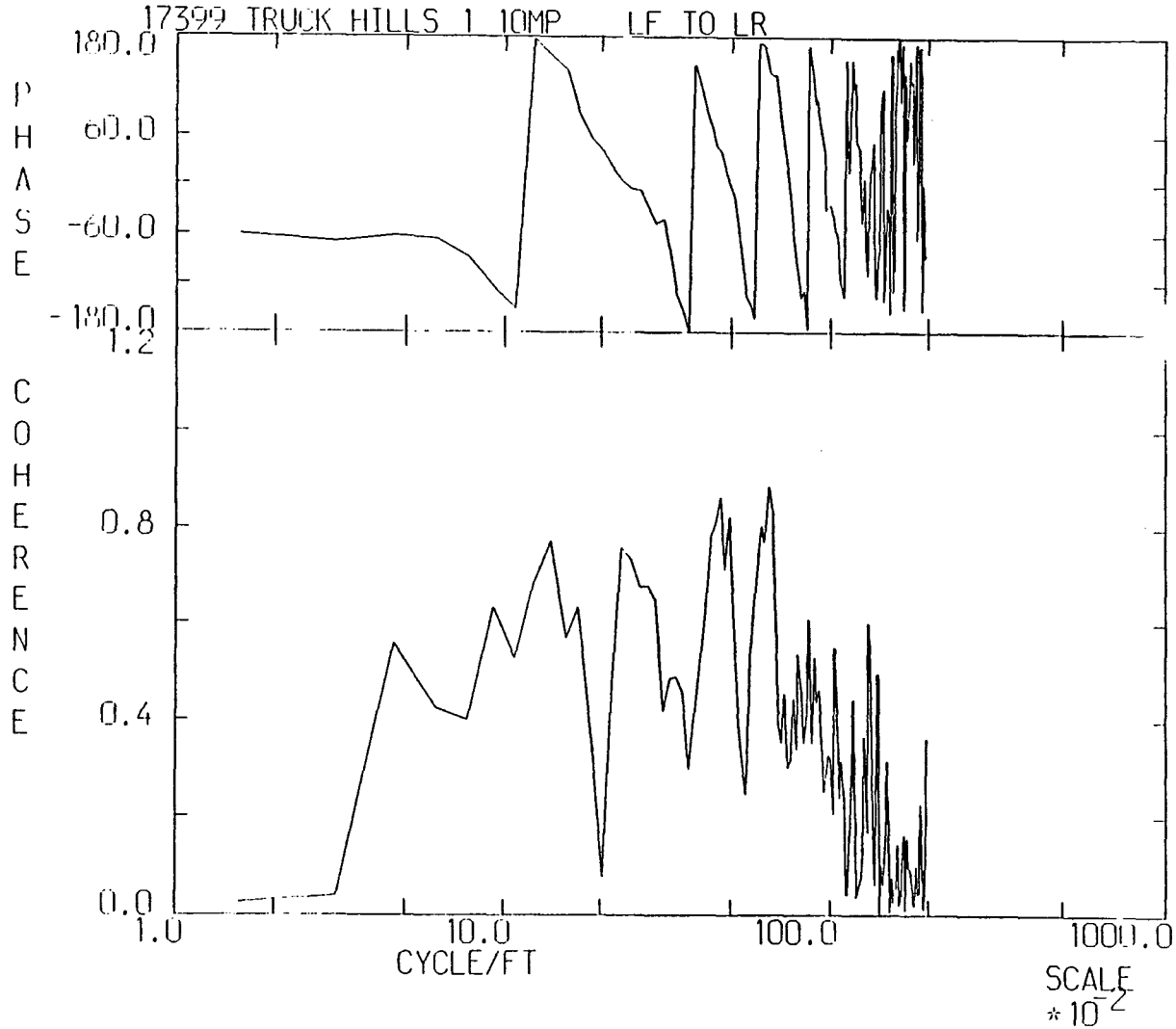
17399 TRUCK HILLS 1 10MP LF TO LR
PHASE
180.0
60.0
-60.0
-180.0
COHERENCE
1.2
0.8
0.4
0.0
1.0
10.0
100.0
1000.0
CYCLE/FT
SCALE
*10^-2

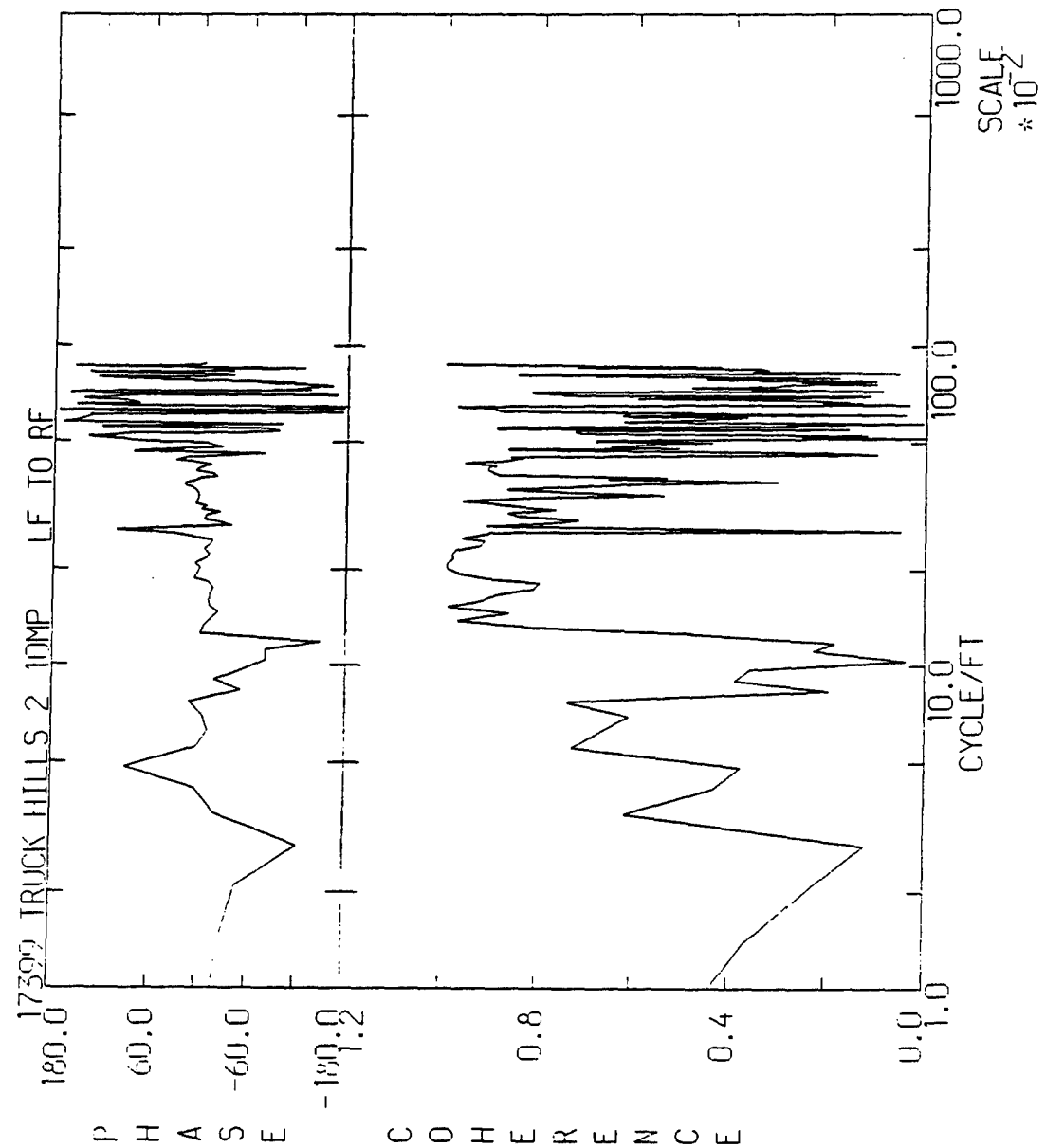
17399 TRUCK HILLS 2 10MP LF TO RF
180.0
60.0
-60.0
-180.0
PHASE
1.2
0.8
0.4
0.0
COHERENCE
1.0
10.0
100.0
1000.0
CYCLE/FT
SCALE
*10^-2

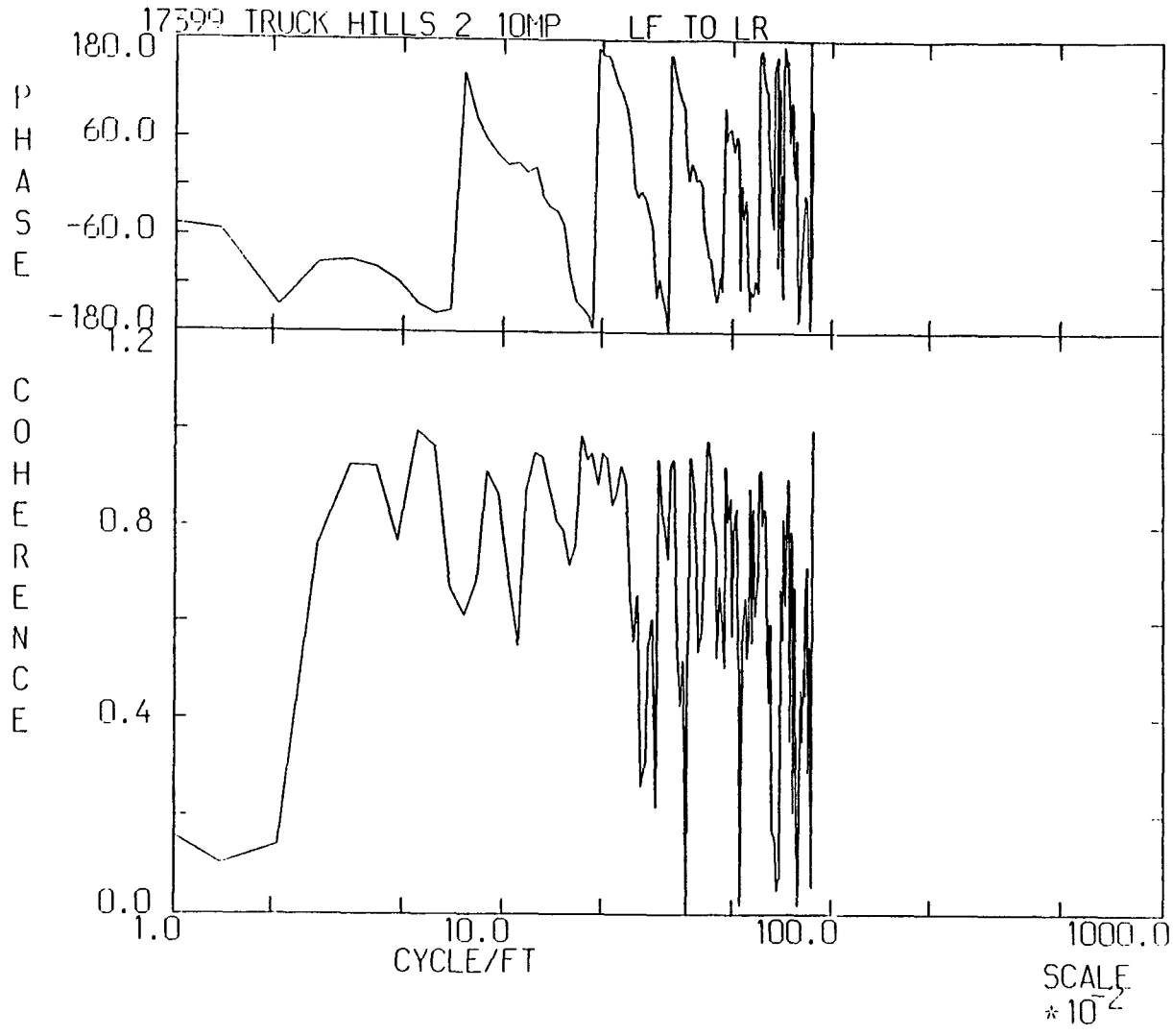
17599 TRUCK HILLS 2 10MP LF TO LR
PHASE
180.0
60.0
-60.0
-180.0
COHERENCE
1.2
0.8
0.4
0.0
1.0
10.0
100.0
1000.0
CYCLE/FT
SCALE
*10^-2

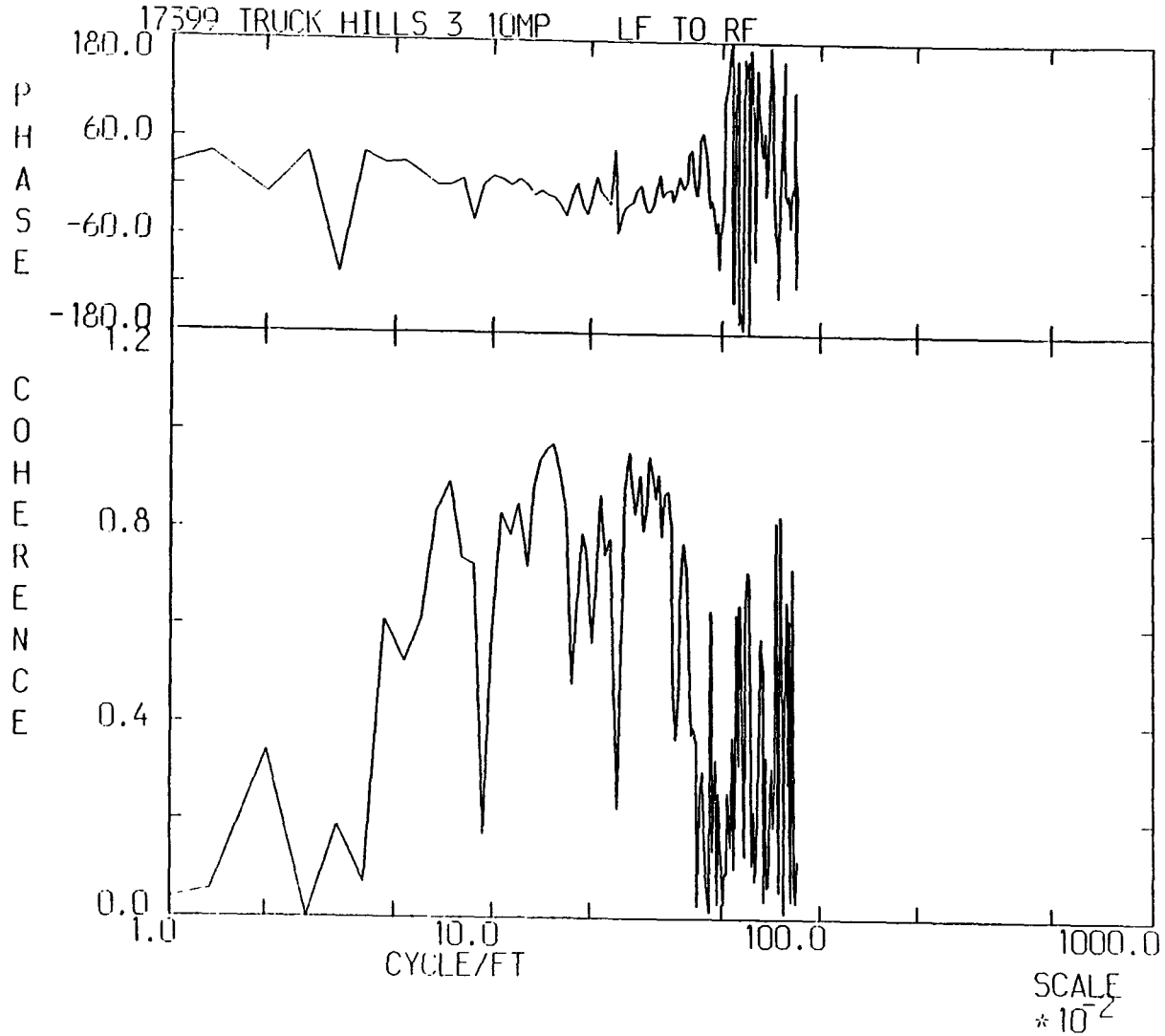
17399 TRUCK HILLS 3 10MP LF TO RF
PHASE
180.0
60.0
-60.0
-180.0
1.2
COHERENCE
0.8
0.4
0.0
1.0
10.0
100.0
1000.0
CYCLE/FT
SCALE
*10^-2

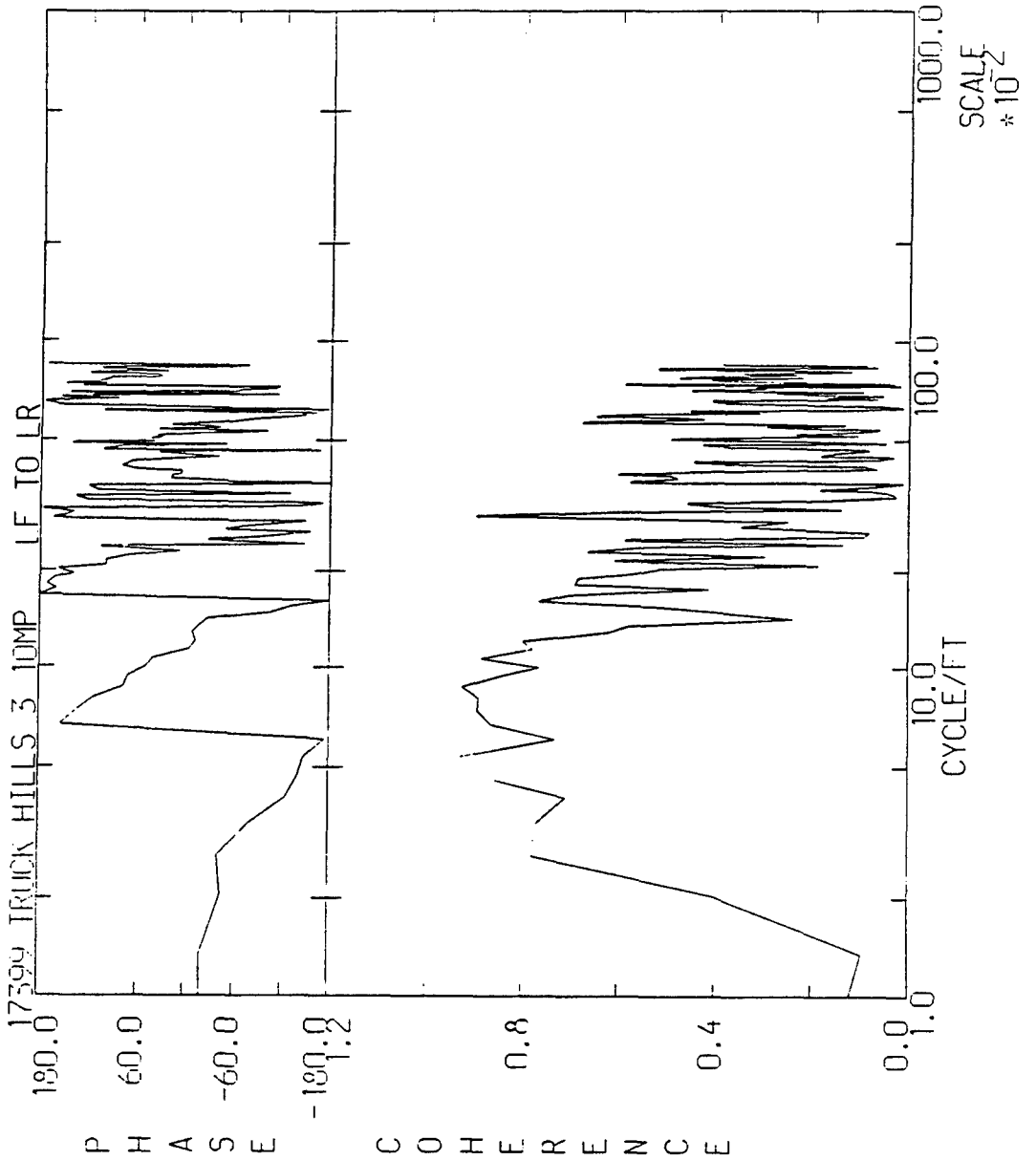
1739 TRUCK HILLS 3 10MP LF TO LR
180.0
60.0
-60.0
-180.0
PHASE
1.2
0.8
0.4
0.0
COHERENCE
1.0
10.0
100.0
1000.0
CYCLE/FT
SCALE
*10^-2

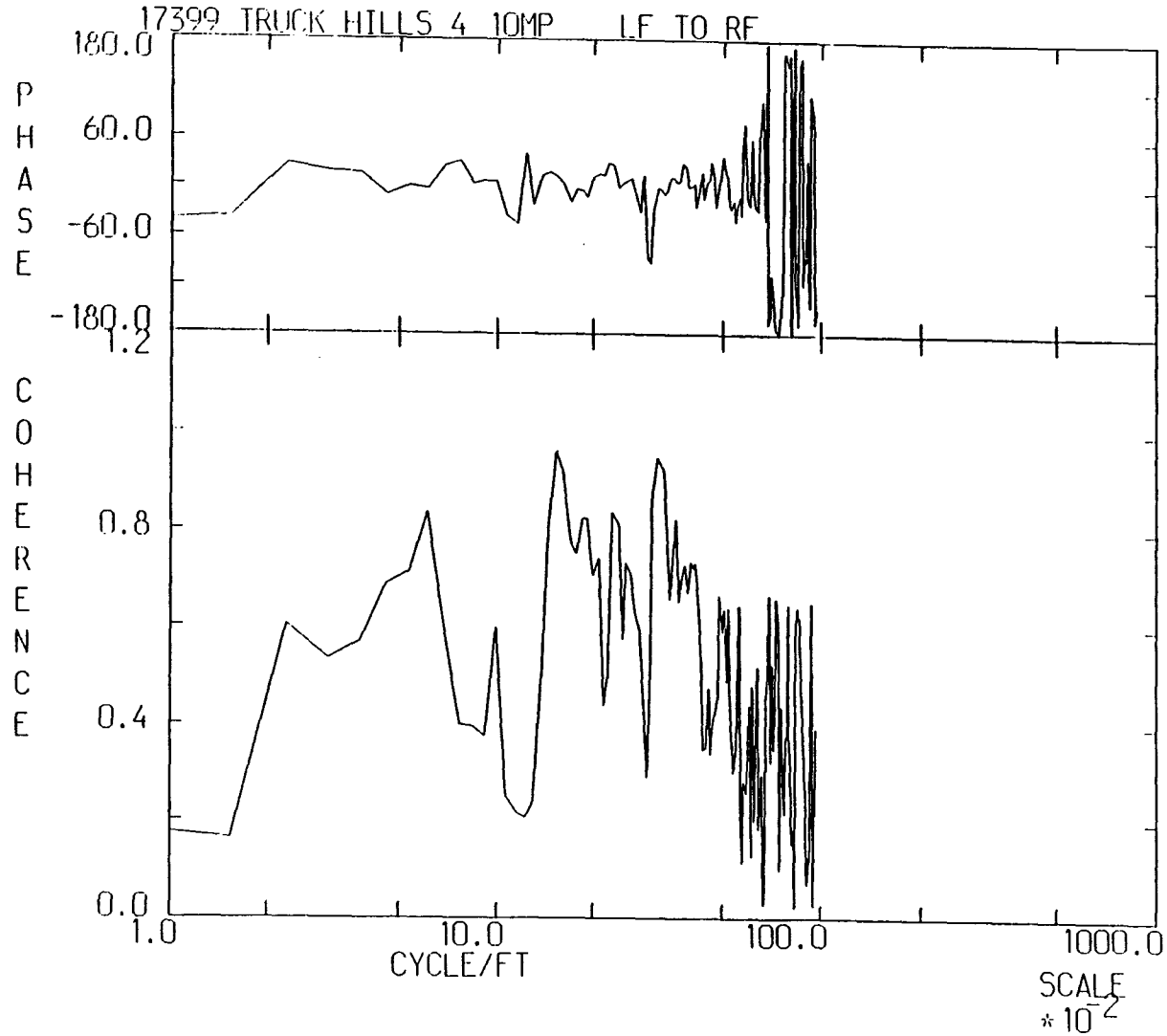
17399 TRUCK HILLS 4 10MP LF TO RF
PHASE
180.0
60.0
-60.0
-180.0
1.2
COHERENCE
0.8
0.4
0.0
1.0
10.0
100.0
1000.0
CYCLE/FT
SCALE
* 10-2

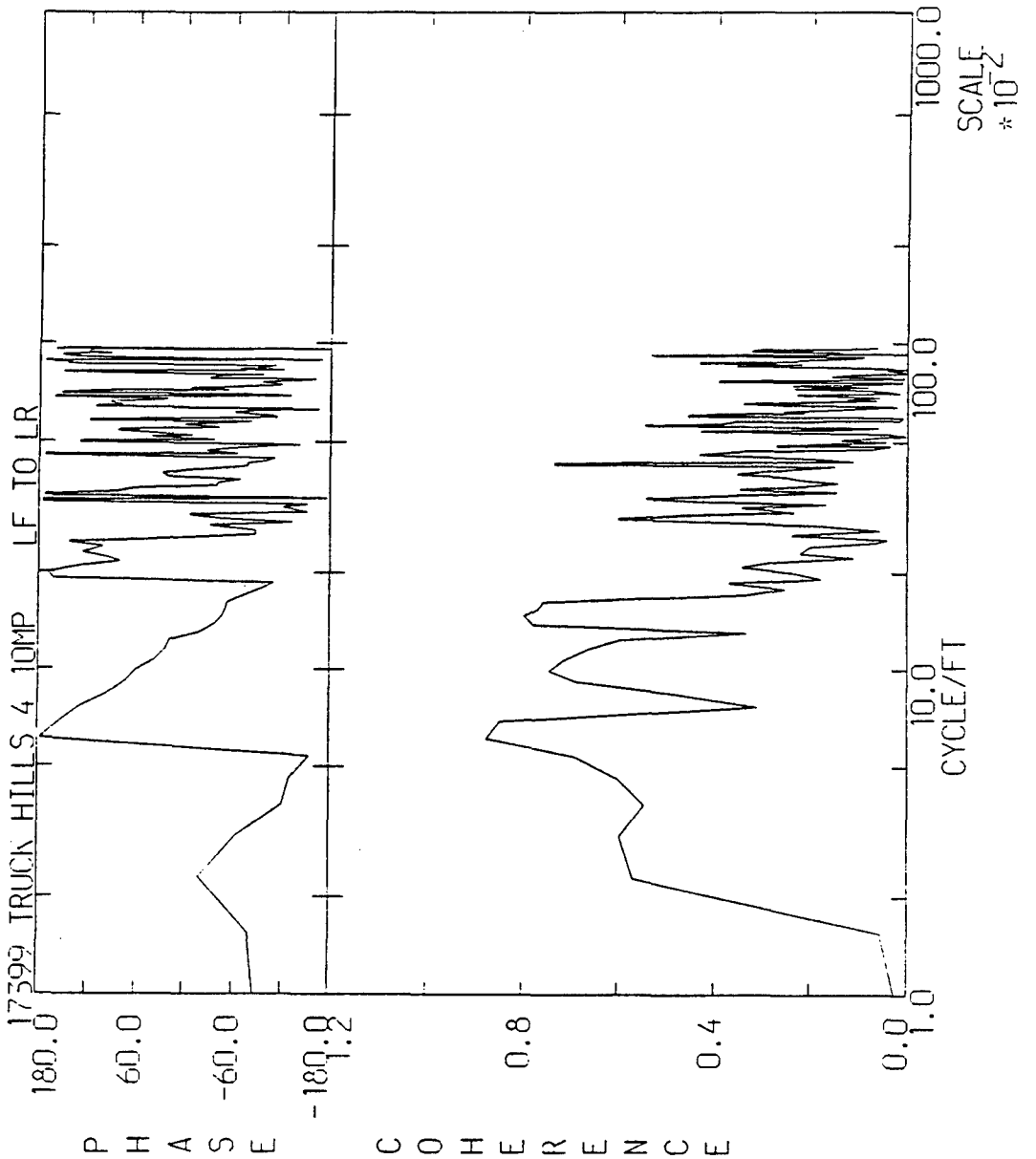
17399 TRUCK HILLS 4 10MP LF TO LR
180.0
60.0
-60.0
-180.0
PHASE
1.2
0.8
0.4
0.0
COHERENCE
1.0
10.0
100.0
1000.0
CYCLE/FT
SCALE
*10⁻²

APPENDIX H

COHERENCE FUNCTION PLOTS - APG PROFILOMETER

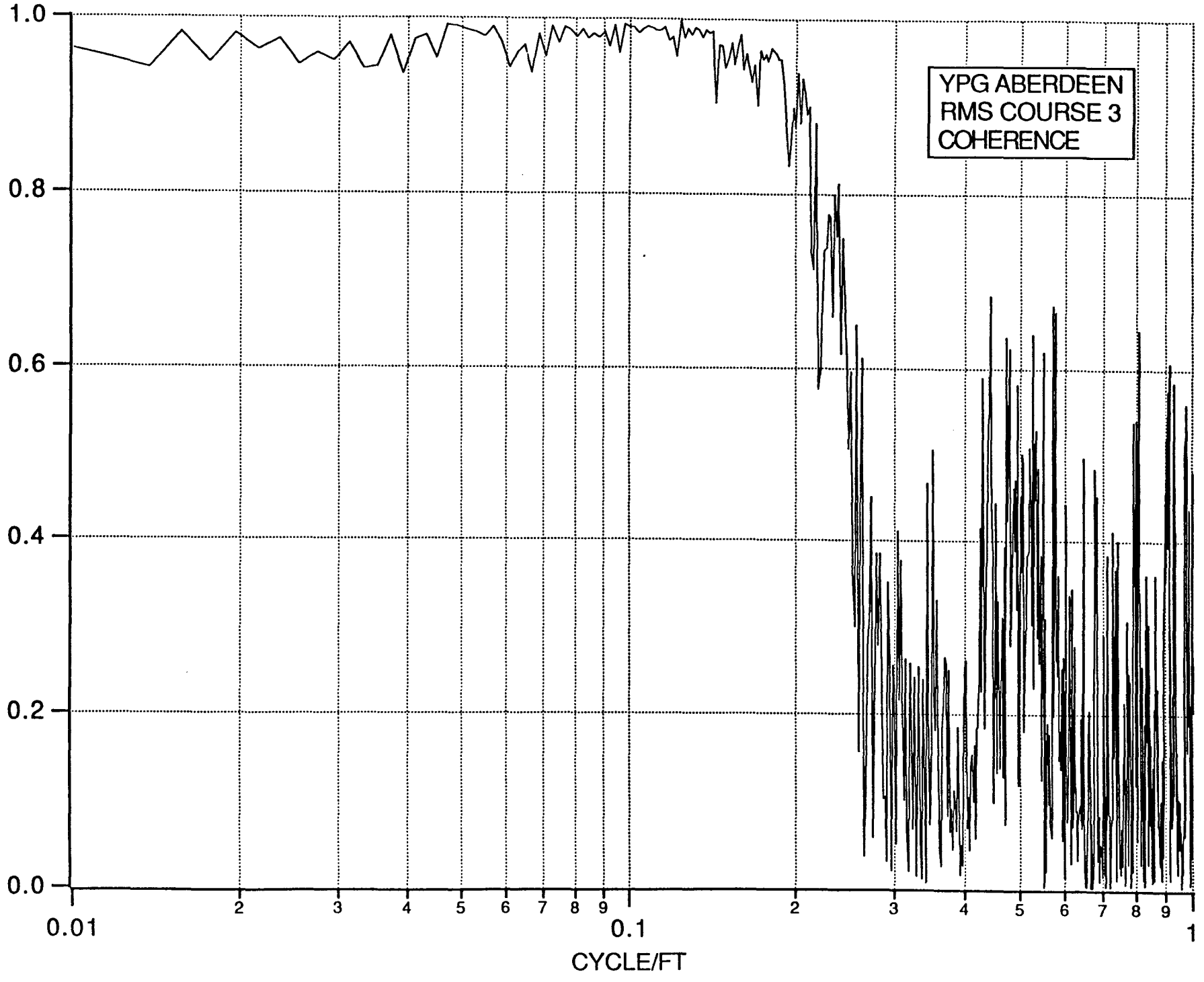
YPG ABERDEEN
RMS COURSE 3
COHERENCE
1.0
0.8
0.6
0.4
0.2
0.0
0.01
0.1
1
2 3 4 5 6 7 8 9
2 3 4 5 6 7 8 9
CYCLE/FT

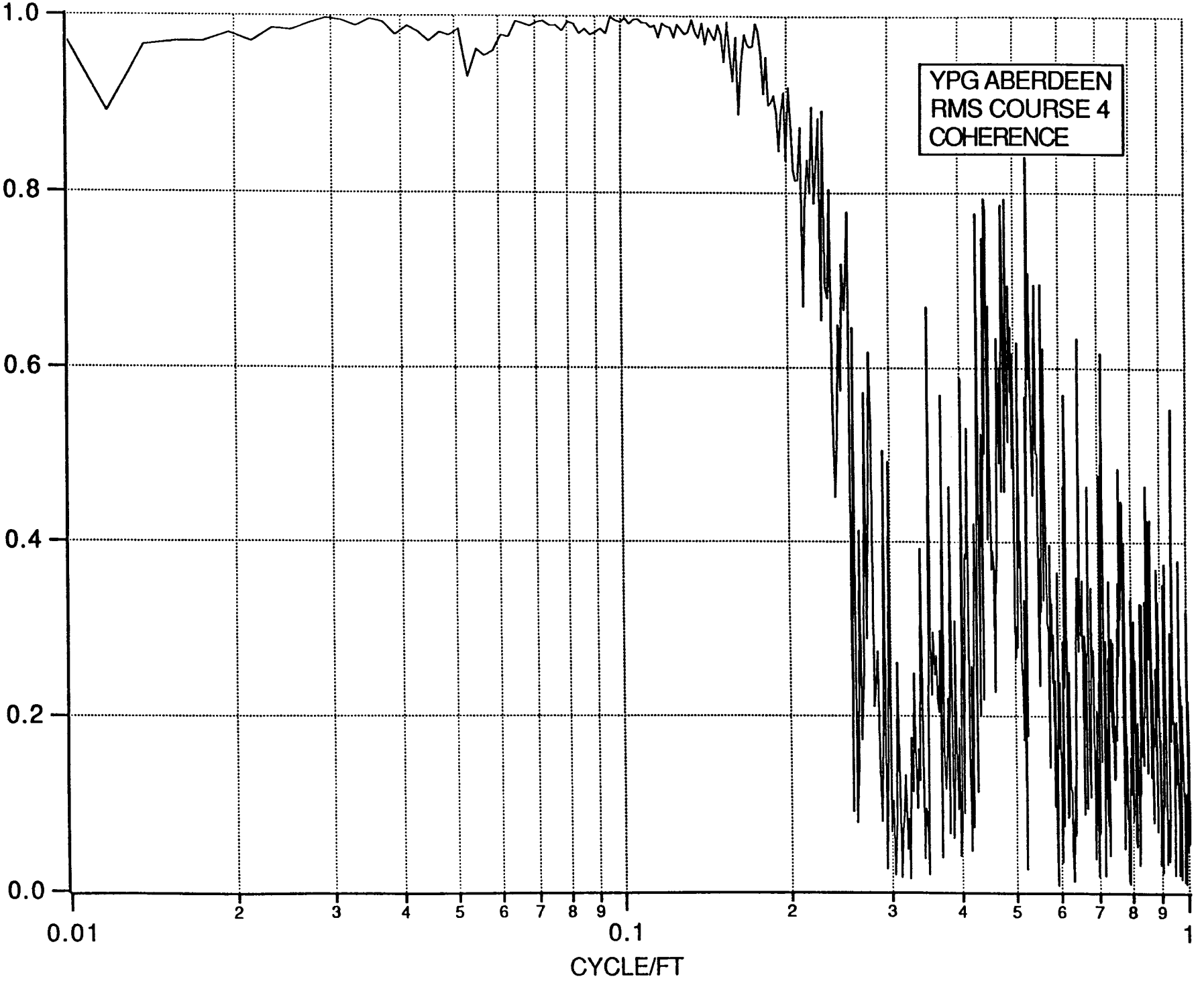
YPG ABERDEEN
RMS COURSE 4
COHERENCE
1.0
0.8
0.6
0.4
0.2
0.0
0.01
0.1
1
2
3
4
5
6
7
8
9
CYCLE/FT

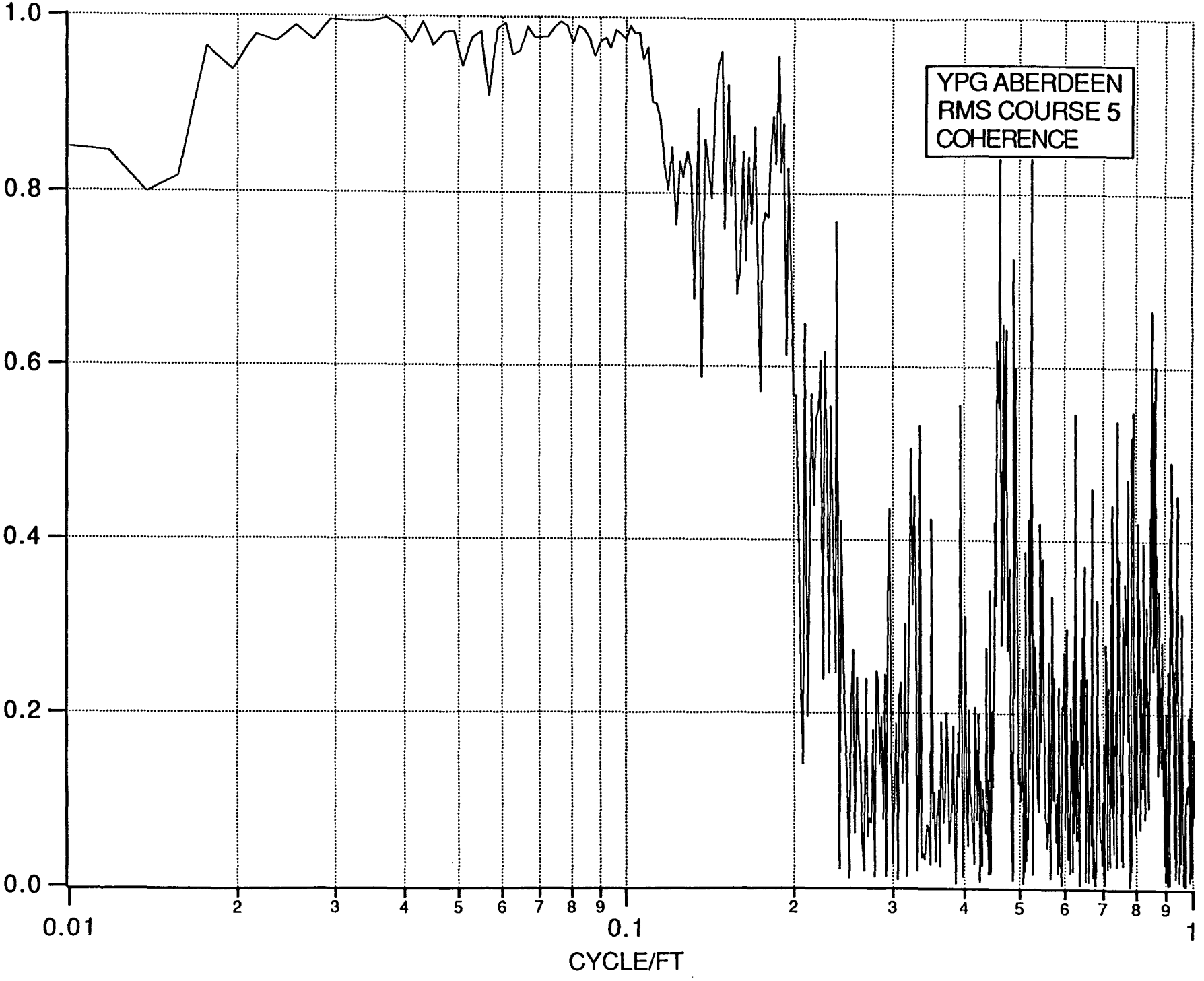
YPG ABERDEEN
RMS COURSE 5
COHERENCE
1.0
0.8
0.6
0.4
0.2
0.0
0.01
2
3
4
5
6
7
8
9
0.1
2
3
4
5
6
7
8
9
1
CYCLE/FT

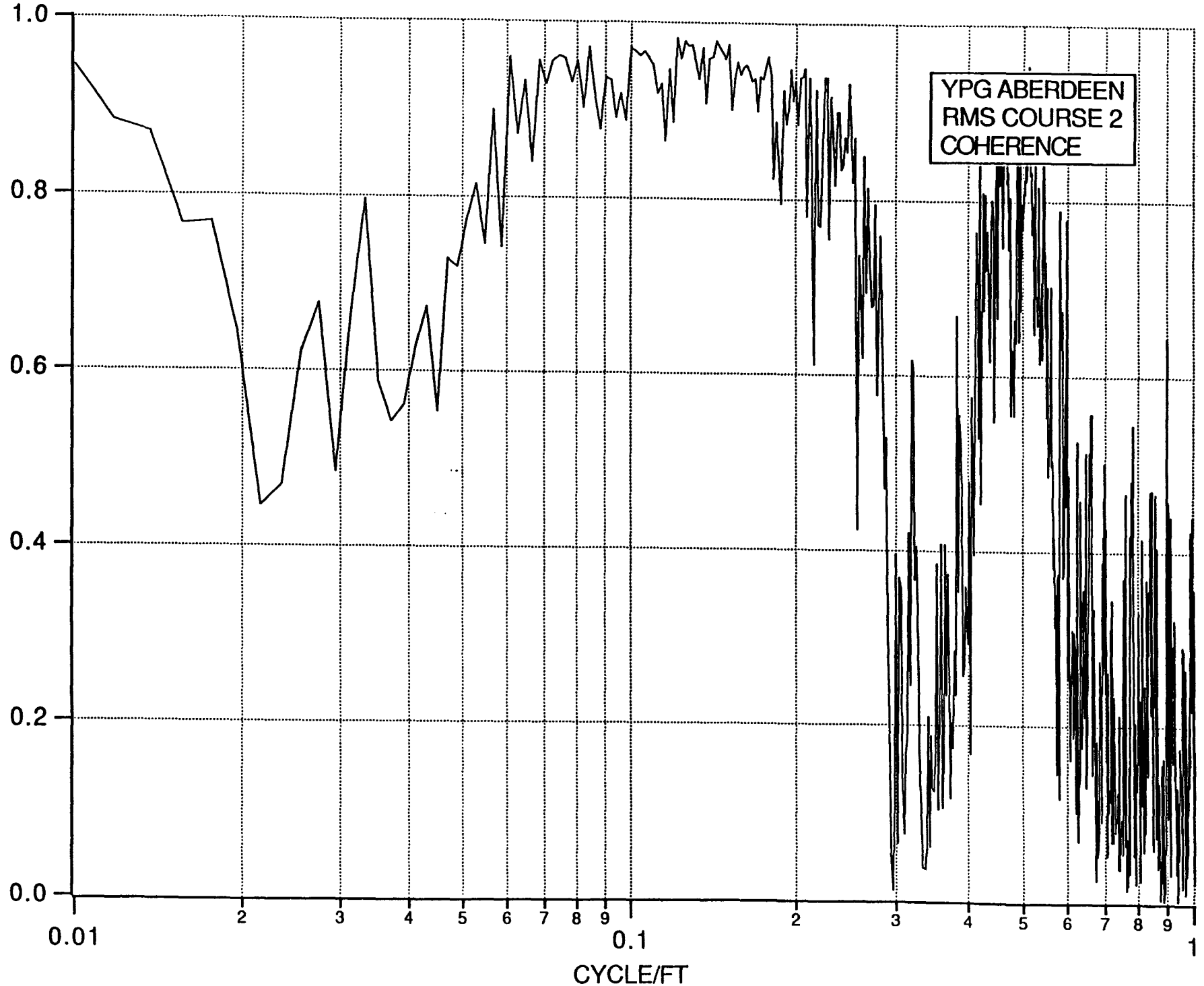
YPG ABERDEEN
RMS COURSE 2
COHERENCE
1.0
0.8
0.6
0.4
0.2
0.0
0.01
2
3
4
5
6
7
8
9
0.1
2
3
4
5
6
7
8
9
1
CYCLE/FT

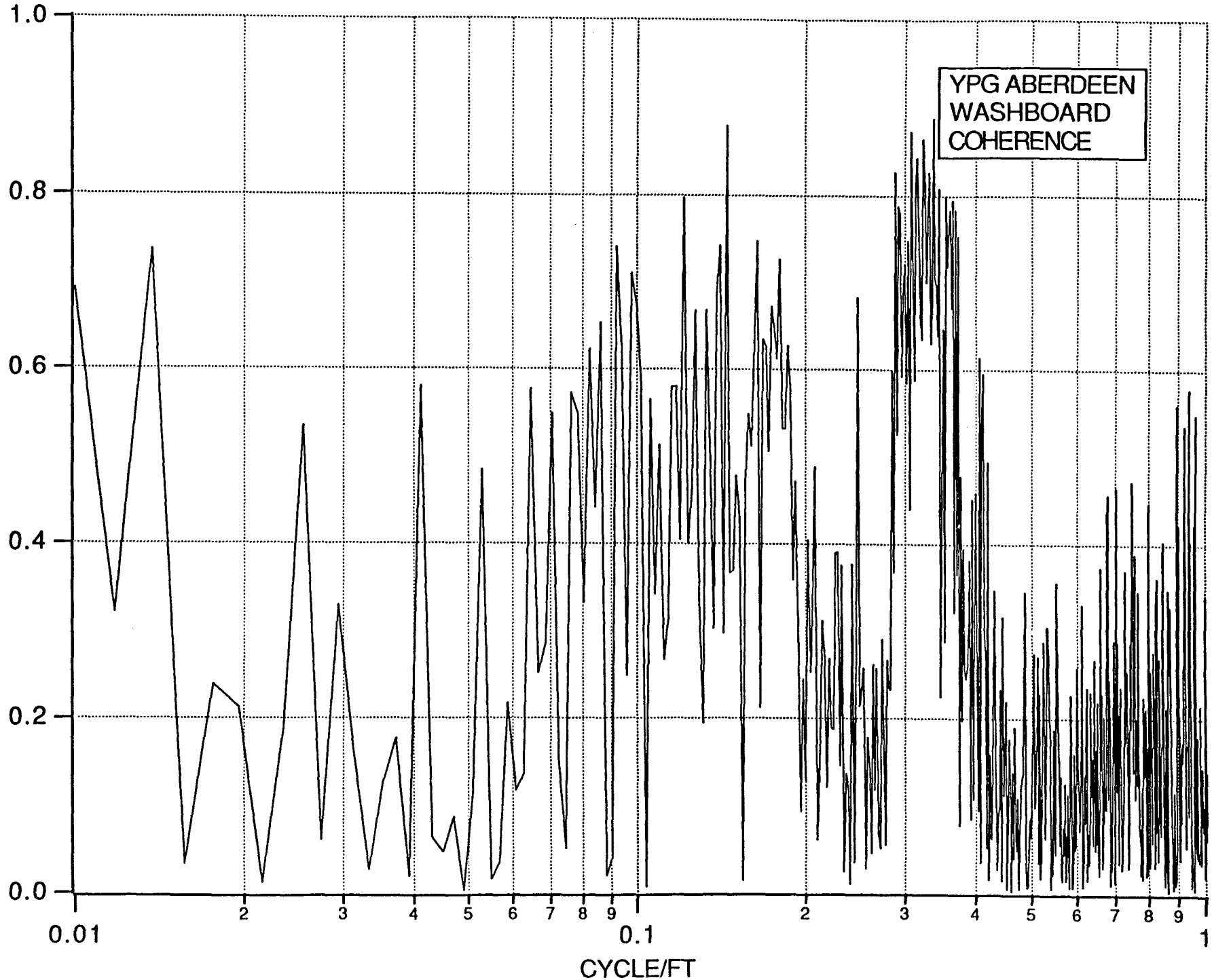
YPG ABERDEEN
WASHBOARD
COHERENCE
1.0
0.8
0.6
0.4
0.2
0.0
0.01
2
3
4
5
6
7
8
9
0.1
2
3
4
5
6
7
8
9
1
CYCLE/FT

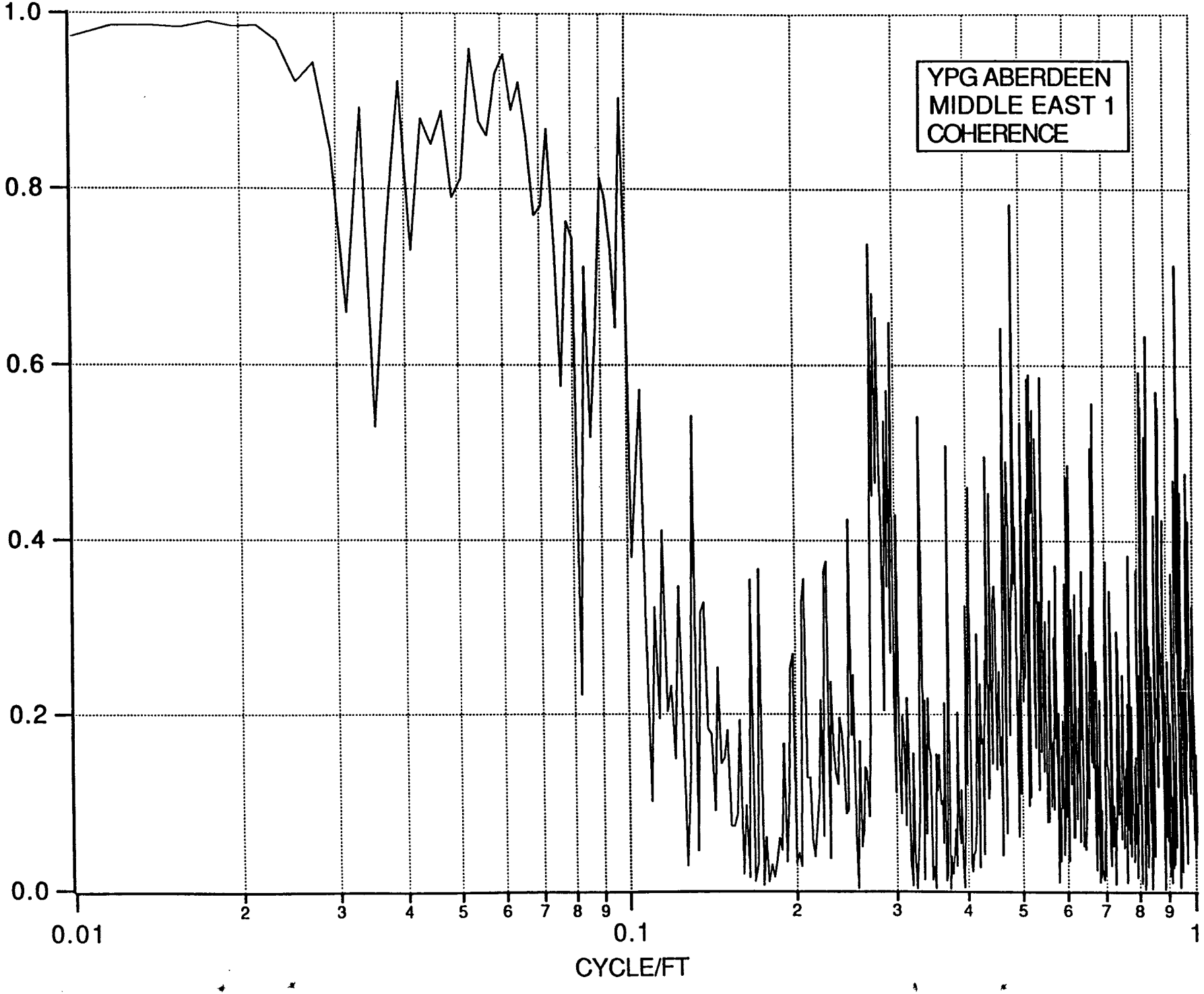
YPG ABERDEEN
MIDDLE EAST 1
COHERENCE
1.0
0.8
0.6
0.4
0.2
0.0
0.01
0.1
1
2
3
4
5
6
7
8
9
CYCLE/FT

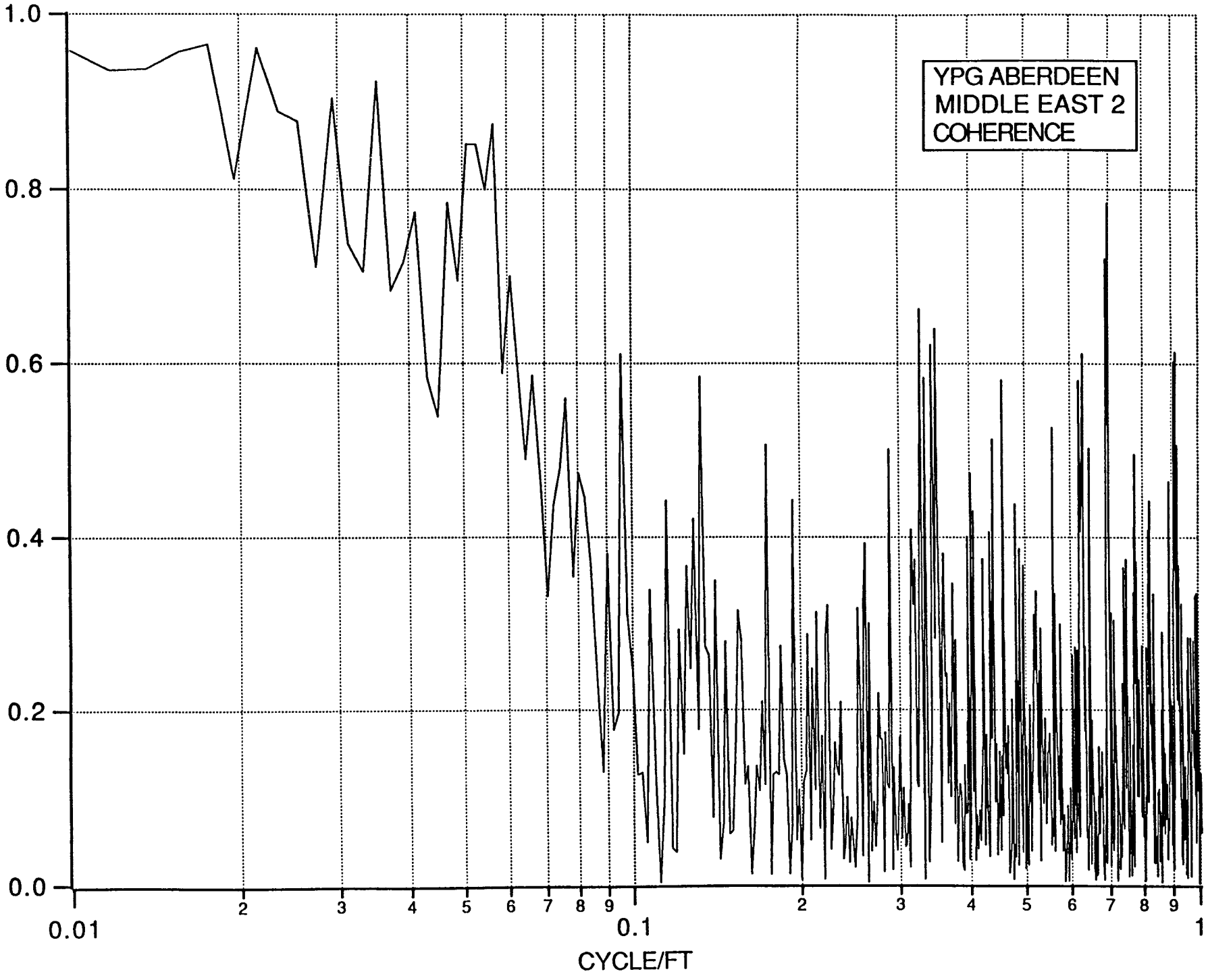
YPG ABERDEEN
MIDDLE EAST 2
COHERENCE
1.0
0.8
0.6
0.4
0.2
0.0
0.01
0.1
1
2
3
4
5
6
7
8
9
CYCLE/FT

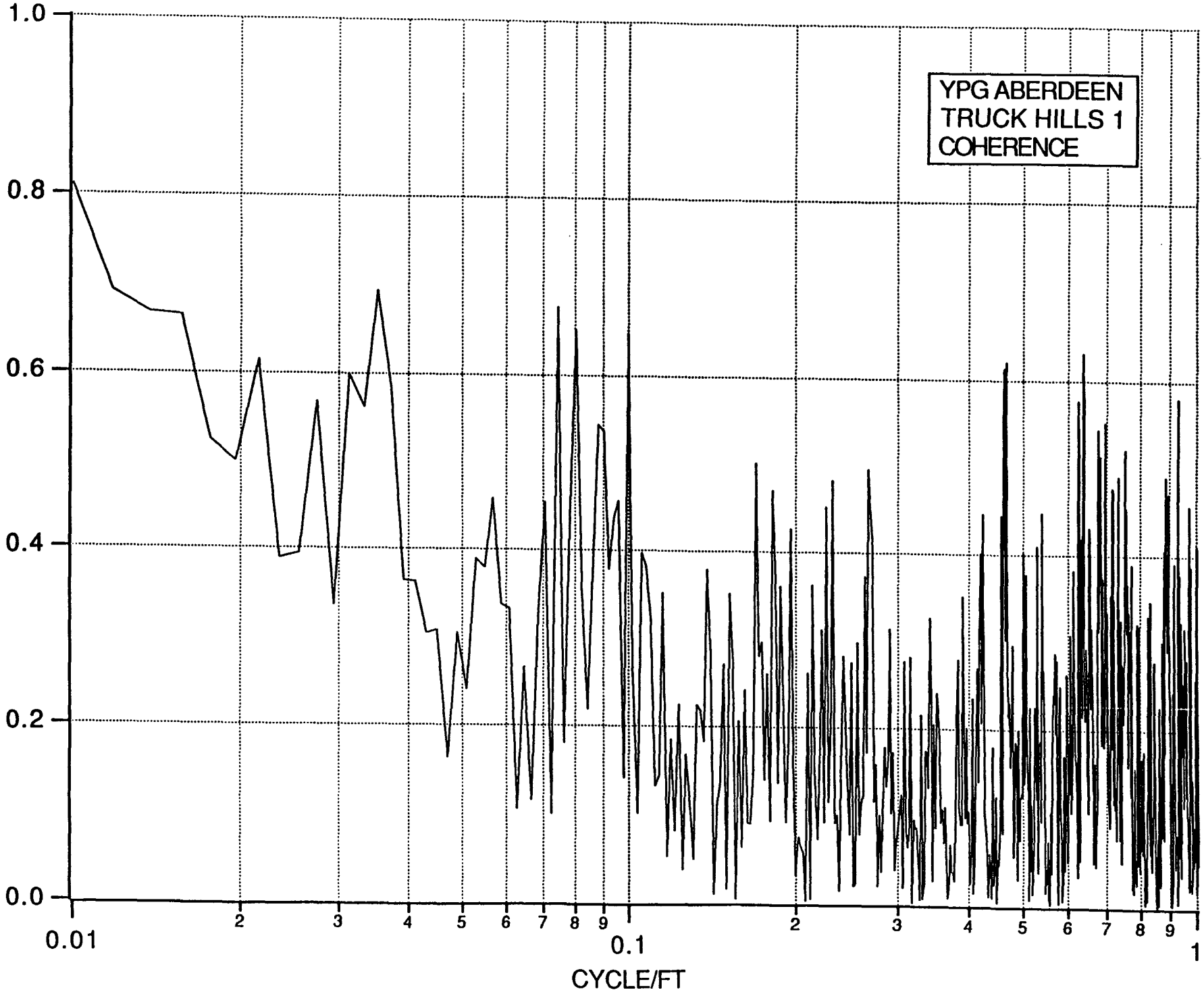
YPG ABERDEEN
TRUCK HILLS 1
COHERENCE
1.0
0.8
0.6
0.4
0.2
0.0
0.01
2
3
4
5
6
7
8
9
0.1
2
3
4
5
6
7
8
9
1
CYCLE/FT

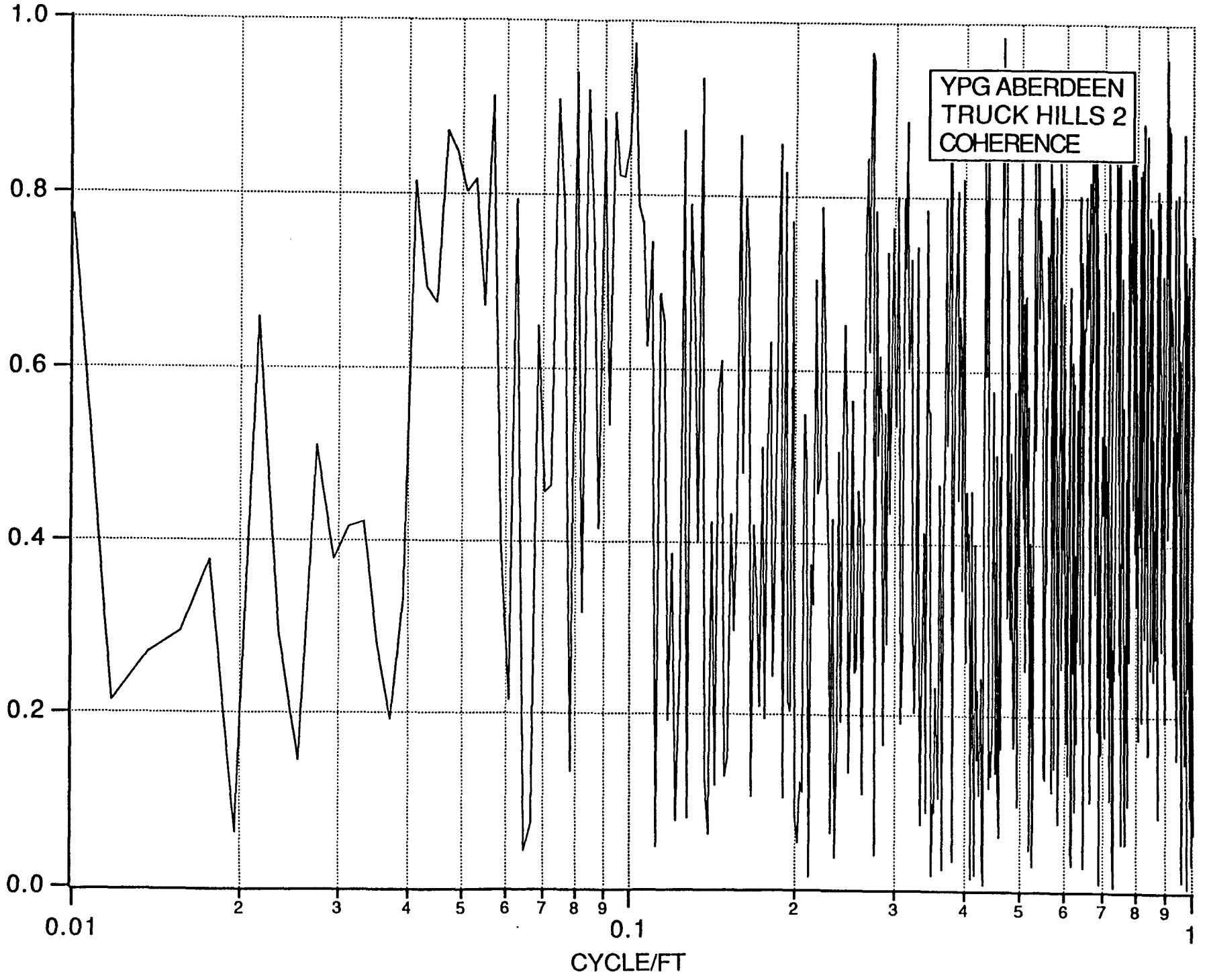
YPG ABERDEEN
TRUCK HILLS 2
COHERENCE
1.0
0.8
0.6
0.4
0.2
0.0
0.01
0.1
1
2
3
4
5
6
7
8
9
CYCLE/FT

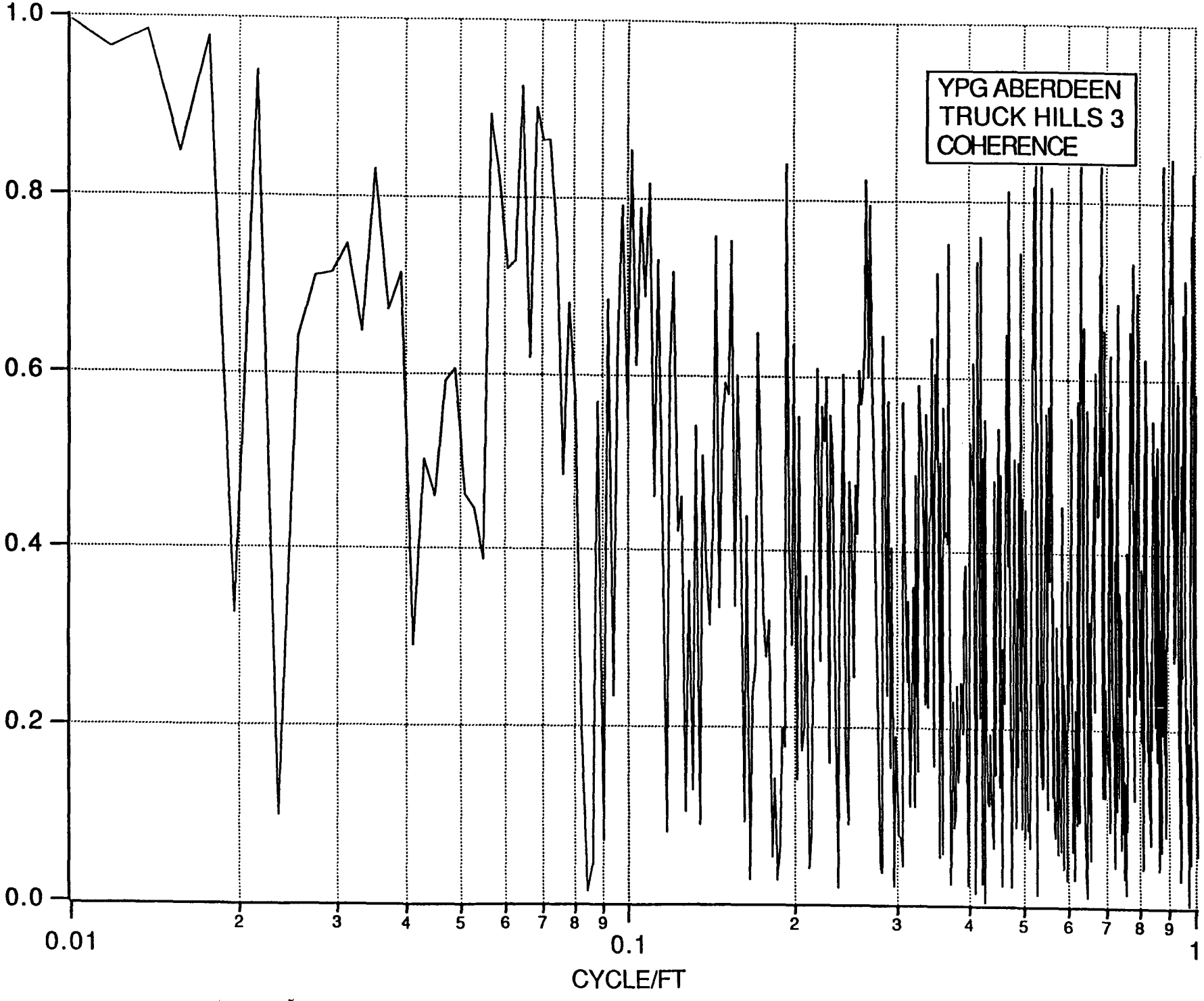
YPG ABERDEEN
TRUCK HILLS 3
COHERENCE
1.0
0.8
0.6
0.4
0.2
0.0
0.01
0.1
1
2
3
4
5
6
7
8
9
CYCLE/FT

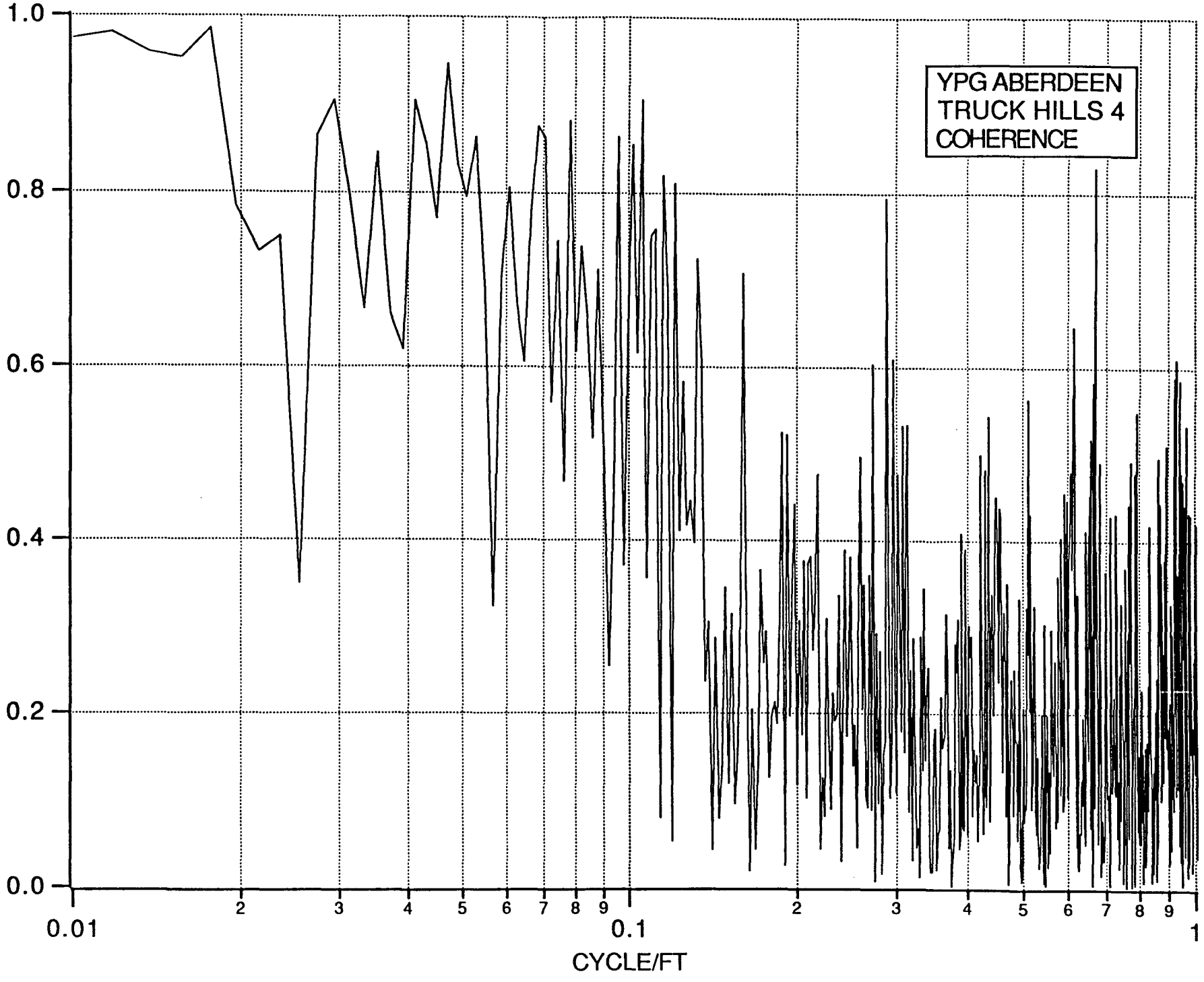
YPG ABERDEEN
TRUCK HILLS 4
COHERENCE
1.0
0.8
0.6
0.4
0.2
0.0
0.01
0.1
1
2
3
4
5
6
7
8
9
CYCLE/FT

APPENDIX I

PHOTOGRAPHIC SUPPLEMENT

PHOTOGRAPH NO. 2017399-01
Aerial View of Middle East No. 1 and 2 Test Courses APG Profilometer, NATC DFMV and NATC Response HMMWV Profiling Course No. 2

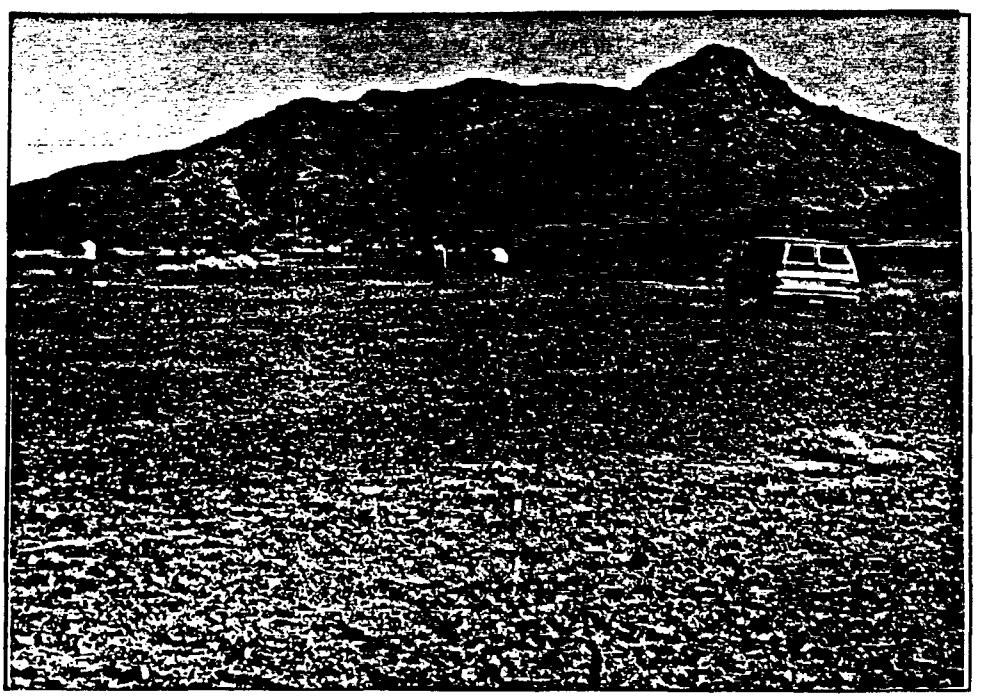

PHOTOGRAPH NO. 2017399-02
Middle East Course No. 2 in Middle of Photograph. Middle East Course No. 1 Across Photograph. Reference of Course Roughness Before Profiling Traffic

PHOTOGRAPH NO. 2017399-03
Middle East Course No. 1
Reference of Course Roughness Before Profiling Traffic

PHOTOGRAPH NO. 2017399-04
APG Profilometer on Middle East Course No. 2

PHOTOGARPH NO. 2017399-05
DFMV Profiling Middle East Course No. 2
Failed APG Profilometer in Background

PHOTOGRAPH NO. 2017399-06
Response HMMWV Negotiating Middle East Course No. 2

PHOTOGRAPH NO. 2017399-07
APG Profilometer on Middle East Course No. 2
Track Width on APG Profilometer Was 48"

PHOTOGRAPH NO. 2017399-08
Middle East Course No. 2
Maximum Extent of Course Deformation After Profile Traffic

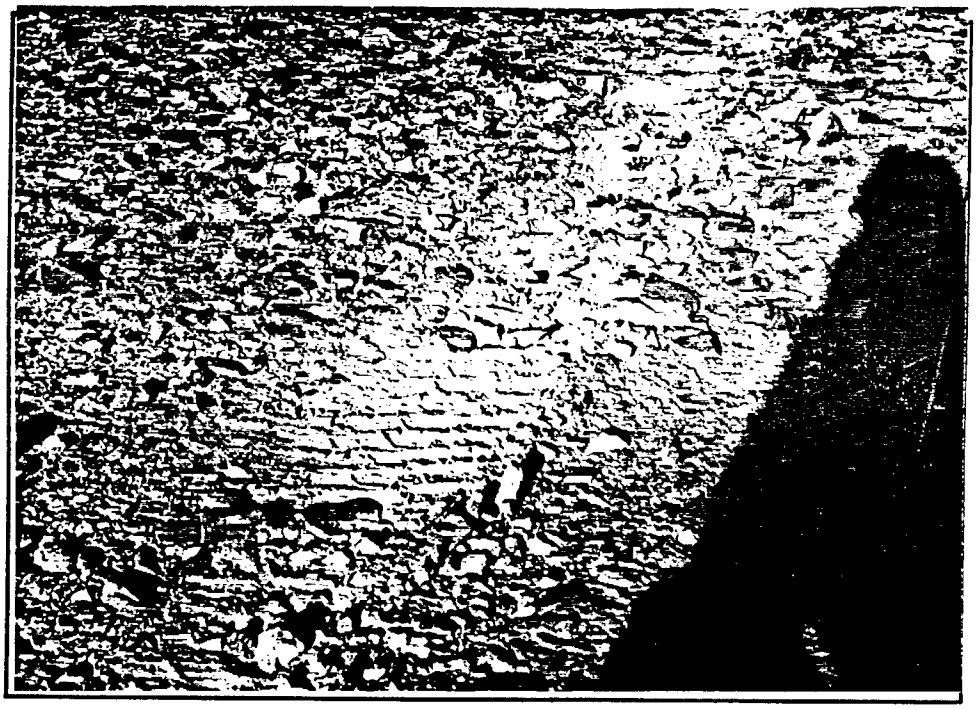

PHOTOGRAPH NO. 2017399-09
Middle East Course No. 2
Localized Deformation After Profile Traffic

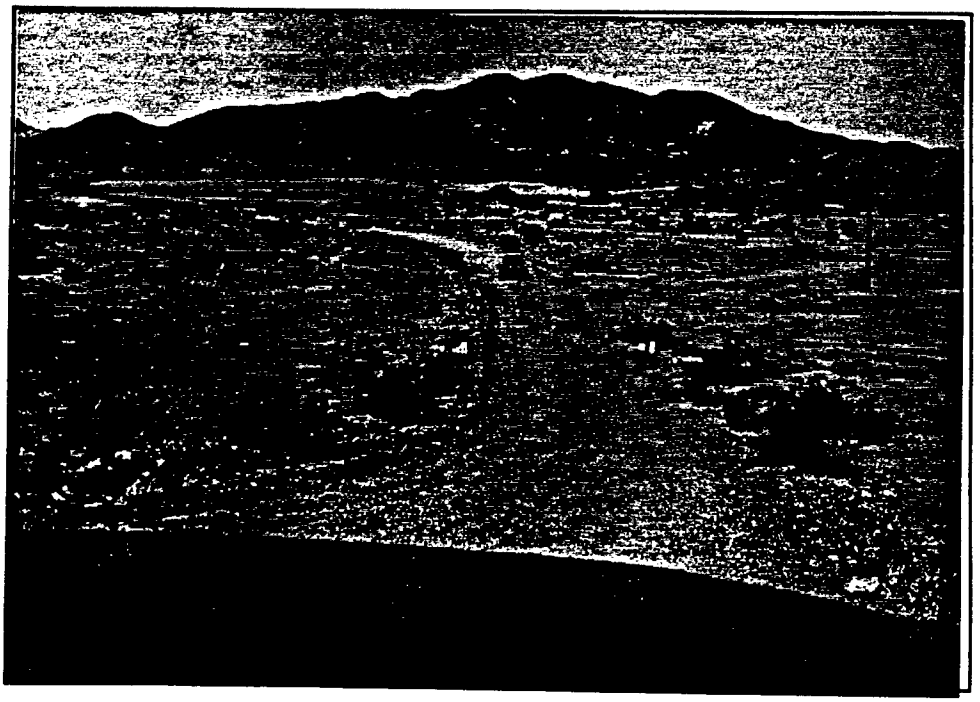

PHOTOGRAPH NO. 2017399-10
DFMV and Response HMMWV on Truck Hill Course No. 1

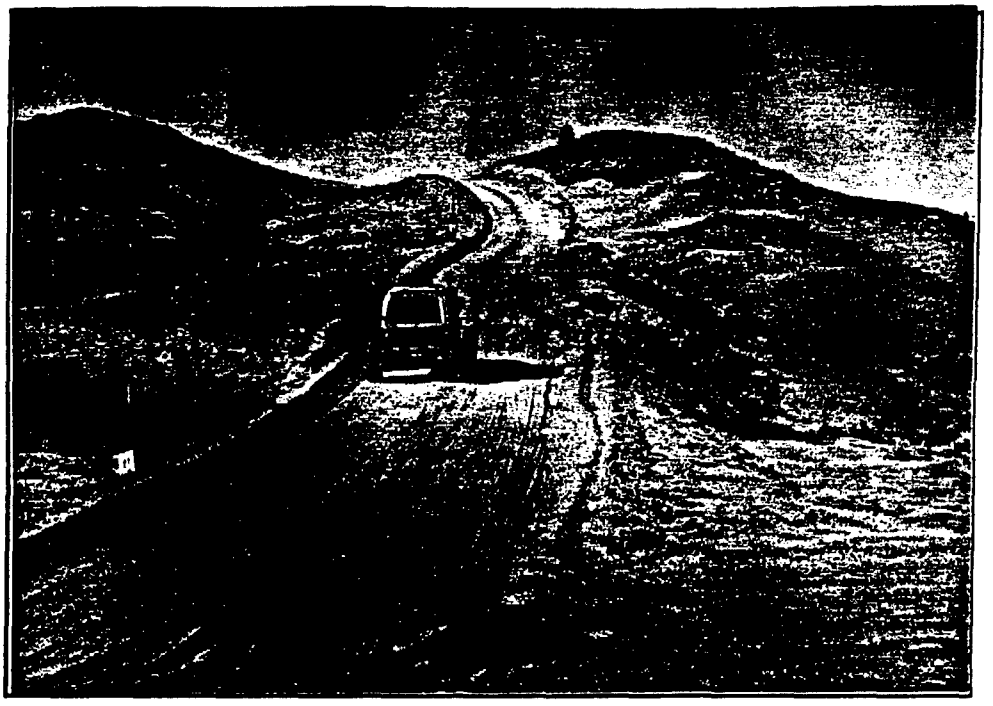

PHOTOGRAPH NO. 2017399-11
DFMV Profiling Truck Hill Course No. 2

PHOTOGRAPH NO. 2017399-12
Response HMMWV Negotiating Truck Hill Course No. 2

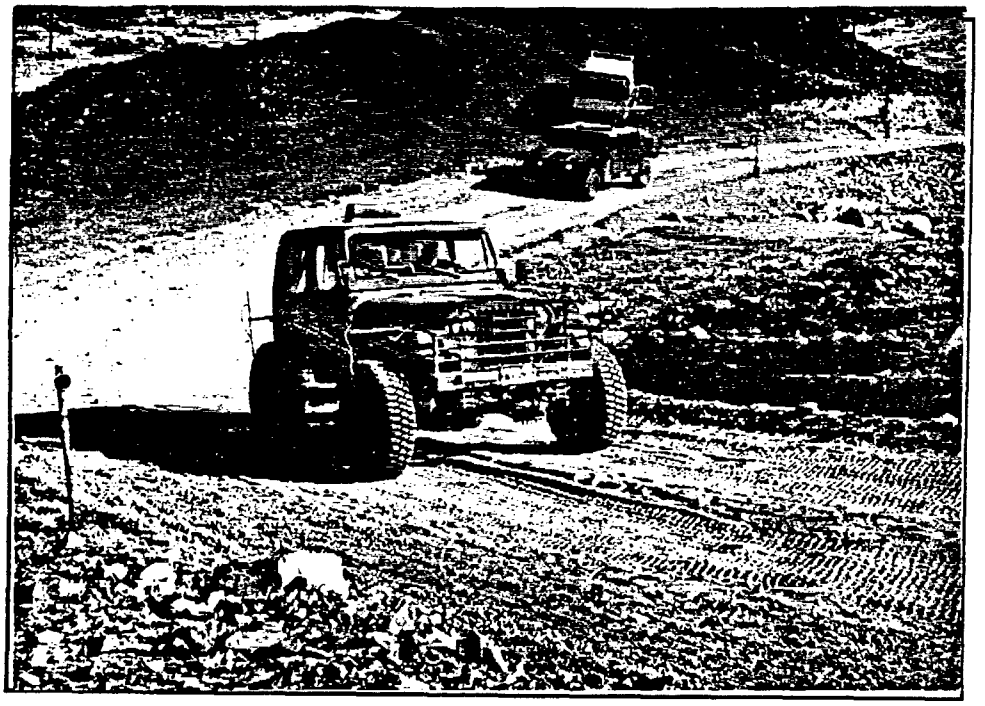

PHOTOGRAPH NO. 2017399-13
DFMV and Response HMMWV on Truck Hill Course No. 3

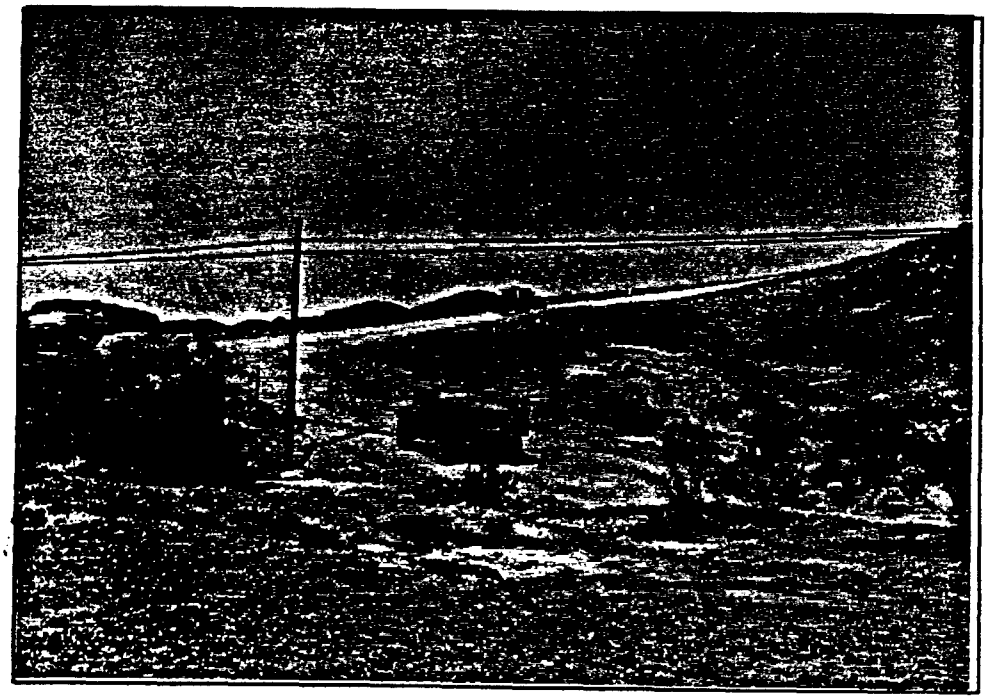

PHOTOGRAPH NO. 2017399-14
DFMV Profiling Truck Hill Course No. 4
Response HMMWV in Foreground

PHOTOGRAPH NO. 2017399-15
DFMV Profiling Truck Hill Course No. 4

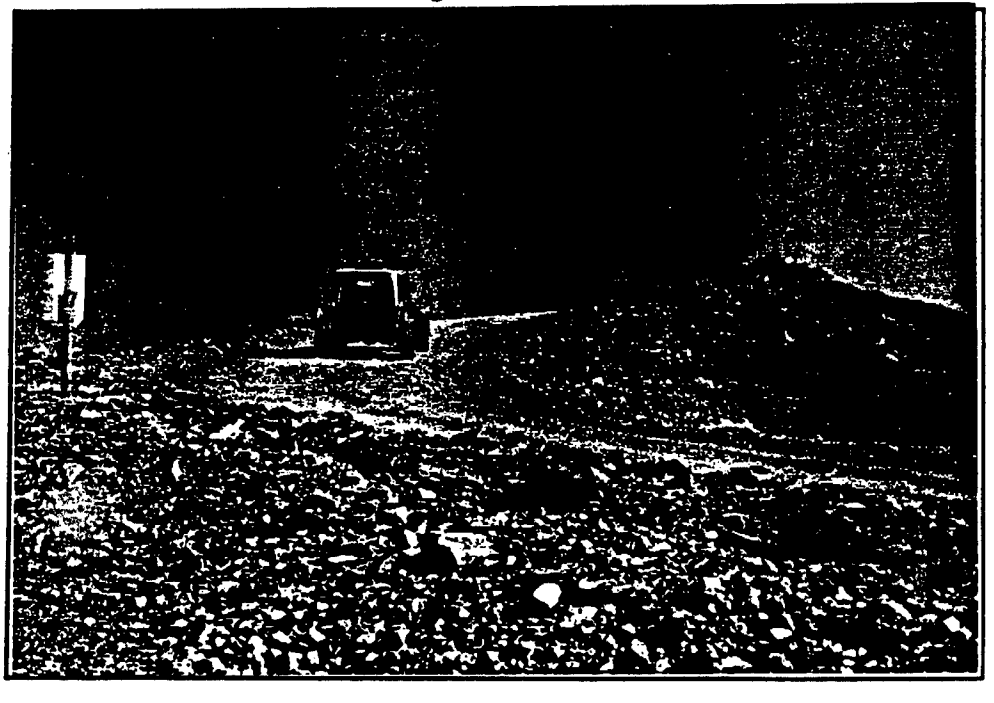

PHOTOGRAPH NO. 2017399-16
DFMV Profiling Upper End of Truck Hill Course No. 4

PHOTOGRAPH NO. 2017399-17
WES Surveying Washboard Course With Rod and Level

PHOTOGRAPH NO. 2017399-18
APG Profilometer on RMS Course No. 5

APPENDIX J

DESCRIPTION OF DFMV INDEPENDENCE

A schematic of the DFMV wheel end is shown in Figure 20. At each wheel end, the vertical, longitudinal and lateral forces at the tire/ground interface are measured through a triaxial load cell machined into the end of the axle. A vertical accelerometer over the load cell measures vertical accelerations at the wheel end. Finally, wheel velocity and thus distance along the test course is measured with an optical encoder that counts 300 pulses per one revolution of the tire. This setup is replicated at all four wheel ends of the DFMV.

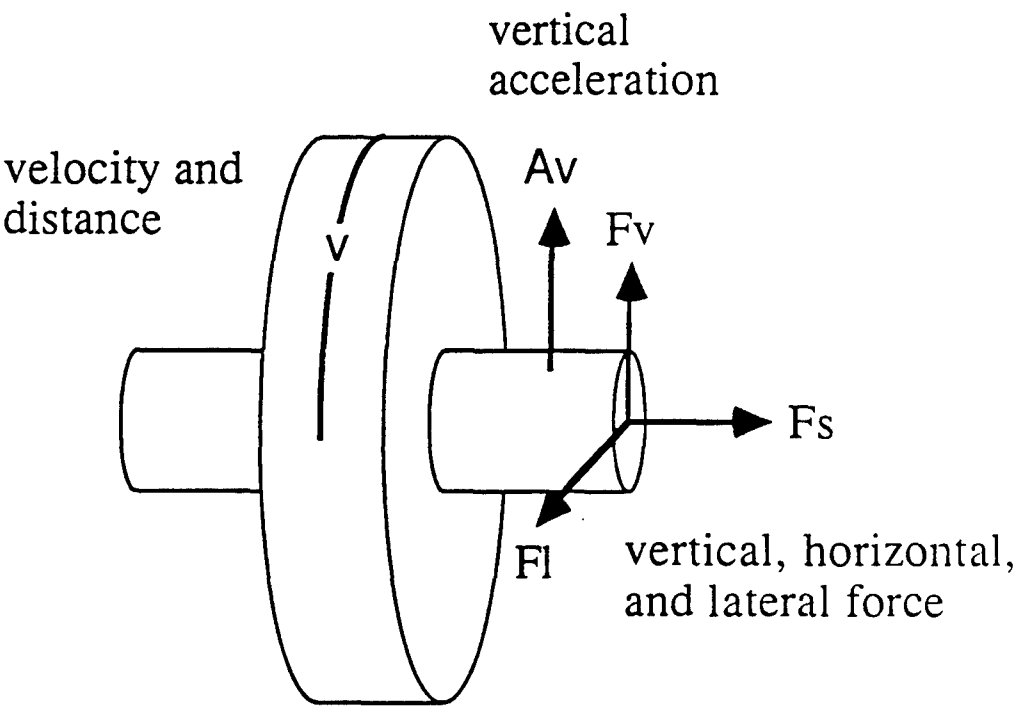

Figure 20. DFMV Wheel End

If the terrain is infinitely hard and straight, then the front tires measure the exact same terrain as the rear tires. If the terrain is deformable, then the front tires measure the first pass over the terrain and the rear tires measure the terrain as deformed by the first pass. Therefore, the tire dynamically interacts with the terrain as it rolls along the path of vehicle travel. The objective of this study was to measure the vertical elevation changes as a function of distance along the test course. In the DFMV measurement, the vertical elevation measurement of the terrain is separated from any suspension or sprung mass vibrations by the position of the triaxial load cell in the axle. As shown in Figure 21, profiling measurements involve a force balance across the load cell (i.e., $F_1 = F_2$). Newton's third law states that "When any force acts on a body, there is created an equal and opposite reaction." If weight is transferred to the front axle, the increase in force on one side of the load cell will be equal and opposite to that on the other side of the load cell. The physical event that equalizes this force is the increase in tire deflection. This is assuming that the reference for the road under the tires does not change. If we establish a set of localized coordinates, this force balance can be studied in terms of the axle moving with respect to a fixed ground plane, the ground plane moving with respect to a fixed axle, or a combination of both. In reality, it is a combination of both.

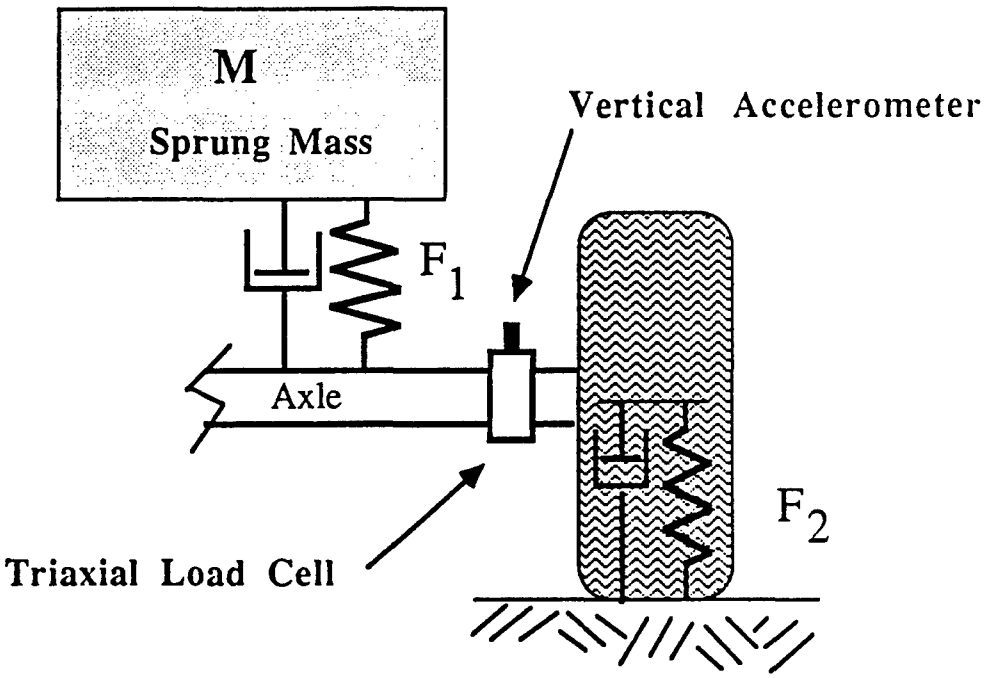

Figure 21. DFMV Wheel End Shown as a Quarter Car Model

Dynamically, if the mass above the suspension bounces or pitches as the vehicle traverses the terrain, and the suspension works at its natural frequency, the forces and motions generated by these excursions will result in opposing deflections and accelerations at the wheel end. The forces from these excursions on either side of the load cell cancel and we are left with the forces and accelerations that are due to vertical changes in the ground with respect to the inertial position of the load cell. In other words, the DFMV measures what the course had to look like under the tire (at that instance in time) to cause the measured forces and accelerations at the wheel end (at that instance in time).

To better understand this cancellation process, consider the DFMV wheel end as a single degree-of-freedom, spring-mass-damper system (Figure 22). The spring rate, k, is the spring rate of the tire. The mass, m, of the system is the mass of everything outside the load cell. The damping rate, c, assumes there is a damping element in the tire similar to a shock absorber. A set of localized coordinates can be established for the DFMV. For this example, assume that the vehicle is static and resting on a hard, level surface. The ground plane becomes a fixed reference and is referred to as x in Figure 22. Similarly, the static height of the centerline of the load cell is established as y in Figure 22. Sitting static in our resting position, the vertical force cell is recording zero force and the accelerometer is recording zero acceleration.

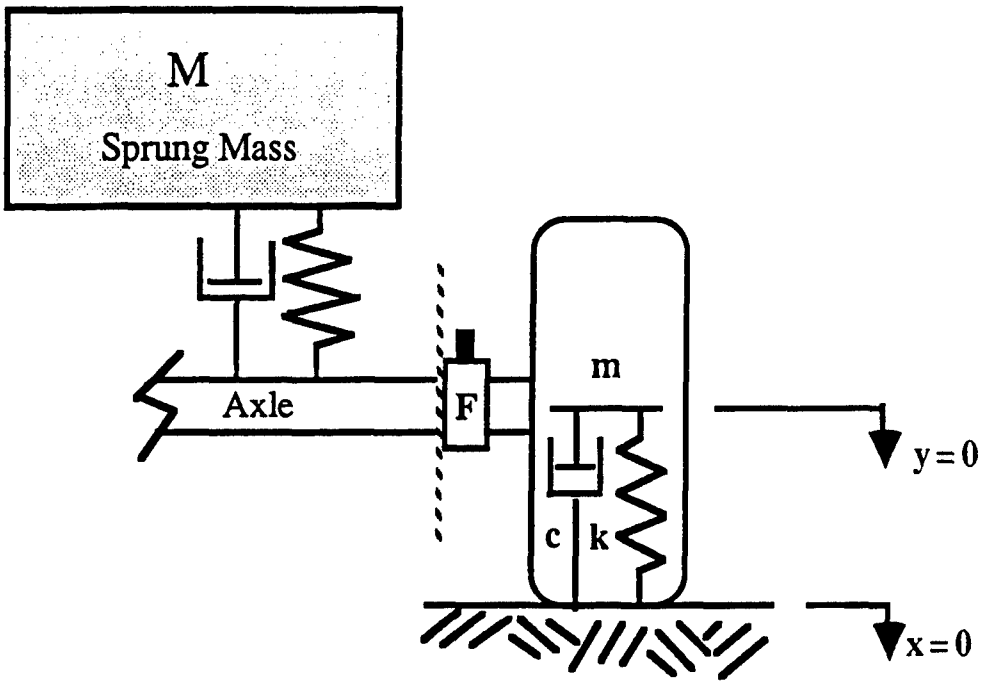

Figure 22. DFMV Wheel End Represented as a Simple Spring-Mass-Damper System

With our measurement system in Figure 22 established and understanding that vehicle dynamic forces cancel on either side of the load cell, we can draw a line through the load cell and disregard all act ity above the load cell. The chassis above the load cell is needed for the force balance in the DFM ystem, but other than that, its only useful purpose is to power and steer the vehicle over the terrain. All vehicle bounce, roll and pitch are balanced, as long as the axle does not hit the bump stop and the tire does not leave the ground. The DFMV system can be thought of as four independent quarter car models, however, phase information left-to-right and front-to-rear are maintained by all measurements being made at the same instance in time, and at fixed distances to each other.

With the DFMV, we are interested in knowing the time history of changes in vertical elevation (x in Figure 22). Knowing ground speed, spatial histories of the vertical elevation (x in Figure 22) can be determined and presented as elevation versus distance plots. We also know that the motion of the sprung mass, M, will generate forces at the load cell that must be supported by the tire. In the simplest terms, this relation is F=ma. However, we have energy stored in the spring and damping elements of the tire, so a relative difference between the local zero at the ground (x in Figure 22) must be compared to a local zero at the center of the load cell (y in Figure 22). Any differences in these localized coordinates will show up as positive or negative forces in our model.

To accomplish the measurement used to calculate the ground elevation profile, the load cell at the wheel hub measures the vertical force, F, continuously as we traverse the terrain. To define the motion response of the tire system, the accelerometer over the load cell is used. The accelerations are measured directly and represent the localized accelerations ($\ddot{y}$ in Figure 22). Recalling that acceleration is the rate of change of velocity, we can integrate the accelerometer output to obtain the localized velocity ($\dot{y}$ in Figure 22). Recalling that velocity is the rate of change of distance, we can integrate velocity to obtain localized position (y in Figure 22).

$$\ddot{y} = \frac{d^2y(t)}{dt^2}$$

$$\dot{y} = \frac{dy(t)}{dt}$$

Knowing that any forces which exist at the load cell must be supported by some combination of static and inertial forces at the wheel end, we develop the following equation of motion from the relationship shown in Figure 22.

$$F = m\ddot{y} + c(\dot{y} - \dot{x}) + k(y - x)$$

To complete the parameters needed for the measurement in Figure 22, NATC measures the mass of the wheel/tire/hub assembly, m on a calibrated scale. The spring rate, k, is measured through a load-deflection curve at the operating inflation pressure. The damping rate, c, of the tire is measured with a specialized test fixture that NATC has developed for tire damping measurements.

We wish to solve for the vertical position of the ground (x in Figure 22) as a function of time, so rearranging terms with x on the left side of the equation yields:

$$c\frac{dx(t)}{dt} + k\,x(t) = m\frac{d^2y(t)}{dt^2} + c\frac{dy(t)}{dt} + k\,y(t) - F(t)$$

This equation is transformed into the frequency domain, as described in Section 8.1 of this final report. Since only the acceleration, $\ddot{y}$, of the wheel hub is measured, the integrations to find $\dot{y}$ and y are done in the frequency domain to eliminate noise generated by time domain numerical integration techniques. Knowing the mass, the damping rate, the spring rate and the position, and velocity and acceleration of the axle end, we can solve the above equation for x, the vertical displacements under the tire. Given the velocity of each wheel end, we can present this data as elevation versus distance or in the frequency-domain as a wave-number spectrum.

APPENDIX K

CORRECTED WES DATA FOR RMS COURSE #5

PAGE	COURSE	TRACK
253	RMS #5	L
254	RMS #5	R
255	RMS #5	COHERENCE PLOT, L TO R

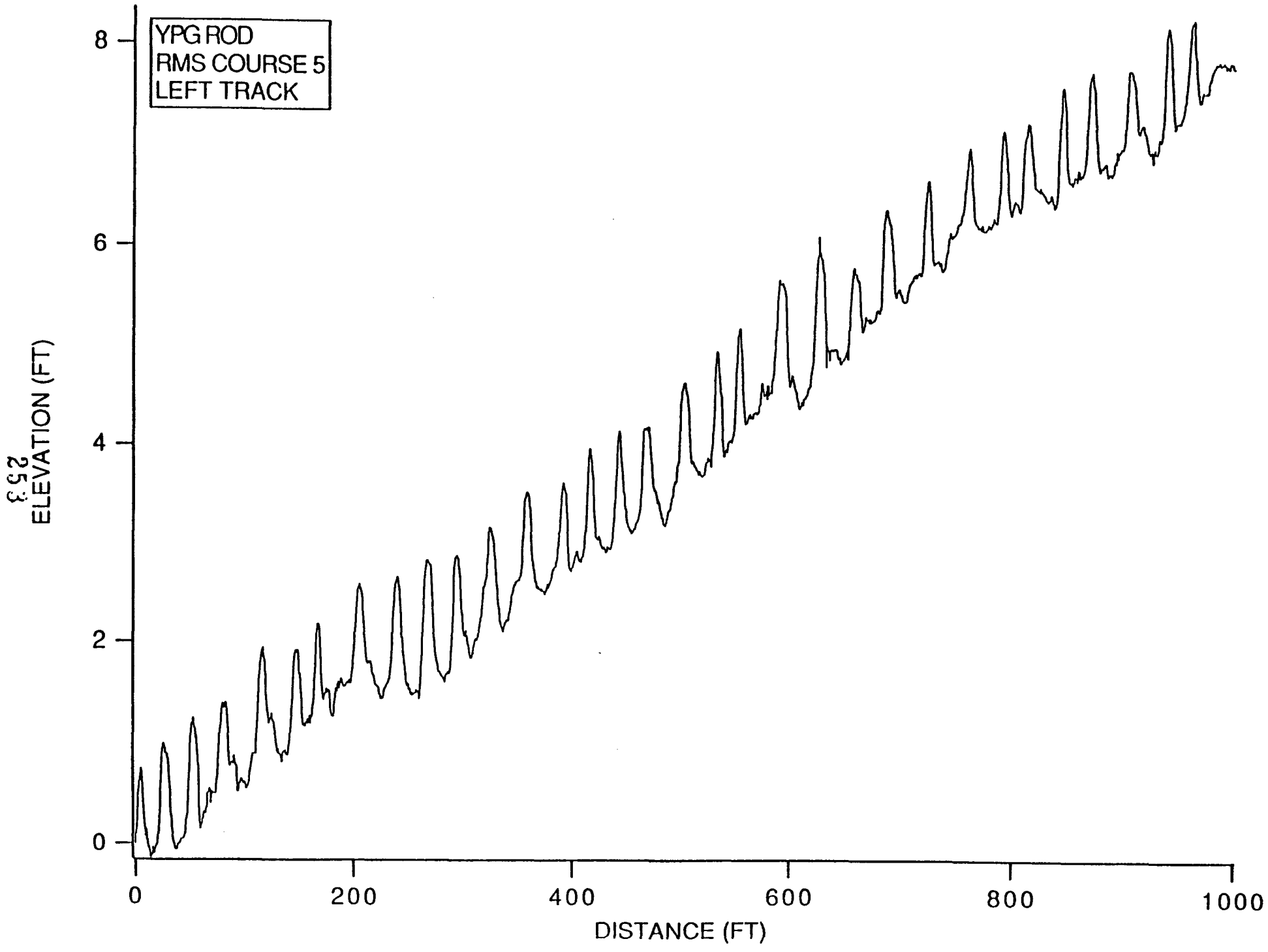
YPG ROD
RMS COURSE 5
LEFT TRACK
8
6
4
2
0
ELEVATION (FT)
0
200
400
600
800
1000
DISTANCE (FT)

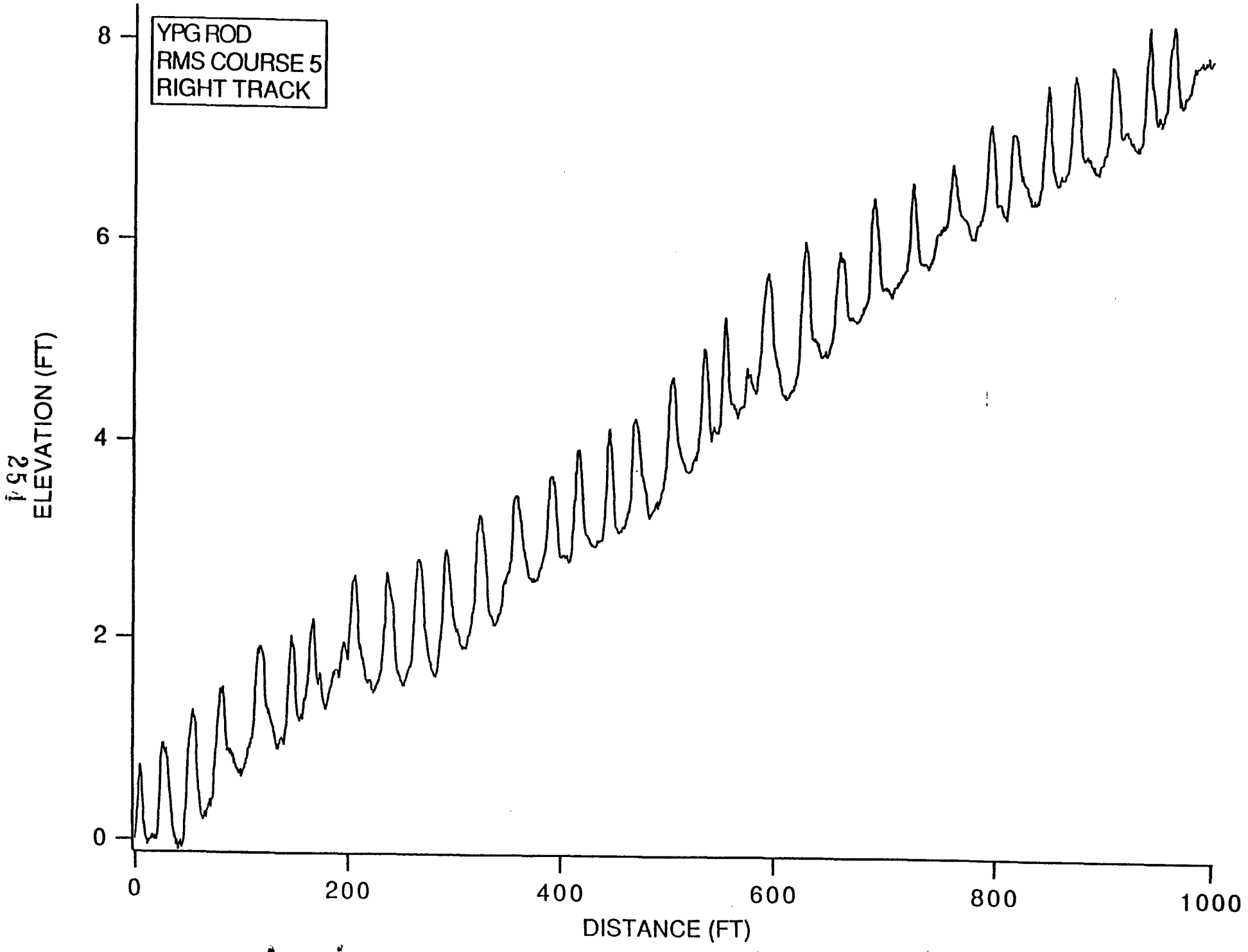
YPG ROD
RMS COURSE 5
RIGHT TRACK
8
6
4
2
0
ELEVATION (FT)
0
200
400
600
800
1000
DISTANCE (FT)

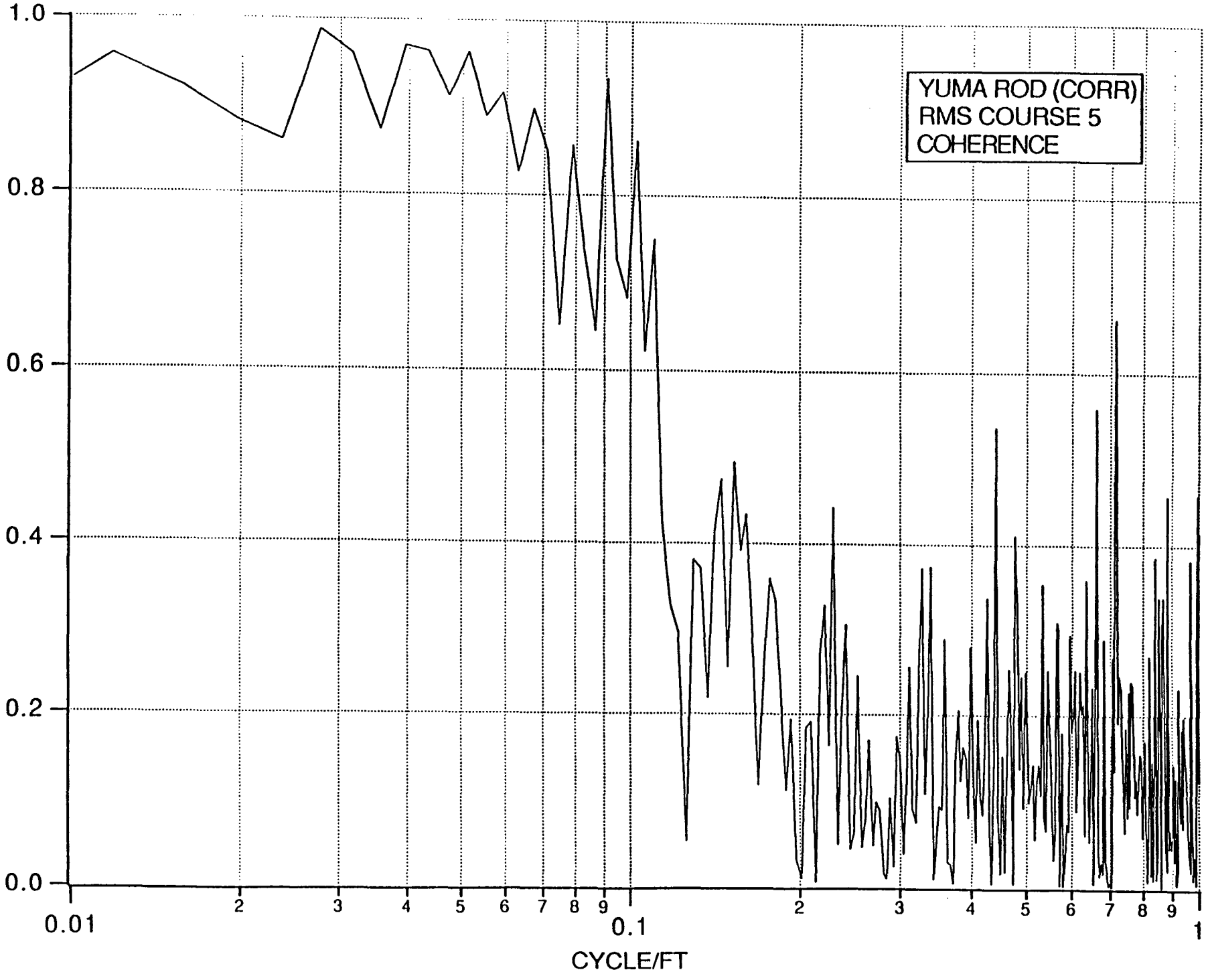
YUMA ROD (CORR)
RMS COURSE 5
COHERENCE
1.0
0.8
0.6
0.4
0.2
0.0
0.01
2
3
4
5
6
7
8
9
0.1
2
3
4
5
6
7
8
9
1
CYCLE/FT

APPENDIX L

INSTRUMENTATION INSTALLED ON DFMV AND HMMWV

The DFMV was instrumented with 33 channels of sensor data (Table 9). For the purposes of this study comparing only vertical roughness measurements, nine (9) channels were required (the vertical force and acceleration at each wheel and left-front-wheel speed). For a complete terrain analysis, twenty-three channels are required. The complete terrain measurements include the vertical, longitudinal and lateral forces at each wheel, the vertical acceleration at each wheel, the speed at each wheel, steering angle to define course curvature, cg inclination angle to define the long wavelengths (drivetrain effects) and vehicle ground speed. The wheel speed and ground speed measurements are necessary for the μ-slip measurements of the test tires on the test surface. Ten additional channels were required for computer simulation comparisons of the DFMV operating over the YPG courses. The measurements included the longitudinal, vertical and lateral accelerations at the vehicle cg, the roll, pitch and yaw rates at the vehicle cg, and the displacement of the axle with respect to the frame.

A 14-channel TEAC XR-5000 analog tape recorder with three Pulse Code Modulation (PCM) cards was mounted in the DFMV. With the three PCM cards, the first 11 channels remained FM channels, while the last three were each 8 digital channels (35 channels total). For the profiling test runs, the 9 channels required for the vertical elevation profiles were on the FM channels. This allowed the sensitivity to be adjusted to give the best resolution. For example, on the vertical force transducers, 1 mv = 1 pound. At the slower speed runs, ±500 pounds was expected, so the input to the tape recorder was set at 0.5 volts. For the same course at the fastest speed run, ±1,400 pounds was expected, so the input to the tape recorder was set at 1.4 volts. This ensured that the signal-to-noise ratio was always at an acceptable level.

The HMMWV was instrumented with 13 channels (Table 10). The HMMWV was operated over each course immediately following the DFMV. After the run at 10 MPH, the HMMWV was operated at several faster speeds. A 14-channel TEAC tape recorder was also mounted in the HMMWV.

Table 9. Instrumentation Installed on the Dynamic Force Measurement Vehicle (DFMV)

Channel No.	Description	Units	
1	Left front vertical wheel force	lbs	FM channel
2	Right front vertical wheel force	lbs	FM channel
3	Left rear vertical wheel force	lbs	FM channel
4	Right rear vertical wheel force	lbs	FM channel
5	Left front wheel speed	MPH	FM channel
6	Left rear wheel speed	MPH	FM channel
7	Left front vertical wheel acceleration	g'S	FM channel
8	Right front vertical wheel acceleration	g's	FM channel
9	Left rear vertical wheel acceleration	g's	FM channel
10	Right rear vertical wheel acceleration	g's	FM channel
11	Left front vertical axle displacement wrt frame	inches	
12	Right front vertical axle displacement wrt frame	inches	
13	Left rear vertical axle displacement wrt frame	inches	
14	Right rear vertical axle displacement wrt frame	inches	
15	Steering angle	inches†	
16	cg longitudinal inclination angle	degrees	
17	cg vertical acceleration	g's	
18	cg longitudinal acceleration	g's	
19	cg lateral acceleration	g's	
20	cg roll rate	degrees/second	
21	cg pitch rate	degrees/second	
22	cg yaw rate	degrees/second	
23	Right front wheel speed	MPH	
24	Right rear wheel speed	MPH	
25	Left front longitudinal wheel force	lbs	
26	Left front lateral wheel force	lbs	
27	Right front longitudinal wheel force	lbs	
28	Right front lateral wheel force	lbs	
29	Left rear longitudinal wheel force	lbs	
30	Left rear lateral wheel force	lbs	
31	Right rear longitudinal wheel force	lbs	
32	Right rear lateral wheel force	lbs	
33	Ground Speed via 5th wheel	MPH	
extra	Identification pulse	on/off	

† Few of the YPG courses had steering input, calibration to degrees of steer will be provided later.

Table 10. Instrumentation Installed on the High Mobility Multi-Purpose Wheeled Vehicle (HMMWV)

Channel No.	Description	Units
1	Vehicle Speed	mph
2	Left front control arm displacement wrt frame	inches
3	Right front control arm displacement wrt frame	inches
4	Left rear control arm displacement wrt frame	inches
5	Right rear control arm displacement wrt frame	inches
6	Left front wheel hub vertical acceleration	g's
7	Right front wheel hub vertical acceleration	g's
8	Left rear wheel hub vertical acceleration	g's
9	Right rear wheel hub vertical acceleration	g's
10	cg vertical acceleration	g's
11	cg longitudinal acceleration	g's
12	cg lateral acceleration	g's
13	steering	inches†

† Few of the YPG courses had steering input, calibration to degrees of steer will be provided later.

Notes:
1. M1025 HMMWV
2. Tire pressure -- 23 PSI front, 22 PSI rear (same tires as on DFMV)
3. 1 person driving (160 lbs)
4. 1 person in right rear seat (200 lbs)
5. Full fuel

PCB PIEZOTRONICS

SPECIFICATIONS

ISOLATOR ACCELEROMETER

REVISIONS

SHEET 1 OF 1

MODEL NO.		348M30
RANGE (FOR ±5V OUTPUT)	±g	50
RESOLUTION	g	.001
SENSITIVITY (±2%)	mV/g	100
RESONANT FREQUENCY (MTD)	kHz	20
FREQUENCY RANGE (±5%)	Hz	.05-2000
DISCHARGE TIME CONSTANT (@R.T.)	s	≥ 10
AMPLITUDE LINEARITY	% FS	1
POLARITY (ACCEL TO BASE)		POSITIVE
OUTPUT IMPEDANCE	ohm	< 100
OUTPUT BIAS	+volt	8 to 14
OVERLOAD RECOVERY	µs	10
TRANSVERSE SENSITIVITY	%	≤ 5
STRAIN SENSITIVITY	g/µin/in	.0005
TEMPERATURE RANGE	°F	-65 to +250
TEMPERATURE COEFFICIENT	%/°F	≤ .03
VIBRATION (MAX)	±g's peak	250
SHOCK (MAX)	g	900
MAGNETIC SUSCEPTIBILITY	g/K GAUSS	.09
STRUCTURE		ISO. STRAIN
SIZE (HEX x HEIGHT)	inch	0.75 x 1.41
SEALING		EPOXY
CASE MATERIAL	st stl	316L
WEIGHT	gram	75
CONNECTOR (micro)	coaxial	10-32
GROUND ISOLATION		YES
EXCITATION	+Vdc/mA	24-27/2-20

SUPPLIED ACCESSORIES:
MOD 081B05 MOUNTING STUDS (2)
MOD 080A24 PETRO WAX

APP'D	[illegible]	[illegible]	SPEC No.
ENGR	[illegible]	[illegible]	348-9300-80
SALES	[illegible]	[illegible]	

ENDEVCO® MODELS 7290-10/7290-30
MICROTRON™ ACCELEROMETERS

Variable Capacitance Low g Rugged

The Model 7290 MICROTRON is a Variable Capacitance Accelerometer specifically designed for the measurement of low level accelerations in a steady state or low frequency environment.

MICROTRON features a pair of unique, patented, silicon sensing elements arranged in a differential configuration, which employs gas damping to maximize frequency response and reduce the effects of spurious high frequency excitation. Using a gas rather than a fluid for damping permits a much more stable damping coefficient over temperature. Integral electronics provide a differential, low impedance, high level output (2 Vdc full scale), and thermal compensation for excellent output stability. The unit can be operated from an unregulated dc power supply of 13 - 18 Vdc.

With an extremely high overrange capability, it is ideal for ballistic, launch and separation dynamics. Applications include missile and aircraft trajectory and flight dynamics measurements, automobile crash testing and weapons effects testing, plus biomedical motion studies, structural evaluation, and other low frequency applications currently served by piezoresistive accelerometers.

This high sensitivity Variable Capacitance Accelerometer offers excellent non-linearity, frequency response, and thermal stability characteristics. MICROTRON is available in Full Scale ranges of ±10 g and ±30 g.

(All values are typical at +75°F [+24°C] unless otherwise specified.)

		MODEL 7290-10	MODEL 7290-30
PERFORMANCE			
RANGE	g	±10	±30
SENSITIVITY (at 10 Vdc excitation, ref 100 Hz)	mV/g	200± 5	66 ±2
NON-LINEARITY & HYSTERESIS (% of reading, max, to full range)	%	±1	±1
FREQUENCY RESPONSE (±5% max, ref 100 Hz)	Hz	0 to 600	0 to 1000
MOUNTED RESONANT FREQ	Hz	2700, typical	3700, typical
DAMPING RATIO		0.7 ±0.2	0.7 ±0.2
TRANSVERSE SENSITIVITY (max)	%	1	1
THERMAL SENSITIVITY SHIFT (−25°C to +75°C)	%	±2	±2
(−55°C to +121°C)	%	−4/REF/−8	−4/REF/−8
ZERO MEASURAND OUTPUT (typical/maximum)	mV	±20/±40	±20/±40
THERMAL ZERO SHIFT[1] (−25°C to +75°C)	% F.S.	±2	±2
ZERO SHIFT DUE TO 10 000 g SHOCK, (max)	% F.S.	0.1%	0.1%
ELECTRICAL			
EXCITATION VOLTAGE	Vdc	13.0 to 18.0	13.0 to 18.0
INPUT CURRENT (max)	mA	15	15
WARMUP TIME (max)	μs	1	1
PHYSICAL			
WEIGHT	oz (gm)	0.43 (12)	0.43 (12)
CASE MATERIAL		Aluminum, Black anodized	
ELECTRICAL CONNECTIONS		Integral cable, 4 conductor, 30 in ±3 in long	
Size	in (cm)	1.00 × 0.85 × 0.25 (2.54 × 2.1 × 0.64)	
MOUNTING TORQUE		Two holes for 4 - 40 mounting screws 6 lbs-in (0.65 Nm)	
ENVIRONMENTAL			
ACCELERATION LIMITS			
Static	g	10 000	10 000
Sinusoidal	g	500	500
Random (20 - 2000 Hz)	rms g	40	40
TEMPERATURE			
Operating	°F (°C)	−65 to +250 (−55 to +121)	−65 to +250 (−55 to +121)
Non-Operating	°F (°C)	−65 to +250 (−55 to +121)	−65 to +250 (−55 to +121)
SHOCK LIMITS (70 μsec duration)	pk g	10 000	10 000
HUMIDITY		Hermetically sealed	

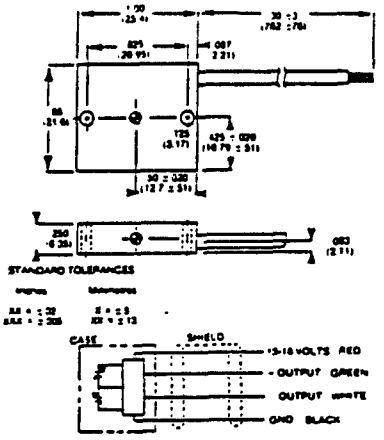

CALIBRATION DATA SUPPLIED
(at 75°F [24°C] and 10.00 Vdc excitation)

FREQUENCY RESPONSE RANGE	Hz
SENSITIVITY (at 100 Hz)	mV/g
ZERO MEASURAND OUTPUT	mV
MAXIMUM TRANSVERSE SENSITIVITY	% of calibrated sensitivity
MOUNTED RESONANT FREQUENCY	Hz
DAMPING COEFFICIENT	Ratio of critical damping

NOTES

[1] ±1% available by special order.

ACCESSORIES INCLUDED

Two each, 4-40 × ¾" cap screws, size-4 washers.
Storage container.

7/87 PS7290-A

30700 Rancho Viejo Road San Juan Capistrano, CA 92675 USA (714) 493-8181 Telex 68-5608 TWX: 910-596-1415

APPENDIX M

DISCUSSION OF SPEED INDEPENDENCE

RMS Course #5 was chosen to illustrate the speed independence of the DFMV measurement. This course was considered worst-case because of its severity. As speed increased, the dynamic forces and accelerations increased significantly (Table 11), and the tires deflected accordingly. The course severely pitched the vehicle and the speed varied due to applying power to go over the bump and then decreasing power on the down side of the bump. RMS Course #5 tested the linearity assumptions of the DFMV spring-mass-damper model and the resonances and response times of the tires.

Table 11. DFMV Force and Acceleration Standard Deviations for RMS Course #5, Left Front DFMV Wheel, Target Speeds of 2, 4, 6 and 8 MPH.

Measurement	------ Average Measurement Speed (MPH) -----			
	3.7	4.5	6.5	7.9
	---------- Standard Deviation ----------			
Force (lbs)	113	146	240	345
Acceleration (g's)	0.16	0.20	0.27	0.36
Speed (MPH)	0.6	0.7	0.7	1.0

A coherence check is the first step for assessing the quality of a given profile, as discussed in Sections 8.3, 10.4 and 11.3. Figures 23 through 26 show the left-front to left-rear coherence plots for the runs at 2, 4, 6 and 8 MPH runs. Note that the coherence starts to drop below 0.8 at the low end at approximately 0.022, 0.021, 0.018 and 0.018 ft^{-1} (45, 48, 56 and 56 ft) for the 2, 4, 6 and 8 MPH runs, respectively. Since the primary wavelength for the RMS Course is 30 ft, a comparison can be made between all speed runs.

Figure 27 shows a displacement PSD for RMS Course #5 for speeds of 2, 4 and 8 MPH . It is important to note that this is the dispersion in the profile information before the data is normalized to a wave-number spectrum. Multiplying the x-axis and dividing the y-axis by velocity yields the spatial presentation that is independent of vehicle speed. Figure 28 is the speed-independent wave-number spectra for the 2, 4, 6 and 8 MPH runs. The remaining discussion in this section will explain the percent error associated with the profile at each speed.

Statistically, the RMS (standard deviation) of the course is the best method for comparing the DFMV measurement to the rod and level measurement, as follows:

> WES calculated the RMS of the course to be 3.6 inches using a 60' window in the RMS program. Calculating the square root of the area under the curve between 60 and 1 foot integration limits for each of the DFMV wave-number spectra yields an equivalent RMS value. Table 12 shows the RMS values calculated from the DFMV and the percent error from the rod and level measurement. Note that the percent error is well within the 38 percent random error calculated from the spectral analysis. Referring to Section 9.4, the normalized random error for four block of data is $\varepsilon = 0.50$. Using a hanning window and 50% overlap processing, the number of blocks is increased to 7, thus a random error of $\varepsilon = 0.38$. The interpretation of this random error is as follows: as a first order of approximation, about two-thirds of the spectral values at the different wave numbers will be within 38% of the average spectral value for all courses of the same design.
>
> This can be further interpreted in terms of the RMS value, as follows:
>
> > The WES RMS value for RMS Course #5 was 3.6 inches. Given a 38% random error, the confidence interval for the RMS of the signal is $2.6 \leq 3.6 \leq 5.0$. As shown in Table 12, the DFMV measurements for speed differences of 2 and 4 times is statistically equivalent.
>
> Ideally, we would like a 90% confidence interval on our course measurements ($3.2 \leq 3.6 \leq 4.0$). There are several options for improving the statistical confidence limits of the DFMV or rod and level measurement. First, the course could be measured 12 times and those 12 spectra averaged. Secondly, if the course were 12,000 feet (2.3 miles) in length versus the measured 1,000 feet, that would also allow a 90% confident interval ($1/\sqrt{(48+(48-1))} = \varepsilon$ of 0.10, given 4 blocks per 1,000 ft, that equates to approximately 12,000 feet). In the report, it was noted that the longer the course, the more accurate the profile.

Table 12. Calculated RMS Values For The DFMV at Speeds of 2, 4, 6 and 8 MPH.

Speed (MPH)	RMS Value (Inches)	Percent Error
2	3.2	10.0
4	3.4	4.7
6	4.2	15.6
8†	4.4	22.0
rod and level	3.6	--

†Judged to be an excessive speed for this course.

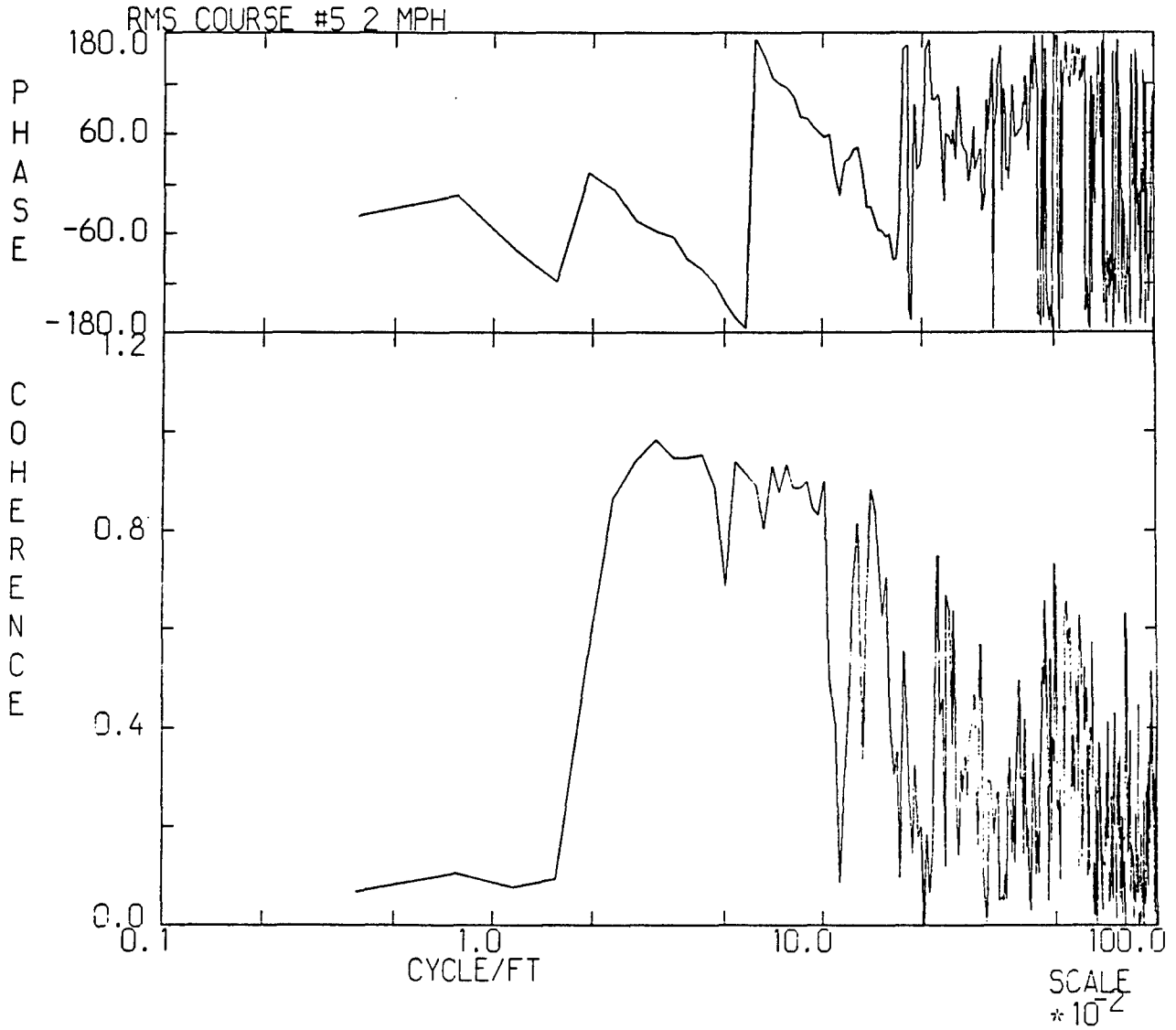

Figure 23. DFMV Left-Front to Left-Rear Coherence of RMS Course #5, 2 MPH

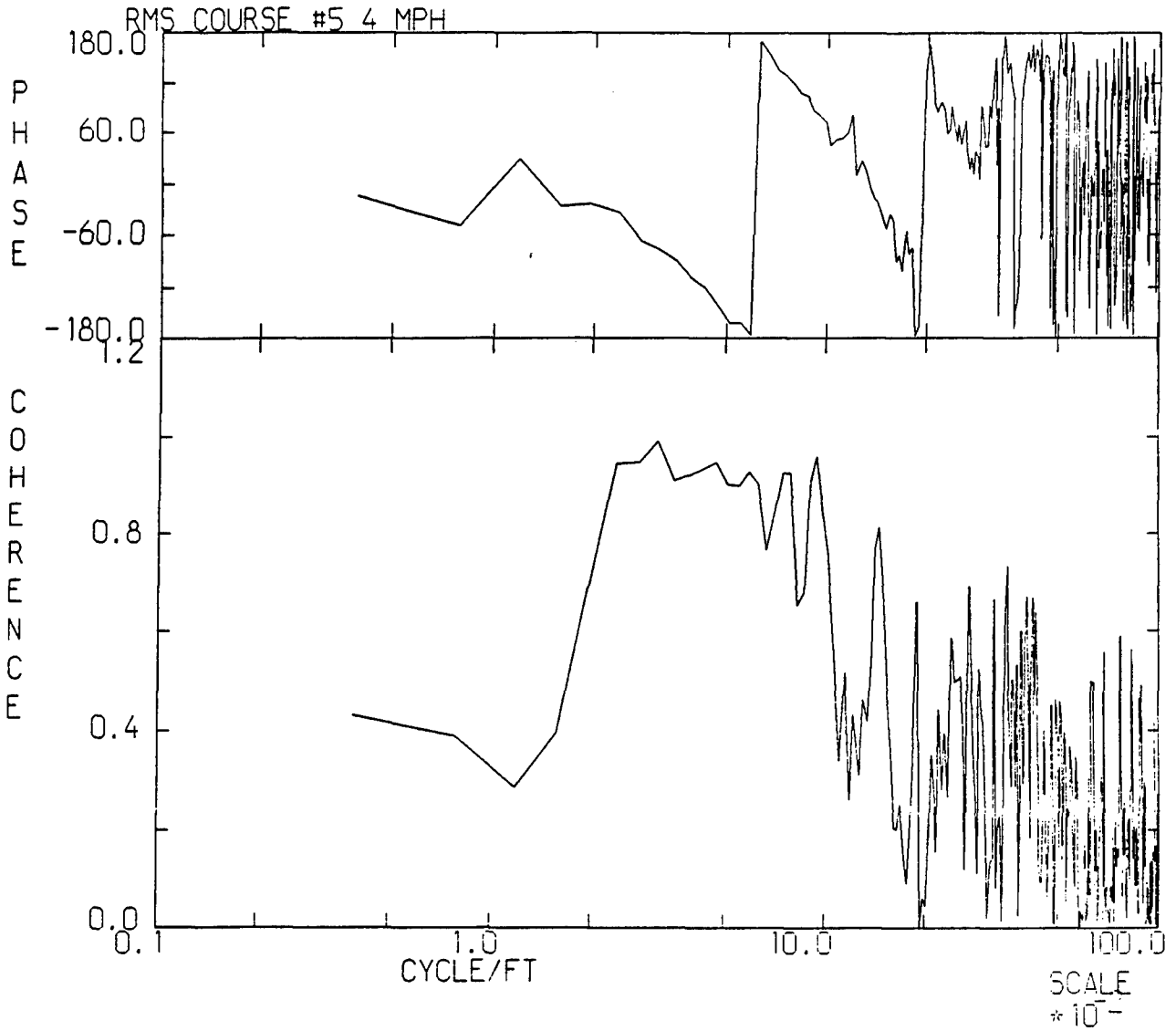

Figure 24. DFMV Left-Front to Left-Rear Coherence of RMS Course #5, 4 MPH

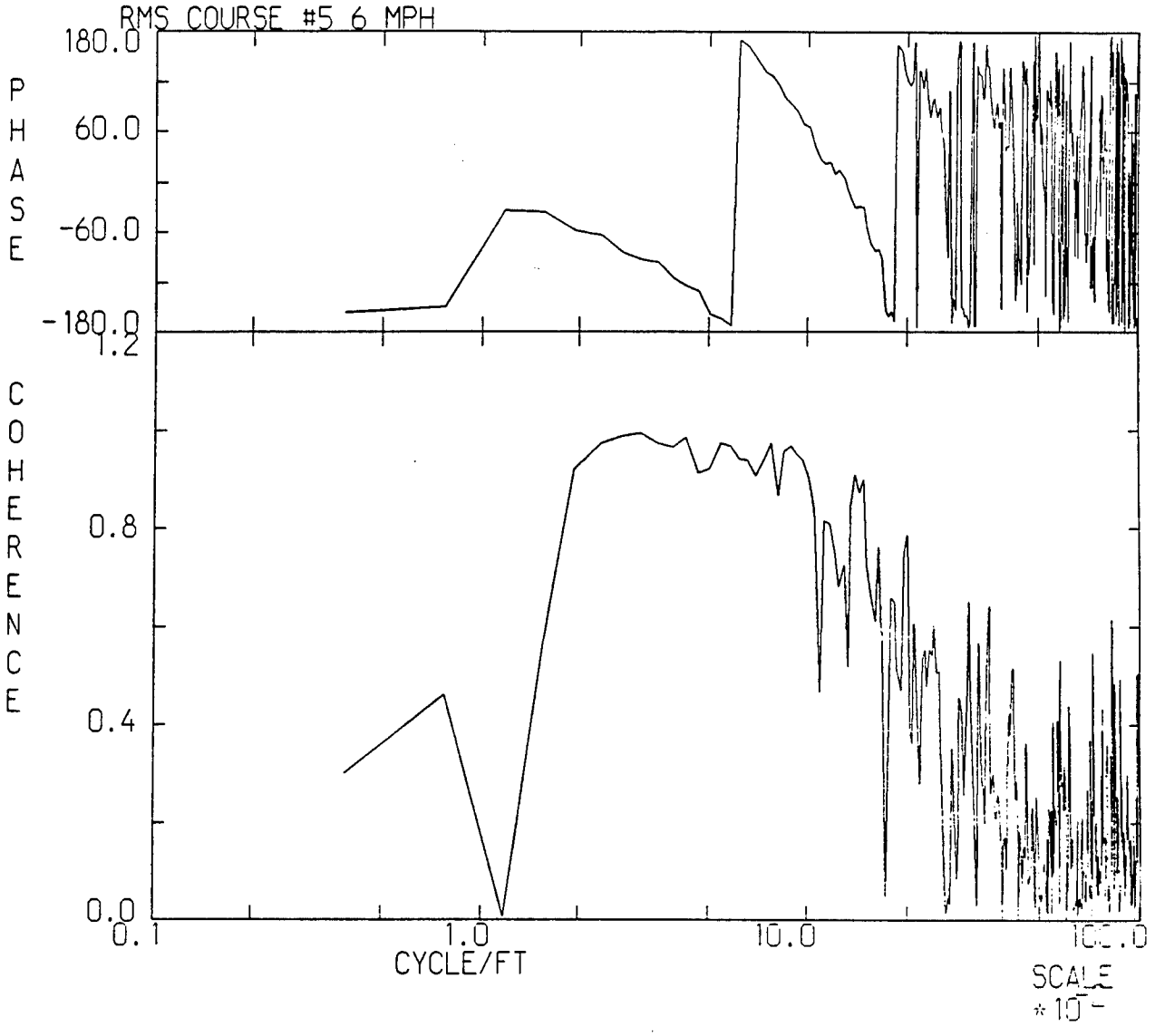

Figure 25. DFMV Left-Front to Left-Rear Coherence of RMS Course #5, 6 MPH

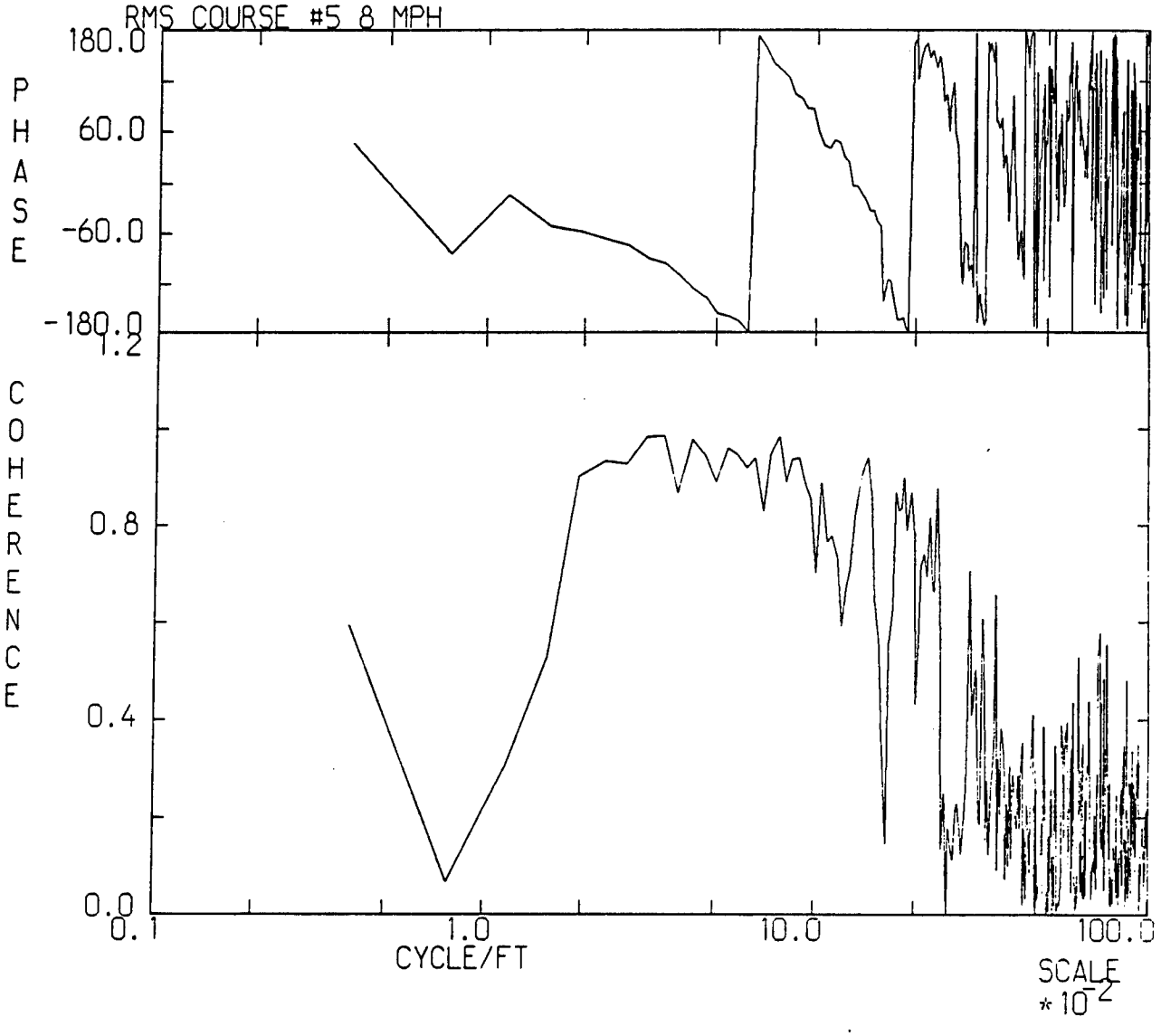

Figure 26. DFMV Left-Front to Left-Rear Coherence of RMS Course #5, 8 MPH

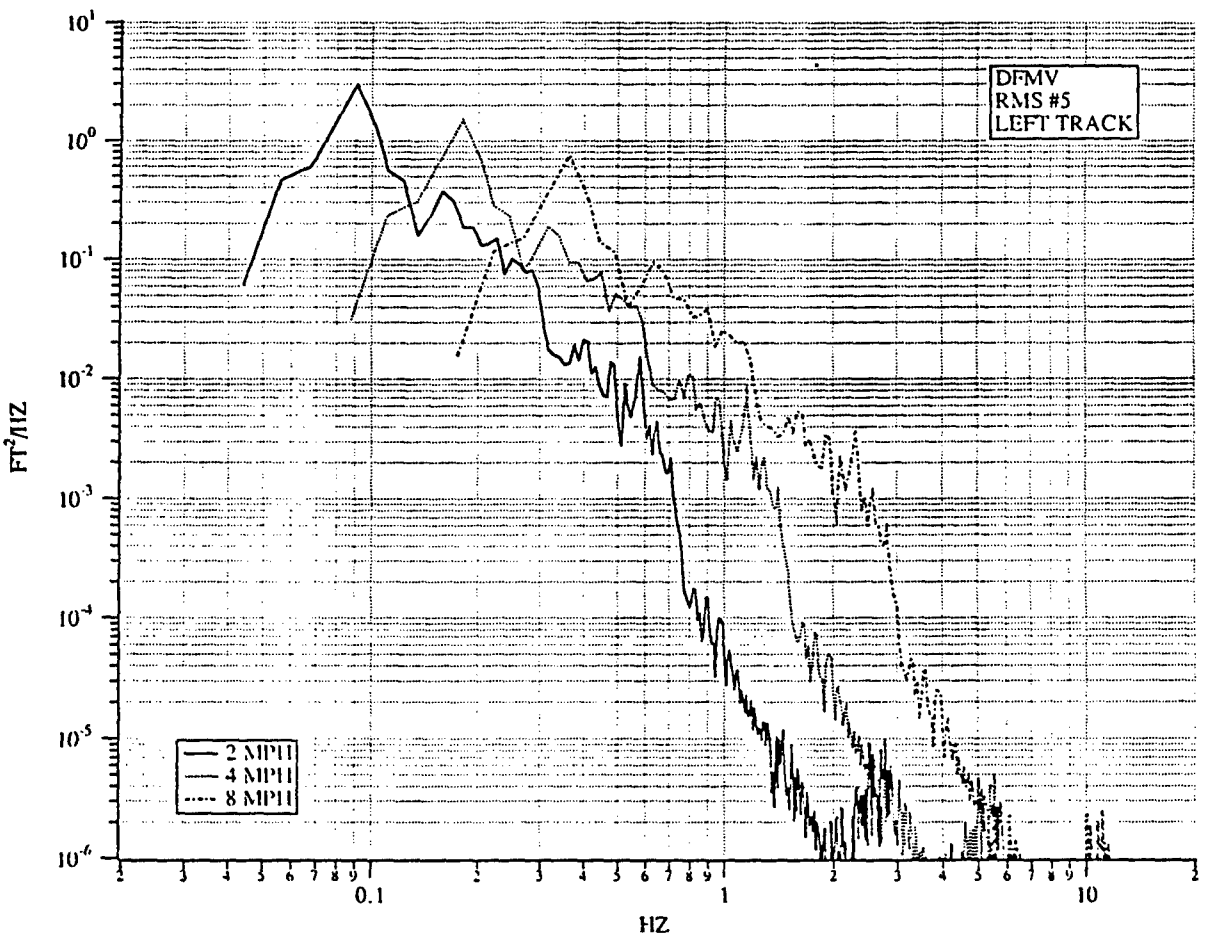

Figure 27. Displacement PSD for RMS Course #5, Speeds of 2, 4 and 8 MPH

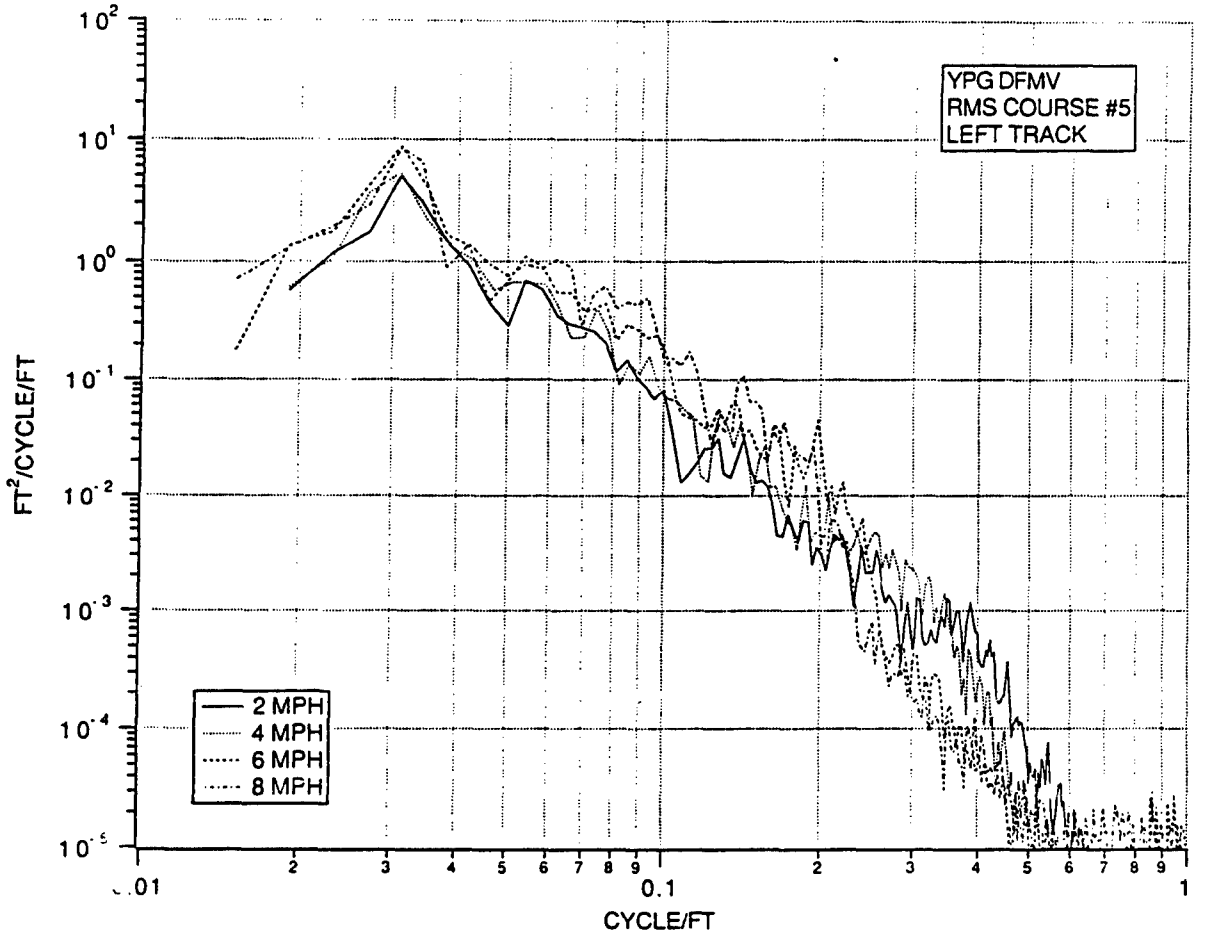

Figure 28. Wave-Number Spectrum for RMS Test Course No. 5 Computed For DFMV Speeds of 2, 4, 6 and 8 MPH.

APPENDIX N

DFMV ELEVATION VERSUS DISTANCE TREND DATA

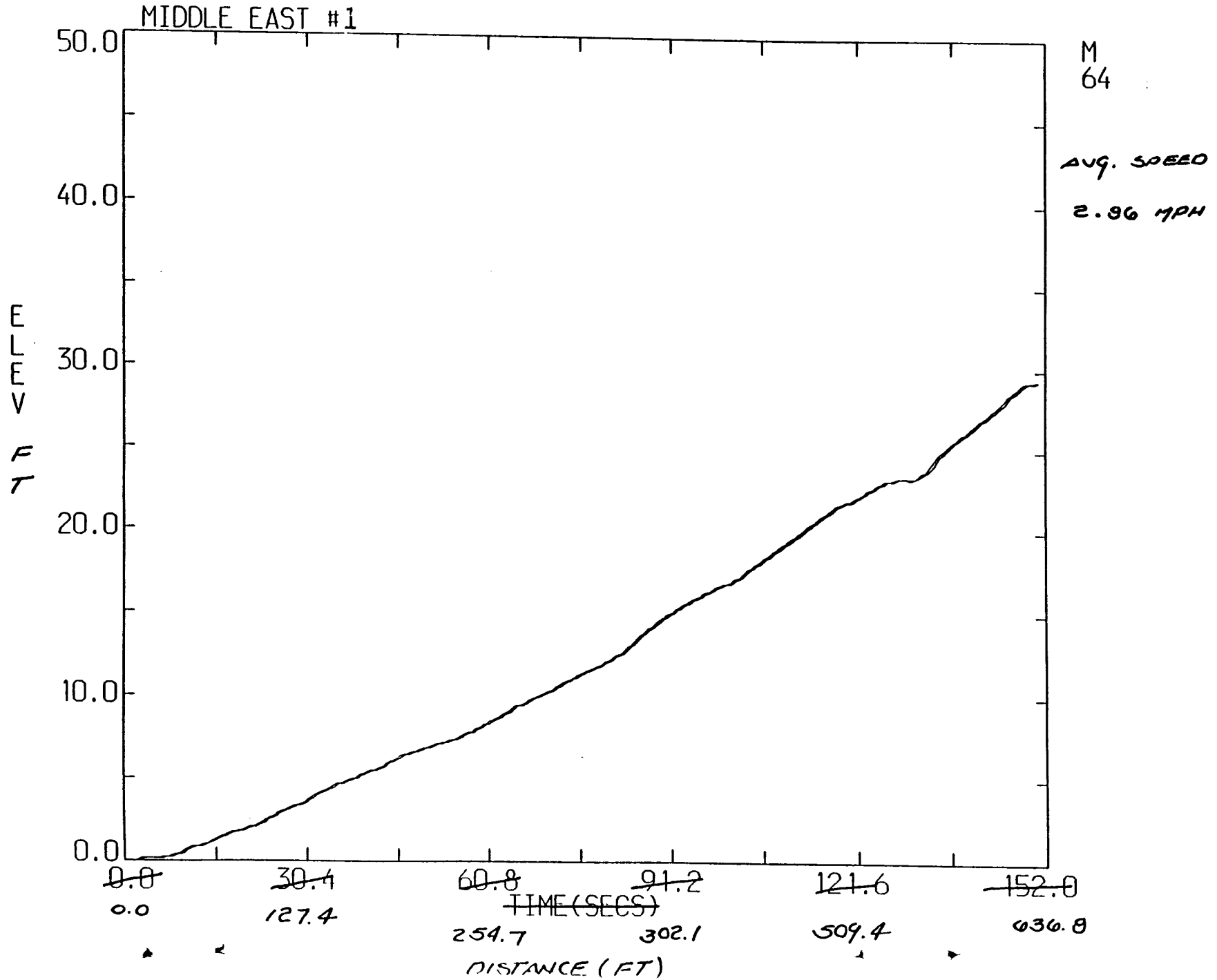
MIDDLE EAST #1
50.0
40.0
30.0
20.0
10.0
0.0
ELEV FT
M
64
AVG. SPEED
2.96 MPH
0.0
30.4
60.8
91.2
121.6
152.0
0.0
127.4
254.7
302.1
509.4
636.8
TIME (SECS)
DISTANCE (FT)

270

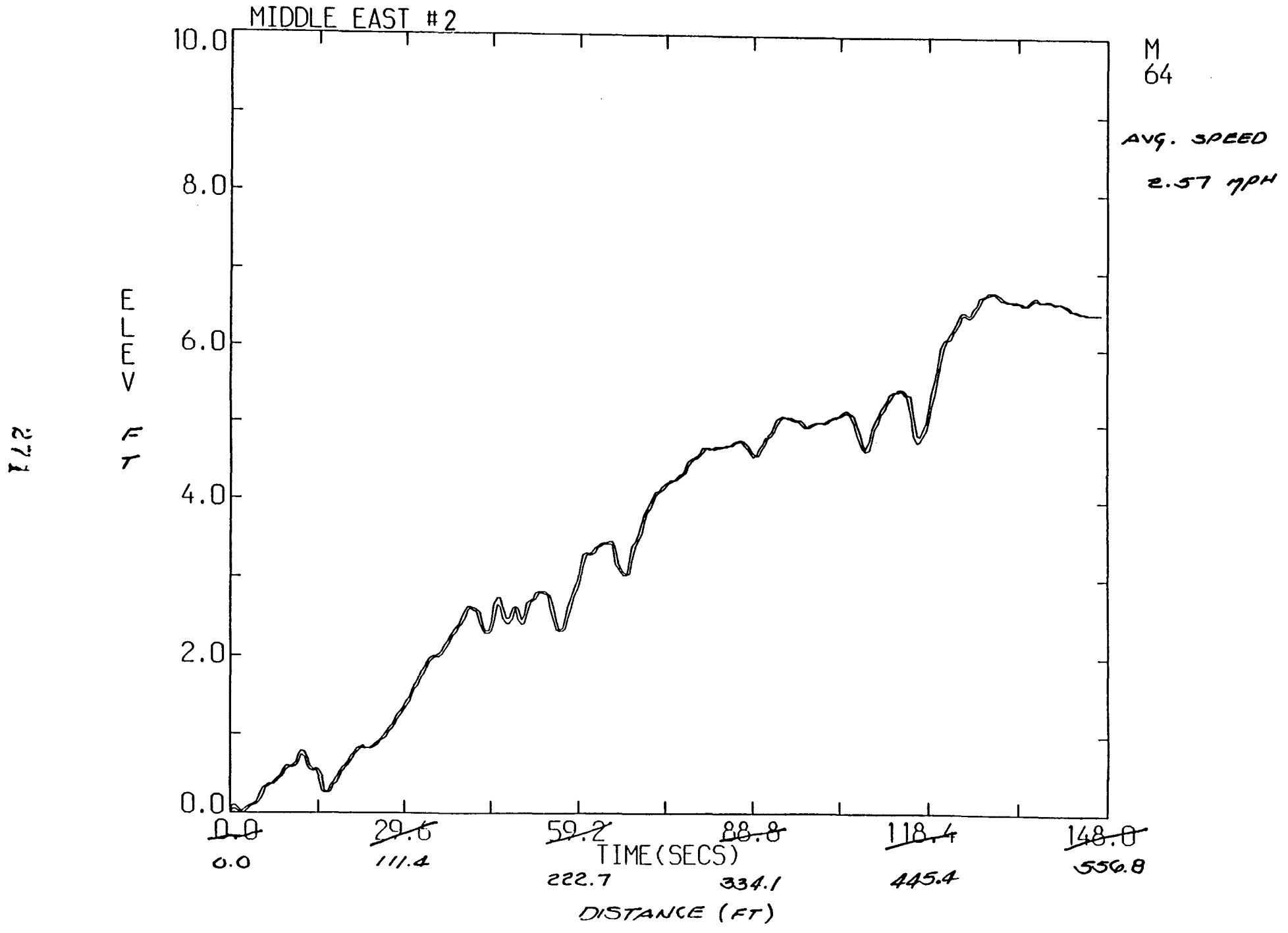
MIDDLE EAST #2
10.0
8.0
6.0
4.0
2.0
0.0
ELEV FT
0.0
29.6
59.2
88.8
118.4
148.0
TIME(SECS)
0.0
111.4
222.7
334.1
445.4
556.8
DISTANCE (FT)
M
64
AVG. SPEED
2.57 MPH

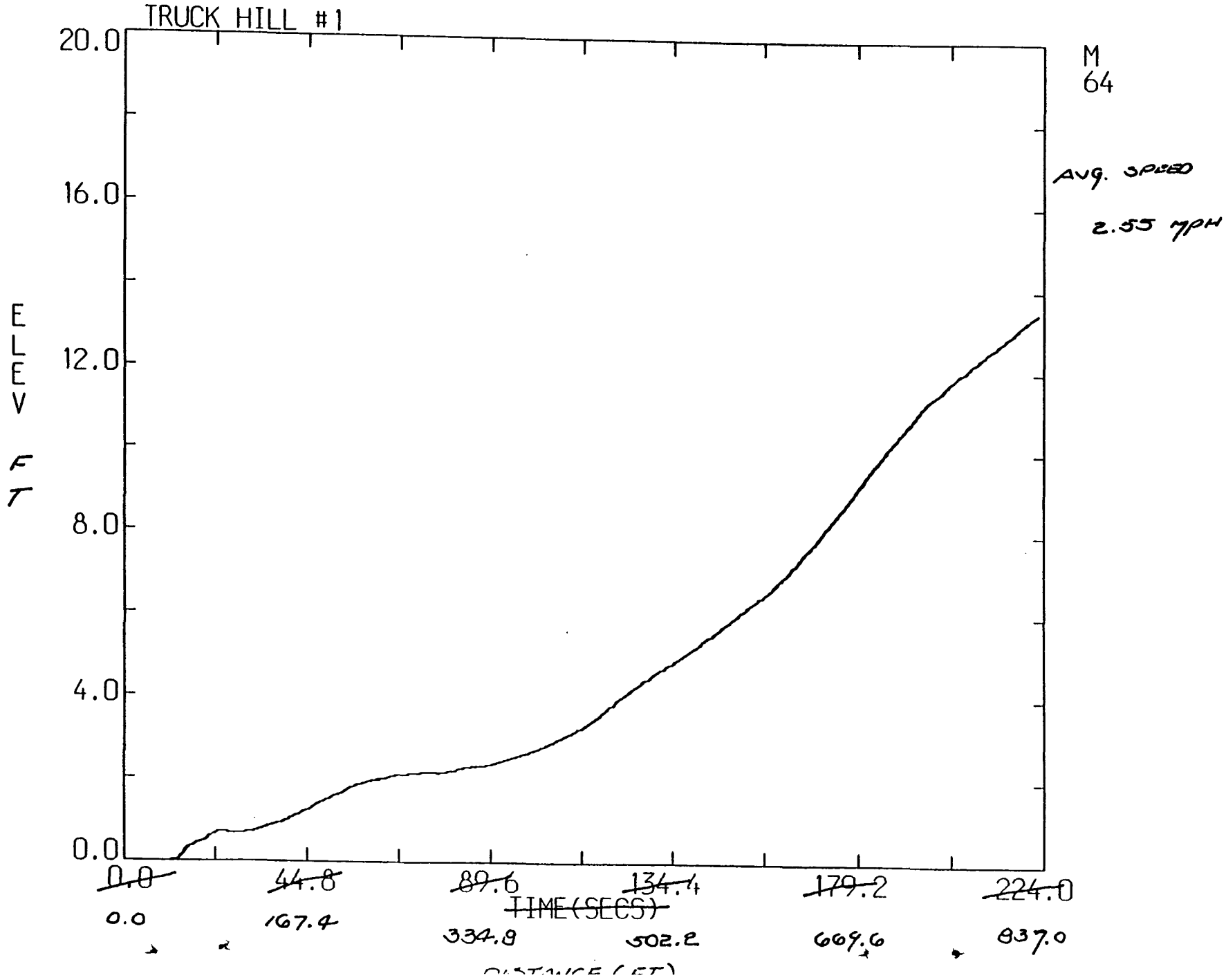
TRUCK HILL #1
20.0
16.0
12.0
8.0
4.0
0.0
ELEV FT
M
64
AVG. SPEED
2.55 MPH
0.0
44.8
89.6
134.4
179.2
224.0
TIME(SECS)
0.0
167.4
334.8
502.2
669.6
837.0

212

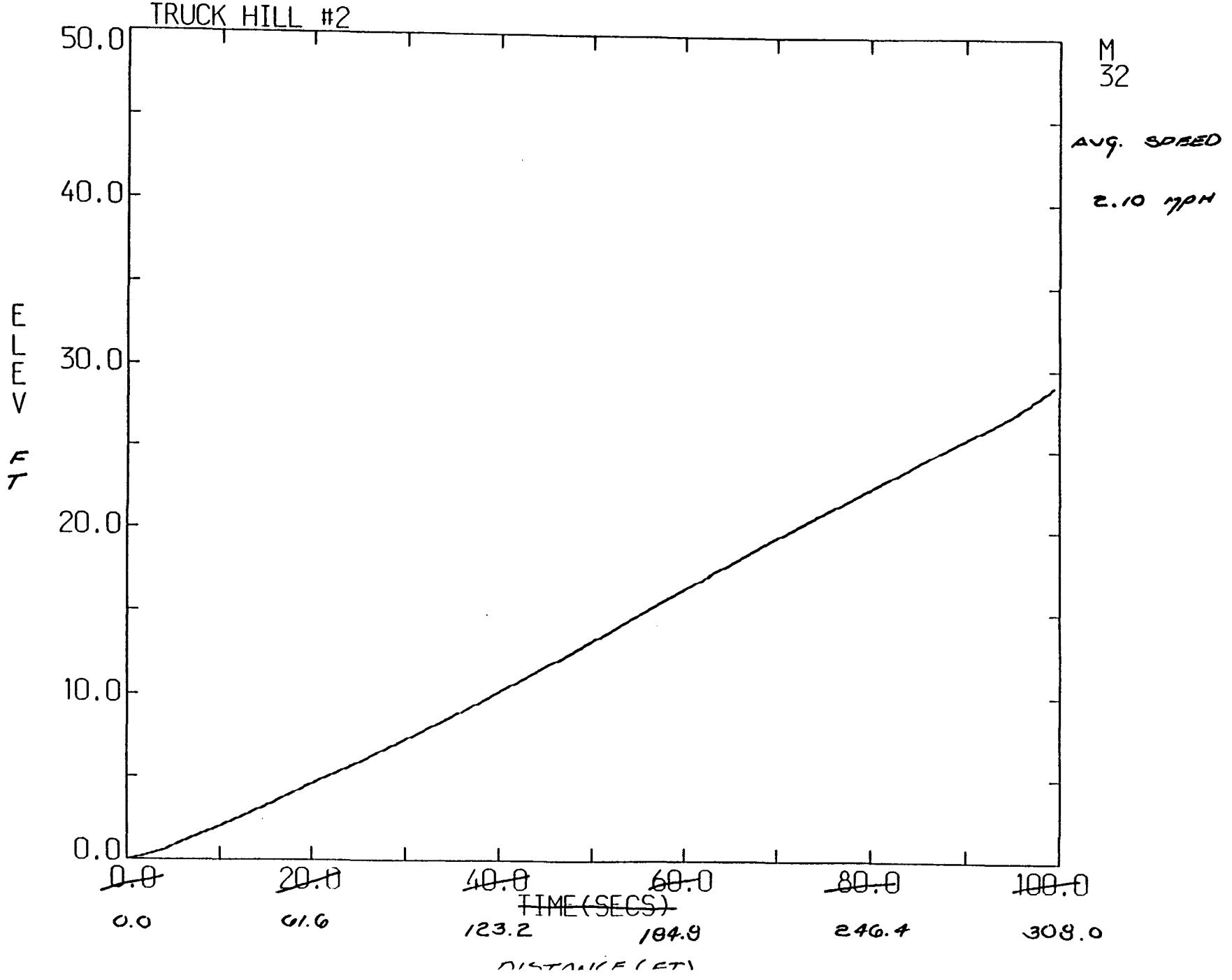
TRUCK HILL #2
50.0
40.0
30.0
20.0
10.0
0.0
ELEV FT
0.0
20.0
40.0
60.0
80.0
100.0
TIME(SECS)
0.0
61.6
123.2
184.9
246.4
308.0
DISTANCE (FT)
M
32
AVG. SPEED
2.10 MPH

273

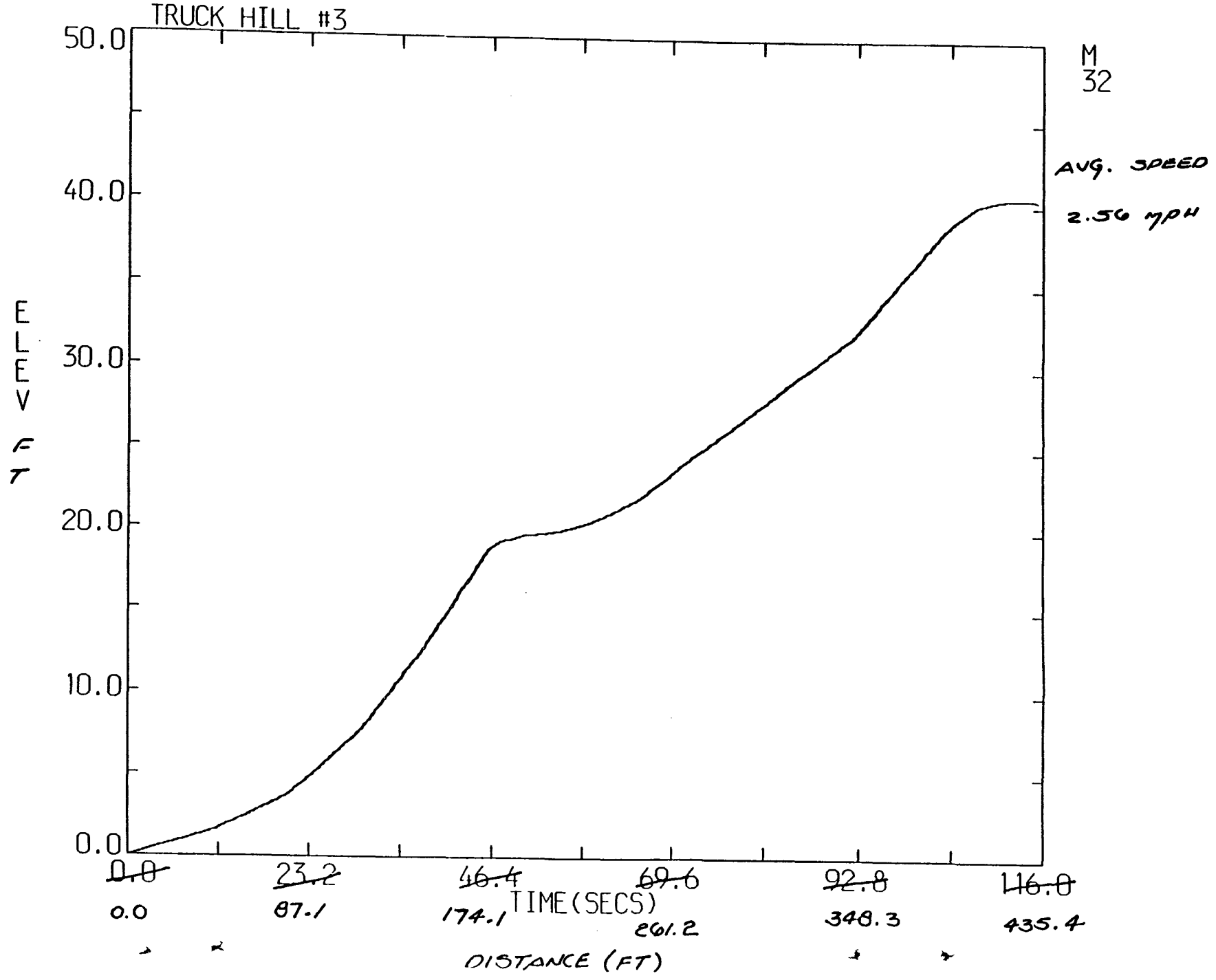
TRUCK HILL #3
M
32
AVG. SPEED
2.56 MPH
50.0
40.0
30.0
20.0
10.0
0.0
ELEV FT
0.0
23.2
46.4
69.6
92.8
116.0
0.0
87.1
174.1
261.2
348.3
435.4
TIME (SECS)
DISTANCE (FT)

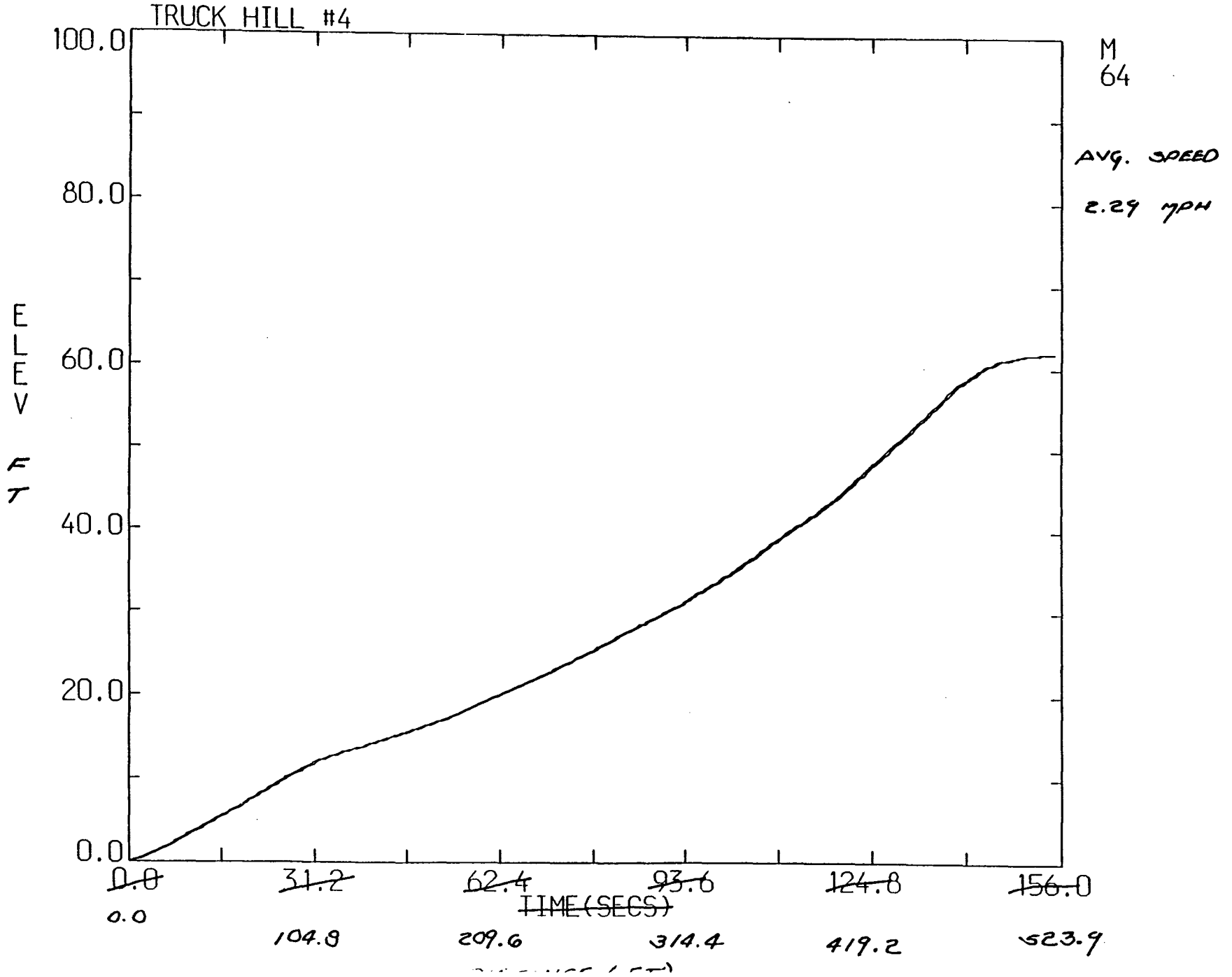
TRUCK HILL #4
100.0
80.0
60.0
40.0
20.0
0.0
ELEVATION
0.0
31.2
62.4
93.6
124.8
156.0
TIME(SECS)
0.0
104.8
209.6
314.4
419.2
523.9
M
64
AVG. SPEED
2.29 MPH

Appendix O

SPRING RATE AND DAMPING CURVES FOR THE GOODYEAR 37X12.50R16.5LT RADIAL-PLY TIRE

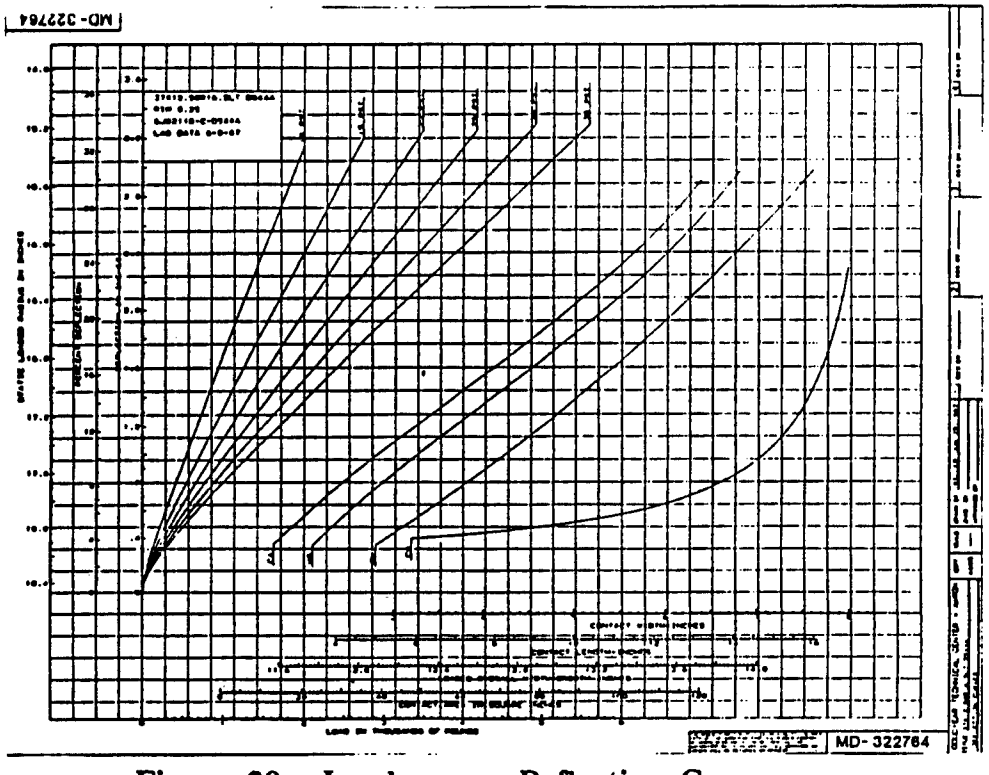

Figure 29. Load versus Deflection Curve

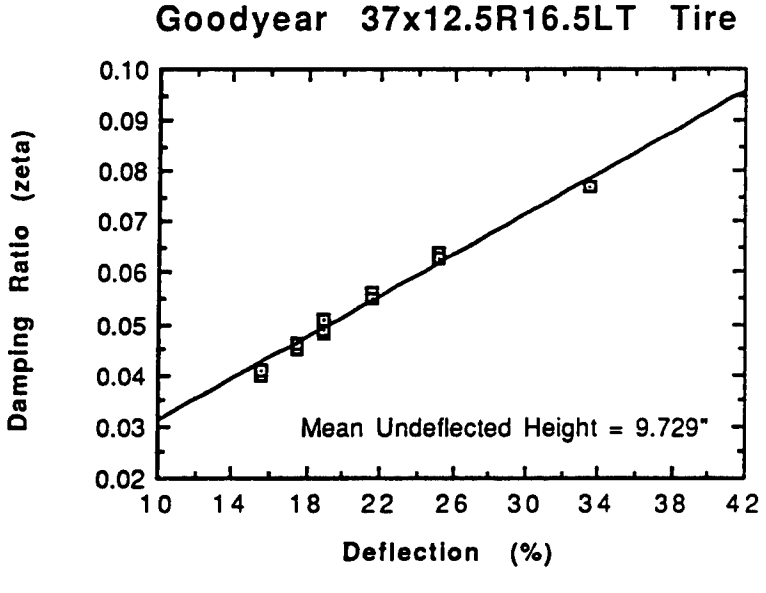

Figure 30. Damping Ratio Versus Deflection Curve

DISTRIBUTION LIST

	Copies
Commander Defense Technical Information Center Building 5, Cameron Station ATTN: DDAC Alexandria, VA 22304-9990	12
Manager Defense Logistics Studies Information Exchange ATTN AMXMC-D Fort Lee, VA 23801-6044	2
Commander U.S. Army Tank-Automotive Command ATTN: ASQNC-TAC-DIT (Technical Library) Warren, MI 48397-5000	2
Commander U.S. Army Tank-Automotive Commend ATTN: AMSTA-CF (Dr. Oscar) Warren, MI 48397-5000	1
Director U.S. Army Materiel Systems Analysis Activity ATTN: AMXSY-MP (Mr. Cohen) Aberdeen Proving Ground, MD 21005-5071	1